# SURFACE IRRIGATION Theory and Practice

WYNN R. WALKER
GAYLORD V. SKOGERBOE

Utah State University

# **Contents**

	PREFACE	X
1	THE PRACTICE OF IRRIGATION	1
	Introduction 1 Objectives of Irrigation 2 Selecting an Irrigation Method 3	
	Advantages and Disadvantages of Surface Irrigation 6	
	References 7	
2	THE IRRIGATION REQUIREMENT	8
	Introduction 8	
	Water Balance 9	
	Soil Characteristics 11	
	Crop Evaporative and Drainage Requirements 20	
	Irrigation Efficiency and Uniformity 22	

	Irrigation Requirement 25	
	Example Problems 25	
	Homework Problems 27	
	References 30	
3	SURFACE IRRIGATION SYSTEMS	32
	Introduction 32	
	Types of Surface Systems 33	
	Water Supply and Management 37	
	Structural Elements 39	
	References 46	
4	FIELD MEASUREMENT TECHNIQUES	47
	Introduction 47	
	Flow Measurement 47	
	Irrigation Events 73	
	Infiltration 80	
	Soil Water 93	
	Example Problems 98	
	Homework Problems 101	
	References 102	
5	EVALUATION OF THE FIELD SYSTEM	104
	Objectives of Evaluation 104	
	Inflow-Outflow 105	
	Advance and Recession 106	
	Advance-Surface Storage 108	
	Infiltration 111	
	Irrigation System Performance 120	
	Alternatives for Improving Hydraulic Performance 124	
	Example Problems 127	

**vi** Contents

	Homework Problems 130	
	References 133	
6	VOLUME BALANCE FIELD DESIGN	134
	Design Objectives 134	
	Design Data 135	
	Preliminary Design 136	
	Detailed Design 138	
	A Rationale for Volume Balance 138	
	Common Design Computations 139	
	Furrow Irrigation Design 142	
	Border Irrigation Design 148	
	Basin Irrigation Design 150	
	Example Problems 152	
	Homework Problems 175	
	References 177	
7	LAND LEVELING	178
	Introduction 178	
	General Considerations 179	
	Land Leveling 180	
	Other Considerations 187	
	Homework Problems 189	
	References 191	

192

Conceptual Approach 192

Automation of Open-Channel Headland Facilities 193

8 OPERATION OF SURFACE IRRIGATION SYSTEMS

Pipeline Automation 197

Controllers 202

Calibration 205

Contents vii

	References 210	
9	SURGE FLOW SURFACE IRRIGATION	212
	Conceptual Development 212	
	Early Field Tests 214	
	Development of Surge Flow Simulation Models 218	
	Surge Flow Management 227	
	Summary 233	
	References 233	
10	HEADLAND FACILITIES	235
	Introduction 235	
	Turnout Structures 235	
	Debris and Sediment Removal 236	
	Open-Channel Irrigation Distribution 239	
	Closed Conduit Irrigation Distribution 264	
	Example Problems 277	
	Homework Problems 286	
	References 287	
11	FUNDAMENTALS OF SURFACE IRRIGATION HYDRAULICS	289
	Introduction 289	
	The Continuity Equation 290	
	Momentum Equation 292	
	Nondimensionalization of Basic Equations 297	
	References 300	

Irrigation Scheduling 206

Monitoring and Evaluation 208

viii

12	THE HYDRODYNAMIC MODEL: CHARACTERISTIC APPROACH	301
	Introduction 301	
	Characteristic Equations 302	
	Numerical Solution for Plane Flow 304	
	Summary 310	
	References 312	
13	THE HYDRODYNAMIC MODEL: EULERIAN INTEGRATION	313
	The Deformable Control Volume 313	
	Definition of Continuity 314	
	Momentum Equation 315	
	Numerical Solution 319	
	Summary 326	
	References 326	
14	THE ZERO-INERTIA MODEL	327
	Introduction 327	
	General Mathematical Approach 328	
	Numerical Solution 336	
	Model Verification 339	
	References 344	
15	THE KINEMATIC-WAVE MODEL	345
	Introduction 345	
	The Characteristic Solution 346	
	The Deformable Control Volume Approach 350	
	Verification 355	
	References 357	

Contents

16 THE VOLUME BALANCE MO	6	THE	VOL	UME	BAL	ANCE	MODEL
--------------------------	---	-----	-----	-----	-----	------	-------

358

Introduction 358

Development of Mass Continuity 358

Numerical Solutions 360

Verification 372

References 373

**INDEX** 

375

# Preface

Surface irrigation methods are the most common for artificially applying water to agricultural lands. They are favored over sprinkle, trickle, and subirrigation methods on the basis of lower capital and operating costs, the simplicity of maintenance, and the utility of unskilled labor. Since World War II, the major growth in irrigated acreage in the United States has been associated with sprinkle and trickle application methods. These pressurized systems reduced the labor requirements, eliminated the need for land leveling, and increased irrigation efficiency substantially. But worldwide, the vast majority of irrigation projects existing, planned, or under development involve surface systems.

Recent developments in surface irrigation technology have largely overcome the irrigation efficiency advantage of pressurized systems and an array of automating devices have reduced labor requirements. The major trade-off between surface methods and the pressurized methods lies in the relative costs of land leveling for effective gravity distribution versus energy for pressurization. Surface methods require less capital investment and are simpler to maintain, but management is more complicated. There is one disadvantage of surface irrigation that confronts every researcher, designer, and irrigator—the soil must be used to convey and infiltrate the water over the field. Unfortunately, soil properties are so highly varied both spatially and temporally that they become extremely difficult to characterize. This creates an engineering problem in which at least two of the primary design variables, discharge and time of application, must be estimated not only at the field layout stage but also prior to or immediately following the initiation of every surface irrigation event. Thus, while it is possible for the new generation

of surface irrigation methods to be attractive alternatives to sprinkle and trickle systems, their associated engineering and management practices are much more difficult to define and implement.

With this challenge in mind, we developed this text for our graduate and undergraduate irrigation engineering students. Being constrained by the time we have had to present the material on surface irrigation, we have used our own selective judgment of pertinent topics. We have tried to provide a framework for study and training while trusting the many other excellent references to the subject will be consulted to explain issues we have not addressed. This text is not a primer. We have assumed that the reader is already familiar with basic soil—water relationships and has been introduced to various surface irrigation methods. The first three chapters are included to remind the reader briefly of these concepts. We have found in our teaching that it helps to review basic principles in order to begin the class on a common footing and to identify any weaknesses in this regard.

We have adopted a mathematical flavor in this text rather than the graphical or tabular format which many may argue is the standard for practicing engineers. We contend, first of all, that in order to reduce surface irrigation engineering to a graphical level, the problem becomes oversimplified because some important parameters tend to be omitted. Further, our own teaching experience has convinced us that a mathematical approach provides the student with a substantially better conceptual understanding. Finally, the popular use of high-capacity programmable calculators and computers requires the mathematical approach and allows more sophisticated design or evaluation techniques to be employed.

The text can be divided into two parts for instructional purposes. Chapters 1 to 10 are presented for the use of practicing irrigation engineers, senior, and M.S.-level students. These chapters cover the fundamentals of volume balance evaluation and design, illustrate methodologies for conducting field measurements, discuss measures involved in surface irrigation operation and maintenance, and describe a unique product of Utah State University, "surge flow."

Chapters 11 to 16 have been provided for the modeler. These chapters summarize the theoretical contributions of the pioneers of modern surface irrigation whose most important work emerged in the early 1960s. We then move into the major numerical solutions developed in the mid-1970s, and finally discuss the computer solutions that evolved in the early 1980s, which have greatly expanded our capability for implementing field programs to improve surface irrigation management.

The reader may be surprised to know that Chapters 11 to 16 did not evolve from a desire to teach these principles in depth at Utah State University; nor were the models developed to exploit modern computer technology. The fact is that in 1980 we were observing the startling impacts of the surge flow regime that our colleagues, Drs. Glen Stringham, Jack Keller, and A. Alvin Bishop, had discovered. We believed this irrigation practice would violate all previously held assumptions regarding existing surface irrigation hydraulic models. We therefore believed that unless the theory were expanded and more fully developed, design and management practices would have to emerge from field experience—a sub-

xii Preface

optimal alternative for a new technology. As a consequence, something beyond our original vision has resulted, which is so often the case. We hope this text will stimulate new seeds that will yield even better ideas in surface irrigation. We look forward to a future of rapidly increasing knowledge in a topic that is vital to a large portion of the world's population.

Wynn R. Walker Gaylord V. Skogerboe Logan, Utah

Preface

# The Practice of Irrigation

#### INTRODUCTION

Approximately 20% of the total cultivated land in the world (about 1.0 billion hectares) is presently irrigated. Historically, civilizations have been dependent on the development of irrigated agriculture to provide the agrarian basis of a society and to enhance the security of their people. When the constraints of the complex soil-water-plant relationship were ignored either through ignorance or lack of planning, the productivity of irrigated agriculture declined. The ancient civilization of Mesopotamia flourished in the Tigris-Euphrates Valley 6000 years ago (Kang, 1972) and then floundered when the soil became saline due to poor irrigation practices and a lack of drainage. It has not recovered to this day. It has been estimated that 6000 years ago it supported as many as 25 million persons. Iraq, which presently occupies much of this same area, today has a population of about 14 million. In fact, the tax records from Mesopotamia show that barley yields were about two to four times present yields in this area (Kovda et al., 1973).

When a reliable and suitable supply of water becomes available for agriculture it can result in vast improvements in agricultural production and assure economic returns to the grower. Effective agronomic practices must be included, such as fertilization and crop rotation. Soil reclamation and management, erosion control, and drainage practices must be developed for the local conditions and applied rigorously. But water management, delivering water to the farms and on the farm itself, is the key to successful irrigation projects.

#### **OBJECTIVES IN IRRIGATION**

Irrigation in arid areas of the world has two primary objectives: (1) to supply the essential moisture for plant growth, which includes the transport of essential nutrients; and (2) to leach or dilute salts in the soil. Irrigation provides a number of side benefits, such as cooling the soil and the atmosphere to create a more favorable environment for plant growth. Irrigation supplements the supply of water received from precipitation and other types of atmospheric water, floodwaters, and groundwater.

The method and timing of irrigations have significant effects on crop production. Annual crops may not germinate if the irrigation method causes a crust over the seedbed. Once established, the stress created by soil moisture tensions can often severely affect yields if they occur during critical periods. Thus, while the first objective of irrigation is to replenish the soil moisture reservoir, the method and its management are important considerations.

Salts are contributed to the irrigation system by two main processes: salt concentration and chemical weathering. Salt concentration effects occur in the soil due to the removal of water by the consumptive use of crops and other natural vegetation. Irrigation along with the interbasin export of high-quality water and evaporation from the water surfaces of streams and lakes are major causes of increased salinity levels caused by concentrating effects. Salts may also accumulate in the soil by the chemical weathering of soil and substrata by irrigation water and natural subsurface flows. Also known as "salt loading," it contributes to the concentrations in water supplies along with excessive fertilizer applications, municipal and industrial wastes, and point sources such as mineral springs, flowing brine wells, and geysers.

If the salts entering and accumulating in the root zone as a result of evaportranspiration or weathering are not periodically leached from the crop root zone, the land will become unproductive. However, the water which passes through the root zone carrying the excess salts may be severely restricted from further travel by subsurface conditions. When this occurs, this leachate will eventually build up into the root zone, causing high salinity levels and poor aeration (waterlogging). In many areas, drainage is more than adequate and the movement of salts from irrigated lands contaminates local groundwater basins and stream flows. Another serious environmental problem associated with irrigated agriculture is the erosion of topsoil and soil nutrients by tailwater into the reservoirs, canals, and laterals of downstream users. Siltation reduces the capacities of drainage and irrigation channels, resulting in costly large-scale maintenance programs and the installation of expensive structures for its removal. The useful lifetime of dams and reservoirs is often computed in terms of the rate of sedimentation.

In view of the needs for irrigation—to increase food and fiber production with all the associated consequences to the stability of a society, as well as the potential for adverse environmental effects, the technology of irrigation is more complex than many nonprofessionals appreciate. It is important that the scope of irrigation engineering not be limited to diversion and conveyance systems, which has been the concern of the civil engineer, nor solely to the irrigated field, which

has been the concern of agricultural engineers and agronomists. Thus it is the "irrigation engineer" who attempts to integrate the delivery, farm, and drainage subsystems into a cohesive discipline.

#### SELECTING AN IRRIGATION METHOD

Irrigation management is often designed to maximize efficiencies and minimize the labor and capital requirements of that particular irrigation system while maintaining a favorable growing environment for the plant. Some managerial inputs are dependent on the type of irrigation system and the design of the system. For example, the degree of automation, the type of system (sprinkle, trickle, or conventional surface irrigation), the reuse of field tailwater, soil type, topographical variations in a field or farm, and the existence and location of management tools such as flow measurement and water control structures can influence the managerial decision-making process.

However, management decisions which are common to all systems, regardless of the types, are the frequency of irrigation, depth of water to be applied, and measures to increase the uniformity of applications such as land leveling or shaping. In addition, individual systems can be manipulated to greatly increase application efficiencies. For example, in furrow irrigation some growers will use two siphon tubes per furrow at the start of irrigation (advance phase) and when the water has reached the end of the row, one tube is removed (wetting phase). This increases the efficiency by minimizing field tailwater runoff, but it requires an additional labor input.

There are a large number of considerations which must be taken into account in the selection of an irrigation system. These factors will vary in importance from location to location and crop to crop. Briefly stated, these considerations include the compatibility of the system with other agricultural operations, economic factors, topographic limitations, soil properties, and several agronomic and external influences.

# Compatibility

The irrigation system for a field or a farm must be compatible with the other existing farm operations, such as land preparation, cultivation, and harvesting practices. For instance, the use of the more efficient, large machinery requires longer and wider fields and even perhaps removable irrigation systems.

#### **Economic Considerations**

The type of irrigation system selected is also an economic decision. Some types of sprinkle systems have high per-acre costs and their use is therefore limited to high-value crops. Other systems have high labor requirements, and some have fairly high operating costs. Some systems have limitations with respect to the type of soil or the topography on which they can be used. The expected life of the

system, fixed costs, and annual operation costs (energy, water depreciation, land preparation, maintenance, labor, taxes, etc.) should also be included in the analysis when selecting an irrigation system.

In considering the economics of irrigation systems it must be kept in mind that the system yielding the highest return is a compromise between the four resources of labor, water, land, and capital. Within limits, each can be traded for the other, with only a marginal change in the gross return of the systems. Thus water can be saved in a surface irrigation system if more labor or labor of greater skill is used to apply the water.

# **Topographic Limitations**

Restrictions on irrigation system selection due to topography include groundwater levels, the location and relative elevation of the water source, field boundaries, acreage in each field, the location of roads and natural gas lines, electricity and water lines and other obstructions, the shape of the field, and the field slope (which can vary dramatically over a field). Field surface conditions such as relative roughness and gullies should also be considered.

The slope of the land is very important. Some types of sprinklers can operate on slopes up to 20% or more, but furrow or graded border irrigation is usually limited to a maximum slope of around 2 to 6%. Trickle irrigation can be used on slopes up to 60%.

The shape of a field also determines the type of system. For instance, level borders, furrows, hand-move or solid-set sprinklers, subsurface, contour ditch, or trickle irrigation systems can be adjusted to fit almost any field shape; whereas a center-pivot sprinkler must have approximately square-shaped fields. For a side-roll sprinkler, level furrow, graded border, or contour furrow, the field should be approximately rectangular in shape.

#### Soil Characteristics

The soil type, soil mositure-holding capacity, the intake rate, and effective soil depth are also criteria which enter into the type of system selected. For example, sandy soils have a high intake rate and will accept high-volume sprinklers which would be unacceptable on a tight clay soil.

The moisture-holding capacity will influence the size of the irrigation sets and frequency of irrigations, as evidenced by a sandy soil with low moisture-holding capacity, which requires frequent, light applications of water. A center-pivot or sideroll sprinkler or even a trickle irrigation system would perform satisfactorily in this case.

A number of other soil properties are also significant factors in considering the type of irrigation system that will be most advantageous in a particular situation. The interaction of water and soils due to physical, biological, and chemical processes has some influence on the hydraulic characteristics and tilth. Crusting and erod-

ibility should be considered in each irrigation system design, and the spatial distribution of soil properties may be an important limitation on some methods of applying irrigation water.

# Water Supply

The quality, quantity, and temporal distribution characteristics of the source of irrigation water have a significant bearing on the irrigation practice. Crop water demands are essentially continuous during the growing season, although varied in magnitude. A small, readily available water supply is best utilized in a small-capacity irrigation system which incorporates frequent applications. The depths applied per irrigation are therefore small in comparison to systems having a large discharge available less frequently.

The quality of water in conjunction with the frequency of irrigations must be evaluated. Salinity is generally the most significant problem, although other elements, such as boron, can be important. A highly saline water supply must be applied more frequently and in larger amounts than a good-quality water.

# **Crop Factors**

Some of the factors associated with the crops being grown which influence the choice of irrigation system and its eventual management are summarized by Corey and Hart (1974):

- 1. The tolerance of the crop during both development and maturation to soil salinity, aeration, and various substances, such as boron
- 2. The magnitude and temporal distribution of water needs for maximum production
- 3. The economic value of the crop

In each case, the allowable investment in the system and the crops which can be irrigated by a specific system are affected by these crop factors.

#### **External Influences**

At times, the selection of an irrigating method may be dictated by considerations somewhat unrelated to agriculture. The irrigation project may be designed from the reservoir to the turnout without regard to what is needed at the farm and thereby force a method of irrigation on the farmers. National concerns about foreign exchange and expatriate consulation may limit import of alternative technologies, and local fabrication capacities may not be adequate. Thus it is easy to find countries where trickle irrigation could be used economically but is prevented

by policy. Some methods may be embedded culturally and used regardless of suitability.

# ADVANTAGES AND DISADVANTAGES OF SURFACE IRRIGATION

The term "surface irrigation" refers to a broad class of irrigation methods in which water is distributed over the field by gravity. A flow is introduced at a high point or along a high edge of the field and allowed to cover the field by overland flow. The rate of coverage is dependent almost entirely on the quantitative differences between inlet discharge and the accumulating infiltration. Secondary factors include field slope and surface roughness.

The practice of surface irrigation is thousands of years old and collectively represents by far the most common irrigation activity today. The easiest water supplies to develop have been stream or river flows which required only a simple river dike and canal to provide water to adjacent lands. These low-lying soils were typically high in clay and silt content and had relatively small slopes. A comparison of irrigation methods at various historical junctures would lead to differing conclusions, but some general advantages and disadvantages of surface irrigation can be outlined.

As alluded to above, surface irrigation systems can be developed with minimal capital investment, although these investments can be very large if the water supply and irrigated fields are some distance apart. At the farm level and even at the conveyance and distribution levels, surface irrigation systems need not require complicated and expensive equipment. Labor requirements for surface irrigation tend to be higher than for the pressurized types, but the labor still need not be high unless maximum efficiencies are sought. However, when water supplies are short, irrigators have developed highly skilled practices which achieve high efficiencies. With the variety of irrigation systems in use today, it is difficult to conclude whether operation and maintenance costs are necessarily lower with surface methods. Generally, energy costs are substantially lower, but inefficiency may very well reverse this factor.

On the negative side, surface irrigation systems are typically less efficient in applying water than either sprinkle or trickle systems. Since many are situated on lower lands with tighter soils, surface systems tend to be more affected by waterlogging and salinity problems. The need to use the field surface as a conveyance and distribution facility requires that fields be well graded. Land leveling costs are high, so the surface irrigation practice tends to be limited to land already having small, even slopes.

A look at expected worldwide irrigation developments shows that most will be oriented toward surface irrigation. New and growing water demands by urban, industrial, energy, and military developments will focus attention on substantial improvements in the performance of surface systems. Surface irrigation is and will continue to be the central focus in irrigation engineering.

#### REFERENCES

- COREY, A. T., and W. E. HART. 1974. Soil-Water Engineering. Undergraduate class notes copyrighted by the authors while at the Department of Agricultural Engineering. Colorado State University, Fort Collins, Colo.
- ISRAELSEN, O. W., V. E. HANSEN, and G. E. STRINGHAM. 1980. Irrigation Principles and Practices, 4th ed. John Wiley & Sons, Inc., New York.
- KANG, S. T. 1972. Irrigation in Ancient Mesopotamia. Water Resour. Bull. 8(3):619-624.
- KOVDA, V. A., C. VANDENBERG, and R. M. HAGAN (eds.). 1973. Irrigation, Drainage and Salinity. An International Source Book. United Nations, Food and Agriculture Organization, Rome.

Chap. 1 References

# The Irrigation Requirement

#### INTRODUCTION

The irrigation system is usually not expected to supply all of the moisture required for maximum crop production. To do so would ignore the valuable contribution of other water sources such as rain and thereby force the irrigation system to be larger and more expensive than necessary. It is also unrealistic that irrigation can or should be practiced without waste. Certainly, the fraction of that supplied which is beneficially used should be maximized, but this fraction or irrigation efficiency cannot be 100% without other serious problems developing.

In arriving at the contribution an irrigation system will make to an irrigated area, particularly a surface irrigation system, four major factors require consideration. These are:

- 1. The concept of water balance in the region encompassing the plant environment
- 2. The body of soil supplying moisture, nutrient, and anchorage for the crop and the associated characteristics of this porous medium
- 3. The crop water requirements, including drainage for aeration and salt leaching
- 4. The efficiency and uniformity of the irrigation system

#### **WATER BALANCE**

The employment of a water balance is a useful concept for characterizing, evaluating, or monitoring any surface irrigation system. A schematic of the water balance parameters used for characterizing a surface-irrigated field is shown in Fig. 2.1. The terms are defined as:

 $D_a$  = depth of applied irrigation water

 $D_{\Delta s}$  = depth of change in soil moisture storage in the root zone where  $D_{\Delta s}$  is positive for increasing soil moisture storage

 $D_{dp}$  = depth of deep percolation

 $D_e$  = depth of evaporation from soil surface or ponded water surface

 $D_{et}$  = depth of evapotranspiration

 $D_{\rm gw}$  = depth of capillary rise from the groundwater table entering the root zone

 $D_p$  = depth of precipitation

 $D_{pl}$  = depth of precipitation intercepted by the plants (crop)

 $D_{pr}$  = depth of precipitation that occurs as surface runoff

 $D_{pz}$  = depth of precipitation that infiltrates into the soil

 $D_t$  = depth of transpiration from plants

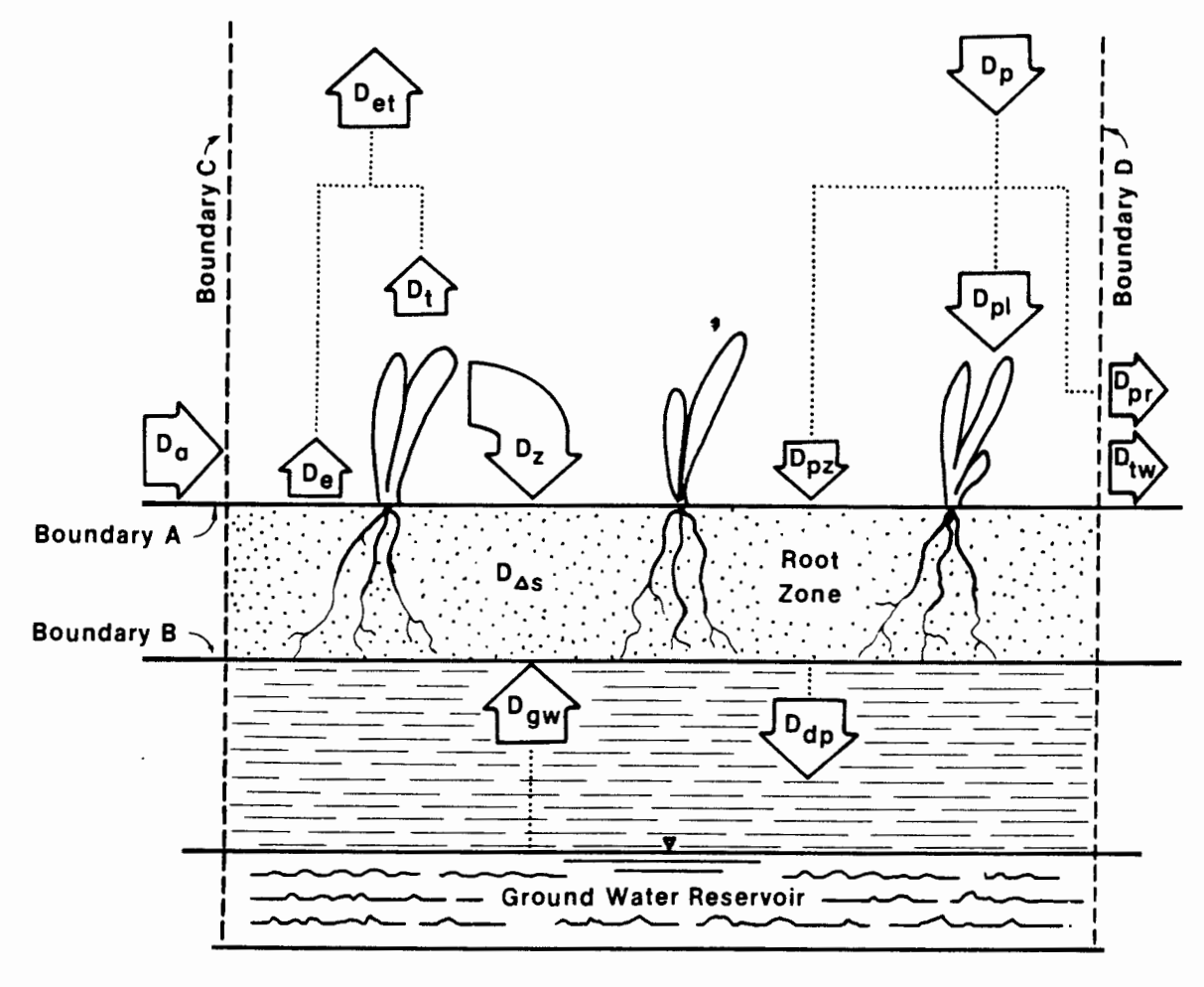


Figure 2.1 The water balance parameters for a surface-irrigated field.

Water Balance 9

- $D_{tw}$  = depth of tailwater (surface) runoff resulting from overland flow of the irrigation water supply
- $D_z$  = depth of infiltrated water resulting from overland flow of the irrigation water supply

There are two additional terms that are useful to define at this point:

- $D_{pn}$  = depth of net precipitation, or the depth of precipitation that is made available to the plant system
- $D_d$  = depth of drainage requirement for maintaining a salt balance in the root zone

The principle of continuity requires that inflow (1) minus outflow (0) equals the change in storage ( $\Delta S$ ) within the defined boundaries of a system:

$$I - O = \Delta S \tag{2.1}$$

Of primary concern in surface irrigation are boundaries A, B, C, and D as shown in Fig. 2.1, for which the continuity equation can be written as

$$(D_a + D_{gw} + D_p) - (D_{et} + D_{pr} + D_{tw} + D_{dp} + D_{pt}) = D_{\Delta s}$$
 (2.2)

in which

$$D_a = D_z + D_{tw} ag{2.3}$$

$$D_p = D_{pz} + D_{pl} + D_{pr} (2.4)$$

and

$$D_{et} = D_e + D_t \tag{2.5}$$

One of the most difficult water balance parameters to measure in the field is the deep percolation,  $D_{dp}$ . Consequently, this parameter is usually the dependent variable in evaluating the water balance for an irrigated field. Rearranging Eq. 2.2 and solving for  $D_{dp}$ , we have

$$D_{dp} = D_a + D_{gw} + D_p - D_{pr} - D_{et} - D_{tw} - D_{\Delta s}$$
 (2.6)

In using the water balance, an important consideration is the time frame in which the computations are made, that is, whether the balance will use annual data, seasonal data, or data describing a single irrigation event. If a mean annual water balance is computed, it becomes reasonable that the change in root zone soil moisture storage,  $D_{\Delta s}$ , could be assumed as zero, thereby eliminating  $D_{\Delta s}$  from Eq. 2.6. In some irrigated areas, precipitation events are so light that the net rainfall  $(D_{np} = D_p - D_{pr})$  can reasonably be assumed as equal to the measured precipitation, and  $D_{pr}$  can be neglected. Under other circumstances, other terms in Eq. 2.6 can be neglected. In fact, time periods are often selected to eliminate as many of the parameters as possible in order to identify the behavior for single parameters. The elimination of parameters from the water balance computations

will result in more accurate predictions of deep percolation,  $D_{dp}$  (or any parameter in the water budget used as the dependent parameter). For instance, the groundwater contributed to the root zone soil moisture,  $D_{gw}$ , can usually be ignored if the groundwater table is more than 7 m below the ground surface for heavy (clay) soils and more than 3 m for light (sandy) soils (unless the crop roots extend to nearly the groundwater table level). Another special case would be the irrigation of sandy desert soils in which the groundwater table is well below the bottom of the root zone and precipitation events are sufficiently light.

#### SOIL CHARACTERISTICS

Soil characteristics of particular importance to irrigated agriculture include (1) the capacity of the soil to hold water and still be well drained; (2) the flow characteristics of water in the soils; (3) the physical properties of the soil matrix, including the organic matter content, soil depth, soil texture, and soil structure; and (4) soil chemical properties, including the translocation and concentration of soluble salts and nutrients due to the movement, use, and evaporation of the soil water. Knowledge of all these relationships and how they influence each other is critical to all who desire to improve irrigation practices and obtain the best, most efficient use of water.

#### **Soil Moisture**

If there is either excessive water (waterlogging) or insufficient water, crop growth will be retarded. As commonly defined, the available moisture for plant use is the range of soil moisture held at a negative apparent pressure of one-tenth to opethird bar (field capacity) and 15 bar (permanent wilting point). However, the soil moisture content within this pressure range will vary from 25 cm per meter of soil depth for some silty loams to as low as 6 cm per meter for some sandy soils.

A simplified schematic of a unit volume of soil, which contains solids (soil particles), liquid (water), and gas (air), is shown in Fig. 2.2. The porosity,  $\phi$ , of the unit volume is

$$\Phi = \frac{V_p}{V} \tag{2.7}$$

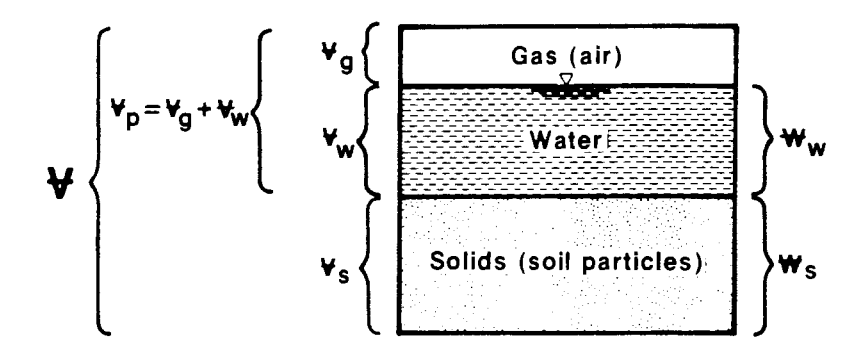
The volumetric water content,  $\theta$ , is

$$\theta = \frac{V_w}{V} \tag{2.8}$$

The saturation, S, which is the portion of the pore space filled with water, is

$$S = \frac{V_w}{V_p} \tag{2.9}$$

Soil Characteristics 11



 $\forall_{q}$  = volume of gas (air)

 $\forall_{p}$  = volume of pores

 $\forall_s$  = volume of soil solids (soil particles)

∀<sub>w</sub>= volume of water

¥ = unit volume

 $W_s$  = weight of solids

₩<sub>w</sub>= weight of water

**Figure 2.2** Simplified schematic of a unit volume of soil.

These terms are related by the expression

$$\theta = S\phi \qquad \qquad (2.10)$$

Whenever field soil moisture samples are collected and the samples ovendried, the soil moisture is reported as a percentage of the dry weight of the soil sample:

$$W = \frac{\text{sample wet wt.} - \text{sample dry wt.}}{\text{sample dry wt.}} = \frac{W_w}{W_c}$$
 (2.11)

where W is the dry weight moisture fraction. To convert these soil moisture measurements into volumes of water, the volumetric moisture content must be computed:

$$\theta = \gamma_b W \tag{2.12}$$

where  $\gamma_b$  is the bulk specific weight of the dry soil. Also,  $\gamma_b$  is related to the specific weight of the soil particles,  $\gamma_s$ , by

$$\gamma_b = \gamma_s (1 - \phi) \tag{2.13}$$

Field capacity is defined as the moisture fraction,  $W_{fc}$ , of the soil when rapid drainage has essentially ceased and any further drainage occurs at a very slow rate. For a soil that has just been fully irrigated, rapid drainage has occurred after approximately 1 day for a "light" sandy soil and after approximately 3 days for a "heavy" soil. This corresponds to a soil moisture tension of  $\frac{1}{10}$  to  $\frac{1}{3}$  atm (bar).

The permanent wilting point,  $W_{wp}$ , is defined as the soil moisture fraction at which permanent wilting of the plant leaf has occurred and applying additional water will not relieve the wilted condition. This point is usually taken as the soil moisture content corresponding to a soil moisture tension of 15 bar.

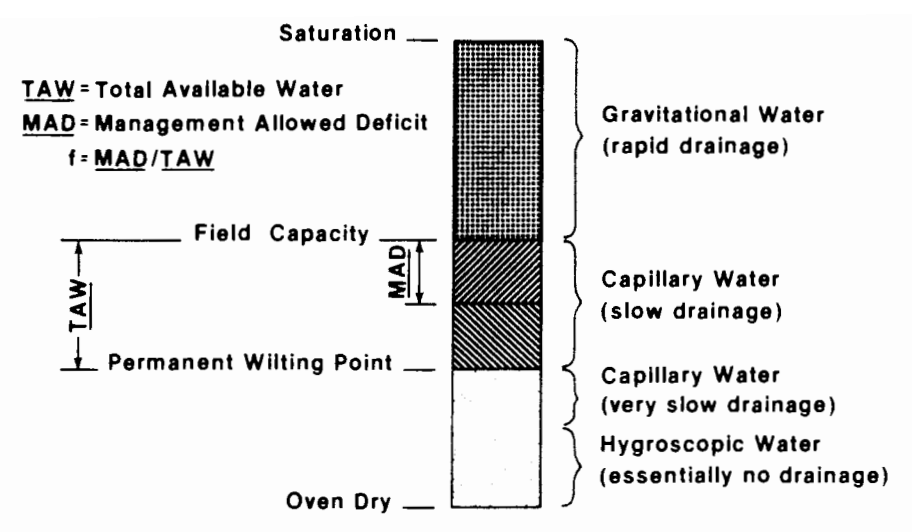


**Figure 2.3** Schematic representation of field capacity and permanent wilting point soil moisture content.

The volumetric moisture contents at field capacity and permanent wilting point become

$$\theta_{fc} = \gamma_b W_{fc} \tag{2.14}$$

$$\theta_{wp} = \gamma_b W_{wp} \tag{2.15}$$

The total available water, TAW, to the plants is approximately the difference in these volumetric moisture contents multiplied by the depth of the root zone, RD:

$$TAW = (\theta_{fc} - \theta_{wp})RD \tag{2.16}$$

Equation 2.16 is not technically exact because crop roots do not extract water uniformly from the soil profile.

The relation between field capacity, permanent wilting point, and total available water is illustrated in Figs. 2.3 and 2.4. Table 2.1 lists some common rooting depths for selected crops.

The management allowed deficit, MAD, is the degree to which the volume of water in the soil is allowed to be depleted before the next irrigation is applied.

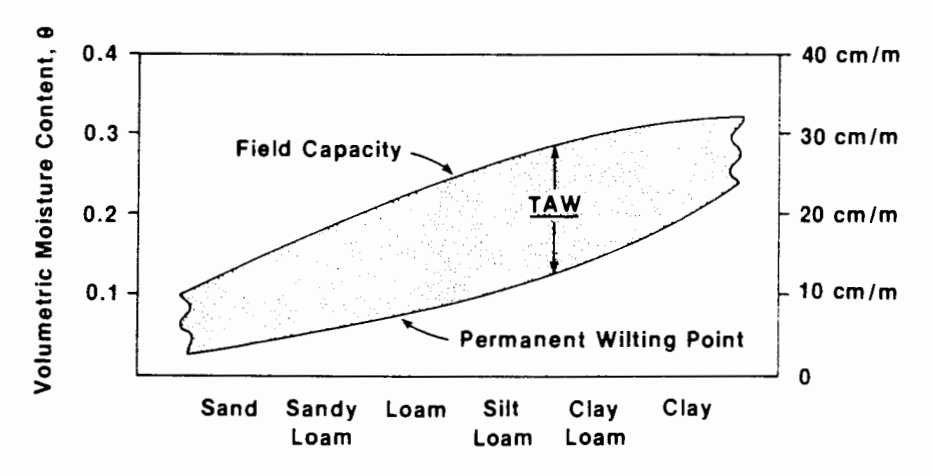


**Figure 2.4** Representative values of total available water, TAW, for different soil types.

Soil Characteristics 13

MAD corresponds to a soil moisture content between field capacity and permanent wilting point, which is primarily dependent on type of crop and crop growth stage:

$$MAD = f \cdot TAW \tag{2.17}$$

The soil moisture deficit, SMD, is the depletion of soil moisture below field capacity at the time that a particular soil moisture content,  $\theta$ , is measured.

$$SMD = (\theta_{fc} - \theta)RD \qquad (2.18)$$

#### Infiltration

Infiltration is the most crucial factor affecting surface irrigation. This single parameter essentially controls not only the amount of water entering the soil, but also the advance rate of the overland flow.

Typical curves of infiltration rate, I, and cumulative infiltration, Z, are shown in Fig. 2.5. In an initially dry soil, the infiltration rate has a very high initial value, but rapidly decreases with time, until finally a fairly steady-state infiltration rate is reached. This steady-state infiltration rate is often referred to as the basic infiltration rate and is close to the value of the saturated hydraulic conductivity of

**TABLE 2.1** AVERAGE ROOTING DEPTHS IN METERS OF SELECTED CROPS IN DEEP, WELL-DRAINED SOILS

Alfalfa	1.5	Grapes	0.9
Almonds	2.0	Ladino clover and grass mix	0.6
Apricots	2.0	Lettuce	0.3
Artichokes	1.4	Melons	1.5
Asparagus	3.0	Milo	1.2
Barley	1.25	Mustard	1.1
Beans (dry)	1.1	Olives	1.5
Beans (green)	0.9	Onions	0.3
Beans (lima)	1.2	Parsnips	1.2
Beets (sugar)	0.8	Peaches	2.0
Beets (table)	0.9	Pears	2.0
Broccoli	0.6	Peas	0.8
Cabbage	0.6	Peppers	0.9
Cantaloupes	1.5	Potatoes (Irish)	0.9
Carrots	0.75	Potatoes (sweet)	1.3
Cauliflower	0.6	Prunes	1.7
Celery	0.6	Pumpkins	1.8
Chard	0.9	Radishes	0.5
Cherries	2.2	Spinach	0.6
Citrus	1.3	Squash (summer)	0.9
Corn (field)	1.2	Strawberries	0.2
Corn (sweet)	0.9	Sudan grass	1.5
Cottoń	1.2	Tomatoes	1.0
Cucumber	1.1	Turnips	0.9
Eggplant	0.9	Walnuts	2.0
Figs	2.0	Watermelon	1.5
Grain and Flax	1.2		

Source: After Doorenbos and Pruitt (1977) and Marr (1967).

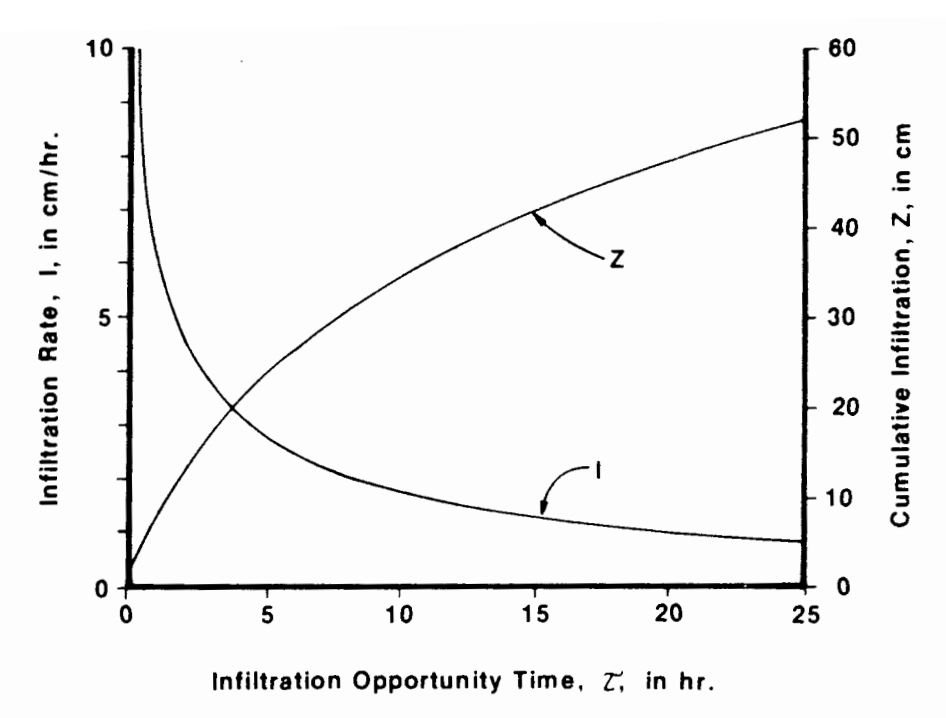


Figure 2.5 Example of infiltration rate, I, and cumulative infiltration, Z.

the surface soil. Infiltration is a complex process dependent on soil properties, physical properties, initial soil moisture content, previous wetting history, permeability changes due to the surface water movement, and air entrapment. For surface-irrigated fields, the infiltration function changes dramatically for each irrigation event. A typical example of this variation is shown in Fig. 2.6. For any particular surface-irrigated field, the infiltration function is further dependent on cultivation practices, the type of crop being grown, and climatic effects (e.g., freezing and thawing action during the winter season in temperate zones). The following summary of infiltration models is taken from Beggs (1981).

\*Bodman and Coleman (1943) described the moisture profile under ponded infiltration into dry soil as consisting of five general zones (see Fig. 2.7):

- 1. The saturated zone, which extends about 1.5 cm below the surface and has a saturated water content
- 2. The transition zone, a region about 5 cm thick below the saturated zone where a rapid decrease in water content occurs
- 3. The transmission zone, where water content varies slowly with both depth and time
- 4. The wetting zone, in which there is a sharp reduction in water content
- 5. The wetting front, a region of very steep moisture gradients where the visible limit of moisture penetration into the soil column can be seen

The transmission zone is particularly interesting because it has been found to have essentially constant hydraulic conductivity (Hansen, 1955) and a fairly uniform hydraulic gradient (Miller and Richard, 1952). The water content in this zone is sometimes called "field saturation" and ranges between 0.8 and 0.9 (Slack, 1980).

Soil Characteristics 15

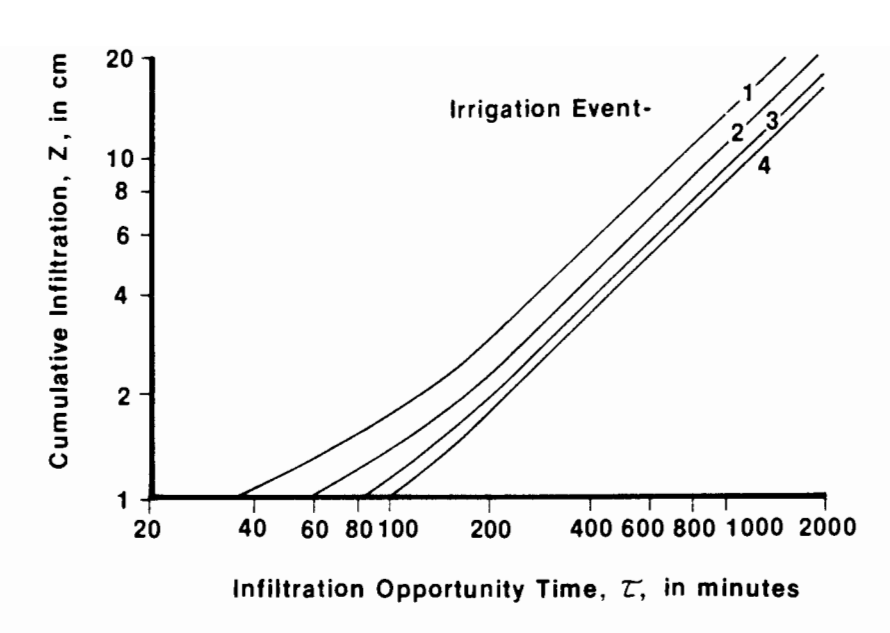
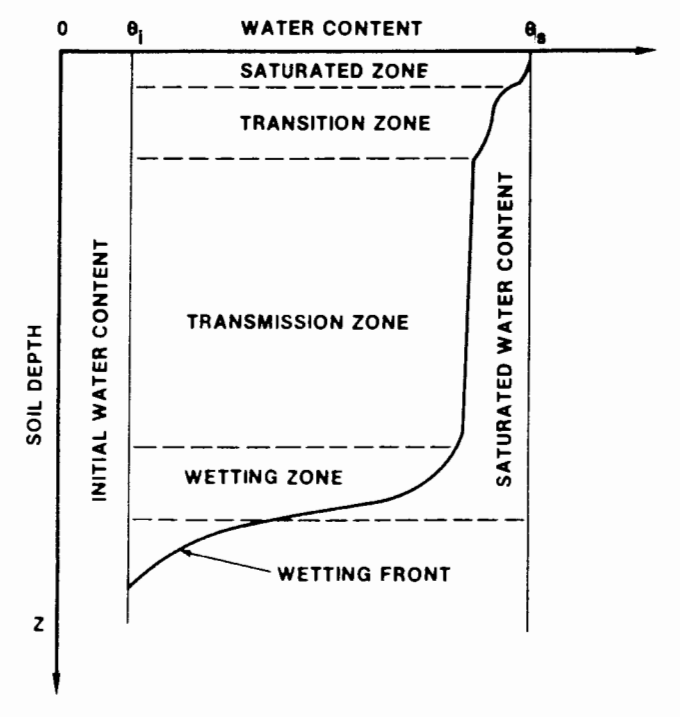


Figure 2.6 Example of seasonal variation in cumulative infiltration, Z, by irrigation event.

The wetting front is a phenomenon unique to porous media flow. It is very sharp and can be easily observed in drier soils (Hanks and Ashcroft, 1976). The reason a sharp wetting front occurs is because the hydraulic conductivity (and consequently water diffusivity) of a soil changes drastically with water content.

Numerous mathematical models have been developed for describing general porous media flow, particularly vertical infiltration. Infiltration equations can generally be broken into three categories: (1) models based on general porous media flow relationships, (2) equations based on assuming a simplified physical model of soil (physically based equations), and (3) those based on data fitting alone (empirical equations).

The most common example of equations in the first category are those based on a single-phase flow solution of the one-dimensional Darcy equation, known as the "Richards equation." The assumption is made that total potential equals the



16

Figure 2.7 Soil-moisture profile during ponded infiltration. (Adapted from Bodman and Coleman, 1943, by permission of the Soil Science Society of America, Inc.)

sum of gravitational and capillary potential. A general flow equation of the following form results:

$$\frac{\partial \theta}{\partial t} = \frac{\partial}{\partial z'} \left[ K(\theta) \left( \frac{\partial h}{\partial z'} - 1 \right) \right] \tag{2.19}$$

where

 $\theta$  = volumetic moisture content

h = total pressure head

K = hydraulic conductivity

z' = vertical distance downward from soil surface (positive downward)

The original assumptions behind Eq. 2.19 also state that the flow into the assumed isotropic, isothermal soil profile is laminar. Unfortunately, equations in this first category are not amenable to analytic solutions except in special cases and must be evaluated by numerical method solutions.

Equations in the second category are similar to or can be derived from the Green and Ampt equation (Green and Ampt, 1911). This equation was based on the assumption that soil could be modeled as a bundle of capillary tubes as follows (Slack, 1980):

$$I = K \left[ 1 + \frac{(\theta_s - \theta_i)h'}{Z} \right]$$
 (2.20)

where

I = infiltration rate

K = hydraulic conductivity in the wetted zone

h' = suction at the wetting front

 $\theta_{\rm v}$  = saturated moisture content

 $\theta_i$  = initial soil moisture content

Z = cumulative depth of infiltration

The third category, empirical equations, is a result of fitting observed infiltration rate behavior with explicit time-dependent functions. The constants in these equations have no physical meaning. One of the earliest infiltration equations was an empirical model developed by Kostiakov (1932). It is a simple equation and is in wide use today. It describes both actual and theoretical infiltration very well at short to medium time spans (Philip, 1957a). The equation has the following form:

$$I = ak\tau^{a-1} \tag{2.21}$$

where  $\tau$  is the intake opportunity time and a and k are empirical parameters obtained from infiltration tests on a given soil.

This equation has two major disadvantages. First, it cannot be adjusted for different field conditions known to have profound effects on infiltration, such as initial water content (Philip, 1957b). Second, it predicts an infiltration rate approaching zero at long times, which is known to be incorrect. A constant term can be added to Eq. 2.21 to correct the latter problem so that the equation becomes

$$I = ak\tau^{a-1} + f_0 (2.22)$$

Soil Characteristics

where  $f_0$  is some value representing the final infiltration as  $\tau$  becomes large. A difficulty with this equation is that it requires one more empirical constant than Eq. 2.21 and is therefore more difficult to calibrate with field data or use in predictive models.

Horton (1940) proposed another empirical equation, using an exponential function of the form

$$I = f_0 + (I_i - f_0)e^{-\beta\tau}$$
 (2.23)

where

 $\beta$  = empirical parameter

 $I_i$  = initial infiltration rate

 $f_0$  = final infiltration rate

Equations 2.21, 2.22, and 2.23 can be integrated to get equations describing cumulative depth of infiltration with time.

An equation similar to the integral form of Eq. 2.22 but with more physical significance was derived by Philip (1957a):

$$Z = S\tau^{0.5} + A\tau \tag{2.24}$$

where S is a soil parameter called sorptivity and A is a soil parameter called transmissivity. This is an approximate equation derived from Eq. 2.19 and some simplifying assumptions about flow velocity and water content profiles. The Green and Ampt equation is actually an intermediate equation in the derivation. It has the advantage of being based on only two soil parameters which also have physical significance. For instance, sorptivity can be adjusted for initial soil-water content by the following relationship (Philip, 1957b):

$$S \propto (\theta_i - \theta_s) \tag{2.25}$$

It can be seen from this relationship that infiltration rate is decreased by higher initial water content. The main disadvantage of Eq. 2.24 is that A is not equal to  $f_0$ , so the equation is not entirely accurate at long times.

Using an approximation from a dimensionless form of the Green and Ampt equation, Hachum and Alfaro (1977) developed another equation with an appearance similar to Eqs. 2.22 and 2.24:

$$Z = F\tau^{0.47} + K(\theta_s)\tau \tag{2.26}$$

where

$$F = 1.2[K(\theta_s)]^{0.47} (\psi_w \ \Delta\theta)^{0.53} \tag{2.27}$$

and  $K(\theta_s) = f_0$  or approximated by the hydraulic conductivity in the field  $\psi_{ij}$  = water entry pressure head of a hypothetical profile  $\Delta \theta = \theta_s - \theta_s$ 

This equation is more accurate than Eq. 2.24 at long times but requires three parameters. It should be noted that Eqs. 2.24 and 2.26 were developed without accounting for soil swelling or structural breakdown.

# Soil Physical Properties

The soil matrix serves several very valuable functions, not the least of which is serving as a foundation to hold the plants upright. It must also furnish nutrients and provide a good balance between aeration and available moisture content.

Soil texture and structure influence the intermolecular forces and "suction" of water in unsaturated soils. These forces can be quite substantial and include the capillary and attractive forces resulting from the close contact of soil particles. Soil texture, primarily soil structure, greatly influences the porosity and distribution of pore sizes, and thereby the permeability of soils to air, water, and roots, which is as important to crop growth as an adequate supply of nutrients. In fact, the entire soil—water—plant system is so interrelated that the failure or lack of one component can cancel the combined benefits of all the others.

Irrigation practices are influenced by the degree of root proliferation since the water supply available to the plant is limited to the soil volume explored in the crop's root system. Different crops have different root growth patterns, hence different moisture extraction patterns. Obviously, a shallow-rooted crop will require more frequent irrigations than will a deep-wide-rooted crop in the same soil.

# Soil Chemical Properties

The chemical properties of soils can greatly influence the irrigability of the soil by affecting the hydraulic characteristics and the suitability of the soil for crop production. Soils having an excess of soluble salts are designated as saline soils, and, if the soil has an excess of exchangeable sodium, it is termed a sodic soil. Sodic soils tend to have very poor soil structure, due to swelling or dispersion of soil particles. For example, the hydraulic conductivity of a soil can change as much as three orders of magnitude when the sodium adsorption ratio (SAR) is reduced from a value of 20 to a value of 1.

Excess soil salinity will delay or prevent crop germination and can substantially reduce the amount and rate of plant growth because of the high osmotic pressures which develop between the soil-water solution and the plant. These pressures, which appear to be independent of the type of salts present, greatly impair the plant's ability to absorb water. In addition, some adverse effects due to salinity can include nutritional imbalances or toxicities caused by specific ions (e.g., boron, which is toxic in very small quantities). In sufficient concentrations, even beneficial salts (fertilizers such as potassium nitrate) can become toxic to plants.

In addition to the soil chemical characteristics mentioned above, the soil must also have an adequate supply of available plant nutrients. Many chemical elements are essential for plant growth and are necessary to obtain large and satisfactory crop yields. These include calcium, carbon, hydrogen, iron, magnesium, nitrogen, oxygen, potassium, phosphorus, sulfur, and many other trace elements, depending on the type of crop. The availability of these nutrients to the plant depends to a large extent upon the moisture content of the soil.

Bacterial activity is also an important part of the soil—water—plant relationship because this action will often convert nitrogen to a usable form (nitrogen-fixing).

Soil Characteristics 19

Bacterial action also breaks down organic matter and converts other cliemical compounds into forms usable by the plants. Soil moisture content, soil structure, and soil aeration directly influence bacterial activity.

#### **CROP EVAPORATIVE AND DRAINAGE REQUIREMENTS**

# **Evapotranspiration**

An important parameter in the water balance equation is the evapotranspiration from the crop and soil surface,  $D_{et}$ . It is dependent on climatic conditions, crop variety and stage of growth, soil moisture depletion, and various physical and chemical properties of the soil. A two-step procedure is generally followed in estimating  $D_{et}$ : (1) computation of the seasonal distribution of "potential evapotranspiration,"  $E_{tp}$ ; and (2) adjustment of  $E_{tp}$  for crop variety and stage of growth. Most of the other factors playing a role, such as soil moisture stress, are ignored for the purposes of design computations. Thus the values of  $D_{et}$  are larger than what might be normally encountered, thereby adding a conservative factor to the design process.

**Potential evapotranspiration.** Potential evapotranspiration is defined as the evapotranspiration rate of a well-watered reference crop which completely shades the soil surface. It is therefore an indication of the climatic evaporative demand calibrated to a vigorously growing crop. Typical reference crops are grass and alfalfa.

There are more than 20 commonly used methods for calculating evapotranspiration, ranging in sophistication from simple temperature correlations, such as the Blaney-Criddle method, to complete equations describing radiant and advective energy balance, such as the Penman method. The Blaney-Criddle method requires field measurements of temperature, whereas the Penman method requires field measurements of temperature, solar radiation, wind, and relative humidity.

The scope of this book does not extend to a thorough review of the various evapotranspiration formulas. For the reader interested in these details, it is suggested that such references as Jensen (1973, 1980) and Doorenbos and Pruitt (1977) be consulted.

Adjusting for crop variety and growth stage. In contrast to potential evapotranspiration  $(E_{ip})$ , which occurs in a well-watered crop at full cover under a given set of climatic conditions, there is the actual field evapotranspiration referenced to a specific crop and its stage of development,  $D_{et}$ .

Crop evapotranspiration,  $D_{et}$ , can be estimated by multiplying  $E_{tp}$  by a crop maturity coefficient,  $k_{co}$ . Values of  $k_{co}$  have been published by Jensen (1969), Kincaid and Heermann (1974), and Doorenbos and Pruitt (1977) for a wide range of crops grown worldwide. Recent results from long-term lysimeter measurements at Kimberly, Idaho, have led to modified  $k_{co}$  values for arid, temperate, intermountain climates (Wright, 1982). For computer applications such as irrigation

scheduling, it has been convenient to express the maturity coefficient in mathematical relationships. Thus, if the potential evapotranspiration,  $E_{ip}$ , has been evaluated over the growing season, the crop evaporative requirement can be estimated as

$$D_{ci}(t) = E_{iv}(t) k_{co}(t) (2.28)$$

# **Drainage Requirement**

The minimum amount of required subsurface drainage water (deep percolation) is usually calculated on the basis of moving as much salt as is applied to the cropland by irrigation. Although measuring total dissolved solids (TDS) in the irrigation water is a more accurate measure of the salt concentration in these waters, more frequently the electrical conductivity (EC) is measured because of ease in making either field or laboratory measurements. Maintaining a salt balance in the root zone then requires that

$$D_{dr} EC_{dp} = D_z EC_z (2.29)$$

where

 $D_{dr}$  = depth of required subsurface drainage

 $EC_{dp}$  = electrical conductivity of deep percolating water

 $D_z$  = depth of infiltrated water resulting from the irrigation water supply

 $EC_z$  = electrical conductivity of the irrigation water supply

The U.S. Salinity Laboratory (1954) defines the leaching requirement, LR, as

$$LR = \frac{D_{dr}}{D_z} = \frac{EC_z}{EC_{dp}}$$
 (2.30)

Referring to the water balance schematic in Fig. 2.1, the root zone water balance can be written as a function of the leaching requirement by substituting  $D_z$  for  $D_{dp}$ . Ignoring the contribution from groundwater and utilizing Eq. 2.29, the required infiltrated depth of irrigation water to satisfy the leaching requirement is

$$D_{zr} = (D_{\Delta s} + D_{et} - D_{pz}) \frac{EC_{dp}}{EC_{dp} - EC_{z}}$$
 (2.31)

This required depth of infiltrated irrigation water does not have to be achieved during each irrigation event. Quite frequently, Eq. 2.31 would be applied on an annual basis, thereby taking into account the large deep percolation losses that usually occur with the first (and second) irrigation events of the season, as well as the benefits from precipitation (and snowmelt) events throughout the year. In some irrigated areas, maintaining a salt balance in the root zone is achieved during years of plentiful water supplies, which may be as long as every 3 to 8 years.

#### IRRIGATION EFFICIENCY AND UNIFORMITY

#### General Discussion

The objective of providing a suitable level of moisture in the soil for plant growth can be achieved by any irrigation system by simply overwatering. The performance of the system is optimized when the moisture level "suitability" is maintained, but the evaporative, runoff, and percolation losses are minimized. To index the performance of the irrigation system, irrigation uniformity and efficiency are defined. However, since an irrigation system is composed of different parts and utilized in different ways, there are a large number of individual expressions for uniformity and efficiency.

Because of the uncertainty associated with the soil infiltration characteristics, the performance of surface irrigation systems is not predictable without assessing the individual system. Even when a level of performance is dictated by design practices, there is no assurance that the field system will perform as intended. In Chapter 5 we describe field evaluation procedures and the interpretation of their data.

# **Application Uniformity and Efficiency**

Among the many factors used to judge the adequacy of an irrigation or the irrigation system, one of the most common is the effectiveness of water applications. Over the years, irrigation engineers have studied irrigation performance and a large number of indices have been proposed. Willardson (1972) stated that at least 20 definitions of irrigation efficiency existed, and probably 5 to 10 have been added subsequently (Hart et al., 1979; Bos, 1979). Uniformity has also been defined in numerous ways, but generally the definitions were first applied to sprinkle irrigation and later used to describe surface irrigation systems. Some of these statistical indicators include Christiansen (1942), Walker (1979), and Elliott et al. (1980).

There does not currently exist a single parameter which is sufficient for evaluating irrigation performance. Conceptually, the adequacy of an irrigation is dependent on the water stored within the crop root zone, the water percolating below the root zone, surface runoff or tailwater, the uniformity of the applied water distribution, and the unused storage capacity of the soil profile following an irrigation. In fact, Hart et al. (1979) have shown that three efficiency terms and one distribution uniformity term are required to adequately describe the hydraulic performance of an irrigation system. To index these factors, the following assumptions are made for surface-irrigated systems:

- 1. The extraction of moisture from the root zone is uniformly distributed with depth and location.
- The infiltration characteristics of the soil surface can be characterized by a unique relationship between depth of water absorbed and intake opportunity time.
- 3. The intent of the irrigation is to completely refill the root zone.

The consequences of these assumptions are that uniformity and efficiency are defined on the basis of surface flow conditions. If an irrigator deliberately underirrigates in the hopes of using precipitation more effectively, the usual measures of uniformity and efficiency do not apply very well, or at least must be interpreted properly.

**Application uniformity.** Consider a field having a uniform slope, soil, and crop density. The field has a total length of L meters. During an irrigation, a steady flow is introduced at the upper end and advances at a monotonically decreasing rate until it reaches the end, runs off for a time, and then recedes following cutoff of the inflow. Figure 2.8 shows the average distribution of infiltrated water along the field length. Because of the differences in intake opportunity time, the applied depths are nonuniformly distributed as shown, with the distribution having a very characteristic shape skewed toward the inlet end of the field.

Application uniformity concerns the distribution of water over the actual field. Most of the commonly used indices were developed for sprinkle irrigation where applied depths tend to have a Gaussian distribution. One uniformity criteria that is applicable to surface irrigation systems is the distribution uniformity, defined as the average infiltrated depth in the low one-quarter of the field divided by the average infiltrated depth over the field (Merriam and Keller, 1978). This term can be represented by the symbol DU. Using values taken from 12 points in Fig. 2.8 between x = 0 and x = L, a DU value of 0.71 can be determined.

There is another view of uniformity that should be noted. Suppose that the uniformity of applied depths is examined along the dimension normal to Fig. 2.8 at locations along the lateral length: x = 0 (inlet), x = 0.8L ( $Z = Z_r$ ), and x = L. Typical distributions are shown in Fig. 2.9. At the field inlet, the applied depth greatly exceeds the storable soil moisture level and uniformity differences tend to be minimized. DU for the inlet distribution shown is 0.98. It should be noted that the larger the average applied length, the more likely DU will have a large value, also due to the redistribution processes of the soil. The DU for the case where the average applied depth and the required depth are equal is 0.93.

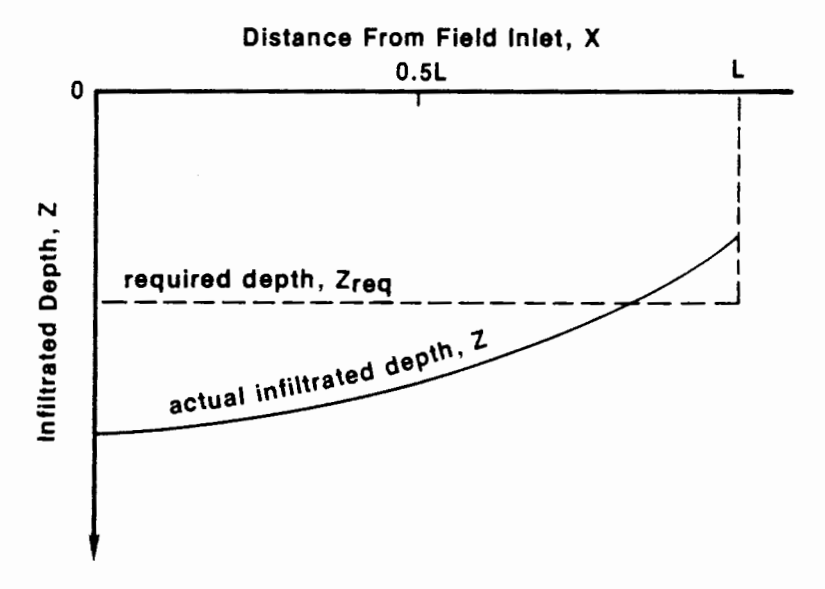


**Figure 2.8** Average distribution of applied water along the advanced length of a surface-irrigated field.

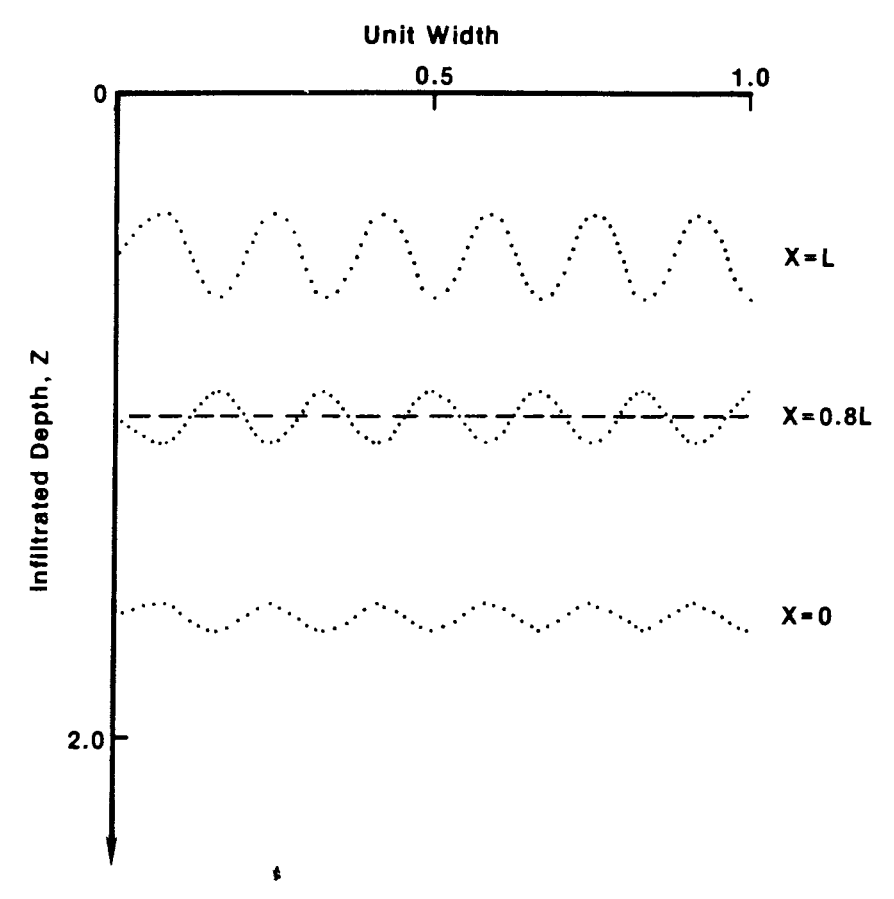


Figure 2.9 Lateral distribution of applied water at three locations along the advance length.

The absolute deviations tend to be larger and the mean is smaller. For the last case, the DU is 0.75.

**Application efficiency.** The definition of application efficiency,  $E_a$ , has been fairly well standardized. It is:

$$E_a = \frac{\text{average depth added to the root zone storage}}{\text{average depth applied to the field}}$$
 (2.32)

 $E_a$  therefore does not include losses due to seepage from conveyance networks leading up to the edge of the field.

Returning to Fig. 2.8, it is noted that losses from the field occur as deep percolation (depths greater than  $Z = Z_r$ ) and as field tailwater. To compute  $E_a$ , it is necessary to identify these losses and the amount of water stored in the root zone. This implies that the total amount of root zone storage capacity and the actual water stored can be segregated, thereby indicating the amount of underirrigation in the soil profile.

The value of  $E_a$  for Fig. 2.8 is 0.71 (about 29% of the applied water is lost). Thus the performance is somewhat diminished over the earlier indications by uniformity alone. In addition, one should be careful in using Eq. 2.32 if for one reason or another the entire field is not evaluated. For instance, Fig. 2.9 shows that if the x = 0.8L location is studied by itself,  $E_a$  would be about 0.98. However,

at x = L,  $E_a$  is 1.0 and at x = 0 it is about 0.62. Thus application efficiency has a spatial connotation that precludes the use of simple averages.

#### Three Additional Indicators

To improve the performance of a surface irrigation system, the measures of uniformity and efficiency must be more qualitative. DU gives minimal information about the magnitudes of losses or underirrigation.  $E_a$  does not allow the engineer to segregate deep percolation losses from tailwater losses and it is difficult to assess the degree of underirrigation. Since these items are important, three additional indicators are proposed: (1) deep percolation ratio, DPR; (2) tailwater ratio, TWR; and (3) water requirement efficiency,  $E_r$ . There are defined as follows:

$$DPR = \frac{\text{average depth of deep percolation}}{\text{average depth applied}}$$
 (2.33)

$$TWR = \frac{\text{average depth of field runoff}}{\text{average depth applied}}$$
 (2.34)

$$E_r = \frac{\text{average depth of root zone moisture stored}}{\text{average depth of potential soil moisture storage}}$$
 (2.35)

#### IRRIGATION REQUIREMENT

It can be observed from the preceding discussion that if the irrigation system could be operated with an application efficiency and water requirement efficiency of 100% (implying that DU = 1.0), the irrigation requirement would be the sum of the crop water requirement and the leaching requirement. Because this is impractical, the irrigation requirement is often defined as:

$$IR = \frac{D_{er} - (D_p - D_{pr})}{E_a}$$
 (2.36)

where IR is the irrigation requirement and  $E_a$  is expressed as a fraction. It is implicitly assumed in Eq. 2.36 that  $E_r$  is generally 100%, so that the natural inefficiency of the system is sufficient to leach salts from the least-watered area. Where soils are relatively well drained, the writers have not observed soil salinization due to underirrigation.

#### **EXAMPLE PROBLEMS**

#### Example 2.1

A moist sand sample has a volume of 464 cm<sup>3</sup> in the natural state and a weight of 793 g. The dry weight is 735 g and the specific gravity of the soil particles is 2.68. Determine the porosity, soil moisture content, volumetric moisture content, and degree of saturation.

Solution. Solving for the porosity,  $\phi$ , from Eq. 2.13, we obtain

$$\Phi = 1 - \frac{\gamma_b}{\gamma_s}$$

Then the bulk specific weight,  $\gamma_b$ , must be determined.

$$\gamma_h = \frac{735 \text{ g}}{464 \text{ cm}^3 (1 \text{ g/cm}^3)} = 1.58$$

Therefore,

$$\phi = 1 - \frac{1.58}{2.68} = 1 - 0.59 = 0.41$$

The soil moisture fraction, W, is determined from Eq. 2.11.

$$W = \frac{793 \text{ g} - 735 \text{ g}}{735 \text{ g}} = \frac{58 \text{ g}}{735 \text{ g}} = 0.079 = 7.9\%$$

The volumetric moisture content,  $\theta$ , is determined from Eq. 2.12.

$$\theta = \gamma_b W = 1.58(0.079) = 0.125 = 12.5\%$$

The saturation, S, can be obtained from Eq. 2.10.

$$S = \frac{\theta}{\Phi} = \frac{0.125}{0.41} = 0.305 = 30.5\%$$

### Example 2.2

For the following data, calculate the total available water, TAW, and soil moisture deficit, SMD.

Soil depth (mm)	$W_{fc}$	$W_{up}$	γ,,	W
0-250	0.25	0.12	1.35	0.15
250-600	0.28	0.15	1.55	0.19
600-925	0.22	0.10	1.45	. 0.16
925-1200	0.16	0.07	1.50	0.12

**Solution.** The rooting depth, RD, in Eqs. 2.16 and 2.18 can be replaced with the thickness of the soil layer to calculate TAW and SMD.

Soil depth (mm)	$\Theta_{tc}$	$\theta_{n_L}$	TAW (mm)	θ	SMD (mm)
250	0.34	0.16	45	0.20	35
350	0.43	0.23	70	().29	49
325	0.32	0.14	58	0.23	29
275	0.24	0.10	$\frac{38}{211}$	0.18	16 129

#### Example 2.3

A 10-ha field is used to grow one crop each year that has a seasonal evapotranspiration

of 550 mm. The average electrical conductivity of the irrigation water supply is 1.2 mmho/cm. This field has a tile drainage system, and based on numerous field measurements throughout a 3-year period, the average electrical conductivity of the drainage outflow is 3.6 mmho/cm. The average annual precipitation is 425 mm, of which it is estimated that 250 mm infiltrates into the soil, mostly between irrigation seasons. What is the required infiltrated depth of irrigation water to satisfy the leaching requirement?

**Solution.** Using mean annual data, it can be assumed that the change in soil moisture storage,  $D_{\Delta s}$ , is zero. Then, using Eq. 2.31, we have

$$D_{zr} = (0 + 550 \text{ mm} - 250 \text{ mm}) \left( \frac{3.6 \text{ mmho/cm}}{3.6 \text{ mmho/cm} - 1.2 \text{ mmho/cm}} \right)$$
  
= (300 mm)(1.5)  
= 450 mm

The seasonal crop evapotranspiration is 550 mm, yet only 450 mm of irrigation water has to be infiltrated into the soil to maintain a salt balance. This level of irrigation would cause salts to accumulate in the root zone during the irrigation season, but these accumulated salts would be leached by precipitation infiltrating into the soil between seasons.

As a check on these computations, the seasonal deep percolation.  $D_{dp}$ , can be calculated using Eq. 2.1 applied to a root zone water balance in Fig. 2.1.

$$(D_z + D_{pz} + D_{gu}) - (D_{et} + D_{dp}) = D_{\Delta s}$$

Assuming that  $D_{cw} = 0$  and  $D_{\Delta x} = 0$ , we have

$$(450 \text{ mm} + 250 \text{ mm} + 0) - (550 \text{ mm} + D_{dp}) = 0$$

Solving for  $D_{dp}$  gives us

$$D_{dp} = 700 \text{ mm} - 550 \text{ mm} = 150 \text{ mm}$$

Now, using Eq. 2.30 to determine the leaching requirement, LR, we obtain

$$LR = \frac{EC_z}{EC_{dn}} = \frac{1.2 \text{ mmho/cm}}{3.6 \text{ mmho/cm}} = 0.33$$

Also,

$$LR = \frac{D_{dr}}{D_{c}} = \frac{150 \text{ mm}}{450 \text{ mm}} = 0.33$$

which shows that the computations are compatible.

If this field is adequately irrigated, then  $D_z$  will exceed 450 mm and a salt balance should easily be maintained; however, many other salinity complications could occur that are beyond the scope of this book.

#### **HOMEWORK PROBLEMS**

2.1. A sharp-edged cylinder 15 cm in diameter is carefully driven into the soil so that negligible compaction occurs. A soil column 20 cm in length is secured. The wet weight is 5780 g and the dry weight is 5180 g. What is the percent moisture on a dry weight basis? What is the bulk specific weight of the soil?

- 2.2. Consider a cylindrical sample of soil having a diameter of 2.54 cm and a length of 6 cm. The specific gravity of the soil particles is 2.65. Before drying the sample weight was 60 g. After drying the weight was 53 g. Calculate φ, S, θ, and W before drying.
- 2.3. A cylinder was carefully pushed into the soil without compressing or distributing the soil. The cross-sectional area of the cylinder was 225 cm². The length of the column of soil within the cylinder was 30 cm. The weight of the soil within the cylinder was 9535 g when it was dried. The weight of the soil before drying was 11,440 g. Determine W, θ, and γ<sub>b</sub> before drying.
- 2.4. (a) A completely saturated clay soil has a soil moisture fraction of 40.0% and a bulk density of 1.34 g/cm<sup>3</sup>. Determine the porosity and the specific gravity of the clay particles.
  - (b) Later, after noticeable compaction of this clay soil, an undistributed soil sample was again taken into the laboratory. The measured bulk density was 1.84 g/cm<sup>3</sup>. Determine the porosity. Then determine the soil moisture when S = 0.85.
- 2.5. For the following data, calculate the total available water and the soil moisture deficit.

Soil depth (cm)	$\gamma_b$	$W_{fc}$	$W_{up}$	W
0-15	1.25	0.24	0.13	0.16
15 - 30	1.30	0.28	0.14	0.18
30-60	1.35	0.31	0.15	0.23
60-90	1.40	0.33	0.15	0.26
90-120	1.40	0.31	0.14	0.28

- 2.6. Soil samples were collected at the site of a field to be planted in grass. Laboratory measurements showed the average field capacity,  $W_{fc}$ , to be 24%, while the average value of the permanent wilting point measurements was  $W_{wp} = 11\%$ . Three field measurements of bulk density were made, with the results being 1.42, 1.51, and 1.45. If the grass that will be planted is estimated to have a potential effective rooting depth of 21 in., what would you estimate the total available water to be in the root zone in millimeters? At what soil moisture content, W, would an irrigation event be scheduled if MAD/TAW = 0.55?
- 2.7. An area of vine plants has an average rooting depth of 1 m. The soil has a field capacity  $W_{ic}$  of 0.32, a permanent wilting point,  $W_{wp}$ , of 0.14, and a bulk density of 1.50. A soil moisture sample weighed 60.13 g and after oven drying, 51.36 g. What depth of irrigation water should be applied to the root zone in order to replenish the soil moisture level to field capacity?
- 2.8. From previous experience on a particular field, it is known that the average volumetric moisture content in the root zone depth of 650 mm will correspond quite reasonably with  $\theta_{\rm h}=0.38$  3 days after completing an irrigation event. The daily evapotranspiration is 8 mm during the hottest month of the season. During this period, what will be the average volumetric moisture content 2 weeks after completing an irrigation event? If the management allowed deficit is 75 mm, what is the required interval between irrigation events during the hottest month? What is the required irrigation interval when the daily evapotranspiration is 5 mm?
- **2.9.** Derive Eq. 2.31 for the required depth of infiltrated irrigation water,  $D_{zz}$ , to satisfy the leaching requirement. State all assumptions.

**2.10.** Water balance studies were conducted on a 6-ha field for 3 years. The data are summarized below for each year.

Year	D <sub>a</sub> (mm)	<i>D<sub>tw</sub></i> (mm)	$D_r$ (mm)	D <sub>er</sub> (mm)	EC, (µmho cm)	$D_{pz}$ (estimated)
2524	1470	845	625	635	1500	$0.5D_p$
2525	920	435	205	670	2450	$1.0D_{\scriptscriptstyle P}^{'}$
2526	1285	710	520	685	. 2100	$0.6D_{p}^{'}$

For each year, what value of  $EC_{dp}$  is required to maintain a salt balance? Assuming 1 mg/l = 0.64\*EC µmhos/cm, how many metric tons of salt must be leached from the root zone during this 3-year period in order to maintain a salt balance? What is the average salt concentration in mg/liter in this leachate over the 3-year period assuming that a salt balance occurs?

- 2.11. A 40-acre field is used to grow two crops annually, with the average seasonal crop evapotranspiration being 725 mm and 450 mm for each crop. The total available irrigation water supply is 200 acre-feet, with all of the tailwater runoff being recycled. This water supply has a total dissolved solids (salts) concentration of 1300 mg/liter. If the subsurface drainage flows have a salt concentration of 3700 mg/liter, is a salt balance being maintained? Calculate the volume of excess or accumulated salts in metric tons per year.
- 2.12. A basin having an area of 0.12 ha is irrigated for 2 hours with a water supply of 30 liters/s. Prior to this irrigation event, the soil moisture deficit, SMD, was 130 mm. Assuming that the soil moisture deficit is completely replenished in the basin  $(E_r = 1.0)$ , what is the application efficiency and deep percolation ratio for this irrigation event?
- 2.13. A border 60 ft wide and 660 ft in length has a soil moisture deficit of 5.2 in. A water supply of 2.38 ft<sup>3</sup>/s was diverted onto this border for 6 h. The measured tailwater runoff was 0.37 acre-foot. Assuming that the soil moisture deficit is replenished along the full length of this border, what are the application efficiency, tailwater ratio, and deep percolation ratio for this irrigation event?
- **2.14.** A furrow-irrigated set consists of 27 furrows spaced 30 in. apart with a furrow length of 1320 ft. At the time that the irrigation event was begun, the soil moisture deficit was 110 mm. Each furrow had an inflow of 13 gal/min for 24 h. The distribution of infiltrated water depth along the furrow length is as follows:

Furrow length, 1/L	0.05	0.15	0.25	0.35	0.45	0.55	0.65	0.75	0.85	0.95
Infiltrated										
depth (mm)										
(mm)	158	153	148	142	136	129	121	110	95	76

What is the volume of deep percolation and tailwater runoff in acre-feet and cubic meters? What is the value of DU,  $E_a$ ,  $E_r$ , DPR and TWR for this irrigation event?

2.15. In Problem 2.14, if the irrigation water supply has an electrical conductivity of 1600  $\mu$ mho/cm and EC<sub>dp</sub> = 5400  $\mu$ mho/cm, what portion of the field is accumulating salts?

### REFERENCES

- BEGGS, R. A. 1981. A Portable Field Sprinkling Infiltrometer. Unpublished M.S. thesis, Agricultural and Irrigation Engineering Department, Utah State University, Logan, Utah.
- BODMAN, G. B., and E. A. COLEMAN. 1943. Moisture and Energy Conditions during Downward Entry of Water into Soils. Soil Sci. Soc. Am. Proc. 8:116–122.
- Bos, M. G. 1979. Standards for Irrigation Efficiencies of ICID. ASCE J. Irrig. Drain. Div. 105(IRI):37-43.
- CHRISTIANSEN, J. E. 1942. Sprinkler Irrigation. Agric. Exp. St. Bull. 670. University of California, Berkeley, Calif. October.
- DOORENBOS, J., and W. O. PRUITT. 1977. Crop Water Requirements (Revised Edition). FAO Irrig. Drain. Pap. 24. United Nations, Food and Agriculture Organization, Rome.
- ELLIOTT, R. L., J. D. NELSON, J. C. LOFTIS, and W. E. HART. 1980. Comparison of Sprinkler Uniformity Models. *ASCE J. Irrig. Drain. Div.* 106(IR4):321–330.
- GREEN, W. H., and G. A. AMPT. 1911. Studies on Soil Physics, 1: The Flow of Air and Water through Soils. J. Agric. Sci. 4(1):1-24.
- HACHUM, A. Y., and J. F. ALFARO. 1977. Water Infiltration and Runoff under Rain Applications. Soil Sci. Soc. Amer. J. 41(5):960–966.
- HANKS, R. J., and G. L. ASHCROFT. 1976. Physical Properties of Soils. Department of Soil Science and Biometeorology. Utah State University Press, Logan, Utah, Chap. 6.
- Hansen, V. 1955. Infiltration and Soil Water Movement during Irrigation. *Soil Sci.* 79:93–104.
- HART, W. E., G. PERI, and G. V. SKOGERBOE. 1979. Irrigation Performance: An Evaluation. ASCE J. Irrig. Drain. Div. 105(IR3):275–288.
- HORTON, R. E. 1940. An Approach towards a Physical Interpretation of Infiltration Capacity. Soil Sci. Soc. Am. Proc. 5:399-417.
- JENSEN, M. E. 1969. Scheduling Irrigations with Computers. J. Soil Water Conserv. 24:193–195.
- JENSEN, M. E. (ed.). 1973. Consumptive Use of Water and Irrigation Water Requirements. American Society of Civil Engineers, New York.
- JENSEN, M. E. (ed.). 1980. Design and Operation of On-Farm Irrigation Systems. Monograph 3. American Society of Agricultural Engineers, St. Joseph, Mich.
- KINCAID, D. C., and D. F. HEERMANN. 1974. Scheduling Irrigations Using a Program-mable Calculator. ARS-NC-12. U.S. Department of Agriculture, Agricultural Research Service, February.
- Kostiakov, A. V. 1932. On the dynamics of the coefficient of water-percolation in soils and on the necessity for studying it from a dynamics point of view for purposes of amelioration. *Trans. Sixth Comm. Int. Soc. Soil Sci.*, Part A., pp. 17–21.
- MARR, J. C. 1967. Furrow Irrigation. Manual 37. California Agricultural Experiment Station, University of California, Davis.

- MERRIAM, J. L., and J. KELLER. 1978. Farm Irrigation System Evaluation: A Guide for Management. Department of Agricultural and Irrigation Engineering, Utah State University, Logan, Utah.
- MILLER, R. D., and F. RICHARD. 1952. Hydraulic Gradients during Infiltration in Soils. Soil Sci. Soc. Am. Proc. 16:33–38.
- PHILIP, J. R. 1957a. The Theory of Infiltration: 4. Sorptivity and the Initial Moisture Content. *Soil Sci.* 84:257–264.
- PHILIP, J. R. 1957b. The Theory of Infiltration: 5. The Influence of the Initial Moisture Content. *Soil Sci.* 84:329–337.
- SLACK, D. C. 1980. Modeling Infiltration under Moving Sprinkler Irrigation Systems. Trans. Am. Soc. Agric. Eng. 23:596-600.
- U.S. Salinity Laboratory. 1954. Diagnosis and Improvement of Saline and Alkali Soils. Agric. Handb. 60. U.S. Department of Agriculture, Riverside, Calif.
- WALKER, W. R. 1979. Explicit Sprinkler Irrigation Uniformity: Efficiency Model. ASCE J. Irrig. Drain. Div. 105(IR2):129–136.
- WILLARDSON, L. S. 1972. Attainable Irrigation Efficiencies. ASCE J. Irrig. Drain. Div. 98(IR2):239-246.
- WRIGHT, J. L. 1982. New Evapotranspiration Crop Coefficients. *ASCE J. Irrig. Drain. Div.* 108(IR1):57–74.

# Surface Irrigation Systems

#### INTRODUCTION

As the oldest and most common method of applying water to croplands, surface irrigation has evolved into an extensive array of configurations. Efforts to classify surface systems differ substantially, but generally include the following: (1) basin irrigation, (2) border irrigation, (3) furrow irrigation, and (4) wild flooding. The distinction between the various types involves substantial overlap and no clear-cut definition of terminology exists. The discussion in this chapter represents the classification used by the writers and is given for illustrative purposes.

The irrigation system as a whole consists of four subsystems, as illustrated in Fig. 3.1. These are: (1) the water supply subsystem, (2) the water delivery subsystem, (3) the water use subsystem, and (4) the water removal subsystem. There are many alternative configurations that are found within each subsystem. For example, the water supply subsystem can also include direct diversions from rivers or streams, pumped flows from groundwater basins, and diversions from surface impoundments, as shown.

The scope of surface irrigation study in this book is limited to the water-use system. It includes the examination of headland facilities (head ditches, etc.), and the method of water application to the field (basin, border, furrow, wild flooding, etc.). It should be noted and carefully understood that the optimal irrigation system in a region can only be realized when each subsystem is properly integrated and managed collectively.

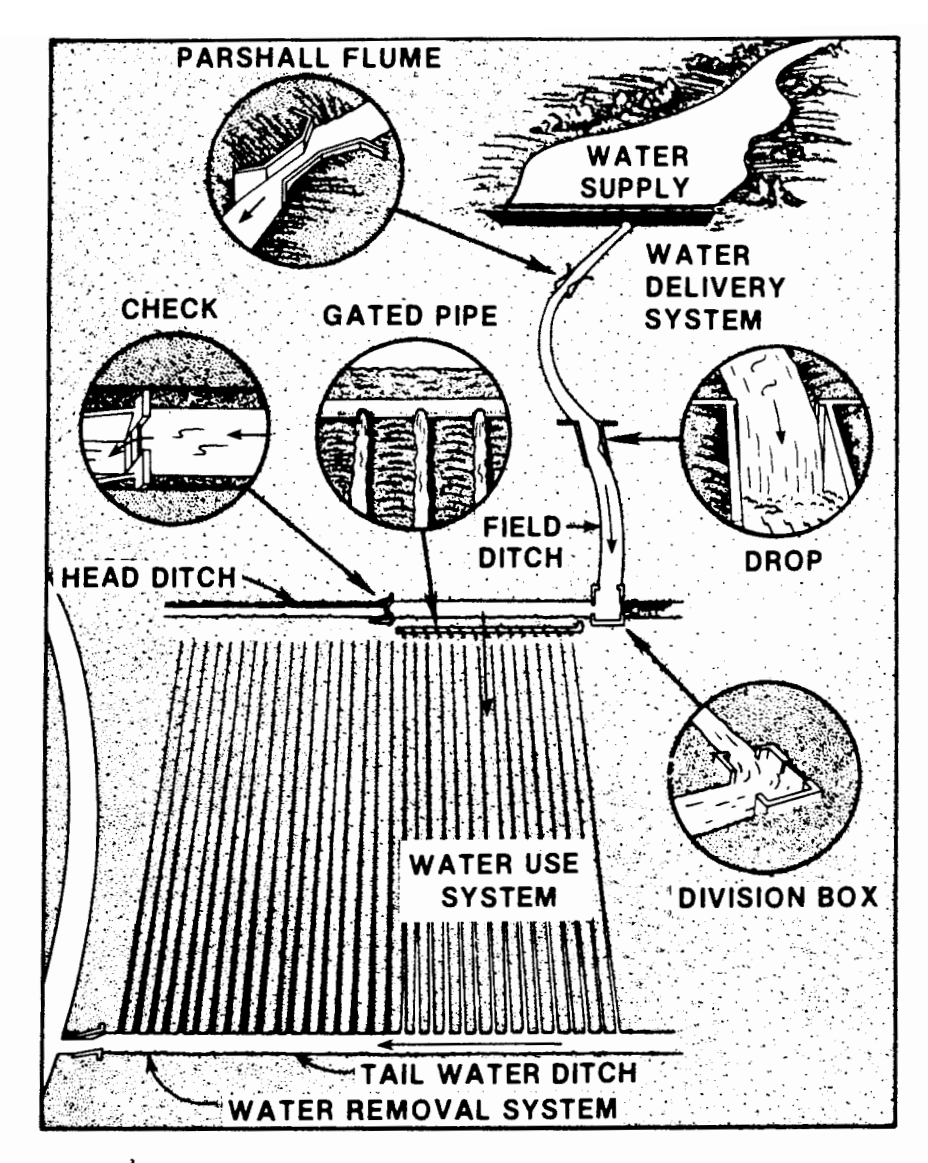


**Figure 3.1** Typical elements of a surface irrigation system. (From U.S. Department of Agriculture, Soil Conservation Service, 1967.)

#### TYPES OF SURFACE SYSTEMS

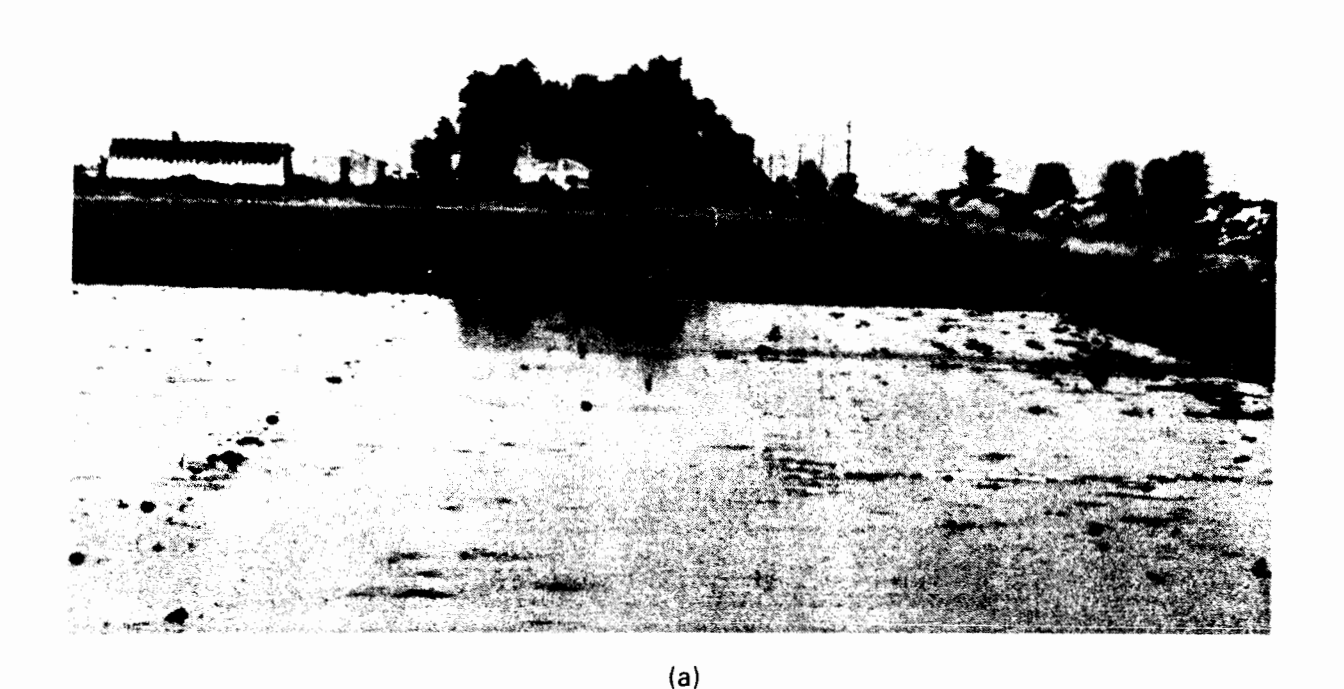
Each surface system has its own unique advantages and disadvantages depending on such factors as (1) initial development costs, (2) size and shape of individual fields, (3) soil characteristics, (4) nature and availability of the water supply, (5) climate, (6) locally grown crops, (7) social preferences and structures, and (8) historical experience. For the purposes of this book, the distinction between types of surface irrigation systems will be based on the physical features of the irrigated fields.

# **Basin Irrigation**

Historically, basin irrigation has been the irrigation of small areas having relatively flat, level surfaces and enclosed by dikes to prevent runoff. Two typical examples

are shown in Fig. 3.2. To segregate basins from level borders (discussed in the next section), the basin terminology will be limited to level areas having complete perimeter dikes to prevent runoff. Figure 3.2a illustrates the most common basin irrigation concept. Water is added to the basin through a gap in the perimeter dike or adjacent ditch. It is important for the water to cover the basin quickly and be shut off when the correct volume has been supplied.

If the basins are small or if the discharge rate available is relatively large, there are few soils not amenable to basin irrigation. Generally, however, basin irrigation is favored by moderate to slow intake soils, and deep-rooted and closely spaced crops. Crops which do not tolerate flooding and soils subject to crusting can be basin irrigated by furrowing or using raised bed planting. Leaching is easily



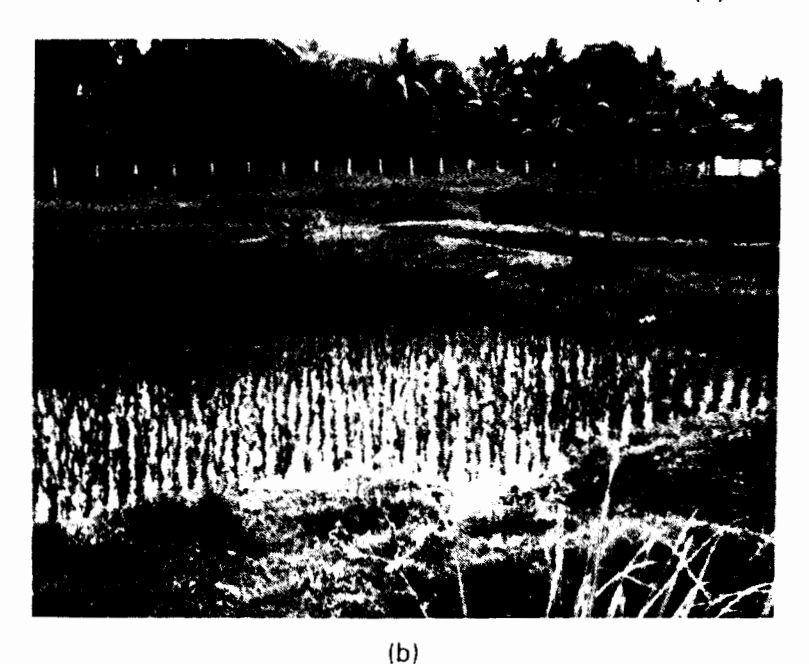


Figure 3.2 Typical basin irrigation systems. (a) Typical large basin irrigation system for field crops. (b) Typical small paddy base.

accomplished with basin irrigation and provision for surface runoff is unnecessary unless rainfall is excessive. Automation is easily applied.

Basin irrigation has a number of limitations that are recognized primarily in association with agriculture in the less developed countries. Accurate land leveling is prerequisite to high uniformities and efficiencies, but this is difficult to accomplish in small areas. The perimeter dikes must be well maintained to eliminate breaching and waste. It is difficult and often infeasible to incorporate the use of modern farm machinery in small basins, thereby limiting small-scale basin irrigation to hand and animal powered cultivation.

# **Border Irrigation**

In many circumstances, border irrigation can be viewed as an expansion of basin irrigation to include long rectangular, or contoured field shapes, longitudinal but no lateral slope, and free draining conditions at the lower end. Figure 3.3. illustrates three typical border irrigation systems.

Figure 3.3a shows a field divided into graded borders. Water is applied to individual borders from the field head ditch and utilizes the elevational differences to traverse the field. When the water is shut off, it recedes from the upper end to the lower end. Graded borders are suited for nearly any crop except those that required prolonged flooding. Soils can have moderately low to moderately high intake rates, but should not crust easily unless the borders are furrowed or the crops are grown on raised beds. The stream size per unit width must be large, particularly following a major tillage operation, in order to achieve rapid field coverage. As with basins, field topography is critical, but the extended areas permit better leveling through the use of farm machinery. Initial land leveling costs may be prohibitive unless the general terrain is relatively flat.

Figure 3.3b and c indicate conditions where the borders are level and water ponds evenly over the soil surface. Level borders or long basins are usually diked at the ends to prevent runoff and thereby achieve high uniformities and efficiencies. Leveling has been a traditional problem, but with the advent of laser technology, level basins and borders have enjoyed an increasing popularity. The limitations are essentially the same as with other forms of basin or border irrigation.

# Furrow Irrigation

An alternative to flooding the entire field surface is to construct small channels along the primary direction of water movement. Water introduced in these "furrows," "creases," or "corrugations" infiltrates through the wetted perimeter and moves vertically and laterally thereafter to refill the soil. Furrows can be used in conjunction with basins and borders, as noted earlier, to overcome topographical variation and crusting. When individual furrows are supplied water as opposed to field spreading prior to the furrows, the method will be called furrow irrigation.

Furrows provide better on-farm water management capabilities under most surface irrigation conditions. Flow rates per unit width can be substantially reduced and topographical conditions can be more severe and variable. A smaller wetted

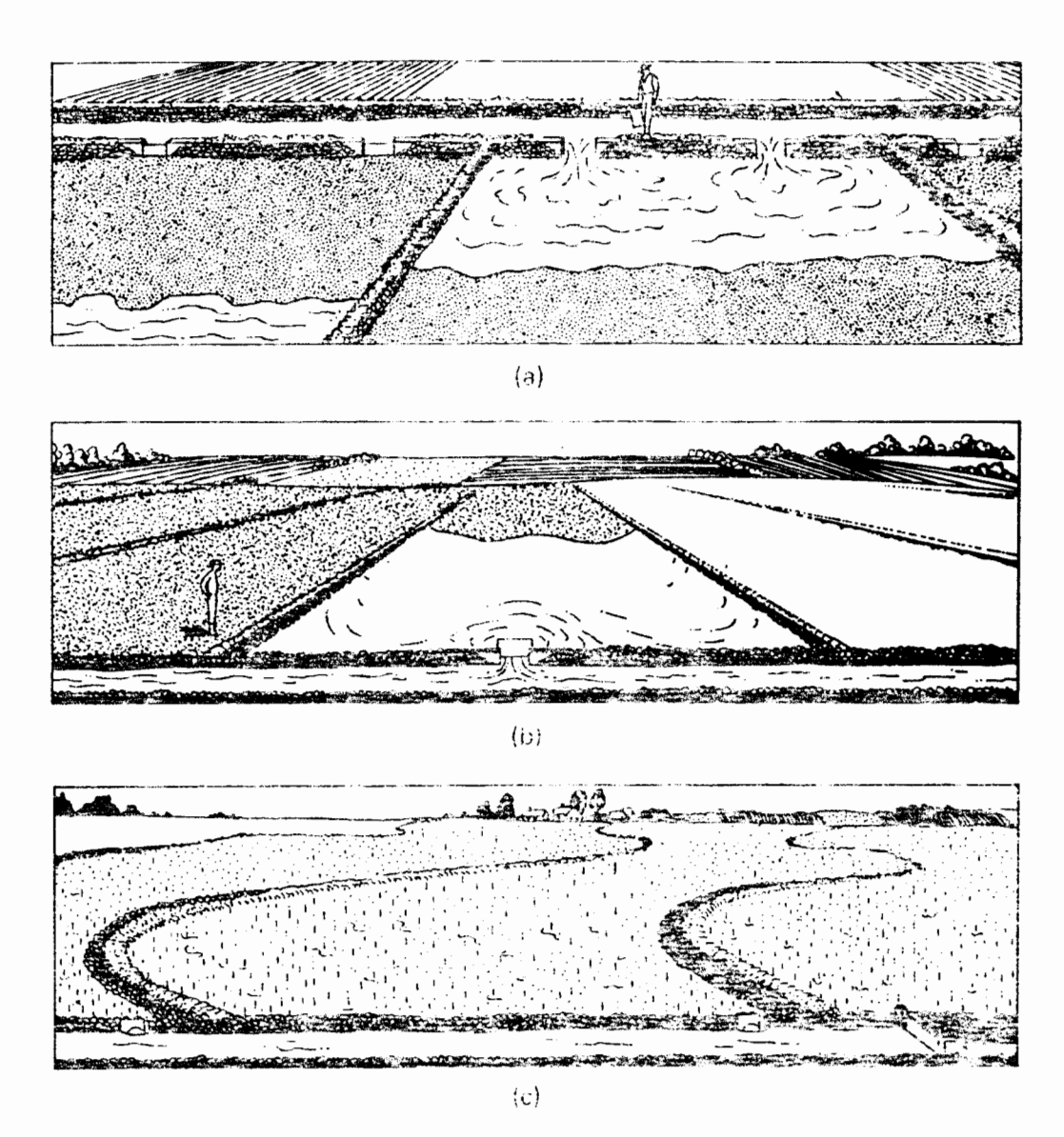
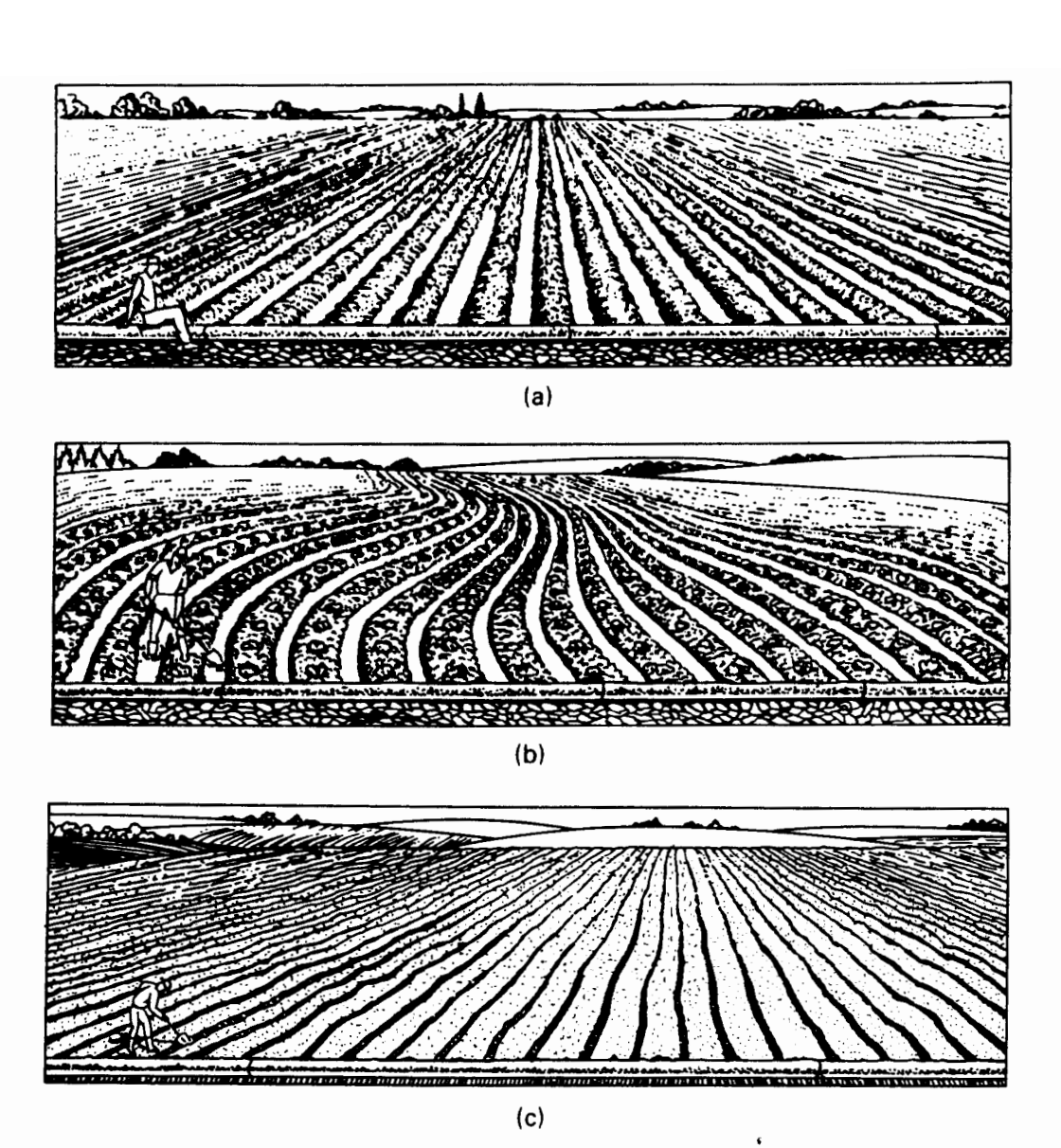


Figure 3.3 Examples of border irrigation systems. (a) Typical graded border irrigation system. (b) Typical level border irrigation system. (c) Typical contour levee or border irrigation system. (After U.S. Department of Agriculture, Soil Conservation Service, 1967.)

area can reduce evaporative losses on widely spaced crops. Furrows provide operational flexibility important for achieving high efficiencies for each irrigation throughout a season. It is a simple (although labor intensive) matter to adjust the furrow stream size to changing intake characteristics by simply changing the number of simultaneously supplied furrows.

The disadvantage of furrows include (1) potential salinity hazards between furrows, (2) greater likelihood of tailwater losses unless end dikes are used, (3) limited machinery mobility across the lateral field direction. (4) the need for one extra tillage practice (furrow construction), and (5) an increased erosion potential. Furrow systems require more labor than border and basin systems and are occasionally more difficult to automate. Figure 3.4 shows three typical furrow-irrigated conditions.



**Figure 3.4** Examples of furrow irrigation systems. (a) Graded or level-furrow irrigation system. (b) Contour furrow irrigation system. (c) Corrugated form of a furrow irrigation system. (After U.S. Department of Agriculture, Soil Conservation Service, 1967.)

## WATER SUPPLY AND MANAGEMENT

Even though it is the oldest and most common method of irrigation, surface irrigation is the least amenable to consistently high levels of performance. Of all the reasons why this is so, probably none have the significance that is associated with the uncertainty of soil infiltration rates. The rate at which water will be absorbed through the soil surface is a nonlinear process which varies both temporally and spatially. It is affected by year-to-year changes in cropping patterns, cultivation, the weathering due to climate, and many other unknown influences. As a result, neither the irrigator nor the engineer can accurately predict the uniformity and efficiency of an irrigation before it occurs, particularly the first water application following planting.

There are other factors limiting surface irrigation system performance, such as a relative lack of standardized equipment for regulation and automation. These and the intake variability noted above place particular emphasis on the management practices applied to surface irrigation, and the art of surface irrigation management is very important. These practices can be classified according to (1) regulation of the field inlet discharge, (2) amending the field surface, and (3) water recovery and reuse.

## **Inlet Discharge Control Practices**

In order to achieve uniform water application, the advancing water front should cover the field during a short interval, certainly not longer than required to infiltrate a depth equal to the soil moisture depletion. A quarter-time rule of thumb was first proposed in published form by Criddle et al. (1956) and has shown promise in some field situations. The rule is generally more applicable to sloping fields than to level ones and may be unnecessary if soil infiltration rates reach a steady-state value very rapidly. The increasing popularity of level basins and borders, which has been facilitated by laser-controlled land-leveling equipment, has shifted the desired advance interval somewhat. Under these conditions, advance is shortened as much as possible.

Although rapid advance is recommended, it imposes serious problems on fields that allow tailwater to flow out of the system. A large fraction of the inlet flow can be lost as tailwater and erosion of the field surface can be substantial. Irrigators can minimize these problems by reducing the inlet discharge by roughly one-half when the flow reaches the end of the field. This practice is called "cutback" irrigation. The first irrigation of the season following planting often requires two or three times the flow rate that subsequent irrigations need to achieve acceptable uniformity.

#### Field Surface Amendments

Surface irrigation performance can be improved by managing the field surface. Where the grade is irregular, causing dry spots and excessive depression storage, land leveling is an important practice. Furrowing borders or basins also reduces the effect of topographical variations. Some soils are too coarse textured for efficient surface irrigation, but practices aimed at incorporating crop residues and animal manures not only reduce intake rates but also improve soil moisture-holding capacity. The water advances over the field better and irrigations need not be applied as often. When water advance over a freshly cultivated field is a problem due to high intake, a limited discharge, or an erosion problem, the surface is often smoothed and compacted by attachments to the planting machinery.

A major cause of inefficiency in furrowed or corrugated surface systems occurs when crops are planted in rows halfway between furrows. The water must move horizontally to the seed location, which requires water-soil contact times much larger than the opportunity time needed to refill the root zone. These types of

problems can be corrected by altering planting and cultivation practices, such as planting nearer the furrow, or planting double rows between furrows.

There are many other amendments to the field surface that might be mentioned. The important point, however, is that the field surface should be maintained in a condition that enhances the ability of the water to move on the field and thereby provide uniform coverage.

## Wastewater Recovery and Reuse

Tailwater storage and recycling are methods that improve surface irrigation practices. They are not widely employed because historically, water and energy have been inexpensive. Today, it is often more economical to cut back the flow rather than pump the unused portion back to the head of the field. Nevertheless, tailwater systems are very cost-effective when the water can be added to the flow serving lower fields.

#### STRUCTURAL ELEMENTS

Surface irrigation systems involve a number of structural elements which control the rate of flow and its energy. To achieve efficient use of the water on the field, these elements should provide a steady, reliable discharge and be capable of effective operation under a number of adverse conditions. The individual elements should be standardized to allow mass production or fabrication.

The elements of a surface irrigation system serve several functions and are generally arranged in the following order: (1) on-off flow control, (2) conveyance, (3) water management, (4) field distribution, and (5) tailwater removal or reuse. To gain a general perception of these structural elements, a brief discussion is included here to illustrate their function. A later chapter deals with their design and installation.

#### **Diversion Structures**

Most surface irrigation systems at the farm level are supplied water from open canal systems operated by irrigation districts, companies, or corporations. Variations include piped delivery systems and groundwater supplies. Diversion structures often perform several tasks. First, they provide on—off water control, which not only allows the district to allocate its water supply, but also protects the fields below the diversion from untimely flooding. Second, diversion structures regulate and stabilize the discharge to the requirements of field conveyance and distribution systems. Flow measurement is usually incorporated at the turnout in order to establish and protect the basic water entitlement. Finally, many diversion structures serve as further protection to downstream structures by controlling sediments and debris as well as dissipating excess kinetic energy in the flow. Two typical canal turnout diversion structures are shown in Fig. 3.5.

Structural Elements 39

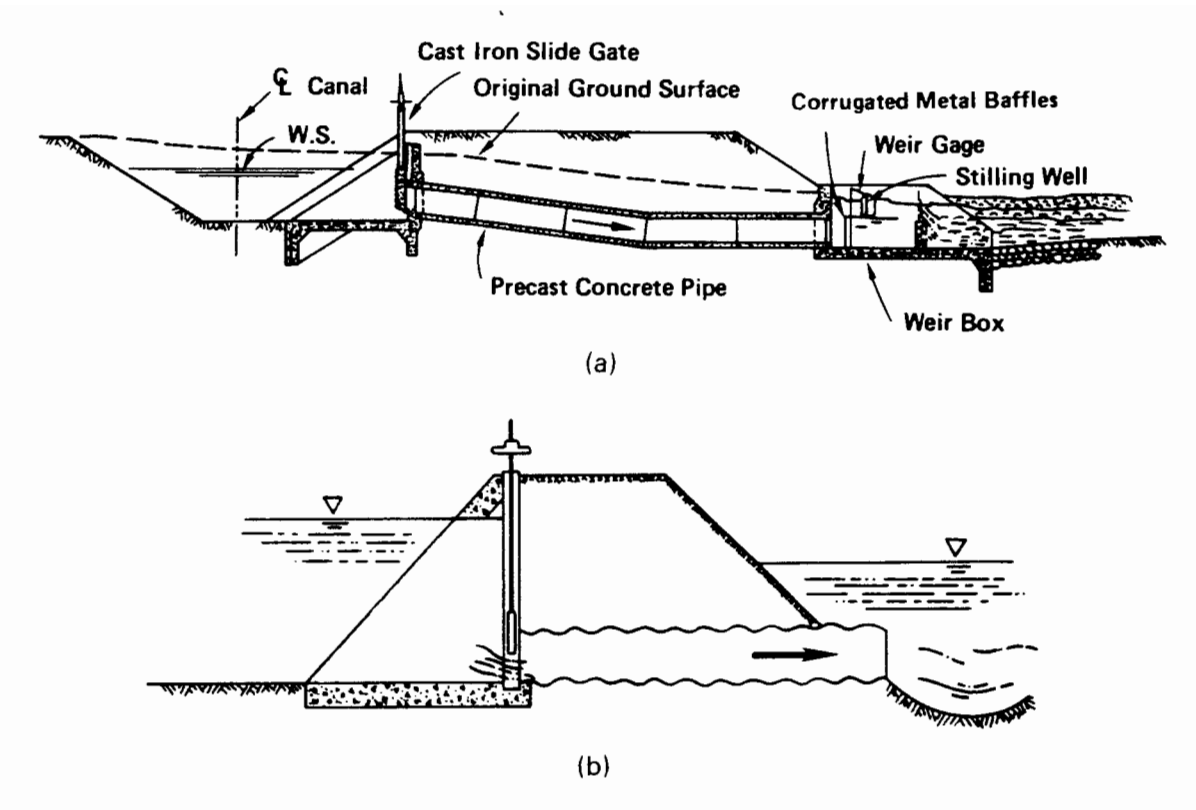


Figure 3.5 Typical canal turnout structure. (a) Pipe turnout into a concrete pipe with downstream flow measurement and energy dissipation. (b) Pipe turnout into a corrugated pipe section. (After Skogerboe et al., 1971.)

## **Conveyance and Management Structures**

The delivery of water from the canal turnout to the field inlet requires the same (although smaller) conveyance and control structures found in major canal networks. The conveyance itself is usually an earthen ditch or lateral, a buried pipe, or a lined ditch. Pipe materials are usually plastic (PVC), concrete, clay, or asbestos cement, but may be as simple as a wooden square or retangular construction. Open-channel linings include slip-form or prefabricated concrete, shotcrete or gunite, asphalt, masonry, surface and buried plastic or rubber membranes, and compacted earth.

The control of water within the conveyance system involves flow measurement, sediment and debris removal, divisions, checks, drops, energy dissipators, and water-level controls. A few of the more common flow-measuring structures for open channels are shown in Figs. 3.6 and 3.7. These include various weirs, flumes, and orifices. An array of checks, drops, dividers, and water-level controllers are shown in Fig. 3.8. The design of these structures is often simple since they are small. The most critical designs are for flow measurement and drop-energy dissipator structures.

# Field Distribution Systems

When the water arrives at the field, it must be transferred and spread across the field within fairly precise limits. Usually, each field has a head ditch or pipeline

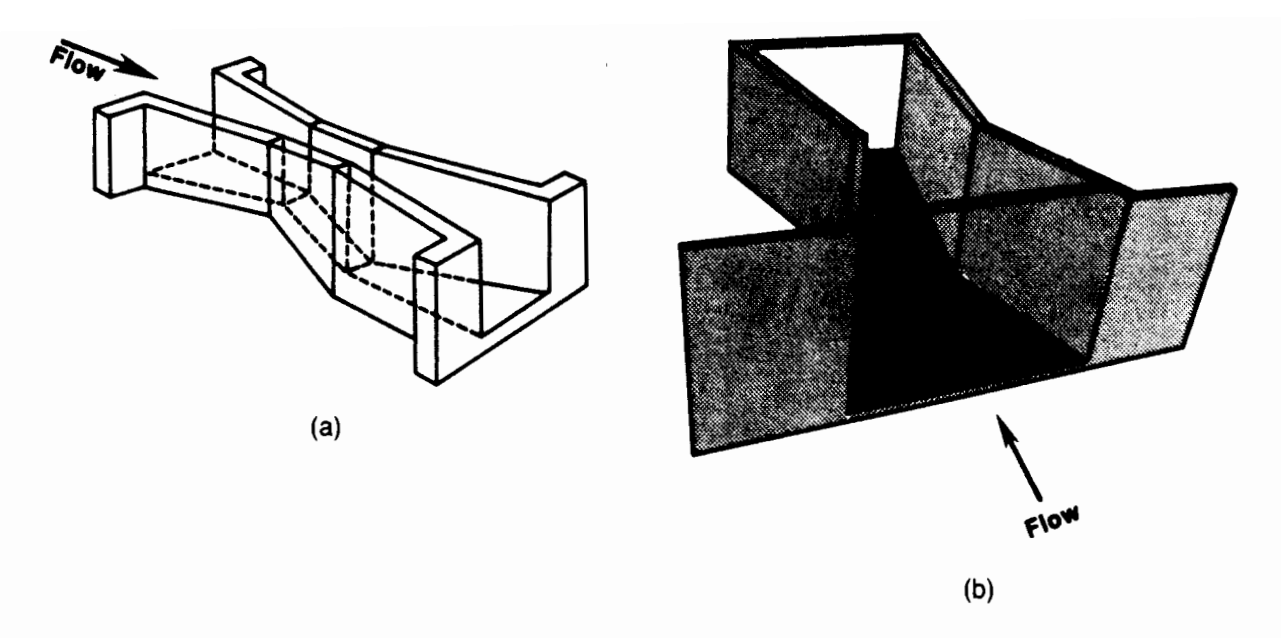
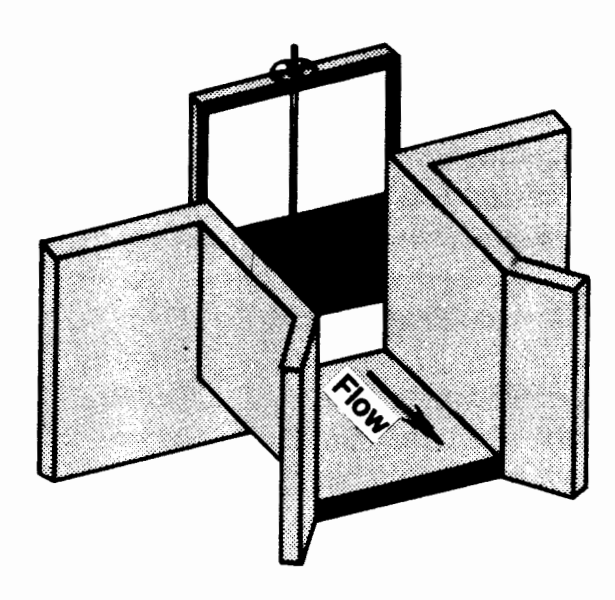


Figure 3.6 Two commonly used flow-measuring flumes. (a) Parshall flume. (b) Cutthroat flume.

running along the upper side of the field. From there the flow is distributed onto the field by a multitude of methods, a few of which will be mentioned here.

If the field is irrigated from a head ditch, the methods used to spread the water over the field depend somewhat on the method of irrigation. For border and basin systems, open or piped outlets are generally used. Figure 3.9 shows two typical configurations, both of which are located in earthen head ditches. If the field is furrow irrigated, outlets like those in Fig. 3.9 may still be used, but it is probably more common to have outlets directed to each furrow or corrugation. Figure 3.10 shows two such systems. In Fig. 3.10a siphon tubes are used to divert the water into each furrow, while in Fig. 3.10b individual pipes or spiles supply each furrow.

The headland facilities for surface irrigation can also consist of surface or



**Figure 3.7** Typical submerged orifice flow control measuring structure.

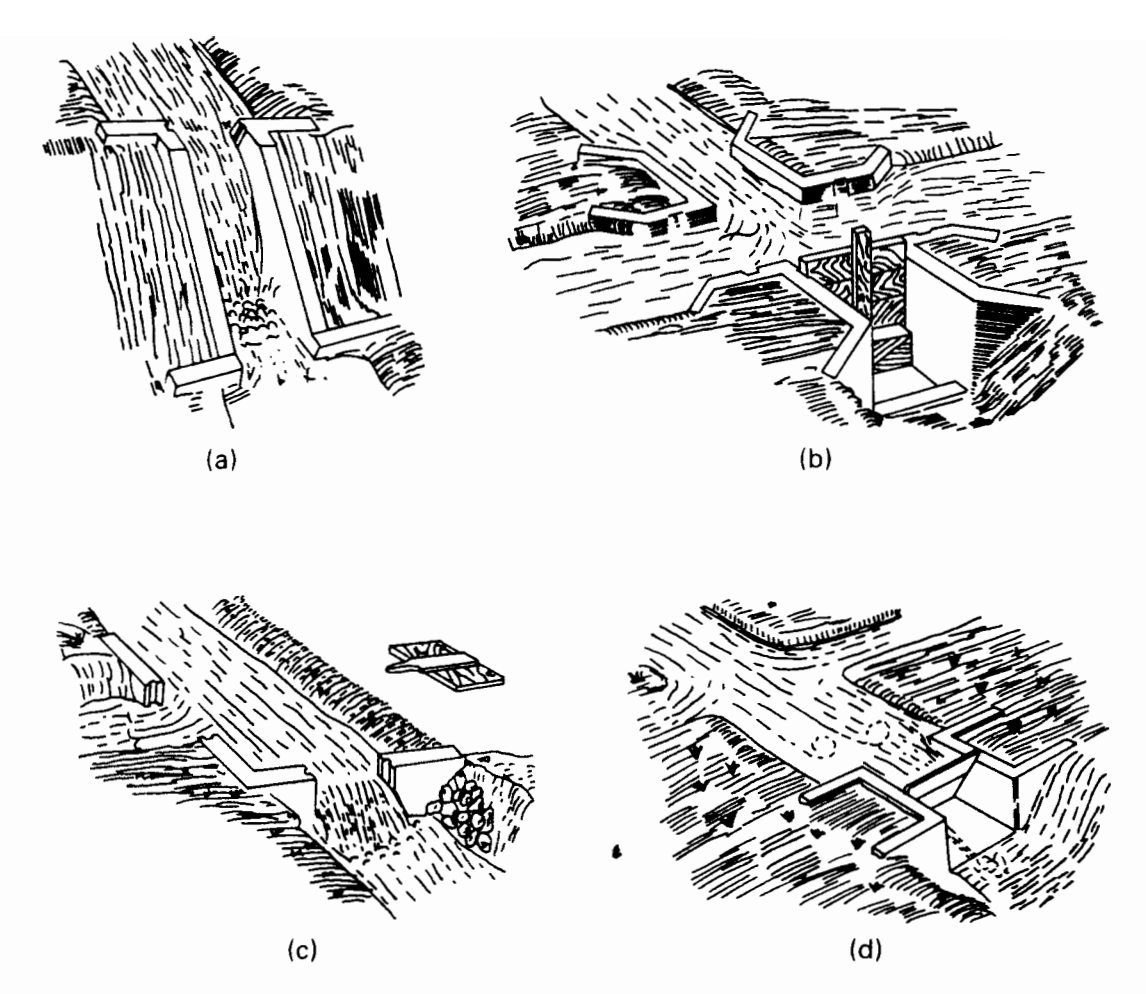


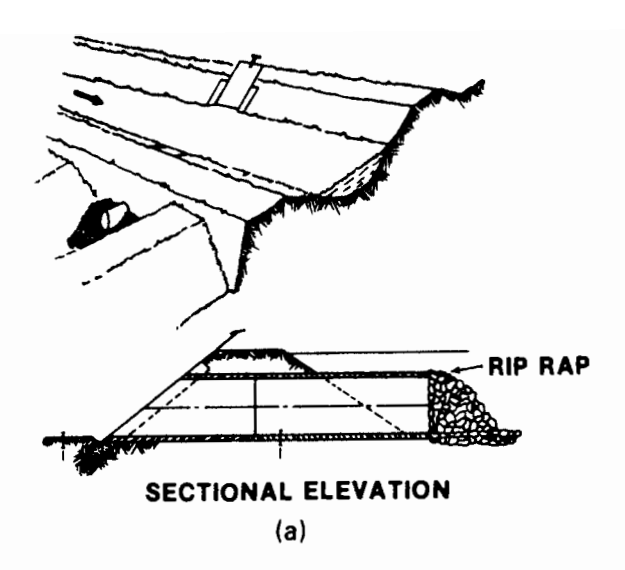
**Figure 3.8** Examples of open-channel water control structures. (a) Simple drop structure. (b) Combination check-flow divider structure. (c) Division structure. (d) Simple check. (After Skogerboe et al., 1971.)

buried pipes. Basin and border irrigation systems usually employ buried pipes serving one or more gated risers within each basin or border. Two typical riser outlets are shown in Fig. 3.11. The most common piped method of furrow irrigation is with the use of plastic or aluminum gated pipe, as shown in Fig. 3.12. The gated pipe may be supplied by a buried pipe to riser assembly such as the one shown in Fig. 3.11 or directly from an open ditch.

A great deal of research and development attention has been given to automating surface irrigation headland facilities. This work and the resultant products are discussed in Chapter 8.

## Tailwater Removal and Reuse Systems

In order to convey water over the field surface rapidly enough to achieve a high degree of application uniformity and efficiency, the discharge at the field inlet must be much larger than the cumulative intake along the direction of advance. As a



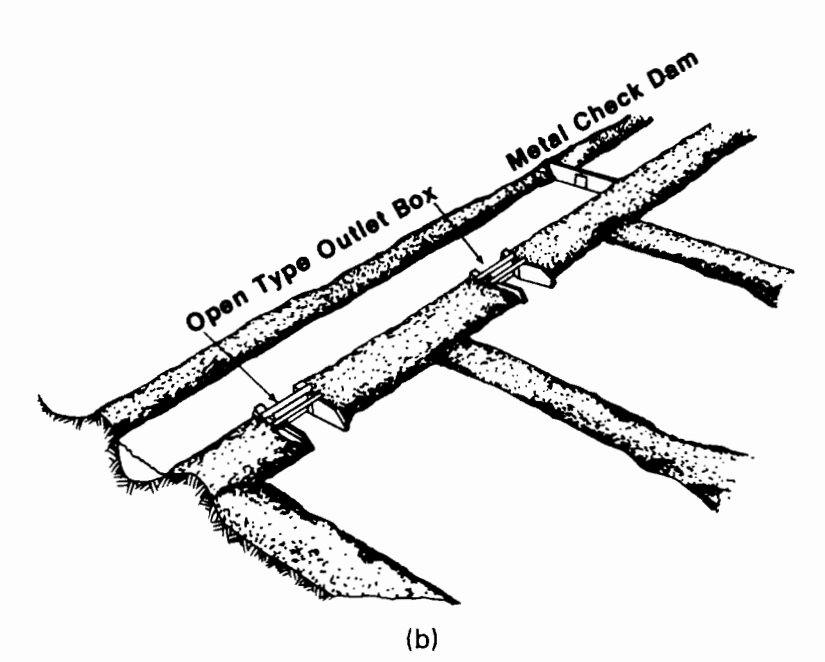
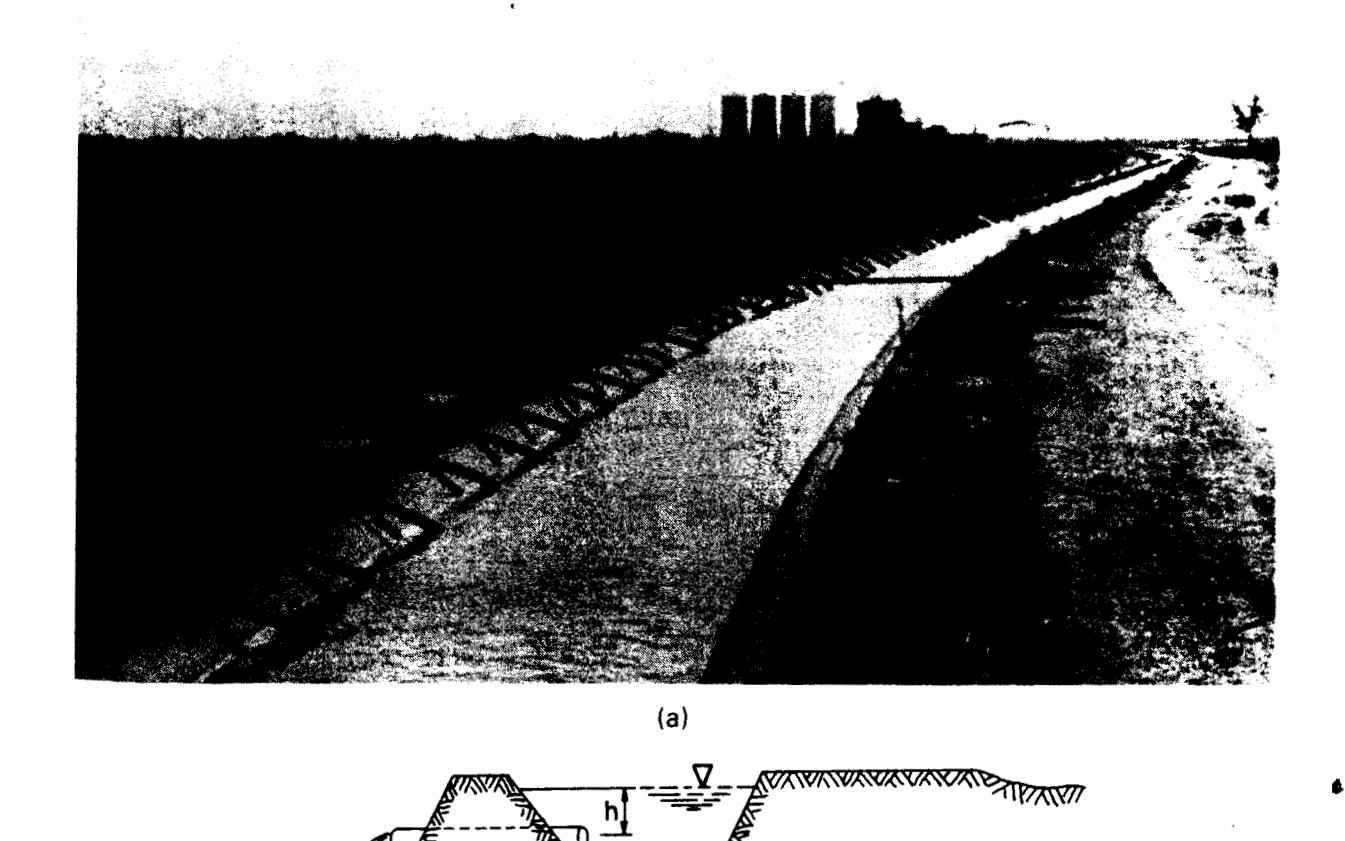


Figure 3.9 Two head ditch outlets for border or basin irrigation. (a) Pipe outlet with gate control. (b) Outlet box with gate control. (U.S. Department of Interior, Bureau of Reclamation, 1951. See also Krautz and Malsajan, 1975.)

result, there remains a significant fraction of the inlet flow at the end of the field which will be wasted unless the field is diked or the tailwater is captured and reused. In many locations, the reason to capture tailwater is not so much for the value of the water but for the soil it has eroded from the field surface. Other conditions exist where erosion is not a problem and the water supply is abundant, so the major emphasis is merely to remove the tailwater before waterlogging and salinity problems emerge. Finally, it may be cost-effective to impound the tailwater and pump it back to the field inlet for reuse or store it for use on lower-lying fields.

Tailwater removal and reuse systems are seldom as complex as headland facilities, often simple earth ditches and pits. There are, of course, times when cross-drainage structures must be provided to convey wastewater by various barriers, such as roads, canals, or pipelines.



**Figure 3.10** Field outlets for furrow irrigation. (a) Furrow irrigation using siphon tubes. (Courtesy of Dr. L. S. Willardson.) (b) Furrow irrigation using spiles.

(b)

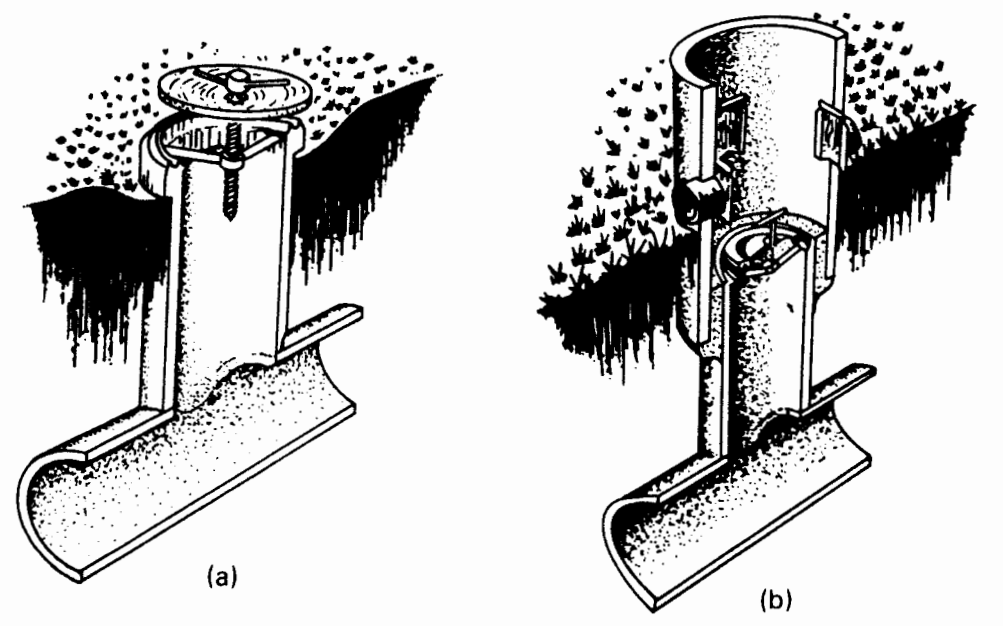
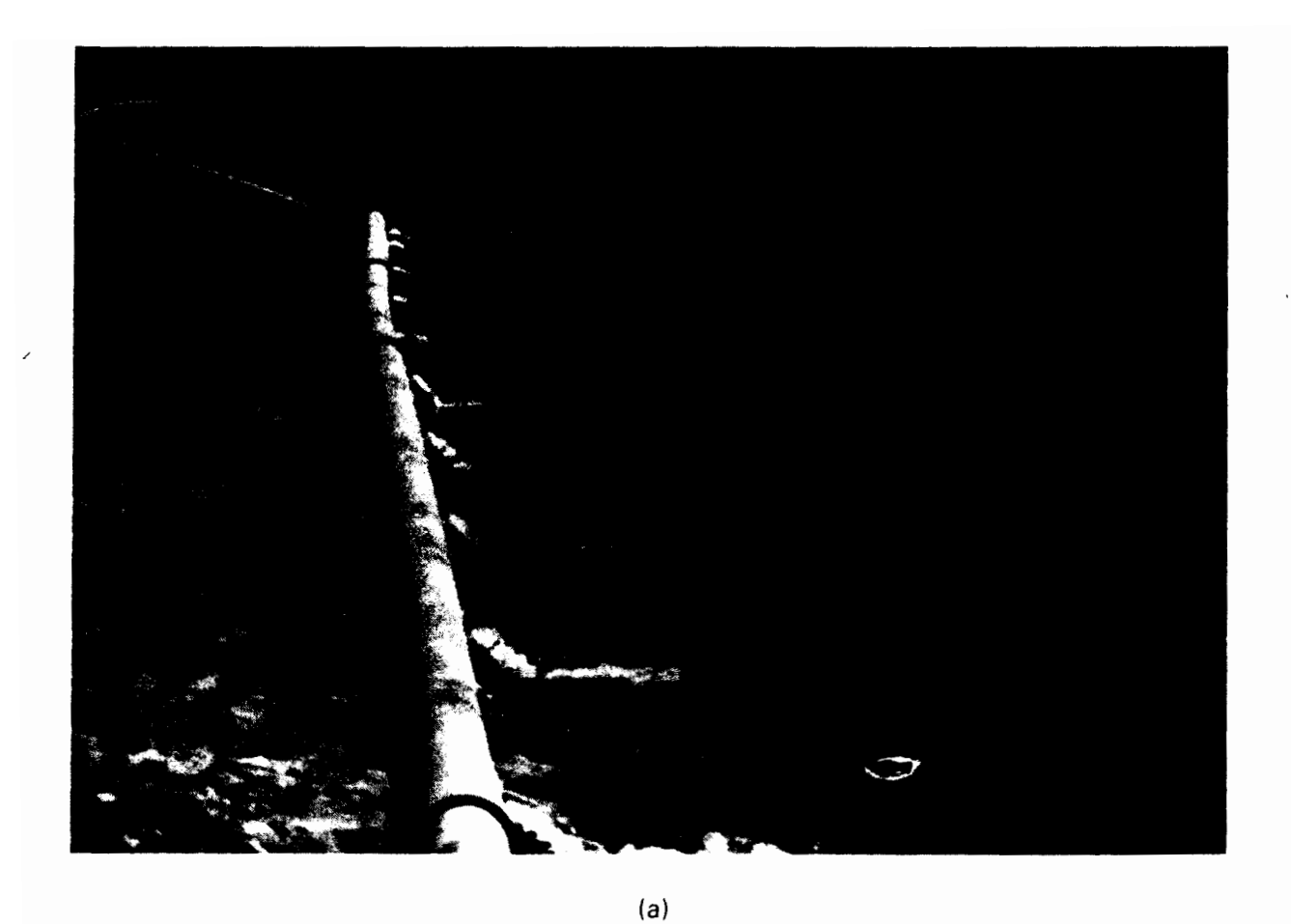


Figure 3.11 Buried pipe headland distribution facilities. (a) Alfalfa-valve-controlled riser. (b) Alfalfa valve riser distributor for orchards. (After Skogerboe et al., 1971.)



(b)

Figure 3.12 Two views of a gated-pipe furrow irrigation system. (Courtesy of Dr. L. S. Willardson.)

Structural Elements 45

#### REFERENCES

- CRIDDLE, W. D., S. DAVIS, C. H. PAIR, and D. L. SHOCKLEY. 1956. Methods of Evaluating Irrigation Systems. USDA-SCS Handb. 82, U.S. Department of Agriculture, Soil Conservation Service, Washington, D.C.
- KRAUTZ, D. G., and V. I. K. MALSAJAN. 1975. Small Hydraulic Structures, Vol. 1. Irrig. Drain. Pap. 26/1, United Nations, Food and Agriculture Organization, Rome.
- SKOGERBOE, G. V., V. T. SOMERAY, and W. R. WALKER. 1971. Check-Drop Energy Dissipation Structures in Irrigation Systems. Water Manage. Tech. Rep. 9. Colorado State University, Fort Collins, Colo., May.
- U.S. Department of Agriculture, Soil Conservation Service. 1967. National Engineering Handbook. "Planning Farm Irrigation Systems." U.S. Government Printing Office, Washington, D.C., July, Sec. 15, Chap. 3.
- U.S. Department of Interior, Bureau of Reclamation. 1951. Irrigation Advisors' Guide. U.S. Government Printing Office, Washington, D.C.

Chap. 3

# Field Measurement Techniques

#### INTRODUCTION

Before proceeding to the procedures for evaluating the hydraulic performance of surface-irrigated fields, it is helpful to review the various field measurement techniques that are commonly employed. The descriptions of various field measurements presented in this chapter are not intended to be exhaustive. Supplementary material can be found in a wide variety of technical publications, including text-books, handbooks, and manuals.

Generally, measuring surface hydrologic parameters is much easier than measuring subsurface hydraulic and hydrologic parameters. The most accurate measurements when evaluating surface-irrigated fields are inflow discharge and tailwater runoff because standardized flow-measuring devices are available that can easily be installed. In contrast, the measurement of infiltration, while easily measured, is complicated by its variability from one location to another in the same field and its variability from one irrigation event to the next during the irrigation season.

#### FLOW MEASUREMENT

There are many standardized flow-measuring devices available for measuring surface water in irrigation systems. Weirs were the first devices, developed more than a century ago. Various flumes have been developed during the twentieth century and have become the most commonly used devices in irrigation systems. Another very common device in irrigation systems is the free or submerged orifice

generally associated with gates for controlling deliveries to individual farms or fields.

### Free Flow and Submerged Flow

The two most significant flow regimes under which any open channel constriction may operate are free flow and submerged flow. The distinguishing difference between the two flow conditions is the occurrence of critical velocity in the vicinity of the constriction (usually, a very short distance upstream from the narrowest portion of the constriction). When this critical flow control occurs, the flow is uniquely related to the flow depth or "head" upstream of the critical section. Thus measurement of a flow depth at some specified location upstream,  $h_u$ , from the point of the critical condition is all that is necessary to obtain the free-flow discharge. Thus

$$Q_f = f(h_u) \tag{4.1}$$

When the flow conditions are such that the downstream flow depth is raised to the extent that the flow velocity at every point through the constriction becomes less than the critical value, the constriction is operating under submerged-flow conditions. With this flow regime an increase in tailwater flow depth,  $\Delta h_d$ , will increase the head upstream of the constriction by  $\Delta h_u$  ( $\Delta h_u$  will be less than  $\Delta h_d$ ). A constriction operating under submerged-flow conditions requires that both upstream depth,  $h_u$ , and downstream depth,  $h_d$ , be measured. The definition given for submergence, S, is

$$S = \frac{h_d}{h_u} \tag{4.2}$$

and may be represented in percent. The submerged-flow discharge,  $Q_s$ , is a function of  $h_u$  and  $h_d$ , generally written as a relation between flow rate, head loss  $(h_u - h_d)$ , and submergence:

$$Q_s = f(h_u, h_d) = f(h_u - h_d, S)$$
 (4.3)

Often, constrictions designed initially to operate under free-flow conditions become submerged in response to unusual operating conditions or the accumulation of moss and vegetation in the open channel. Care should always be taken to note the operating condition of the constriction in order to determine which rating should be used. The value of submergence marking the change from free flow to submerged flow, or vice versa, is referred to as the transition submergence,  $S_t$ . At this condition, the discharge given by the free-flow equation is exactly the same as that given by the submerged-flow equation. Hence, if discharge equations are known for both the free-flow and submerged-flow conditions, a definite value of the transition submergence can be obtained by setting the equations equal to one another and solving for  $S_t$ . It should be noted that this derived value of  $S_t$  is highly sensitive to slight errors in the coefficients or exponents of either equation.

The difference between free flow, the transition state, and submerged-flow water surface profiles is illustrated for a simple channel constriction in Fig. 4.1.

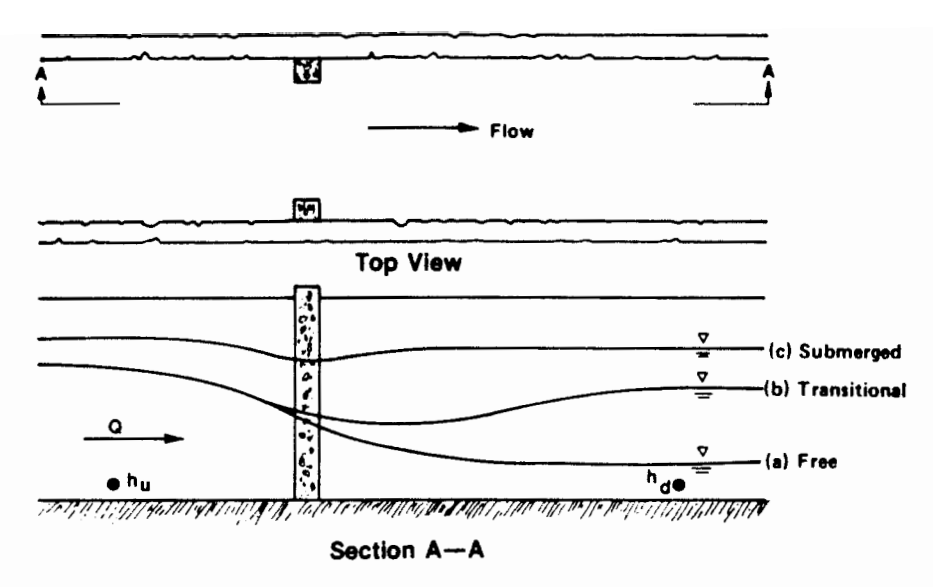


Figure 4.1 Flow conditions in an open-channel constriction.

Water surface profile (a) illustrates free flow and (b) indicates the transition submergence condition. Both profiles (a) and (b) have the same upstream depth of flow, with profile (b) having the maximum submergence value for which the free-flow condition can exist. The submerged-flow condition is illustrated by profile (c), where an increase in the tailwater depth has also increased the depth of flow at the upstream station.

#### **Flumes**

There are two classes of flumes included in this section: (1) the long-throated flume in which the critical depth condition is created in a region of parallel flow, and (2) the variety of flumes in which critical conditions occur in regions of curvilinear flow. The significant difference in these two classes of flumes is that linear stream flow conditions are much better defined theoretically. Rating relations can be reasonably well predicted and thereby some advantage is gained due to the ease of dealing with field installations that may not be constructed precisely to specifications. The curvilinear flumes require individual ratings for specific geometries and must therefore be constructed accurately and installed correctly. Each class of flume and its respective configuration are accurate and effective when utilized properly. Each has its own set of conditions for optimum use.

**Parshall flumes.** The Parshall flume (Fig. 3.6a) is the most commonly used flow-measuring device in irrigation systems in the United States. This flume was developed between roughly 1917 and 1925 and was first called "the improved Venturi flume" (Parshall, 1926). The two most desirable features of the Parshall flume are that it operates satisfactorily with a loss of head much less than that required for a weir, and that under normal operating conditions the discharge can be determined with an accuracy of 2 to 5%. The primary disadvantage of a Parshall flume is the size of the structure (Fig. 4.2 and Table 4.1). Normally, the Parshall flume is operated under free-flow conditions, although submerged-flow ratings have

Flow Measurement 49

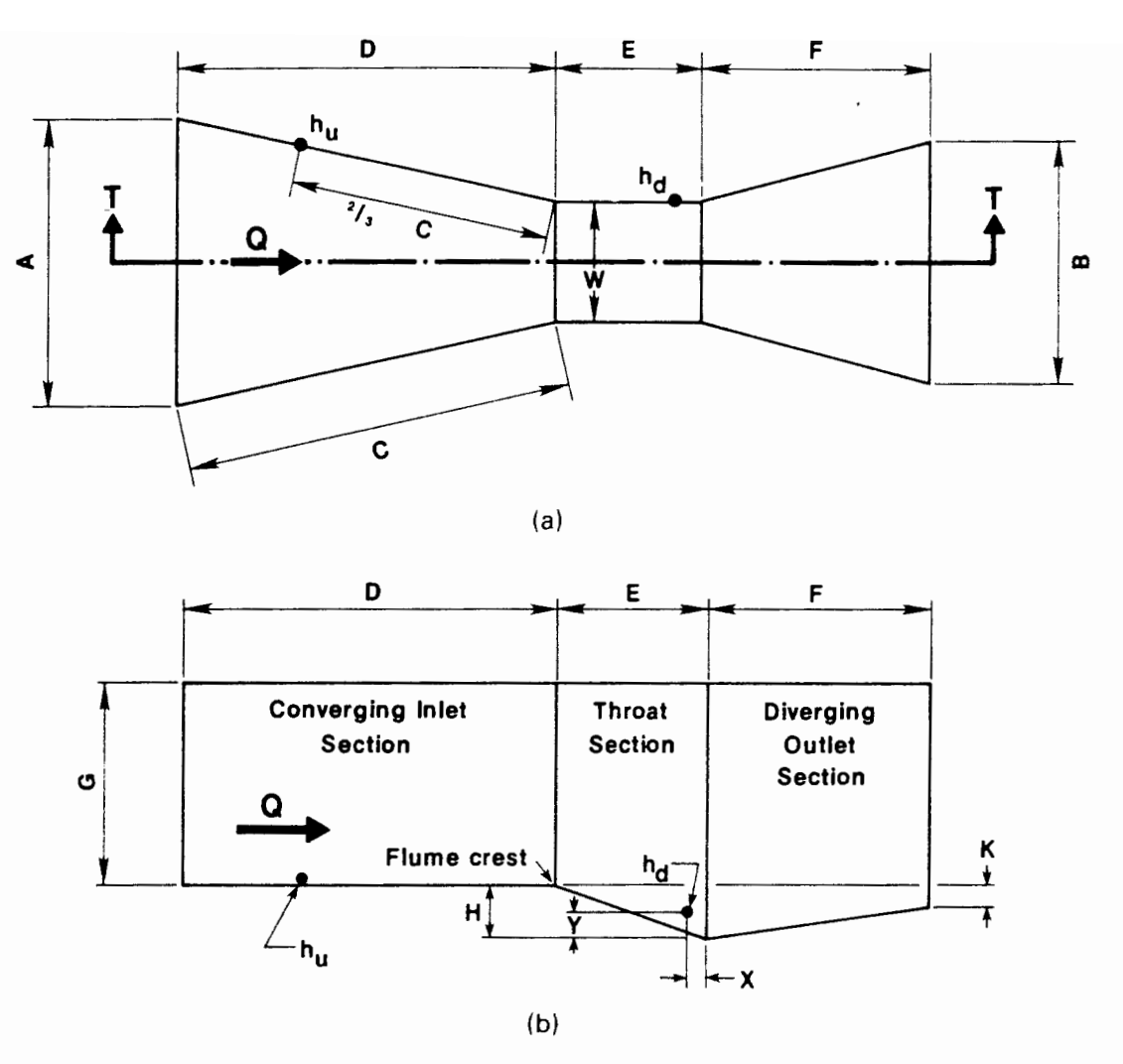


Figure 4.2 Physical layout of a Parshall flume. (a) Plan view of a Parshall flume. (b) Sectional view of a Parshall flume.

been developed using the location,  $h_d$ , for the downstream flow depth (Fig. 4.2). The water is highly turbulent at this location, which adds to the likely errors in determining  $h_d$  and consequently the submerged-flow discharge.

The free-flow and submerged-flow coefficients and exponents for Parshall flumes are presented in Table 4.2, where the general form of the free-flow equation is

$$Q_f = C_f h_u^{n_f} \tag{4.4}$$

and the general form of the submerged-flow equation (Skogerboe et al., 1967c) is

$$Q_s = \frac{C_1(h_u - h_d)^{n_f}}{[-(\log S + C_2)]^{n_s}}$$
(4.5)

**Cutthroat flumes.** A flow-measuring device which has been recently developed is the cutthroat flume (Skogerboe et al., 1967a). The original studies were extended by Bennett (1972) in rating a group of cutthroat flumes which have the same geometric shape. Because of this similarity, the behavior of all flumes

TABLE 4.1 DIMENSIONS AND CAPACITIES FOR PARSHALL FLUMES IN ENGLISH UNITS\*

width (fi.in.) $A=B=C=A+D=E=F=G=H=$ $\frac{3}{5}(W/2+)$ $A=B=C=A+D=E=F=G=H=$ $0.17$ $0.06\frac{19}{12}$ $0.73\frac{1}{12}$ $0.13\frac{1}{12}$ $0.12\frac{1}{12}$ $0.10\frac{1}{12}$ $0.10\frac{1}{12$						Dimensio	Dimensions (feet and inches)	nd inches						Free capa	Free-flow capacities
$\begin{array}{cccccccccccccccccccccccccccccccccccc$	Throat width				$\frac{2}{3}C \text{ or }$ $\frac{2}{3}(W/2 +$									M.	No.
$\begin{array}{cccccccccccccccccccccccccccccccccccc$	(ft.in.)	A	В	C	4)	D	E	F	$\mathcal{G}$	Н	×	×	^	(ft <sup>3</sup> /s)	(ft³/s)
$\begin{array}{cccccccccccccccccccccccccccccccccccc$	0′1″	$0.6\frac{19}{32}$ "	$0'3\frac{21}{32}''$	$1'2\frac{9}{32}''$	$0.9\frac{17}{32}$ "	1.2"	0′3″	0.8″	0,6″	0'1#"	0.0	0,5"	0' \frac{1}{3}"	0.01	0.2
$\begin{array}{cccccccccccccccccccccccccccccccccccc$	0'2"	$0.8\frac{13}{32}$ "	$0.5\frac{2}{16}$ "	1′4 ™3₁	$0'10_8''$	1'4"	$0'4^{\frac{1}{2}''}$	0.10"	0′8″	$0'1\frac{11}{16}''$	$0'0^{\frac{7}{8}}$ "	0′ <u>§</u> "	0′1″	0.02	0.4
$ \begin{array}{cccccccccccccccccccccccccccccccccccc$	0′3″	$0'10\frac{1}{16}''$		$1'6\frac{3}{8}''$	$1'0^{\frac{1}{4}''}$	1,6″	.9.0	1'0"	1′3″	$0'2^{\frac{1}{4}''}$	0′1″	0.1"	$0'1^{\frac{1}{2}}$ "	0.03	9.0
$1'10_8^{14}$ $1'3'$ $2'10_8^{14}$ $1'11_8^{14}$ $2'10'$ $1'6'$ $2'0'$ $2'0_4^{14}$ $2'0'$ $4'6'$ $3'0'$ $4'4_8^{14}$ $2'0'$ $3'0'$ $3'0'$ $3'4_8^{14}$ $2'6'$ $4'9'$ $3'2''$ $4'7_8^{14}$ $2'0'$ $3'0'$ $3'0'$ $3'11_2^{14}$ $3'6'$ $3'4'$ $4'10_8^{14}$ $2'0'$ $3'0'$ $3'0'$ $4'6_4^{14}$ $3'6'$ $3'4'$ $5'3'$ $2'0'$ $3'0'$ $3'0'$ $5'1_8^{14}$ $3'6'$ $3'6'$ $3'6'$ $3'0'$ $3'0'$ $3'0'$ $5'1_8^{14}$ $5'0'$ $4'0'$ $5'10_8^{14}$ $2'0'$ $3'0'$ $3'0'$ $5'1_8^{14}$ $5'0'$ $4'0'$ $5'10_8^{14}$ $2'0'$ $3'0'$ $3'0'$ $7'6_8^{14}$ $5'0'$ $4'4'$ $6'4_2^{14}$ $2'0'$ $3'0'$ $3'0'$ $7'6_8^{14}$ $5'0'$ $4'4'$ $6'4_2^{14}$ $2'0'$ $3'0'$ $3'0'$ $8'0'$ $7'0'$ $7'0'$ $7'0'$ $7'0'$ $7'0'$ <	,,9,,0	$1'3^{\frac{1}{2}}_{\frac{1}{2}}$ "	$1'3\frac{1}{2}''$	$2'0^{L}_{16}$ "	1'45"	2.0"	1′0″	2'0"	1,6″	$0'4\frac{1}{2}"$	0'3"	0.2"	0.3"	0.05	2.9
$ 2.9\frac{1}{4}, \qquad 2.0^{\circ} \qquad 4.6^{\circ}, \qquad 3.0^{\circ} \qquad 4.4\frac{3}{8}, \qquad 2.0^{\circ} \qquad 3.0^{\circ} \qquad 3.4\frac{3}{8}, \qquad 3.4^{\circ} \qquad 3.2^{\circ} \qquad 4.4\frac{3}{8}, \qquad 2.0^{\circ} \qquad 3.0^{\circ} \qquad 3.0^{\circ} \qquad 3.0^{\circ} \qquad 3.11\frac{1}{2}, \qquad 3.0^{\circ} \qquad 3$	.6,0	$1'10\frac{5}{8}"$	1'3"	$2'10^{\frac{5}{8}''}$	$1'11\frac{1}{8}"$	2′10″	1'0"	1'6"	2'0"	$0'4^{\frac{1}{2}}$ "	0,3"	0.2"	0'3"	0.1	5.1
$3^44\frac{8}{8}$ , $2^46^{\prime\prime\prime}$ $4^49^{\prime\prime\prime}$ $3^42^{\prime\prime\prime}$ $4^77^{\prime\prime\prime}$ $2^{\prime\prime\prime\prime}$ $3^{\prime\prime\prime\prime}$ $3^{\prime\prime\prime\prime}$ $3^{\prime\prime\prime\prime}$ $3^{\prime\prime\prime\prime}$ $3^{\prime\prime\prime\prime}$ $3^{\prime\prime\prime\prime}$ $3^{\prime\prime\prime\prime}$ $3^{\prime\prime\prime\prime}$ $3^{\prime\prime\prime\prime}$ $3^{\prime\prime\prime\prime\prime}$ $3^{\prime\prime\prime\prime\prime}$ $3^{\prime\prime\prime\prime\prime}$ $3^{\prime\prime\prime\prime\prime}$ $3^{\prime\prime\prime\prime\prime}$ $3^{\prime\prime\prime\prime\prime}$ $3^{\prime\prime\prime\prime\prime}$ $3^{\prime\prime\prime\prime\prime\prime}$ $3^{\prime\prime\prime\prime\prime\prime}$ $3^{\prime\prime\prime\prime\prime\prime}$ $3^{\prime\prime\prime\prime\prime\prime}$ $3^{\prime$	12"	$2'9^{\frac{1}{4}}$ "	2'0"	4,6"	3.0"	$4'4\frac{7}{8}"$	2'0"	3.0"	3'0"	.6.0	0'3"	0'2"	0.3"	0.4	16.0
$3'111\frac{1}{2}''$ $3'0''$ $5'0''$ $3'4''$ $4'10^2_8''$ $2'0''$ $3'0''$ $3'0''$ $4'6\frac{1}{4}''$ $3'6\frac{1}{4}''$ $3'6\frac{1}{4}''$ $3'6\frac{1}{4}''$ $3'6\frac{1}{4}''$ $3'6\frac{1}{4}''$ $3'6\frac{1}{4}''$ $3'6\frac{1}{4}''$ $3'6\frac{1}{4}''$ $3'6^2''$ $3'0''$ $3'0''$ $3'0''$ $4'0''$ $5'10\frac{1}{8}''$ $2'0''$ $3'0''$ $3'0''$ $3'0''$ $7'6\frac{1}{8}''$ $6'0''$ $4'4''$ $6'4\frac{1}{4}''$ $2'0''$ $3'0''$ $3'0''$ $3'0''$ $9'11\frac{1}{8}''$ $8'0''$ $7'6''$ $5'0''$ $7'4\frac{1}{4}''$ $2'0''$ $3'0''$ $3'0''$ $1'1'1\frac{1}{4}''$ $9'0''$ $8'0''$ $5'4''$ $7'10\frac{1}{8}''$ $2'0''$ $3'0''$ $3'0''$ $1'1'1\frac{1}{4}''$ $9'0''$ $8'0''$ $5'4''$ $7'10\frac{1}{8}''$ $2'0''$ $3'0''$ $1'1'1\frac{1}{4}''$ $1'2'0'$ $1'4'3\frac{1}{4}''$ $6'0''$ $1'4'0''$ $3'0''$ $6'0''$ $1'1'1^2''$ $1'1'1'1'$ $1'1'1'1'$ $1'1'1'1'$ $1'1'$ $1'1'1'$ $1'1'1'$ $1'1'1'$ $1'1'1'$ $1'1'1'$ $1'1'1'$ $1'1'1'$ $1'1'1'$ $1'1'1'$ $1'1'1'$ $1'1'$	18″	3'48"	5,6"	4.6″	3'2"	$4'7\frac{7}{8}''$	2'0"	3.0"	3.0"	.6,0	0'3"	0.2"	0.3"	0.5	24.0
$4^{6\frac{1}{2}n}$ $3^{6}$ $5^{6}$ $3^{6}$ $5^{6}$ $3^{6$	24"	$3'11^{\frac{1}{2}''}$	3.0"	2.0,	3'4"	$4'10^{\frac{7}{8}''}$	2'0"	3.0"	3.0"	,6,0	0'3"	0.5"	0'3"	0.7	33.0
$5.1\frac{1}{8}$ , $4'0'$ , $5'6'$ , $3'8'$ , $5'4\frac{1}{4}$ , $2'0'$ , $3'0'$ , $3'0'$ , $6'4\frac{1}{4}$ , $5'0'$ , $6'0'$ , $4'0'$ , $5'10\frac{1}{8}$ , $2'0'$ , $3'0'$ , $3'0'$ , $3'0'$ , $7'6\frac{1}{8}$ , $6'0'$ , $6'6'$ , $4'4'$ , $6'4\frac{1}{2}$ , $2'0'$ , $3'0'$ , $3'0'$ , $3'0'$ , $9'11\frac{3}{8}$ , $8'0'$ , $7'0'$ , $7'0'$ , $4'8'$ , $6'10\frac{3}{8}$ , $2'0'$ , $3'0'$ , $3'0'$ , $3'0'$ , $11'1\frac{1}{4}$ , $9'0'$ , $8'0'$ , $5'4''$ , $7'10\frac{1}{8}$ , $2'0'$ , $3'0'$ , $3'0'$ , $3'0'$ , $11'1\frac{1}{4}$ , $9'0'$ , $8'0'$ , $5'4''$ , $7'10\frac{1}{8}$ , $2'0'$ , $3'0'$ , $3'0'$ , $3'0'$ , $11'1\frac{1}{4}$ , $12'0'$ , $14'3\frac{1}{4}$ , $6'0'$ , $14'0'$ , $3'0'$ , $6'0'$ , $13'0'$ , $6'0'$ , $18'4^{\frac{3}{4}}$ , $16'3\frac{1}{4}$ , $6'8''$ , $16'0'$ , $3'0'$ , $6'0'$ , $10'0'$ , $6'0'$ , $10'0'$ , $6'0'$ , $10'0'$ , $6'0'$ , $11'0'$ , $11'0'$	30″	$4'6\frac{5}{4}''$	3,6"	5'4 <u>1</u> "	3′6¾″	2,3"	2'0"	3.0"	3.0"	0.6,	0'3"	0.2"	0'3"	8.0	41.0
$64\frac{1}{8}$ $5'0''$ $6'0''$ $4'0''$ $7'6\frac{5}{8}$ $8'9''$ $7'0''$ $7'0''$ $9'11\frac{3}{8}$ $8'0''$ $11'1\frac{1}{4}$ $9'0''$ $8'0''$ $15'7\frac{1}{4}$ $12'0''$ $14'3\frac{1}{4}$ $6'0''$ $14'0''$ $25'0''$ $3'0'''$ $3'0'''$ $3'0'''$ $3'0'''$ $3'0''''$ $3'0'''''$ $3'0''''''''''''''''''''''''''''$	3,0"	$5'1\frac{i}{8}''$	4.0″	2,6"	3′8″	$5'4\frac{3}{4}"$	2′0″	3.0,,	3'0"	0,6	0'3"	0.2"	0'3"	1.0	50.0
7.6 $\frac{8}{8}$ , 6'0" 6'6" 4'4" 6'4 $\frac{1}{2}$ " 2'0" 3'0" 3'0" 8'9" 7'0" 7'0" 4'8" 6'10 $\frac{3}{8}$ , 2'0" 3'0" 3'0" 3'0" 11'1 $\frac{3}{4}$ , 8'0" 7'6" 5'0" 7'4 $\frac{1}{4}$ , 2'0" 3'0" 3'0" 3'0" 15'7 $\frac{1}{4}$ , 12'0" 14'3 $\frac{1}{4}$ , 6'0" 14'0" 3'0" 6'0" 4'0" 18'4 $\frac{3}{4}$ , 16'3" 6'8" 16'0" 3'0" 6'0" 10'0" 6'0" 3'0" 25'0" 18'4" 25'6" 9'4" 25'0" 6'0" 12'0" 7'0" 3'0" 24'0" 25'6" 9'4" 25'0" 6'0" 13'0" 7'0" 8'0" 5'0" 15'0" 10'0" 6'0" 13'0" 7'0" 5'0" 10'0" 6'0" 14'0" 7'0" 5'0" 15'0" 15'0" 7'0" 10'0"	4,0,,	$6'4^{\frac{1}{4}}$ "	2.0,	.0.9	4.0"	$5'10\frac{5}{8}"$	2'0"	3.0"	3'0"	.,6,0	0'3"	0.5"	0.3"	1.3	0.89
8'9" 7'0" 7'0" 4'8" $6'10\frac{3}{8}$ " 2'0" 3'0" 3'0" 3'0" $9'11\frac{3}{8}$ " 8'0" 7'6" 5'0" $7'4\frac{1}{4}$ " 2'0" 3'0" 3'0" 3'0" 11'1 $\frac{1}{4}$ " 9'0" 8'0" 5'4" $7'10\frac{1}{8}$ " 2'0" 3'0" 3'0" 3'0" 2'0" 3'0" $15'7\frac{1}{4}$ " 12'0" 14'3 $\frac{1}{4}$ " 6'0" 14'0" 3'0" 6'0" 10'0" 6'0" 25'0" 18'4" 25'6" 7'8" 25'0" 6'0" 12'0" 7'0" 3'0" 29'4" 25'6" 11'0" 25'0" 6'0" 13'0" 7'0" 5'0" 20'4" 27'6 $\frac{1}{4}$ " 12'8" 26'0" 6'0" 13'0" 7'0" 5'0" 5'0" 16'0" 17'0" 5'0" 10'0" 6'0" 14'0" 7'0" 6'0" 16'0" 16'0" 7'0" 6'0" 16'0" 16'0" 7'0" 6'0" 16'0" 7'0" 6'0" 16'0" 7'0" 6'0" 16'0" 7'0" 6'0" 16'0" 7'0" 6'0" 16'0" 7'0" 6'0" 16'0" 7'0" 6'0" 16'0" 7'0" 6'0" 16'0" 7'0" 6'0" 16'0" 7'0" 6'0" 16'0" 7'0" 6'0" 16'0" 7'0" 6'0" 16'0" 7'0" 6'0" 16'0" 7'0" 6'0" 16'0" 7'0" 6'0" 16'0" 7'0" 6'0" 16'0" 7'0" 6'0" 16'0" 7'0" 6'0" 16'0" 7'0" 6'0" 7'0" 6'0" 16'0" 7'0" 6'0" 7'0" 6'0" 7'0" 7'0" 6'0" 7'0" 7'0" 6'0" 7'0" 7'0" 6'0" 7'0" 7'0" 6'0" 7'0" 7'0" 6'0" 7'0" 7'0" 6'0" 7'0" 7'0" 6'0" 7'0" 7'0" 6'0" 7'0" 7'0" 6'0" 7'0" 7'0" 6'0" 7'0" 7'0" 6'0" 7'0" 7'0" 6'0" 7'0" 7'0" 6'0" 7'0" 7'0" 7'0" 7'0" 7'0" 7'0" 7'0" 7	5'0"	$7'6\frac{2}{8}''$	,0,9	.9,9	4,4"	$6'4\frac{1}{2}''$	2'0"	3.0"	3'0"	.6.0	0'3"	0.2"	0'3"	2.2	86.0
$\begin{array}{cccccccccccccccccccccccccccccccccccc$	,0,9	% <sub>,</sub>	7.0,,	7.0"	4′8″	$6'10^{\frac{3}{8}''}$	2'0"	3.0"	3.0"	,6,0	0'3"	0.2"	0.3"	2.6	104.0
$\begin{array}{cccccccccccccccccccccccccccccccccccc$	7.0,,	$9'11\frac{3}{8}''$	8,0,,	1.6"	2.0"	$7'4^{\frac{1}{4}''}$	2'0"	3'0"	3'0"	.6.0	0'3"	0.2"	0.3"	4.1	121.0
$157\frac{1}{4}$ 12'0" 14'3\frac{1}{4}\$ 6'0" 14'0" 3'0" 6'0" 4'0" 18'4\frac{3}{4}\$ 6'8" 16'0" 3'0" 8'0" 5'0" 5'0" 5'0" 5'0" 5'0" 5'0" 5'0" 5	8.0″	$11'1\frac{1}{4}''$	9.0″	8.0″	5'4"	$7'10^{\frac{1}{8}''}$	2'0"	3'0"	3'0"	.6.0	0'3"	0.2"	0,3"	4.6	140.0
$184_{4}^{5}$ $1484_{4}^{5}$ $1478''$ $16.3_{4}^{3}$ $6.8''$ $16.0''$ $3.0''$ $30.0''$ $24.0''$ $25.6''$ $4.0''$ $10.0''$ $6.0''$ $12.0''$ $7.0''$ $35.0''$ $40.4_{4}^{5}$ $35.0''$ $25.6''$ $40.4_{4}^{5}$ $10.0''$ $7.0''$ $40.4_{4}^{5}$ $10.0''$ $7.0''$ $40.4_{4}^{5}$ $10.0''$ $10.$	10′0″	$15'7\frac{1}{4}''$	12'0"	$14'3^{\frac{1}{4}}$ "	,0,9	14'0'	3.0"	.0,9	4,0,	$1'1^{\frac{1}{2}''}$	.9.0	1.0″	0,6,	0.9	200.0
$25.0''$ $18'4''$ $25'6''$ $7'8''$ $25'0''$ $4'0''$ $10'0''$ $6'0''$ $30'0''$ $24'0'$ $25'6''$ $9'4''$ $25'0''$ $6'0''$ $12'0''$ $7'0''$ $40'4\frac{1}{4}$ $34'8''$ $26'6\frac{1}{4}$ $11'0''$ $25'0''$ $6'0''$ $13'0''$ $7'0''$ $50'0\frac{1}{2}$ $45'4''$ $27'6\frac{1}{2}$ $16'0''$ $27'0''$ $6'0''$ $16'0''$ $7'0''$ $6'0''$ $16'0''$ $7'0''$	12'0"	$18'4\frac{5}{4}''$	14'8"	$16'3^{\frac{3}{4}''}$	,,8,9	16.0"	3'0"	8'0"	5'0"	$1'1^{\frac{1}{2}''}$	.9,0	1.0"	0.6	8.0	350.0
$30.0$ " $24'0$ " $25'6$ " $9'4$ " $25'0$ " $6'0$ " $12'0$ " $7'0$ " $35'0$ " $29'4$ " $25'6$ " $11'0$ " $25'0$ " $6'0$ " $13'0$ " $7'0$ " $40'4\frac{3}{4}$ " $34'8$ " $26'6\frac{1}{4}$ " $12'8$ " $26'0$ " $6'0$ " $14'0$ " $7'0$ " $50'9\frac{1}{2}$ " $45'4$ " $27'6\frac{1}{4}$ " $16'0$ " $27'0$ " $6'0$ " $16'0$ " $17'0$ " $6'0$ " $16'0$ " $17'0$ "	15'0"	25'0"	18'4"	25'6"	7.8"	25'0"	4'0"	10'0'	.0,9	1,6"	0,6,	1.0"	0,6,	8.0	0.009
$35.0''$ $29'4''$ $25'6''$ $11'0''$ $25'0''$ $6'0''$ $13'0''$ $7'0''$ $40'4\frac{1}{4}''$ $34'8''$ $26'6\frac{1}{4}''$ $12'8''$ $26'0''$ $6'0''$ $14'0''$ $7'0''$ $50'9\frac{1}{2}''$ $45'4''$ $27'6\frac{1}{2}''$ $16'0''$ $27'0''$ $6'0''$ $16'0''$ $7'0''$ $6'0''$ $16'0''$ $17'0''$	20'0"	30'0"	24'0"	25'6"	9'4"	25'0"	.0,9	12'0"	7.0"	2'3"	1'0"	1.0,	0.6	10.0	1000.0
$40^{4}4^{2}$ $34^{8}$ $26^{6}4^{2}$ $12^{8}$ $26^{6}0^{2}$ $6^{6}$ $14^{4}$ $7^{6}$ $50^{9}4^{2}$ $45^{4}$ $27^{6}4^{2}$ $16^{6}$ $16^{6}$ $27^{6}$ $6^{6}$ $16^{6}$ $16^{6}$ $7^{6}$ $20^{6}$	25'0"	35'0"	29′4″	25'6"	11'0"	25'0"	,0,9	13'0"	7.0"	2'3"	1,0,,	1.0″	.6.0	15.0	1200.0
$50'9^{\frac{1}{2}}$ $45'4''$ $27'6^{\frac{1}{2}}$ $16'0''$ $27'0''$ $6'0''$ $16'0''$ $7'0''$	30′0″	40'4 <u>÷</u> "	34'8"	26'64"	12′8″	26'0"	,0,9	14'0'	7.0′	2'3"	1'0"	1.0"	0.6,	15.0	1500.0
" " " " " " " " " " " " " " " " " " "	40′0″	$50.9\frac{1}{2}$ "	45'4"	$27'6\frac{1}{2}''$	16'0"	27'0"	,0,9	16'0''	7.0"	2'3"	1.0″	1'0"	0.6,	20.0	2000.0
$0.05_2$ $0.05$ $2/10^2$ $0.07$ $0.07$ $0.07$	20.0″	$\frac{5}{2}$ , $\frac{5}{2}$ , $\frac{5}{2}$	.8,95	$27'6\frac{1}{2}''$	19′4″	27'0"	,0,9	20'0"	7.0"	2'3"	1.0"	1'0"	0.6	25.0	3000.0

<sup>4</sup>1 in. = 2.54 cm; 1 ft = 0.3048 m; 1 ft<sup>3</sup>/s = 28.32 liters/s.

**TABLE 4.2** FREE-FLOW AND SUBMERGED-FLOW COEFFICIENTS AND EXPONENTS FOR PARSHALL FLUMES

$W^{a}$	$C_f$	$C_1$	$C_2$	$n_f$	$n_s$	$S_{i}$
1"	0.338	0.299	0.0044	1.55	1.000	0.56
2"	0.676	0.612	0.0044	1.55	1.000	0.61
3"	0.992	0.915	0.0044	1.55	1.000	0.64
6"	2.06	1.66	0.0044	1.58	1.080	0.55
9"	3.07	2.51	0.0044	1.53	1.060	0.63
12"	4.00	3.11	0.0044	1.52	1.080	0.62
18"	6.00	4.42	0.0044	1.54	1.115	0.64
24"	8.00	5.94	0.0044	1.55	1.140	0.66
30"	10.00	7.22	0.0044	1.555	1.150	0.67
3'	12.00	8.60	0.0044	1.56	1.160	0.68
4'	16.00	11.10	0.0044	1.57	1.185	0.70
5′	20.00	13.55	0.0044	1.58	1.205	0.72
6'	24.00	15.85	0.0044	1.59	1.230	0.74
7'	28.00	18.15	0.0044	1.60	1.250	0.76
8′	32.00	20.40	0.0044	1.60	1.260	0.78
10'	40.13	24.79	0.0044	1.59	1.275	0.80
12'	47.50	29.34	0.0044	1.59	1.275	0.80
15'	58.56	36.17	0.0044	1.59	1.275	0.80
20'	77.00	47.56	0.0044	1.59	1.275	0.80
25'	95.44	58.95	0.0044	1.59	1.275	0.80
30'	113.88	70.34	0.0044	1.59	1.275	0.80
40'	150.75	93.11	0.0044	1.59	1.275	0.80
50'	187.63	115.89	0.0044	1.59	1.275	0.80

<sup>&</sup>lt;sup>a</sup>English units are utilized to be consistent with the original equipment development.

intermediate in size to those tested can be interpolated and have been shown to be within a degree of accuracy suitable for field use (Skogerboe et al., 1972, 1973).

The cutthroat flume was developed to operate satisfactorily under both freeflow and submerged-flow conditions based on previous studies by Robinson and Chamberlain (1960) and Hyatt (1965). The advantages of a level flume floor, as opposed to the inclined floor in the throat and exit sections of the Parshall flume, are: (1) ease of construction, (2) the flume can be placed inside a concrete-lined channel, and (3) the flume can be placed on the channel bed.

Earlier studies regarding the length of the throat section in flow-measuring flumes, discussed by Skogerboe et al. (1967b), showed that flow depths measured in the exit section of a flume resulted in more accurate submerged flow ratings than calibrations employing flow-depth measurements in the throat section. Consequently, there appeared to be no apparent advantage in having a throat section. In fact, one distinct hydraulic advantage of removing the throat section was the improved flow conditions in the exit section. The rectangular flat-bottomed flume, which resulted from the testing program, is illustrated in Fig. 4.3. Since the flume has no throat section (zero throat length), the flume was given the name "cutthroat" by the developers (Skogerboe et al., 1967a).

Source: From Skogerboe et al. (1967c).

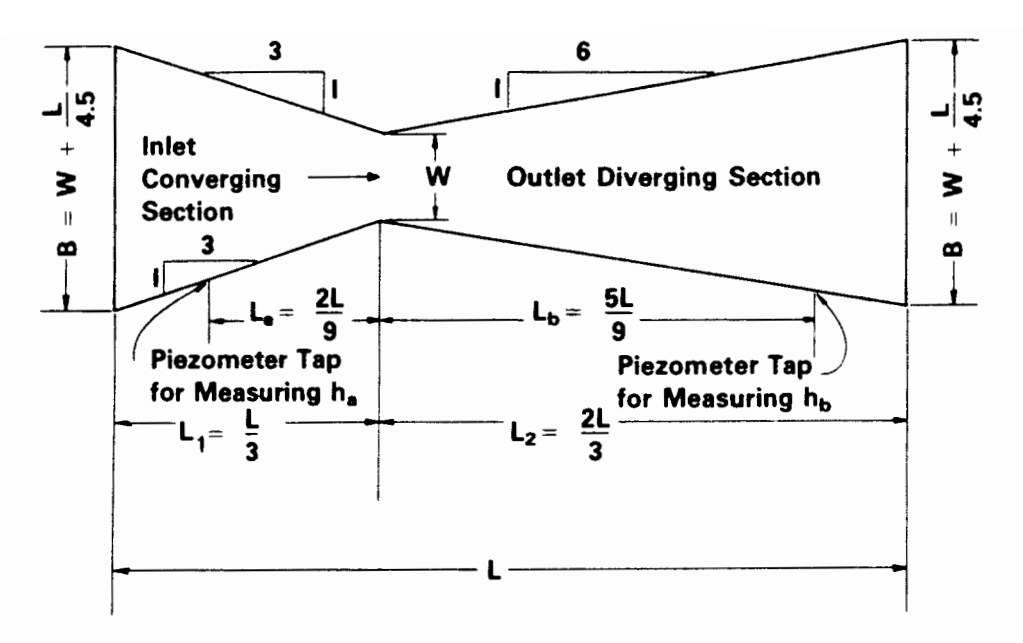


Figure 4.3 Definition sketch of a cutthroat flume.

The free-flow equation for cutthroat flumes can be described by Eq. 4.4, where  $Q_f$  is the flow rate in cubic feet per second. The value of  $n_f$  was found to be dependent only on the flume length, as shown in Fig. 4.4.

The value of the free-flow coefficient,  $C_f$ , is a function of both flume length and throat width:

$$C_f = K_f W^{1.025} (4.6)$$

where

 $C_f$  = free-flow coefficient

 $K_f$  = flume length coefficient, ft (Fig. 4.4)

W =throat width, ft

For accurate discharge measurements, the recommended ratio of flow depth to flume length  $(h_u/L)$  should be equal to or less than 0.33, with increasing values of this ratio resulting in greater inaccuracies because of higher approach velocities and a more rapidly changing water surface profile at the flume cross section where  $h_u$  is measured.

For submerged flow analyses, Eq. 4.5 is also applied to the cutthroat flume. However, the coefficient  $C_2$  is generally neglected. The value of  $n_s$  was found to be dependent only on the flume length, and therefore, like  $n_f$ , can be obtained for any flume length between 1.5 and 9 ft simply by reading the value from the graph in Fig. 4.4. The submerged coefficient,  $K_s$ , and the transition submergence,  $S_t$ , are also plotted in Fig. 4.4. This allows computation of the submerged-flow coefficient as follows:

$$C_s = K_s W^{1.025} (4.7)$$

At high values of submergence (above 95%), small errors in reading  $h_u$  and  $h_d$  result in significant errors in calculating the discharge. Thus, as the submergence is increased above 95%, the discharge error becomes greater, and flumes are not very reliable.

Flow Measurement

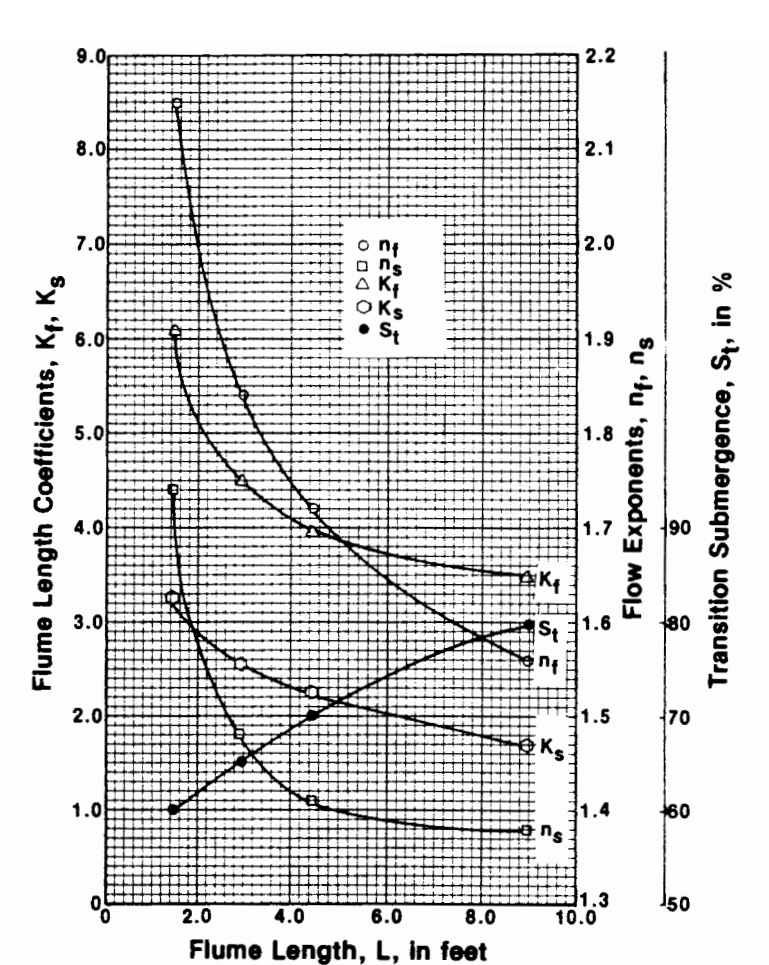


**Figure 4.4** Generalized free-flow and submerged-flow coefficients and exponents and *S*, for cutthroat flumes.

**Trapezoidal flumes.** The American Society of Agricultural Engineers (ASAE) Standard S359.1, "Trapezoidal Flumes for Irrigation Flow Measurement," presents calibrations for many sizes of trapezoidal flumes. Only four standard calibrated trapezoidal flow measuring flumes will be presented herein. The reader should consult ASAE (1980–1981) for details regarding 30 standard parallel-flow trapezoidal measuring flumes for use with standard ASAE S289, "Concrete Slip-Form Canal and Ditch Linings." In addition, an analysis from Replogle (1975) will be described in which a more generalized trapezoidal measuring configuration can be employed.

For the four experimentally developed and calibrated flumes, 1, 2, 3, and 4, the essential flume dimensions are identified by a code containing the throat cross section and the approach cross section, both of which are described by the floor width and sidewall slopes (Fig. 4.5 and Table 4.3). Thus flume 1 is designated by 0.4 (1:1) - 1.0 (1:1), meaning that the throat floor width,  $b_3$ , is 0.4 ft with wall slopes of 1:1, and the approach floor width,  $b_1$ , is 1.0 ft with wall slopes of 1:1.

Recommended standard calibrated flumes 1 and 2 are designed for use with two commonly used concrete-lined ditch sections as listed in ASAE Standard S289. Flumes 3 and 4 are recommended primarily for use in unlined channels. Flume 4 has a zero-width throat section and is intended for measuring small flow rates, such as in individual furrows.

Trapezoidal flumes measure discharge with an accuracy of 5% under freeflow conditions. The discharge accuracy is dependent on the tolerances in con-

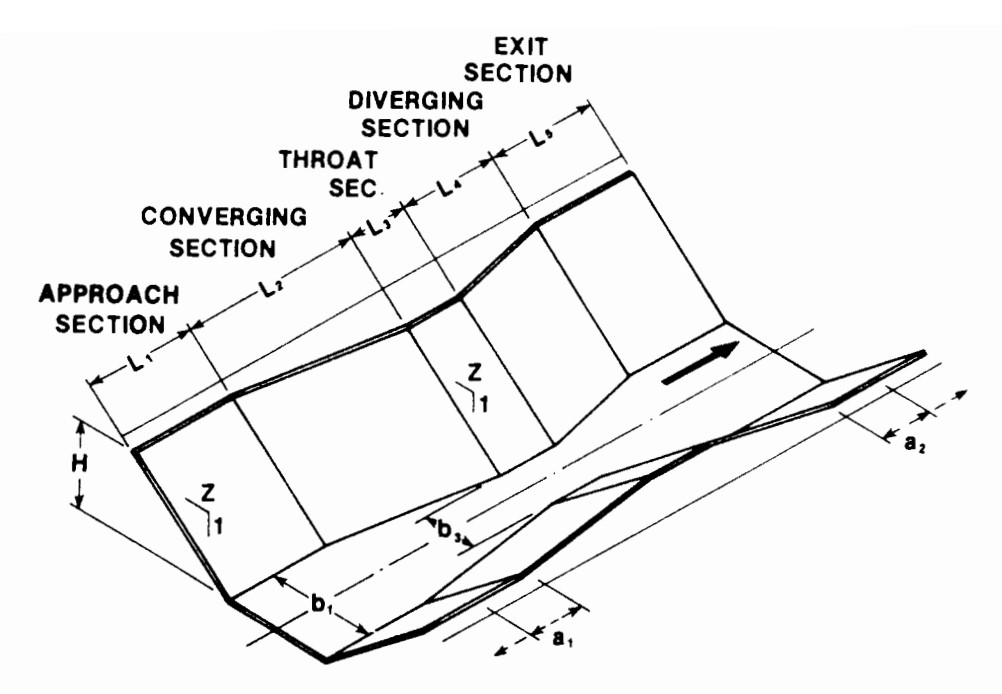


**Figure 4.5** Typical standard calibrated trapezoidal flume. (From American Society of Agricultural Engineers, 1980–1981.)

structing the throat section, accuracy of stage measurement  $(h_u \text{ and } h_d)$ , and proper installation. Dimensional deviations in flume construction will result in measurement errors approximately proportional to throat area errors. For flumes with a triangular throat section, discharge errors are approximately 2.5 times the error in stage reading. For flumes with vertical sidewalls (such as Parshall flumes and cutthroat flumes), discharge errors are approximately 1.5 times the error in stage reading. Thus for flumes having a trapezoidal throat section with a flat floor, the discharge error ranges between these two values.

The free-flow discharge,  $Q_f$ , equations for the four standard calibrated trapezoidal measuring flumes are listed in Fable 4.4. The upstream flow depth,  $h_u$ , is a vertical (stage) flow depth measured in the approach section at a distance  $a_1$  feet upstream from the converging section, as shown in Fig. 4.5 and listed in Table 4.3.

The submerged flow discharge,  $Q_s$ , can be obtained for flumes 1, 2, and 3 by using the discharge correction factors in Table 4.5. The downstream flow depth,  $h_d$ , is a vertical depth measured in the exit section at a distance  $a_2$  feet downstream from the diverging section, as shown in Fig. 4.5 and listed in Table 4.3. For submerged flow, the measured value of  $h_u$  is used in the free-flow discharge equation (Table 4.4) to obtain  $Q_f$ . Then from the calculated value of submergence, S, the discharge correction factor  $K_{sf}$  is obtained from Table 4.5. The submerged flow discharge,  $Q_s$ , is calculated from

$$Q_s = Q_f K_{sf} (4.8)$$

55

Another trapezoidal measuring flume is the 60° v-notch flume originally developed by Robinson and Chamberlain (1960). The Soil Conservation Service of the U.S. Department of Agriculture (USDA) has reported on the use of a small

TABLE 4.3 DIMENSIONS OF STANDARD CALIBRATED TRAPEZOIDAL MEASURING FLUMES (FEET)

	<b>a</b> 54	0.063	0.50	0.25	1
	a <sub>l</sub> a	0.146	0.50	0.25	0.125
	$L_{\varsigma}$	0.50	9.	0.50	0.25
	$L_4$	1.42	2.00	1.33	0.58
	$L_3$	1.00	2.50	1.67	0.58
	$L_2$	1.42	3.00	2.31	0.56
	$L_1$	1.25	2.00	1.50	0.58
	Н	1.33	3.00	2.31	0.56
	Z	1.00	1.25	0.58	0.58
	$p_{_3}$	0.40	1.0	0.67	1
	$p_1$	1.0	2.00	1.33	0.167
Designation	Approach section	-1.0(1:)	-2.0(1.25:1)	-1.33(0.58:1)	-0.17(0.58:1)
Desig	Throat section	0.4(1:)	1.00(1.25:1)	0.67(0.58:1)	0.0(0.58:1)
	No.	-	2	8	4

\*Distance to point of depth measurement,  $h_{n}$  and  $h_{d}$ . Source: American Society of Agricultural Engineers (1980–1981).

**TABLE 4.4** FREE-FLOW DISCHARGE EQUATIONS OF STANDARD CALIBRATED TRAPEZOIDAL MEASURING FLUMES

Flume no.	Equation	h <sub>u</sub> range (ft)	Calibrated flow range (cfs)
1	$Q_f = 3.23h_u^{2.5} + 0.63u_0^{1.5} + 0.050$	0.20-1.20	0.05-5.96
2	$Q_f = 4.27h_u^{2.5} + 1.67h_u^{1.5} + 0.19$	0.30 - 2.70	0.54-58.8
3	$Q_f = 1.46h_u^{2.5} + 2.22h_u^{1.5}$	0.20 - 2.20	0.24-17.4
4	$Q_f = 1.55h_u^{2.58}$	0.15 - 0.50	0.012-0.26

Source: American Society of Agricultural Engineers (1980-1981).

60° v-notch flume for measuring water in furrows (SCS, 1962). The free-flow ratings for these flumes vary somewhat by author. Trout (1983) recalibrated the flume shown in Fig. 4.6 and summarized the results against previous ratings and a theoretical model. The rating proposed by Trout (1983) is

$$Q = 0.249 (h_u - 0.15)^{2.61} (4.9)$$

where Q is the discharge in liters per minute,  $h_u$  is the gage reading in centimeters, and a 0.15-cm correction is made for meniscus distortion.

Modified broad-crested weir. Replogle (1975) introduced a compendium of critical depth hydraulics for the linear stream flow condition. The computational procedure was generalized for flumes or channel geometries of rather complex shape. Thus the ratings of the previously described trapezoidal flumes can be evaluated. Possibly the most significant contribution was the introduction of a simple broad-crested weir to the bottom of a trapezoidal canal section as shown in Fig. 4.7. The increased flow velocities found in concrete-lined irrigation canals had for some time complicated flow measurement in new or rehabilitated systems. In some cases, for instance, lining earthen channels to prevent seepage actually

**TABLE 4.5** EFFECT OF SUBMERGENCE ON THE DISCHARGE CORRECTION FACTOR  $(K_{sr})$  FOR STANDARD CALIBRATED TRAPEZOIDAL MEASURING FLUMES

Percent submergence		Discharge correction factor, $K_{sf} = Q_{s}/Q_{f}$			
$S = (h_d/h_a) \times 100$	Flumes 1 and 2	Flume 3			
70	0.993	1.000			
75	0.984	1.000			
80	0.970	0.996			
85	0.945	0.988			
90	0.902	0.972			
92	0.875	0.964			
94	0.838	0.953			
95	0.815	0.946			

Source: American Society of Agricultural Engineers (1980-1981).

Flow Measurement 57

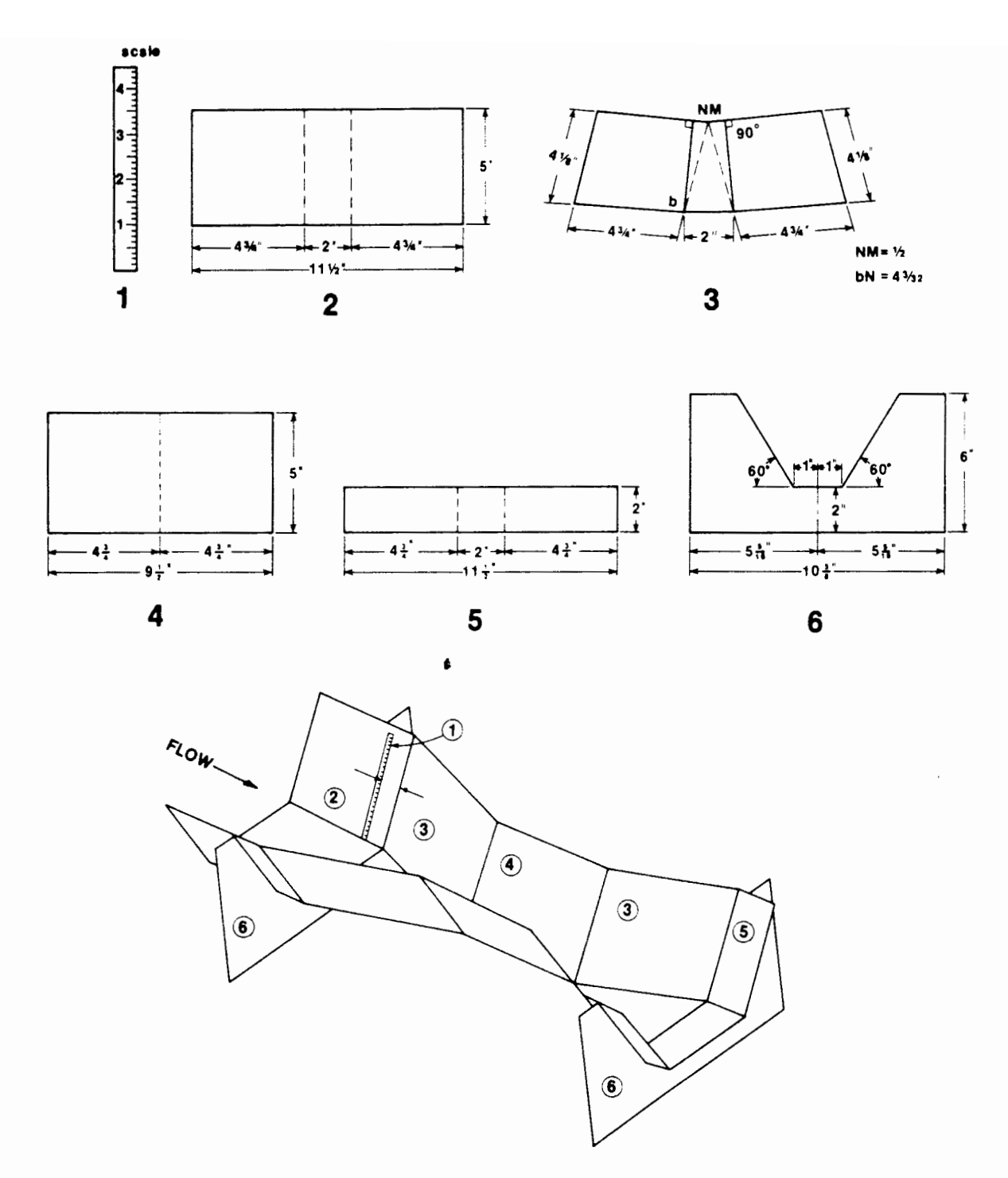


**Figure 4.6** Physical layout and dimensions of the small 60° V-notch flume. Scale is in inches. (From U.S. Department of Agriculture, Soil Conservation Service, 196?)

resulted in higher system losses due to complications with existing flow measurements.

Replogle and colleagues have developed some selected designs for commonly encountered conditions, but too few to cover the conditions in which one might use such a device. As a result, the mathematical rating and design procedure developed by Replogle (1975) will be repeated herein. The authors also feel that this review of hydraulic principles is useful. The discussion will, however, be

limited to the trapezoidal condition depicted in Fig. 4.7, and since Replogle has yet to name this measuring system, it will be referred to herein as the trapezoidal broad-crested weir. It is described in this section on flumes because of its hydraulic similarity.

The weir is divided into three sections: (1) the approach, (2) the transition, and (3) the critical-flow or throat section. It is assumed that somewhere in the throat the flow passes through critical depth, so that

$$Q = \left(\frac{gA_3^3}{\alpha_3 T_3}\right)^{.5} \tag{4.10}$$

where

 $Q = \text{discharge in m}^3/\text{s}$ 

 $g = acceleration of gravity, 9.807 \text{ m/s}^2$ 

 $A_3$  = cross-sectional flow area in m<sup>2</sup> (see Fig. 4.7).

$$A_3 = (b_3 + zy_3)y_3 (4.11)$$

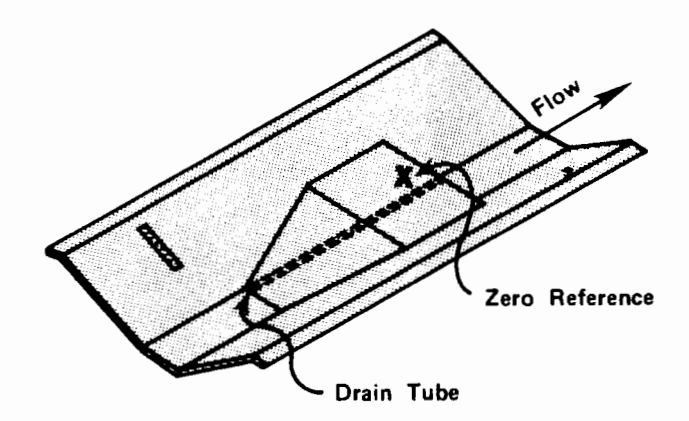
 $T_3$  = top width of the flow,

$$T_3 = b_3 + 2zy_3 \tag{4.12}$$

 $\alpha_3$  = energy distribution coefficient

The width of the trapezoidal base in the throat,  $b_3$ , and the flow depth,  $y_3$ , are measured in meters, while z is the trapezoidal side slope.

It is usually most practical to evaluate conditions in the approach section and relate these to discharge since the flow profile is more stable. The difference in



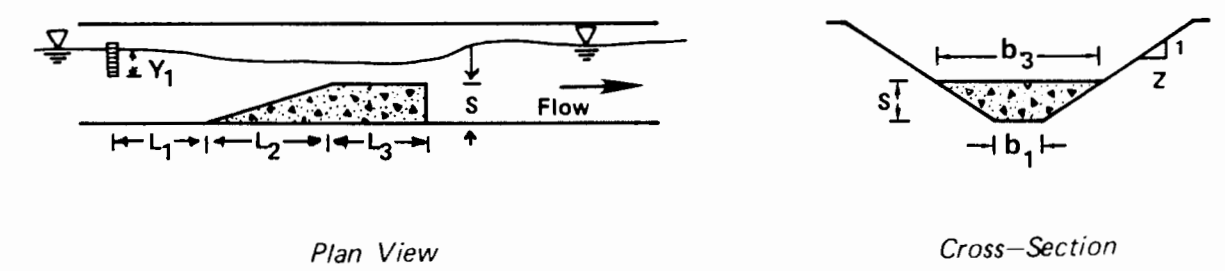


Figure 4.7 Definition sketch of trapezoidal broad-crested weir.

Flow Measurement 59

specific energy between the approach and critical section can be written and then rearranged as follows:

$$y_3 = y_1 + \frac{\alpha_1 Q^2}{2gA_1^2} - \frac{\alpha_3 Q^2}{2gA_3^2} - H_f \tag{4.13}$$

in which  $H_f$  is the friction loss between the two sections:

$$H_f = h_{f1} + h_{f2} + h_{f3} \tag{4.14}$$

Replogle (1975) presents a discussion of the theory allowing calculation of  $H_f$  in Eq. 4.13 based on the drag force, boundary layer analysis. This will not be repeated here. The friction losses in each section, using a drag force relation, are described by

$$h_{fi} = \frac{C_{fi} W P_i L_i Q^2}{2g A_i^3} \tag{4.15}$$

where  $C_{fi}$  is the drag coefficient associated with the *i*th section and WP<sub>i</sub> is the wetted perimeter m. For the approach section, the boundary layer is assumed to be a fully turbulent layer and  $C_{f1} = 0.00235$ . The drag coefficient for the transition section,  $C_{f2}$ , is also assumed to equal 0.00235. However, the wetted perimeter and area are more complex, due to the bottom and side convergence in the flow. Replogle (1975) rationalizes that the flow depth at the end of the transition section can be defined as

$$y_2 = y_3 + 0.625(y_1 - y_3) \tag{4.16}$$

The friction loss in the transition section is assumed to be based on the average loss rates defined at the section's inlet and exit, multiplied by its lengths,  $L_2$ .

Thus

$$h_{f_2} = \frac{0.00235 L_2 Q^2}{4g} \left( \frac{WP_1}{A_1^3} + \frac{WP_2}{A_2^3} \right)$$
 (4.17)

where

$$WP_2 = b_3 + 2y_1(1+z^2)^{0.5}$$
 (4.18)

$$A_2 = (b_3 + zy_2)y_2 (4.19)$$

$$WP_1 = b_1 + 2(y_1 + s)(1 + z^2)^{0.5}$$
 (4.20)

$$A_1 = (b_1 + (y_1 + s)z)(y_1 + s) \tag{4.21}$$

The drag coefficient for the throat section is more complicated because it is assumed that laminar flow exists in the throat section for a distance of  $X_c$  meters before the flow becomes turbulent. The computations necessary to compute  $C_{f3}$  are as follows. First, the kinematic viscosity of the water is determined enroute to computing both a laminar and turbulent Reynold's number:

$$\nu = \frac{0.0001655}{t^{0.09477}} - 0.0001 \tag{4.22}$$

where t is the water temperature in °F. For laminar flow the Reynold's number,  $R_L$ , is

$$R_L = \frac{QL_3}{A_3\nu} \tag{4.23}$$

The turbulent Reynold's number,  $R_c$ , is found from

$$R_c = 350,000 + \frac{L_3}{k} \tag{4.24}$$

in which k is the absolute roughness height for the surface of the flume. For typical concrete canal sections, k is about 0.0005 m.

If  $R_L$  is less than  $R_c$ , the drag coefficient for the throat section is

$$C_{f_3} = \frac{1.328}{R_L^{0.5}} \tag{4.25}$$

If, on the other hand,  $R_L$  is greater than  $R_c$ , estimation of  $C_{f3}$  proceeds as follows. First, the following expression is solved iteratively for  $C_1$ :

$$C_1 = \frac{0.544C_1^{0.5}}{5.61C_1^{0.5} - 0.638 - \ln\left[1/(R_L C_1) + k/(4.84C_1^{0.5} L_3)\right]}$$
(4.26)

Next,  $X_c$  is estimated from

$$X_c = \frac{R_c \nu A_3}{Q} \tag{4.27}$$

Then  $C_2$  is found using Eq. 4.26, by substituting  $X_c$  for  $L_3$ ,  $R_c$  for  $R_L$ , and  $C_2$  for  $C_1$ . Finally,

$$C_{f_3} = C_1 - \frac{R_c}{R_L} (C_2 - C_3) \tag{4.28}$$

The value of  $C_3$  in Eq. 4.28 is equal to  $C_{f3}$  found from Eq. 4.25.

The energy distribution coefficients are defined as

$$\alpha_1 = 1.04 \tag{4.29}$$

and

$$\alpha_3 = 1 + (3E^2 - 2E^3) \left( \frac{1.5WP_3}{T_3} - 0.5 \right) \left( \frac{0.025L_3WP_3}{A_3} - 0.05 \right)$$
 (4.30)

in which

$$E = 1.77C_1^{0.5} (4.31)$$

$$\frac{1.5\text{WP}_3}{T_3} - 0.5 < 2.0 \tag{4.32}$$

Flow Measurement

and

$$0 < \frac{.025L_3WP_3}{A_3} - 0.05 < 1.0 \tag{4.33}$$

The broad-crested weir rating must also be checked to ensure that free-flow conditions are maintained over the range of discharge the structure is designed to handle. The free flow-submerged flow transition submergence, called the "modular limit" by Bos et al. (1984), must be checked to ensure a free-flow design. The procedure follows. First, a reference section is established downstream of the structure at a distance  $L_4$  meters, where Bos et al. (1984) recommend that

$$L_4 = 10 \left( \frac{s + L_3}{2} \right) \tag{4.34}$$

Then Eq. 4.15 is used to calculate the friction losses over the distance  $L_3$  to  $L_4$ :

$$h_{f4} = \frac{0.00235 \text{WP}_4 L_4 Q^2}{2g A_4^3} \tag{4.35}$$

Next, the energy losses associated with the sudden expansion of the flow are determined:

$$h_k = \frac{1.2Q^2(1/A_3 - 1/A_4)^2}{2g} \tag{4.36}$$

Then the sill referenced energy at section 4 is determined by

$$H_4 = H_1 - H_f - h_{f4} - h_k \tag{4.37}$$

in which  $H_1$  is the sill referenced energy at the inlet gage:

$$H_1 = y_1 + \frac{Q^2}{2gA_1^2} \tag{4.38}$$

and  $H_f$  represents the energy losses from the inlet gage to the critical section computed earlier.

The modular limit is

$$ML = \frac{H_4}{H_1} \tag{4.39}$$

Solution of Eqs. 4.10 to 4.39 is a trial-and-error procedure. Bos et al. (1984) present a FORTRAN computer code that can be used to predict the flow ratings of the broad-crested weir configured in Fig. 4.7 as well as similar structures. Essentially, the procedure begins with the definition of the channel and weir geometry  $(L_1, L_2, L_3, s, b_1, z)$ , material roughness (k), the water temperature (t), and the upstream vertical gage reading  $(y_1)$  for which a flow rate is to be calculated. Values of  $\alpha_1$ ,  $\alpha_3$ , and  $H_f$  are initialized and Eqs. 4.10 and 4.13 are solved for values of Q and  $Q_3$ . Then Eqs. 4.14 to 4.28 are used to refine the estimate of  $Q_3$  and  $Q_4$  and Eqs. 4.29 to 4.33 to define  $Q_4$  and  $Q_4$  and  $Q_5$ . The procedure is to repeat these two basic steps until they have converged on  $Q_5$ . Finally, Eqs. 4.34 to 4.39 are iteratively solved

to find the modular limit or transition submergences and should not exceed about 0.90.

**H flumes.** Holtan et al. (1962) report on the earlier development of HS, H, and HL flumes for measuring open-channel discharges (Fig. 4.8). The designations S and L refer to small and large discharge capacities. These flumes were

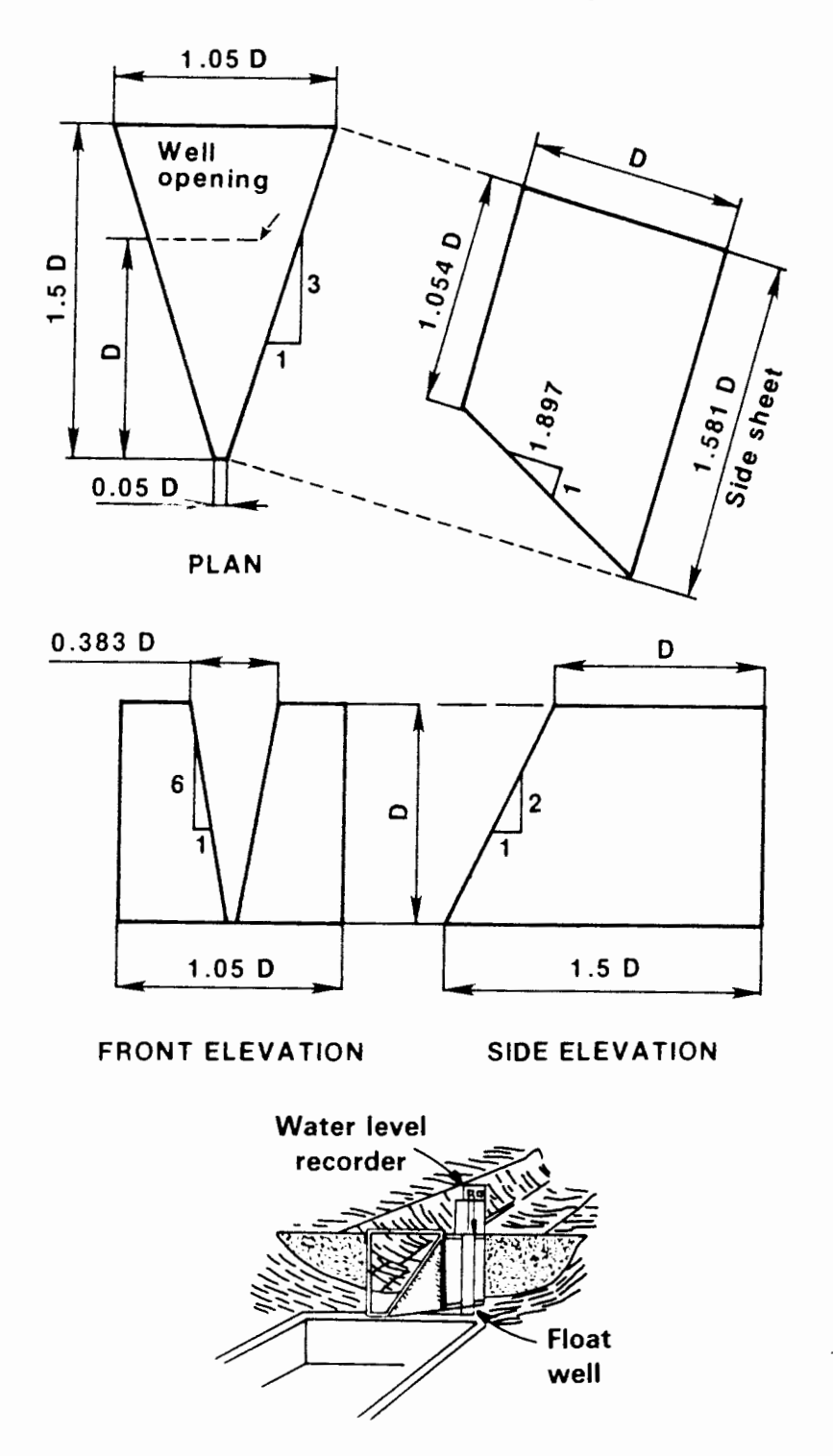


Figure 4.8 Physical layout of the HS flume. (After Holtan et al., 1962.)

TABLE 4.6 CHARACTERISTICS OF FOUR HS FLUMES

Flume depth.  D (cm)	Max. Q (liters s)	A	В	С
12.2	2.27	-0.4361	2.5151	0.1379
18.3	6.14	-0.4430	2.4908	0.1657
24.4	12.7	-0.4410	2.4571	0.1762
30.5	22.3	-0.4382	2.4193	0.1790

1 liter's = 15.851 gal/min.

Source: From Bos (1976).

developed primarily for measuring runoff on agricultural watersheds, but they are also useful for measuring furrow flows in irrigated agriculture.

Free-flow ratings for various sizes of H flumes can be described by (Bos, 1976)

$$\log Q = A + B \log h_u + C(\log h_u)^2 \tag{4.40}$$

in which Q is the discharge in  $m^3/s$  and  $h_u$  is the gage reading in meters. Table 4.6 gives the values of A, B, and C for four of the small (HS) H flumes

The location for measuring the upstream flow depth,  $h_u$ , is shown in Fig. 4.8 as a distance 0.5D downstream from the entrance to the HS flume. A piezometer tap should be constructed just above the flume floor. A rectangular approach channel is required that has a width of  $1.05\ D$  for HS flumes and a minimum length of  $2\ D$ .

#### Weirs

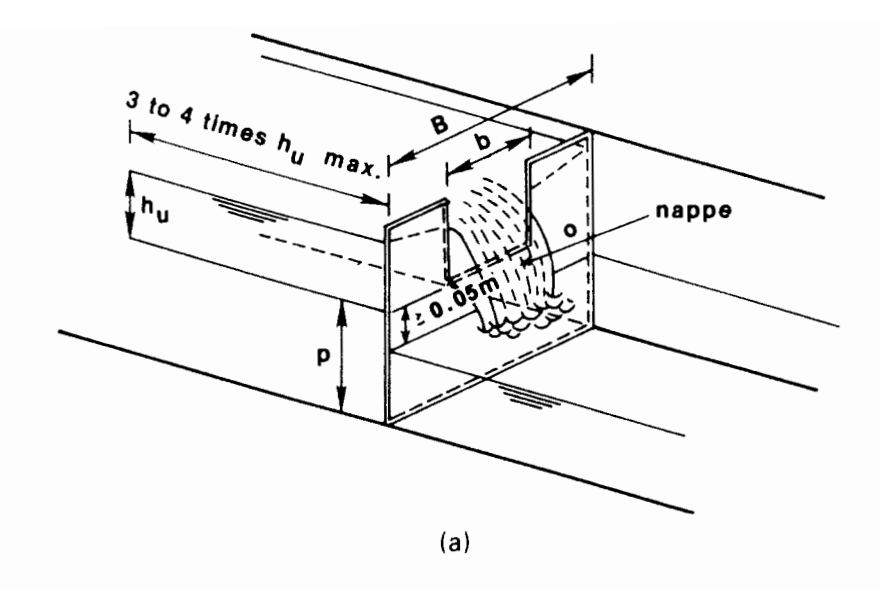
Weir structures are commonly encountered in irrigation systems, most frequently at check structures in the water delivery network. The greatest disadvantage in using weirs for discharge measurements in an irrigation system is the amount of head required, particularly for free-flow operation. However, weir structures tend to provide more accurate discharge ratings than flumes and orifices.

There are some excellent references on weirs, such as the U.S. Bureau of Reclamation (USBR, 1974), Bos (1976) and the book by Ackers et al. (1978). In this book, only two types of weir structures will be presented, a rectangular thin-plate weir and a thin-plate V-notch weir.

Rectangular thin-plate weirs. Kindsvater and Carter (1957) made extensive laboratory studies in order to develop highly accurate free-flow discharge ratings for rectangular thin-plate weirs. A definition sketch is shown in Fig. 4.9. The free-flow discharge equation is

$$Q_f = \frac{2}{3} (2g)^{0.5} C_e b_e h_e^{1.5}$$

$$= 2.9524 C_e b_e h_e^{1.5}$$
(4.41)



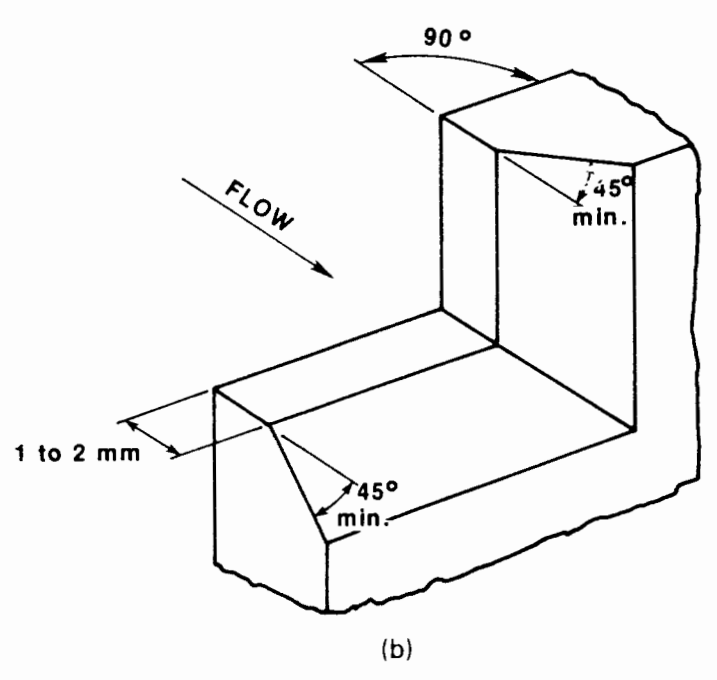


Figure 4.9 Definition sketch of a rectangular thin-plate weir. (a) Rectangular sharp-crested weir (thin-plate weir). (b) Enlarged view of crest and side of rectangular sharp-crested weir. (From Bos, 1976.)

where

 $Q_f = \text{flow, m}^3/\text{s}$ 

 $C_e$  = effective free-flow discharge coefficient

 $b_e$  = effective width of the constriction, m

 $h_e$  = effective head, m

The effective free-flow discharge coefficient,  $C_e$ , is a function of the ratios b/B and  $h_u/p$ , which can be determined graphically from Fig. 4.10, the units are again meters. The effective constriction width,  $b_e$ , is given by

$$b_{\epsilon} = b + K_b \tag{4.42}$$

The relationship between  $K_b$  and the constriction ratio, b/B, is presented in Fig. 4.11. Finally, the effective head,  $h_e$ , is given by

$$h_e = h_u + K_h \tag{4.43}$$

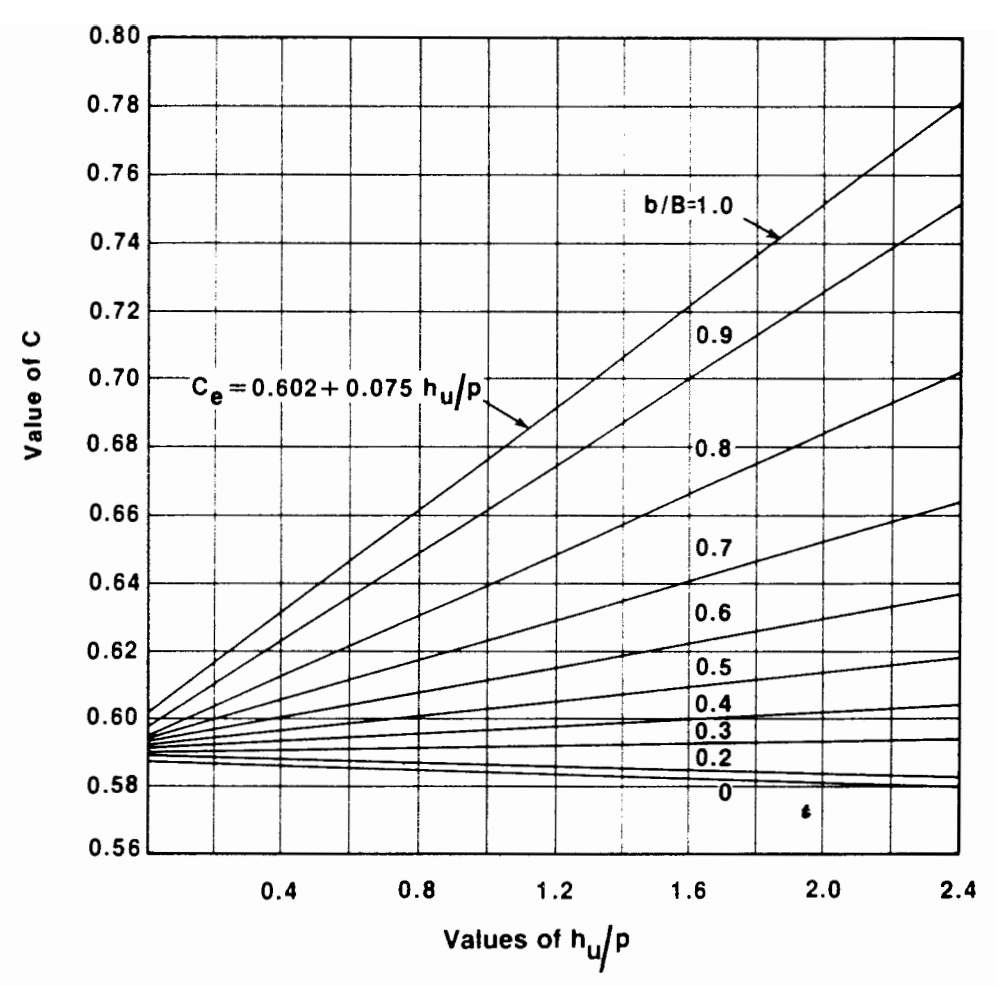


**Figure 4.10** Effective free-flow discharge coefficient,  $C_e$ , as a function of the constriction ratio, b B, and weir height ratio,  $h_a/p$ , for rectangular thin-plate weirs. (Reprinted from Kindsvater and Carter, 1957, with permission of ASCE.)

in which  $h_u$  is in meters and where a constant value of  $K_h = 0.001$  m is recommended.

**V-notch weirs.** All other things being equal, the most accurate open-channel constriction for measuring discharge is the V-notch weir (Fig. 4.12). Some of the most notable research on the hydraulics of weirs occurred at the Georgia Institute of Technology (Kindsvater and Carter, 1957; Shen, 1981). These workers found that much of the earlier research on V-notch weirs coincided with their results. As a consequence, a high degree of reliability can be placed on the discharge ratings.

Shen (1981) presented the generalized discharge equation for V-notch weirs in the following form (the units are the same as for Eq. 4.41):

$$Q_f = \frac{8}{15} (2g)^{0.5} C_e \tan \frac{\theta}{2} h_e^{2.5}$$

$$= 2.3619 C_e \tan \frac{\theta}{2} h_e^{2.5}$$
(4.44)

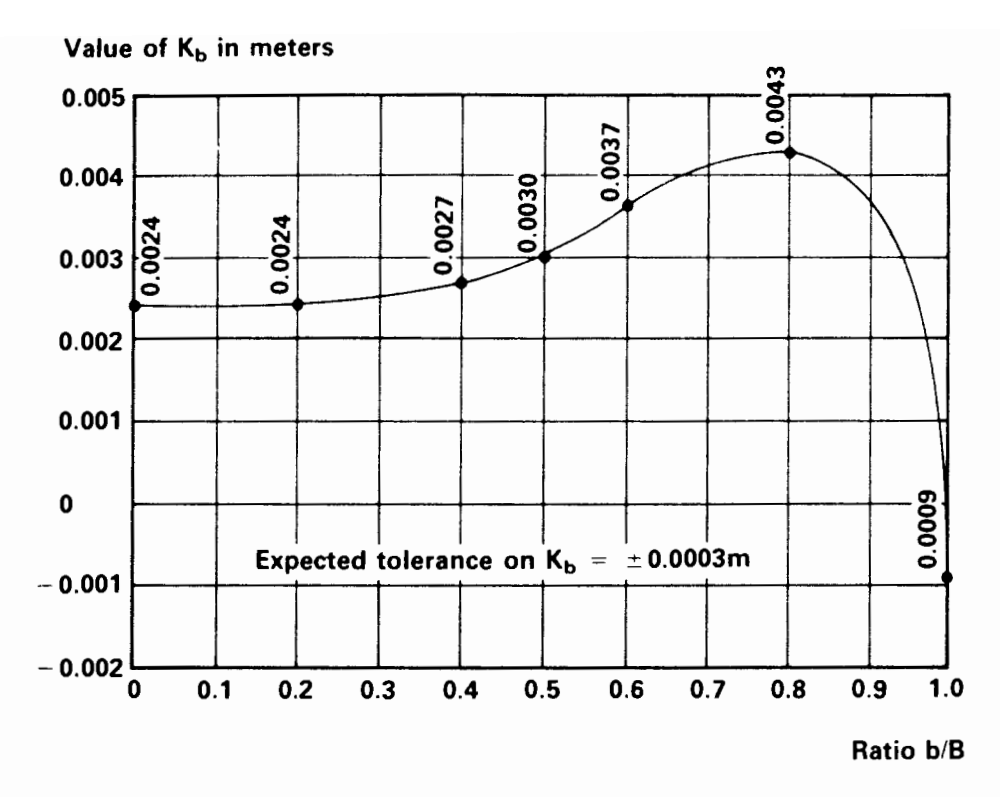


**Figure 4.11** Relationship between the constriction width correction,  $K_b$ , and the constriction ratio, b B, for rectangular thin-plate weirs. (Reprinted from Kindsvater and Carter, 1957, with permission of ASCE.)

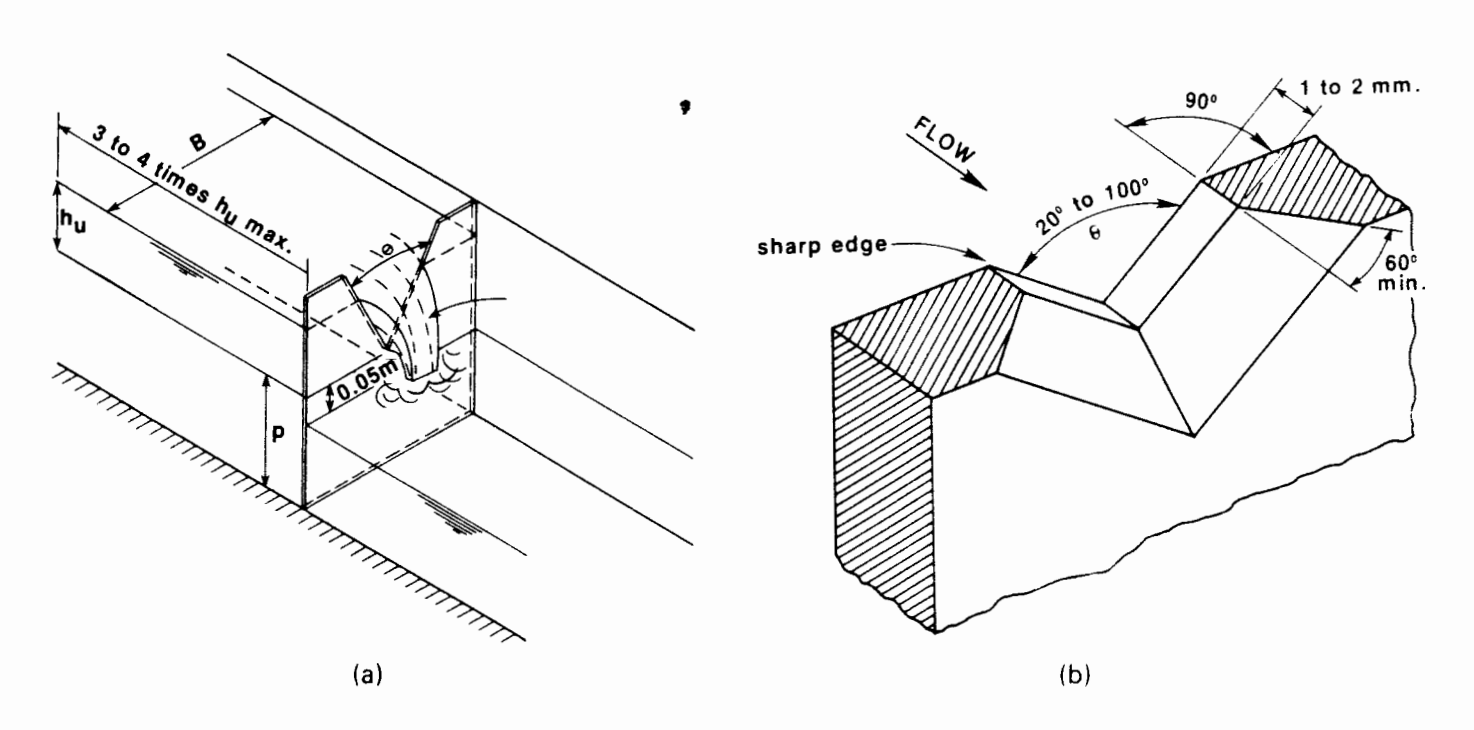
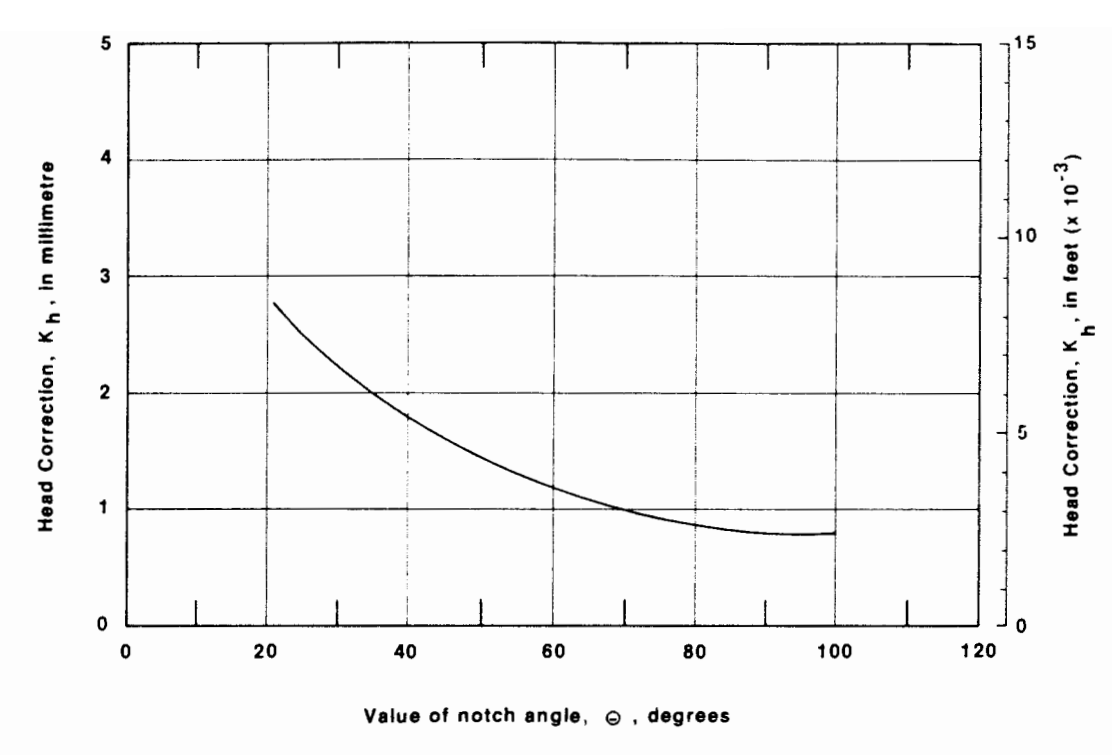


Figure 4.12 Definition sketch of a V-notch weir. (a) V-notch sharp-crested weir. (b) Enlarged view of a V-notch. (From Bos, 1976.)

Flow Measurement 67



**Figure 4.13** Head correction as a function of the notch angle,  $\theta$ , for V-notch weirs. (From Shen, 1981.)

where  $\theta$  is the central angle of the notch. The parameter  $K_h$  can be obtained from Fig. 4.13, and  $C_e$  is obtained from Fig. 4.14. Both  $K_h$  and  $C_e$  are dependent only on the notch angle,  $\theta$ , as long as

$$\frac{h_u}{p} \le 0.4 \tag{4.45}$$

$$\frac{p}{B} \le 0.2 \tag{4.46}$$

When a V-notch weir has been fabricated, the central angle,  $\theta$ , can easily be determined by measuring the top width and the vertical depth of the notch. The term tan  $(\theta/2)$  is equal to half the top width divided by the vertical depth to the notch.

## **Orifices**

Any type of opening in which the upstream water level is higher than the top of the opening is referred to as an orifice. In this case, if the jet of water emanating from the orifice discharges freely into the air or downstream channel without

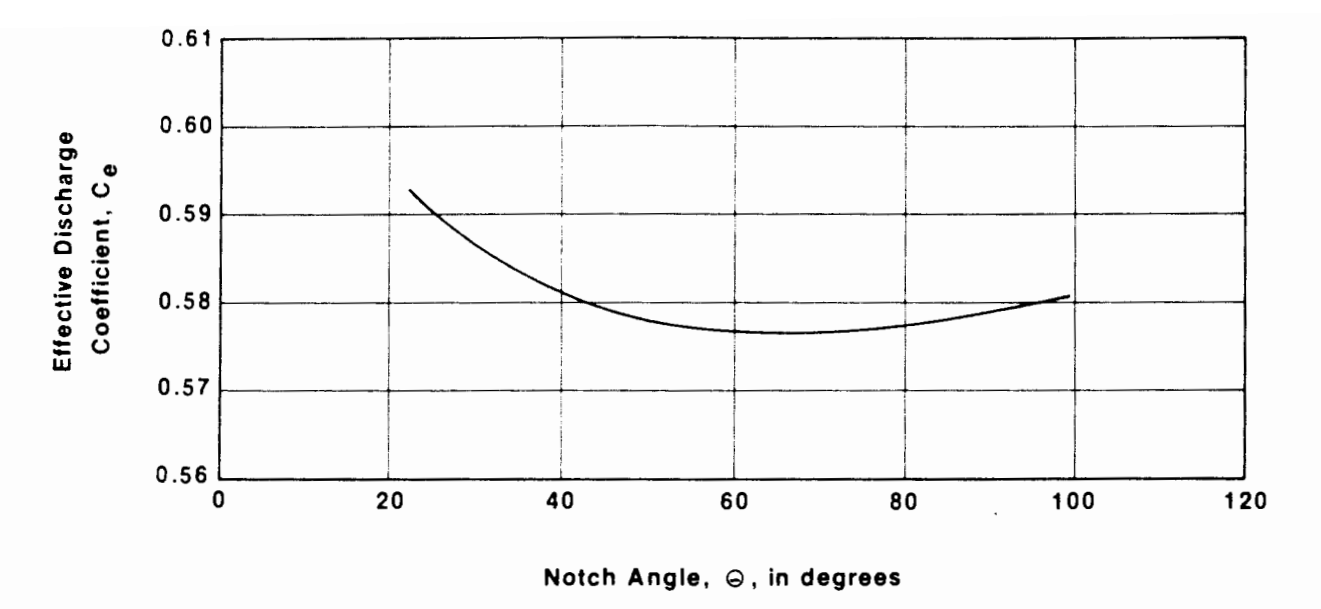


Figure 4.14 Effective coefficient of discharge,  $C_c$ , as a function of the notch angle,  $\theta$ , for V-notch weirs. (From Shen, 1981.)

backwater or tailwater effects, the orifice is operating under free-flow conditions. If the upstream water level is below the top of the opening, the opening is performing hydraulically as a weir structure. For free-flow conditions in an orifice, the discharge equation is

$$Q_t = C_d C_r A (2gh_u)^{0.5} (4.47)$$

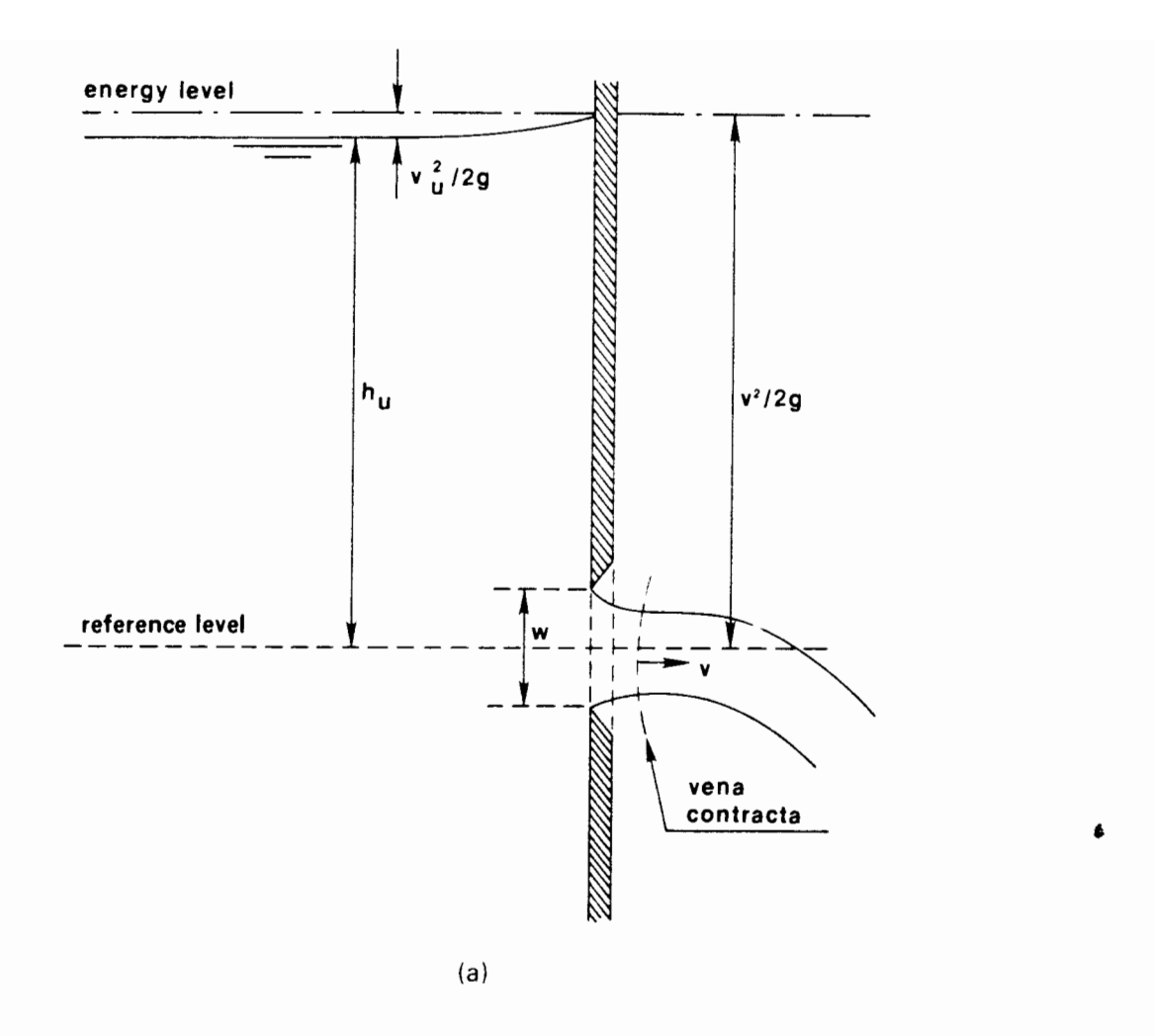
where  $h_u$  is measured from the center of the orifice to the upstream water level. If the downstream water level is also above the top of the orifice (Fig. 4.15), submerged conditions exist and the discharge equation becomes

$$Q_s = C_d C_i A [2g(h_u - h_d)]^{0.5}$$
 (4.48)

The velocity head coefficient,  $C_v$ , approaches unity as the approach velocity to the orifice approaches zero. In irrigation systems,  $C_v$  can usually be assumed as unity since most irrigation channels have very flat gradients and the flow velocities are low (usually less than 1 m/s).

An orifice can be used as a highly accurate flow-measuring devivce in an irrigation system. If the orifice structure has not been rated previously in the laboratory, it can easily be rated in the field. The hydraulic head term,  $h_u$  or  $h_u - h_d$ , can be relied on to have the exponent  $\frac{1}{2}$ , which means that a single field rating measurement, if accurately made, will provide an accurate determination of the coefficient of discharge,  $C_d$ . Generally, orifices have  $C_d$  values of about 0.60 to 0.80, depending on the geometry of the orifice structure.

Flow Measurement 69



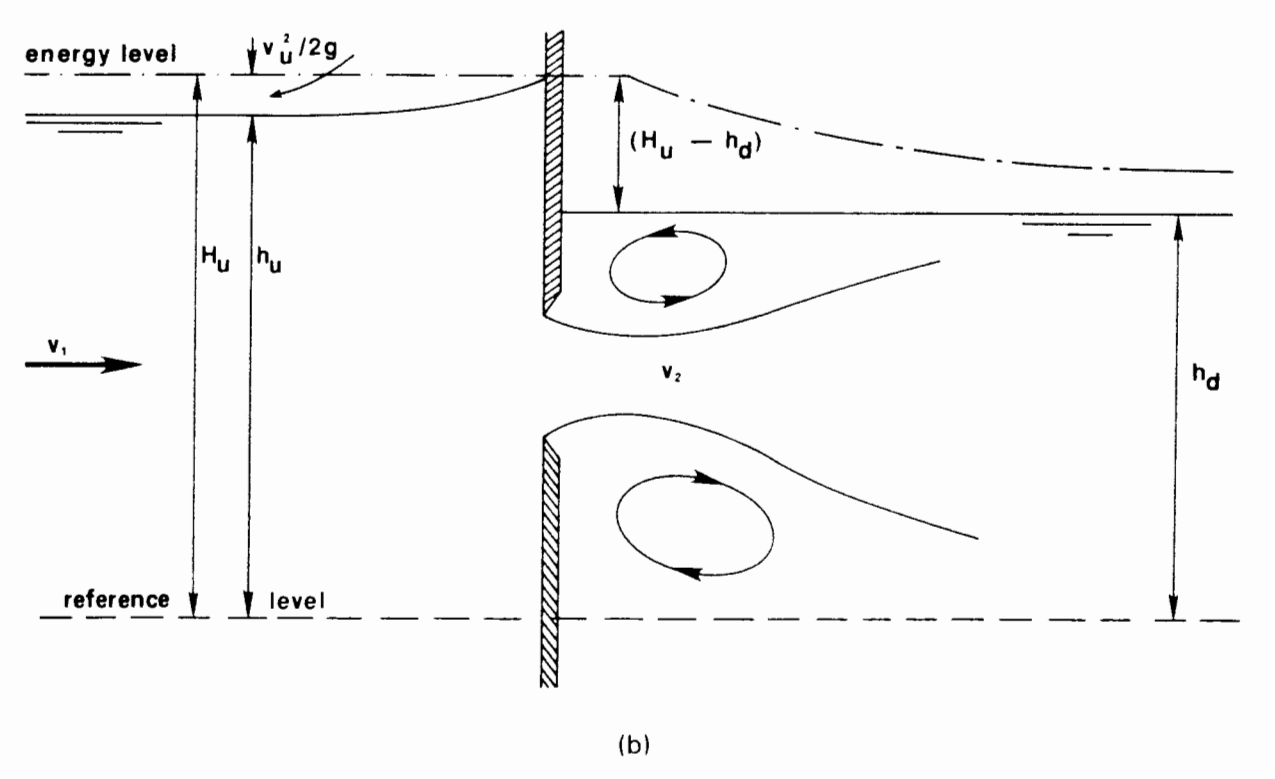


Figure 4.15 Definition sketch for orifice flow. (a) Free flow. (b) Submerged flow.

### **Closed-Conduit Devices**

Closed-conduit flow-measuring devices are needed to measure the discharge from irrigation pumps and irrigation pipeline delivery networks. Only three types of devices are described below: orifices, Venturi meters, and propeller meters. For other devices and techniques the reader is referred to U.S. Department of Agriculture, Soil Conservation Service (1962) and U.S. Bureau of Reclamation (1974).

**Orifices.** The discussion in the preceding section regarding free-flow and submerged-flow orifices would apply to closed-conduit orifices. Taking the results from a number of researchers, Bos (1976) developed Table 4.7, which presents average discharge coefficients,  $C_d$ , for circular orifices under both free-flow and submerged-flow conditions. The values of  $C_d$  in Table 4.7 are valid primarily for negligible approach velocity, which frequently is not the case. The U.S. Department of Agriculture, Soil Conservation Service (1962) has published some free-flow orifice discharge ratings for pipeline sizes frequently encountered in irrigation systems (Table 4.8).

**Venturi meters.** The most accurate closed-conduit device is the Venturi meter shown in Fig. 4.16. The generalized discharge equation for Venturi meters is

$$Q = C_d K d^2 (h_u - h_d)^{0.5} (4.49)$$

where

 $C_d$  = coefficient of discharge obtained from Table 4.9

 $d_2$  = diameter of the throat section

 $h_u$  = pressure head in the entrance section

 $h_t$  = pressure head in the throat section

K = a factor obtained from the equation

$$K = \frac{\pi}{4} \left[ \frac{2g}{1 - (d_2/d_1)^4} \right]^{0.5} \tag{4.50}$$

**TABLE 4.7** AVERAGE DISCHARGE COEFFICIENTS,  $C_{\sigma}$ , FOR CIRCULAR ORIFICES HAVING NEGLIGIBLE APPROACH VELOCITY

Orifice diameter.	Free-flow $C_d$	Submerged-flow $C_d$
0.020	0.61	0.57
0.025	0.62	0.58
0.035	0.64	0.61
0.045	0.63	0.61
0.050	0.62	0.61
0.065	0.61	0.60
> 0.075	0.60	0.60

Source: From Bos (1976).

Flow Measurement 71

**TABLE 4.8** FREE-FLOW DISCHARGE RATINGS (GAL/MIN) FOR VARIOUS COMBINATIONS OF ORIFICE AND PIPELINE DIAMETERS FREQUENTLY ENCOUNTERED IN IRRIGATION SYSTEMS

		in. fice		in. fice		in. fice		-in. ifice	7-in.	8-in.
Head (in.)	4-in. pipe	6-in. pipe	6-in. pipe	8-in. pipe	6-in. pipe	8-in. pipe	8-in. pipe	10-in. pipe	10-in. pipe	10-in. pipe
6	108	82	160	150	305	240	408	345		
8	122	94	185	170	350	280	458	395	600	935
10	133	104	205	190	393	316	508	445	666	1040
12	146	114	225	208	430	346	556	490	728	1120
14	157	123	243	224	465	376	599	530	785	1194
16	167	132	257	238	495	402	636	568	838	1266
18	178	140	271	252	524	426	672	604	887	1336
20	187	148	285	266	548	449	708	636	933	1404
22	197	156	299	279	572	470	744	664	979	1471
24	205	164	310	291	596	488	776	692	1022	1529
26	214	171	323	303	620	504	805	720	1064	1585
28	222	177	335	314	644	520	831	747	1104	1641
30	230	183	346	325	668	536	857	773	1143	1697
32	239	189	357	335	692	552	882	799	1181	1753
34	246	195	369	345	715	568	907	824	1218	1809
36	254	200	380	354	737	584	931	<b>\$847</b>	1251	1865
38	260	205	390	363	759	600	955	867	1281	1000
40	266	210	401	371	781	616	979	887	1311	
42	272	214	411	380	800	631	1001	906	1341	
44	278	219	420	388	820	645	1023	925	1371	
46	284	224	429	396	837	659	1045	944	1401	
48	290	229	440	405	855	672	1067	963	1431	
50	296	234	448	413	872	686	1089	982	1461	
52	302	238	457	421	888	700	1110	1000	1491	
54	307	243	465	429	904	714	1130	1018	1520	
56	313	248	472	437	919	727	1150	1036	1548	
58	317	252	480	445	934	739	1170	1052	1574	
60	323	257	489	453	948	751	1190	1068	1598	
62	328	262	496	461	961	763	1209	1084	23.70	
64	333	266	504	469	97 <b>4</b>	775	1227	1099		
66	338	271	513	475	988	787	1245	1133		
68	343	275	520	483	1002	799	1263	1127		
70	349	280	525	491	1016	811	1280	1140		

Source: From U.S. Department of Agriculture, Soil Conservation Service (1962); originally published in "Layne Well Water Systems," Layne and Bowler, Inc., Memphis, Tenn., 1951.

in which  $d_1$  is the diameter of the entrance section. The entrance cone has a central angle of about 21°, while the exit cone has a central angle of 5 to 7°.

**Propeller meters.** An illustration of a propeller meter is shown in Fig. 4.17. A propeller meter measures velocity which when combined with the cross-sectional area of the pipeline section surrounding the meter provides the discharge rate. One of the principal advantages of a propeller meter is the direct reading of discharge and the capability to totalize the total volume of water discharged

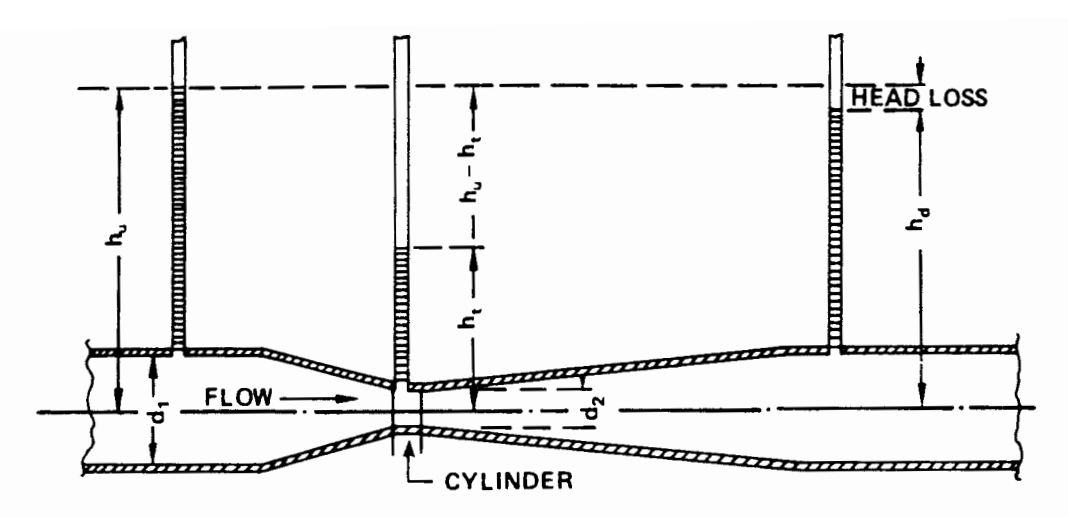


Figure 4.16 Schematic of a Venturi meter.

over time. The principal disadvantage of propeller meters for irrigation pipelines occurs when the water supply contains sediment or debris. Proper location of the inlet structure should prevent bedload sediments, but not suspended sediments, from entering the pipeline. Attention must be given to these details; otherwise, the propeller meters will function for only a short time.

## **IRRIGATION EVENTS**

The hydraulic phases of an irrigation event were listed in Chapter 3, as (1) advance. (2) wetting or ponding, (3) depletion, and (4) recession. The typical field measurements employed for evaluating each of these phases are described below.

## **Advance Phase**

Rate of advance. To measure the rate which the advancing front moves across a surface-irrigated field, stakes are placed along the width and length of the field. A common spacing of these stakes is 30 m, except for small fields (<2ha).

**TABLE 4.9** COEFFICIENTS OF DISCHARGE,  $C_d$ , FOR VENTURI METERS

Diameter				Thro	at velocity	(ft/s)			
of throat (in.)	3	4	5	10	15	20	30	40	50
I	0.935	0.945	0.949	0.958	0.963	0.966	0.969	0.970	0.972
2	0.939	0.948	0.953	0.965	0.970	0.973	0.974	0.975	0.977
4	0.943	0.952	0.957	0.970	0.975	0.977	0.978	0.979	0.980
8	0.948	0.957	0.962	0.974	0.978	0.980	0.981	0.982	0.983
12	0.955	0.962	0.967	0.978	0.981	0.982	0.983	0.985	0.985
18	0.963	0.969	0.973	0.981	0.983	0.984	0.985	0.986	0.986
48	0.970	0.977	0.980	9.984	0.985	0.986	0.987	0.988	0.988

Source: From U.S. Department of Agriculture, Soil Conservation Service (1962).

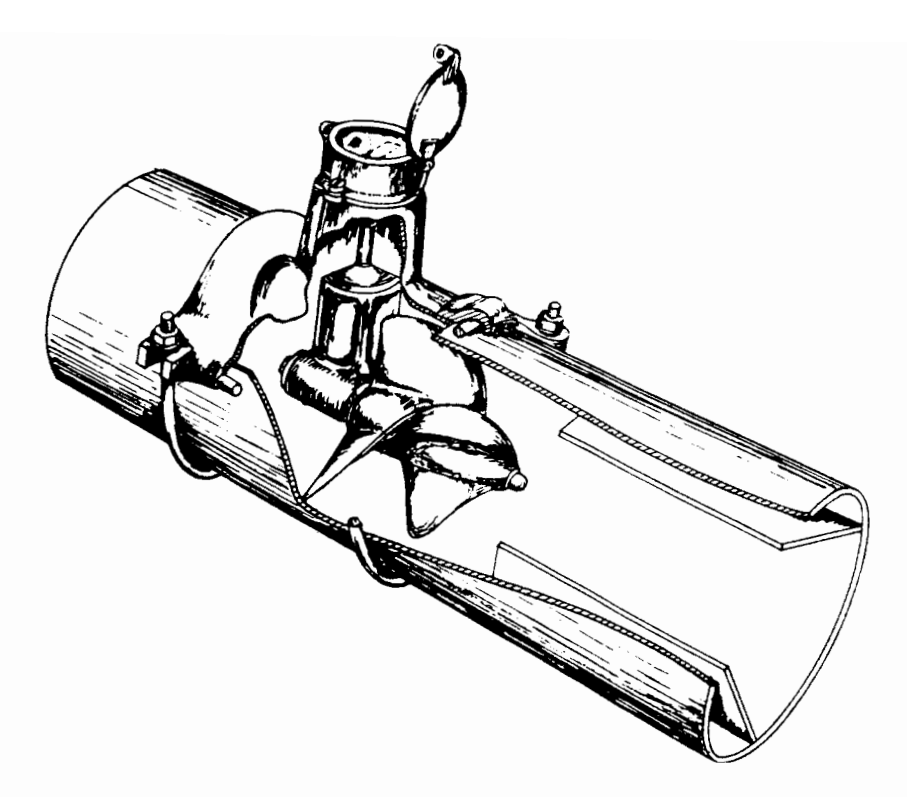


Figure 4.17 Low-pressure propeller meter. (From U.S. Department of Agriculture, Soil Conservation Service, 1962.)

where the spacing would be reduced to 1/6 to 1/10 of the field in order to provide a sufficient number of measuring points (six or more). The ground surface elevation at each stake should be surveyed to determine the grade of the irrigated field and any undulations in the ground surface.

The clock time is recorded when the irrigation water supply is diverted onto the field and when the advancing front reaches each stake. A format for recording water advance data on furrow-irrigated fields is shown in Table 4.10. The format used for border- or basin-irrigated fields is shown in Table 4.11, in which each of the three columns in the table represents a line of stakes along the field length (rather than the stakes along an individual furrow).

In Tables 4.10 to 4.13, the identification code  $(R_E, F_A, F_I, I, \text{ and } F_u)$  is a means of accurately locating the particular furrow being measured:

 $R_E$  = region

 $F_A$  = site (or farmer's name or number)

 $F_I$  = field at site

I = irrigation event number

 $F_{\mu}$  = furrow number

Another technique for measuring the rate of advance is to plot contours of the advancing front at periodic time intervals. Early in the irrigation season, prior to plant cover, the advancing front can be photographed to assist with the advance contouring. A grid of stakes is still needed and should be marked in such a manner that they can readily be identified, either for purposes of sketching or photograph-

 TABLE 4.10
 FORMAT FOR RECORDING WATER ADVANCE AND RECESSION DATA

 ON FURROW-IRRIGATED FIELDS

					WATER,	WATER ADVANCE/RECESSION DATA	ECESSIC	N DATA						
Identification (R <sub>E</sub> , F <sub>A</sub> , F <sub>I</sub> , I): _	A, F <sub>1</sub> , I):				Date:	1	Crop:		1		Irrigation Start:	n Start:		
Soil:					Observer:					Fin	Finish:			
Comments:										Total	Total Time:			
Furrow:			1		Furrow:					Furre	Furrow:			
Stream Size:					Stream Size:					Strea	Stream Size:			
Charle	Advance		Recession	sion		Advance	ince	Recession	ē		Advance	1 7	Recession	sion
Station	-	=	- Lime		Station		E E			Station		Time		
	CIOCK	5	200 200 400	Ę		clock	Ę	Sock	E S		clock	CUM	clock	E
												1		
											_			
												T		
												1		
					3									
Source: From Ley (1978).	Lev (1978	<u>ئ</u> ىر												

Source: From Ley (1978).

**TABLE 4.11** FORMAT FOR RECORDING WATER ADVANCE, PONDING, DEPLETION, AND RECESSION DATA ON BASIN-IRRIGATED FIELDS

$ entification (R_E, F_A, F_I, I): $			Date: _			Cro	Crop:			Soil:			
bserver:				Irrigation Start:	n Start:				Time of Advance: _	vance:			
ime of Cutoff:	W.S.	W.S. Elev. (a t <sub>co</sub> : _			Tin	Time of Depletion:	etion: _			Total	Total Time:		
low Path:			Flow Path:	<b>h</b> :				<b>T</b> 1	Flow Path:				
low Stream		Advance	Recession	]3		Advance		Recession		Advance		Recession	
clock cum mm lps	Sidion	clock cum	clock	cum	ordiron	clock	cum clock	cum	Station	clock	cum	clock	E C
				<u> </u>				_			_		
											-		
				<u></u>									
						<u></u>							
				<u> </u> 									
				<u> </u> 									
				<u> </u> 									
				<u> </u> T		\$					_		
				1							-		
				1			-				+		
				<u> </u> 									
				<u> </u> 									
						_							

Source: From Ley (1978).

ing. Some typical examples of the advancing front in regular-shaped and irregular-shaped basins are shown in Fig. 4.18.

Cross-sectional surface flow area. The cross-sectional geometry of furrows and corrugations is important when evaluating hydraulic flow characteristics and surface storage. For each furrow selected for evaluation, the cross-sectional geometry should be measured at two or three stations. A useful apparatus for determining the cross-section of furrows is shown in Fig. 4.19, and the format for recording the data is shown in Table 4.12. To minimize time in the field, this

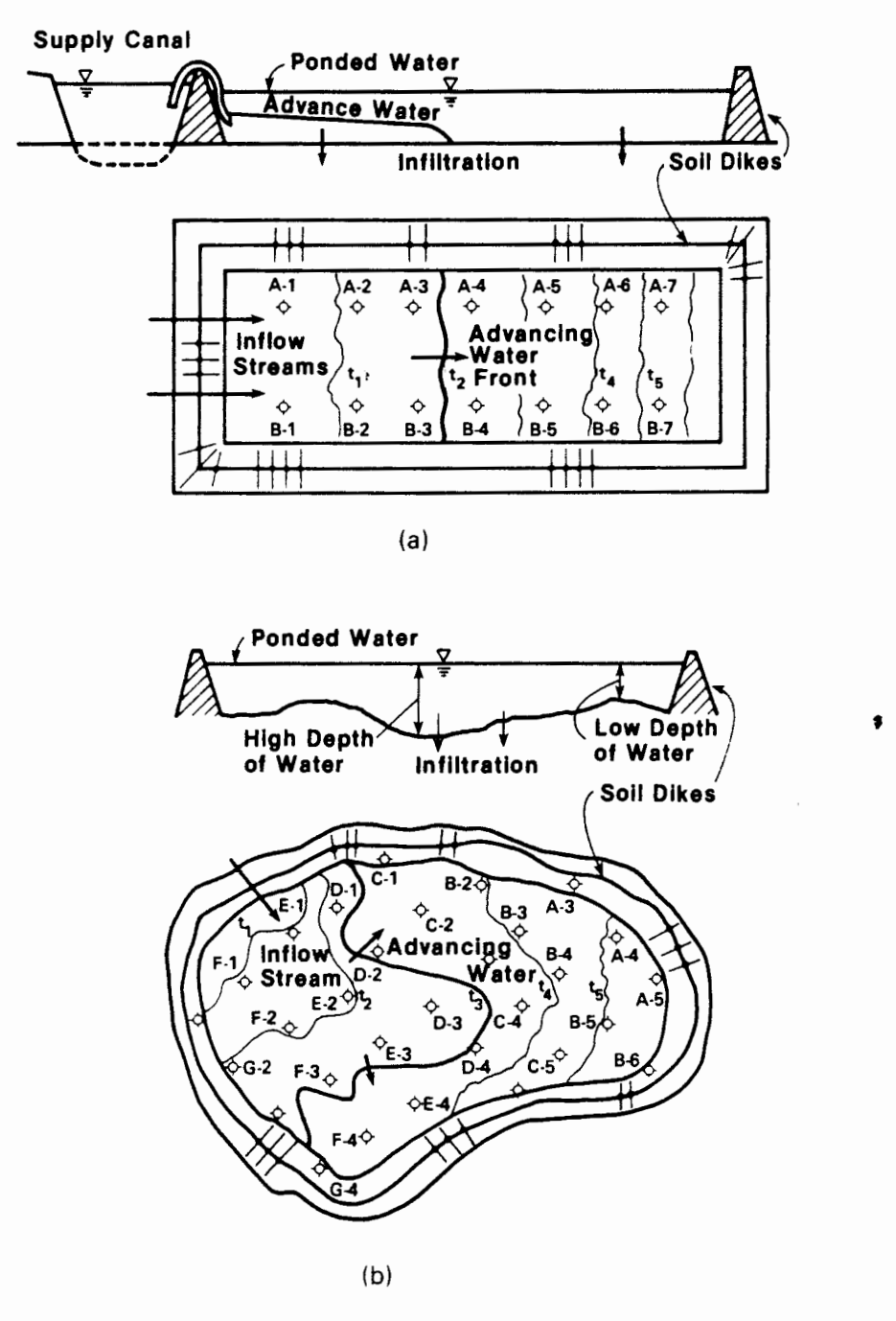


**Figure 4.18** Schematic description of the advance phase in regular and irregular basins. (a) Regular basin. (b) Irregular basin. (Adapted from Peri et al., 1979.)

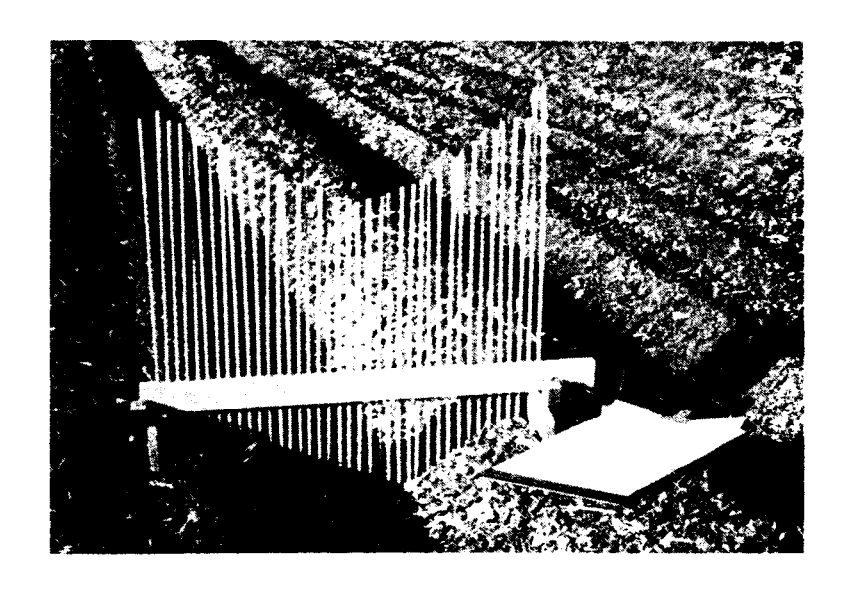


Figure 4.19 Furrow profilometer for determining cross-sectional area. (Courtesv of G. P. Merkley.)

apparatus can be placed in the furrow and a photograph taken, which can then be analyzed in the office at a later date.

During irrigation of basins, borders, or furrows, the flow depth and water surface top width should be measured periodically at selected stations. These data can be combined with cross-sectional flow areas to compute the surface storage at different times. A useful technique for measuring flow depth in basins and borders is to have a scale on each stake, which can consist of a metal staff gage or strips of colored tape around the stake.

# **Ponding Phase or Wetting**

The term "wetting phase" is usually used for furrow and border irrigation where tailwater runoff can occur, whereas "ponding" is the preferred term for basin irrigation (no tailwater runoff). This phase begins when the advance phase is completed and ends when the irrigation water supply is cut off. After the advance phase is complete, the amount of surface water storage may be measured periodically using the techniques described above.

# **Depletion Phase**

The depletion phase begins at the time of cutoff, after which the ponded water surface elevation declines and is recorded periodically. The depletion phase ends when any portion of the ground surface is bare of water.

## Recession Phase

For surface-irrigated fields the recession phase ends when surface water disappears at each measuring station and is recorded, as shown in Table 4.10. The time difference at each measuring station between the clock time or cumulative time for advance and recession is the opportunity time,  $\tau$ , for infiltration to occur. An example of advance, recession, and infiltration opportunity time for a furrowirrigated field is shown in Fig. 4.20.

TABLE 4.12 FORMAT FOR RECORDING FURROW CROSS-SECTIONAL DATA

Before Irrigation After	X X X X X X X X X X X X X X X X X X X	X X X Y Y Y Y Y Y Y Y Y Y Y Y Y Y Y Y Y
Furrow Spacing:	X	X
Ident (Location) (R <sub>E</sub> , F <sub>A</sub> , F <sub>I</sub> , I, F <sub>u</sub> ):Observer:	X	X X X X X X X X X X X X X X X X X X X

Source: From Ley (1978).

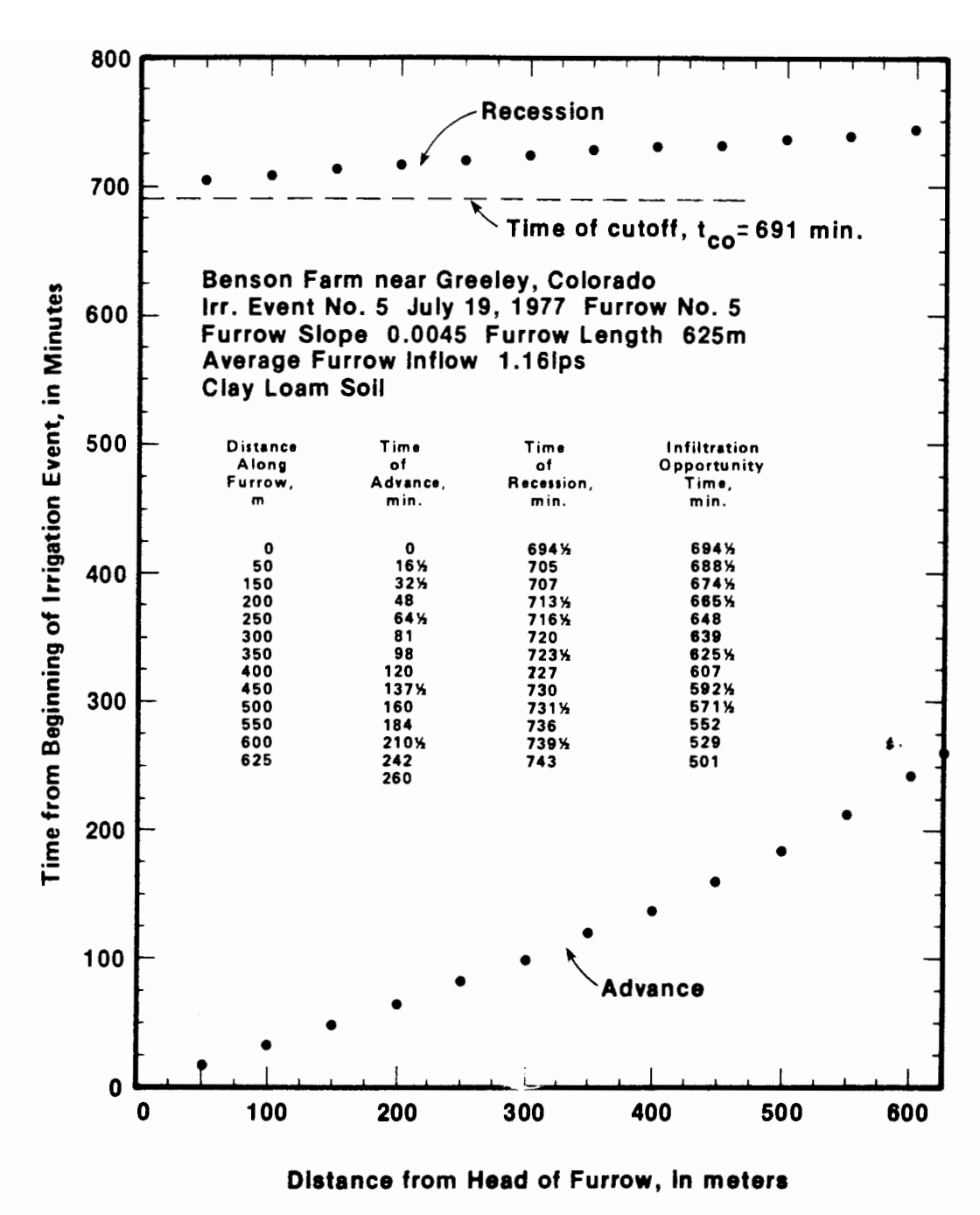


Figure 4.20 Advance and recession curves and infiltration opportunity times based on actual data for a furrow-irrigated field. (From Salazar, 1977.)

For basin irrigation, it is advantageous to draw contours of the receding front at various times. Examples of advance and recession contours for a level basin are shown in Fig. 4.21. A format for basin irrigation, wherein the data for all four hydraulic phases of an irrigation event can be recorded, is presented in Table 4.12.

#### INFILTRATION

Not only is infiltration one of the most crucial hydraulic parameters affecting surface irrigation, but unfortunately, it is also one of the most difficult parameters to assess accurately in the field. The importance of knowing the infiltration function in

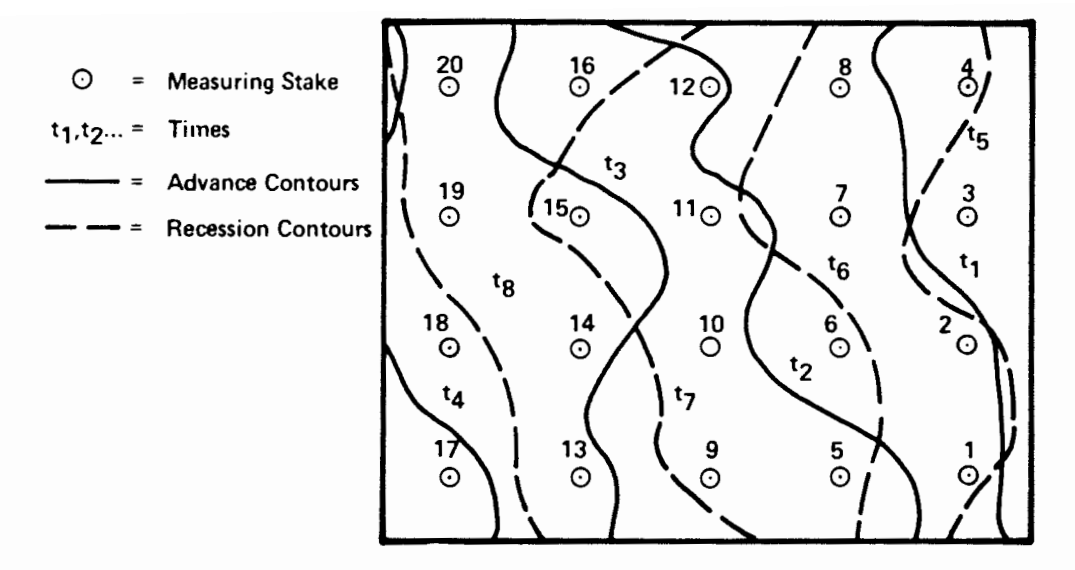


Figure 4.21 Advance and recession contours as measured in the field at various times for a regular graded basin irrigated field. (From Peri et al., 1979.)

order to describe the hydraulics of a surface irrigation event, along with the inherent difficulties in obtaining reliable estimates of this parameter, means that the investigator should expect to spend considerable time and effort in assessing infiltration before proceeding with the design of a surface irrigation system.

In the past, the three most commonly employed techniques for measuring infiltration were cylinder infiltrometers, ponding, and inflow-outflow field measurements. For furrow irrigation, the blocked furrow method has been used, while a more recent technique refined at Utah State University is the recycling furrow infiltrometer. These field measurement techniques are described below. In Chapter 5, analytical techniques for deriving the infiltration function based on field measurements collected during the advance phase are presented.

# Cylinder Infiltrometer

**Installation.** One of the most complete treatises on the use of cylinder infiltrometers for measuring infiltration was presented by Haise et al. (1956). The material below was taken largely from their publication, but with a few modifications based on more recent field experiences.

A metal cylinder (Fig. 4.22) is used having a diameter of 30 cm or more and a height of about 40 cm. The cylinders should be constructed of smooth material to minimize skin friction when driving the cylinder into the soil. Commonly, cold-rolled steel is used. The wall thickness of the cylinder should not exceed 2 mm (0.08 in., which is approximately 14 gage), unless a sharpened cutting edge is provided, as shown in Fig. 4.22.

A driving plate is advantageous for setting on top of the infiltrometer to drive the cylinder into the ground. A piece of steel plate at least 10 to 15 mm thick (about 1/2 in.) is satisfactory for this purpose. The dimensions of this typically square plate should be 5 to 10 cm greater than the diameter of the cylinder. Placing lugs on the underside of the plate keeps it centered over the cylinder when driving

Infiltration 81

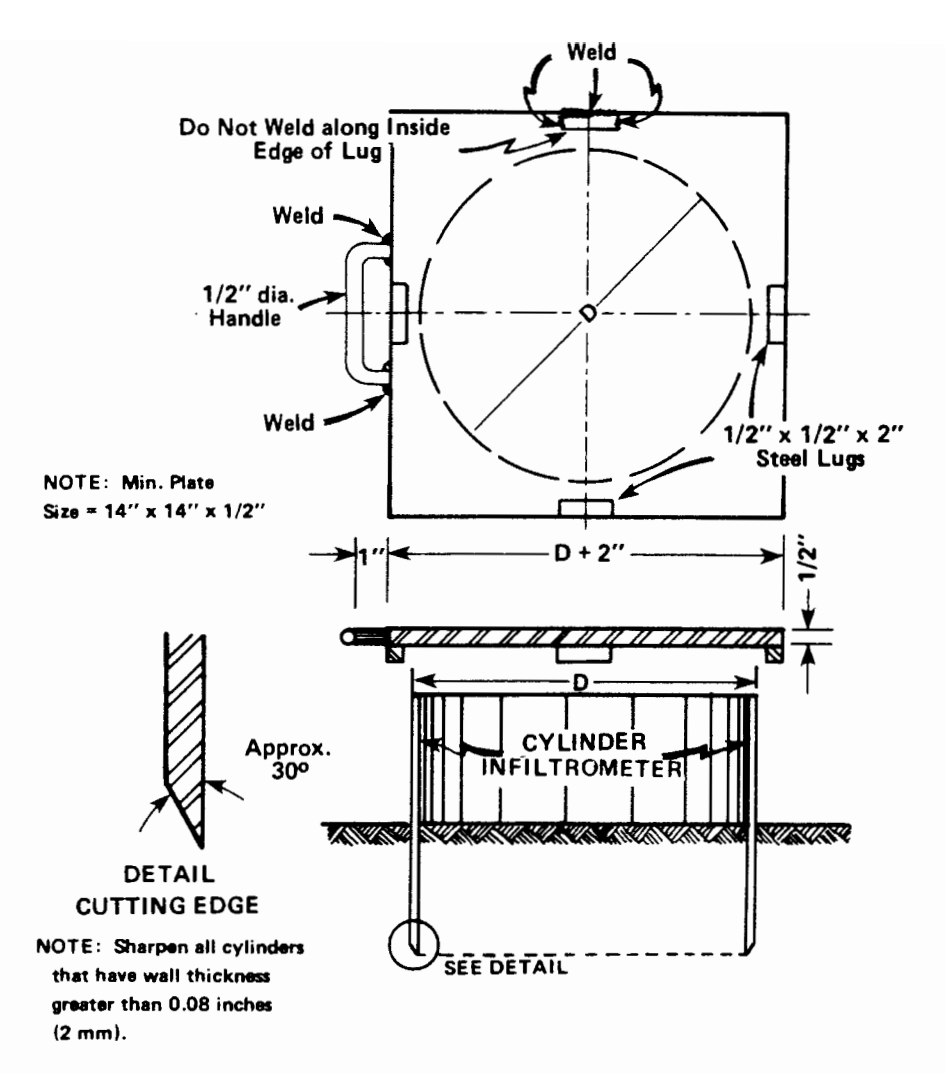


**Figure 4.22** Details for fabricating a cylinder infiltrometer and a driving plate. (From Haise et al., 1956.)

the infiltrometer. Fabricating a handle on the plate provides for greater ease in carrying.

A heavy driving hammer is needed for inserting the infiltrometer. Two types of suitable hammers are illustrated in Fig. 4.23. The steel block hammer will weigh nearly 14 kg (about 30 lb). The weight of the galvanized pipe hammer is dependent on the amount of lead placed inside the pipe, but normally this hammer would weigh slightly less than the steel block hammer.

When installing cylinder infiltrometers, the procedure should be:

- 1. Select possible locations for three to five cylinders and examine the sites carefully for signs of unusual surface disturbance, animal burrows, stones that might damage the cylinder, and so on. Avoid areas that may have been affected by unusual animal or machinery traffic. The individual cylinders used for a single test should be set close enough together so that they can conveniently be run simultaneously. Normally, they should be set within a 0.2 ha (½ acre) area.
- 2. Set a cylinder in place and press it firmly into the soil.

- 3. Place the driving plate over the cylinder and tamp with the driving hammer until the cylinder is driven to the desired depth. The level of the cylinder should be checked frequently to keep it oriented properly.
- 4. Construct a buffer pond unless the infiltrated water is not expected to reach the bottom of the cylinder prior to the end of the test. A satisfactory buffer pond can be constructed by throwing up a low dike around the cylinder. The inside toe of the dike should be at least 15 cm from the cylinder. In cropped fields or in areas where water supplies must be hauled to the test site, it may be desirable to use a metal cylinder to form the buffer pond. These buffer cylinders should be at least 30 cm larger in diameter than the cylinder infiltrometers. Outside cylinders, however, need not be as long as the cylinder infiltrometer nor driven as deep. Generally, buffer cylinders 20 cm long driven 5 to 10 cm into the soil will be adequate. Since these large-diameter cylinders are usually driven by tamping blows around their circumference, they should be constructed of 10-gage or heavier metal, or they should have a reinforcing strip welded around the top.

**Operation.** One or two water buckets, each having a capacity of roughly 10 liters, are needed to convey water to the infiltrometer. The usual irrigation water supply should be used since the chemical characteristics of the water can affect the infiltration rate.

A point gage can be used for measuring the water surface elevation in the cylinder and is easily fabricated as shown in Fig. 4.24. Instead of using a triangular

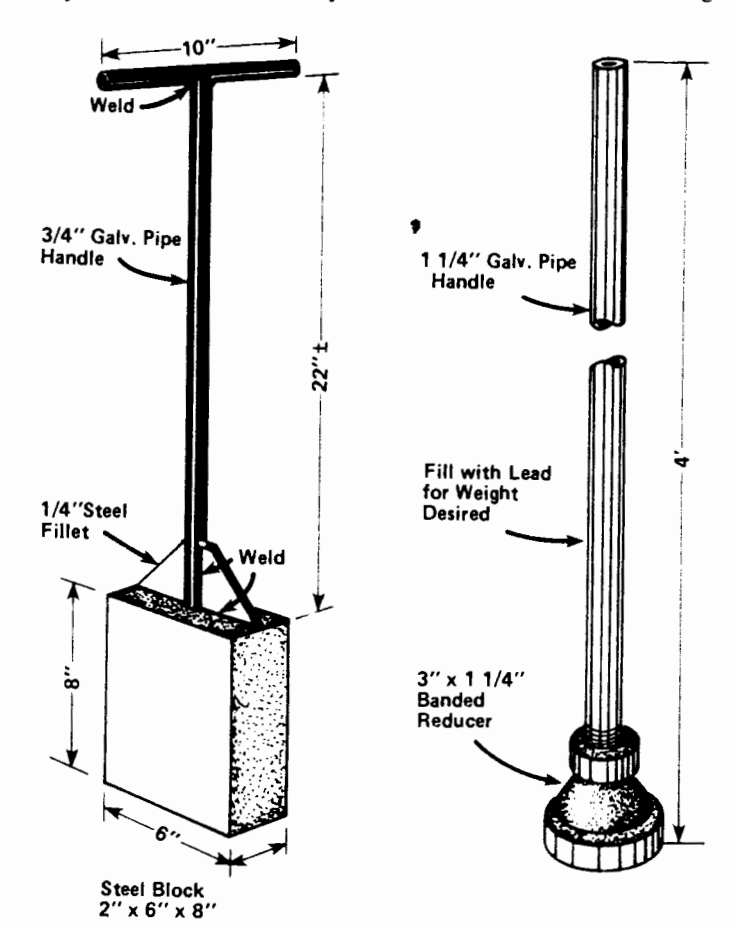


Figure 4.23 Two types of suitable driving hammers for installing a cylinder infiltrometer. (From Haise et al., 1956.)

Infiltration 83

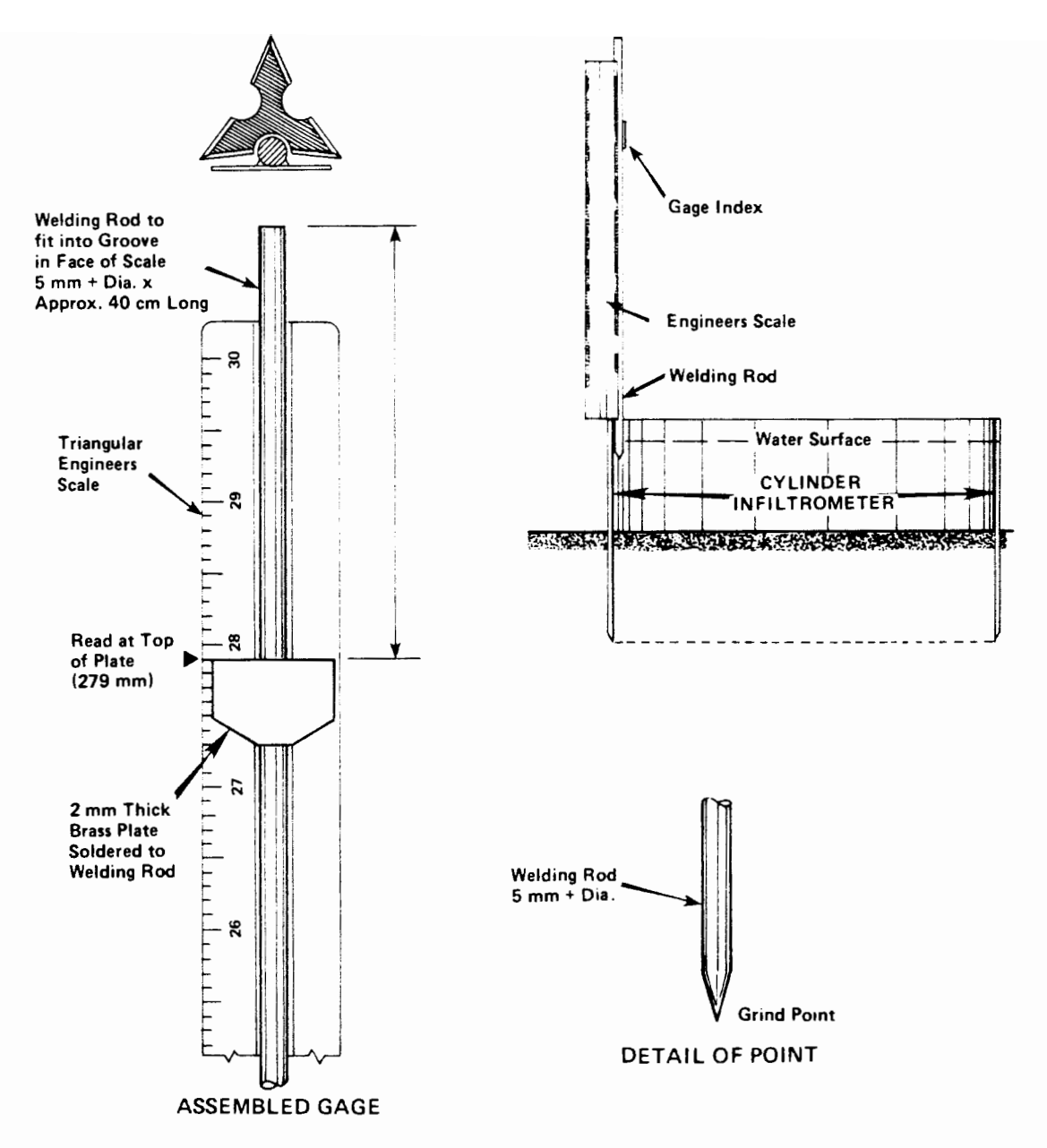
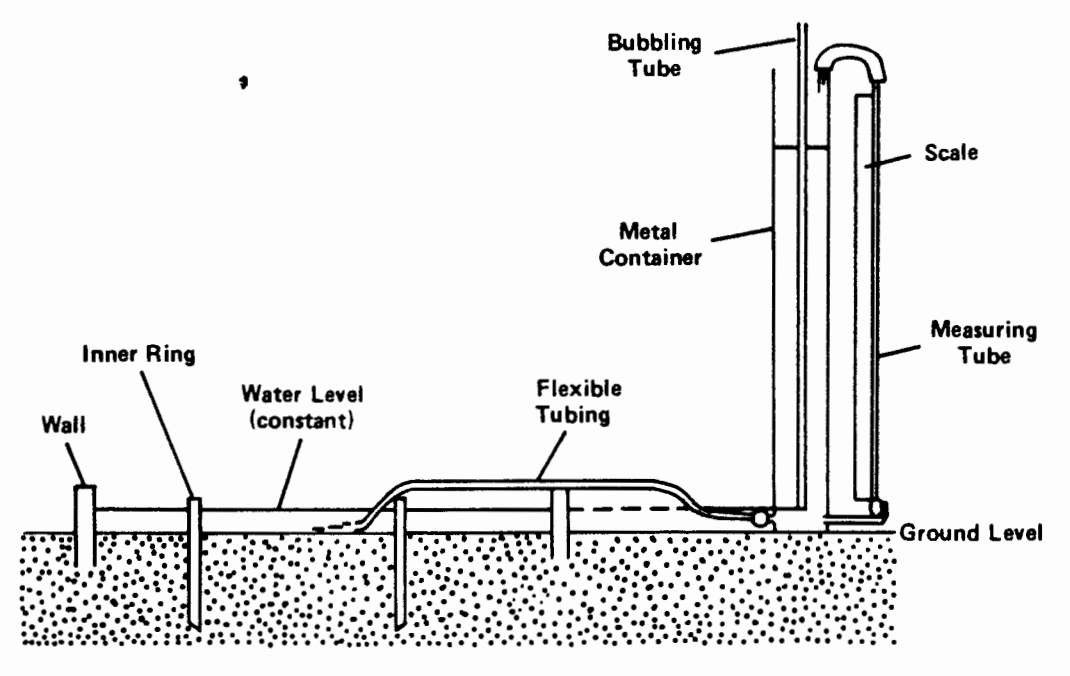


Figure 4.24 Details for fabricating a point gage for measuring the water surface elevation in an infiltrometer. (Adapted from Haise et al., 1956.)

engineer's scale, almost any type of scale could be used. Another technique is to use a Mariotte bottle for maintaining a constant water surface elevation in the infiltrometer, as shown in Fig. 4.25. Since the water level in the measuring burette corresponds with the water level in the calibrated metal container, the volume of water infiltrating into the soil is determined by recording the change of water level in the burette. After the infiltrometers have been installed, the following operational procedure should be followed.

1. Fill the buffer pond (if used) with water to a depth approximately the same as will be used in the cylinder infiltrometer, as a safety precaution against leakage between the two surface reservoirs.

- 2. Fill the cylinder infiltrometer with a known volume of water (a depth of about 10 cm) so that the initial depth at time zero can be calculated.
- 3. Make a point gage measurement, or a gage reading in the metal container if a Mariotte tube is used, of the water surface elevation. (Use a cylinder edge for the point gage datum point and mark the cylinder so that all subsequent measurements can be made at the same point on the cylinder.) The cylinder should be filled quickly and the initial water surface observation made immediately, to reduce errors due to infiltration during this period.
- 4. Record the point gage or metal container gage reading and the time at which the observation was made (Table 4.13).
- 5. Make additional measurements at periodic intervals and record the data. Intervals between observations usually should be short (5 to 10 min) at the start of the test. After two or three measurements the intervals may be increased. After about the first hour, measurements at 30- to 60-min intervals will usually be sufficient. Observation frequencies should be adjusted to infiltration rates. For most soils, observations made at the end of 5, 10, 20, 30, 45, 60, 90, and 120 min and hourly thereafter, will provide good data. As a general rule, the infiltration between measurements should not be more than 2 cm (about 1 in.). Measurements should usually be continued until 4 h has elapsed. It is seldom necessary to extend the tests beyond the time required to put about 15 cm of water into the soil.
- 6. When the water level has dropped a few centimeters (2 to 5) in the cylinder, add sufficient water to return the water surface to its approximate initial elevation. Maintain the depth of water in the cylinder between 6 and 10 cm throughout the entire test. When water is added, be sure to record the level



**Figure 4.25** Cylinder infiltrometer with buffer area and Mariotte bottle for maintaining a constant water surface elevation.

Infiltration 85

TABLE 4.13 FORMAT FOR RECORDING CYLINDER INFILTROMETER DATA

Identification (R <sub>E</sub> , F <sub>A</sub> , F <sub>I</sub> , I):	Days Since Last Irr. Event: Date:
Crop:	Soil:
Cultivation Practices:	
Soil Moisture: 0-15 cm % 15-30 cm	- %;30-60 cm %; 60-90 cm %; 90-120 cm %
General Comments:	

5	ée	eun Fin	
Cylinder Inf. No. 5	Intake	gage	
der Ir		e E i	
Cylin	Time	clock	
4	0	e E i E	
Cylinder Inf. No. 4	Intake	gage cum mm min	
der Ir		nin Ti	
Cylin	Time	clock	
2	e	cum min	
Cylinder Inf. No. 3	Intake	gage cum mm min	
der Ir	0	cum min	
Cylin	Time	clock	
2	ê	cum min	
Cylinder Inf. No. 2	Intake	gage	
der ir	6)	cum min	
Cylin	Time	clock	
-	é	n E i	
Cylinder Inf. No. 1	Intal	gage	
der 1	e)	min T	
Cylir	Time	clock	

Source: Adapted from Haise et al. (1956).

- before and after filling. Keep the interval between these two readings as short as possible to avoid errors due to infiltration during the refilling period. In using the data, the refilling is assumed to be instantaneous.
- Where an abnormally high or low infiltration value is indicated by a cylinder, it should be removed and the soil examined for possible causes and observations recorded.
- 8. At the conclusion of a test, remove the cylinders and clean them thoroughly. Mud-encrusted cylinders are difficult to drive and are apt to cause excessive soil disturbance. If the cylinders will not be used again for a week or more, a cloth soaked in oil should be used to coat the inside cylinder wall.

# **Ponding Methods**

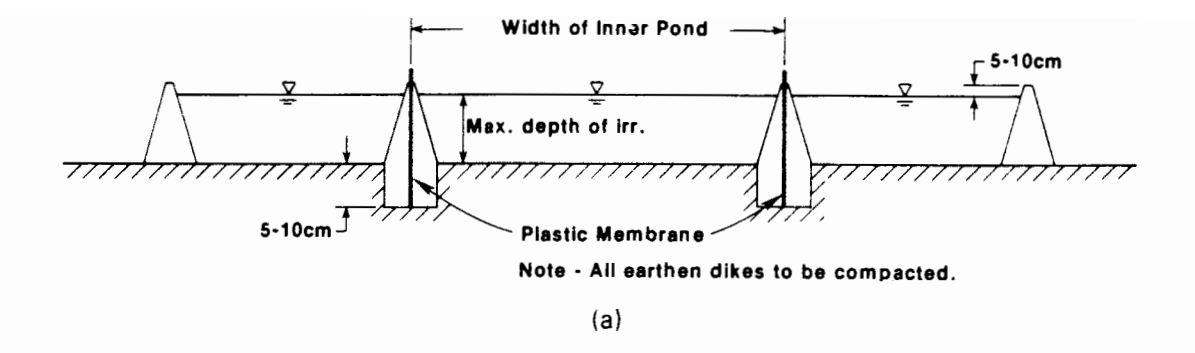
Utilizing ponds constructed on the ground surface involves the same principles and procedures as discussed above for cylinder infiltrometers. The principal advantages of the ponding method is the ability to use larger ground surface areas, and metal cylinders are not required. The greatest disadvantage of this technique is that using a single pond, rather than two concentric ponds, may result in larger overestimations of the true infiltration rate. This problem can be overcome by excavating a trench, which is then made at least relatively impermeable. Both a double-pond and single-pond technique are described below.

The double-pond technique involves the simple construction of two concentric ponds, usually square, but they can have any desired geometric shape. The dikes are constructed from soils which have been collected outside the area of the ponds. with their height being 5 to 10 cm greater than the maximum depth of irrigation water applied during the test. In fact, care must be taken not to disturb the ground surface inside the ponds, particularly the inner pond. The investigator should be aware that boundary effects will cause a difference in infiltration rates between the two ponds. These soil\*dikes should be compacted to minimize seepage between the two ponds; however, the greatest leakage will occur at the interface between the original ground surface and the soil dikes. To minimize this leakage, it is desirable to excavate the soil where the dikes will be located to a depth of 5 to 15 cm and then start backfilling with the same soil in layers of about 5 cm, compacting with a hand-held weight before placing the next soil laver. Another technique for reducing seepage between the two concentric ponds is the use a simple impermeable barrier such as plastic strips (Fig. 4.26a) or wood planks. The ground surface area of each pond should be measured and the volume of water required to provide a depth equal to, or greater than, the maximum depth applied during an irrigation event should be readied.

The single-pond technique requires the construction of a trench around the periphery of the pond as shown in Fig. 4.26b. Instead of using a plastic membrane, any other relatively impermeable barrier could be used, including compacted clays provided that they are much more impermeable than the soil underneath the pond.

For monitoring the drop in pond water surface elevation, the point gage shown in Fig. 4.24 can be employed. For the ponding methods, the point gage should be used in conjunction with some type of stilling well, as illustrated in Fig. 4.27.

Infiltration 87



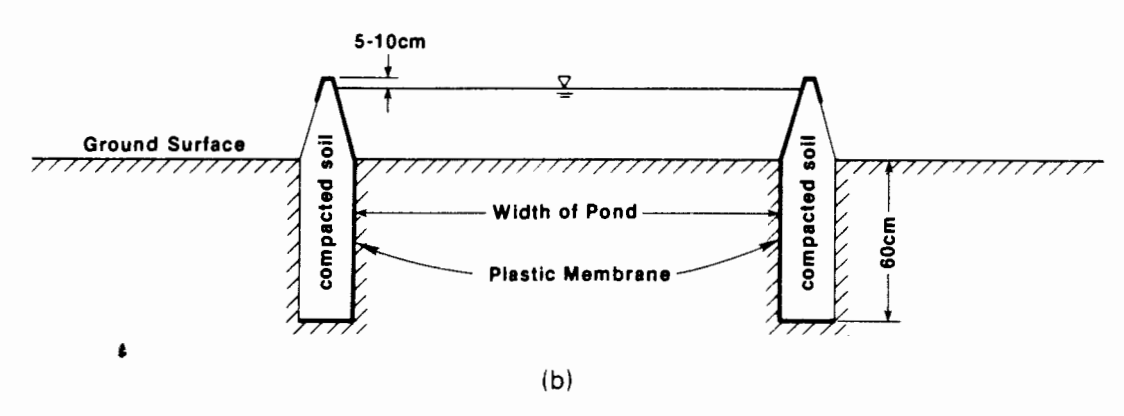


**Figure 4.26** Schematic of ponding techniques for measuring infiltration. (a) Double-pond technique. (b) Single-pond technique.

The data can be recorded on the same format as that used with cylinder infiltrometers (Table 4.13).

#### Inflow-Outflow Methods

Inflow-outflow methods for determining infiltration provide good measures of total infiltration, but not necessarily the distribution of infiltration along the length of an irrigated field. To estimate infiltration distribution, inflow-outflow measurements must be combined with field measurements of advance in order to derive the infiltration function. These analytical techniques are presented in Chapter 5.

For basin irrigation, the volume of inflow is equal to the volume of infiltration. For small basins, where the time of advance is small compared to the total irrigation time, the infiltration can be assumed as essentially uniform over the basin area. Otherwise, the alternatives for evaluating the infiltration distribution are: (1) use cylinder infiltrometers; (2) employ the ponding method; or (3) combine inflow and advance data to derive the infiltration function (Chapter 5).

For border irrigation, the difference between inflow and tailwater runoff measurements is an accurate measure of the total infiltration with time. However, to determine the infiltration distribution along the border length, either cylinder infiltrometers or ponds would have to be used (with some adjustment based on inflow-outflow measurements as described in Chapter 5), or the infiltration function would be derived from a combination of inflow-outflow and advance data.

The measurement of infiltration for furrow irrigation differs from border irrigation in that it is feasible to make inflow-outflow measurements over a relatively short furrow length, say 30 to 100 m. One of the simplest techniques is to use WSC flumes (Fig. 4.6) at the head and tail of a furrow length. The greatest concern relates to the amount of backwater resulting from the downstream flume, which would result in more water intake than under normal operating conditions. To alleviate the backwater resulting from installing a constriction in the furrow, the outflow can be measured volumetrically as shown in Fig. 4.28. Two other techniques for measuring infiltration from irrigated furrows are described below.

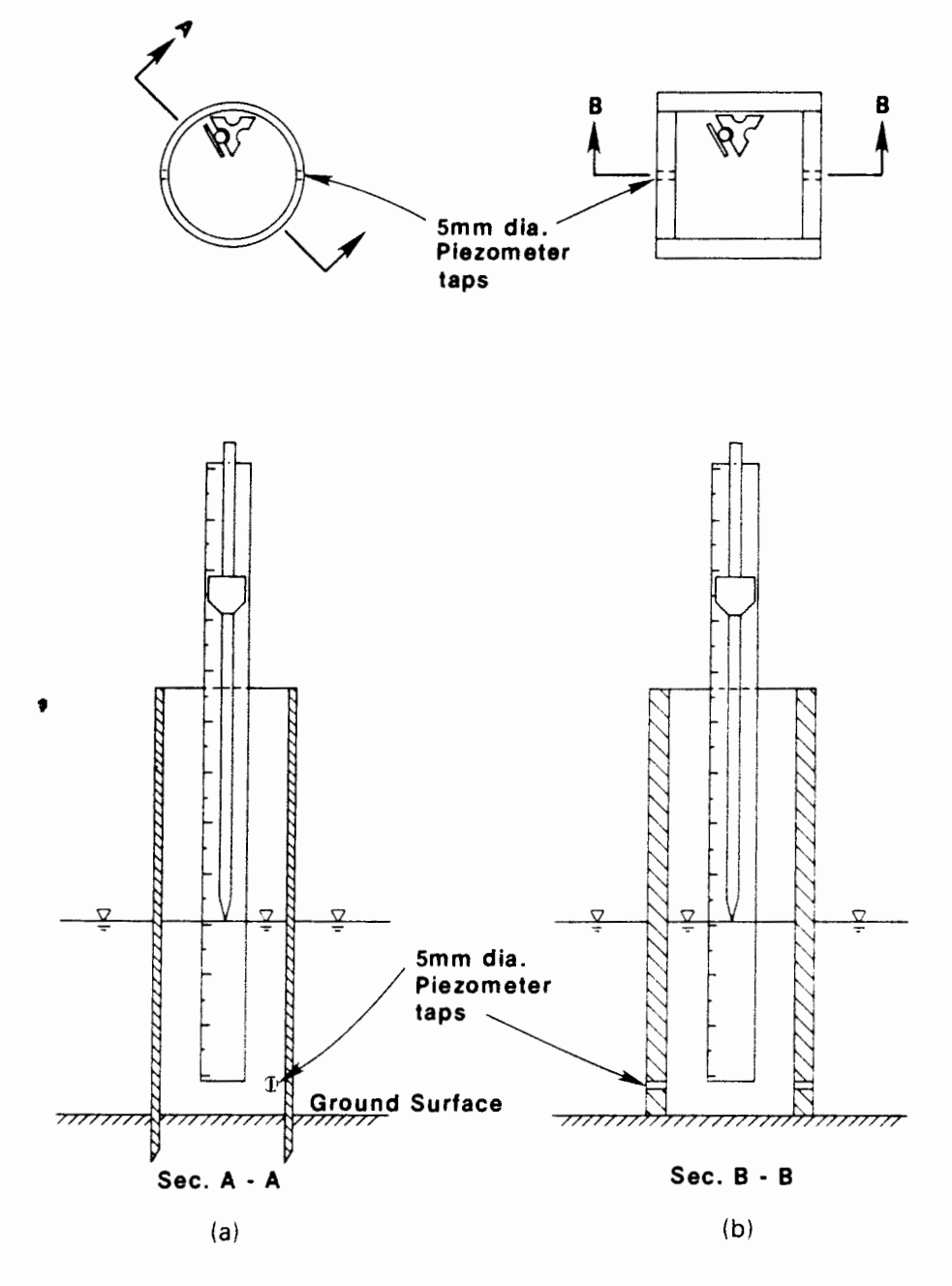


Figure 4.27 Alternative stilling well configurations for monitoring water surface elevation in a pond using a point gage. (a) Metal or PVC stilling well. (b) Wooden stilling well.

Infiltration 89

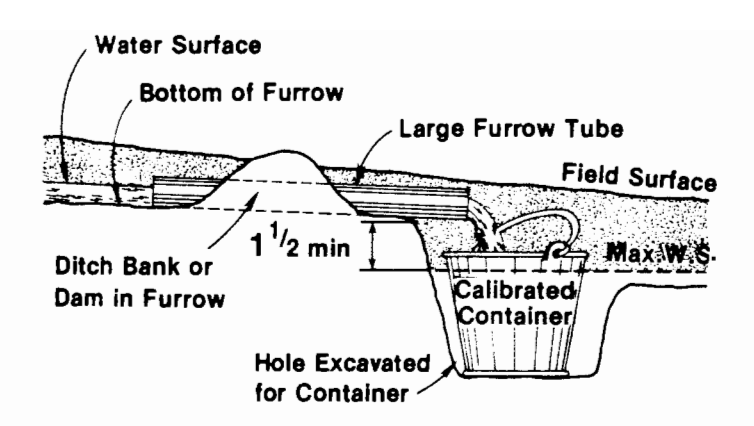


Figure 4.28 Volumetric measurement for outflow from an irrigated furrow. (From Shockley et al., 1959.)

#### **Blocked Furrow Method**

The cylinder infiltrometer and ponding methods for measuring infiltration do not simulate the geometric conditions in a furrow. Infiltration from a furrow occurs around the wetted perimeter, which means that a significant portion of the total infiltration moves laterally through the furrow sides rather than vertically downward. Recognizing this problem, Bondurant (1957) developed a furrow infiltrometer which has come to be known as the blocked furrow method for measuring intake.

The schematic shown in Fig. 4.29 has been adapted from Bondurant (1957). In particular, the end plates have been made taller to reduce boundary effects (lateral subsurface soil moisture movement underneath the end plates). The float valve, reservoir, and water stage recorder are not mandatory since water can be placed by hand in the furrow being studied, using any type of container. However, whenever placing water in the furrow, the volume should be known. Also, prior to beginning the test, the relationship between depth and volume in the measure furrow should be established. For this purpose, furrow profilometer (Fig. 4.19) measurements could be made every 10 cm of furrow length, depending on the uniformity of furrow cross section. With this information, every time a known volume of water is placed in the measure furrow, the water surface elevation can be computed.

After installing the physical arrangement shown in Fig. 4.29, the procedure for the blocked furrow method would be:

- 1. Have the known volumes of water supply available for each of the buffer furrows, and the volumes that will fill the measure furrow to the desired depth.
- 2. Fill the water reservoir and adjust the water stage recorder.
- 3. Start the infiltrometer test by quickly, but carefully pouring the known volume of water into the measure furrow by hand.
- 4. Turn on the water supply from the reservoir and adjust the float to maintain the desired water level in the measure furrow.
- 5. Fill the buffer furrows to the same depth as the measure furrow and maintain this level in the buffer furrows. (*Note*: If sufficient personnel are available, step 5 could coincide with step 3.)

In analyzing the data, a format similar to that for cylinder infiltrometers can be used (Table 4.13). The water stage recorder data are used to record clock time and cumulative volume of intake, which can be converted into a cumulative intake for the measure furrow.

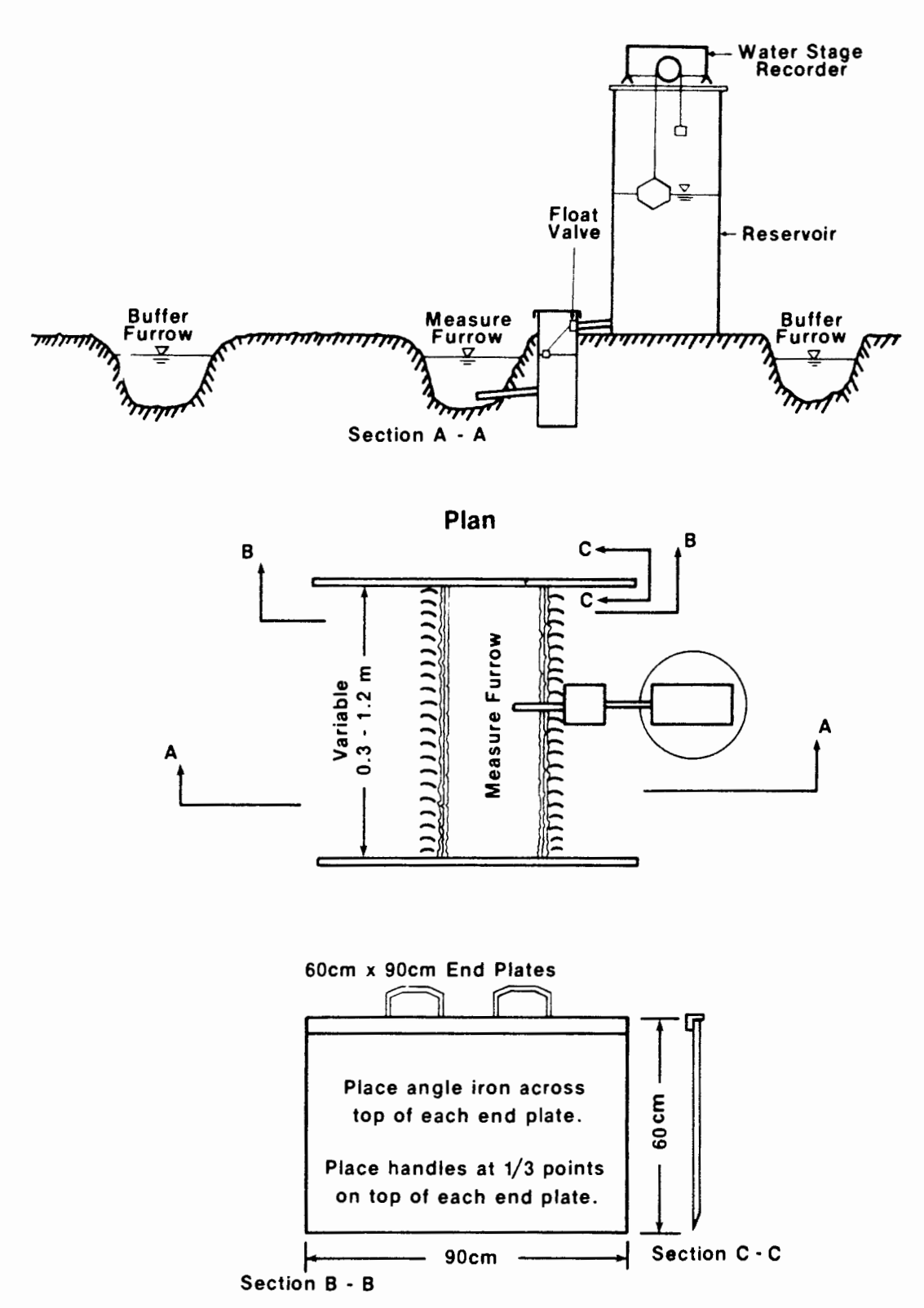


**Figure 4.29** Schematic of blocked furrow method of measuring infiltration. (Adapted from Bondurant, 1957.)

Infiltration 91

# Recycling Furrow Infiltrometer

A recent innovation for evaluating infiltration from furrows is the recycling furrow infiltrometer. The primary advantage of this device is that both the geometric and hydraulic conditions in the field furrow are simulated. Thus the soil—water interface is being simulated more realistically. Suspended particles are kept in suspension rather than being filtered at the soil surface during infiltration and forming a more impermeable soil surface layer than would occur under usual conditions of furrow flow.

A schematic of the recycling furrow infiltrometer is shown in Fig. 4.30. A sump is excavated at each end of a furrow section roughly 5 to 6 m in length. The sumps should be carefully buried in the ground so that the sump inverts correspond with the furrow bed elevation, to avoid erosion at both ends of the furrow test section. Water is released from the water supply reservoir by opening the gate valve, and then regulated using the globe valve. The centrifugal pump then discharges the water via a hose into the furrow inflow sump, where it advances across the furrow test section and is collected in a tailwater sump. The sump pump then discharges the tailwater back into the water supply reservoir. The discharge volume from the sump pump is regulated by a float valve so that a constant water level is maintained in the tailwater sump.

The initial operation of this device creates some problems because of the short period required to complete the advance phase. To minimize this effect, the furrow inflow discharge rate can be set higher for a few minutes and then decreased to a constant level. Once the advance phase has been completed, the

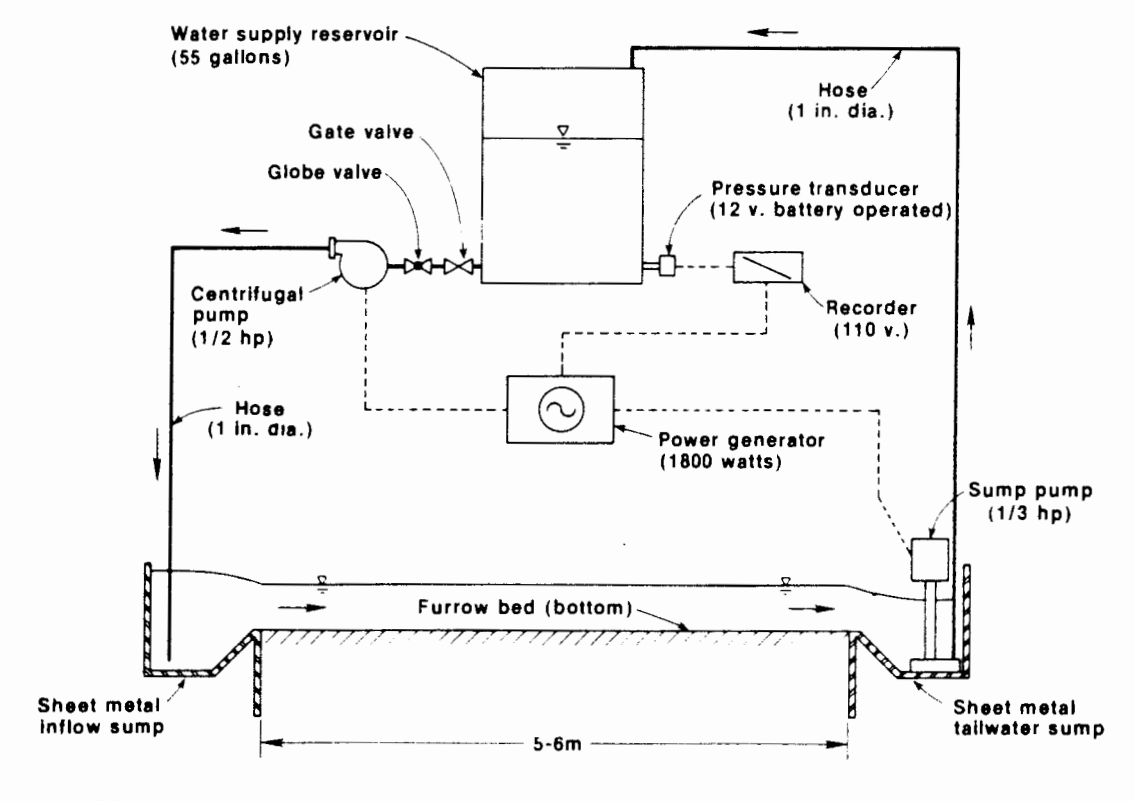


Figure 4.30 Schematic of a recycling furrow infiltrometer. (From Malano, 1982.)

system will provide the necessary information about the rate of infiltration into the furrow as reflected in the rate at which the water surface is dropping in the water supply reservoir.

A water balance can be written at any time after completion of the advance phase:

$$Q_{\rm in} = Q_z + Q_{tw} \tag{4.51}$$

where

 $Q_{\text{in}}$  = discharge rate from the centrifugal pump to the inflow sump,  $\frac{\text{m}^3}{\text{min}}$ 

 $Q_z$  = discharge rate infiltrating into the soil, m<sup>3</sup>/min

 $Q_{tw}$  = tailwater being discharged by the sump pump, m<sup>3</sup>/min

The infiltration discharge rate can also be written as

$$Q_z = A_t I (4.52)$$

where I is the infiltration rate in m/min and  $A_f$  is the ground surface area in m<sup>2</sup> being served by the furrow. Since the rate of fall in the water supply reservoir is also a measure of the infiltration rate,  $Q_z$ ,

$$Q_z = A_r \frac{dh}{dt} \tag{4.53}$$

where  $A_r$  is the cross-sectional area of the water supply reservoir in m<sup>2</sup> and dh/dt is the recession rate of the water level in the supply reservoir in m/min. Setting Eqs. 4.51 and 4.53 equal to one another yields

$$A_f I = A_r \frac{dh}{dt} \tag{4.54}$$

or

$$I = \frac{A_r}{A_t} \frac{dh}{dt} = C \frac{dh}{dt} \tag{4.55}$$

This also implies, then, that the cumulative infiltration in meters becomes

$$Z = Ch (4.56)$$

where h is the total change in water level drop in the water supply reservoir.

## **SOIL WATER**

The primary concern with water in irrigated agriculture is the replenishment of soil moisture in the plant root zone. The discussions above regarding flow measurement, infiltration, advance, recession, and so on, were intended to provide tools that can be used in conjunction with analytical techniques to predict soil moisture status. To calibrate or to verify these predictions, the soil moisture status must be measured periodically. More commonly, the soil moisture status is measured

to determine when the next irrigation event should occur and how much water should be applied. For these purposes, the minimum number of soil-water parameters that must be measured are soil moisture content, bulk density, field capacity, and permanent wilting point.

# Soil Moisture Content

Numerous techniques have been developed for evaluating soil moisture content,  $\theta$ , in the soil profile. In this book, only gravimetric sampling, neutron probe, and the touch-and-feel method will be described. Tensiometers are generally not suitable for evaluating the soil moisture status under commonly employed surface irrigation practices, although they would be useful once the technology for high-frequency surface irrigation applications has been developed.

**Gravimetric sampling.** The standard method for determining soil moisture content is the gravimetric sampling method. The samples are usually collected using some type of sampling tube, either manually or power driven. In many cases, a shovel is used to collect a composite sample over some depth interval (e.g., 30 to 60 cm). The soil sample (approximately 100 to 200 g) is placed in an airtight container and weighted prior to placing in an oven maintained at 105°C (with the container cover removed so that the soil can dry). Usually, the soil sample is left in the oven for 24 hours, although a constant dry weight (less than 0.1 % in weight during an hour) is usually achieved prior to this. The soil sample, with container and cover, is again weighed. Then using the predetermined tare weight of the container and cover, the soil moisture content is determined as discussed in Chapter 2.

**Neutron probe.** When a source of fast neutrons is placed in a medium of moist soil, the emitted neutrons collide with the nuclei of the medium, thereby losing energy. Neutrons that have been slowed down are called thermal or slow neutrons. The ability of nuclei in the moist soil medium to reduce the speed of neutrons varies considerably, but the ability of the soil nuclei is small compared with hydrogen. Therefore, the more hydrogen nuclei that exist in a soil, the more the neutrons emitted from a source will be slowed down, and a greater number of slow neutrons will be concentrated near the neutron source. If the soil medium surrounding the neutron source is low in soil moisture (which means that the soil medium is also low in hydrogen nuclei), the cloud of slow neutrons surrounding the neutron sources will be less dense than for higher soil moisture contents (Van Bavel et al., 1963).

The neutron probe and scaler for making soil moisture measurements are illustrated in Fig. 4.31. The neutron probe is inserted into an access tube at each desired depth and the neutron count rate is read from the scaler.

The manufacturers of neutron probe equipment furnish a calibration curve that relates neutron count rate to volumetric soil moisture content,  $\theta$ . However, it is advisable for the investigator to develop an individual calibration for each soil type in the region being studied. Theoretically, these calibration curves are linear,

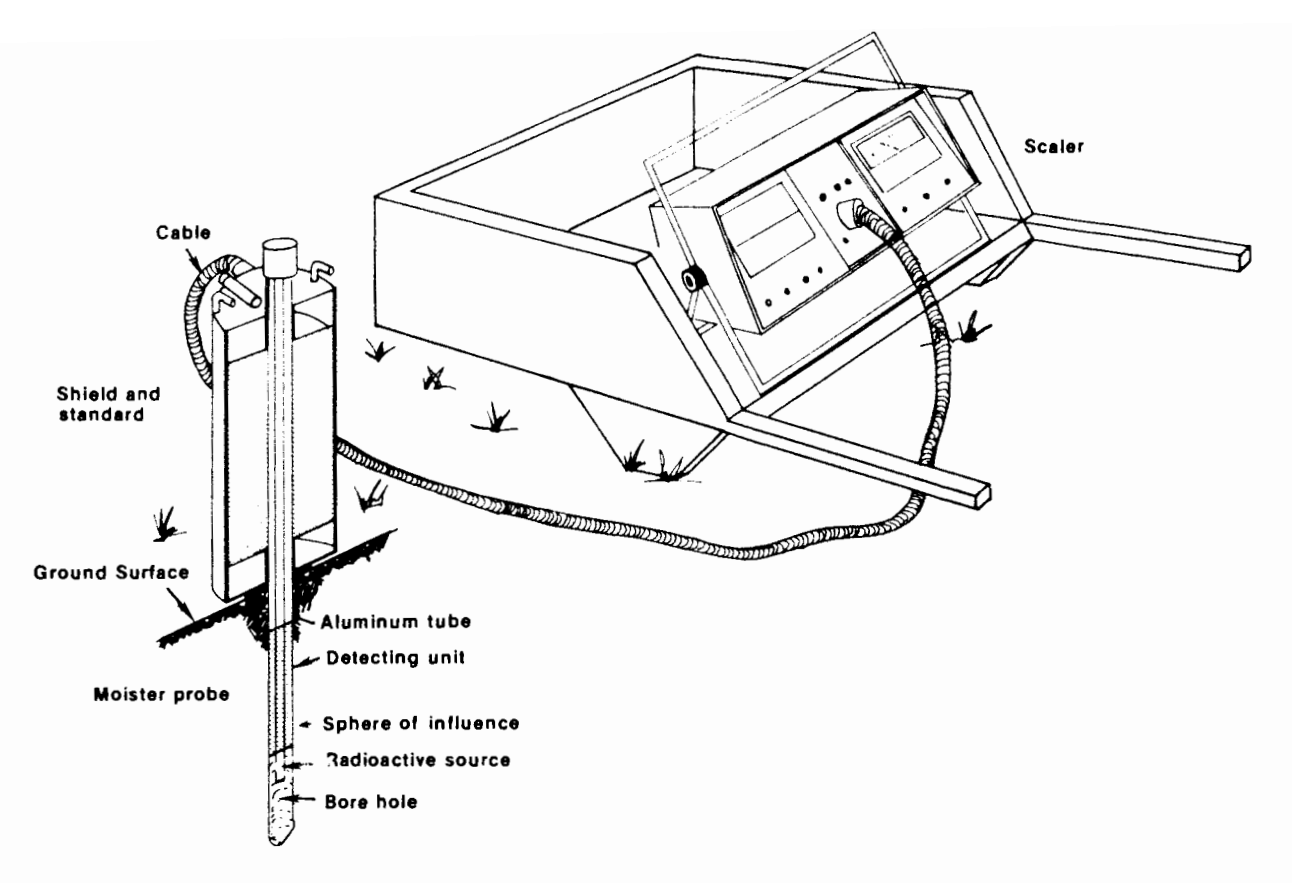


Figure 4.31 Schematic of a neutron probe and scaler for measuring soil moisture.

but in actual practice they are frequently slightly curvilinear (Van Bavel et al., 1963). Field and laboratory calibration procedures are described by Van Bavel et al. (1963).

The sphere of influence for soil moisture readings by the neutron probe is affected by the mositure content of the soil, with this sphere increasing with decreasing soil moisture. This phenomenon affects the accuracy of soil moisture determinations near the ground surface, thereby affecting measurements made prior to an irrigation event more than afterward. As a consequence, soil moisture measurements with a neutron probe are usually unreliable within 10 to 30 cm of the ground surface and the first neutron probe reading is usually taken at a depth of 30 cm and the soil moisture content above this depth is measured gravimetrically.

**Touch-and-feel.** As a means of developing a rough estimate of soil moisture status, the touch-and-feel method is frequently used. A handful of soil is taken and squeezed into a ball about 2 to 3 cm in diameter. Then, knowing the soil type, the response of the squeezed soil can be related to the descriptions listed in Table 4.14 to arrive at the estimated depletion level. Merriam (1960) has developed a similar table which gives the moisture deficiency in in./ft.

A person can develop a calibration for various soil types in a local region by collecting gravimetric samples whenever the touch-and-feel method is used. In this manner, the person will improve the accuracy of soil moisture status estimates at a later date when only the touch-and-feel method is used.

Soil Water 95

TABLE 4.14 ESTIMATING SOIL MOISTURE STATUS BY THE TOUCH-AND-FEEL METHOD

	Feel or appe	Feel or appearance of soil by general texture groups	
Percent depletion	Light loamy fine sand- fine sandy loam	Medium very fine sandy loam-silt	Fine and very fine sandy clay loam-clay
100-75	Dry; loose; flows through fingers	Powdery; dry; will not form a ball*	Hard, baked, cracked; some- times has loose crumbs on surface
75-50	Appears to be dry; will not form a ball*	Dry, almost powdery; a ball can be formed under pressure; the ball is very crumbly and hardly holds its shape; will not ribbon; soil too crumbly <sup>b</sup>	Somewhat pliable; will ball under pressure <sup>a</sup>
50-25	Tends to ball under pressure but seldom holds together	Forms a pliable ball; soil does not stick to hand; no moisture on hand, just damp feeling; ribbons readily; soil has no slick feeling	Forms a pliable ball; ribbons readily; soil sometimes has a slick feeling
25-0	Forms a weak ball; breaks easily; has no slick feeling	Forms tight plastic ball; slightly sticky; ribbons easily; solid; slick feeling, with moist particles left on hands	Easily ribbons out between fingers; has a slick feeling
0 (field capacity)	Upon squeezing no free water appears on soil but wet outline of ball is left on hand	Same as Light	Same as Light

"Ball is formed by squeezing a handful of soil firmly.

<sup>b</sup>Ribbon is formed by squeezing soil out between thumb and forefinger.

Source: After Merriam (1960).

# **Bulk Density**

The bulk density, or bulk specific weight, of a soil mass,  $\gamma_b$ , is the dry weight of soil per unit bulk volume (in Fig. 2.2), which is expressed g/cm<sup>3</sup>. Measurements of bulk specific weight are commonly made by extracting a soil sample, then measuring the bulk volume, and drying the sample in an oven to determine the soil moisture content. The dry weight of soil,  $W_b$ , is then used as follows to establish  $\gamma_b$ :

$$\gamma_b = \frac{W_b}{V} \tag{4.57}$$

Many methods have been developed for determining bulk density; most use a metal cylinder sampler that is driven to the desired depth in the soil profile either manually or mechanically. Since bulk density can vary considerably with depth and over an irrigated field, it is necessary to make a number of measurements in order to develop reasonable estimates of volumetric moisture content in the root zone.

# Field Capacity

Field capacity is a useful concept in irrigation, but cannot be precisely defined. The most common method of determining field capacity is using a pressure plate system that will apply a pressure to a saturated soil sample. When water is no longer leaving the soil sample, the soil sample is removed and placed in an airtight container for weighing. Then it is placed in an 105°C oven to determine the soil moisture content. This test should be run at  $\frac{1}{10}$  atm for a light sandy soil and  $\frac{1}{3}$  atm for a heavy clay loam soil. Frequently, the pressure plate system will be used to determine  $\theta$  for many capillary pressures (e.g.,  $\frac{1}{10}$ ,  $\frac{1}{3}$ ,  $\frac{1}{2}$ , 1, 2, 5, 10, and 15 atm), so that the soil moisture retention curve can be drawn for the particular soil type.

A more reliable technique for establishing field capacity is to irrigate a test plot in the field. The irrigation should continue until the soil profile has been wetted for a depth of about 1 m or more. The ponds illustrated in Fig. 4.26 for measuring infiltration would be suitable provided that the pond width was at least 1 to 3 m. (In fact, if the ponding method is used for measuring infiltration, the test could be continued, as described below, to measure field capacity.) Once the irrigation water has infiltrated into the soil, the plot (or pond) is covered with a plastic membrane that will prevent soil evaporation. Then, every 24 h afterward, the soil moisture is measured until there is very little change, thus yielding an estimate of  $\theta_{fc}$ .

# Permanent Wilting Point

Most commonly, the soil moisture content at the permanent wilting point,  $\theta_{wp}$ , is taken as the moisture content corresponding to -15 bar. Although  $\theta_{wp}$  can be somewhere between -10 and -20 bar, the soil moisture content normally varies very little in this range, so that using the data for -15 bar provides a reasonable

Soil Water 97

estimate. Also, an irrigation event usually occurs well before the root zone soil moisture has been reduced to  $\theta_{wp}$ , unless the water is not available when required.

The actual measure of permanent wilting point requires the growing of a reference crop (dwarf sunflower) in a series of watertight containers with an opening in each lid for a single plant to pass through (the air space between the opening and plant stem is filled with cotton to reduce soil evaporation). The soil moisture corresponding to  $-\frac{1}{3}$  bar is maintained until the third pair of leaves have developed. Then the plant is no longer watered. When all three pairs of leaves have wilted (without regaining turgor after 10 to 15 h in a dark, humid chamber), the plant is cut at the soil surface and the soil moisture content measured and correlated to the permanent wilting point.

## **EXAMPLE PROBLEMS**

# Example 4.1

A cutthroat flume is located in an irrigation canal. It is 6 ft long and has a throat width of 2 ft. Measurements of upstream depth  $(h_u)$  and downstream depth  $(h_d)$  reveal a submergence  $(h_d/h_u)$  of 80%. If the  $h_u$  reading were used in the free-flow equation, the discharge would be 10 ft<sup>3</sup>/s. What is the actual flow passing through the flume?

First, Fig. 4.4 is consulted to identify the rating of the flume:  $n_f = 1.645$ ,  $n_s = 1.389$ ,  $K_f = 3.72$ ,  $K_s = 2.03$ , and  $S_t = 74.3\%$ . From these parameters the free-flow and submerged-flow coefficients,  $C_f$  and  $C_s$ , in Eqs. 4.6 and 4.7 can be determined:

$$C_f = K_f W^{1.025} = 3.72(2)^{1.025} = 7.57$$
  
 $C_s = K_s W^{1.025} = 2.03(2)^{1.025} = 4.131$ 

The problem states that if the flow regime in the flume were free, using  $h_u$  in Eq. 4.4 along with the appropriate value of  $C_f$  and  $N_f$  would yield a discharge of 10 ft<sup>3</sup>/s. Thus, by rearranging Eq. 4.4,  $h_u$  can be computed:

$$h_u = \left(\frac{Q}{C_t}\right)^{1/n_t} = \left(\frac{10}{7.57}\right)^{1/1.645} = 1.184 \text{ ft}$$

The value of  $h_d$  is found by rearranging Eq. 4.2:

$$h_d = Sh_u = 0.80(1.184) = 0.948 \text{ ft}$$

The actual discharge is now found from Eq. 4.5 (with  $C_2 = 0$  for cutthroat flumes):

$$Q_{\text{actual}} = \frac{C_s (h_u - h_d)^{n_t}}{(-\log s)^{n_s}} = \frac{4.131(1.184 - 0.948)^{1.645}}{[-\log (0.8)]^{1.389}} = 9.89 \text{ ft}^3/\text{s}$$

#### Example 4.2

A Parshall flume installation is to be designed for a canal condition in which the following conditions are expected: constructed depth of canal is 1.45 ft; minimum freeboard is 0.17 ft (2 in.); maximum discharge is 12.5 ft<sup>3</sup>/s; and normal flow depth is 0.95 ft at the 12.5-ft<sup>3</sup>/s flow. What flume would you select, and how would you install it?

The installation of the flume in the canal will increase the upstream depth but not the downstream depth. The maximum allowable upstream depth is the constructed depth minus the necessary freeboard, or 1.45 - 0.17 = 1.28 ft. The Parshall flumes that will pass 12.5 ft<sup>3</sup>/s under free-flow conditions with a  $h_u$  value of 1.28 or less can be determined using Eq. 4.4 and the rating coefficients found in Table 4.2. For example, a 2-ft flume will pass only 11.7 ft<sup>3</sup>/s at a head of 1.28 ft. The smallest flume that can be used is the 30-in. (14.68 ft<sup>3</sup>/s at  $h_u = 1.28$  ft). If the 30-in, flume is used, the  $h_u$  value for the 12.5-ft<sup>3</sup>/s flow will be  $(n_f = 1.555, C_f = 10.0)$ 

$$h_u = \left(\frac{12.5}{10.0}\right)^{1.1.555} = 1.15 \text{ ft}$$

If the flume is located in the canal such that the base of the throat section rests on the bottom, then from examining Fig. 4.2, the inlet will rest 9 in. or 0.75 ft above the bottom. This will cause the water depth upstream of the flume to be 1.15 ft plus 0.75 ft, or 1.90 ft, which exceeds the constructed depth. Thus the flume installer must carefully consider the raise in water level upstream in the placement of the inlet relative to the canal bottom. Suppose the flume is installed so that the inlet rests on the channel bottom. In this case the downstream depth in the flume would be 0.95 ft. (Note that while  $h_d$  is measured below the inlet, it must be referenced to that elevation.) The submergence ratio, S, would be 0.95/1.15 = 82.6%, which from Table 4.2 exceeds the transition submergence. This is a workable solution but not optimal since the flow would be submerged. Thus one must similarly be careful about the elevation of the flume, to avoid submerged flow if possible. The solution to this problem is to raise the flume above the channel bottom until the submergence is below the transition value while selecting flumes which do not raise the water level upstream above the freeboard level (1.28 ft). The following table illustrates the iterative process of the design-selection procedure.

Flume	$h_{\mu}{}^{\mathrm{a}}$	$\Delta E^{h}$	Sc
30 in.	1.154	0.126	71.4%
3 ft	1.027	0.253	67.9%
4 ft	0.8545	0.4255	61.4%

<sup>&</sup>lt;sup>a</sup>Upstream head for the design flow of 12.5 ft<sup>3</sup>/s.

One will now observe that the 30-in. flume will not operate in the free-flow range, whereas both the 3- and 4-ft flumes will. Since the 3-ft flume would normally be less expensive than the 4-ft flume, this is the selection for the problem. In its installation, the inlet invert should be situated 0.253 in. (3 in.) above the channel bottom.

This type of design installation problem is common to all free measuring flumes. The consideration and technique involved are also applicable to weir installations. In summary, the design task is to achieve a free-flow condition with minimum head loss and without exceeding a maximum allowable upstream water level.

<sup>&</sup>lt;sup>b</sup>Maximum difference between the elevation of the channel bottom and the flume inlet,  $\Delta E = 1.28$ 

<sup>-</sup>h

 $<sup>^{\</sup>circ}$ Minimum submergence at the design flow = (0.95)

 $<sup>-\</sup>Delta E)/h_u$ .

### Example 4.3

The recycling infiltrometer shown in Fig. 4.30 was installed to measure the infiltration in a field being furrow irrigated. The furrows in the field were spaced 0.75 m apart. The section of furrow actually tested was 6.5 m long with a cross-sectional shape that led to the following simplification of the Manning equation:

$$Q = (34.295) \frac{S_0^{0.5}}{n} A^{1.36^{-}}$$

in which  $S_0$  is the slope of the furrow (0.8%), n is the Manning roughness coefficient (taken to be 0.04 in these measurements), A is the cross-sectional area in  $m^2$ , and Q is the flow in  $m^3$ /min. The infiltrometer tank was circular with a 60-cm diameter. Water from it was pumped at a rate of 2.0 liters's for a period of 6 hrs. The recorded water-level readings in the infiltrometer tank were as follows:

Elapsed time of reading (min)	Tank reading (cm)
0	150
5	138.6
10	133.5
20	126.1
30	120.3
60	107.0
90	96.6
120	87.8
240	59.9
360	38.1

Using these data, find the parameters for the cumulative Kostiakov infiltration function (the integrated form of Eq. 2.21).

The solution to this problem must begin by recognizing that when Eq. 2.21 is integrated, the resulting function is

$$Z = k\tau^a$$

in which k and a are the same empirical parameters,  $\tau$  is the intake opportunity time in minutes, and Z is the cumulative infiltration in meters. Water infiltrating into the 6.5-m furrow actually does so through the furrow's wetted perimeters, but for mathematical purposes we assume that it occurs into a strip equal to the furrow spacing wide and the 6.5 m long. Thus  $A_t$  in Eq. 4.54 is

$$A_f = 6.5 \text{ m} \times 0.75 \text{ m} = 4.875 \text{ m}^2$$

The cross-sectional area of the reservoir,  $A_r$ , is

$$\frac{\pi d^2}{4} = \frac{\pi (0.60 \text{ m})^2}{4} = 0.28274 \text{ m}^2$$

Utilizing the data above and Eq. 4.56 where C = A, A, yields the following values of Z as a function of  $\tau$ :

Z	τ
(m)	(min)
0	0
0.00661	.5
0.00958	10
0.01386	20
0.01722	3()
0.02493	60
0.03095	90
0.03690	120
0.05226	240
0.06490	360

The Z versus  $\tau$  results can be plotted on log-log paper to find the values of k and a, or one can use the linear regression capability of most hand-held calculators. Either way, the results yield

$$Z = 0.0028 \tau^{0.534}$$

# **HOMEWORK PROBLEMS**

- **4.1.** (a) A channel carries a flow of about 10 ft<sup>3</sup>/s. Which Parshall flumes could be used to measure this flow?
  - (b) Knowing that the flume is to operate in the free-flow regime, what would the  $h_u$  reading be for each flume that you selected in part (a)?
- **4.2.** Determine the free-flow and submerged-flow rating equation (Eqs. 4.4 and 4.5) for a cutthroat flume 6 ft long and having a 2.5-ft throat width. What would be the free-flow  $h_u$  reading with a discharge of 5 ft<sup>3</sup>/s? If a submerged flow regime existed at this discharge, submergence being 80%, what would the  $h_u$  value be?
- **4.3.** Would trapezoidal flume 2 carry the flow given in Problem 4.1? What would  $h_u$  be?
- **4.4.** A cutthroat flume is being used to measure irrigation water in a local lateral. The flume is 2.13 m long. A technician who did not know about flume hydraulics read  $h_u$ , looked in his tables, and recorded a discharge of 0.709 m<sup>3</sup>/s. He also recorded  $h_d$  because he was so instructed. Sometime later an engineer checked the data and found the flume submergence to be 85% and had to adjust the recorded discharge. How much adjustment was necessary?
- **4.5.** The broad-crested weir installation shown in Fig. 4.7 is operating in a trapezoidal canal with the following characteristics:  $b_1 = 1.3$  m. z = 1.5:1, and the constructed depth is 1.5 m. The dimensions of the weir are  $L_1 = 2.0$  m, s = 0.50 m,  $L_2 = 1.0$  m, and  $L_3 = 2.0$  m. What is the discharge passing over the weir if the vertical gage reading,  $y_1$ , is 0.60 m? Assume an absolute roughness height of 0.0002.
- **4.6.** The upstream head on a rectangular sharp-crested weir is 0.40 m. The weir has a crest

- width, b, of 2 m and is located in a channel 4 m wide. What is the discharge passing over the structure? Assume that the value of p is 0.5 m.
- **4.7.** Design a V-notch weir that will pass the flow you found in Problem 4.5 as its maximum discharge.
- **4.8.** A contracted rectangular sharp-crested weir is needed to measure up to 0.20 m<sup>3</sup>/s in an irrigation system. The weir is being placed in a rectangular channel 2 m wide and 54.3 cm deep. The weir crest must be 5 cm above the downstream water depth, which under normal flow conditions is 26.1 cm. (No provisions for free board are needed and no additional free board is allowed.) It is desirable to constrict the flow as much as possible to improve the weir accuracy. What dimensions would you recommend?
- **4.9** As a laboratory exercise, arrange with a local irrigator an evaluation of one of his fields during an upcoming irrigation. Collect data on soil moisture, field topography, and geometry prior to irrigation. If you can, make an infiltration measurement prior to the irrigation. During and immediately following the irrigation, measure the inflow, outflow, advance, recession, and furrow shape (if the field has furrows). Prepare a detailed professional report on the activity.

### REFERENCES

- ACKERS, P., W. R., WHITE, J. A. PERKINS, and A. J. M. HARRISON. 1978. Weirs and Flumes for Flow Measurement. John Wiley & Sons Ltd., Chichester, West Sussex, England.
- American Society of Agricultural Engineers (ASAE). 1980–1981. Agricultural Engineer's Yearbook, 27th ed. St. Joseph, Mich.
- Bennett, R. S. 1972. Cutthroat Flume Discharge Relations. Unpublished M.S. thesis, Colorado State University, Fort Collins, Colo.
- BONDURANT, J. A. 1957. Developing a Furrow Infiltrometer. Agric. Eng. 602-604. August.
- Bos, M. G. (ed.). 1976. Discharge Measurement Structures. Publ. 20, International Institute for Land Reclamation and Improvement (ILRI), Wageningen, The Netherlands.
- Bos, M. G., R. A. Replogle, and A. J. Clemmens. 1984. Flow Measuring Fluries for Open Channel Systems. John Wiley & Sons, Inc., New York.
- HAISE, H. R., W. W. DONNAN, J. T. PHELAN, L. F. LAWHON, and D. G. SHOCKLEY. 1956. The Use of Cylinder Infiltrometers to Determine the Intake Characteristics of Irrigated Soils. Publ. ARS 41-7. U.S. Department of Agriculture, Agricultural Research Service and Soil Conservation Service, Washington, D.C., May.
- HOLTAN, H. N., N. E. MARSHALL, and L. L. HARROLD. 1962. Field Manual for Research in Agricultural Hydrology. Agric. Handb. 224, U.S. Department of Agriculture, Agricultural Research Service, Washington, D.C., June.
- HYATT, M. L. 1965. Design, Calibration, and Evaluation of a Trapezoidal Measuring Flume by Model Study. Unpublished M.S. thesis, Utah State University, Logan, Utah.
- KINDSVATER, C. E., and R. W. C. CARTER. 1957. Discharge Characteristics of Rectangular Thin-Plate Weirs. ASCE J. Hydraul. Div. 83 (HY6):1–36.
- LEY, T. W. 1978. Sensitivity of Furrow Irrigation Performance to Field and Operation Variables. Unpublished M.S. thesis, Colorado State University, Fort Collins, Colo.
- MALANO, H. M. 1982. Comparison of the Infiltration Process Under Continuous and Surge Flow. Unpublished M.S. thesis, Utah State University, Logan, Utah.

- MERRIAM, J. L. 1960. Field Method of Approximating Soil Moisture for Irrigation. *Trans. ASAE* 3(1):31–32.
- PARSHALL, R. L. 1926. The Improved Venturi Flumes. Trans. Am. Soc. Civ. Eng. 89:841–880.
- Peri, G., G. V. Skogerboe, and D. I. Norum. 1979. Evaluation and Improvement of Basin Irrigation. Water Manage. Tech. Rep. 49B. Water Management Research Project, Colorado State University, Fort Collins, Colo., June.
- REPLOGLE, J. A. 1975. Critical-Flow Flumes with Complex Cross Section. *Proc. ASCE Irrig. Drain. Div. Spec. Conf.* Logan, Utah, August 13–15, pp. 336–388.
- ROBINSON, A. R., and A. R. CHAMBERLAIN. 1960. Trapezoidal Flumes for Open Channel Flow Measurement. *Trans. ASAE* 3(2):120–124, 128.
- SALAZAR, L. J. 1977. Spatial Distribution of Applied Water in Surface Irrigation. Unpublished M.S. thesis, Department of Agricultural and Chemical Engineering, Colorado State University, Fort Collins, Colo.
- SHEN, J. 1981. Discharge Characteristics of Triangular-Notch Thin-Plate Weirs. Water Supply Pap. 1617-B. U.S. Geological Survey.
- SHOCKLEY, D. G., J. T. PHELAN, L. F. LAWHON, H.R. HAISE, W. W. DONNAN, and L. L. MYERS. 1959. A Method for Determining Intake Characteristics of Irrigation Furrows. Publ. ARS 41-31. U.S. Department of Agriculture, Agricultural Research Service and Soil Conservation Service, Washington, D.C., April.
- SKOGERBOE, G. V., M. L. HYATT, R. K. ANDERSON, and K. O. EGGLESTON. 1967a. Design and Calibration of Submerged Open Channel Flow Measurement Structures: Part 3, Cutthroat Flumes. Rep. WG31-4. Utah Water Research Laboratory, Utah State University, Logan, Utah, April.
- SKOGERBOE, G. V., M. L. HYATT, and K. O. EGGLESTON. 1967b. Design and Calibration of Submerged Open Channel Flow Measurement Structures: Part 1, Submerged Flow. Rep. WG31-2, Utah Water Research Laboratory, Utah State University, Logan, Utah, February.
- SKOGERBOE, G. V., M. L. HYATT, J. D. ENGLAND, and J. R. JOHNSON. 1967c. Design and Calibration of Submerged Open Channel Flow Measurement Structures: Part 2, Parshall Flumes. Rep. WG31-3, Utah Water Research Laboratory, College of Engineering, Utah State University, Logan, Utah, May.
- SKOGERBOE, G. V., R. S. BENNETT, and W. R. WALKER. 1972. Generalized Discharge Relations for Cutthroat Flumes. ASCE J. Irrig. Drain. Div. 98(IR4):569–583.
- SKOGERBOE, G. V., R. S. BENNETT. and W. R. WALKER. 1973. Selection and Installation of Cutthroat Flumes for Measuring Irrigation and Drainage Water. Tech. Bull. 120, Experiment Station, Colorado State University, Fort Collins, Colo.
- TROUT, T. 1983. Recalibration of the Powlus Fiberglass V-notch Furrow Flume. Personal communication, May.
- U.S. Bureau of Reclamation (USBR). 1974. Water Measurement Manual. 2nd ed., Revised Reprint. U.S. Government Printing Office, Washington, D.C.
- U.S. Department of Agriculture, Soil Conservation Service. 1962. Measurement of Irrigation Water. Irrigation, SCS National Engineering Handbook. U.S. Government Printing Office, February, Sec. 15, Chap. 9.
- VAN BAVEL, C. H. M., P. R. NIXON, and V. L. HAUSER. 1963. Soil Moisture Measurement with the Neutron Method. Publ. ARS 41-70. U.S. Department of Agriculture, Agricultural Research Service. Washington, D.C., June.

# Evaluation of the Field System

### **OBJECTIVES OF EVALUATION**

The principal objective of evaluating an irrigation system is to identify alternatives that may be both effective and feasible in improving the system's performance. For instance, the evaluation may reveal that the application efficiency could be improved by limiting the duration of the irrigation. Uniformity may be improved by adjusting the flow rate. It also may be discovered that the field length or slope requires modification for the existing system to operate more effectively. Evaluations of surface-irrigated fields yield not only data which can be used to detect problems but also information essential to achieving high levels of management and control. Repeated evaluations indicate the dynamic behavior of the field over a season and from year to year. In the more intensive investigations, important data describing the basic infiltration characteristics of the field are collected.

Several approaches to a surface irrigation evaluation can be taken depending on the time and effort that can be invested in the study. This chapter outlines a basic methodology for estimating the application efficiency, deep percolation ratio, field tailwater ratio, and water requirement efficiency from the volume balance theory outlined in Chapter 16. Various alternatives for estimating the components in the performance equations are described. For this chapter to be useful by itself, many of the mathematical relations pertinent to the analysis will be previewed. For a more detailed discussion, the reader is referred to Chapter 16.

The field measurement techniques outlined in Chapter 4 provide the means for defining the following six important elements in a volume balance evaluation:

- 1. The inflow discharge (per furrow or per unit width in a border or basin)
- 2. The advance and recession of the water over the field surface
- 3. The tailwater discharge (if allowed by the system)
- 4. The soil moisture deficit prior to the irrigation
- 5. The volume of water on the soil surface at various times
- 6. An indication of the infiltration characteristics of the soil surface

Individual measurement of these six elements is both time consuming and expensive, so a number of procedures have been developed for estimating one or more from a limited study of the rest. Thus, before describing the analyses for computing the measures of efficiency, four intermediate evaluations will be discussed. These are an inflow-outflow analysis, the advance-recession trajectories, an advance-surface storage assessment, and an investigation of infiltration. Of the six parameters listed above, only the inflow discharge and soil moisture deficit must be known in all cases.

## INFLOW-OUTFLOW

The inflow discharge onto a field can be measured with various flow-measuring devices. The data yield a hydrograph which can be integrated to determine the total volume of water applied. Usually, the inflows are maintained at a steady rate and the volume applied is simply the discharge multiplied by time. A tailwater runoff (outflow) hydrograph can be obtained in a similar manner (except where the end of the field is diked). An example of an inflow-outflow hydrograph for a single furrow on an irrigated field in northeastern Colorado is shown in Fig. 5.1.

Three useful pieces of information can be obtained from the inflow-outflow hydrograph. First, the integration of the individual hydrographs, and then their comparison, provide an accurate measurement of the total volume of water infiltrating into the soil:

$$V_z = V_{\rm in} - V_{\rm tw} \tag{5.1}$$

in which  $V_z$ ,  $V_{\rm in}$ , and  $V_{\rm iw}$  are the total volume of infiltration, inflow, and runoff, respectively. Thus the inflow-outflow hydrographs establish the aggregate volume balance.

The second parameter defined by the inflow-outflow hydrograph is the steady-state or "basic" infiltration rate. Note in Fig. 5.1 that the difference between the constant portion of the two hydrographs is approximately 46.2 liters/min. Thus, in the 625 m of furrow, the average basic intake rate,  $f_0$ , is 0.0739 liters/min per meter.

Finally, the inflow-outflow hydrographs can be used in conjunction with the value of  $f_0$  to yield an estimate of the surface water storage at the time of cutoff,  $t_{co}$ . Again, using Fig. 5.1 as an example, the volume of tailwater runoff occurring after  $t_{co}$  can be found from integrating the runoff hydrograph from t = 691 min to

Inflow-Outflow

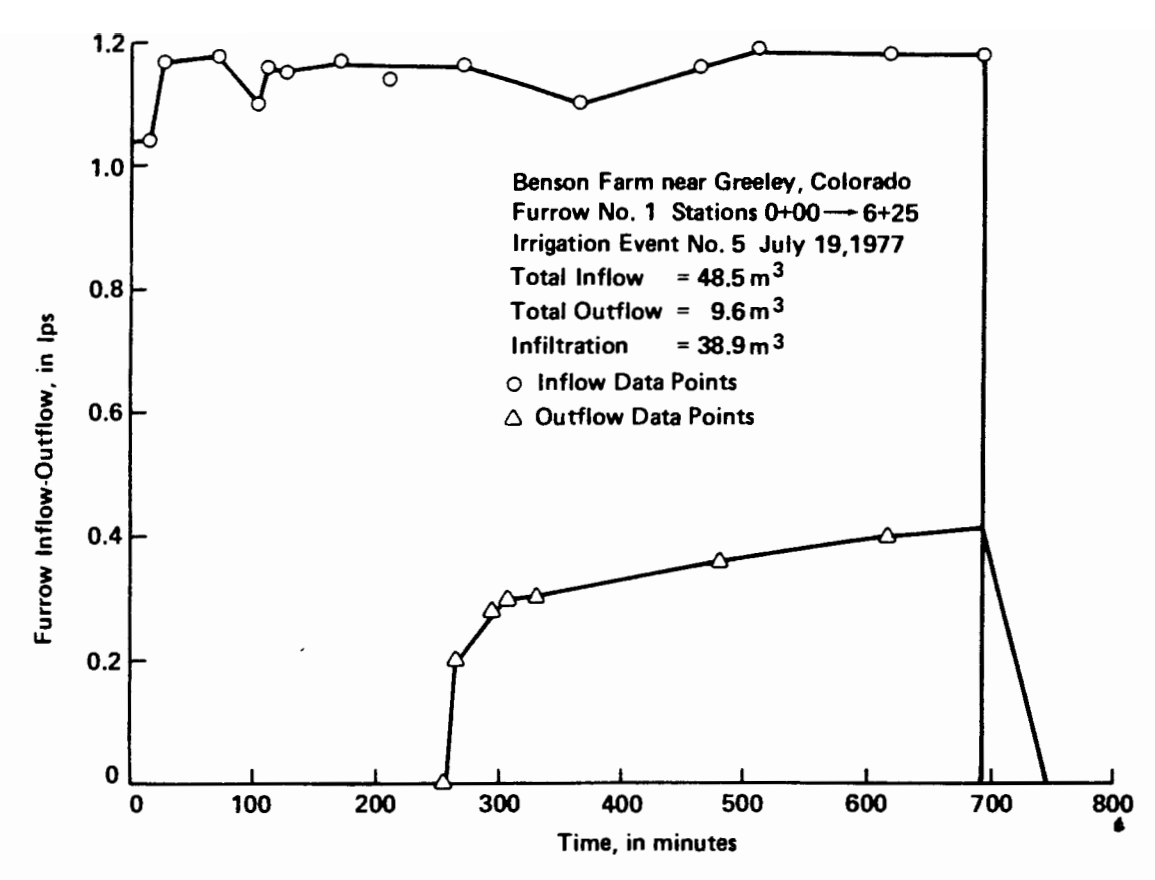


Figure 5.1 Example of an inflow-runoff hydrograph for a furrow-irrigated field. (From Salazar, 1977.)

t = 745 (the time of recession). This value is found to be 648 liters. If the recession rate is assumed to be linear, the volume of infiltration during recession,  $(V_z)_{rec}$ , is

$$(V_z)_{\text{rec}} = \frac{(46.2 \text{ liters/min}) (54 \text{ min})}{2} = 1247 \text{ liters}$$
 (5.2)

Therefore, the estimated surface storage at  $t_{co}$  is 1895 liters (648 liters + 1247 liters).

#### ADVANCE AND RECESSION

Under surface-irrigated systems, the time interval during which water will infiltrate at a specified location is defined by the time water flow first reaches the point (advance) and the time following cutoff when water eventually drains from the point (recession). The advance and recession trajectory or the time-space distribution of irrigation water thereby defines the intake opportunity time over the entire field surface and yields information necessary in the evaluation application efficiencies and uniformities.

The advance of water over the surface is also an important consideration in managing surface irrigation systems. The time that it takes for water to reach the end of the field is very often a close approximation of the cutoff time. It provides the time of field tailwater flow or lower-end ponding. Consequently, the advance

Chap. 5

trajectory is often described mathematically for input to system management. The most common approximation is the simple power function

$$(t_a)_x = p'x^{r'} (5.3)$$

where x is the advance distance (m) achieved in  $t_a$  minutes of inflow, and p' and r' are fitting parameters. Elliott and Walker (1982) concluded after various comparisons of Eq. 5.3 with more elaborate forms and methods of fitting that the best results are achieved by a two-point fitting of the equation. The time of advance to one-half the field length, L/2, and the advance to the end, L, can be solved simultaneously to define the empirical parameters, p' and r':

$$r' = \frac{\ln(t_{0.5L}/t_L)}{\ln(0.5)} \tag{5.4}$$

and

$$p' = \frac{t_L}{L'} \tag{5.5}$$

in which  $t_{0.5L}$  and  $t_L$  are the advance times to the middistance and field end, respectively. An alternative form using an exponential parameter is

$$(t_a)_x = p'' x e^{r'' x} ag{5.6}$$

where p'' and r'' are again fitting parameters. It is probably worthwhile to note that estimation of  $t_L$  is more important than exactly matching intermediate points. An example of two sets of advance data fitted by Eqs. 5.3 and 5.6 is given in Fig. 5.2.

For basin irrigation, advance and recession usually have to be plotted differently than for furrow or border irrigation. Since basins are normally intended to be level, the undulations in the ground surface have a major effect on both advance and recession. Thus, rather than plotting the length of travel of the advancing front against time, the watered and dewatered area of the basin are plotted against time.

To illustrate the collection and interpretation of advance-recession data in basins, an actual field study will be presented (Kundu and Skogerboe, 1980). A basin 36.6 m wide and 36.6 m long was constructed immediately following precision land leveling. The soil was a silty clay loam having a bulk density of  $1.50 \text{ g/cm}^3$  and a porosity of 45%. The basin was staked with a 6- by 6-m grid and then irrigated with a 13.84-liter/s inflow. Table 5.1 lists data for time of advance,  $t_a$ , and time of recession,  $t_r$ , for each station, along with the infiltration opportunity time,  $\tau$ . Contours drawn at different times during advance and recession are shown in Figs. 5.3 and 5.4, respectively.

For this example, the data from the advance contours were plotted on logarithmic paper as illustrated in Fig. 5.5 and described by the following power function:

$$A_x = 33.92(t_a)_x^{0.74} (5.7)$$

in which  $A_x$  is the area wetted (m<sup>2</sup>) in  $t_a$  minutes. A comparison of the contour

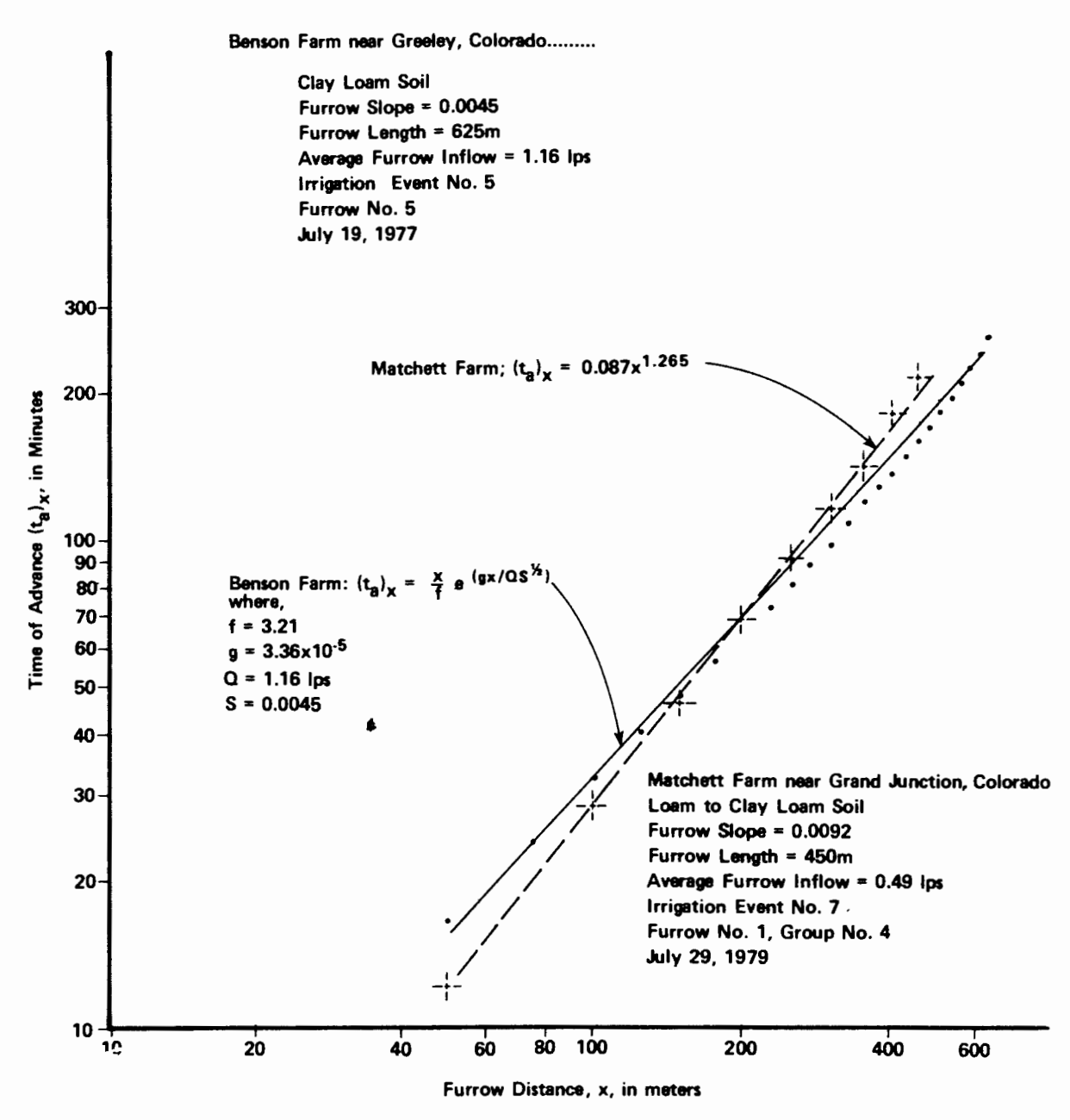


Figure 5.2 Examples of logarithmic plot of advance field data for furrow irrigation. (From Salazar, 1977, and Elliott, 1980.)

data and station data clearly shows the advantage in drawing periodic contours during advance (and also recession).

### ADVANCE-SURFACE STORAGE

The surface storage volume at any time during an irrigation event is an important factor in conducting surface irrigation evaluations. For sloping fields, as in many furrow and border systems, it is generally sufficient to multiply the inlet cross-sectional area by a "shape factor" and then the advance distance to get the surface

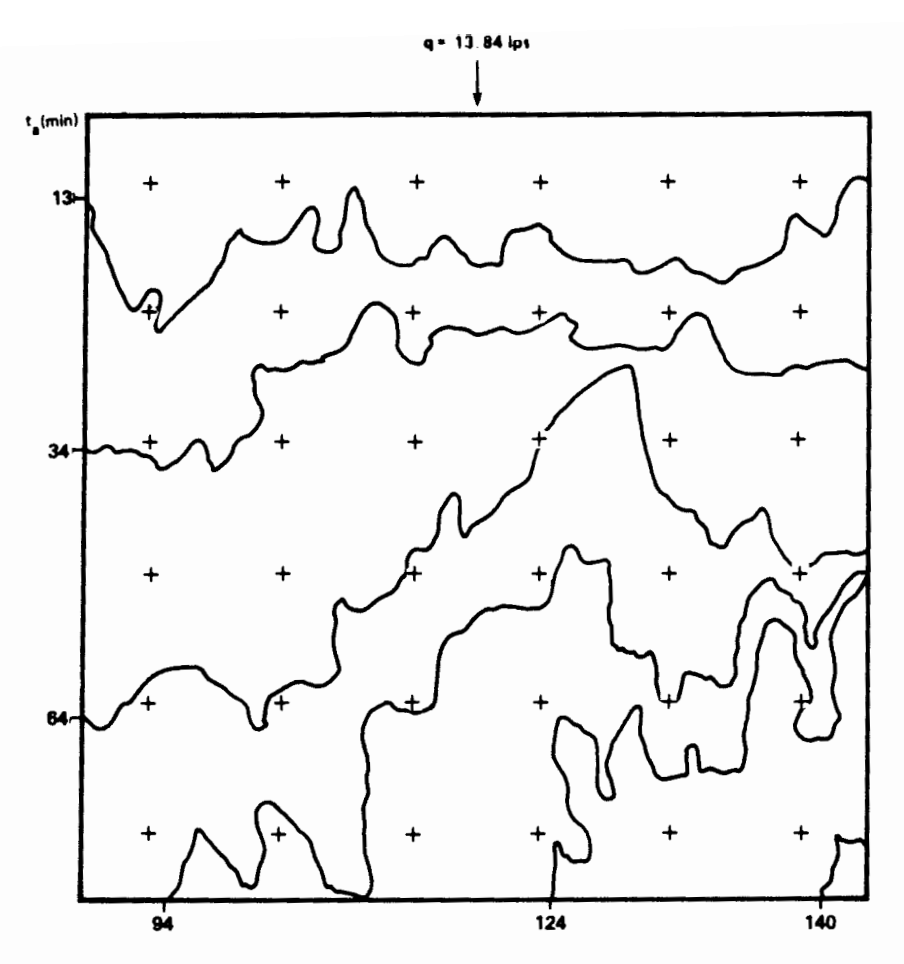


Figure 5.3 Advance contours for the example basin.

storage volume. The inlet area can be found with a uniform flow formula such as the Manning equation.

For low-gradient or level fields such as basins, the surface storage volume may be more accurately estimated by careful monitoring. For the example basin test discussed above, the monitored flow-depth data for the first irrigation event of the season were recorded from a grid of marked stakes. The data, listed in Table 5.2, can be combined with the advance contours in Fig. 5.3 to determine the surface storage volume,  $V_{ss}$ , for each time period during the advance phase. The results for the Colorado tests were as follows:

$(t_a)_x$ (min)	$V_{ss}$ (m <sup>3</sup> )
13	5.6
34	13.7
64	24.8
94	31.2
124	43.8
145	52.9

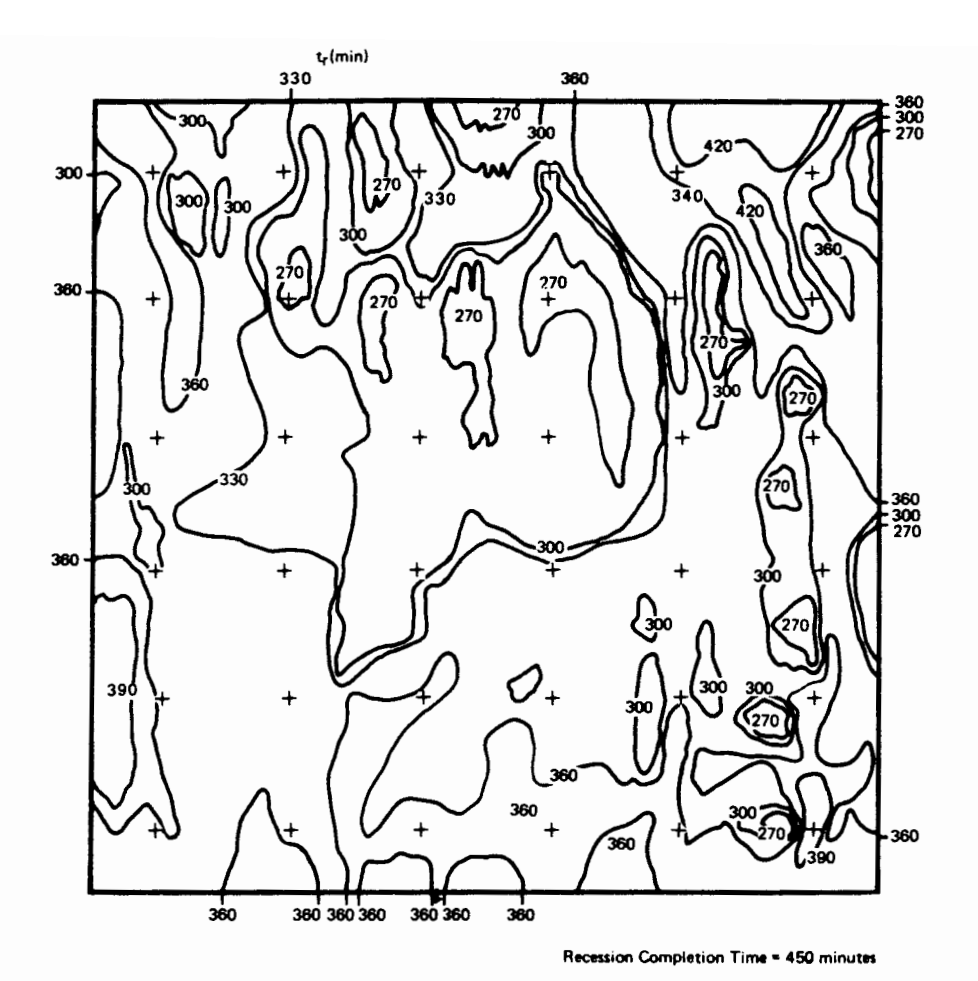


Figure 5.4 Recession contours for the example basin irrigated field.

**TABLE 5.1** TIME OF ADVANCE AND RECESSION MEASURED AT EACH BASIN STATION DURING THE IRRIGATION EVENT

Station	t <sub>a</sub> (min)	t, (min)	τ (min)	τ (rank)	Station	t <sub>a</sub> (min)	t, (min)	τ (min)	τ (rank)
11	3	385	382	4	41	64	300	236	34
12	2	410	408	1	42	77	320	243	28
13	4	315	311	8	43	90	335	245	27
14	6	310	304	9	44	69	308	239	31
15	7	335	328	7	45	51	335	284	13
16	3	400	397	2	46	54	295	241	30
21	19	405	386	3	51	123	375	252	25
22	20	365	345	5	52	94	350	256	23
23	28	265	237	32	53	119	350	231	35
24	18	295	277	19	54	92	360	268	21
25	29	265	236	33	55	67	345	278	18
26	17	350	333	6	56	71	360	289	12
31	37	315	278	17	61	139	405	266	22
32	48	340	292	11	62	132	375	243	29
33	64	285	221	36	63	122	405	283	14
34	40	285	245	26	64	105	385	280	16
35	40	322	282	15	65	99	355	256	24
36	28	330	302	10	66	84	355	271	20

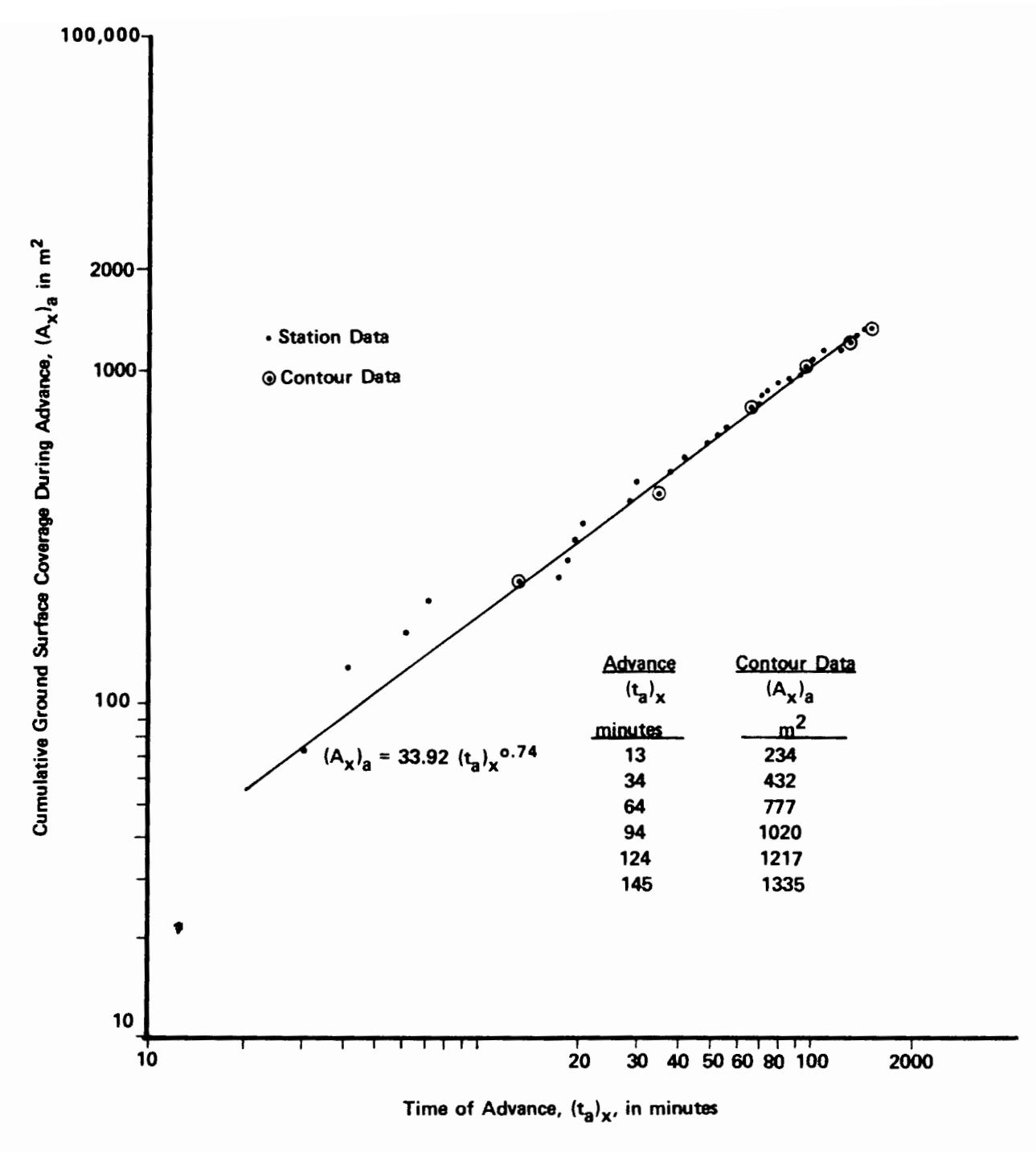


Figure 5.5 Logarithmic plot of advance data for the example basin irrigated field.

This information can be used to determine the basin's infiltration parameters, as will be shown below. Thus measures of uniformity and efficiency can also be computed.

## **INFILTRATION**

The most crucial and often the most difficult parameter to evaluate under the surface-irrigation condition is infiltration, particularly the variation of infiltration characteristics spatially and temporally. In general, a relatively large number of

Infiltration 111

**TABLE 5.2** OBSERVED FLOW DEPTHS (mm) AT SEVERAL TIMES DURING ADVANCE FOR THE FIRST IRRIGATION EVENT ON THE EXAMPLE BASIN IRRIGATED

	36	1 2 2 8 8 4 4 4 8 8   8 4 4 8 4   8 4		99	1		29	38	41
	35	33 30 40 40		65			1	38	41
	34			45	ļ		l	32	41
	33	17 17 40 40		63	1		١	35	48
	32			62	ŀ		1		35
	31	1 1 8 8 8 8 8		61	ı		I	١	51
	26	32 32 33 33 33 33 33 33 33 33 33 33 33 3		99	1		38	4	84
	25	16 3 3 3 5 5 5 5 5 5 5 5 5 5 5 5 5 5 5 5		55	ı		32	35	38
Station number	24	32 22 23 33 34 34 34 34 34 34 34 34 34 34 34 34	Station number	54	ı	1 1	10	35	4
tation 1	23	25 25 25 25 25 25 25 25 25 25 25 25 25 2	tation	53	1		1	59	41
S	22	32 25 27 33 32 33 33 33 33 33 33 33 33 33 33 33	S	52	ı			19	32
	21	14 48 48 48 48 48 48 48 48 48 48 48 48 48		51	ı		١	1	44
	16	32 38 44 88 84 84 84 84		46	١	16	25	53	30
	15	29 35 41 44 44 44		45	I	74	32	32	38
	14	44 48 48 48 15 15		44	1		24	25	30
	13	29 14 44 44 44 44		43	1	1	3	27	32
	12	8 5 5 5 5 5 5 5 5 5 5 5 5 5 5 5 5 5 5 5		42	1		32	38	4
	=	35 44 14 14 44 44		41	I		21	25	25
Time of	advance (t <sub>u</sub> ) <sub>1</sub> (min)	13 34 64 94 124 145	Time of	advance (t <sub>a</sub> ) <sub>t</sub> (min)	13	¥ \$	94	124	145

field measurements of infiltration are required to represent the average field condition. Methods that use a static water condition (such as ring infiltration) often fail to indicate the typically dynamic field condition. As a result, there are two approaches to obtaining field representative infiltration functions based on the response of the field to an actual watering. The first is to adjust the results of point measurements with inflow. The second is to determine the infiltration formula directly from the inflow-outflow, advance-recession, and advance-surface storage volume field data.

# The Adjusted Infiltration Approach

Merriam and Keller (1978) presented cylinder infiltrometer data taken presumably from tests on a border-irrigated field. Some of the data plot as a straight line after a logarithmic transformation, implying that the Kostiakov function is an appropriate model for these data. For other data, curvilinear relations result and were approximated as two linear functions, although such data imply that a Kostiakov–Lewis type of equation employing a basic intake rate term should be used to describe the data. To simplify the illustration of the adjustment approach, the Kostiakov equation will be used in the following discussion.

Merriam and Keller (1978) suggest that a "typical" curve be plotted, on a judgment basis, as a linear fit of the measurements using log-log paper. The slope of the "typical" curve is dictated by the slope of the cylinder infiltrometer data at greater intake opportunity times, while vertical placement of the curve is dictated largely by the data for lower opportunity times (<30 min).

If the infiltration curves found from cylinder infiltrometer data are representative of the field condition, an estimate of the total infiltrated volume during the irrigation should be the same as indicated by the inflow-outflow analysis and/or the advance surface storage analysis. For the basin irrigation example, the results of two cylinder infiltrometer tests were conducted near the center of the basin and are shown in Fig. 5.6. The infiltrometer test data fit a linear relationship on logarithmic paper, yielding the coefficient, k, and exponent, a, for the Kostiakov relation. Then plotting a "typical" curve through both data sets yielded the following intake relation:

$$Z_{\text{typ}} = 2.25 \, \tau^{0.676} \tag{5.8}$$

where  $Z_{\rm typ}$  is the cumulative infiltration in mm and  $\tau$  is the intake opportunity time in min. Equation 5.8 was then used to compute the depth applied at each station as shown in Table 5.3. Based on inflow measurements, the average cumulative infiltrated depth was 111.97 mm compared to an average value of 102.34 mm found from using Eq. 5.8. The coefficient, k, was adjusted as follows:

adjusted 
$$k = 2.25 \left( \frac{111.97 \text{ mm}}{102.34 \text{ mm}} \right) = 2.46$$
 (5.9)

producing the adjusted cumulative infiltration function  $Z_{ad}$ :

$$Z_{ad} = 2.46\tau^{0.676} \tag{5.10}$$

Infiltration

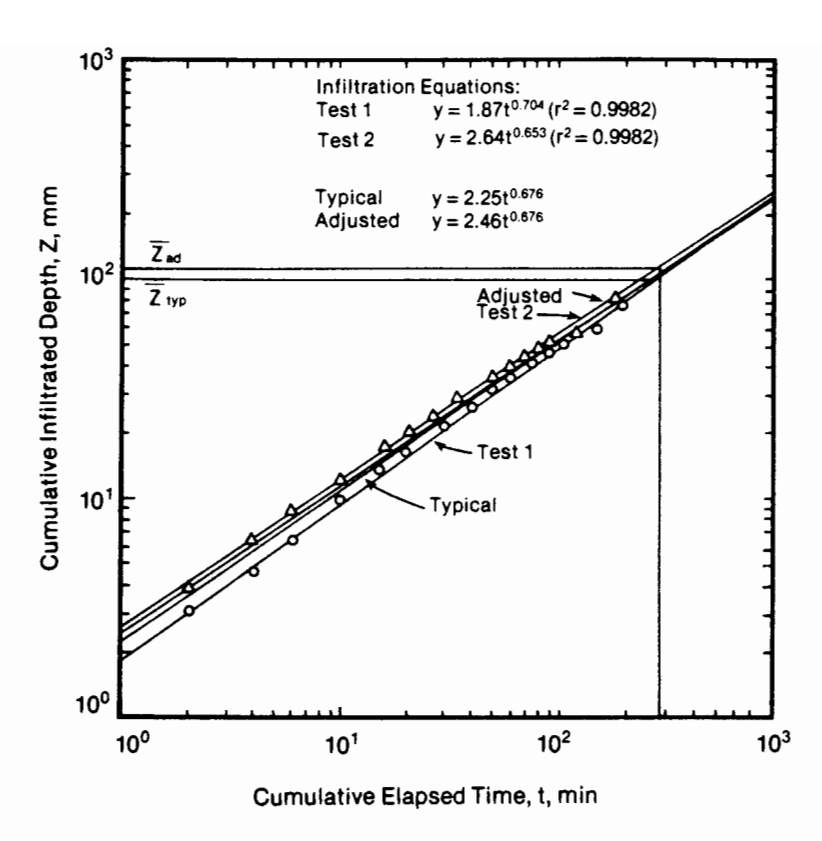


Figure 5.6 Cumulative infiltration curves for irrigation L1.

The remaining question relates to the calculated distribution of infiltrated depths throughout the basin. In this particular case, since the cylinder infiltrometer data provided similar infiltration functions, and because the typical infiltration equation had to be adjusted upward by only 10% (usually, much greater adjustments are required), the investigator can be fairly confident about the calculated distribution of infiltrated depths.

The infiltration equation derived from the infiltrometer measurements and adjusted by mass balance at a specified time can also be checked by advance-surface storage analysis (Table 5.2). Based on inflow measurements, advance contours, and surface storage measurements, the cumulative infiltrated depth during advance is listed in Table 5.4 and plotted in Fig. 5.7 together with Eq. 5.10. In addition, the point corresponding to the termination of the irrigation event (112 mm at 450 min) has been plotted. Equation 5.10 is expected to pass through the point (112 mm, 283.4 min), which is the average infiltrated depth and average opportunity time. Although the comparative fit is not too good, the two methods do yield similar results and illustrate the techniques of adjusting point measurements with larger-scale field observations.

## Infiltration from Advance Data

Elliott and Walker (1982) and their colleagues made a large number of point measurements of infiltration rates using blocked furrow and cylinder infiltrometers. These data did not provide a satisfactory simulation of actual furrow advance nor an accurate prediction of tailwater volume. Consequently, it was concluded that the most effective evaluation methodology is to measure advance rates, hydraulic

**TABLE 5.3** CUMULATIVE INFILTRATE DEPTHS AT EACH STATION IN THE EXAMPLE BASIN IRRIGATED FIELD USING THE "TYPICAL" AND "ADJUSTED" INFILTRATION EQUATIONS•

2 md (mm)	8	101	[0]	86	112	100	103	5 5	6	108	110	113	107	101	112	10	5 5	106
Z <sub>typ</sub> (mm)	8	92	33	6	103	92	95	8	£ &	8	101	104	86	6	102	801	8	8
t (min)	236	243	245	239	284	241	252	256	231	268	278	289	266	243	283	280	256	271
t <sub>a</sub> (min)	\$	11	8	69	51	54	123	94	119	92	<i>L</i> 9	71	139	132	122	105	8	\$
<i>t,</i> (min)	300	320	335	308	335	295	375	350	350	360	345	360	405	375	405	385	355	355
Station	41	42	43	4	45	46	51	52	53	\$	55	99	61	62	63	\$	9	<b>9</b> 8
(mm)	137	143	119	117	124	141	138	128	66	110	66	125	110	114	95	101	112	117
z <sub>typ</sub> (mm)	125	131	109	107	113	129	126	117	91	101	8	114	101	5	87	93	102	107
f (min)	382	408	311	304	328	397	386	345	237	277	236	333	278	292	221	245	282	302
t <sub>a</sub> (min)	3	2	4	9	7	3	19	70	28	18	53	17	37	48	\$	40	40	28
<i>t,</i> (min)	385	410	315	310	335	400	405	365	265	295	265	350	315	340	285	282	322	330
Station	=	12	13	14	15	16	21	22	23	24	25	26	31	32	33	34	35	36

 $\bar{a} = 283.4; \bar{z}_{\text{typ}} = 102.34 \text{ mm}; \bar{z} = \bar{z} = 111.97 \text{ mm}.$ 

**TABLE 5.4** CUMULATIVE INFILTRATED DEPTHS AT SEVERAL TIMES DURING ADVANCE FOR THE EXAMPLE BASIN IRRIGATION

Time, t (min)	Cumulative inflow volume, Qt (m³)	Surface storage volume, $Vp(t)$ (m³)	Cumulative infiltrated volume, $V(t)$ $(m^3)$	Area of infiltration,  Aj  (m²)	Cumulative infiltrated, $Z(t)$ (mm)
13.0	10.795	5.636	5.159	233.592	22.09
34.0	28.234	13.683	14.551	432.234	33.66
64.0	53.146	23.755	28.391	777.168	36.53
94.0	78.058	31.240	46.818	1019.825	45.91
124.0	102.970	43.793	59.177	1217.224	48.62
145.0	120.408	52.874	67.534	1334.950	50.59

cross sections, and tailwater volumes. From these data one can then deduce an average furrow infiltration relation based on volume balance calculations. In evaluating well over 100 comprehensive furrow tests during a 3-year period, the mathematical form and the calibration procedures were found to have an important bearing on the effectiveness of the volume balance method. The experience of these investigations led to the following methodology for evaluating infiltration functions. This analysis is limited to sloping fields.

Volume balance equation. In Chapter 16 the kinematic concept of the "volume balance" is developed and reviewed. Several mathematical approaches

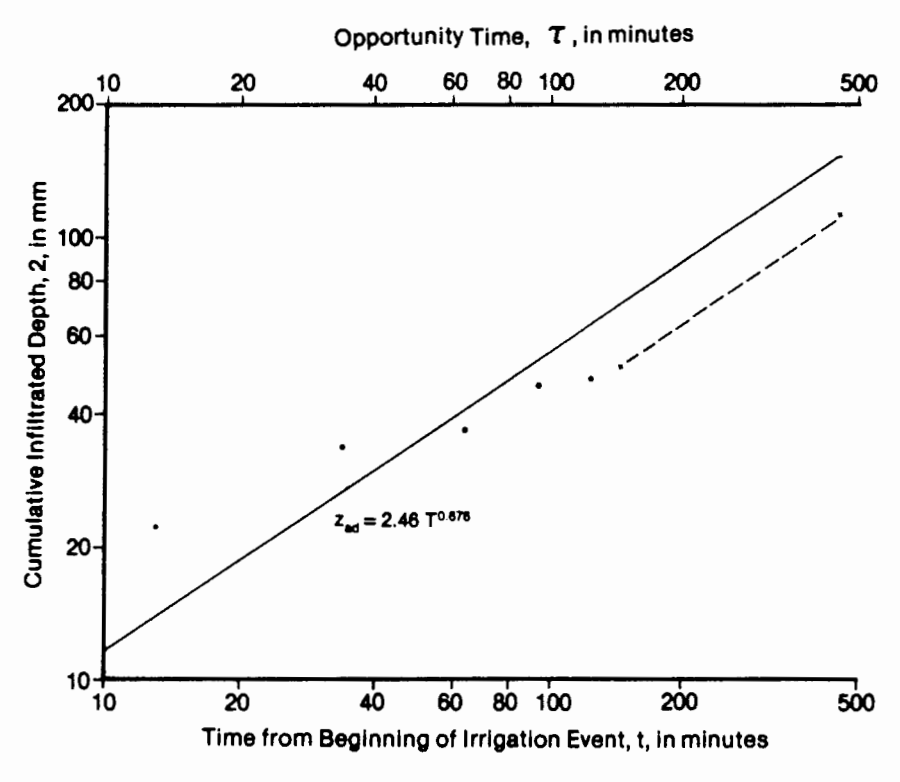


Figure 5.7 Cumulative infiltrated depth based on volume balance for the example basin irrigated field.

are described in which the "power advance" is the simplest to employ in the field evaluation of infiltration parameters. A preview of the equations will be helpful.

The power advance solution of the volume balance analysis is based on the following two assumptions:

1. The trajectory of the advance of the water front in a furrow or border can be described as the simple power function given as Eq. 5.3 but written with distance as the dependent parameter:

$$x = p(t_a)_r^r (5.11)$$

where x is the distance the front has advanced in time  $t_a$ , and r and p are empirical fitting parameters  $[r = 1/r' \text{ and } p = (1/p')^r \text{ in Eq. 5.3}].$ 

2. The infiltration function has the Kostiakov-Lewis characteristic form

$$Z = k\tau^a + f_0\tau \tag{5.12}$$

where

Z = infiltrated volume per unit length after an infiltration opportunity time  $\tau$ 

 $f_0$  = basic intake rate in units of volume per unit length per unit time

k, a = empirical fitting parameters

Utilizing these two assumptions, the volume balance equation can be written for any time:

$$Q_0 t = \sigma_y A_0 x + \sigma_z k t^a x + \frac{f_0 t x}{1 + r}$$
 (5.13)

where

 $A_0$  = cross-sectional area of flow at the inlet,  $m^2$ 

 $Q_0$  = inlet discharge, m<sup>3</sup>/min

t = elapsed time since the irrigation started, min

 $\sigma_y$  = surface storage shape factor, which is defined as a constant of 0.70 to 0.80

 $\sigma_z$  = subsurface shape factor, defined as

$$\sigma_z = \frac{a + r(1 - a) + 1}{(1 + a)(1 + r)}$$
 (5.14)

$$A = \sigma_1 y^{\sigma_2} \tag{5.15}$$

or

$$y = \sigma_1' A^{\sigma_2'} \tag{5.16}$$

where

$$\sigma_2' = \frac{1}{\sigma_2} \qquad \sigma_1' = \left(\frac{1}{\sigma_1}\right)^{\sigma_2'} \tag{5.17}$$

and

$$WP = \gamma_1 y^{\gamma_2} \tag{5.18}$$

Infiltration

in which y is depth in meters and WP is wetted perimeter in meters. The coefficients and exponents are empirical. It should be noted that for border-irrigation systems,  $\sigma_1$ ,  $\sigma_2$ , and  $\gamma_1$  are equal to 1.0 and  $\gamma_2$  is zero. The inlet flow area is

$$A_0 = C_1 \left( \frac{Q_0 n}{60 \sqrt{S_0}} \right)^{C_2} \tag{5.19}$$

where

$$C_2 = \frac{3\sigma_2}{5\sigma_2 - 2\gamma_2} \tag{5.20}$$

and

$$C_1 = \sigma_1 \left( \frac{\gamma_1^{0.67}}{\sigma_1^{1.67}} \right)^{C_2} \tag{5.21}$$

Values of the Manning roughness coefficient, n, range from about 0.02 for previously irrigated and smooth soil, to about 0.04 for freshly tilled soil, to about 0.15 for conditions where dense growth obstructs the water movement.

**Evaluating the infiltration parameters.** Christiansen et al. (1966) presented a volume balance approach for determining the constants k, a, and  $f_0$ . Ley (1978) modified this approach using the Fibonacci search method to find optimal parameter values which not only match the furrow advance but also minimize the error between the predicted and measured infiltrated volumes. Using precision furrows, Fangmeier and Ramsey (1978) also determined the constants of Eq. 5.12 with the volume balance approach. The reader may wish to consult these references for comparison with the analysis that follows.

Elliott and Walker (1982) propose a "two-point" method of evaluating the parameters in Eq. 5.12 and then proceed to show that the approach is indeed more accurate than traditional methods. The procedure begins by defining  $f_0$  from the inflow-outflow hydrograph or by other means which are noted below. Then Eq. 5.13 is written for two advance points using advance rate measurements to define the parameters in Eq. 5.11. The two common points are the middistance of the field and the end of the field. Thus for the middistance,

$$Q_0(t_{0.5L}) = \frac{\sigma_y A_0 L}{2} + \sigma_z \frac{k(t_{0.5L})^a L}{2} + \frac{f_0(t_{0.5L}) L}{2(1+r)}$$
 (5.22)

and for the end of the field,

$$Q_0 t_L = \sigma_y A_0 L + \sigma_z k t_L^a L + \frac{f_0 t_L L}{1 + r}$$
 (5.23)

where

 $t_{0.5L}$  = advance time to one-half the field length, min

 $t_L$  = advance time to the end of the field, min

L = field length, m

The unknowns in Eqs. 5.22 and 5.23 are the parameters k and a. Solving these

two equations simultaneously using a logarithmic transformation to linearize them yields

$$a = \frac{\ln (V_L/V_{0.5L})}{\ln (t_L/t_{0.5L})}$$
 (5.24)

where

$$V_L = \frac{Q_0 t_L}{L} - \sigma_y A_0 - \frac{f_0 t_L}{1+r}$$
 (5.25)

$$V_{0.5L} = \frac{2Q_0 t_{0.5L}}{L} - \sigma_y A_0 - \frac{f_0 t_{0.5L}}{(1+r)}$$
 (5.26)

Then  $\sigma_z$  is found directly from Eq. 5.14 and the parameter k is found by

$$k = \frac{V_L}{\sigma_z t_L^a} \tag{5.27}$$

**Evaluating the basic intake rate.** Several approaches can be used for determining a value for  $f_0$  in the infiltration equation. One method utilizes the data from blocked furrow infiltrometer tests made the day before irrigation. After an infiltrometer test has been run for several hours (the time being dependent on soil type), the essentially constant rate of infiltration can be taken to be  $f_0$ . Elliott and Walker (1982) report on  $f_0$  values obtained from eight blocked furrow tests on a clay loam soil and 15 tests on a loamy sand soil. Although the  $f_0$  values seemed to have had reasonable magnitudes, they appeared to fluctuate much too greatly on a given soil. This might be partially attributable to the shortness of the block furrow segments and the accompanying edge effects. The variability involved in the blocked furrow method for determining  $f_0$  prevented further use of the data in that evaluation.

The second method of estimating  $f_0$  is based on the fact that by knowing only the soil type, one can obtain published values of the basic infiltration rate.

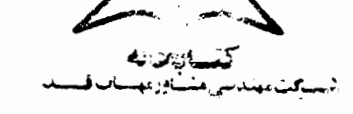
The third technique for determining  $f_0$  is the inflow-outflow method, in which the entire furrow is used essentially as an infiltrometer. This method is based on the assumption that late in the irrigation the soil has reached its basic infiltration rate. Then  $f_0$  can be found using the following equation:

$$f_0 = \frac{Q_{\rm in} - Q_{\rm out}}{L} \tag{5.28}$$

where  $Q_{\rm in}$  and  $Q_{\rm out}$  are the inflow and outflow rates, respectively, in m<sup>3</sup>/min.

The report then gives the results of the inflow-outflow method used on 135 individual furrow evaluations at three Colorado locations (the Benson Farm, the Printz Farm, and the Matchett Farm). The irrigation practices were to irrigate every other furrow at the Benson and Printz farms and every furrow at the Matchett Farm. A two-way analysis of variance was carried out on the  $f_0$  values from each farm to check for significant differences between irrigations and between individual furrows. The results indicated that the value of  $f_0$  is statistically constant

Infiltration



field, not changing significantly from irrigation to irrigation nor from furrow to furrow. One generally expects significant differences between "hard" furrows (those compacted by machinery) and "soft" furrows, between furrows where the flows are substantially different, or between furrows where debris varies. On the other hand, perhaps these variations are found primarily in the  $kt^a$  term. Certainly, the largest potential error in estimating an infiltration function for a field lies in the a and k term of Eq. 5.12.

### IRRIGATION SYSTEM PERFORMANCE

Analysis of the field data allows quantitative definition of the irrigation system performance. Such performance reflects, of course, not only the physical features of the system but its management as well. The models discussed in later chapters provide the capability of assessing the changes in performances that are associated with alterations in design or operational parameters. Field data analysis provides only an indication of the single event, and therefore tends to be related specifically to the surface irrigation method.

Three typical results of surface irrigation are illustrated in Fig. 5.8. Occasionally, the inflow is cut off shortly after completion of the advance phase, and

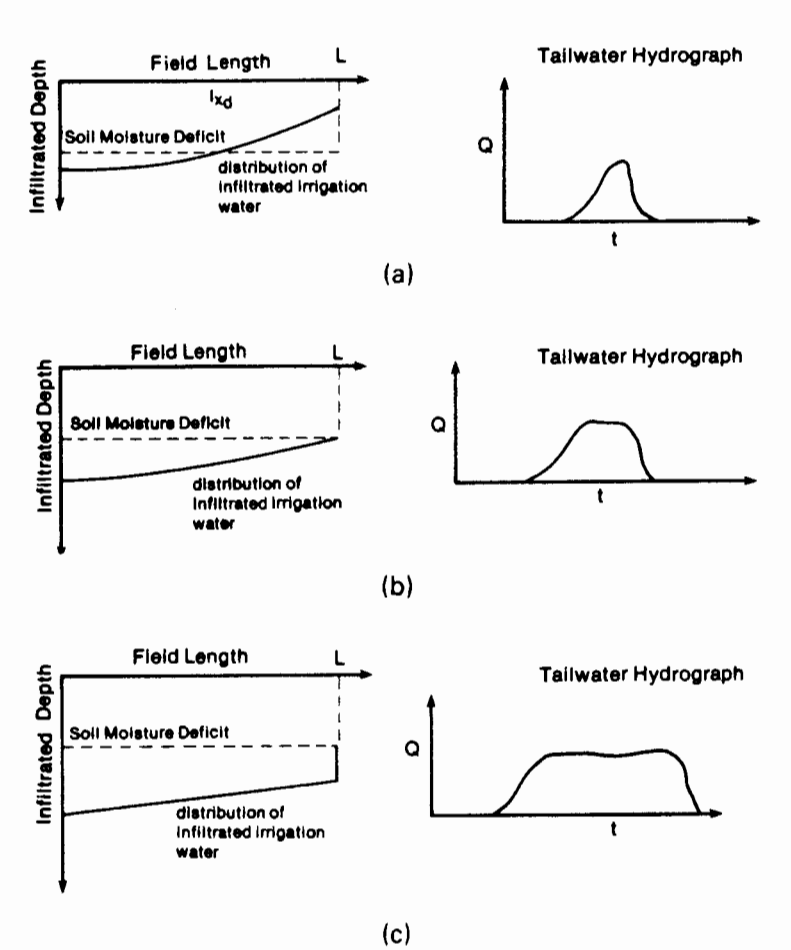


Figure 5.8 The relationship between required water application and actual moisture distribution for three typical irrigation regimes. (a) Under-irrigation case. (b) Complete-irrigation case. (c) Over-irrigation case.

the application at some point in the field is inadequate to meet the requirements (Fig. 5.8a). At other times, the requirement is met, with the least watered areas just receiving the required amount of water (Fig. 5.8b). Finally, and most often, the applied depths exceed the requirement at all locations (Fig. 5.8c). Because of the large differences in economic, physical, social, and operational conditions that occur relative to surface irrigation, it is impossible to place quantitative judgments on any of these three cases. One can identify situations in which underirrigation or overirrigation are both desirable and undesirable. Consequently, the suggested evaluation of performance is the numerical definition of the four efficiency parameters described in Chapter 2 and then a case-by-case professional judgment of their values.

# Furrow-Irrigation Evaluation

Furrow systems are generally found on sloping fields and allow water to drain freely from the end of the furrow after completing the advance phase. Evaluation data would normally include the inflow, furrow geometry, advance trajectory, and runoff hydrograph. The information would lead to a definition of intake characteristics or the appropriate adjustment of infiltrometer measurements. Many evaluations assume that lateral wetting occurs between furrows in a uniform manner and that recession time is a negligible addition to the intake opportunity time along the furrow.

The total infiltrated volume can be found by integrating the subsurface moisture distribution by the trapezoidal rule:

$$V_z = \frac{L}{2n} \left( Z_0 + 2Z_1 + 2Z_2 + \dots + Z_n \right) \tag{5.29}$$

where

L =furrow length, m

 $Z_i$  = cumulative intake at the *i*th point, m<sup>3</sup>/m

n = number of increments used to subdivide the furrow

Values for cumulative intake are determined by

$$Z_i = k[t_r - (t_a)_i]^a + f_0[t_r - (t_a)_i]$$
 (5.30)

in which k, a, and  $f_0$  are as defined for Eq. 5.2,  $t_r$  is the recession time in minutes, and  $(t_a)_i$  is the advance time to the *i*th station in minutes. If recession is to be neglected, the cutoff time,  $t_{co}$ , is used instead of  $t_r$ .

When the applied depth does not completely satisfy the requirement, the infiltrated volume must be computed in two segments. First, the location of the inadequate area must be defined (see Fig. 5.8a for  $x_d$ ). Then Eq. 5.29 is utilized to integrate the infiltrated volume over the adequately irrigated area,  $V_{za}$ , and over the inadequate area,  $V_{zi}$ , such that

$$V_z = V_{za} + V_{zi} \tag{5.31}$$

The four standard measures of performance can be computed as follows:

## For complete and overirrigation

$$E_a$$
 = application efficiency  
=  $\frac{Z_{\text{req}}L}{Q_0 t_{co}} \times 100$  (5.32)

where  $Z_{reg}$  is the required depth of application to the furrows in m<sup>3</sup>/m.

DPR = deep percolation ratio
$$= \frac{V_z - Z_{\text{req}}L}{Q_0 t_{co}} \times 100$$
(5.33)

TWR = tailwater ratio  
= 
$$100 - E_a - DPR$$
  
 $E_r$  = water requirement efficiency  
=  $100\%$  (5.34)

# 2. For the underirrigation case,

$$E_a = \frac{Z_{\text{req}} x_d + V_{zi}}{Q_0 t_{co}} \times 100 \tag{5.35}$$

DPR = 
$$\frac{V_{za} - Z_{req}x_d}{Q_0t_{co}} \times 100$$
 (5.36)

$$TWR = 100 - E_a - DPR (5.37)$$

$$E_r = \frac{Z_{\text{req}} x_d + V_{zi}}{Z_{\text{req}} L} \times 100 \tag{5.38}$$

# **Border Irrigation Evaluation**

The analysis of border irrigation data follows the same procedures as outlined previously for furrow systems. Simplication can be made in using discharge per unit width instead of furrow flow, and the cross-sectional area is rectangular. This analysis, of course, assumes a free-draining outflow condition at the outlet. For ponded conditions caused by end diking, the analysis follows the procedure outlined below for basins.

In the evaluation of furrow systems, the infiltration during recession was considered negligible. For border irrigation, the infiltration during the drainage period following cutoff must be considered. The post-cutoff period is divided into a depletion phase and a recession phase, as illustrated in Fig. 5.9.

Water is introduced to the border at time zero, reaches the end at time  $t_L$ ,

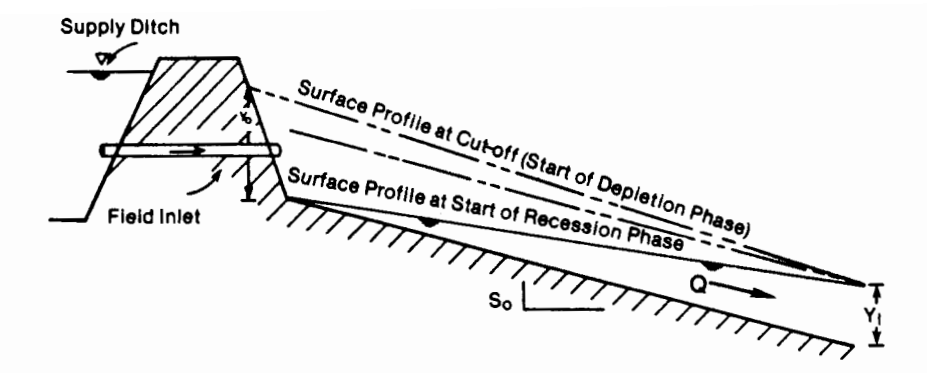


Figure 5.9 Schematic illustration of two phases of post-shutoff period for border irrigation, indicating the depletion and recession phases.

and is allowed to continue until the cutoff time,  $t_{\rm co}$ . Then water begins to drain from the field until the surface is just exposed at the upper end,  $t_d$ , and then recedes from the entire surface until  $t_r$ . The Manning formula can be used to estimate the flow depths of the inlet to the border  $(y_0 \text{ in meters})$  as a function of the unit discharge  $(q_0 \text{ in m}^3/\text{min})$ . Under the assumptions made by Strelkoff (1977), the time until the end of the depletion phase and the beginning of recession is given by

$$t_d = t_{co} + \frac{y_0 L}{2q_0} \tag{5.39}$$

The time interval  $t_r - t_d$ , in minutes, can then be derived and presented as follows:

$$t_r - t_d = \frac{0.095 n^{0.47565} S_y^{0.20735} L^{0.6829}}{I^{0.52435} S_0^{0.237825}}$$
(5.40)

in which

$$S_{y} = \frac{y_{1}}{L} \tag{5.41}$$

$$=\frac{[(q_L n)/(60\sqrt{S_0})]^{0.6}}{L} \tag{5.42}$$

$$q_L = q_0 - IL \tag{5.43}$$

and

$$I = \frac{ak}{2} \left[ t_d^{a-1} + (t_d - t_L)^{a-1} \right] + f_0$$
 (5.44)

Once the depletion and recession times  $(t_d \text{ and } t_r)$  have been determined, estimates for  $E_a$ , DPR, TWR, and  $E_r$  can be developed as in Eqs. 5.29 to 5.38.

# **Basin Irrigation Evaluation**

The estimate of basin application efficiencies is somewhat simplified by the small field slope and the prevention of runoff. Water first entering the basin would advance to the end dike and then pond on the surface, as illustrated in Fig. 5.10.

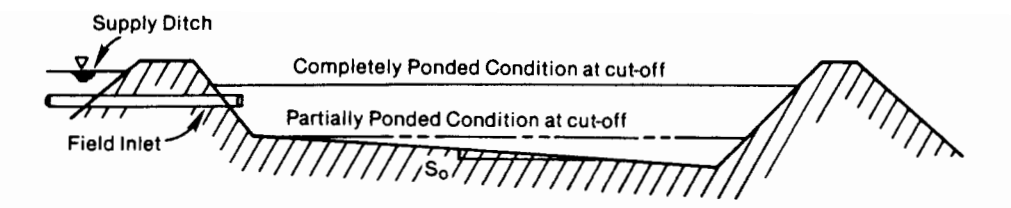


Figure 5.10 Schematic representation of a typical basin irrigation condition.

As the water surface rises, it will approach a horizontal orientation. Thus it can be seen that during the depletion and recession phases the surface water has little or no movement, and the subsurface profile can be determined by adding the surface depths to the profile that developed during the advance phase.

Because the slope of most basins is zero or very flat, the uniform flow equations cannot be used to determine the depth of flow at the field inlet. If it is assumed that at the time of cutoff the subsurface moisture distribution is approximately linearly distributed, a volume balance will determine the surface depths of flow:

$$q_0 t_{co} - \frac{Z_0 + Z_L}{2} L = \frac{y_0 + y_1}{2} L \tag{5.45}$$

where

$$Z_0 = k t_{co}^a + f_0 t_{co} (5.46)$$

$$Z_L = k(t_{co} - t_L)^a + f_0(t_{co} - t_L)$$
 (5.47)

and  $y_0$  and  $y_1$  are the flow depths at the inlet and end of the field, respectively. Assuming that the water surface is horizontal,

$$y_1 = y_0 + S_0 L ag{5.48}$$

which can be substituted into Eq. 5.45 and solved for  $y_0$  as follows:

$$y_0 = \frac{q_0 t_{co}}{L} - \frac{Z_0 - Z_L}{2} - \frac{S_0 L}{2} \tag{5.49}$$

The final distribution of subsurface water is then based on adding  $y_0$  to  $Z_0$  and  $y_1$  to  $Z_L$ . The application efficiency and deep percolation ratios can be found from Eqs. 5.29 to 5.38. The tailwater ratio for basin irrigation is zero.

# ALTERNATIVES FOR IMPROVING HYDRAULIC PERFORMANCE

The field evaluation of a surface irrigation system will identify modifications that will enhance hydraulic performance. Besides the easily identified problems of applying too much or too little water onto the soil, the distribution of infiltrated

water over the field may vary considerably, tailwater runoff may be excessive, or significant deep percolation losses may occur. Solutions to these problems are numerous. In fact, the optimal solution is usually a combination of several remedies.

# **Modifying Hydraulic Conditions**

In any discussion of modifying individual hydraulic parameters to improve irrigation performance, it must be recognized that all of the parameters are interdependent. Therefore, when discussing changes in discharge, time of cutoff, slope and length of run, any alteration in one of these parameters will affect one, or more, of the other parameters.

**Discharge.** Changing the discharge rate available for use on an irrigated field will significantly affect the time of advance. In most field situations, the maximum discharge rate used should not result in significant soil erosion. Utilizing high flow rates maximizes the potential for tailwater losses (except for basin irrigation), but minimizes the time of advance and thereby the variation in opportunity time along the field length, so a more uniform depth of water is applied.

To reduce the tailwater runoff from border or furrow irrigated fields, a high discharge rate can be used during the advance phase and then the discharge can be "cut back" (reduced) for the surface storage phase. The ideal situation would be to reduce the discharge rate continuously during the surface storage phase so that no tailwater runoff occurs.

Frequently, the discharge rate available to a farmer is fixed, so that increasing the discharge rate onto an irrigated field is difficult. In such cases, construction of a small storage pond may be a feasible alternative. The pond might hold a few hours or a few days of storage for the available discharge. Then, during an irrigation event, a higher discharge rate could be used.

**Time of cutoff.** For whatever discharge is being used, the ideal time of cutoff,  $t_{co}$ , occurs when the infiltrated depth in the least-watered portion of the field is equal to the irrigation requirement, taking into account the infiltration that will occur during the depletion and recession phases for basin and border irrigation. Discharge and time of cutoff are the two operational hydraulic parameters, and they are strongly interdependent, with  $t_{co}$  being the easiest for the irrigator to modify. In design, or in operation, this interdependence between  $Q_0$  and  $t_{co}$  must be known to design a surface irrigation system properly, but even more important, to operate the system properly.

**Length of run.** Changing the length of run may be one means of maximizing hydraulic performance. However, a farmer is usually motivated to maximize the

length of run in order to have more land available for growing crops and to accomplish cultivation and harvesting more efficiently.

**Topography.** Basin irrigation is particularly affected by topography. The minimum depth of irrigation water applied to a basin is dictated by covering the "high spots" so that they do not become saline. Consequently, instead of applying the irrigation requirement, much greater depths must be applied, particularly in the early part of the irrigation season. For basin irrigation, the alternatives are improved land-leveling techniques or basin-furrow irrigation.

For border- or furrow-irrigated fields, the slope, or grade, of the field may not be uniform and have a significant effect on time of advance. Usually, the most desirable solution is land preparation to a uniform grade. In some cases it may be more desirable to break the field into two fields to avoid the expense of land leveling.

Time of advance. For border and furrow irrigation, time of advance is the hydraulic parameter likely to receive the most attention for modification; whereas for basin irrigation the advance time is second only to topography in terms of modification for improving hydraulic performance. The effects on time of advance of modifying discharge, length of run, and topography have been discussed above. A major innovation for affecting time of advance is surge flow irrigation. Other means for reducing advance time are: (1) for furrow irrigation, compact and smooth the furrows so that there is a lower intake rate and less flow resistance; (2) for border irrigation, convert to furrow irrigation; and (3) for basin irrigation, employ basin-furrow irrigation.

Infiltration. The ideal situation is to have the infiltrated depth equal over all portions of a field. Given the usual variation of infiltration opportunity time along the length of a field, this would require that the infiltration function vary in a continuous manner along the length rather than be a single function. One means for accomplishing this would be to compact the soil surface, with the greatest compaction being applied at the head of the field and the compactive energy being continuously reduced toward the end of the field. Such a measure would be more suitably applied to furrows than to border or basin irrigation or basin-furrow irrigation. The infiltration function will be affected the most during the first irrigation event after soil compaction, with rapidly declining effects on infiltration thereafter.

Tailwater runoff. In some cases, tailwater runoff will be the most significant hydraulic parameter to be controlled. For example, if the tailwater runoff is not reused and there is a shortage of water, either minimizing or reusing tailwater runoff will be important. Also, minimizing or recycling tailwater runoff is important if significant topsoil erosion is occurring. Another important impact of tailwater runoff is the transport of nutrients or biocides to downstream water bodies.

There are usually two possibilities for tailwater recovery systems. The runoff is collected in a pond and either (1) pumped back to the head of the field to be reused for irrigation, or (2) conveyed by gravity for use on the next field or farm downstream.

**Deep percolation**. A certain amount of subsurface drainage is required in order to maintain a salt balance. In most surface irrigation systems, though, significant quantities of deep percolation occur that result in wasting of water, waterlogging, and soil salinization. To eliminate deep percolation losses completely is extremely difficult because of variations in intake opportunity time and soil intake properties which generally result in overirrigation over a significant fraction of the field. If deep percolation losses are contributing to other significant water problems, the goal in improving hydraulic performance would be to minimize deep percolation losses.

Reducing the time of advance results, in a more uniform opportunity time along the length of a field, which in turn will result in a more uniform infiltrated depth if the soils are similar over a field. Then, cutting off the inflow discharge when the irrigation requirement has been satisfied will keep deep percolation losses at a minimum. Also, the measures described above for soil compaction to provide more uniform infiltrated depths would also be highly beneficial.

# **EXAMPLE PROBLEMS**

## Example 5.1

An evaluation was made of a furrow irrigation system to determine the infiltration characteristics of the field and the performance of the system. Prior to the evaluation the topography of the field was established (slope was 0.8% and uniform, the length of furrows was 200 m, and the furrow spacing was 0.75 m) and gravimetric soil samples were taken to determine the soil depletion (10 cm). On the day of the irrigation test, a steady flow of 0.12 m³/min was introduced into the furrow and the advance-recession trajectories were observed. Measured advance and recession are as follows:

Distance (m)	Advance time (min)	Recession time (min)
0	0	390 (time of cutoff)
50	6	396
110	18	402
150	30	405
200	55	408

The tests also included measurements of the runoff (a steady value of  $0.0822 \text{ m}^3/\text{min}$  was

reached by the time the flow was shut off). Following the irrigation, a measure of the furrow cross section was made, with the following average results.

Elevation from furrow bottom (m)	Horizontal width of furrow (m)
0	0
0.01	0.058
0.02	0.097
0.03	0.130
0.04	0.161
0.05	0.190
0.06	0.217
0.07	0.243
0.08	0.268
0.09	0.292
0.10	0.316
0.11	0.339
0.12	0.361

What is the infiltration characteristic of this furrow and the resulting application efficiency?

The first step in the analysis of this and similar problems is to develop the areadischarge relationship (Eq. 5.19). One can plot the cross-sectional data given above and derive such a relation. For the purposes of this example, an approximate shortcut will be used. The reader may wish to perform a more accurate analysis and compare results.

The shortcut method assumes that one can write a series of simple power relations as follows (T is top width, y is depth, A is area, and WP is the wetted perimeter):

$$T = a_1 y^{a_2}$$
  
 $T = 0.361$   $y = 0.12$   
 $T = 0.217$   $y = 0.06$ 

Using a logarithmic transformation and a two-point fit yields

$$a_2 = \frac{\log (0.361/0.217)}{\log (0.12/0.06)} = 0.734$$
$$a_1 = \frac{0.361}{(0.12)^{0.734}} = 1.712$$

Then

$$A = \sigma_1 y^{\sigma_2}$$
  $\sigma_1 = \frac{a_1}{a_2 + 1} = \frac{1.712}{1.734}$   
= 0.987  
 $\sigma_2 = a_2 + 1 = 1.734$ 

Next,

$$WP = \gamma_1 y^{\gamma_2}$$

Chap. 5

This calculation is more rigorous and is accomplished as follows:

$$WP|_{0.06} = \sum_{i=0}^{6} \{2[(y_i - y_{i-1})^2 + [0.5(T_i - T_{i-1})]^2]^{0.5}\} = 0.249 \,\mathrm{m}$$

and

$$WP|_{.12} = \sum_{i=1}^{12} \{2[(y_i - y_{i-1})^2 + [0.5(T_i - T_{i-1})]^2]^{0.5}\} = 0.437 \,\mathrm{m}$$

$$\gamma_2 = \frac{\log(0.437/0.249)}{\log(0.12/0.06)} = 0.811$$

$$\gamma_1 = \frac{0.437}{(0.12)^{0.811}} = 2.439$$

Finally, we can define  $C_1$  and  $C_2$  in Eqs. 5.20 and 5.21:

$$C_2 = \frac{3(1.734)}{5(1.734) - 2(0.811)} = 0.738$$

$$C_1 = 0.987 \left[ \frac{(2.439)^{0.67}}{(0.987)^{1.67}} \right]^{0.738} = 1.555$$

Thus

$$A = 1.555 \left( \frac{Qn}{60S_0^{0.5}} \right)^{0.738} = 1.555 \left[ \frac{.12(0.04)}{60(0.008)^{0.5}} \right]^{0.738} = 0.009 \text{ m}^2$$

The next step is to calculate the value of r in Eq. 5.11. Again the two-point method can be utilized:

$$x = 200$$
  $t_x = 55 \text{ min}$   
 $x = 110$   $t_x = 18$   
 $r = \frac{\log(200/110)}{\log(55/18)} = 0.535$ 

The basic intake,  $f_0$ , can be determined using inflow and outflow hydrographs as described in Eq. 5.28. The reader is cautioned, however, that one must be sure the tailwater hydrographed has stabilized. This may require many hours. It is better at this point to assume a value typical of the soil than to compute  $f_0$  before it is reached in the furrow. If sufficient care is not taken,  $f_0$  will be too big and the analysis will correct it by making the value of a too small, possibly even negative. It appears in the hydrograph for this example that a stable runoff of  $0.0822 \, \text{m}^3/\text{min}$  was reached, so from Eq. 5.28,

$$f_0 = \frac{0.12 - 0.0822}{200} = 0.00019 \text{ m}^3/\text{m/min}$$

We are now ready to compute the values of k and a from Eqs. 5.24 to 5.27:

$$V_L = \frac{(0.12 \,\mathrm{m}^3/\mathrm{min})(55 \,\mathrm{min})}{200 \,\mathrm{m}} - 0.77(0.009 \,\mathrm{m}^2) - \frac{0.00019(55)}{1 + 0.535} = 0.0193$$

$$V_{0.5L} = \frac{0.12(18)}{110} - 0.77(0.009) - \frac{0.00019(18)}{1.535} = 0.0105$$

This calculation is more rigorous and is accomplished as follows:

$$WP|_{0.06} = \sum_{i=0}^{6} \{2[(y_i - y_{i-1})^2 + [0.5(T_i - T_{i-1})]^2]^{0.5}\} = 0.249 \,\mathrm{m}$$

and

$$WP|_{.12} = \sum_{i=1}^{12} \{2[(y_i - y_{i-1})^2 + [0.5(T_i - T_{i-1})]^2]^{0.5}\} = 0.437 \,\mathrm{m}$$

$$\gamma_2 = \frac{\log(0.437/0.249)}{\log(0.12/0.06)} = 0.811$$

$$\gamma_1 = \frac{0.437}{(0.12)^{0.811}} = 2.439$$

Finally, we can define  $C_1$  and  $C_2$  in Eqs. 5.20 and 5.21:

$$C_2 = \frac{3(1.734)}{5(1.734) - 2(0.811)} = 0.738$$

$$C_1 = 0.987 \left[ \frac{(2.439)^{0.67}}{(0.987)^{1.67}} \right]^{0.738} = 1.555$$

Thus

$$A = 1.555 \left(\frac{Qn}{60S_0^{0.5}}\right)^{0.738} = 1.555 \left[\frac{.12(0.04)}{60(0.008)^{0.5}}\right]^{0.738} = 0.009 \text{ m}^2$$

The next step is to calculate the value of r in Eq. 5.11. Again the two-point method can be utilized:

$$x = 200$$
  $t_x = 55 \text{ min}$   
 $x = 110$   $t_x = 18$   
 $r = \frac{\log (200/110)}{\log (55/18)} = 0.535$ 

The basic intake,  $f_0$ , can be determined using inflow and outflow hydrographs as described in Eq. 5.28. The reader is cautioned, however, that one must be sure the tailwater hydrographed has stabilized. This may require many hours. It is better at this point to assume a value typical of the soil than to compute  $f_0$  before it is reached in the furrow. If sufficient care is not taken,  $f_0$  will be too big and the analysis will correct it by making the value of a too small, possibly even negative. It appears in the hydrograph for this example that a stable runoff of  $0.0822 \, \text{m}^3/\text{min}$  was reached, so from Eq. 5.28,

$$f_0 = \frac{0.12 - 0.0822}{200} = 0.00019 \text{ m}^3/\text{m/min}$$

We are now ready to compute the values of k and a from Eqs. 5.24 to 5.27:

$$V_L = \frac{(0.12 \,\mathrm{m}^3/\mathrm{min})(55 \,\mathrm{min})}{200 \,\mathrm{m}} - 0.77(0.009 \,\mathrm{m}^2) - \frac{0.00019(55)}{1 + 0.535} = 0.0193$$

$$V_{0.5L} = \frac{0.12(18)}{110} - 0.77(0.009) - \frac{0.00019(18)}{1.525} = 0.0105$$

$$a = \frac{\log(0.0193/0.0105)}{\log(200/110)} = 0.545$$

$$\sigma_z = \frac{0.545 + 0.535(1 - 0.545) + 1}{1.545(1.535)} = 0.754$$

$$k = \frac{0.0193}{1.754(55)^{0.545}} = 0.00124$$

The final infiltration that characterizes the furrow during the test is

$$Z = 0.00124\tau^{0.535} + 0.00019\tau$$

where Z has units of  $m^3/m$  of furrow length/furrow spacing. At the end of the furrow, the intake opportunity time is 408 - 55 = 353 min. Substituting this into the relation above yields a value of Z = 0.0974 m<sup>3</sup>/m. This is equivalent to a uniform depth of

$$\frac{0.0974 \text{ m}^3/\text{m}}{0.75 \text{ m (spacing)}} = 0.130 \text{ m} \text{ or } 13.0 \text{ cm}$$

We thus see that the field was overirrigated and the application efficiency from Eq. 5.32 is

$$E_a = \frac{10 \text{ cm}(0.01 \text{ m/cm})(0.75 \text{ m})(200 \text{ m})}{(0.12 \text{ m}^3/\text{min})(390)} = 0.321 \text{ or } 32.1\%$$

This is not a good performance and should be improved. The most obvious step is to reduce the application time. If Z in the relation above is set to 0.075, the required depth (10 cm  $\times$  0.75 m spacing) and  $\tau$  is solved for (using principles in Chapter 6). The correct opportunity time is 231 min. If the recession time (409 - 390 = 18 min) is about the same, the cutoff time should be

$$t_{co} = \tau_{reo} + t_a - (t_r - t_{co}) = 260 + 55 - 18 = 297 \text{ min}$$

With this value of cutoff time, the application efficiency can be recomputed:

$$E_a = \frac{0.075(200)}{0.12(297)} = 0.42$$
 or 42%

This is a substantial improvement but not a very good value either. Now we must adjust the inflow. This is a design problem and will be taken up in Chapter 6.

### **HOMEWORK PROBLEMS**

**5.1.** An infiltration study was conducted on a surface-irrigated field yielding the following cumulative intake function:

$$Z = 0.00884\tau^{0.212} + 0.00017\tau$$

in which Z has units of  $m^3/m^2$  and  $\tau$  has units of minutes. Later during the irrigation of this field it was observed that the flow advanced to the end of the field in 125 min and then runoff for a time before the inflow was shut off. Following cutoff, it took 15 more minutes for the surface water to recede from the end of the field. If the irrigator wished to apply 7.5 cm to the lower end of the field, when should he or she have stopped the irrigation?

- **5.2.** What is the cross-sectional flow area in a furrow under the following conditions:  $Q_0 = 1.5$  liters/s, L = 300 m,  $S_0 = 0.01$ , n = 0.04, WP =  $1.389y^{0.564}$  (y is depth, WP is wetted perimeter), and  $A = 1.066y^{1.654}$ ?
- 5.3. The following furrow evaluation data were developed:

Test location: Fort Morgan, Colorado Irrigation: number 8 in the season Furrow: number 2 in test group

Date: August 26, 1979

Soil: loamy sand Crop: maize

Field length: 350 m Furrow spacing: 1.5 m

Surface roughness: n = 0.04

FIELD MEASUREMENTS OF ELEVATION, ADVANCE, AND RECESSION

Station (m)	Δ Elevation (m)	Time of advance (min)	Time of recession (min)
0	0	0	171
25	0.107	6.5	177
50	0.168	10.0	180
75	0.226	16.0	183
100	0.280	22.0	185
125	0.344	27.0	188
150	0.387	32.0	192
175	0.445	37.0	196
200	0.485	43.0	198
225	0.567	49.0	200
250	0.664	57.0	201
275	0.765	63.0	202
300	0.817	73.0	203
325	0.838	89.0	204
350	0.869	116.0	205

#### INFLOW HYDROGRAPH

Time (min)	Inflow (liters/s)	Time Inflow (liters/s)		Time (min)	Inflow (liters/s)
0.0	0.0	15.0	2.692	47	2.692
2.5	1.887	18.0	2.876	61	2.875
3.5	2.517	21.0	2.875	89	2.875
5.0	2.642	24.0	2.875	113	2.875
8.0	2.349	36.0	2.875	165	2.875
10.0	2.349	42.0	2.969	170	0
13.0	2.349	45.0	2.517		

#### **OUTFLOW HYDROGRAPH**

Time (min)	Outflow (liters/s)	Time (min)	Outflow (liters/s)
111	0 .	172	0.498
114	0.162	174	0.498
118	0.255	176	0.498
131	0.343	178	0.496
135	0.392	180	0.496
139	0.443	182	0.402
143	0.496	184	0.389
149	0.496	186	0.358
156	0.496	188	0.301
165	0.496	190	0.219
170	0.496	194	0

Furrow cross section (data are x-y pairs, furrow centerline is x = 0, y = 0. x is the + or - lateral direction, y is the depth above the furrow bottom at the centerline, and the units are in centimeters).

x	у	x	•	
0	0.0	- 20	7	
2	0.0	-18	6	
4	0.0	- 16	5	
6	0.0	- 14	3	
8	0.0	- 12	1	
10	0.0	′ –10	1	
12	0.5	-8	1	
14	1.5	-6	0	
16	3.0	-4	0	
20	6.5	-2	0	
22	8.0			

The average soil moisture depletion prior to the irrigation was 6.0 cm. From these data, perform the following analyses and submit the results as an engineering report:

- (a) Identify the infiltration parameters using the two-point method.
- (b) Plot the subsurface distribution of applied water.
- (c) Calculate the application efficiency, deep percolation ratio, tailwater ratio, and water requirement efficiency.
- **5.4.** A furrow irrigation is evaluated yielding the following results:

length of the advance phase = 2.5 h length of the recession phase = 0.5 h length of the depletion phase = 3 min soil moisture deficit prior to irrigation = 10 cm furrow spacing = 0.75 m infiltration function

$$Z = 0.003\tau^{0.651} + 0.00022\tau$$

- where Z has units of m<sup>3</sup>/m of furrow length and  $\tau$  is in minutes, when should the inflow be shut off?
- 5.5. Figures 4.20 and 5.1 contain data from an evaluation in Colorado. The furrow cross section was also evaluated and found to have  $\rho_1$  and  $\rho_2$  (Eq. 6.7) values of 0.3469 and 2.871, respectively. The soil moisture depletion was 9 cm and the furrow spacing was 1.5 m. What were the application efficiency, deep percolation ratio, tailwater runoff ratio, and water requirement efficiency for this test? Assume n = 0.04.
- **5.6.** A border 360 m long, lying on a slope of 0.5% with an estimated n value of 0.04 was evaluated. A flow of 0.357 m<sup>3</sup>/min/m of width was applied and it advanced to the end of the border in 108 min. The flow was cutoff at 226 min. The soil's infiltration rate was measured and the following function derived:

$$Z = 0.00875\tau^{0.413} + 0.0005\tau$$

where Z is in meters and  $\tau$  is in minutes. If the required depth of application was 15 cm, what was the application efficiency?

#### REFERENCES

- CHRISTIANSEN, J. E., A. A. BISHOP, F. W. KIEFER, JR., and Y. S. FOK. 1966. Evaluation of Intake Rate Constants as Related to Advance of Water in Surface Irrigation. *Trans.* ASAE 9(5):671-674.
- ELLIOTT, R. L. 1980. Furrow Irrigation Field Evaluation Data. Report, Department of Agricultural and Chemical Engineering, Colorado State University, Fort Collins, Colo., August.
- ELLIOTT, R. L., and W. R. WALKER. 1982. Field Evaluation of Furrow Infiltration and Advance Functions. *Trans. ASAE* 25(2):396–400.
- FANGMEIER, D. D., and M. K. RAMSEY. 1978. Intake Characteristics of Irrigation Furrows. *Trans. ASAE* 21(4):696-700, 705.
- KUNDU, S. S., and G. V. SKOGERBOE. 1980. Field Evaluation Methods for Measuring Basin Irrigation Performance. Tech. Rep. 59. Water Management Research Project, Colorado State University, Fort Collins, Colo., February.
- LEY, T. W. 1978. Sensitivity of Furrow Irrigation Performance to Field and Operation Variables. Unpublished M.S. thesis, Department of Agricultural and Chemical Engineering, Colorado State University, Fort Collins, Colo.
- MERRIAM, J. L., and J. KELLER. 1978. Farm Irrigation System Evaluation: A Guide for Management. Department of Agricultural and Irrigation Engineering, Utah State University, Logan, Utah.
- SALAZAR, L. J. 1977. Spatial Distribution of Applied Water in Surface Irrigation. Unpublished M.S. thesis, Department of Agricultural and Chemical Engineering, Colorado State University, Fort Collins, Colo.
- STRELKOFF, T. 1977. Algebraic Computations of Flow in Border Irrigation. ASCE J. Irrig. Drain. Div. 103(IR3):357-377.

# Volume Balance Field Design

### **DESIGN OBJECTIVES**

The principal purpose of irrigating croplands is to replenish the root zone reservoir frequently enough to avoid crop stress but uniformly and efficiently enough to conserve energy, water, nutrients, and labor. Irrigation significantly affects the local environment in which the crop exists, and therefore, irrigating may be for other reasons than satisfying crop water demands. Lands may be watered to cool the atmosphere surrounding sensitive fruit and vegetable crops, or to heat the atmosphere to prevent their damage by frost. An irrigation may be intended to leach salts accumulated in the root zone, soften the soil prior to planting, or to even fertilize the field and spread pesticides.

The design of a surface irrigation system implies that a previous consideration has been made of the expected system performance. In other words, implicit in the design practice is the assumption that uniformity and efficiency can be predicted from such parameters as discharge, application time, infiltration characteristics, field slope and length, and the depth required to refill the root zone. Such a predictive capability requires evaluation of two major processes: (1) advance, and (2) recession. A typical plot of the advance and recession trajectories for a surface-irrigated field was shown in Fig. 4.20, and in Fig. 5.8 some typical distributions of infiltrated water and runoff hydrographs that can result from the irrigation were shown.

The design procedures in this chapter are based on the following assumption. The irrigation is intended to apply a depth equivalent to the soil moisture deficit over the entire field. Maximum application efficiencies will occur, therefore, when

the least-watered areas are just refilled. The design intake opportunity time can be defined as

$$Z_{\text{reg}} = k\tau_{\text{reg}}^a + f_0\tau_{\text{reg}} \tag{6.1}$$

where

 $Z_{\text{req}}$  = required infiltrated volume per unit length (and is equal to the soil moisture deficit in similar units)

 $\tau_{reg}$  = design intake opportunity time

k and  $\dot{a}$  = empirical parameters

 $f_0$  = basic intake rate in units of volume per unit time per unit length

For most surface-irrigated conditions,

$$\tau_{\text{reg}} = t_r - t_L \tag{6.2}$$

in which  $t_r$  and  $t_L$  are the recession and advance times, respectively, at the lower end of the field. If the minimum intake opportunity time actually occurs at the field inlet because of a diked downstream boundary or a relatively flat field, then

$$\tau_{\text{req}} = t_{\text{co}} + t_d \tag{6.3}$$

where  $t_{co}$  is the time of cutoff and  $t_d$  is the vertical recession (or depletion) time at the field inlet.

The application efficiency,  $E_a$ , is defined as

$$E_a = \frac{Z_{\text{req}}L}{Q_0 t_{co}} \tag{6.4}$$

where L is the field length and  $Q_0$  is the field inflow (discharge per unit width for borders and basins or discharge per furrow). The design objectives become clearer when viewing Eq. 6.4.  $E_a$  is to be maximized by careful selection of L,  $Q_0$ , and  $t_{co}$ . However, by assuming the definition of  $Z_{req}$  in Eq. 6.1,  $t_{co}$  is dependent on  $Q_0$ , thereby reducing the independent parameters by one.

### **DESIGN DATA**

There are two situations where an engineer may have an opportunity to design a surface irrigation system: (1) a new irrigation project may be planned where one of the surface methods has been selected, or (2) the performance of an existing irrigation system requires improvement by redesign. In the latter situation, the planned system may not be the same as the one already existing, and in fact, may not even be a surface irrigation system.

At the stage in a new irrigation project where the surface irrigation system design is initiated, a great deal of irrigation engineering has already taken place. The selection of surface irrigation for a specific location is an integral part of the project planning process. Some of the various aspects of planning associated with surface irrigation selection were dealt with in Chapters 1 and 3 and can be found in several other books.

Design Data 135

If a new or modified surface system is anticipated on lands already irrigated, it is likely that the decision is based at least partially on the results of an evaluation of the existing system as described in Chapter 5. Such evaluations not only identify the performance of the existing method of water application but also generate the data necessary for the improved practices.

Whether the system is part of a new project or one that is to be improved, the data required fall into six general categories:

- 1. The nature of the water resources to be used, including the annual allotment, method of delivery and charge, flow rate and duration, and period of use. (The quality of the irrigation water is also an important aspect of the water resource.)
- 2. The topography of the land surface, including major slopes, undulations, locations of water delivery, and surface drainage points
- 3. The physical and chemical characteristics of the soil, particularly the infiltration characteristics, moisture-holding capacities, salinity, and internal drainage
- 4. The expected cropping pattern and its temporal water demands, and special factors such as sensitivity to prolonged soil saturation, harvesting and cultivation needs, germination problems, and critical growth periods
- 5. The economic and marketing conditions in the area as well as the availability of labor (and its skill), maintenance and replacement services, capital of construction and operation, and energy, fertilizers, and so on
- 6. The cultural practices employed in the overall farming enterprise, especially where they may prohibit a specific element of the design or operation of the surface irrigation system

The surface irrigation design process begins as a procedure in which the most desirable watering frequency and depth are matched with the capacity and availability of the water supply. The "matching" involves the intermediate analysis of field distribution design and field layouts.

### PRELIMINARY DESIGN

Before setting the design parameters associated with each component of the surface irrigation system, a preliminary operating scenario should be established. The optimal operation is the one that supplies water to the crop root zone in variable depths and according to a flexible schedule. This regime allows the irrigator to manage the soil moisture depletion for maximum yields as well as to save water, labor, and energy. Although probably not as major a factor, system flexibility provides a better integration of irrigation functions in other farming tasks.

Some irrigation systems are supplied water on continuous or rotational schedules. The flow rate and duration are usually fixed, so flexibility in scheduling

irrigation is limited to what each farmer or group of farmers can accomplish within their own systems. At the preliminary design stage, the designer should determine the limits of the water supply in satisfying an optimal irrigation schedule throughout a season.

### Net Irrigation Requirements and Schedules

As a first step in the design process, local climatological, soil, and cropping pattern data can be used to evaluate the temporal distribution of crop water demands. This analysis should yield the amount of water the system should supply as a function of time during the season or by individual irrigation events. The capacity of the system will be dictated by either the first irrigation or the period of maximum crop demand. The former limitation will not be known until the final design stage.

With a tentative schedule produced by considering only the crop demands (minus expected precipitation), the next consideration is the capability of the water delivery system to supply water according to its schedule. Complete demand systems should have little trouble, while continuous or rotational water supplies may be difficult to match to the crop demand.

Whichever criterion (crop demand or water availability) governs the operating policy at the farm level will then dictate the primary operational schedule. This information will provide the timing and depth to be applied during the irrigation season and the application efficiency of the system as well.

### Selecting the System and Its Layout

With a schedule of typical irrigation events and the soil and topographical characteristics of the location, the type of surface irrigation system to employ can be carefully considered. Furrow systems would be favored on most sloping conditions where row crops are being grown as well as in flat areas where small applied depths are required. Border and basin systems apply larger depths during most irrigations and therefore may be better suited to rotational water supplies. These and many other considerations go into a decision as to the best surface irrigation technology to apply.

A great deal of management can be applied in all cases where flexibility in irrigation frequency and depth are important. For example, suppose that a 100-ha field was to be designed to apply 100 mm of water using level basins. Suppose further that the irrigation district would supply 1.16 m³/s for 24 h at 10-day intervals. If the hydraulics would permit, the irrigator could apply the flow to one basin of 100 ha for the entire 24 h in order to apply the 100 mm. Or, he could divide the field into ten 10-ha basins, irrigate each one for 2.4 h and achieve the same result. The difference in the two alternatives is that the discharge per hectare in the former is 0.0116 m³/s/ha, while in the latter it is 0.116 m³/s/ha. This difference may be immensely important in how well the system will perform and the water be utilized to support comparable levels of production. Thus, at the preliminary design stage, it is important to evaluate possible field subdivisions.

### **DETAILED DESIGN**

The detailed design process involves four steps: (1) determine the slope of the field, (2) establish the flow per unit width onto the field and its duration, (3) locate and design headland structures and miscellaneous facilities, and (4) provide surface drainage facilities to either collected tailwater for subsequent reuse or to dispose of these flows. Individual sections and chapters follow which deal with these four design requirements (together with a managerial discussion chapter). For this section, a design philosophy will be stated briefly to justify the procedures outlined later.

## **Land Leveling**

Land leveling can easily be the most expensive improvement that a farmer makes on his fields. It is, however, absolutely prerequisite to the satisfactory performance of the surface irrigation system. The philosophy of this text is simply that the slope of the field should be designed to result in minimum earth movement. The one exception would be where long-term considerations dictate that basin irrigation will yield sufficient benefits to offset the added leveling cost. We discuss the land-leveling problem in Chapter 7.

# Flow Rates and Time of Application

Once the field slope is set and the applied depths are anticipated from the irrigation scheduling, the remaining design variables are flow rate per unit width of border or basin or furrow flow, the time of cutoff, and the field length. Because most farmers resist subdividing fields in length due to reduced machinery efficiency, length will not be treated as a design variable unless a combination of flow rate and cutoff time cannot be found which provide satisfactory system performance.

### A RATIONALE FOR VOLUME BALANCE

Surface irrigation design always seems to be in a transitional stage. Since 1977, major advances in the technology of modeling have been made which allow design and evaluation to be conducted at a substantially higher theoretical level. For instance, historical design practices based primarily on volume balance concepts can now be replaced with the hydrodynamic, zero-inertia, and kinematic-wave models, all of which are considered in following chapters.

There are several fundamental reasons why a volume balance design methodology has been included when, as stated, the state-of-the-art technology has superseded the volume balance concept. For the beginning irrigation engineer, the volume balance methodology provides a view of design procedures without the cumbersome detail of advanced theory. Design issues such as the maximization of application efficiencies with proper choices of inflow rates and cutoff time can be illustrated. The influence of other variables, such as field slopes and length, roughness of the field surface, and infiltration characteristics of the soil can be ascertained easily. Finally, volume balance provides an evaluation methodology and a design procedure within the framework of the same mathematical formulas.

The essential difference between irrigation evaluation and design using the volume balance procedure is as follows. Data collected during an evaluation include inflows and outflows, flow geometry, length and slope of the field, soil moisture depletion, and advance and recession rates. From these data, the infiltration characteristics of the field surface are deduced and then the system performance is determined. Design procedures begin with known or estimated infiltration parameters (including their changes during the season) and expected flow geometry, field slope, and field length. Then the rates of advance and recession, as well as field performance levels, are estimated for various combinations of inflow discharge and cutoff times. The values selected for design are those that maximize efficiency and will vary over the irrigation season as desired application depths and infiltration parameters change.

The irrigation designer faces a problem consisting of three distinct phases. First, the characteristics of the site must be identified, including the most likely field slopes and lengths. Then the flow parameters, inflow discharge, and cutoff times must be computed, to maximize efficiency. Finally, the field parameters must be reconciled with the prevailing conditions of the water supply and general farming practices. The first phase was discussed earlier. Selection of field parameters will be described here for furrow, border, and basin systems. The furrow analysis will include designs with and without cutback or tailwater reuse subsystems. Border irrigation design will be limited to the free-draining case and it will be assumed that cutback and tailwater reuse principles described in the furrow section can be applied by the reader.

### **COMMON DESIGN COMPUTATIONS**

Two of the surface irrigation design computations are similar for furrow, border, and basin systems. These are the calculations of the required intake opportunity time and the duration of the advance phase. A step-by-step procedure for these computations will be given in this section and then simply referred to in the following system design methodologies.

### Intake Opportunity Time

The basic mathematical model of infiltration utilized in this text is the Kostenkov-Lewis relation (Eq. 6.1), in which Z has units of  $m^3/m$ ,  $\tau$  has units of minutes, and  $f_0$  has units of  $m^3/\min/m$ . To express intake as a depth of application, Z must be divided by the unit width. For furrows, the "unit width" is the furrow spacing, w, where for borders and basins it is 1 m. Values of k, a, and  $f_0$ , and unit width are design input data, as is the volume per unit length required to refill the root zone,  $Z_{\text{reg}}$ .

The volume balance design procedure requires that the intake opportunity

time associated with  $Z_{\text{req}}$  be known. This time, represented by  $\tau_{\text{req}}$ , requires a nonlinear solution to Eq. 6.1. A convenient method is the Newton-Raphson procedure:

- 1. Make an initial estimate of  $\tau_{req}$  and label it  $(\tau_{req})_i$ .
- 2. Compute a revised estimate,  $(\tau_{req})_{i+1}$ , based on the following formula:

$$(\tau_{\text{req}})_{i+1} = (\tau_{\text{req}})_i + \frac{Z_{\text{req}} - k(\tau_{\text{req}})_i^a - f_0(\tau_{\text{req}})_i}{\frac{ak}{(\tau_{\text{reg}})_i^{1-a}} + f_0}$$
(6.5)

3. Compare the values of the initial and revised estimates. If they are equal to each other, or within an acceptable tolerance, the value of  $\tau_{req}$  is determined. If they are not sufficiently equal in value, replace the initial value of  $\tau_{req}$  with the revised value,  $(\tau_{req})_i = (\tau_{req})_{i+1}$ , and repeat steps 2 and 3.

### **Advance Time**

Water will be distributed over a surface-irrigated field nonuniformly due to the differential time required for water to cover the field. To account for these differences in the design procedures, it is necessary to calculate the advance trajectory.

It is first necessary to describe the flow cross section using two of the following functions, given in Chapter 5:

$$A = \sigma_1 y^{\sigma_2} \tag{5.15}$$

and

$$WP = \gamma_1 y^{\gamma_2} \tag{5.18}$$

or as a simpler substitute,

$$A^2 R^{1.33} = \rho_1 A^{\rho_2} \tag{6.6}$$

where

A =cross-sectioned flow area, m<sup>2</sup>

y = flow depth, m

WP = wetted perimeter, m

 $\sigma_1, \sigma_2, \gamma_1, \gamma_2, \rho_1, \rho_2$  = empirical shape coefficients

For border and basin systems,  $\sigma_1$ ,  $\sigma_2$ ,  $\gamma_1$ , and  $\rho_1$  are equal to 1.0. The value of  $\gamma_2$  is 0.0 and  $\rho_2$  is 3.3333.

The next step is to determine the cross-sectional flow area at the field inlet,  $A_0$ . For sloping fields, this can be accomplished with the Manning equation as follows:

$$A_0 = C_1 \left(\frac{Q_0 n}{60 S_0^{0.5}}\right)^{C_2} \tag{5.19}$$

where

$$C_2 = \frac{3\sigma_2}{5\sigma_2 - 2\gamma_2} \tag{5.20}$$

and

$$C_1 = \sigma_1 \left( \frac{\gamma_1^{0.67}}{\sigma_1^{1.67}} \right)^{C_2} \tag{5.21}$$

or,

$$A_0 = \left(\frac{Q^2 n^2}{3600 \rho_1 S_0}\right)^{1/\rho_2} \tag{6.7}$$

where

 $Q_0$  = field inlet discharge, m<sup>3</sup>/min/unit width

n = Manning roughness coefficient

 $S_0$  = field slope

In a level-slope condition, such as in a basin, it is assumed that the friction slope is equal to the inlet depth,  $y_0$ , divided by the distance covered by water, x. This leads to the following expression for  $A_0$ :

$$A_0 = \left(\frac{Q_0^2 n^2 x}{3600}\right)^{0.23} \tag{6.8}$$

It can be seen that  $A_0$  increases during the advance phase and must therefore be calculated at each time step used to evaluate the advance trajectory. For sloping field conditions  $A_0$  is assumed to be constant.

The design input data required at this point are  $\sigma_1$ ,  $\sigma_2$ , and  $\gamma_1$ ,  $\gamma_2$ , or  $\rho_1$ ,  $\rho_2$ , field length, (L), S, n, and  $Q_0$ . This information can be used to solve the volume balance equation (Eq. 5.23) for the time of advance,  $t_I$ :

$$Q_0 t_L - 0.77 A_0 L - \sigma_z k t_L^a L - \sigma_z' f_0 t_L L = 0$$
 (5.23)

where  $\sigma_z$  is evaluated by Eq. 5.14 and  $\sigma_z' = 1/(1 + r)$ , where r is defined in Eq. 5.11.

Equation 5.23 contains two unknowns,  $t_L$  and r, which are related. To solve for them, a two-point advance trajectory is defined in the following procedure:

- 1. The power advance exponent r typically has a value of 0.3 to 0.9. The first step is to make an initial estimate of its value and label this value  $r_i$ . Then a revised estimate is computed and compared as follows.
- 2. Calculate  $\sigma_z$  and  $\sigma_z'$ .
- 3. Calculate the time of advance,  $t_L$ , using the following Newton-Raphson procedure:

a. 
$$(t_L)_i = 5.0(A_0 L/Q_0)$$

b. 
$$(t_L)_{i+1} = (t_L)_i -$$

$$\frac{Q_0(t_L)_i - 0.77A_0L - \sigma_z k(t_L)_i^a L - \sigma_z' f_0(t_L)_i L}{Q_0 - \frac{ak\sigma_z L}{(t_L)_i^{1-a}} - \sigma_z' f_0 L}$$
(6.9)

c. Compare the initial estimate of advance time,  $(t_L)_i$ , with the revised estimate,  $(t_L)_{i+1}$ . If they are sufficiently equal, proceed to step 4. If not,

- define  $(t_L)_i = (t_L)_{i+1}$  and repeat steps b and c. Note that should the inflow,  $Q_0$ , be too small for the field length, this procedure will fail to converge. This is an indication that either  $Q_0$  must be increased or L reduced.
- d. Calculate the time of advance to the field midpoint,  $t_{0.5L}$ , in the same manner as finding  $t_L$  by replacing L by 0.5L and  $t_L$  with  $t_{0.5L}$ . For level field conditions, the midpoint length and the inlet area,  $A_0$ , must be substituted. Equation 6.8 is used with L and 0.5L to find the appropriate values of  $t_L$  and  $t_{0.5L}$  respectively.
- 4. Compute a revised estimate of r as follows:

$$r_{i+1} = \frac{\ln(2)}{\ln(t_L/t_{0.5L})} \tag{6.10}$$

5. Compare the initial estimate with the revised estimate. If they are sufficiently equal, the procedure for finding  $t_L$  is concluded. If not, let  $r_i = r_{i+1}$  and repeat steps 2 to 4.

Determination of  $t_L$  is the basic volume balance calculation. It is used at the beginning of a design to ensure that the maximum flow will be able to complete the advance phase adequately. Similarly, it is used to find a minimum field inflow, as well as a cutback flow if used in the design. The  $t_L$  computations are used repeatedly in optimization of the design or its operations.

When designing manually or with some of the simpler programmable calculators, it is often worthwhile to begin with maximum flow and increment downward with the  $t_L$  procedure until a minimum is reached. Then  $Q_0$  versus  $t_L$  can be plotted, for later reference in the design procedures.

### FURROW IRRIGATION DESIGN

Beginning with the information gained from evaluating the farm system, decisions must be made concerning the following parameters: (1) furrow flow rate, (2) furrow length, (3) time of application (duration of the inflow to each furrow), (4) furrow slope, and (5) degree of automation.

The number of furrow parameters needing evaluation can generally be reduced to furrow inlet discharge and cutoff time. Land leveling is so expensive that farmers usually grade on the basis of least earth movement, so furrow slope is generally a specified value. Similarly, field length is often specified by farmers because it significantly affects the efficiency of equipment operations. Occasionally, the intake rates are high enough to prevent the flow from advancing to the end of the furrow, and either slope or field length may require adjustment. Automation tends to follow the choice of furrow system being implemented.

There are three primary furrow designs: (1) furrow systems without cutback or tailwater reuse facilities, (2) the cutback system, and (3) the tailwater recirculation system. Each of these systems must have substantial flexibility to adequately irrigate fields in which the surface roughness and intake rates vary so widely from

irrigation to irrigation. The philosophy of design suggested in this book is to select flow rates and cutoff times for at least two expected field conditions which need to be evaluated as part of the design process. For instance, a furrow discharge and cutoff time should be found for the first irrigation following planting or cultivation, when roughness and intake are maximum, and for the third or fourth irrigation, when these conditions are minimal.

# Furrow Design Procedure for Systems without Cutback or Reuse

A step-by-step procedure for selecting the furrow inflow and cutoff time for traditional systems is as follows:

1. Input data required, in addition to those noted previously, include the system discharge,  $Q_T$  (m<sup>3</sup>/min), and the field width,  $W_f$ . The number of furrows,  $N_f$ , is then

$$N_f = \frac{W_f}{w} \tag{6.11}$$

2. The maximum flow velocity in furrows,  $v_{\rm max}$ , is suggested as being about 8 m/min in erosive silt soils to about 13 m/min in the more stable clay and sandy soils. An initial value of furrow inlet flow,  $Q_0$  (m³/min), should be selected that will produce velocities near the maximum allowable. From continuity and Eq. 5.19, this is

$$Q_0 = \left\{ v_{\text{max}} C_1 \left( \frac{n}{60 S_0^{0.5}} \right)^{C_2} \right\}^{1/(1 - C_2)} = Q_{\text{max}}$$
 (6.12)

or from continuity and Eq. 6.7,

$$Q_0 = \left(v_{\text{max}}^{\rho_2} \frac{n^2}{3600\rho_1 S_0}\right)^{1/(\rho_2 - 2)} = Q_{\text{max}}$$
 (6.13)

The value of  $Q_0$  should be adjusted so that the number of sets is an integer number, that is,  $N_f Q_0/Q_T$  should be an integer.

- 3. Compute the advance time,  $t_L$ .
- 4. Compute the required intake opportunity time,  $\tau_{req}$ .
- 5. Compute time of cutoff,  $t_{co}$  (min):

$$t_{co} = \tau_{req} + t_L \tag{6.14}$$

6. Compute application efficiency,  $E_a$ , from Eq. 6.4:

$$E_a = \frac{Z_{\text{req}}L}{Q_0 t_{co}} \tag{6.4}$$

7. The application efficiency should be maximized subject to the limitations on erosive velocity, the availability and total discharge of the water supply, and other farming practices. The inflow should be reduced and the procedure

repeated until a maximum  $E_a$  is determined. The reduction in inflow per furrow should correspond again to flows that result in integer values of the field sets.

# **Cutback Furrow Design Procedure**

The application efficiency maximizing procedure described above basically determines the minimal waste trade-off point between tailwater and deep percolation. For example, a small value of  $Q_0$  will result in low tailwater losses but high deep percolation losses, due to the large differences in intake opportunity times. Large furrow flows advance over the field rapidly, thereby providing the potential for greater application uniformity and less deep percolation, but also greater tailwater losses as the water flows from the field for a longer time.

One of the most common methods of minimizing tailwater is to reduce the furrow inflow when the advance phase is completed. There are two cutback strategies that can be designed. The first is used in cases where sufficient labor is available (or a relatively high level of automation) to accomplish a complex schedule of adjusting furrow flows and set sizes. This strategy is to provide sufficient flow to complete the advance phase in about one-fourth of the required intake opportunity time, then cut back to a soaking flow and add a new set. As soon as the second set has completed advance, the flow is cut back and a third set is added. It is therefore possible to have four simultaneous operating sets, and a high level of irrigation management is important. The design procedure is basically the same as for the second strategy, which is described below.

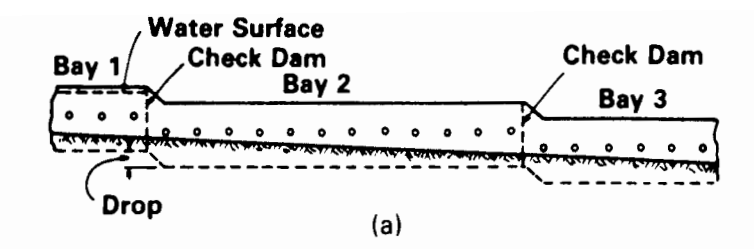
Most cutback systems are designed to operate in sets of two, one advance phase set and one soaking set. Thus the advance phase and the soaking phase are both equal to the required intake opportunity time. This irrigation regime also just refills the root zone reservoir in the least watered areas. One of the most common cutback systems is that proposed by Garton (1966) and illustrated in Fig. 6.1. The head ditch is divided into a series of level bays with spiles or other means of diverting water into the furrows. As shown, the differences in bay elevations are such that the water level is sufficient to flow into the furrows of only two bays simultaneously. In the lowest bay, the head of the outlets needs to be sufficient to provide the desired advance phase flow while the reduced head in the upstream bay provides the soaking flow.

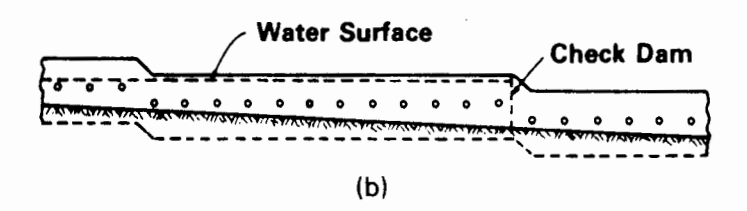
The cutback design procedure for the system illustrated in Fig. 6.1 is as follows:

 In addition to the information required by the previous procedure, the relationship between head ditch water level and furrow flow rate must be defined:

$$Q_0 = c_1 h^{c_2} (6.15)$$

where  $c_1$  and  $c_2$  are empirical coefficients and h is the head ditch water level above the outlet invert.





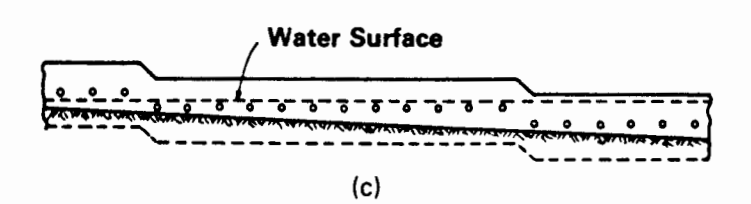


Figure 6.1 Elevation view of one cutback furrow irrigation system. In view (a), bay 1 is delivering the advance furrow flow, while a check between bays 1 and 2 prevents water from going to the downstream bays. In view (b) the check has been moved to the downstream end of the bay 2 and the flow is divided between bay 1 (receiving the cutback flow) and bay 2 (receiving the advance flow). In view (c) the check has been moved to the downstream end of bay 3. Bay 1 now receives no water, bay 2 is in the cutback phase, and bay 3 is in the advance phase. (From Garton, 1966.)

- 2. Compute the required intake opportunity time,  $\tau_{req}$ , and note that for two-bay cutback systems,  $t_L = \tau_{req}$ .
- 3. Compute the discharge required to complete the advance phase in  $t_L$  minutes. This can be accomplished iteratively using the procedure for finding  $t_L$  given previously. If a number of  $Q_0$  versus  $t_L$  values have been determined and plotted as suggested, it is generally sufficient to select the appropriate value from this curve or interpolate it from the earlier results.
- 4. Compute the cutback flow,  $Q_0'$ :

$$Q_0' = 1.1 f_0 L (6.16)$$

It is usually necessary to increase the cutback flow slightly above the basic intake rate to keep the furrow wet over its entire length.

5. Compute the number of furrows in each field set:

$$N_{1} = \frac{Q_{T}}{Q_{0}}$$

$$N_{2} = \frac{Q_{T} - N_{1}Q_{0}'}{Q_{0}}$$

$$N_{3} = \frac{Q_{T} - N_{2}Q_{0}'}{Q_{0}}$$

$$N_{i} = \frac{Q_{T} - N_{i-1}Q_{0}'}{Q_{0}}$$
(6.17)

- 6. If the field set division does not result in an even number of sets, adjust the total supply discharge  $Q_T$  if possible or adjust the  $Q_0$  value until the system is satisfactory.
- 7. Compute the application efficiency:

$$E_a = \frac{Z_{\text{req}}L}{t_L(Q_0 + Q_0')} \tag{6.18}$$

## Design of Furrow Systems with Tailwater Reuse

Substantial improvements in the application efficiency of furrow irrigation systems are possible when tailwater is no longer a waste. The design of such systems is much more complex than the procedure given above because of the need to utilize effectively two sources of water simultaneously.

Reuse systems, such as that illustrated in Fig. 6.2, have an inherent economic trade-off that must be recognized. To minimize deep percolation losses and achieve high uniformities, the furrow velocity should be nearly that of the maximum erosive velocity. Such a flow will require a potentially costly tailwater reservoir and pumpback system. Thus an optimal reuse system generally involves a furrow flow rate that advances the field in 30 to 40% of the required intake opportunity time.

One of the major complexities of reuse systems is the strategy for recirculating the captured tailwater. A popular option is to pump the tailwater into the primary supply and then open additional furrows to utilize the additional flow. Another is to irrigate separate sections of the field with the tailwater. The primary difficulty is that the tailwater reservoir and pumping system need to be carefully controlled.

To illustrate the design strategy for reuse systems, a design procedure for a common configuration is outlined. The reuse system is intended to capture tailwater from one set and combine it with the supply to a second set. A similar

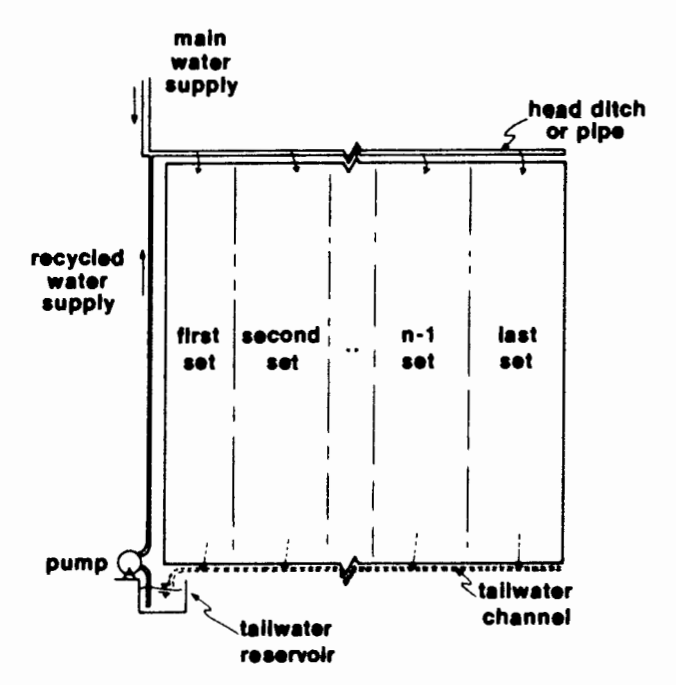


**Figure 6.2** Typical tailwater reuse configuration.

operating scenario will prevail for each subsequent pair until the last set is irrigated. For this set, the tailwater must either be stored until the next irrigation, dumped into a wasteway, or used elsewhere.

The total volume of tailwater recycled will be held at a constant volume of the runoff from the first set. This requires that the difference in tailwater volume between the first and subsequent sets be wasted. The recycled flow can thus be held constant to simplify the pump-back system and the overall management strategy.

The following steps comprise the furrow reuse system design:

- 1. Input data are the same as for the cutback system.
- 2. Compute the required intake opportunity time,  $\tau_{req}$ , as outlined previously.
- 3. Compute the inlet discharge required to complete the advance phase in approximately 30% of  $\tau_{req}$ , correcting if necessary for nonerosive stream velocities.
- 4. Compute the tailwater volume as follows:
  - a. The time of cutoff is  $t_{co} = \tau_{req} + t_L$ .
  - b. The infiltrated depths at the field inlet and outlet are

$$Z_{\text{in}} = k(t_{co})^a + f_0 t_{co}$$
$$Z_{\text{out}} = Z_{\text{rec}}$$

c. The volume of tailwater is

$$V_{\text{tw}} = N_f Q_0 t_{co} - \frac{0.77 A_0 L}{2} - \frac{Z_{\text{in}} + Z_{\text{out}}}{2} L$$
 (6.19)

where

$$N_f = \frac{Q_T}{Q_0} \tag{6.20}$$

5. Compute the pump-back discharge,  $Q_{nb}$ :

$$Q_{pb} = \frac{V_{tw}}{t_{co}} \tag{6.21}$$

6. Compute the number of furrows in the second or subsequent sets:

$$N_i = \frac{Q_T + Q_{pb}}{Q_0} {(6.22)}$$

7. The field should be in evenly divided sets, which may require repetition of the procedure with a modified furrow discharge.

# Integration with Water Supply

The water supply has characteristics that must be reconciled with the furrow discharges and cutoff times evaluated during the second design phase described above. These characteristics include discharge, availability, and duration. There are many

operational policies utilized by irrigation districts today and the designer must be aware of the one affecting the system being designed.

The first consideration is the supply discharge. A field has a fixed number of furrows each to receive the design flow. Thus the number of sets is the total number of furrows divided by the ratio of supply discharge to furrow discharge. For instance, a field with a supply of 250 liters/s and 1000 furrows each requiring 1 liter/s will irrigate in four sets (250 furrows being irrigated simultaneously). Because the number of sets must be an integer number, the furrow discharge may need to be modified slightly. It should also be noted that since furrow discharge will change during the season, the number of sets may also change. Similar modifications may be necessary if the water supply also varies.

The availability of the water supply affects primarily the depth to be applied during each irrigation. Rotational systems must be capable of applying variable requirements, whereas demand systems can apply fixed requirements.

In many irrigation systems, the duration of the water supply is also fixed, along with discharge and availability. When this is the case, the furrow discharge and cutoff time must not only lead to a proper set distribution and refill the root zone, but also irrigate the field in the allotted time.

All of these matters are site specific and require careful exercise of judgment. In every aspect, furrow irrigation system design is an iterative process in which an evaluation of field operating procedures must fall within the limits imposed by site conditions, the water supply, and the multifaceted farming enterprise. Border and basin irrigation are also governed by these considerations.

### **BORDER IRRIGATION DESIGN**

The design of borders is similar to that for furrow systems, with two notable differences. First, the geometry of the flow is simpler because it can be treated as wide, plane flow. This difference leads to some simplifications in the computations while the second complicates calculations. This second difference is that while the depletion and recession phases can generally be neglected in furrow irrigation design, both phases are important in border irrigation.

Borders can be diked at their lower end or allowed to drain freely. The diked condition is similar to that of basins and is treated in the next section. Freedraining borders are also amenable to cutback and tailwater reuse methodologies. Only the design of the free-draining case will be described in this section.

The step-by-step design procedure for borders is as follows:

- 1. Identify the following input data:
  - a. Soil infiltration characteristics, a, k, and  $f_0$
  - b. Field slope,  $S_0$ ; length, L; surface roughness coefficient, n
  - c. Soil moisture depletion at the time of irrigation,  $Z_{\text{req}}$
  - d. Total supply flow rate,  $Q_T$
  - e. Total width of the field,  $W_f$
- 2. Select the border inflow rate per unit width,  $Q_0$  (m<sup>3</sup>/min/m), near a value

allowed by maximum erosive velocities. Hart et al. (1980) suggest an empirical equation to assist in this choice:

$$Q_{\text{max}} = \frac{0.01059}{S_0^{0.75}} \tag{6.23}$$

for non-sod-forming crops, and a value twice this large for sod crops. Note also that a minimum  $Q_0$  is suggested to ensure adequate spreading:

$$Q_{\min} = \frac{0.000357L\sqrt{S_0}}{n} \tag{6.24}$$

3. Compute the inflow depth,  $y_0$ , in meters, as follows:

$$y_0 = \left(\frac{Q_0 n}{60 S_0^{0.5}}\right)^{0.6} \tag{6.25}$$

and check to ensure that this value does not exceed the probable border dike heights.

- 4. Compute the required intake opportunity time,  $\tau_{req}$ .
- 5. Compute the time of advance,  $t_L$  (min).
- 6. Assume that the design will just refill the soil moisture storage at the end of the border and then calculate the time of recession as follows:

$$t_r = \tau_{\text{reg}} + t_L \tag{6.26}$$

where  $t_r$  is the recession time in minutes since the beginning of the irrigation.

- 7. Calculate the depletion time,  $t_d$  (min), as follows:
  - a.  $T_1 = t_r$

b. 
$$I = \frac{ak}{2} [T_1^{a-1} + (T_1 - t_L)^{a-1}] + f_0$$
 (6.27)

c. 
$$S_y = \frac{1}{L} \left[ \frac{(Q_0 - IL)n}{60S_0^{0.5}} \right]^{0.6}$$
 (6.28)

d. 
$$T_2 = t_r - \frac{0.095n^{.47565}S_y^{0.20735}L^{0.6829}}{I^{0.52435}S_0^{0.237825}}$$
 (6.29)  
e. Is  $T_1 = T_2$ ? no, then assign  $T_1 = T_2$  and repeat steps (b) through (e) ves. then  $t_1 = T_2$ 

- yes, then  $t_d = T_2$
- 8. Calculate the infiltrated depths at the border inlet and determine whether the design leads to complete, over-, or underirrigation.

$$Z_0 = kt_d^a + f_0t_d$$
 if  $Z_0 \ge Z_{\text{req}}$ , irrigation is complete (CI) (6.30)  
if  $Z_0 < Z_{\text{reg}}$ , underirrigation (UI)

9. If the irrigation is complete, compute the application efficiency,  $E_a$ , using Eq. 6.4 and the time of cutoff as follows:

$$t_{\rm co} = t_d - \frac{y_0 L}{2Q_0} \tag{6.31}$$

10. If the irrigation is not complete, the cutoff time must be increased so that the intake at the inlet is equal to the required depth. The computation proceeds as follows:

a. 
$$t_{co} = \tau_{req} - \frac{y_0 L}{2Q_0}$$
 (6.32)

b. 
$$I = \frac{ak}{2} \left[ \tau_{\text{req}}^{a-1} + (\tau_{\text{req}} - t_L)^{a-1} \right] + f_0$$
 (6.33)

c. Compute  $S_v$  from Eq. 6.28.

d. 
$$t_r = \tau_{\text{req}} + \frac{0.095 n^{0.47565} S_y^{0.20735} L^{0.6829}}{I^{0.52435} S_0^{0.237825}}$$
 (6.34)

e. 
$$Z_L = k(t_r - t_L) + f_0(t_r - t_L)$$
 (6.35)

f. Compute  $E_a$  from Eq. 6.4.

11. Compute the border width,  $W_0$ , in meters and the number of borders,  $N_b$ :

$$W_0 = \frac{Q_T}{Q_0} \tag{6.36}$$

$$N_b = \frac{W_f}{W_0} \tag{6.37}$$

If  $N_b$  is not an even number or the width is unsatisfactory for other reasons, modify the unit width inflow,  $Q_0$ , or plan to adjust the system discharge,  $Q_T$ . Note that because infiltration generally declines during the irrigation season, the number of simultaneously irrigated borders may increase for later water applications.

### **BASIN IRRIGATION DESIGN**

Basin irrigation design is somewhat simpler than either furrow or border design since tailwater is prevented from exiting the field and the slopes are usually very small or zero. Thus, recession and depletion are accomplished at the same time and nearly uniform over the entire basin. Because longitudinal and transverse slopes are small or zero, the driving force in the flow is limited to the hydraulic slope of the water surface. Consequently, the uniformity of the field surface topography is critically important.

An effort will not be made in this section to describe a design procedure for irregularly shaped basins. It will be assumed that water movement over the basin will occur in a single direction as with furrows and borders. Three further assumptions will be made specifically for basin irrigation. The first is that the friction slope during the advance phase of the flow can be approximated by

$$S_f = \frac{y_0}{x} \tag{6.38}$$

where

 $y_0$  = depth of flow at the basin inlet, m

x = distance from inlet to the advancing front, m

 $S_f$  = friction slope

Utilizing the result of Eq. 6.38 in the Manning equation yields

$$Q_0 = \frac{60y_0^{2.167}}{nx^{0.5}} \tag{6.39}$$

or

$$y_0 = \left(\frac{Q_0^2 n^2 x}{3600}\right)^{0.23} \tag{6.40}$$

The second assumption is that immediately upon cessation of inflow, the water surface assumes a horizontal orientation and infiltrates vertically. In other words, the infiltrated depths over the basin are equal to the infiltration during advance, plus the average depth of water remaining on the soil surface at the time of advance, plus the average depth added to the basin following completion of advance. At the inlet to the basin, the infiltrated depth is

$$Z_0 = kt_L^a + f_0 t_L + 0.80 y_0 + \frac{Q_0 (t_{co} - t_L)}{L}$$
 (6.41)

(note that  $t_{co} - t_L \ge 0$ ). The first two terms of Eq. 6.41 represent the infiltrated depth during the advance phase. The third term is the average depth of surface water at the time of advance. The final term is the average depth of water added to the basin following completion of the advance phase.

Finally, it is assumed that the design is made just to refill the root zone deficit in the least watered areas, in this case, the downstream end of the basin. Equation 6.41 can be simplified and then used to solve for the time cut off by omitting the first two terms and then solving for  $t_{co}$ :

$$t_{co} = \frac{Z_{\text{req}}L - 0.8y_0L}{Q_0} + t_L \tag{6.42}$$

It is apparent that the time cutoff must be greater than or equal to the time of advance, which limits the minimum depth that can be applied during a basin irrigation.

The procedure for basin design is as follows:

- 1. Identify the same input data as described earlier.
- 2. Select a basin inflow rate per unit width,  $Q_0$  (m<sup>3</sup>/min/m), near a value allowed by the maximum erosive velocities and the height of the basin dike. Check by finding the maximum basin depth at the inlet during the advance phase using Eq. 6.40 with L/2 substituted for x.

$$Q_{\text{max}} = \left[ v_{\text{max}} \left( \frac{n^2 L}{7200} \right)^{0.23} \right]^{1.857}$$
 (6.43)

- 3. Compute the advance time,  $t_L$  (min).
- 4. Assume that the design will just refill the soil moisture storage at the end of the basin and then calculate the time of cutoff using Eq. 6.42. If  $t_{co}$  is less than or equal to  $t_L$ , set  $t_{co} = t_L$ .
- 5. Calculate the basin application efficiency using Eq. 6.4.
- 6. Repeat steps 2 to 5 until a maximum value of  $E_a$  is found.
- 7. Compute the basin size consistent with the available water supply and overall field dimensions. Then adjust  $Q_0$  or  $Q_T$  accordingly, if necessary.

### **EXAMPLE PROBLEMS**

### Example 6.1: Fixed Inflow Furrow Irrigation Design

There are three surface irrigation design configurations that an engineer must consider. These are the fixed inflow design, the reduced or cutback inflow design, and the runoff recycling design. Because basins usually dike the entire field perimeter to prevent runoff, the last two designs are generally applicable only to furrows and borders. To illustrate the essential elements of the design process, the three configurations will be demonstrated for furrow irrigation and then only the first system layout for borders and basins.

The Problem. A few years ago a farmer converted several of his irrigation systems from a sprinkler to furrow systems. His motivation was to generate more net revenues. The first of the fields shown in layout in Fig. 6.3, is irrigated by the furrow method and was comprised of a loam soil, sloped 0.8% east to west (over the 200-m length) and 0.1% north to south. The furrows were spaced at 1.5-m intervals along the 200-m length and typically had a parabolic shape which was described during several evaluations as follows (Eq. 6.6):

$$A^2R^{1.67} = 0.325A^{2.734}$$

During the evaluations noted, the infiltration function characteristic of the field was divided into two relations to describe the first irrigation following cultivation and then the subsequent irrigations. These relations were

$$Z = 0.0028\tau^{0.534} + 0.00022\tau$$
 m<sup>3</sup>/m (first irrigation)

and

$$Z = 0.0021\tau^{0.331} + 0.00015\tau$$
 m<sup>3</sup>/m (later irrigations)

The evaluation used a Manning coefficient of 0.04 for all analyses.

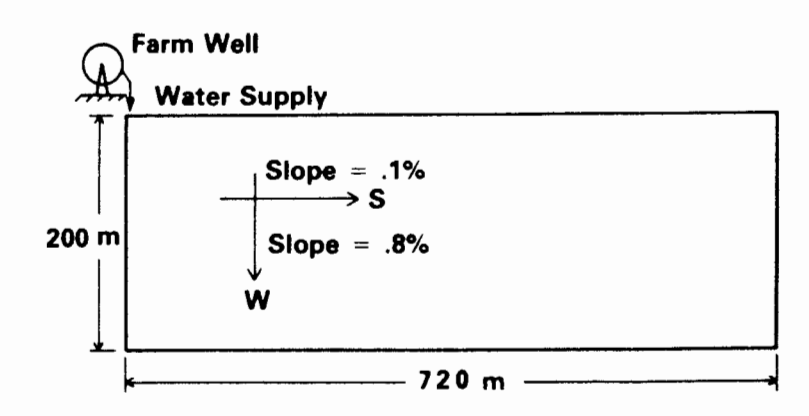


Figure 6.3 Furrow design example field layout.

The well supplying irrigation water to the field had a capacity of 6 m³/min with no quality limitations. In most cases, the irrigator preferred to apply irrigations of 10 cm, which appeared to give him the highest yield response as well as fit conveniently into his other operations. During the first year of operation, major problems emerged that required a comprehensive review of the design. The problem is most interesting when undertaken as if the initial design were being developed.

Initial Design Calculations. At the beginning of a design process, the limitations on the design parameters need to be determined. The first of these is the maximum allowable flow in the furrow. These soils are relatively stable, so the maximum flow velocity could be as high as 13 m/min. Equation 6.13 provides the means of evaluating the corresponding maximum flow rate:

$$Q_{\text{max}} = \left(\frac{v_{\text{max}}^{\rho_2} n^2}{3600 S_0 \rho_1}\right)^{1/(\rho_2 - 2)}$$
$$= \left[\frac{13^{2.734} (0.04)^2}{3600 (0.008) (0.325)}\right]^{1/0.734}$$
$$= 0.104 \text{ m}^3/\text{min}$$

The field is 720 m wide, so that using a 1.5-m furrow spacing results in 720/1.5 = 480 furrows. The well capacity of  $6.0 \text{ m}^3/\text{min}$  would service 6.0/0.104 = 57.69 furrows per set, or the field would be divided into 480/57.69 = 8.32 sets (obviously impractical since the sets must be comprised of an integer number of furrows and the field needs to be subdivided into n integer number of sets). The minimum number of sets is eight, consisting of 60 furrows each and having a maximum flow of  $0.10 \text{ m}^3/\text{min}$ . (It is assumed in this example that it is desirable to utilize the full water supply rather than regulate it.) Beyond this condition are the following options:

Number of sets	Furrows per set	Furrow flow (m <sup>3</sup> /min)
6	80	0.075
5	96	0.0625
4	120	0.05
3	160	0.0375
2	240	0.025
1	480	0.0125

The second limitation on the design procedure is whether or not the flow will complete the advance phase in a reasonable time, say 24 h. In this regard, what minimum flow will complete the advance phase within this limit? If the maximum flow is too small to complete the advance, the furrow length must be reduced.

The second common design computation provides a means of determining the time of advance  $t_L$  as a function of furrow inflow,  $Q_0$ . The maximum inflow can be used to calculate the minimum advance time, but since the minimum flow conditions are not known, the maximum advance time must be established by searching. The computation of  $t_L$  for each  $Q_0$  is somewhat tedious by hand and one may wonder if this phase of the design might be shortened. In the absence of at least a microcomputer, the minimum computational aid is a programmable calculator. With such, the computations are lengthy but not impossible,

and the outcome is most useful, as will be seen. One set of computations will be given for illustrative purposes using the first irrigation condition:

1.  $Q_0 = 0.10 \text{ m}^3/\text{min maximum flow allowable for eight sets.}$ 

2.

$$A_0 = \left[ \frac{Q_0^2 n^2}{3600 S_0 \rho_1} \right]^{1/\rho_2}$$

$$= \left[ \frac{0.10^2 (0.04)^2}{3600 (0.008) (0.325)} \right]^{1/2.734}$$

$$= 0.0077 \text{ m}^2$$
(6.7)

3. Assign the initial value of r = 0.5.

4.

$$\sigma_z = \frac{a + r(1 - a) + 1}{(1 + a)(1 + r)} = \frac{0.534 + 0.5(1 - 0.534) + 1}{1.5(1.534)}$$

$$= 0.76793$$
(5.14)

5. a. Let  $T_1$  be the initial estimate of  $t_L$ :

$$T_1 = 5A_0 \frac{L}{Q_0} = 5(0.00777) \frac{200}{0.1}$$
$$= 80 \text{ min}$$

b. Compute a revised estimate of  $t_L$  as  $T_2$ .

$$T_{2} = T_{1} - \frac{Q_{0}T_{1} - 0.77A_{0}L - \sigma_{z}kT_{1}^{a}L - [f_{0}T_{1}L/(1+r)]}{Q_{0} - (\sigma_{z}akL/T_{1}^{1-a}) - [f_{0}L/(1+r)]L}$$

$$= 80 -$$
(6.9)

$$\frac{0.1(80) - 0.77(0.0077)(200) - 0.76793(0.0028)(80)^{0.534}(200) - [0.00022(80)(200)/1.5]}{0.1 - [0.76793(0.534)(0.0028)(200)/80^{1-0.534}] - [0.00022(200)/1.5]}$$
= 80.19 min

- c. Compare  $T_1$  and  $T_2$ . They differ by less than 1 min, and so another iteration is not needed. Usually, it will be necessary to let  $T_2 = T_1$  and repeat steps 5a and 5b.
- 6. The next step is to find the advance time required to reach one-half the field length,  $t_{5L}$ . The procedure is exactly the same as that given above for  $t_L$ , steps 5a to 5c.
- 5a. Let  $T_1$  be the initial estimate of  $t_{.5L}$ .

$$T_1 = 2.5A_0 \frac{L}{Q_0} = 2.5(0.0077) \frac{200}{0.1}$$
  
= 40 min

5b. 
$$T_2 = 40 -$$

$$\frac{0.1(40) - 0.77(0.0077)(100) - 0.76793(0.0028)(40)^{0.534}(100) - [0.00022(40)(100)/1.5]}{0.1 - \frac{0.76793(0.534)(0.0028)(100)}{40^{1-0.534}} - \frac{0.00022(100)}{1.5}$$

$$= 40 - (19.74) = 20.3 \text{ min}$$

5c. This time the difference between  $T_1$  and  $T_2$  is too great, and steps 5b and 5c must be repeated.

$$T_1 = T_2 = 20.3$$

5b. 
$$T_2 = 20.3 -$$

$$\frac{0.1(20.3) - 0.77(0.0077)(100) - 0.76793(0.0028)(20.3)^{0.534}(100) - [0.00022(20.3)(100)/1.5]}{0.1 - [0.76793(0.534)(0.0028)(100)/20.3^{1-0.534}] - [0.00022(100)/1.5]}$$
= 19.2

- 5c. The two values are now sufficiently close and we define  $t_{5L}$  as 19.2 min.
- 7. The estimation of  $t_L$  and  $t_{.5L}$  above is based on the assumption that the advance exponent r was 0.5. This assumption can be checked.

$$r = \frac{\log(2)}{\log(t_L/t_{SL})} = \frac{\log(2)}{\log(80/19.7)} = 0.4838 \tag{6.10}$$

In this case the initial estimate of r was quite good. Occasionally, however, greater differences will be noted after the first iterations and another pass through steps 1 to 7 will be necessary. In most cases, the value of r should be converged to about  $\pm 0.0001$  in order to estimate the furrow design accurately. Even with relatively poor estimates of r, this procedure converges within three to four iterations. If the stated precision is followed in this case,  $t_L$  will be 80.2 min, which is not significantly different than estimated above. In fact, this result is achieved with one additional repetition of steps 1 to 7.

At this point in the furrow design process it is advisable to repeat these calculations for each flow that might be employed in the design. For the two irrigation conditions, the results are as follows:

Furrow inflow (m³/min)	First irrigation advance time (min)	Subsequent irrigation advance times (min)
0.075	198.6	36.0
0.0625	441.6	46.3
0.05	3	68.2
0.0375	a	143.5
0.025	a	a
0.0125	a	a

<sup>&</sup>lt;sup>a</sup>These flow conditions fail to complete the advance phase in 24 hours without reducing the field length.

The Field Design. There are now three flows and set layouts feasible for the initial field condition and five for the later conditions. The design question at this stage is: Which one leads to the optimal design? The answer is determined by computing the application efficiency for each alternative. First, the required intake opportunity time for each condition is determined using Eq. 6.5. For the first field condition, assume initially that  $\tau_{req} = 300$  min  $(T_1 = 300)$ . Then noting that  $Z_{req} = 10$  cm  $\times$  1.5 m (furrow spacing) or 0.15 m<sup>3</sup>/m of length, Eq. 6.5 becomes

$$T_2 = 300 + \frac{0.15 - 0.0028(300)^{0.534} - 0.00022(300)}{[0.534(0.0028)/300^{0.466}] + 0.00022}$$

$$= 300 + 77.35 = 377.35$$

$$T_2 = 377.35 + \frac{0.15 - 0.0028(377.35)^{0.534} - 0.00022(377.35)}{[0.534(0.0028)/377.35^{0.466}] + 0.00022}$$

$$= \frac{377}{35} + \frac{1}{383} = 378.73$$

$$T_2 = 378.73 + \frac{0.15 - 0.0028(378.73)^{0.534} - 0.00022(378.73)}{[0.538(0.0028)/0.378.73^{0.466}] + 0.00022}$$

$$= 378.73 + 0.00273 = 378.73 = \tau_{reg}$$

Similarly, for the later applications,  $\tau_{req} = 868.5$  min.

The application efficiency for each of the possible field configurations can now be computed. The results, shown below, indicate that the best design is to divide the field into six individual subunits or sets of 80 furrows and utilize an inflow of  $0.075 \, \text{m}^3/\text{min}$ . Then during the subsequent irrigations, two of these sets should be irrigated simultaneously, with half the field supply flow to each set, or a  $Q_0$  of  $0.0375 \, \text{m}^3/\text{min}$ . Figure 6.4 imposes this layout on the field as shown earlier.

APPLICATION EFFICIENCIES FOR FURROW EXAMPLE

$Q_0$ (m <sup>3</sup> /min)	$t_L \pmod{\min}$	t <sub>req</sub> (min)	$\frac{Z_{\text{req}}}{(\text{m}^3/\text{min})}$	<i>L</i> (m)	E., (%)
	Fir	rst irrigation	condition		
0.10	80.2	378.73	0.15	200	65.4
0.075	198.6	378.73	0.15	200	69.3(six sets)
0.0625	441.6	378.73	0.15	200	58.5
	Subsec	quent irrigati	on conditions		
0.10	26.2	868.5	0.15	200	33.5
0.075	36.0	868.5	0.15	200	44.2
0.0625	46.3	868.5	0.15	200	52.5
0.05	68.2	868.5	0.15	200	64.1
0.0375	143.5	868.5	0.15	200	79.1(three sets)

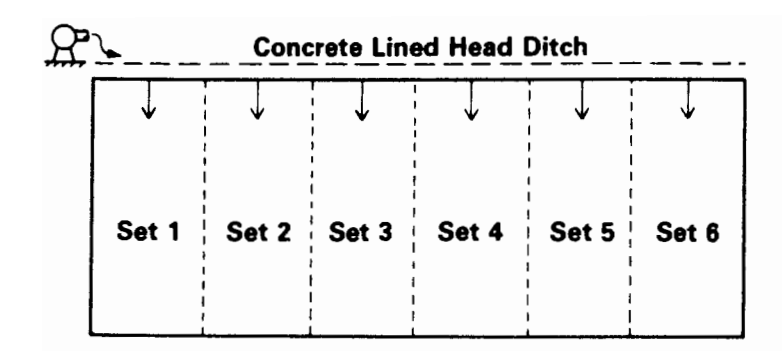


**Figure 6.4** Final furrow design field layout.

The frequency and duration of each irrigation needs to be checked and then the headland facilities selected and designed. During the first irrigation, the field will require just fewer than 60 hours to complete the irrigation. The later waterings will require just over 50 h. If evapotranspiration rates were 1 cm/day, the irrigation interval would be something like 10 days, and one can see that the design waters the field well within these limits. Since the water supply is a tubewell, presumably controlled by the irrigator, the duration of the design is also well within the limits. It should be noted, however, that many irrigation systems do not provide flexible flow rates, adjustable watering frequencies, or variable durations to individual irrigators. As a result, the design parameters that optimize application efficiency may not be feasible. The design should be viewed from a number of perspectives before finalization and implementation.

It may be useful to examine briefly the performance of this design. If the actual irrigations evolve as these design computations indicate, the farmer will waste 20 to 30% of his pumped water as either tailwater or deep percolation. By today's standards, these losses are not great and it may not be cost-effective to add cutback or reuse to the system to reduce these losses further. During the initial waterings, the losses will be about evenly split between runoff and deep percolation. During the later irrigations, runoff will be most of the field loss and runoff recovery and reuse or cutback may yield further savings.

After the field has been configured and the flows set, the designer selects and sizes the field headland facilities. This illustration will be given in Examples 6.2 and 6.3.

### Example 6.2: Cutback Furrow Design

The furrow design developed in Example 6.1, if implemented and carefully managed, would yield an efficient furrow irrigation system. It is not always obvious, but maximum surface irrigation application efficiencies are directly proportioned to the depth of application. To maximize efficiency for a small required depth, high flows of short duration are used. For larger applications, optimizing efficiency implies reducing the flow and increasing the duration of the irrigation. This trend is illustrated in Example 6.1.

There is another point that is also hidden in the peculiarities of the surface irrigation hydraulics. The movement of the water over the soil surface is very sensitive to the relative magnitude of the field inflow and the accumulation of that flow entering the soil profile via infiltration. The outcome of this relationship is that irrigation practices that modify the field inflow, such as cutback, may actually reduce the performance of the system. In more practical terms, if the advance rate is slowed to accommodate a cutback regime, the gains in efficiency derived from reduced tailwater may be more than offset by increases in deep percolation losses. The user of this book might repeat the following cutback design example using all the data and field conditions of Example 6.1 to illustrate this problem.

The Problem. To demonstrate the cutback design concept, the essential features of Example 6.1 can be modified as follows. Suppose that the field soil is a clay or clay loam rather than the sandy loam. The furrows would probably be closer, say 0.75 m apart, in order to increase the infiltrating surface. For example, the 10-cm required application from 1.5-m furrows required a 0.15-m<sup>3</sup>/m cumulative application through the individual furrows of Example 6.1. For the heavier soil, the individual furrow intake is reduced to 0.075 m<sup>3</sup>/m. Let us assume for this problem that the field conditions are the same as in the fixed inflow design problem except for the furrow spacing and the infiltration characteristic of the soil. Initially,

$$Z = 0.0036\tau^{0.357} + 0.000046\tau$$

and thereafter.

$$Z = 0.00383\tau^{0.317} + 0.000035\tau$$

in which the same system of units apply.

Let us further assume the head distribution will be a lined trapezoidal open ditch with spiles installed in the field side to supply each furrow. The hydraulics of these tubes will be determined as part of the design. The system configuration will be the two-bay system illustrated in Fig. 6.1. This design has the advantage that it can easily be automated or simply operated by hand if desired. It minimizes the complexity of irrigating and keeps labor to a minimum. The inherent limitation of the design is that the advance phase and the wetting phase must have the same duration. To facilitate these conditions, it will be assumed that the field water supply from the tube well can be adjusted downward from the 6-m³/min capacity.

Initial Design Calculations. The initial design computations for the cutback system are fundamentally the same procedure as outlined in Example 6.1. The  $\tau_{req}$  for the first irrigation is 785 min and for the subsequent irrigations is 1127 min. If the two-set system is envisioned (one set in the advance phase and one in the wetting), the advance time and cutoff times for the first irrigation are, respectively,  $t_L = \tau_{req} = 785$  min and  $t_{co} = t_L + \tau_{req} = 1570$  min. For subsequent irrigations,  $t_L = 1127$  min and  $t_{co} = 2254$  min.

The next computation is the maximum flow,  $Q_{\text{max}}$ . Since the field and furrow geometries have not changed, the value of  $Q_{\text{max}} = 0.104 \text{ m}^3/\text{min}$ . Of course, the soil might be less stable and rather than a maximum flow velocity of 13 m/min, a lower value of 8 m/min must be used. For this problem assume that the field is indeed easily eroded. Then from Eq. 6.13,

$$Q_{\text{max}} = \left\{ 8^{2.734} \left[ \frac{0.04^2}{3600(0.008)(0.325)} \right] \right\}^{1/0.734}$$
$$= 0.017 \text{ m}^3/\text{min}$$

The next step is to compute the relationship between the inflow and the advance time. Rather than specifying a range of discharges and computing the associated advance times as above, the cutback design looks for a unique flow that yields the  $t_L$  already determined as 785 or 1127 min. This may appear simpler to some and more difficult to others. It is, in fact, the same effort with a slightly different aspect. The detail of the computations will not be given again. For the first irrigation,  $Q_{\text{max}}$  was substituted into the second common design procedure with the time of advance defined as  $t_L = 555$  min after four iterations. This is, of course, faster than the desired advance, so the flow must be decreased. How much is a matter of judgment. Here we will assume a series of 10% reductions from 0.017. For example, if Q = 0.0145 m³/min, the advance time,  $t_L$ , is 860 min. For computerized

design systems the exact  $Q_0$  leading to a  $t_L$  of 785 min can be calculated quickly. By hand it is adequate simply to interpolate. The results of this exercise are summarized below.

ADVANCE TIME	FOR VARIOUS FURR	ow
INFLOWS		

Furrow inflow (m <sup>3</sup> /min)	Advance time (min)
Firs	st irrigation
0.017	555
0.0153	735
0.0145	860
0.015	785 (linearly
	interpolated value)
Late	er irrigations
0.017	347
0.0153	429
0.0136	554
0.0119	764
0.01	1253
0.106	1127 (linearly interpolated value)

It is worthwhile noting that in the case where the maximum flow resulted in an advance time greater than the value required for the system to work, the field length would have to be reduced.

The Field Design. Once the advance phase inflows are established, the field design or layout begins, with an estimate of the cutback flow. The one important constraint on the cutback or wetting phase flow is that it should not be so small as to be less than the intake along the furrow, therefore causing dewatering or recession at the downstream end. Equation 6.16 was given to assist the designer in avoiding this problem. Thus, for the first irrigation the cutback flow must be at least

$$Q_{ch} = 1.1(0.000046)(200) = 0.0101 \text{ m}^3/\text{min}$$

In other words, the flow can only be cut back to 0.0101/0.015 = 67% of the advance phase flow. In subsequent irrigations,

$$Q_{cb} = 1.1(0.000035)(200) = 0.0077 \text{ m}^3/\text{min}$$

or cut back to 73% of the advance flow.

There are several unique features of cutback systems that need to be considered at the design stage. Of particular concern is the fact that the number of furrows per set must vary over the field if the water supply is to be held constant. The number of furrows per set can be the same only if the field supply is varied for each change in sets across the field. This is an option that is feasible but generally not practical. To illustrate this, let us develop a field layout for the cutback irrigation system shown in Fig. 6.2.

Using Eqs. 6.17 and the design information developed previously, the field layout for the system is as summarized below. The  $Q_{cb}/Q_0$  ratio was taken as 0.73, reflecting the constraint imposed by the later irrigations. This ratio must be the same for all irrigations.

CUTBACK FURROW IRRIGATION CONFIGURATION FOR EXAMPLE 6.2

No. of		Number of furrows per set by: Set number							$Q_T$ for first	$Q_{\scriptscriptstyle T}$ for	
sets in field	1	2	3	4	5	6	7	8	9	irrigation later irrigations (m³/min) (m³/min)	
2	756	204								11.34	8.01
3	463	125	372							6.95	4.91
4	386	104	310	160						5.79	4.09
5	301	81	242	125	211					4.52	3.19
6	261	71	210	108	182	128				3.92	2.77
7	222	60	178	93	155	109	143			3.34	2.36
. 8	198	54	159	82	138	97	127	105		2.97	2.10
9	176	48	140	73	123	86	103	94	108	2.64	1.86

One can see that given the 6-m<sup>3</sup>/min capacity of the well supply, the field must be divided into at least four sets to accommodate the first irrigation condition. The upper limit on the number of sets can be evaluated by examining the duration and frequency of the irrigations. The time of cutoff for each set during the first irrigation was determined previously as 26.17 h (1570 min). For the later irrigations,  $t_{co} = 37.67$  h (2254 min).

Except during the advance phase of the first set and the wetting phase of the last, two sets are always operating simultaneously. The duration of the irrigation, therefore, is 1 plus the number of sets times the advance time. For this example:

No. of sers	Duration of first irrigation (days)	Duration of later irrigations (days)
4	2.4	3.9
5	2.9	4.7
6	3.4	5.5
7	3.9	6.3
8	4.9	7.0
9	5.4	7.8

The designer must consider the availability of water and suitability of irrigations of various durations. For example, the application to the root zone is designed to be 10 cm. It is not unusual to have crop evapotranspiration rates of 1 cm/day, so the irrigation may supply only 10 days of water to the field. If this is the case here, the number of sets cannot exceed 6. Let us decide to divide the field into five sets, which falls within the constraints on water supply and irrigation frequency.

This system will involve five sections of headland ditch or pipe. The first section will

be 301 furrows (0.75 m/furrow) = 226 m. The remaining sections or bays will be 61 m, 181 m, 94 m, and 158 m, respectively.

The final steps in the design are to size the headland channel and furrow outlets. Let us assume that a trapezoidal concrete ditch is to be used with spiles to convey the water to each furrow. Let us assume further that local contractors can construct the concrete ditch as desired but have available forms for sections having side slopes of 1:1 and bottom widths of 30 cm. The usual constructed depth is 32 cm. The average cross-field slope was given in Example 6.1 as 0.001. For a maximum flow of 4.52 m³/min (0.07533 m³/s) the depth of flow in the 30-cm section is found by trial and error to be 22 cm. Thus the standard size should be adequate and is probably cheaper than a special shape.

For the purpose of this illustration, the field outlets can be assumed to be spiles with a discharge coefficient of 0.8 and the available sizes are assumed to be 18, 25, and 32 mm, inside diameter. Using this information, the design heads are determined for the advance and wetting phase flows during the first and subsequent irrigations. Note that the cutback-to-advanced flow ratio is 0.73.

		Head	(cm)	
Spile size	First irrigation		Later im	rigations
(mm ID)	Advance	Wetting	Advance	Wetting
18	7.69	4.10	3.39	2.03
25	2.07	1.10	1.03	0.54
32	0.77	0.41	0.38	0.20

In the interests of minimizing the system costs, the 18-mm spile appears to offer the best choice, but it will need to be operated near the freeboard level of the ditch.

We now come to one of the major problems in using cutback systems. The difference in head between any two sets during the first irrigation (one advancing and one wetting) is 3.59 cm. During the later irrigations this value decreases to 1.36 cm. If the difference in head is supplied entirely by a difference in the bay elevation, as often suggested, the system will only be capable of providing one of the design conditions. Of course the system could be designed for an average infiltration condition rather than two, or possibly other configurations which require variable field supply rates would yield a common elevation difference between sets. It must be concluded, however, that the cutback system illustrated is not easily suited to field conditions where the intake rates change substantially during the course of the irrigation season unless water level regulation is provided at the junction of each pair of sets. One will find this a necessity of any cutback system.

Thus, for the system being illustrated here we view first the head ditch layout. It runs 720 m across the upper end of the field, in which the slope is 0.1%. The total change in elevation is therefore 0.72 m, which can be shared proportionally among five sets of bays. Figure 6.5 shows one possible configuration. The first bay runs horizontally from the inlet end of the field, then drops 18 cm into the second bay. There are three additional drops 18 cm leading to the last bay, whose end terminates at the edge of field elevation. Details of the spile locations are also shown in Fig. 6.5. Between each of the bays there must be an adjustable check structure to adjust the system for the variation in outlet flows.

The operation of the cutback system proceeds as follows. During the advance phase of the first set, the check between bays 1 and 2 is closed. At the end of the first-set advance

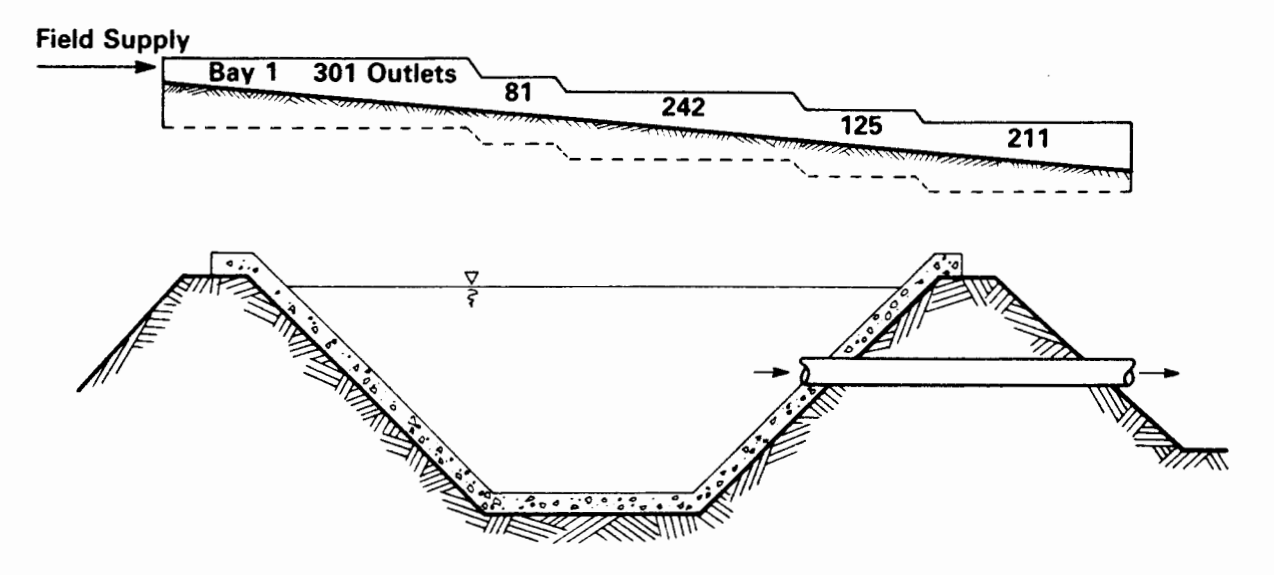


Figure 6.5 Example cutback system head ditch and outlet configuration.

phase, the flow is partially released into the second bay. The check between bays 2 and 3 is closed and the check between 1 and 2 is adjusted until the depth of flow in bay 1 (for the first irrigation) is 22 cm + 4.1 = 26 cm, so the flow from each outlet will equal the cutback flow. During later irrigations the depth in bay 1 is adjusted to 24 cm. This procedure is repeated through each of the bays up to bay 5. When its advance phase is completed, the check between bays 4 and 5 is opened so that all of the flow goes to bay 5. This continues until its wetting phase is concluded and the system is turned off. Some additional tailwater losses are thus experienced during the wetting phase of the last irrigation.

System Performance. All of the computations needed to determine the performance of this system will not be given. During the first irrigation, the design calls for an advance phase flow of  $0.015 \, \text{m}^3/\text{min}$  for 13 h and then a flow of  $0.73(0.015) = 0.011 \, \text{m}^3/\text{min}$  for another 13 hours. This regime is designed to apply a required depth of 10 cm at the end of the field. The application efficiency is therefore (Eq. 6.4)

$$E_a = \frac{Z_{\text{req}}L}{t_L(Q_0 + Q_{ch})} \times 100 = \frac{0.10(0.75)(200)}{785(0.015 + 0.0101)} \times 100 = 76.1\%$$

On the last set,

$$E_a = \frac{0.10(0.75)(200)}{785(0.015 + 0.015)} \times 100 = 63.7\%$$

Later irrigations are designed to achieve application efficiencies based on advance flow of 0.0106 m<sup>3</sup>/min for 18.8 h (1127 min) and a cutback flow of 0.0077 m<sup>3</sup>/min for the same duration. For the first four sets,

$$E_a = \frac{0.10(0.75)(200)}{1127(0.0106 + 0.00770)} \times 100 = 72.7\%$$

and for the last set,  $E_a = 67.8\%$ .

It is clear that cutback design is cumbersome. The operation is, however, not difficult, and the attainable application efficiencies are good.

### Example 6.3: Furrow Reuse Design

A third furrow irrigation option where tailwater is inevitable is to capture it in a small reservoir at the end of the field and either pump it back to the upper end to be used along with the primary supply or divert it to another field nearby. Although cutback is a natural tendency of irrigators, there are fewer actual cutback systems than reuse systems. Some of the new automation techniques, however, are based on cutback so this relative use may change. For illustrative purposes, assume that the design is to be applied to the same field conditions as prescribed in Example 6.2.

The Problem. The system envisioned for this reuse example will use gated pipe connected to the water supply at the high-elevation corner of the field. The irrigator will introduce water to the first set using only well water. The surface runoff from the first set will be collected and then pumped back and combined with the well supply to irrigate the remainder of the sets. The field layout will be similar to the schematic system shown in Fig. 6.2.

The pertinent field data were given earlier but are presented again for the convenience of the reader. One change is made with regard to the water supply. The well capacity has been reduced to 2.4 m<sup>3</sup>/min. The field characteristics are as follows:

```
Length = 200

Width = 720 m

Furrow spacing = 0.75 m

Slope in 200-m direction = 0.8%

Slope in 720-m direction = 0.1%
```

## Irrigation factors:

Infiltration during first irrigation:

$$Z = 0.0036\tau^{0.357} = 0.000046\tau$$

Infiltration during later irrigations:

$$Z = 0.00383\tau^{0.317} + 0.000035\tau$$

Required depth of application = 10 cm

Water supply: deep tubewell with capacity of 2.4 m<sup>3</sup>/min, quality good.

*Initial Calculations*. Initial calculations begin again with the required intake opportunity. These results were determined in Example 6.2.

$$\tau_{req} = 785 \text{ min during first irrigations}$$

 $\tau_{req} = 1127 \text{ min during later irrigations}$ 

The maximum allowable furrow flows are also the same, 0.017 m<sup>3</sup>/min, and result in the following advance times:

 $t_L = 555$  min during first irrigation

 $t_L = 347 \text{ min during later irrigations}$ 

An old rule of thumb states that  $t_L$  should be approximately 25% of  $\tau_{\rm req}$ . For the first irrigation the maximum allowable flow is only able to complete the advance phase in 71% of  $\tau_{\rm req}$ , while for the later irrigations the figure is 31%. Usually, a designer selects the advance ratio and finds a flow that will approximate it. When the maximum flow fails this criterion, one should design the system around the maximum flow. As in the cutback case, the right flow for the design must be sought by trial and error, and the design flow needs to yield an integer field division, which is somewhat more difficult for the reuse configuration.

As with both previous cases, it is worthwhile at the initial design stage to compute a series of advance trajectories using the common computational procedure. More detailed results need to be recorded, specifically the advance function:

$$x = p(t_a)_x^r (5.11)$$

where x is the advance distance achieved in  $(t_a)_x$  minutes and p and r are empirical coefficients. The advance computations yield two points for this relation,  $(t_L, L)$  and  $(t_{0.5L}, L/2)$ . From the analyses made for the cutback example, the advance times, p and r, are listed for corresponding values of furrow inflow in the following table.

Furrow inflow (m³/min)	Advance time (min)	p	r
	First irrigation	on	
0.017	555	8.9977	0.4908
0.0153	735	9.3125	0.4647
0.0145	860	9.5481	0.4502
0.015	778	9.3954	0.4594
	Later irrigation	ons	
0.017	347	6.8352	0.5772
0.0153	429	6.8601	0.5564
0.0136	554	6.9508	0.5318
0.0119	764	7.2406	0.4999
0.0106	1048	7.7233	0.4679
0.01	1253	8.14099	0.4488

The application efficiency and field layouts under the reuse regime are not as easily computed as before because of the runoff recycling, which alters the field water supply. To evaluate these components of the design, it is necessary to compute the deep percolation ratio and the tailwater runoff ratio for the possible range of flows. This will be illustrated for the first irrigation condition using a furrow inflow of 0.017 m<sup>3</sup>/min.

With a required intake opportunity time of 785 min and an advance time of 555 min, the time of cutoff on all furrows is 1340 min (22.3 hours). (For practical purposes it is recognized that an irrigator would change sets under this design every 24 hours, but for illustrative purposes the example will retain the computed numbers.) Using the advance

function and the appropriate intake relation, the distribution of applied water is given as follows:

Distance from field inlet (m)	Computed opportunity time (min) <sup>a</sup>	Computed application (m³/m) <sup>b</sup>
0	1340	0.1087
20	1339	0.1084
40	1319	0.1075
60	1292	0.1059
100	1205	0.1007
120	1144	0.0971
140	1072	0.0928
160	988	0.0876
180	892	0.0817
200	785	0.0750

 $at_{op} = t_{co} - t_L$ 

Using the trapezoidal integration (Eq. 5.29) of the applied water, the amount infiltrated over the field length is

$$V_Z = \frac{200}{2(10)} \left[ 0.1087 + 2(0.1084 + 0.1075 + 0.1059 + 0.1037 + 0.1007 + 0.0971 + 0.0928 + 0.0876 + 0.0817) + 0.075 \right]$$

 $= 19.545 \text{ m}^3 \text{ per furrow}$ 

The required application is

$$0.10 \text{ m} \times (0.75 \text{ m})(200 \text{ m}) = 15 \text{ m}^3 \text{ per furrow}$$

The total inflow to each furrow is

$$0.017 \text{ m/min}(1340 \text{ min}) = 22.78 \text{ m}^3 \text{ per furrow}$$

The deep percolation and runoff ratios are thus

$$DPR = \frac{19.45 - 15.0}{22.78} \times 100 = 20\%$$
 (5.33)

The application efficiency based on no runoff losses is

$$E_a = 100 - 20 = 80\%$$

The runoff fraction is

$$TWR = \frac{22.78 - 19.545}{22.78} \times 100 = 14.2\%$$
 (5.34)

Thus the volume of tailwater per furrow is

$$0.142(22.78) = 3.235 \text{ m}^3 \text{ per furrow}$$

<sup>&</sup>lt;sup>b</sup>Application = depth × furrow spacing per meter of width.

A similar calculation can be made for each of the field conditions and inflow rates given above. A summary of these results follows.

Furrow inflow (m³/min)	DPR (%)	TWR (%)	Runoff volume per furrow (m³)	E <sub>a</sub> (%)
	I	First irrigation	on	
0.017	20	14.2	3.2	80
0.0153	25.3	10.3	2.4	74.7
0.015	26.6	9.4	2.2	73.4
0.0145	29	8	1.9	71
	L	ater irrigatio	ons	
0.017	7	33	8.3	93.0
0.0153	9.5	27.5	6.6	90.5
0.0136	13	21.3	4.9	87
0.0119	18.9	14.5	3.3	81.1
0.0106	25.8	9.1	2.1	34.2
0.01	30.3	6.7	1.6	69.7

The Field Design. The operation of the reuse system will be such that the volume of the runoff reservoir will only need to be as large as the runoff from the first set. Following the first set, the pump-back system will be operating continuously and some excess capacity will always exist in the reservoir even though the total runoff from subsequent sets will be greater than that from the first. The field design involves determining a field layout, sizing the runoff reservoir and pump-back system, and sizing the headland facilities (gated pipe in this case).

The field layout can be found by trial and error or calculated. If the layout is calculated, one approach is to fix a furrow flow and determine the well supply needed. For the problem at hand during the first irrigation, it appears that a  $Q_0$  of 0.017 m<sup>3</sup>/min maximizes the application efficiency. For this value, the following layouts are possible:

Number of sets	Required flow from well (m³/min)
10	1.447
9	1.610
8	1.815
7	2.079
6	2.4322 (exceeds capacity)

Choosing seven sets, the number of furrows in the first set is

$$N_1 = \frac{Q_T}{Q_0} = \frac{2.079}{0.017} = 122 \tag{6.20}$$

The volume of the runoff reservoir must be, for the first irrigation,

$$V_m = 3.2 \,\text{m}^3 \,\text{per furrow} \times 122 = 390 \,\text{m}^3$$

Recalling that for a first irrigation condition, the time of cutoff is 785 min  $(\tau_{req})$  + 555 min  $(t_L)$  = 1340 min, the capacity of the pump-back system is

$$Q_{pb} = \frac{390 \text{ m}^3}{1340 \text{ min}} = 0.291 \text{ m}^3/\text{min}$$

The number of furrows per set for the subsequent sets is

$$N_2 = N_3 = N_4 = \cdots = N_i = \frac{Q_T(1 + \text{TWR})}{Q_0} = \frac{2(1.142)}{0.017} = 140$$

There are 960 furrows in the field. Six sets contain 140 furrows, one set contains 122. This is 962 furrows, so it is necessary to reduce one of the sets by two furrows.

Now the system must be configured for the later irrigating conditions. If the individual furrow flows are again set at 0.017 m/min to maximize application efficiency, the field water supply from the well as a function of the number of subsets is as follows:

Number of sets	Required flow from well (m/min)
10	1.2583
9	1.4021
8	1.5829
7	1.8174
6	2.1333
5	2.5823 (exceeds capacity)

Again choosing seven sets, the number of furrows in the first is

$$N = \frac{1817}{0.017} = 107$$

The volume of the runoff reservoir needs to be

$$V_{\rm ro} = 107 \times 8.3 \, \text{m}^3 \, \text{per furrow} = 888 \, \text{m}^3$$

The capacity of the pump-back system must be

$$Q_{\rm pb} = \frac{888 \text{ m}^3}{1474 \text{ min}} = 0.602 \text{ m}^3/\text{min}$$

It will therefore be necessary to regulate the pump-back system during the first irrigation to a value slightly less than half of the capacity. The runoff reservoir is governed by the later irrigations.

The number of furrows in subsequent sets is

$$N_i = \frac{1.817(1.33)}{0.017} = 142$$

This layout adds up to 959 furrows, so the number in the last set can be increased to 143.

We now see the design for the field layout and the reuse system. The final design is to size the gated pipe for the field. For the flows envisioned, most of the standard adjustable orifices with which gated pipe are equipped would be sufficient. Most of the orifice outlets will have dimensions of at least  $2.5 \text{ cm} \times 4.0 \text{ cm}$ . Using the orifice relations

given earlier, the minimum head required to pass a design furrow flow of 0.017 m<sup>3</sup>/min is determined as follows:

$$Q = CA(2gH)^{0.5}$$

$$H = \left[\frac{Q}{CA(2g)^{0.5}}\right]^2$$

$$= \frac{(0.017/60)^2}{[0.8(0.025)(0.04)]^2(2)(9.81)} = 0.0064 \text{ m}$$
(4.47)

Thus the maximum orifice openings will easily pass the flow.

To facilitate water management along the pipeline, the pipe should flow full with at least 30 cm of pressure head. Standard gated pipe sizes are typically 15, 20, 25, and 30 cm inside diameter. Using a design flow of 2.4 m³/min, which is approximately the combined flow during the first irrigation, the following head losses are computed for each 720-m length of pipe [minor losses due to fittings and gates are neglected (see Eq. 10.36)]:

Gated pipe diameter (cm)	Friction loss (m)
30	0.643
25.4	1.436
20.3	4.237
15.2	17.130

If the supply to the system from the well and the pump-back system is assumed to occur at a pressure of 1 m, the allowable head loss across the field is

$$H_L = (H_{in} - H_{end}) + (elev_{inlet} - elev_{end})$$
  
= 1 - 0.3 + 0.001(720) = 1.42 m

Thus the 25.4-cm pipe would be the best choice. Multiple sizes might be considered to reduce costs.

#### Example 6.4: Border Irrigation Design

In some ways border irrigation design and management is similar to furrow irrigation. There are, however, three unique features that both simplify and complicate the design computations. First, depletion and recession should not be neglected. Because water covers the entire soil surface, it drains from the field more slowly and adds more to the intake opportunity time. Second, the design flow must be restricted by a minimum value that will spread over the field and cover isolated undulations in the surface topography. Without the channelization made possible by furrows, border irrigation is more sensitive to surface microtopography. Third, the potential runoff from borders is substantially higher than that from furrows because there is substantially more water on the field that can drain. Cutback and runoff reuse are practices that can be applied, but the usual practice is to dike the downstream end of the field. This results in a basin type of system, and its design is illustrated next. However, one should be aware that on sloping fields that are diked, a relatively small error on the cutoff time will create a large pond at the end of the field, causing potential crop loss and drainage problems.

**The Problem.** A border irrigation system is being considered for a new irrigation project. A detailed predesign assessment has been made, yielding the following input data. The soil is a deep silty-clay loam with estimated infiltration functions as follows:

First irrigation:  $Z = 0.00320\tau^{0.490} + 0.000107\tau$ Later irrigation:  $Z = 0.00327\tau^{0.474} + 0.000098\tau$ 

The individual fields are to be laid out within 360- by 360-m blocks. The prevailing land topography is such that in one direction the field slopes will be 0.1% and in the other they will be level. The borders will therefore be laid out for the irrigation water to advance along the slope. From other local projects of similar conditions, the anticipated application per irrigation is 5.25 cm. This is based largely on calculations of evapotranspiration during peak demand periods of 0.75 cm/day. The water supply system is to be a canal network which will be designed and operated on a 7-day rotation. Each block is planned to receive water for 24 hours on each seventh day. Water is short, so night and holiday irrigations are considered essential during the peak periods. The discharge to each block is not defined at this time. One of the tasks of this design is to determine a total supply rate for each block.

*Initial Calculations*. The first calculation is the time needed to refill the root zone. Using the data provided and the procedure outlined, the intake opportunity times for the two field conditions are as follows:

First irrigations:  $\tau_{req} = 146.4 \text{ min}$ Later irrigations:  $\tau_{req} = 162.8 \text{ min}$ 

As with furrow systems, the  $\tau_{req}$  value indicates something of the system's operational times. For free-draining borders, the  $\tau_{req}$  value is equal to the time of recession,  $t_r$ , at the end of the field. If this end is the downstream end of the field,

$$\tau_{\text{reg}} = t_r - t_L \tag{6.26}$$

If the least watered area is at the inlet,

$$\tau_{reg} = t_d$$

where  $t_d$  is the depletion time.

The second initial calculation is of the maximum flows. According to Eq. 6.23, the maximum flows per meter of width are

$$Q_{\text{max}} = \frac{0.01059}{S_0^{0.75}} = \frac{0.01059}{0.001^{0.75}} = 1.88 \text{ m}^3/\text{min}$$

If the  $Q_{\text{max}}$  inflow is selected, the inlet depth should not exceed the height of typical field dikes. From Eq. 6.25,

$$y_{\text{max}} = \left[ \frac{1.88(0.04)}{60(0.001)^{0.5}} \right]^{0.6} = 0.144 \text{ m}$$

This should be within the limits of most field dikes.

The next calculation is to determine the relationships between discharge and advance. This step is like earlier furrow design calculations and will not be undertaken here. It is important to note that the border advance in essence assumes a furrow-like condition. The flow is 1 m wide and has  $\rho_1$  and  $\rho_2$  values of 1.0 and 3.333, respectively. Beyond that, the

computational procedures are the same. Figure 6.6 summarizes discharge-advance results for two field lengths (180 and 360 m) and the two irrigation conditions. The changes in infiltration rate for this soil are not substantial enough to affect significantly the advance rates for borders. Consequently, a design based on the first irrigation should suffice. The advance relation can also be evaluated for field lengths of 120 and 90 m. The differences are higher at the 360-m length, but the application efficiency is lower than at the shorter lengths.

The limitations imposed by the field water supply have not been The Field Design. set, so the field layout can be one of several combinations. The next step in the design process is to calculate the depletion and recession times for various values of inflow. One illustration should demonstrate this procedure adequately. For an inflow of 0.14 m<sup>3</sup>/min (per meter of width), the advance time is about 158 min. From Eq. 6.7,

$$A_0 = \left(\frac{Q_0^2 n^2}{3600 \rho_1 S_0}\right)^{1/\rho_2}$$
$$= \left[\frac{0.14^2 (0.04)^2}{60^2 (1)(0.001)}\right]^{1/3.33} = 0.0303 \text{ m}^2$$

The time of recession at the lower end of the field,  $t_r$ , is determined as

$$t_r = \tau_{req} + t_L = 158 + 146 = 304 \text{ min}$$
 (6.26)

The time of depletion must be iteratively determined from Eqs. 6.27 to 6.29:

a. 
$$T_1 = t_r = 304 \text{ min}$$
  
b.  $I = \frac{0.490(0.0032)}{2} [304^{-0.51} + (304 - 158)^{-0.51}] + 0.000107$   
 $= 0.00021 \text{ m}^3/\text{min/m}$   
c.  $S_y = \frac{\left[0.14 - 0.00021(360)](0.04)}{60(0.001)^{0.5}}\right]^{0.6}$   
 $= 0.00005289$   
d.  $T_2 = 304 - \frac{0.095(0.04)^{0.47565}(0.00005289)^{0.20735}(360)^{0.6829}}{0.00021^{0.52435}(0.001)^{0.237825}}$ 

e. Since  $T_1$  is not close to  $T_2$ , steps b to e must be repeated with  $T_1 = 238.8$  min.

b. 
$$I = \frac{0.490(0.0032)}{2} [238.8^{-0.51} + (238.8 - 158)^{-0.51}] + 0.000107$$
  
 $= 0.0002389 \text{ m}^3/\text{min/m}$   
c.  $S_y = \frac{\left[0.14 - 0.0002389(360)](0.04)}{60(0.001)^{0.5}}\right]^{0.6}$   
 $= 0.00004576$   
d.  $T_2 = 304 - \frac{0.095(0.04)^{0.47565}(0.00004576)^{0.20735}(360)^{0.6829}}{0.0002389^{0.52435}(0.001)^{0.237825}}$ 

d. 
$$T_2 = 304 - \frac{0.095(0.04)^{0.47565}(0.00004576)^{0.20735}(360)^{0.6829}}{0.0002389^{0.52435}(0.001)^{0.237825}}$$
  
= 304 - 59.6 = 244.4 min

e. Again the estimate of  $t_d$  can be improved by another iteration. If this is done, the new value is 243.7 min.

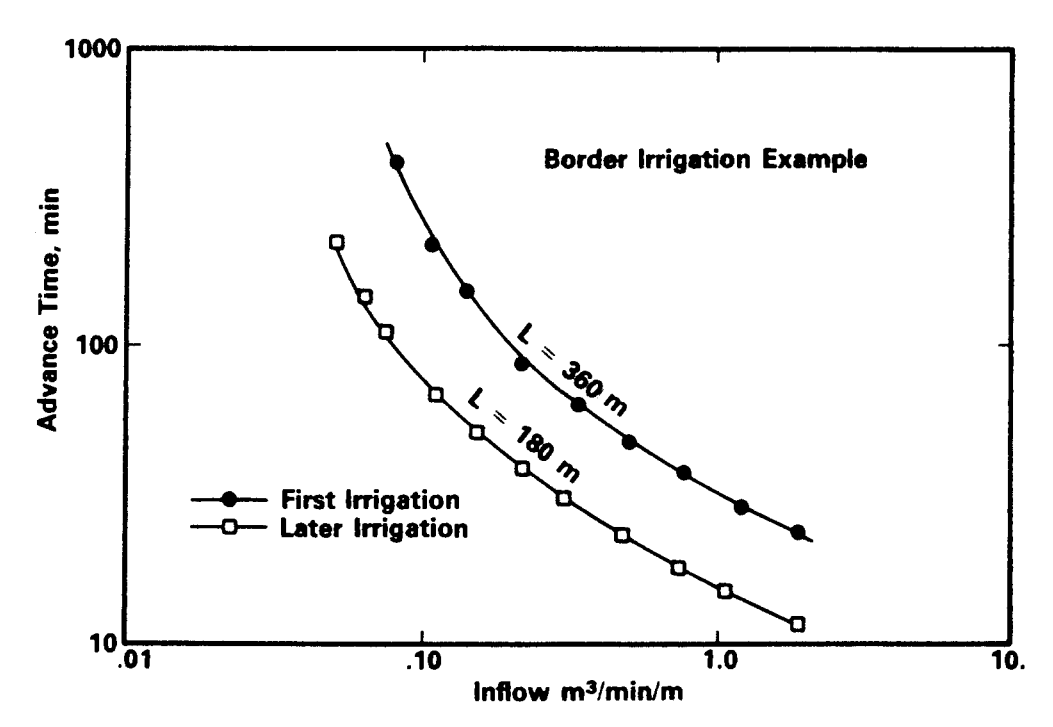


Figure 6.6 Discharge-advance time relations for two example border field conditions.

The time of cutoff,  $t_{co}$ , is found from Eq. 6.31:

$$t_{co} = t_d - A_0 \frac{L}{2Q_0} = 244 - 0.0303 \frac{360}{0.28} = 205 \text{ min}$$

The application efficiency of the irrigation is (Eq. 6.4)

$$E_a = \frac{Z_{\text{req}}L}{t_{co}Q_0} \times 100 = \frac{0.0525(360)}{205(0.14)} \times 100 = 66\%$$

This series of computations should be repeated for the range of discharge and field lengths to find the design giving the maximum  $E_a$ . It turns out that the results are not too different.

Field length (m)	Optimum inflow (m³/min)	Optimum efficiency (%)
360	0.144	66
180	0.075	65.9
120	0.043	65.4
90	0.034	65.5

Selecting the 360-m borders will mean that a relatively large field supply will be needed if the individual widths are to be of a reasonable value. A summary of the 360- and 180-m border configurations is given below. The cutoff time for 360-m borders is 210 min. For 180-m borders it is 190 min.

The choice of layout may depend on many factors unrelated to irrigation, but generally the longer the border the better. Thus one might logically choose the 360- by 60-m layout using six borders. The field supply will need to be 8.64 m³/min for optimum efficiency and the block would be completely irrigated within the day.

The design of headworks to operate this design is similar to the earlier furrow discussion and will not be repeated.

POSSIBLE BORDER LAYOUTS

Field supply (m³/min)	Field length (m)	Border width (m)	Number	Irrigation time (h)
8.64	360	60	6	21
10.37		72	5	17.5
12.96		90	4	14
17.28		120	3	10.5
25.92		180	2	7.0
51.84		360	1	3.5
9.0	180	120	6	19.3
13.5		180	4	12.7
27.0		360	2	6.3

## Example 6.5: Basin Irrigation Design

Basin irrigation is probably the most common method of surface irrigation because of its widespread use on small landholdings. Large basin systems were substantially less popular auntil the introduction of laser-controlled land-grading equipment. It is interesting to compare the performance of basins against that of border and furrow systems. They have the obvious advantage of eliminating tailwater, but they do not have field slope to assist the water movements over the field. For the purposes of this design example, assume that the basin alternative is to be considered for the area described in the border design problem of Example 6.4. However, the required depth of application is 10 cm, as in the furrow problems, and the water supply is limited to 12.6 m³/min and is available for one day in seven. By way of summary:

Field dimensions:  $360 \times 360 \text{ m}$ 

Field slope: 0.001% and 0% in the two dimensions, respectively

First irrigation condition:  $Z = 0.0032\tau^{0.490} + 0.000107\tau$ Later irrigation condition:  $Z = 0.00327\tau^{0.474} + 0.000098\tau$ 

In addition, the following information is provided:

Land leveling costs =  $$0.50/m^3$  of earth moved

Irrigation water costs =  $$0.25/1000 \text{ m}^3$$ 

Total seasonal requirement by crops = 0.46 m

Initial Calculations. Basin design is the simplest of the computational procedures. The most important limitation of this procedure is that the advance time must be less than the cutoff time; that is, the advance phase must be completed before the inflow is cut off.

The first calculation is the required intake opportunity time,  $\tau_{req}$ . It is required in the design calculations to about the same extent that it is in furrow and border systems. For the first irrigation condition,  $\tau_{req} = 383$  min, and for later irrigations this is  $\tau_{req} = 430$  min.

Next, the advance rate as a function of inflow per unit width is needed. This cal-

culation is only slightly more detailed than it is for furrows and borders. The only difference is that the inlet cross-sectional area,  $A_0$ , changes with advance distance. Thus  $A_0$  must be calculated for each  $Q_0$  selected and for both of the two advance points in the procedure. It might be assumed that the maximum and minimum flows would be in the same range as in the border example:

$$0.05 \text{ m}^3/\text{min/m} < Q_0 < 1.88 \text{ m}^3/\text{min/m}$$

Actually, the upper limit is more restricted by the field supply. Before proceeding with these calculations, which are long and tedious except by computer, one should consider the problem carefully. The flow rate and duration of the field supply are fixed, and therefore the unit flow rate one might select must yield an integer field subdivision as in all the problems examined thus far. Consequently, these calculations can be deferred until the field layout stage.

The Field Design. The designer has at this point to formulate an initial field layout. It is a judgment exercise unless he or she has a computer to calculate quickly the design of a broad range of basin dimensions. For this exercise, a basin length of 180 m is selected. A basin the full 360-m length may be difficult to irrigate with small unit width flows, and increasing these may require construction of very narrow basins. Shorter basins also increase the number of basins on the field, which may create a lot of work for the irrigator. It is a matter of judgment.

With 180-m basins, the possible configurations are as fo	follows:
--	----------

Basin width (m)	Number of basins	Unit flow (m³/min/m)	Inlet flow area, $A_0$ $(m^2)^a$
90	8	0.14	0.046
120	6	0.105	0.041
180	4	0.070	0.034
360	2	0.035	0.024

 $<sup>^{</sup>a}$ Eq. 6.40 with n = 0.04.

These unit flows were used individually to compute the advance using the procedure already illustrated. These results are as follows:

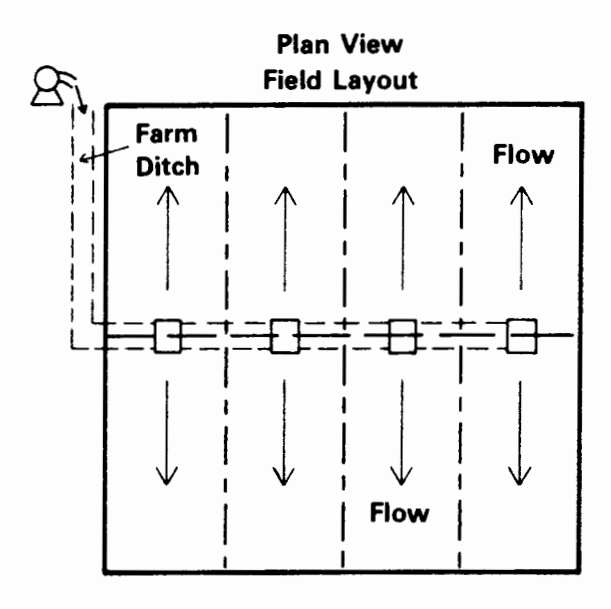
Basin configuration	Advance time (min)	Time of cutoff (min) <sup>a</sup> .	Total time (h)
	First irrigati	on	
$180 \times 90 (8)$	77	158	21.1
$180 \times 120 (6)$	104	220	22.0
$180 \times 180 (4)$	173	362	24.1
$180 \times 360 (2)$	664	1079	36.0
	Later irrigati	ons	
$180 \times 90 (8)$	74	156	20.8
$180 \times 120 (6)$	99	216	21.8
$180 \times 180 (4)$	160	349	23.3
$180 \times 360 (2)$	535	950	31.7

<sup>&</sup>lt;sup>a</sup>Eq. 6.42.

One sees that the first two field layouts are feasible. The choice should rest on the performance of each layout as computed from Eq. 6.4. These results are as follows:

Field layout	Application efficiency (%)
Fi	rst irrigation
180 × 90	81.2
$180 \times 180$	77.8
La	ter irrigations
180 × 90	82.5
$180 \times 120$	79.5

The design selected is therefore an eight-basin layout of 180- by 90-m basins. The design question at this point has to do with how one would organize the system. In all the previous examples, the field was irrigated along the direction of slope to minimize the land-leveling costs. Suppose that the fields were organized as shown in Fig. 6.7, so that the flow advanced in the direction of natural slope. As shown, the volume of earth needing to be relocated for the basins (assuming a cut-fill ratio of 1.3) is  $5.265 \, \text{m}^3/\text{m}$  of width, or  $5.265 \, \times 90 \, \text{m} \, \times \, 8 \, \text{basins} = 3790.8 \, \text{m}^3$ . At a cost of \$0.50/m³, the land-leveling cost on this field would be nearly \$2000, or \$146 per hectare. If the basins are oriented in the other direction, as shown in Fig. 6.8, the earth-moving requirements are  $1.316 \, \text{m}^3/\text{m}$  of length  $\times 180 \, \text{m} \, \times \, 8 \, \text{basins} = 1895.4 \, \text{m}^3$  or one-half the cost (less than \$1000, or \$73/per hectare).



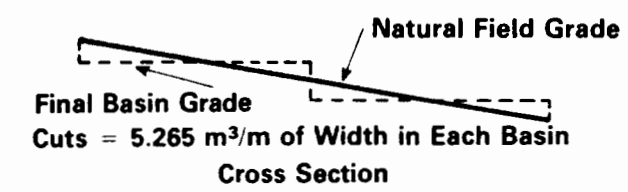
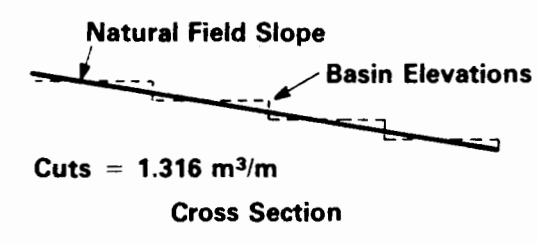


Figure 6.7 Field layout and cross section for example basin design problem irrigation in the direction of the natural slope.

# Farm Ditch

Plan View



**Figure 6.8** Alternative layout and cross section for the example basin irrigating in the cross-slope direction.

One of the interesting economic issues in surface irrigation is whether the added land grading costs for basin irrigation can be justified. The differences in application efficiency between the borders and basins is about 15%. During a season requiring about 60,000 m<sup>3</sup> of irrigation water to supply crop requirements, the borders will utilize more than 17,000 m<sup>3</sup> more than the basins. At a cost of \$25/per 1000 m<sup>3</sup>, this water saving results in an economic advantage to basins of \$425 per year. Thus the land grading is paid for in about 2 years if all other factors (e.g., production) are equal.

Another advantage of basins is the ease in which the on-farm conveyance and distribution is accomplished. Figure 6.8 shows one such layout. The length of this ditch system is just more than one-half the length required for a border or furrow system of similar field subdivision. Basins can be irrigated in any direction and from one outlet.

## **HOMEWORK PROBLEMS**

**6.1.** An infiltration study was conducted on a surface-irrigated field yielding the following cumulative intake function:

$$Z = 0.00884\tau^{0.212} + 0.00017\tau$$

in which Z has units of  $m^3/m$  and  $\tau$  has units of minutes. Later, during the irrigation of this field, it was observed that the flow advanced to the end of the field in 125 min and then ran off for a time before the inflow was shut off. Following cutoff, it took 15 more minutes for the surface water to recede from the field. If the irrigator wished to apply 7.5 cm to the lower end of the field, when should he have shut off the inflow?

- 6.2. A corn crop needs to be irrigated in the near future. Its root depth is 0.8 m and the soil in which it is growing is a clay loam (TAW = 15 cm/m). An irrigation scheduling service estimates that the average evapotranspiration for corn over the next 7 days should be 12 mm/day. The irrigator wishes MAD to be no greater than 60% and no less than 50% of TAW. A student visited the field today and took a gravimetric soil sample 30 cm long and 2.5 cm in diameter. It weighed 260 g in the laboratory. She found that the volume of water necessary to saturate the sample after it had been oven dried was 58.9 cm<sup>3</sup>. The specific weight of the soil particles was 2.65 g/cm. She put a -1/3 atm pressure on the saturated sample until drainage stopped and found that the sample had lost 24.7 g of water. How many days until the irrigator should expect to irrigate?
- **6.3.** How long will it take for the advance phase to be completed in a furrow system with the following characteristics?

$$Q_0 = 1.5$$
 liters/s  $\rho_1 = 0.664$   $k = 0.00884 \text{ m}^3/\text{min}^a/\text{m}$   $n = 0.04$   $\rho_2 = 2.8787$   $f_0 = 0.00017 \text{ m}^3/\text{min}/\text{m}$   $S_0 = 0.01$   $a = 0.212$  furrow spacing = 76 cm  $L = 300 \text{ m}$ 

- 6.4. If the inflow to the furrow in Problem 6.3 was cut off at 300 min and recession was negligible, what depth of water would have been applied on the lower end of the field? When should it be cut off to apply 8 cm at the lower end? With the 8-cm depth, what would be the application efficiency?
- 6.5. Design a free-draining border irrigation system and a level-basin irrigation system for the following field conditions (i.e., choose optimal parameters for achieving maximum application efficiency). Assume that tailwater, if any, cannot be reused.

Soil: silt-loam.

Infiltration: first irrigation ( $Z = 0.00546\tau^{0.315} + 0.00005 \tau$  in m<sup>3</sup>/m); later irrigation ( $Z = 00417\tau^{0.256} + 0.00003 \tau$ ).

Field topography: slope = 0.002; no cross slope; n = 0.04; L = 360 m; field width is 360 m.

Water supply: gravity canal supply to open ditch distribution system to each border or basin; available discharge  $= 0.25 \text{ m}^3/\text{s}$  on 3-day notice.

Cropping pattern: alfalfa, small grains, and other livestock crops.

Irrigation pattern: irrigator likes to apply 10 cm during each irrigation.

6.6. A few years ago Farmer Brown converted several of his field systems from sprinkler to furrow systems. His motivation was to reduce energy costs, and since his crops were always planted in rows, it seemed better to make this move. Annual water demands were about 750 mm in potential crop use. Sprinkler application efficiency averaged 65% over the year. Water is supplied to the farm from the farmer's own well, using a 75-hp pumping system, lifting water from a depth of 20 m. The farmer uses 308-mm pipe to convey water to the various fields. The total flow of the pump that can be delivered to the fields in 6 m³/min. The cost of electric energy is \$0.05/kWh. For the fields still having sprinkler systems, another 50-hp pump is used downstream to pressurize the flow to 40 m of head. Both pumping plants were tested and each found to have an efficiency of 57%. The individual fields on the farm were

irrigated by furrows before the farmer purchased the land, so it had already been graded. One field of interest is 400 m by 720 m. It slopes 0.8% in the 400-m direction and 0.1% in the 720-m direction.

An evaluation of furrow irrigation at the site was made last year. Briefly, it was found that:

- 1. Furrows were spaced 1.5 m apart and aligned in the 400-m direction.
- 2. Typical furrow shapes were such that  $A^2R^{1.33} = 0.325A^{2.734}$ .
- 3. First irrigation (preplant) infiltration functions for the sandy loam soil were typically  $Z = 0028 \tau^{0.534} + 0.00022 \tau$ .
- 4. Subsequent infiltration functions were typically  $Z = 0.0021 \tau^{0.331} + 0.00015 \tau$  (m<sup>3</sup>/m).
- 5.  $Z_{reg}$  was usually about 10 cm.

Major problems have been experienced. The furrow flow advance did not extend to the end of the fields during the first irrigation, so that yields on about 25% of the field have been poor. Last year, for example, yields on the part of the field receiving adequate water (75%) were 150 bushels per acre, and nil on the remainder. The price for the crop was \$5.50 per bushel. Thus the loss was \$14,680. Average application efficiencies were only 41%, so that although he used less pressure, he had to pump 24% more water. You may want to investigate the net energy savings or costs of existing sprinklers and furrow systems.

The farmer has heard of high efficiencies being achieved in laser-leveled basins. Local land-leveling costs are presently running about \$0.50/m³ of cut. Infiltration rates on this soil under basin conditions were estimated from some ring infiltrometer tests as

$$Z = 0.0032\tau^{0.490} + 0.00017\tau$$
 m<sup>3</sup>/m for first irrigation

and

$$Z = 0$$
 f  $00323$   $\tau^{0.474} + 0.000098$   $\tau^{-3}$  m for later waterings

The farmer has another field nearby on which he would like to test a basin irrigation system. Its dimensions are 360 m by 720 m with a slope of 0.1% in the 360-m direction and 0% slope in the 720-m direction. The farmer has a sideroll sprinkler system that he could put on either field, so his economic choice does not include the sprinkle equipment cost. What would you recommend for each field?

### REFERENCES

GARTON, J. E. 1966. Designing an Automatic Cut-back Furrow Irrigation System. Bull. B-651, Oklahoma Agricultural Experiment Station, Oklahoma State University, Stillwater, Okla., October.

HART, W.E., H. G. COLLINS, G. WOODARD, and A. J. HUMPHERYS. 1980. Design and Operation of Gravity on Surface Systems. In *Design and Operation of Farm Irrigation Systems*. ASAE Monograph 3, St. Joseph, Mich, Chap. 13.

## Land Leveling

## INTRODUCTION

Because the land surface must serve as the major conveyance in all surface irrigation systems, it must be formed so that water movements will be as uniform as possible. This is equivalent to the design of laterals and manifolds for a sprinkle or trickle irrigation system when pipe diameters are selected so that pressure and discharge variations over the field fall within prescribed limits.

There are two land-leveling philosophies. The first is to provide a slope which maximizes the effectiveness of an existing or planned irrigation system. The second is to grade the field to its best condition with minimal earth movement. In the latter program, the design of the irrigation system is undertaken to make the system as efficient as possible with the improved field topography. Because land leveling is expensive and large earth movements leave significant areas of the field without fertile topsoil, the general practice has been the second approach. It will also be the approach described in this chapter.

The topographical modification of a field surface is described by several terms. A major earth-moving project is usually called "land leveling" or "grading," whereas the smoothing of small irregularities and roughness is referred to as "land planing," "smoothing," or "floating." In this book the terminology will be simplified by

aggregating each of these operations into a general term, "land leveling," following the U.S. Department of Agriculture (1970).

## **GENERAL CONSIDERATIONS**

Land leveling may very well provide farmers with the capability to utilize water, labor, and energy resources more effectively. However, in the near term, the land-leveling operation can prove to be the most intensive and disruptive practice that will be applied to the field. As a result, several factors should be considered before the land-leveling operation begins.

Major topographical changes are almost certain to reduce crop production unless special attention is given to improving fertility in the cut areas with added fertilizers. Topsoil will be removed from some locations and deposited at others, thereby removing the primary source of nutrients for the crop. The authors have seen cuts as shallow as 5 cm reduce yields to practically nothing for several years following land leveling. Similarly, areas where leveling equipment passes repeatedly can be so compacted or pulverized that water penetration is reduced for some time, thereby reducing yields. Thus a land-leveling operation should be preceded by attention to soil characteristics.

The climate of the area must be carefully considered prior to land leveling. Regions of short intense rainfall probably should have limited land slopes, while areas with very large annual rainfalls should avoid any land leveling that hinders surface drainage. The existing slope and the method of surface irrigation should be consistent. Relatively steep slopes are usually more amenable to furrow irrigation than either border or basin irrigation. To utilize the border or basin method on slopes, terraces are likely to be required in order to minimize cuts and fills. The cropping pattern will also affect leveling decisions. High valued crops justify greater leveling costs whereas low valued crops may not be able to be profitable with more than minor leveling.

Farmers have many operations that require their skill and labor. The irrigation system should be designed with their practices and preferences in mind. A field leveled to high standards is generally more easily irrigated than one where undulations require special attention in order to water satisfactorily. Some areas have been leveled several times as irrigators change their operations in response to new technologies and the need for modified irrigation frequencies.

Finally, new equipment is continually being introduced which provides the capability for more precise land-leveling operations. One of the most significant advances has been the adaption of laser control in land-leveling equipment. The equipment has made level basin irrigation particularly attractive since the final field grade can be very precise. It is not unusual to see the marks of a planter show evenly across a 5 to 10-ha field as the water infiltrates into the soil. These marks may be less than 5 cm high.

## LAND LEVELING

After the engineer and the farmer have studied the field conditions and decided on overall irrigation strategy, the land-leveling program can be initiated. Hart (1975) outlines five general steps as follows:

- 1. The land must be cleared of vegetation that would impede equipment operation as well as any large debris located on the field. Depending on the equipment being used and the density of the surface, the soil may require cultivation. If the equipment loads earth and carries it to fill areas, it is better not to have loose surface conditions. However, if a planing operation is involved, a loose soil is preferable.
- 2. The existing topography needs to be determined. For manual control equipment, leveling will also necessitate staking the field in a uniform grid, whereas laser-controlled systems need only measure and record the field profile.
- 3. The modified field surface should be determined based on computation of longitudinal and lateral slopes.
- 4. Cut-and-fill volumes need to be calculated. Based on this information, the grid stakes must be marked with cut-and-fill depths for the operators. Note
- that laser-controlled operations need only determine the balanced cut-fill volume.
- 5. The leveling operation is undertaken and followed by a check on the finished grade to ensure that the design has been achieved.

In the sections that follow, steps 2 through 5 will be outlined as if each were required.

## Land Survey and Mapping

The first step in surveying and mapping the field is to set a uniform grid system on the field. One corner of the field is chosen as a starting point and a stake is located one-half spacing from either boundary. This is illustrated in Fig. 7.1 by the stake A. Then a row of stakes is measured and set using an engineer's level and a tape. The level is set up over stake A and sighted along a line parallel to the boundary. Usually, this is accomplished by going to the opposite edge and locating a stake one-half grid spacing from the edge (see stake R in Fig. 7.1). Then, using the level for alignment, the first row of stakes is measured into place (A, B, C, and D).

With the instrument located over stake A and aligned along the A, B, C, D row, the next step is to turn the alignment 90° by either measuring a 3-4-5 triangle, as shown, or by using the instrument angle indicators if available. The new alignment is used to locate the stake row, A, E, I, K, as before. The instrument can then be located over stakes E and F to orient rows E, F, G, H and B, F, J, L. Each of the remaining stakes can be placed visually by sighting against the two stakes at the field edges.

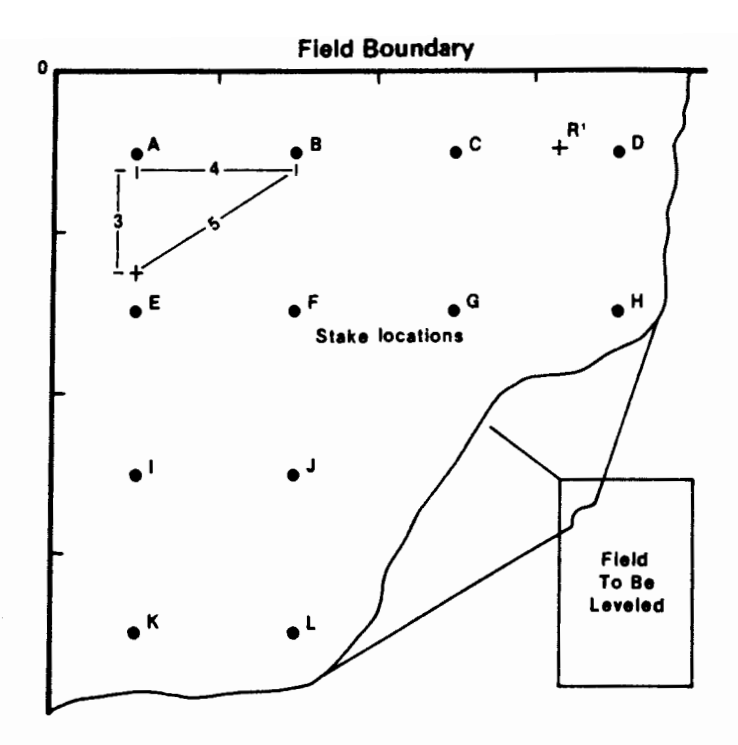


Figure 7.1 Field staking process for field surveying and mapping.

The field stakes provide the basis of the field survey. The level or transit can be located in a central area and rod readings taken from each stake position. It is generally advisable to locate a benchmark near the field from which to reference the readings as elevations. Readings taken from the location of water supply structures are also useful for designing the headland facilities of the surface irrigation system. It is assumed that the basic principles of land surveying are known and practiced during this phase of the land-leveling operation.

## Selecting Field Slopes

An initial decision as to the specific type of surface irrigation system to be utilized will limit field slope. Basins are designed without slopes in either the advance direction or across the field. Borders are similar in having zero cross-slope, but may have advance slopes of 0.5 to 1%, depending on crop and soil conditions. Furrow irrigation systems work well with advance slopes of 1 to 3% and cross-slopes of 0.5 to 1.5%. If the average natural slopes are greater than these ranges, terraces or benches should be constructed.

From a theoretical viewpoint, land slopes can be designed to improve the performance of the surface irrigation system. However, the infiltration rates and roughness change so drastically during the course of an irrigation season that it is generally more practical to shape the field for minimum disturbance or least cost and then adapt an efficient irrigation design and operation for the resulting condition. There are several ways to determine the "new" field shape, including some that are inspection methods requiring experienced judgment. A formal method, called the "plane method," will be used here.

The plane method is a least-squares fit of field elevations to a two-dimensional plane with subsequent adjustments for variable cut-fill ratios. If the field has a

Land Leveling 181

basic X-Y orientation, the plane equation is written as

$$EL(X, Y) = AX + BY + C \tag{7.1}$$

where

EL = elevation of the X, Y coordinate

A, B = regression coefficients

C = elevation of the origin

Evaluation of the A, B, and C constants can be accomplished using a four-step procedure. The first is to determine the weighted-average elevations of each stake row in both field directions—the advance-slope and cross-slope directions, respectively. The purpose of the weighting is to adjust for the boundary grid points that may represent larger or smaller areas than given by the standard grid dimension due to irregular field shapes and sizes. The weighting factor is defined as the ratio of actual area represented by a grid point to the standard area:

$$\theta_{ij} = \frac{A_{ij}}{A_s} \tag{7.2}$$

where

 $\theta_{ij}$  = weighting factor of the grid point identified as the *i*th advance-slope stake row and the *j*th cross-slope stake row

 $A_{ij}$  = area represented by the (i, j) grid point

 $A_s$  = area represented by the standard grid dimensions

Using Eq. 7.2, the average elevation of the *i*th row,  $EL_i$ , is

$$EL_{i} = \frac{\sum_{j=1}^{N'} \theta_{ij} EL_{ij}}{\sum_{j=1}^{N'} \theta_{ij}}$$
(7.3)

where N' is the number of cross-slope rows and  $\mathrm{EL}_{ij}$  is the elevation of the (i, j) coordinate found from field measurements  $\mathrm{EL}(X, Y)$ .

A similar expression can be written for finding the average elevation of the jth cross-slope row,  $EL_j$ :

$$EL_{j} = \frac{\sum_{i=1}^{N''} \theta_{ij} EL_{ij}}{\sum_{i=1}^{N''} \theta_{ij}}$$
(7.4)

where N'' is the number of stake rows in the cross-slope direction.

The second step is to locate the centroid of the field with respect to the grid system. For convenience, an origin can be located one grid spacing in each direction from the first stake position (i.e., stake A in Fig. 7.1). The distance from the origin to the centroid in the X dimension is found by

$$X = \frac{\sum_{j=1}^{N'} \theta_j X_j}{\sum_{j=1}^{N'} \theta_j}$$
(7.5)

where X is the distance from origin to centroid,  $X_j$  is the X distance from origin to the jth stake row position, and

$$\theta_j = \sum_{i=1}^{N''} \theta_{ij} \tag{7.6}$$

Similarly,

$$Y = \frac{\sum_{i=1}^{N''} \theta_i Y_i}{\sum_{i=1}^{N''} \theta_i}$$
 (7.7)

where Y is the Y distance from the origin to centroid,  $Y_i$  is the Y distance from origin to the *i*th stake row position, and

$$\theta_i = \sum_{j=1}^{N'} \theta_{ij} \tag{7.8}$$

The third step is to compute a least-squares line through the average row elevations in both field directions. The slope of the best-fit line through the average X-direction elevation (EL<sub>i</sub>) is A and is found by

$$A = \frac{\sum_{j=1}^{N'} X_{j} EL_{j} - \left(\sum_{j=1}^{N'} X_{j}\right) \left(\sum_{j=1}^{N'} EL_{j}\right) / N'}{\sum_{j=1}^{N'} X_{j}^{2} - \left(\sum_{j=1}^{N'} X_{j}\right)^{2} / N'}$$
(7.9)

For the best-fit slope in the Y-direction, the slope, B, is

$$B = \frac{\sum_{i=1}^{N''} Y_i EL_i - \left(\sum_{i=1}^{N''} Y_i\right) \left(\sum_{i=1}^{N''} EL_i\right) / N''}{\sum_{i=1}^{N''} Y_i^2 - \left(\sum_{i=1}^{N''} Y_i\right)^2 / N'}$$
(7.10)

Finally, the definition of the best-fit plane represented by Eq. 7.1 is completed by determining C. The average field elevation can be found by summing either  $\mathrm{EL}_i$  or  $\mathrm{EL}_j$  and dividing by the appropriate number of grid rows. This elevation corresponds to the elevation of the field centroid (X, Y). Thus Eq. 7.1 can be solved for C as follows:

$$C = EL_F - AX - BY (7.11)$$

where  $EL_F$  is the average field (or centroid) elevation.

The value of each grid point elevation can be recomputed with Eq. 7.1 and compared to the measured values. The differences are the necessary cuts (computed EL smaller than measured E) or fills. Before these computations are undertaken, however, the slopes in both field directions must be checked to see if

Land Leveling 183

they are within satisfactory limits. If they are not, adjustments must be made. For example, if the intended system is a border irrigation system, the cross-slope should be zero (A=0) and the cuts and fills would need to be based on this condition. A second note concerns the fact that cuts and fills do not balance because of variations in soil density. This adjustment is discussed in a subsequent section.

## **Example Field Slope Computations**

A small rectangular field illustrated in Fig. 7.2 has been staked on a 30- by 30-m grid spacing. The first stake, located at the upper left-hand corner, was placed one-half spacing from both sides of the field to start the staking. An engineer's level and rod were used to measure elevation at each stake, as shown in the figure. The field is to be furrow irrigated and the least disturbing cut-fill plane is to be determined. The field is most likely to be irrigated from bottom to top as they appear in the figure.

The first step is to calculate the average row elevations. Weighting factors are as follows:

		4	i	
i	1	2	3	4
1	1.0	1.0	1.0	1.33
2	1.0	1.0	1.0	1.33
3	1.0	1.0	1.0	1.33
4	1.0	1.0	1.0	1.33
5	1.17	1.17	1.17	1.56

Using Eqs. 7.3 and 7.4, the average advance-slope and cross-slope row elevations are as follows:

i	$EL_i$			
1	10.156			
2	10.850			
3	11.425			
4	11.654			
5	11.783			
	1	2	3	4
EL,	10.671	11.255	11.392	11.392
,	Ave	rage field ele	evation = 11	.176

The second step is to calculate the centroid coordinates assuming that the origin is one spacing from the first stake. This requires that the sum of the

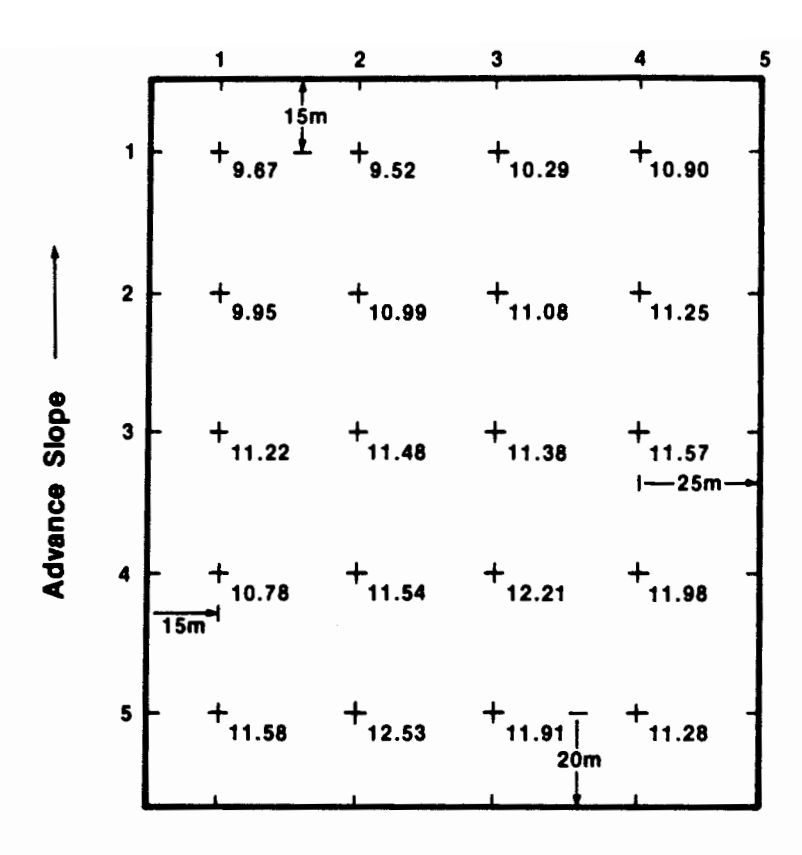


Figure 7.2 Typical grid of surveying stakes on a rectangular field. Normal grid spacing is 30 m by 30 m.

weighting factors (Eqs. 7.6 and 7.8) be calculated and then Eqs. 7.5 and 7.7 applied. The results of these calculations are X = 78.437 and Y = 91.983.

Next, the slope of the plane in both directions is calculated from Eqs. 7.9 and 7.10, resulting in A = 0.0076667 and B = 0.013527. With these values, the coordinates of the centroid and the average field evaluation, the value of C is 9.3304. Temporarily ignoring the need to make adjustments for slope limitations and cut/fill ratios, the measured elevations can be subtracted from the computed elevations to identify cuts (negative numbers) and fills (positive numbers). A summary of these results is illustrated in Fig. 7.3.

This example is a case in which some of the grid areas are larger than others and the total volume of cuts exceeds the total volume of fills. A simple and rapid calculation of these respective volumes can be made as follows:

$$V_c = \sum_{m=1}^{N_c} A_m C_m (7.12)$$

and

$$V_f = \sum_{n=1}^{N_f} A_n F_n (7.13)$$

where

 $V_c$  = volume of cuts, m<sup>3</sup>

 $V_f$  = volume of fills, m<sup>3</sup>

 $A = \text{grid area } m \text{ or } n, m^2$ 

 $C_m$  = depth of cut at grid point m, m  $F_n$  = depth of fill at grid point n, m

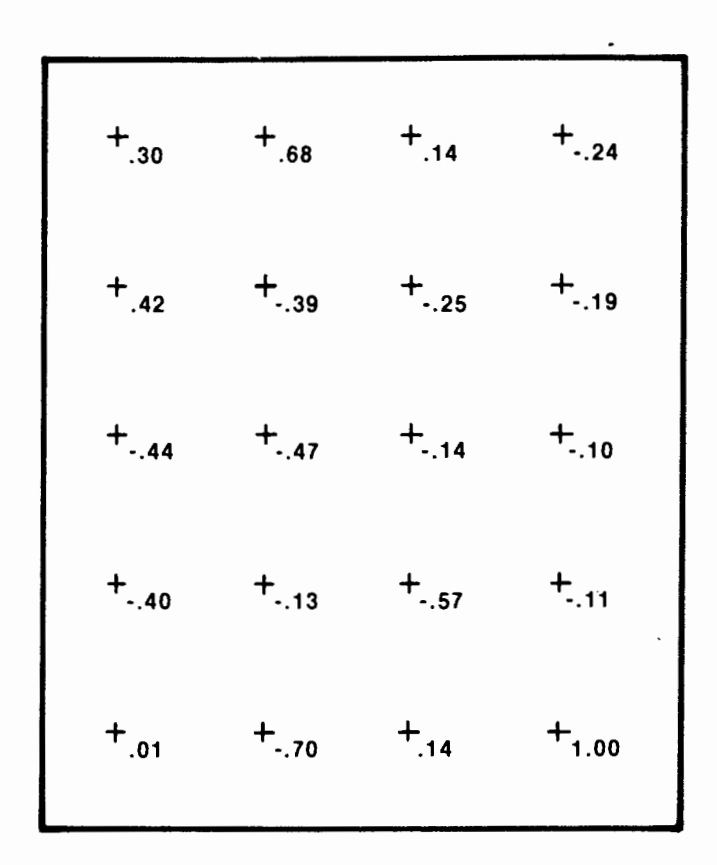


Figure 7.3 Summary of cuts (-) and fills (+) for the field in Figure 7.2. All units in meters.

The cut/fill ratio R is

$$R = \frac{V_c}{V_f} \tag{7.14}$$

and should be in the range 1.1 to 1.5, depending on the soil type and its condition.

For the example above, the volume of cuts is  $3,664.5 \text{ m}^3$  and the volume of fills is 3303.50, which yield a cut/fill ratio of 1.11. If this value is too low, the plane is lowered and the cuts and fills recomputed. If R is too high, the adjustment proceeds in the opposite direction. A methodology to adjust R is given in the next section.

## **Adjusting Cut/Fill Ratios**

Hart (1975) and Marr (1967) discuss the necessity of having cut/fill ratios greater than 1 for land-leveling operations. Specific reasons are not identified, but machinery compaction in the fill areas and an optical illusion leading to excess fill are cited. However, even laser plane systems, where fill area compaction is minimal and no operator optics are involved, required cut/fill ratios greater than 1. Consequently, one must conclude that the disturbance of the soil reduces its density, contrary to what one might expect.

Selecting a cut/fill ratio remains a matter of judgment. If the value arrived at by least squares requires modification, the procedure is to find the adjustment

Land Leveling Chap. 7

to original elevation (C), which yields the new value of R. For an increase in R,

$$\delta = \frac{RV_f - V_c}{\sum_{i=1}^{N_c} A_i (1+R)}$$
 (7.15)

Equations 7.14 and 7.15 assume that none of the cut grid points become fill points, and vice versa.

## **Computing Cut Volumes for Contractors**

Equation 7.12 is usually less formal for contracting purposes than is required. Some more complete estimators include the prismoidal formula, the "average-end-area method," and the "four-corners method." The four-corners method is simplest to use and is suggested by the USDA (1970). The formula for all complete grid spacings is

$$V_{ci} = \frac{A_i}{4} \frac{\left(\sum_{j=1}^{N_c} C_j\right)^2}{\sum_{j=1}^{N_c} C_j + \sum_{m=1}^{4-N_c} F_m}$$
(7.16)

where  $A_i$  is the area of the grid square i in  $m^2$  and  $N_c$  is the number of cuts at the four corners of the grid square.

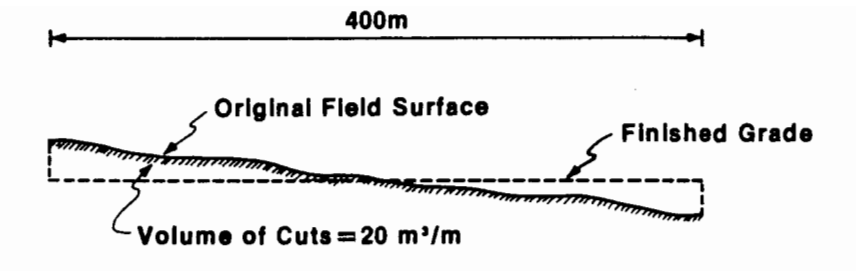
At the field edges and corners, if complete grid spacings are not present, the cut volume must be computed separately. The procedure is to assume that the elevation of the field boundaries are the same as those of the nearest stake and would thereby have the same cut or fill dimensions. Equation  $\P$ .17 is then utilized with the appropriate  $A_i$  value corresponding to the actual edge area.

## OTHER CONSIDERATIONS

Anderson et al. (1980) present a very good discussion of a number of miscellaneous factors that need to be considered in land leveling. Four of these factors are summarized in this chapter: (1) subdividing a field to minimize earth movements, (2) field operations, (3) miscellaneous earth requirements, and (4) maintenance.

## Field Subdivision

As noted previously, land leveling is likely to be not only the most disruptive operation applied to the field but also the most costly. One method of reducing cut volumes is to subdivide the field in the cross-slope direction and level the field





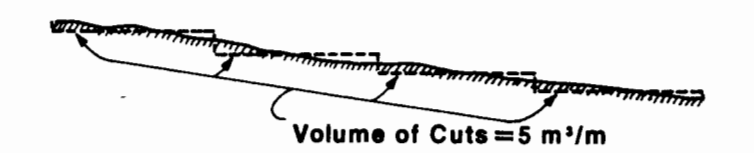


**Figure 7.4** Field subdivisioning to reduce land-leveling requirements.

in terraces. Figure 7.4 shows a field with a 0.1% cross-slope and three alternative subdivisions, along with the cut volume per meter of field length. It can be seen that subdividing the field proportionately reduces the cut volume.

## Field Operations

It is possible, and computer codes have been developed, to minimize equipment movement for any field situation. However, few operators utilize these procedures but prefer instead to develop field movement patterns based on their own judgment and experience. A cut-haul-fill pattern of travel that maximizes the efficiency of the land-leveling operation tends to be one in which the routes are of nearly equal length. Such a strategy prevents the overuse of travel lanes and minimizes the haul and return distances.

Where manually controlled equipment is used, many operators establish a benchmark grid over the field by cutting and filling strips on both sides of a stake to the desired grade. Then the median areas can be leveled to grade visually with better precision. Nevertheless, the effectiveness of manually controlled operations is dependent on the skill and experience of the operator. Good operators make cut-and-fill passes which are relatively uniform and their equipment is seen to operate at fairly uniform speeds, particularly during loading passes.

Laser-controlled equipment eliminates the need for operator skill in setting grades but not that required for maximizing the operation efficiency. Efficient

cut-haul-fill routes are still required, and where cuts are indicated greater than the power of the equipment, the operator must temporarily override the laser control. In central Utah, where laser-controlled equipment is now in widespread use to convert sloping borders to level basins and used to improve the grade of the borders, it has become common practice to employ both manual and laser-controlled equipment on the same job. A reference grid of single-width strips is made by the laser equipment, then the manually controlled equipment is used to make the major cuts and fills ("roughing in" the field), and finally, the laser-controlled machinery comes back and smooths the field to its finished grade. This practice stems from the type of equipment being used. The laser machinery is often designed to operate mainly in planing rather than in cut-and-haul and is therefore not particularly efficient where a large volume of earth must be moved.

## Miscellaneous Earth Requirements

Land leveling is often accompanied by improvements or changes in other components of the surface irrigation system. Earth may be used to raise the elevation of roadways or to prepare a raised pad for headland facilities. In the computations setting field cuts and fills, the volume of the earth needed for these miscellaneous requirements should be deducted in the cut-fill ratio calculation.

## Maintenance

The topography of surface-irrigated fields, even after leveling, is not a static feature of the land. Year-to-year variations in tillage operations, such as plowing, disking, chiseling, or cultivation, disturb the surface layers as well as shifting their lateral position. The loose soils may settle differently depending on equipment travel or depths of irrigation water applied. Consequently, a major land-leveling operation will correct the macrotopographical problems but annual leveling or planing is needed to maintain the field surface by correcting microtopographical variations.

Because the land-leveling operation disturbs the topsoil on a field, an important aspect of field maintenance is fertility management. In cut areas, additional fertilizers and organic matter should be applied to restore fertility and soil tilth. Cut areas also tend to exhibit the effects of soil salinity, and measures aimed at increasing the leaching fraction in these areas may be worthwhile.

## **HOMEWORK PROBLEMS**

7.1. Figure 7.5 gives the ground surface elevations in feet and tenths of feet for a 45-acre field. Experience with the soils present suggests a cut/fill ratio of 1:1. Develop a land-leveling plan for this field. Present a map showing the cuts and fills, and a map showing the final ground surface topography. Assume that the field will be furrow irrigated and can accommodate field slopes in any direction. Do not use compound

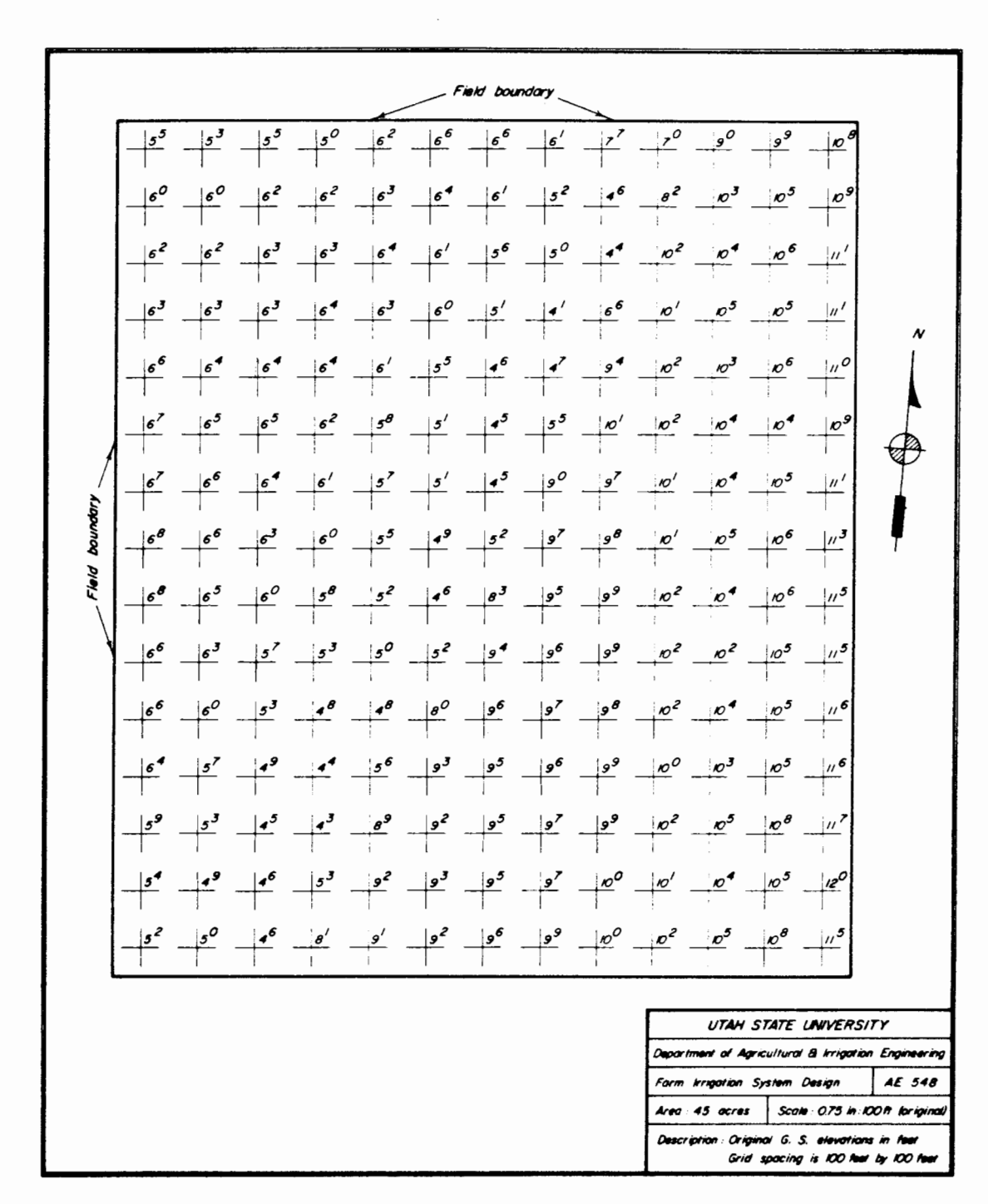


Figure 7.5 Field layout and elevation for Problem 7.1. (Courtesy of Dr. G. E. Stringham.)

slopes. Estimate the earthwork quantities and price the land-leveling job assuming \$0.50 per cubic yard.

7.2. The irrigator who owns the field would like to evaluate the land-leveling costs associated with border and basin irrigation. Repeat Problem 7.1 for these irrigation methods. Assume that both borders and basins will be about 5 acres each and prepare the least-cost designs. Irrigation water is expected to be delivered to the southeast corner of the field. Show how the water will be distributed over the field.

## REFERENCES

- ANDERSON, C. L., A. D. HALDERMAN, H. A. PAUL, and E. RAPP. 1980. Land Shaping Requirements. Design and Operation of Farm Irrigation Systems. ASAE Monogr. 3, St. Joseph, Mich., Chap. 8.
- HART, W. E. 1975. Irrigation System Design. Department of Agricultural and Chemical Engineering, Colorado State University, Fort Collins, Colo.
- MARR, J. C. 1967. Grading Land for Surface Irrigation. Circ. 408. California Agricultural Experiment Station, University of California, Davis, Calif.
- U.S. Department of Agriculture, Soil Conservation Service. 1970. Land Leveling, *National Engineering Handbook*, U.S. Government Printing Office, Washington, D.C., Chap. 12.

# Operation of Surface Irrigation Systems

## **CONCEPTUAL APPROACH**

After designing a new, improved, or automated surface irrigation system, there is a need to *calibrate* the system during the first irrigation season following installation by measuring the hydraulic performance. These field data would also be used to:

- 1. Check against the original design assumptions so that the designers gain more sensitivity to local conditions
- 2. Enlarge the data base for local calibration of design parameters
- 3. Provide a data base for implementing an effective irrigation scheduling program the following irrigation season

Calibration is also the process of adjusting the new "hardware" so that it operates properly (e.g., the gates on the individual ports supplying water to a furrow should be adjusted so that the advance rate is fairly uniform for all the furrows in a set).

An irrigation scheduling program should be implemented along with the system's structural improvements. Historically, the typical irrigation scheduling program has advised a farmer when to irrigate and how much to apply as an average depth. How much to irrigate is usually calculated from the soil moisture depletion divided by an application efficiency which is assumed constant throughout the season rather than varying with each irrigation event. This is *not* sufficient. The farmer must also be provided with information relating the available water supply at the time of irrigation to the time of cutoff in order to fulfill the crop water requirement while minimizing water and fertilizer losses. This requires information

regarding the variation in time of advance and the infiltration function for each irrigation event throughout the season.

If many farm irrigation systems are being improved in an area as part of a large-scale project, there will usually be a "monitoring and evaluation" program to measure the effectiveness of the project in achieving stated goals and as a means of providing feedback that allows continual refinement of the implementation process. An effective irrigation scheduling program, properly done, provides much of the data required for a monitoring and evaluation program.

Increasing attention has been given in recent decades to the research and development of automated "hardware" for surface irrigation methods. The objectives for these developments have been to reduce irrigation labor costs and to increase irrigation application efficiencies. Without automation to implement present-day state-of-the-art technologies, reducing either tailwater runoff or deep percolation would require additional irrigation labor costs, something not palatable to irrigators unless water is very expensive. Generally, both objectives must be achieved in order for irrigators to adopt automated irrigated systems. Reliability of the automated systems are crucial for irrigators to continue their use year after year.

A large fraction of the existing automated surface irrigation equipment in the United States has been developed by the U.S. Department of Agriculture's Agricultural Research Service (USDA-ARS) since the early 1960s. Some automating concepts and devices have originated in agricultural universities and the commercial irrigation equipment industry. In the following sections, a very limited illustration of surface irrigation automation is given. Surface irrigation automation has not been extremely successful as judged by the use of automating equipment in the surface-irrigated agriculture of any country in the world. Among the reasons one might note, the lack of reliability and the failure of most devices to make a substantial impact on labor or system performance are cited most often. New concepts, such as surge flow (discussed separately in Chapter 9), may remedy the historical lack of enthusiasm by farmers by providing a complete system of automation rather than the system of partial automation that is generally available.

## **AUTOMATION OF OPEN-CHANNEL HEADLAND FACILITIES**

Most surface irrigation systems incorporate a ditch or lateral along the high sides of the fields. Water is then diverted onto the fields. Automated diversion usually employs automated gates in the channel to regulate water levels, or along the channel to control outlet flows, or both. Some of the more common structures for automating the head ditch are drop-open and drop-closed gates, and trapezoidal, rectangular, and circular slide gates.

## **Drop-Open Gate**

Most of the work in developing drop-open gates (and drop-closed gates) was accomplished by Humpherys (1969, 1971). One interesting refinement was made by Evans (1977) (an associate of the authors), working in conjunction with Alu-

minum Specialties, Inc., of Grand Junction, Colorado. This drop-open gate is composed of three pieces of aluminum or other lightweight metal attached to a metal frame slightly smaller than the perimeter of the shaped gate guide which has been fixed into the channel. The complete gate and the gate guide are shown in Fig. 8.1. The center panel of the gate overlaps the two side panels when in the closed position. The center panel, in turn, is held in the upright position by a pivoting angle, thereby controlling the entire gate at one location. The side panels have rubber flaps on the upstream side which seal against the center panel when sufficient water pressure is exerted against the gate. However, when less water

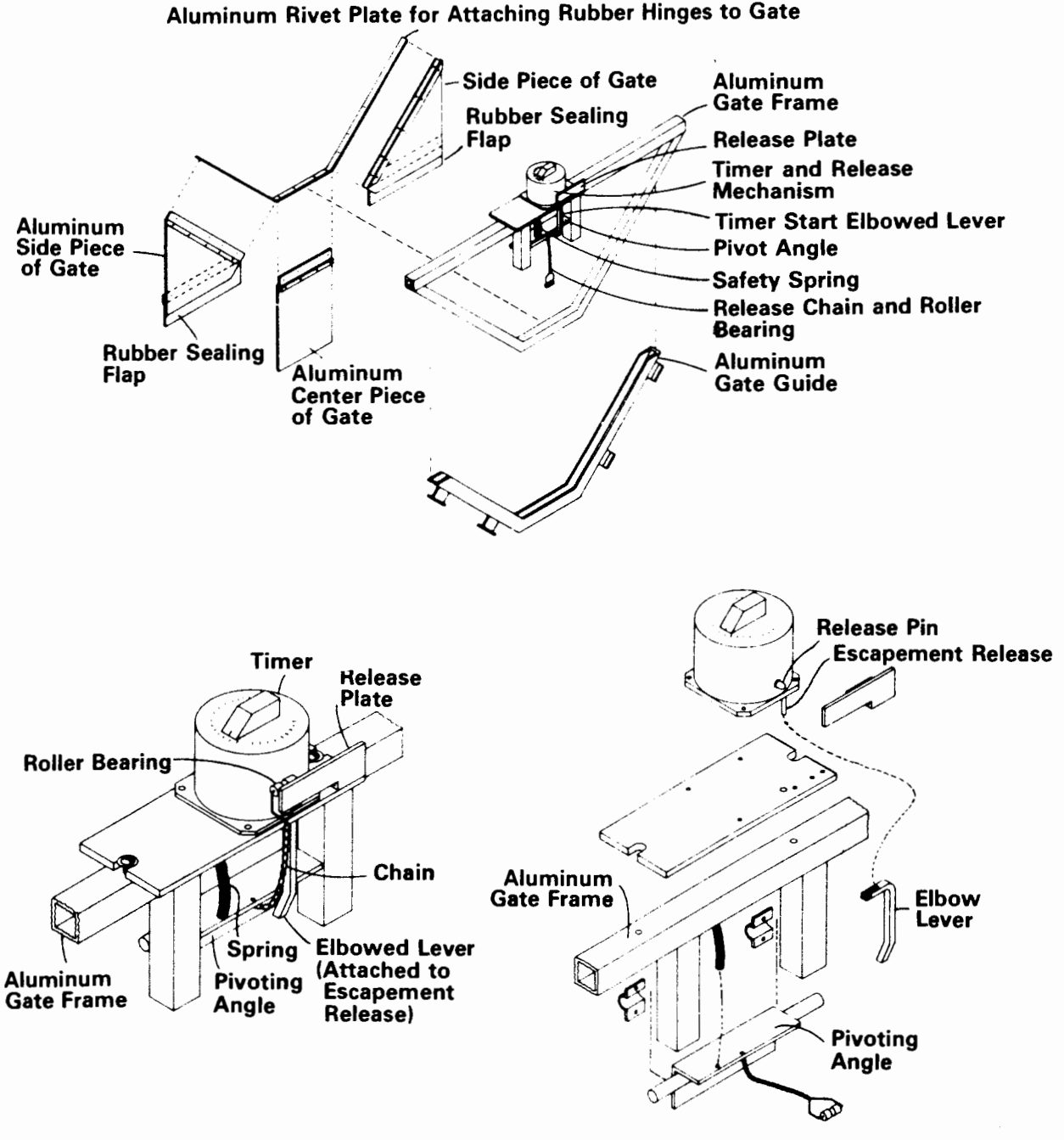


Figure 8.1 Schematic drawing of the drop-open gate reported by Evans (1977) and an exploded view of its timing mechanism.

pressure is applied to the gate, these rubber flaps permit leakage through the gate to prevent activation of the timing mechanism. The panels are hinged at the bottom by heavy nylon-reinforced butyl rubber to provide a strong but flexible and leak-proof hinge.

The timing mechanism is composed of four basic parts. For the gate described by Evans (1977), a 24-hour Coret timer is mounted on the top, horizontal frame of the gate assembly. The timer is equipped with a horizontal release pin which is withdrawn when the preset time on the clock has elapsed. The third part is a short length of chain with a small grooved roller bearing connecting the timer at the release pin to the short angle, which pivots about its vertex and holds the gate center panel. A short, elbowed lever is extended vertically downward from the timer's escapement device (an internally levered arrangement which will start or stop the timer) to a position below the pivoting angle. Any displacement due to a surge of water, or the increasing pressure due to water depth increases on the center gate panel, will cause a small rotation in the pivot, which then activates the clock by releasing the escapement device. At the end of the specified time interval, the release pin retracts and allows the roller bearing and chain to fall free, thereby releasing the pivoted angle. The force of the water against the gate forces the pivot to rotate, and the gate panels fall open and allow the water to proceed to the next gate.

Another type of drop-open gate developed by the U.S. Department of Agriculture, Agricultural Research Service, is shown in Fig. 8.2 and utilizes a canvas or plastic material on the gate. The drop-open gates are particularly useful with the cutback furrow systems described in Chapter 6.

## **Drop-Closed Gate**

If properly designed, a network utilizing both drop-open and drop-closed gates would automate an entire gravity irrigation system, changing ditches as well as sets. A simplified drop-closed type of gate has also been developed and tested under field conditions. The drop-closed gate is quite similar in concept to the drop-open gate. The basic difference is that the gate closes by rotating to the vertically downward position. The gate is a single unit, as shown in Fig. 8.3. The weight of the gate will cause it to drop when the release pin is retracted, and the force of the water will cause it to seal. This gate was originally constructed of aluminum. This same concept of drop mechanism can also be utilized on gate types which sit on the side of the concrete ditch and fall into the ditch. This type of gate would be designed to work on the timer only and not be actuated by a float or water-level sensor.

## Slide-Gate Turnouts

Slide gates are commercially available for use as flow-regulating structures in irrigation channels. The gate consists of a rectangular, trapezoidal, or circular slide gate with either a notched or threaded stem mounted on top of the gate frame. The slide gate is raised or lowered by operation of the jack along the notched stem

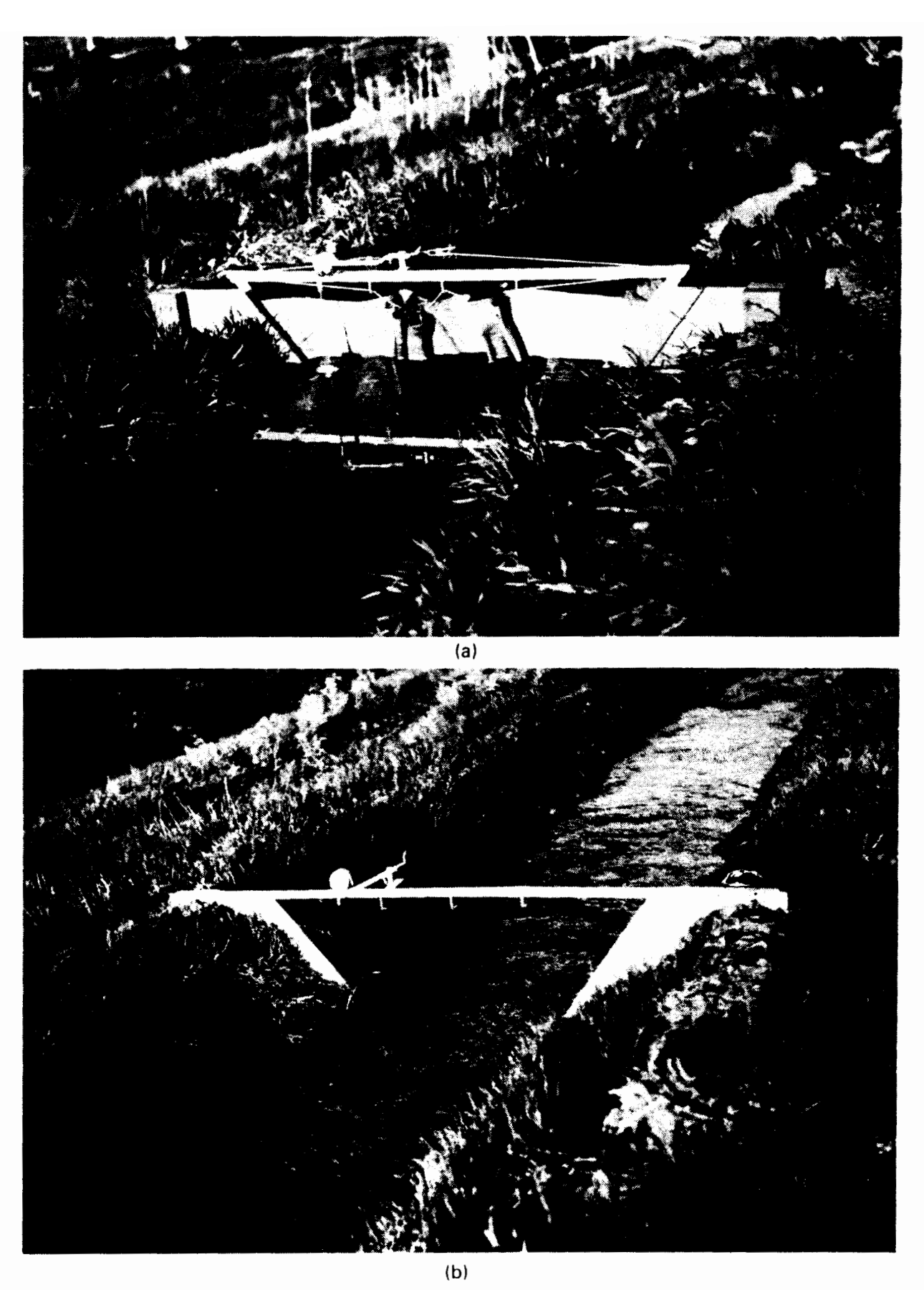


Figure 8.2 Field installation of a drop-open gate using a flexible barrier. (Courtesy of Dr. E. G. Kruse, U.S. Department of Agriculture, Agricultural Research Service.)

196

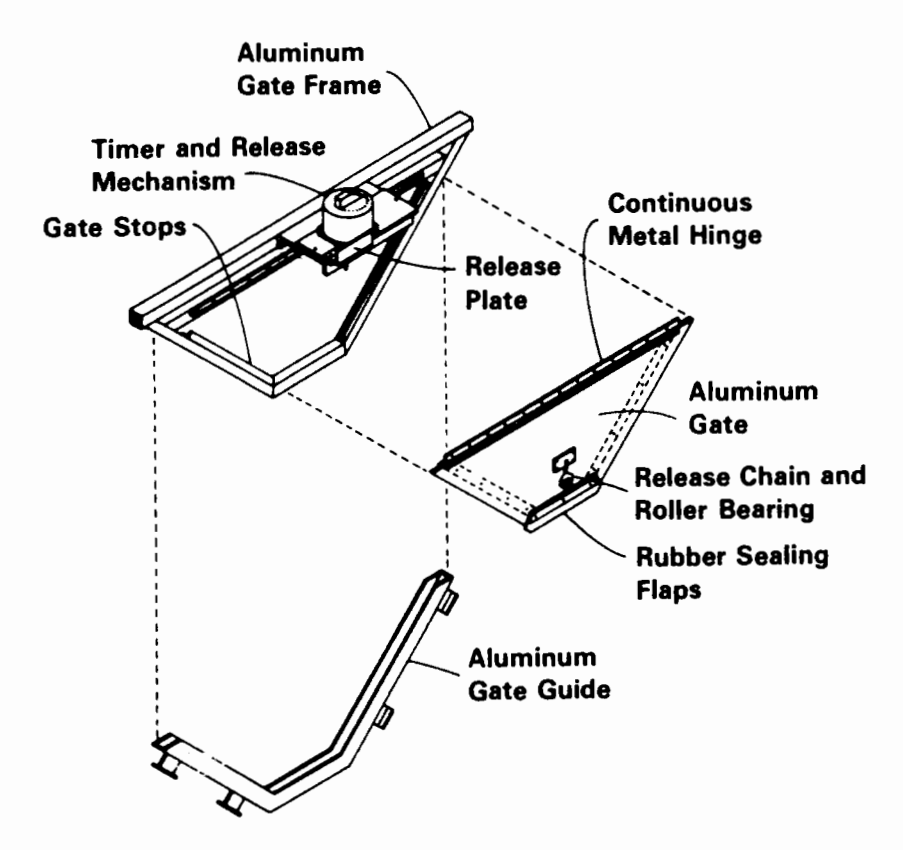


Figure 8.3 Schematic drawing of drop-closed gate. (From Evans, 1977.)

or by rotating a wheel along the threaded stem. Two typical slide gates are illustrated in Fig. 8.4; either could be automated by installing pneumatic, hydraulic, or electric actuators or motors to move the stem.

In Arizona, pneumatically operated jack gates are used as farm turnouts onto level basins (Fig. 8.5). USDA-ARS personnel perfected the automation of jack gates by a pneumatic system, although the manually operated jack gate is offset from the gate centerline for use in case of a breakdown by the automated equipment.

## PIPELINE AUTOMATION

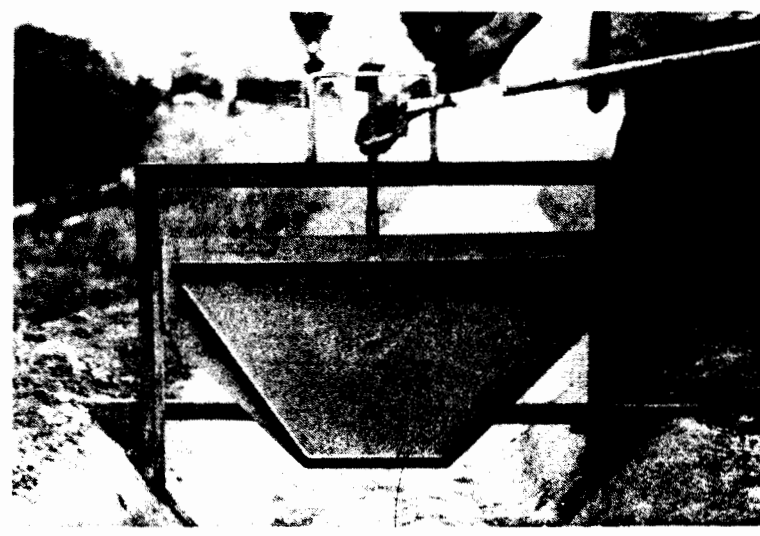
In recent years, a growing number of furrow irrigation systems have been designed or modified to utilize pipelines to convey and distribute water on the farm. The piped system can be automated with valves at either major division points or at each furrow or field outlet. Usually, pipeline automation is more reliable when only a small number of flow points are automated.

## **USDA Inflatable Pneumatic O-Ring**

One of the early developments in surface irrigation automation was the USDA pneumatic valve portrayed in Fig. 8.6. This inflatable O-ring is a product produced by Carlyle Tire and Rubber Co. for the USDA (Haise et al., 1980). Pneumatic



Figure 8.4 Two typical slide gates for surface irrigation systems. (a) Screw gate from central Utah. (b) Trapezoidal jack gate. (Courtesy of Dr. G. E. Stringham.)



O-rings were fabricated for a 4-in. orchard valve and 12- to 18-in.-diameter alfalfa valves. A major problem in using the lay-flat pneumatic O-ring in commercially available gated pipe hydrants is size (e.g., a 20-in.-diameter diaphragm is needed for a 12-in.-diameter alfalfa valve when opened 4 in.). More recent designs utilize a cover that more nearly conforms to the shape of the inner tube (Fig. 8.7). Hydrants can be placed directly over the O-ring without the need for lacing, a marked improvement over the original USDA inflable pneumatic O-ring. The Colorado Valve Co. has a license to manufacture the newly designed valve under the original USDA patent (Haise et al., 1980).

## Water-Operated Snake River Valve

(b)

Water-operated valves can operate as independent units that utilize water pressure from the pipeline to open or close diaphragm valves. The valve closes when the rubber diaphragm or bladder filled with water expands against the valve seats, and opens when water is drained from the diaphram. A three-way pilot valve is used



Figure 8.5 Pneumatically controlled automated jack gate. (Courtesy of Dr. A. Dedrick, U.S. Department of Agriculture, Agricultural Research Service.)

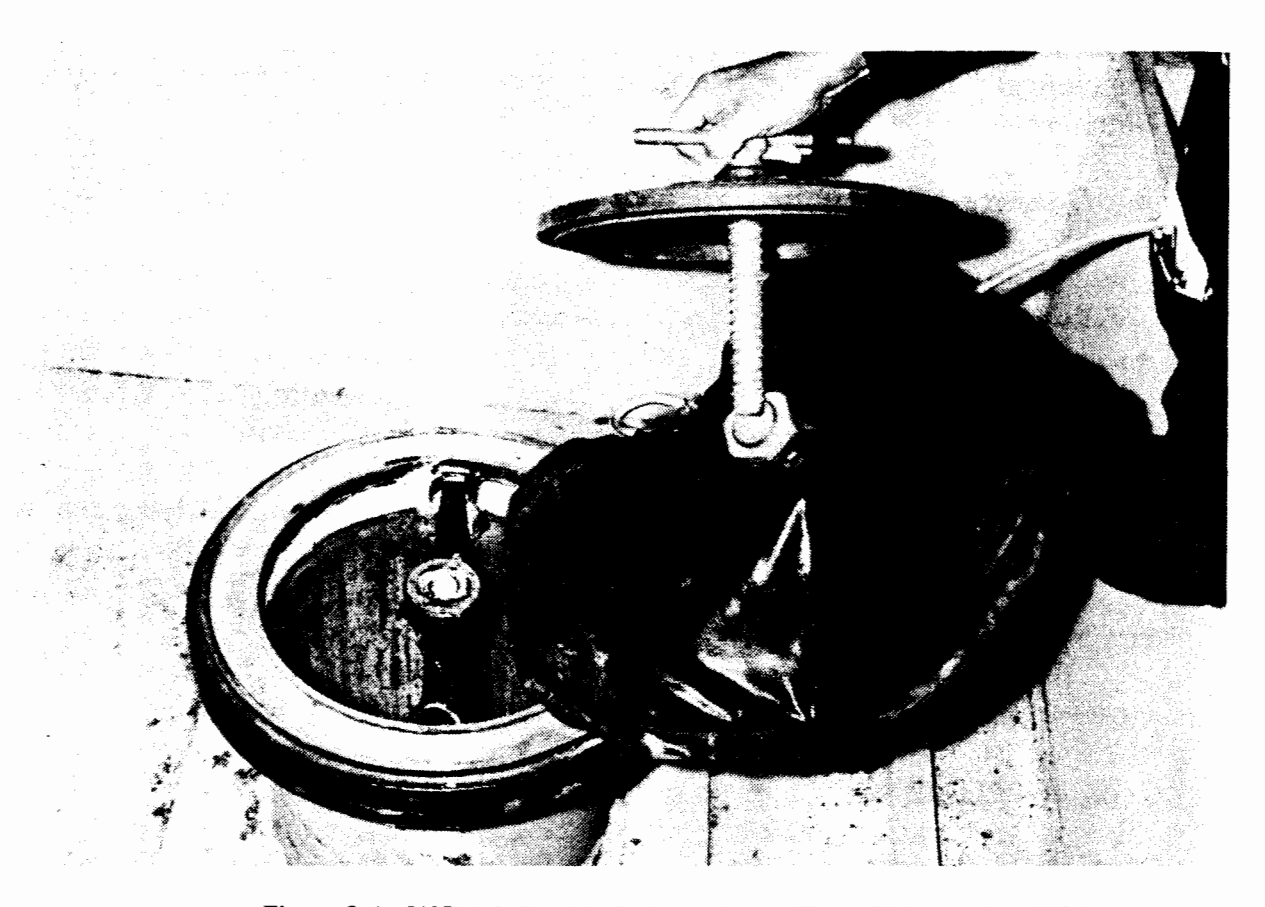


Figure 8.6 USDA inflatable O-ring valve. (From Haise et al., 1980.)



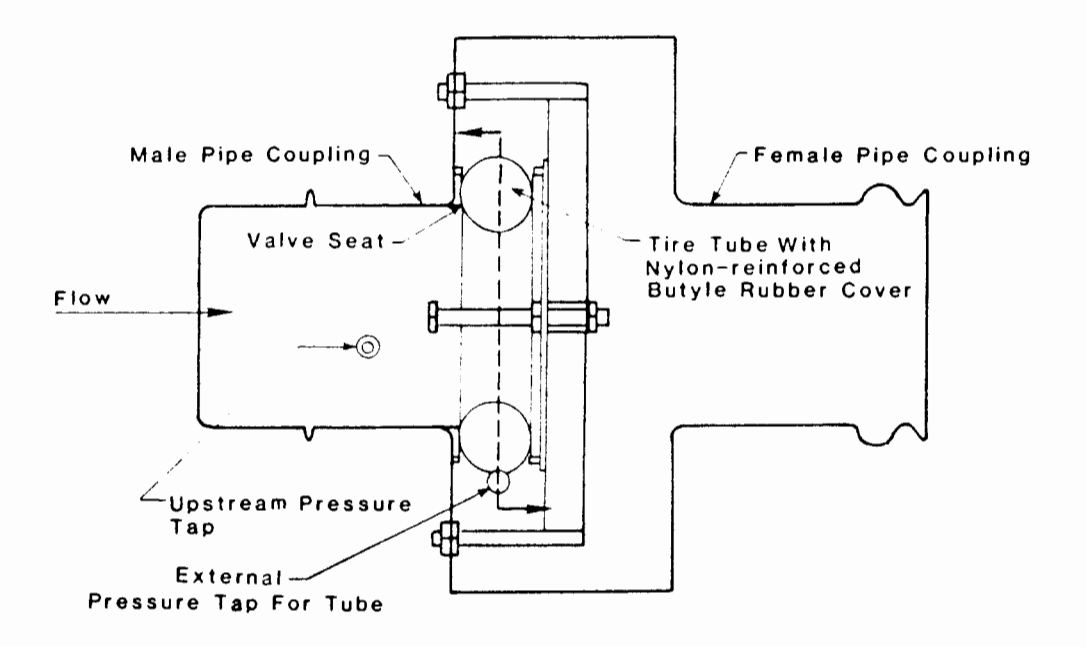
Figure 8.7 Improved USDA inflatable pneumatic O-ring valve. (From Haise et al., 1980.)

for the opening and closing processes. Snake River valves are available in diameters of 4, 6, 8, and 10 in. The fabrication details are shown in Fig. 8.8. The type A nonreinforced bladder is used for pressure heads of less than 9 ft (approx. 3 m), while the type B reinforced bladder is used for 16 ft (5 m) of maximum pressure head (Humpherys and Stacey, 1975). The Snake River valve is now commercially fabricated by the Hastings Irrigation Pipe Company of Hastings, Nebraska.

## Air-Operated Butterfly Valve

Low-pressure butterfly valves commonly used in gravity irrigation systems are usually operated by hand but can be controlled automatically or semiautomatically if fitted with suitable operators. The valves can be located in a tee to switch water to adjacent sets or in-line to control placement and pressure. Two types of operators are used to automate these valves. The first is a standard piston-type cylinder and the second is a relatively new spring-actuated valve. The air cylinders are pivot mounted on the rear with the rod attached to the butterfly lever arm with a rod clevis (Fig. 8.9). For field service, the cylinders have stainless steel rods covered with a boot, and either stainless steel or brass bodies. Portable air tanks can be used to supply air to the cylinders (Humpherys, 1983).

The air cylinders are designed to provide sufficient operating force at an air pressure of approximately 30 lb/in.<sup>2</sup> even though the air tanks are charged to about 120 lb/in.<sup>2</sup> At the higher pressures, cylinder output force exceeds that needed, but since tank pressure decreases with time and usage, this design assures satisfactory valve operation at low tank pressures. The cylinders are mounted and operated so that they open the valve in the push direction. For cylinder uniformity and standardization, a stroke of 6 in. is used for all cylinder and valve sizes. Cylinders



## Valve Cross Section

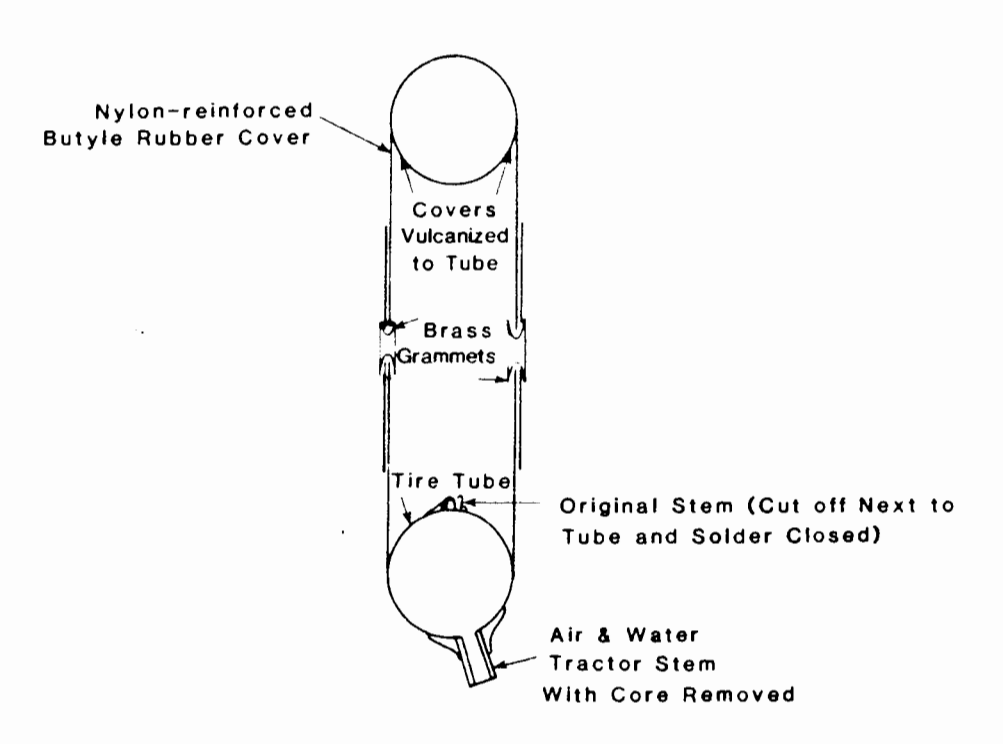


**Figure 8.8** Schematic detail of Snake River valve. (Courtesy of Allan S. Humpherys. See also Humpherys and Stacey, 1975.)

having a 1.5-in. bore diameter are used for both the 6- and 8-in. pipeline valves, while 1.75-in. cylinders are used on both 8- and 10-in. valves. Since not all manufacturers provide 1.75-in. cylinders, 10-in. valves are often operated with 2-in. cylinders.

Humpherys (1983) has also developed a spring-operated butterfly valve for use in automated surface irrigation systems. The unit differs from the valve in

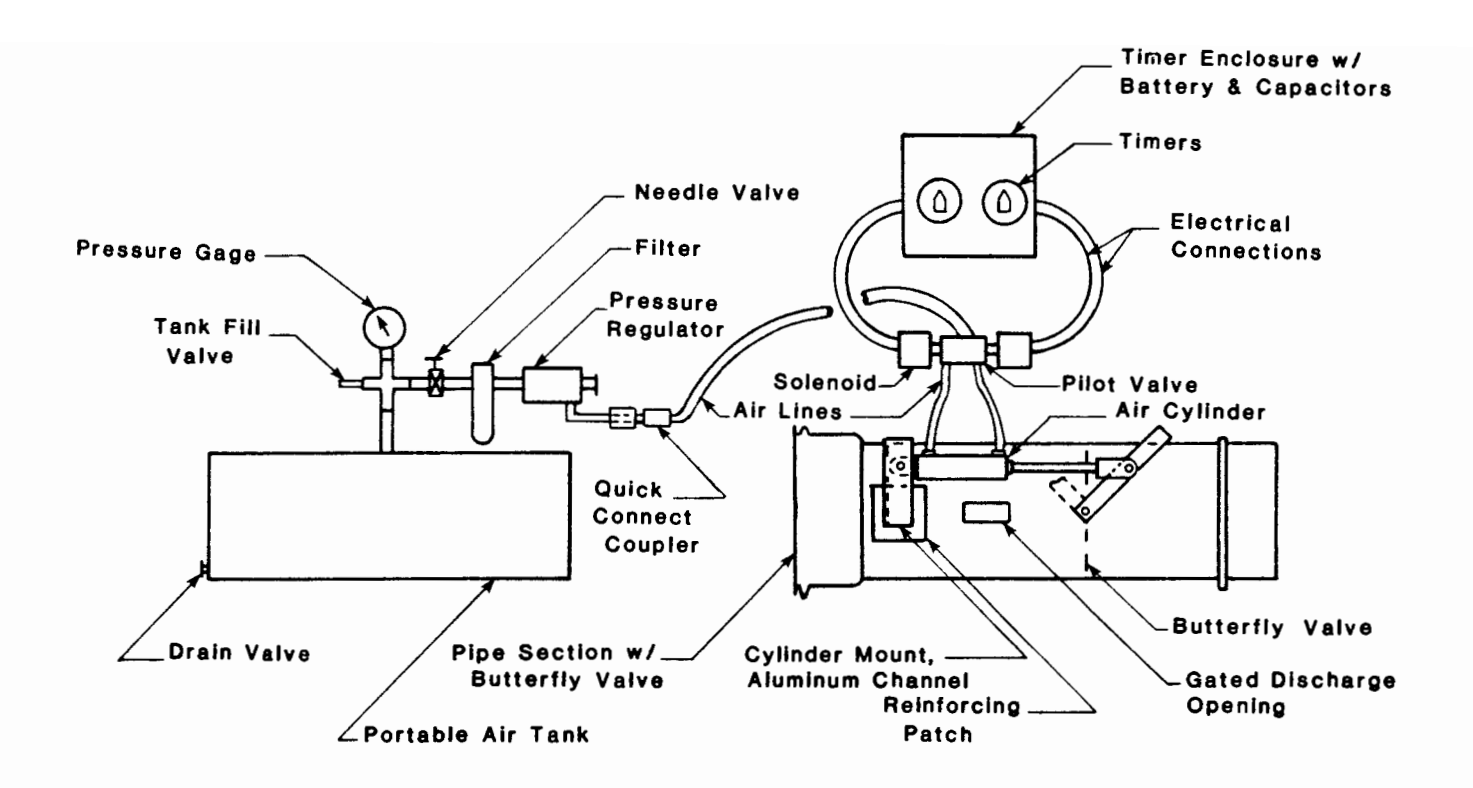


Figure 8.9 Schematic piston-operated butterfly valve. (After Humpherys, 1983.)

Fig. 8.8 primarily in the use of a short section of pipe containing the torsion-spring operator and a trip-release mechanism on a 24-hr mechanical timer instead of the pneumatic actuating system. The torsion springs rotate the valve disk through the necessary angular distance one time and then must be manually reset.

## **Gated Pipe Outlets**

Haise et al. (1980) describe research and development efforts by USDA-ARS personnel regarding the automation of gated pipe outlets for furrow-irrigated fields. One of the innovations is the modified Epp-fly gated pipe valve shown in Fig. 8.10. The valve is operated on and off by a pneumatic pillow inside the valve body. Similar arrangements and modifications have been made by several others. Stringham and Keller (1979) modified commercial sprinkler valves by replacing a standard diaphragm with a more flexible one and then using pressure to actuate the on-off flow control for the first surge flow system.

## **CONTROLLERS**

A final component of automation is the logic device or controller. Control systems can be utilized in the automation of an entire irrigation system or simply applied to a single flow-regulating device. Thus controllers range in complexity from a

simple timer as in the drop-open gate, to a controller incorporating a microprocessor unit to link many regulators and manage both their openings and closings.

## **System Controllers**

USDA-ARS personnel have also been prominently involved in the development and application of controllers to the automation of surface-irrigated fields. In one of the earliest developments in system automation, shown in Fig. 8.11, tone te-

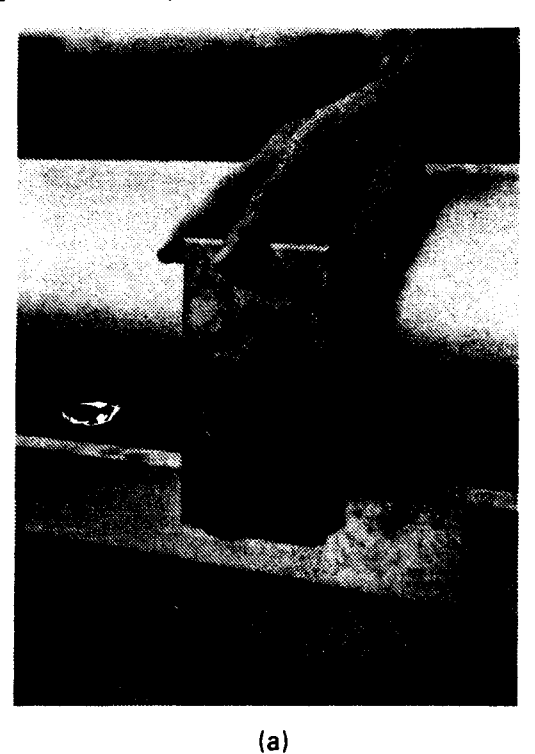




Figure 8.10 (a) Modified Epp-fly valve installed in metal transition box on 8-in. aluminum pipe. (b) Inside view of valve showing pillow, flowing water, and valve inlet lever to adjust discharge. (From Haise et al., 1980.)

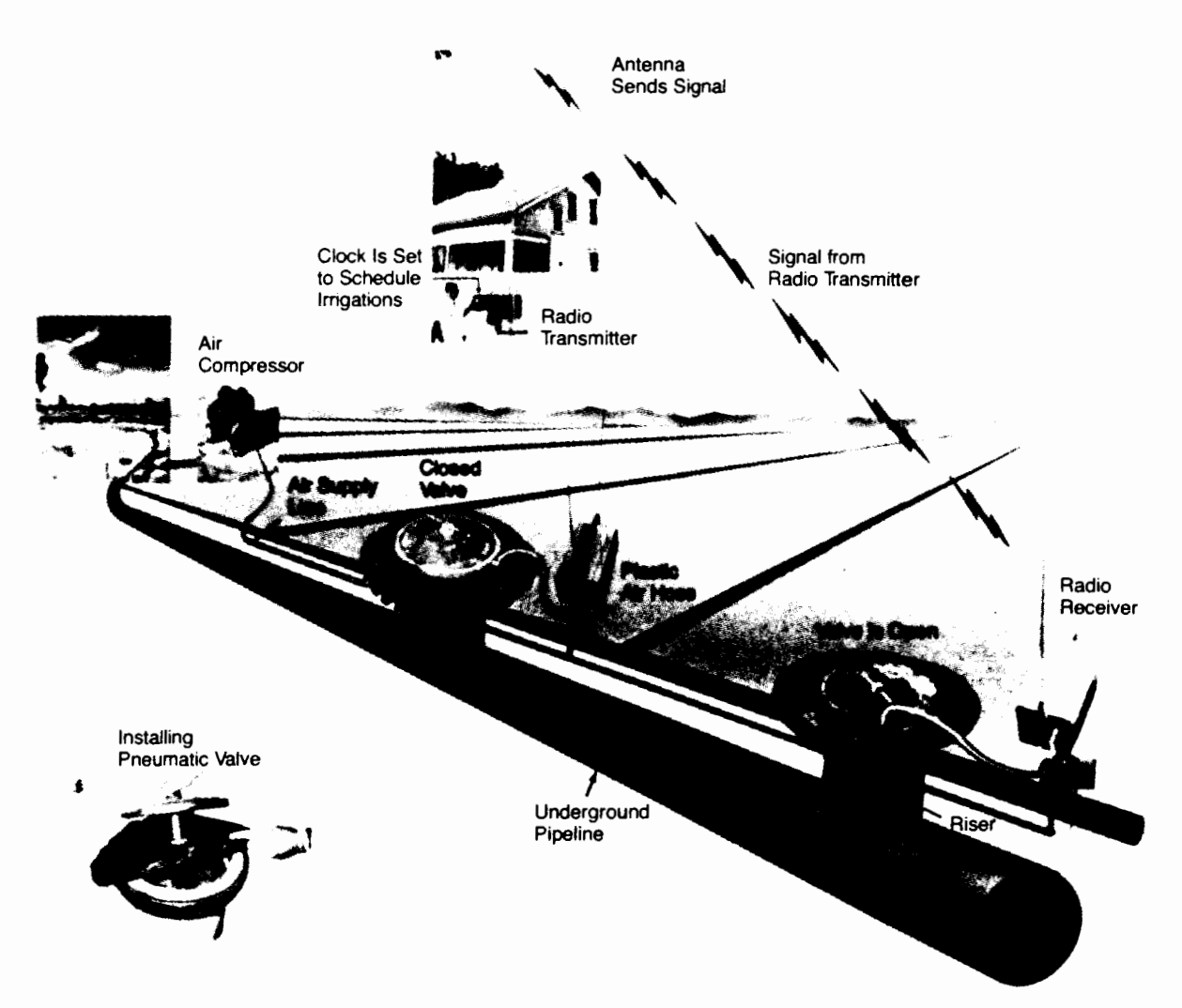


Figure 8.11 Radio tone controlled pipeline irrigation system. (From Haise et al., 1980; system patented by H. R. Haise and E. G. Kruse on May 23, 1967, as a USDA patent.)

lemetry was employed. There were some difficulties with these controllers (Haise et al., 1980), but many of these problems could be circumvented today with the electronic circuitry presently available.

Whereas system controllers for surface systems have been generally unsuccessful, those for sprinkle and trickle systems have been widely accepted and applied. With the advent of better surface irrigation practices such as surge flow and precision land leveling, it is certain that reliable system level automation will emerge for surface irrigation as well.

## Station Controllers

If the primary flow control is directed only toward the headland facilities, controllers which actuate a single valve may be all that is necessary for automation. A small portable system including a compressed air energy source is shown in Fig. 8.12. Most of these controllers are butterfly operated and are somewhat similar to (if not actually derived from) sprinkler irrigation controllers.

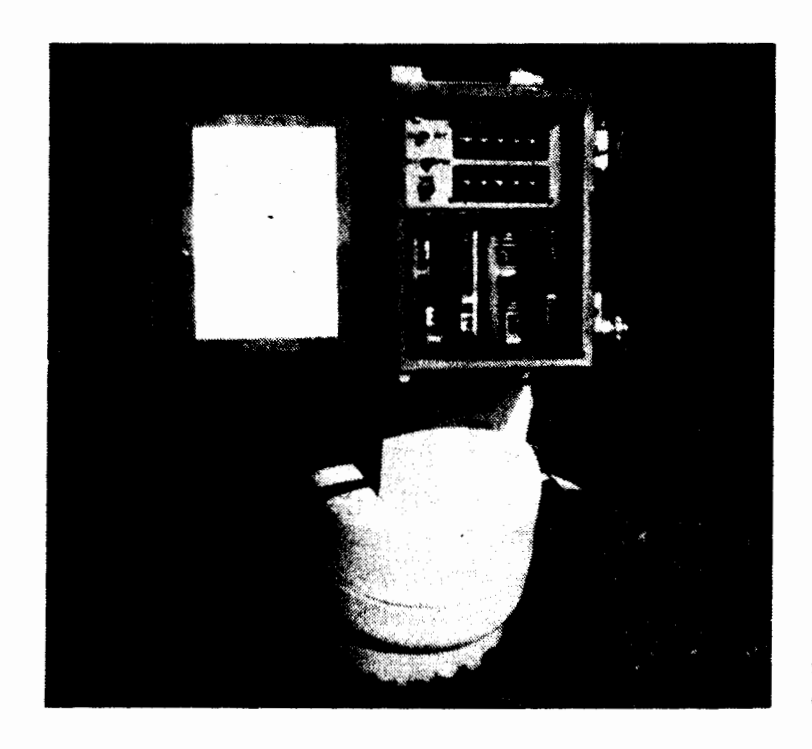


Figure 8.12 Portable battery-powered single-station controller. (From Haise et al., 1980.)

## Summary

Nearly any description of surface irrigation automation quickly becomes outdated due to the continual development of control and actuating equipment. A sample of surface irrigation automation has been given in this chapter to illustrate (but not exhaustively detail) the present state of the art. New concepts, such as surge flow (Chapter 9), will require new automating devices. Application of microprocessor controllers coupled to system performance sensors will soon be realities.

## CALIBRATION

In calibrating a new or improved surface irrigation system, the first interest is in evaluating the "hardware" contained in the headland and tailwater facilities. During installation, this hardware should have been checked for proper dimensions and elevation. Also, any mechanical or electrical devices should have been inspected for proper functioning. In some cases, the system would have been checked for proper hydraulic functioning. If not, this should be undertaken during the first irrigation event following installation.

As a first step, the flow-measuring device at the field or farm inlet should be checked. If this is an open-channel flow-measuring device, the zero-flow depth should be checked, probably with an engineer's level. Should there be any question regarding the accuracy of the flow-measuring device, the discharge rating should be evaluated by temporarily installing another primary flow-measuring device or checking the flow rate with devices such as a current meter.

Any structures that have been installed for trash removal or sediment removal should be checked during each irrigation event to evaluate their effectiveness. At

the same time, all mechanical or electrical components in the headland or tailwater facilities should be checked for any signs of malfunction.

Data regarding field capacity (FC), permanent wilting point (PWP), and soil bulk density ( $\gamma_b$ ) should have been collected prior to design of the surface irrigation system. These data, combined with soil moisture monitoring, allow computation of the soil moisture deficit that should be replenished during the subsequent irrigation event.

During each irrigation event, the hydraulic performance should be evaluated based on measurements of:

- 1. Available water supply to the irrigation set
- 2. Time of advance at midfield and at the end of the field
- 3. Time of cutoff
- 4. Time of recession

If there will be tailwater runoff from the surface-irrigated field, it is highly desirable to install a flow-measuring device to monitor this runoff. For a furrow-irrigated field, the inflow to several furrows should be measured, together with the advance time to midfield and end of field. The measured inflow to the irrigated basin, border, or set, and the time of advance to the end of the field and the recession time, should be compared with the values used in designing the system. The time of advance data to midfield and end of field can be used to derive an infiltration function. Average values can be used for the basin, border, or set to derive the infiltration function, which should be compared with the design infiltration function for that particular irrigation event.

For furrow irrigation, the infiltration function for each furrow can also be derived, or a sample of furrows can be used having a wide range of furrow inflow and time of advance to the end of the field. The sampling should include furrows having nearly similar values of flow but with a large variation in time of advance, and vice versa. These data can also be used to adjust the flow in each furrow in order to achieve a more uniform time of advance for all furrows.

## IRRIGATION SCHEDULING

The purpose of irrigation scheduling is to maintain a good soil moisture status in the root zone reservoir and thereby provide near optimum environmental conditions for crop growth. Advising farmers "when to irrigate" and "how much to irrigate" is satisfactory for pressurized irrigation systems such as sprinkle irrigation and trickle irrigation, where the water application can be controlled by the network of closed conduits. For surface irrigation systems, the control is not the method of applying water but rather the soil surface. More specifically, the infiltration function is the major concern in replenishing the root zone reservoir. The combination of infiltration function and time of advance function dictates the hydraulic performance for an irrigation event. Unfortunately, both of these functions change

dramatically from one irrigation event to the next during a season, as well as showing year-to-year variations. As a consequence, scheduling irrigation events for a surface-irrigated field is considerably more difficult than scheduling sprinkle or trickle irrigation events.

## **Crop Water Requirements**

In any irrigated area, the best available information is used in calculating evapotranspiration  $(E_t)$ . If the available data base is insufficient for the required accuracy in calculating crop water requirements, better field measurements will have to be undertaken, preferably prior to implementation of an irrigation scheduling program (e.g., during the calibration phase) and perhaps continued during the early years of the program. In some areas, field data may have to be collected on crop rooting depths because of unique soil characteristics and cultivation practices.

A combination water budgeting and irrigation scheduling computer program is particularly useful in predicting crop water requirements and the next irrigation event. A flow diagram for such a computer program is shown in Fig. 8.13. Historical climatic data are used to calculate average values of reference evapotranspiration for each day of the season. Then using the typical planting date in the local area for each crop, and combining with crop growth coefficients, the crop evapotranspiration can be estimated daily between planting and harvesting. This is only a guide to  $E_t$  values for the area. For any particular field included in an irrigation scheduling program, the planting date will probably not correspond with the usual date in the local area, but a new estimate of daily  $E_t$  can quickly be obtained. The computer program is continually updated throughout the season by inputting measured climatic data and measured soil moisture data.

## Application of Irrigation Water

In answering the question of how to apply the proper amount of irrigation water, the flow rate available for the next irrigation event must be estimated. If the water source is a pumped well, the discharge should be known based on measurements during the calibration phase. If surface water supplies are used for irrigation, there may be considerable variation in available flow rate during the season as well as from season to season. Historical data will be required in conjunction with forecasted water supplies to estimate the available flow rate at the time of the next irrigation event. In addition, the operational characteristics of each irrigated area can have a dramatic effect on the discharge rate at a field or farm inlet.

During the calibration phase, field data can be collected to verify the design procedure. In essence, whichever model was used in the design procedure should be calibrated for the particular field being investigated. The calibrated model can be used to generate time of advance relationships, which are a function of irrigation event and flow rate. A typical example is shown in Fig. 8.14. The calibrated model can also be used to generate infiltration relationships, which are a function of irrigation events (Fig. 8.15). These functional relationships are the basis for advising the irrigator on how to apply the proper amount of irrigation water.

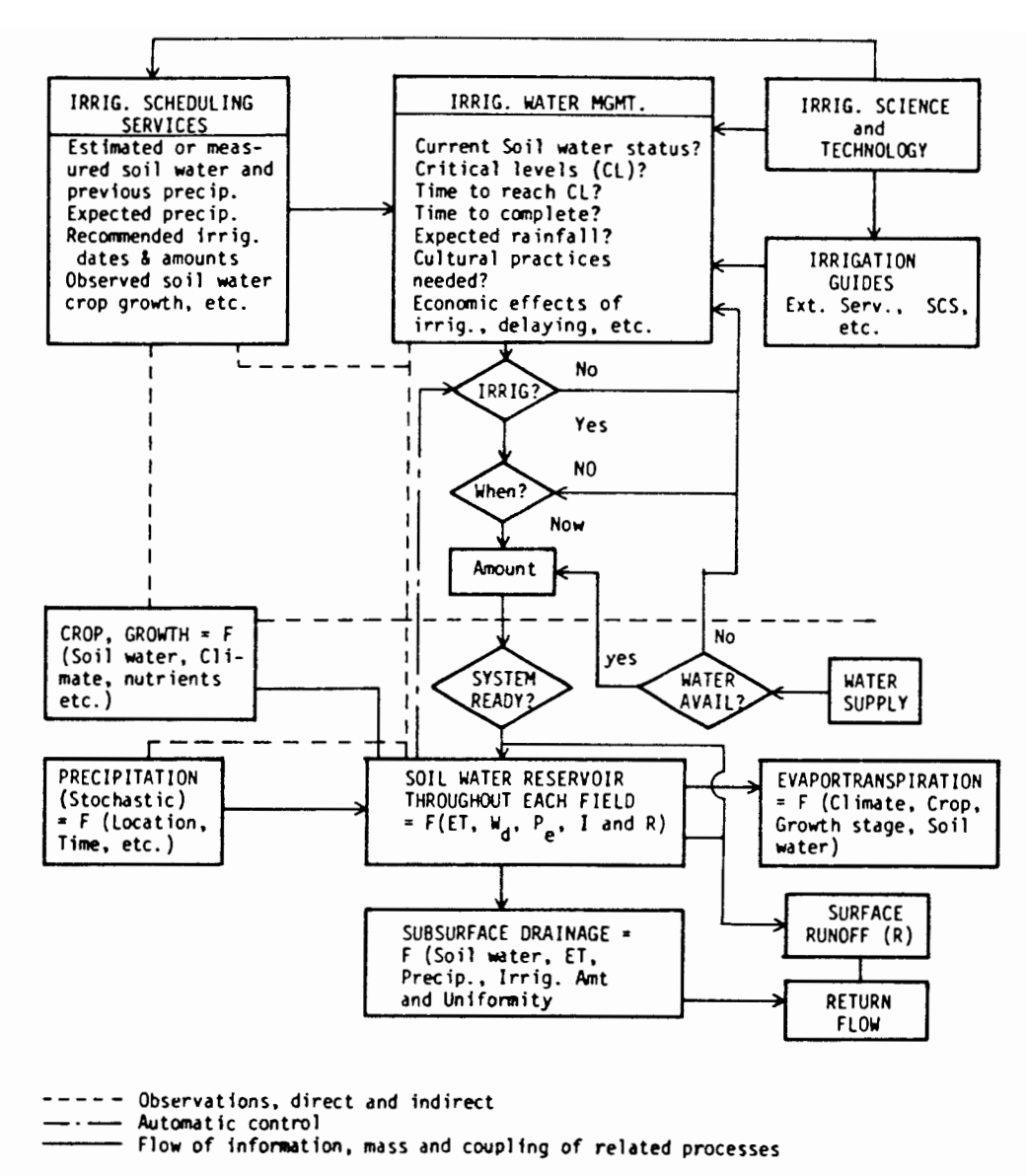


Figure 8.13 Flow diagram for water budgeting and irrigation scheduling computer program. (After Jensen, 1975.)

### **MONITORING AND EVALUATION**

Any project can be expected to benefit from a monitoring and evaluation program. This mechanism is beneficial in documenting the effectiveness of the project, but more important, to provide feedback for refining the implementation process.

For projects that have involved physical improvements to the farm surface irrigation systems, followed by calibration and irrigation scheduling, monitoring and evaluation become a relatively simple process. Primarily, a sample of fields would have flow-measuring devices temporarily installed for recording tailwater runoff, unless, of course, basin irrigation was being employed. In addition, the inflow discharge and time of cutoff would be monitored to compare farmer practices with the advice provided by the irrigation scheduling program. Also, there would be considerable value in interviewing farmer participants in the project to learn of

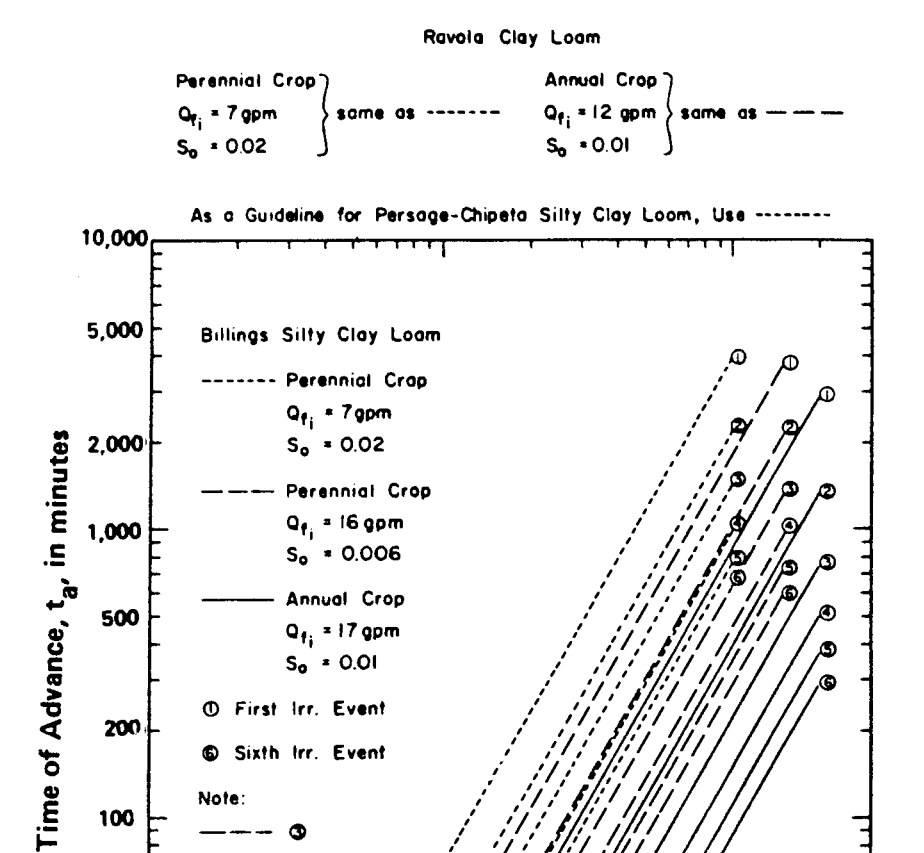


Figure 8.14 Example of variation in time of advance functions with irrigation event for a particular soil type, crop, and constant furrow inflow discharge rate.

Furrow Length, L, in feet

their perceptions regarding the project and to obtain their suggestions for improving the implementation process.

In contrast, irrigation scheduling programs have been implemented in surface-irrigated areas without the benefit of field data describing the hydraulic performance of farm irrigation systems. Most of those programs have had very little impact on improving irrigation practices, let alone gain farmer acceptance and long-term adoption of the irrigation scheduling program. In such situations, irrigation scheduling can be only marginally effective until proper field data have been collected, such as the data recommended under the calibration process. Calibrating a field will result in dramatic improvement that can be achieved by irrigation scheduling. When many fields have been calibrated in an irrigated area, general relationships can be developed between inflow discharge, time of advance functions, and the

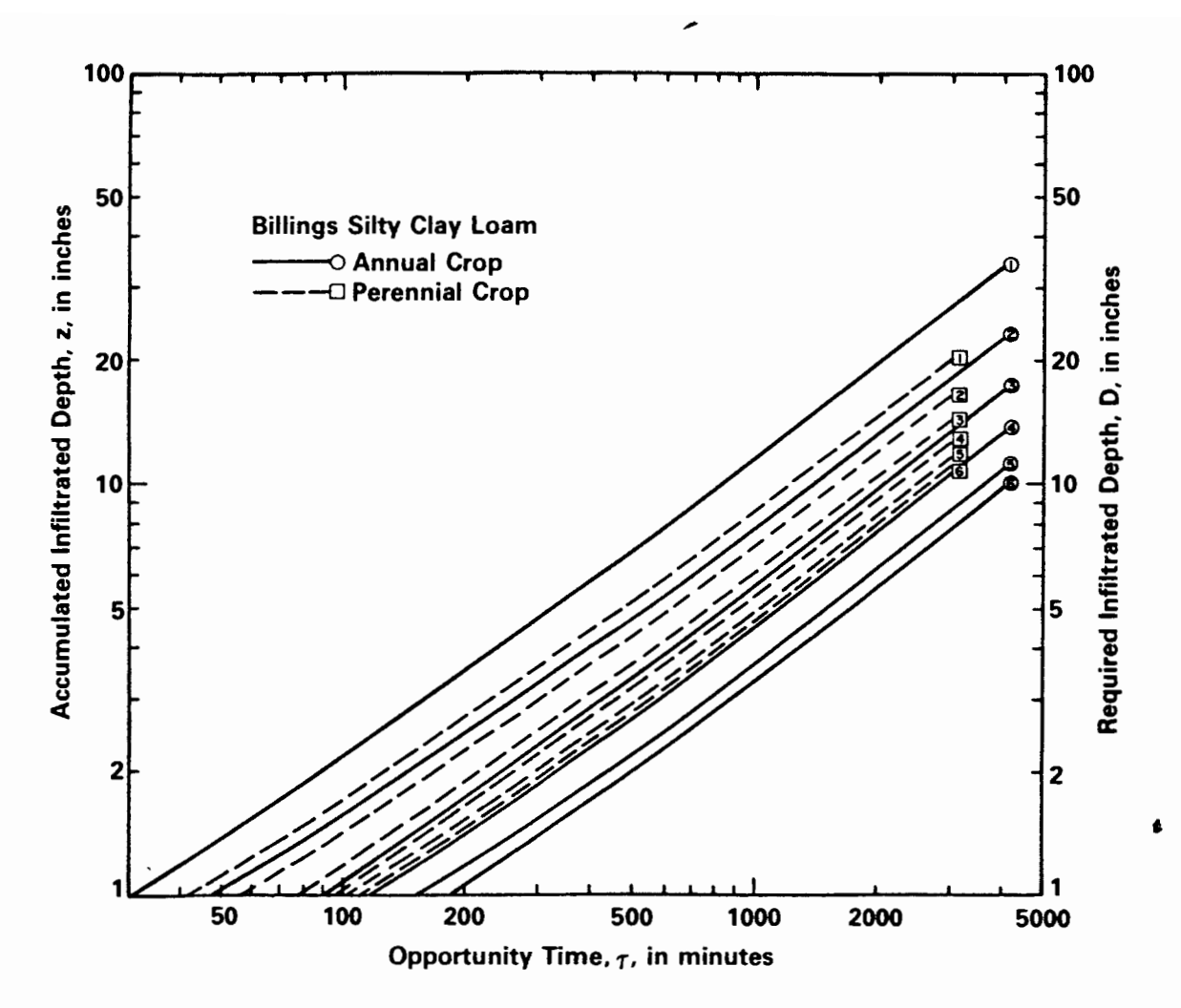


Figure 8.15 Example of infiltration functions for a particular soil type.

infiltration functions for various soil types, crops, and cultivation practices. Again, such field data could also be incorporated into one of the surface irrigation models, which would then allow general relationships for the local area to be generated.

### REFERENCES

EVANS, R. G. 1977. Improved Semi-automatic Gates for Cut-Back Surface Irrigation Systems. *Trans. ASAE* 20(1):105-108, 112.

HAISE, H. R., E. G. KRUSE, M. L. PAYNE, and H. R. DUKE. 1980. Automation of Surface Irrigation: 15 Years of USDA Research and Development at Fort Collins, Colorado. Prod. Res. Rep. 179. U.S. Department of Agriculture.

HUMPHERYS, A. S. 1969. Mechanical Structures for Farm Irrigation. ASCE J. Irrig. Drain. Div. 95(IR4):463-479. Proc. Pap. 6944.

HUMPHERYS, A. S. 1971. Automatic Furrow Irrigation Systems. *Trans. ASAE* 14(3):446, 470.

- HUMPHERYS, A. S. 1983. Automated Air-Powered Irrigation Butterfly Valves. *Trans.* ASAE 26(4): 1135-1139.
- HUMPHERYS, A. S., and R. L. STACEY. 1975. Automated Valves for Surface Irrigation Pipelines. ASCE J. Irrig. Drain. Div. 101(IR2): 95-100.
- JENSEN, M. E. 1975. Scientific Irrigation Scheduling for Salinity Control of Irrigation Return Flows. Rep. EPA-600/2-75-064. U.S. Environmental Protection Agency, Robert S. Kerr Environmental Research Laboratory, Ada, Okla., November.
- STRINGHAM, G. E., and J. KELLER. 1979. Surge Flow for Automatic Irrigation. *Proc. 1979 ASCE Irrig. Drain. Div. Spec. Conf.* Albuquerque, N.M., July.

# Surge Flow<sup>1</sup> Surface Irrigation

#### CONCEPTUAL DEVELOPMENT

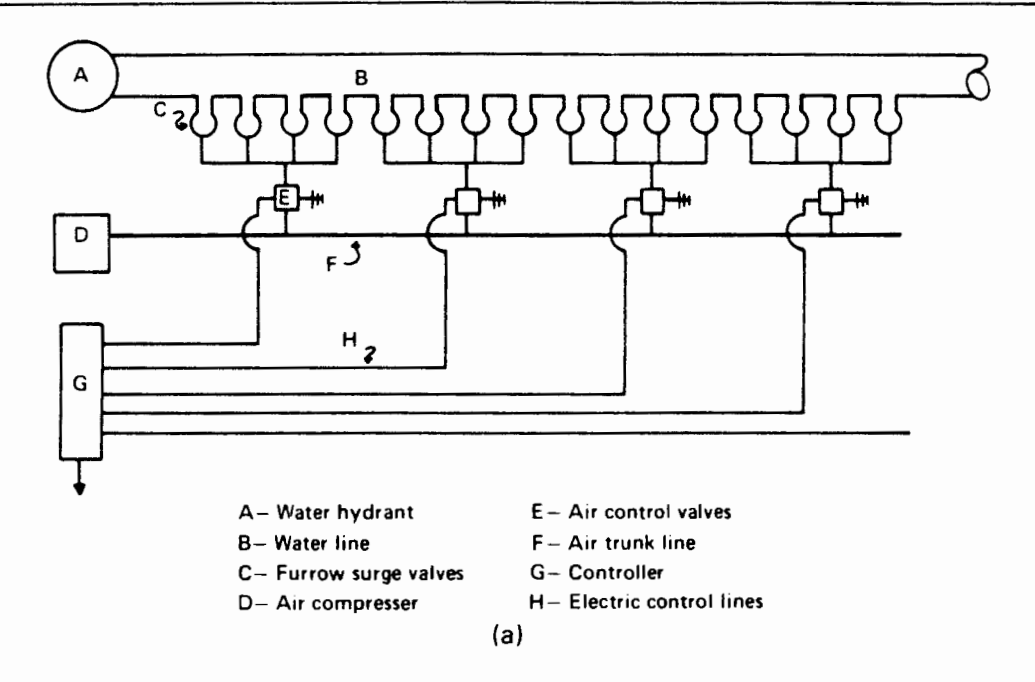
Stringham and Keller (1979) introduced the concept of surge flow in the 1979 Irrigation and Drainage Specialty Conference of the American Society of Civil Engineers.<sup>2</sup> The report was a preliminary discussion of a promising automating technique for achieving cutback in furrow irrigation. Their basic premise was stated as follows:

Previous attempts to develop automatic cutback irrigation systems have concentrated on reducing the steady state stream size. However, simple automatic irrigation valves can only turn water on or off, but not half on or half off. Therefore, we concluded that it would be simpler to cycle the valves to reduce the average flow rate instead of partially closing the valves.

The surge flow system discussed by Stringham and Keller (1979) is illustrated in Fig. 9.1. Pneumatic valves were modified for low pressure by replacing the diaphragm and then were installed on a PVC pipeline. Banks of valves were operated in coordination with a microprocessor-based controller to achieve a cycling

<sup>1</sup>SURGE FLOW<sup>®</sup> is the registered trademark of the Utah State University Foundation, but the term "surge flow" also refers to an irrigation practice. This chapter refers primarily to the practice and therefore will not utilize the trademark designation.

<sup>2</sup>In March 1986, the U.S. Patent Office issued patent number 4,577,802, titled "Method and System for Furrow Irrigation," listing Drs. Jack Keller and G. E. Stringham as inventors and the Utah State University Foundation as assignee.



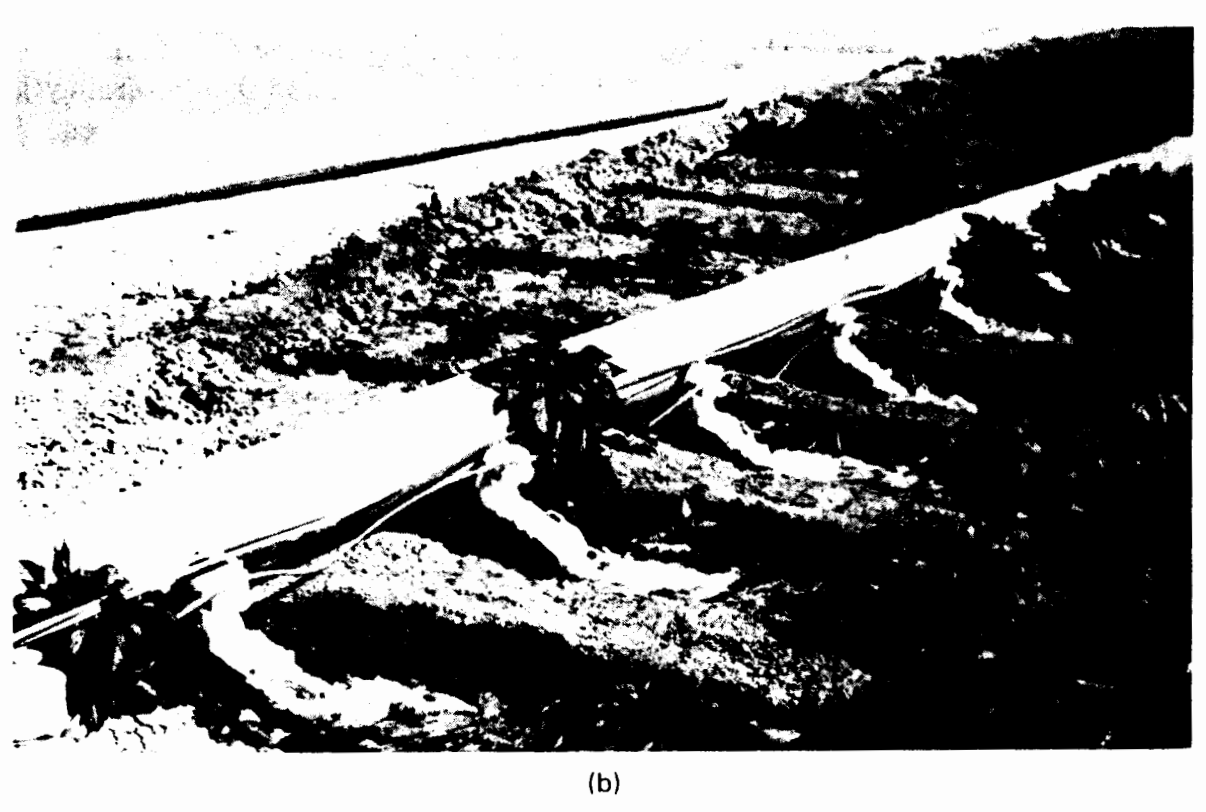


**Figure 9.1** USUF-Kubota surge flow system and the automating valves. (a) From Stringham and Keller, 1979, with permission of ASCE. (b) Courtesy of Dr. Glen E. Stringham.

sequence ranging from a few seconds to several hours. To test the equipment, a small unit was set up on 12 furrows, 600 ft long, in late 1978. The furrows were divided into three sets each having a valve discharge of 13 gal/min. The first bank was allowed to run continuously until completion of the advance phase. The second was cycled approximately 8 s on and off to achieve an average flow rate in the

furrow of 6.3 gal/min. The third set was cycled approximately 16 s on and 8 s off, yielding an average furrow flow of 8.6 gal/min. In addition to observing the operation of the system, limited field data were collected to record the advance rate.

In retrospect, the interpretation of the field data demonstrated considerable insight. The advance rates under the 16-8 cycling were faster than for continuous flow. The continuous flow, however, advanced more rapidly than the 8-8 cycled furrows. Stringham and Keller (1979) stated: "If subsequent tests verify this phenomenon [faster advance rate due to cycling], the implications are extremely interesting in terms of distribution uniformity along furrows and runoff rates." The phenomenon they perceived is hardly indicated by their data, since natural variability could have produced the same result. Nevertheless, they speculated that cycling the inflows somehow created an advantage not theretofore understood—a conclusion that has since been proven with remarkable clarity.

Actually, the surge flow phenomenon had been observed by irrigators for more than two decades prior to the initial research (Stringham and Keller were also aware of these practices). Many irrigators found it impossible to complete the advance phase of an irrigation following a major cultivation because of the high intake rate. They discovered that by diverting the flow to another set for a few hours or a day when the advance rate stopped, and then returning the flow to the partially wetted field later, the advance phase could be completed. The most common term for this practice is "bumping."

Today, surge flow is a management practice that can be applied to many surface-irrigated conditions. It can be used either to "cut back" the inflow at the completion of advance and minimize tailwater, and/or to accelerate the advance phase on problem soils. A large number of researchers, primarily in the western United States have investigated this practice. In this chapter we present the state of the art of surge flow as developed sequentially. Some of the major questions affecting implementation on a system scale are discussed.

#### **EARLY FIELD TESTS**

In 1979 the first field tests were initiated at Utah State University (Allen, 1980; Poole, 1981). A 600-ft-long system comprised of the piping, valves, and controls developed the preceding year was installed on a university-operated cornfield. The furrows were on a slope of 1.5% and the field soil was Millville silt loam. Four tests were conducted in late June and early July using a cycle time of 10 minutes for three surge treatments per test and continuous flow. The surge tests included cycle ratios of one-third, one-half, and two-thirds. Each surge and continuous flow treatment had time-averaged discharges of 10 gal/min and were replicated in wheel and nonwheel furrows. Field data were collected to identify advance rates and tailwater runoff. Advance trajectories for a first and second irrigation in the nonwheel furrows are shown in Figs. 9.2 and 9.3 (the individual surge-front locations are connected with a solid line to illustrate the differences between surge and continuous flow treatments). An analysis of the field data provided an interesting

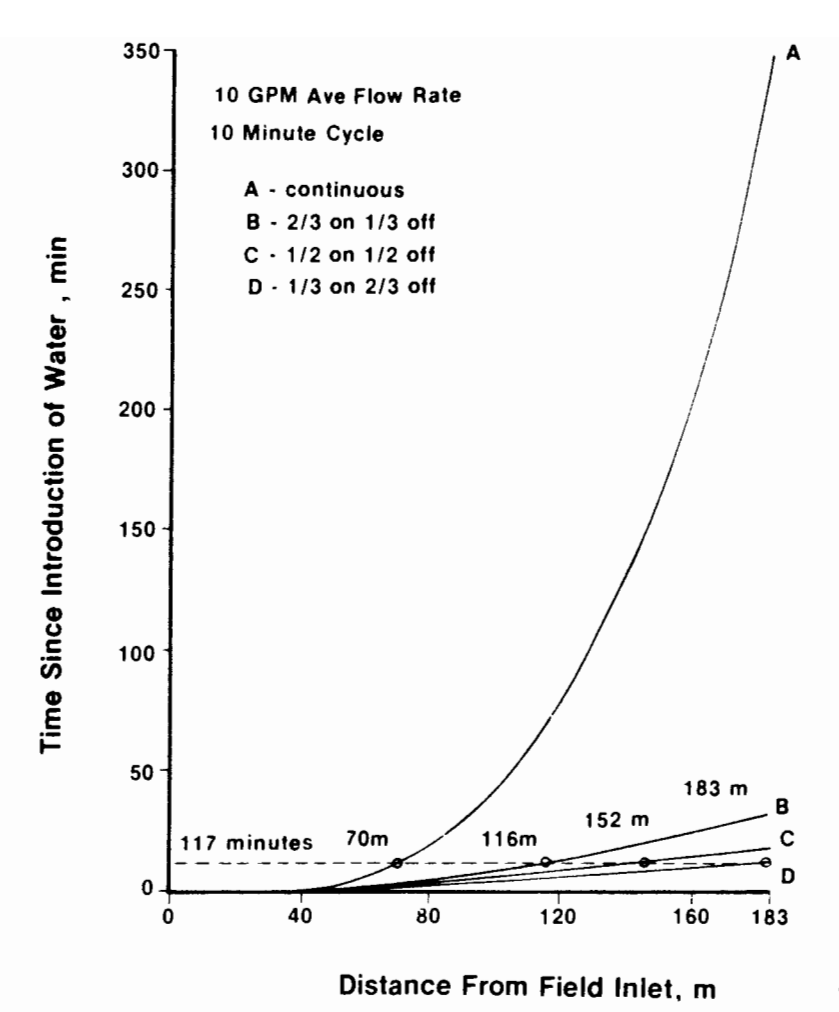


Figure 9.2 Advance rates on July 3, 1979, first irrigation, newly dug non-wheel furrows. (After Allen, 1980.)

comparison. Soil samples were taken prior to the irrigation to determine the soil moisture deficit, and the inflow-outflow hydrographs were subtracted to identify the total infiltrated volume. For the one-third-on/two-thirds off surge and continuous flow tests shown in Fig. 9.2, the results were as follows: an application efficiency of 87% under surge flow and a 9% performance for the continuous flow. Although not all the tests were this profound, the promise of surge flow was certainly evident.

A second set of experiments was conducted with the system in 1979 to consider whether or not the surge flow effect was due primarily to the higher instantaneous flow rate. Poole (1981) utilized 2-, 5-, 10-, and 20-min cycle times with a cycle ratio of one-half for all tests. The instantaneous discharge for both surged and continuous inflows was 20 gal/min, so the surged tests actually had a time-averaged flow of one-half that of the continuous flow furrows. The field conditions were the same as those noted above, and the same field data collection procedures were utilized. The advance trajectories for the July 3 nonwheel test are shown in Fig. 9.4, and as seen, do not differ much from Fig. 9.2. However, an analysis of the variability among the various replications produced a very interesting result. Over the season, over the field, and over all replications, the time required for the continuous flows to reach the end of the furrow ranged from 270 to 3490 min, an order-of-magnitude variation. This variation was reduced substantially under surge flow. For instance, the advance time for the 20-min cycle ranged from 60 to 120

Early Field Tests 215

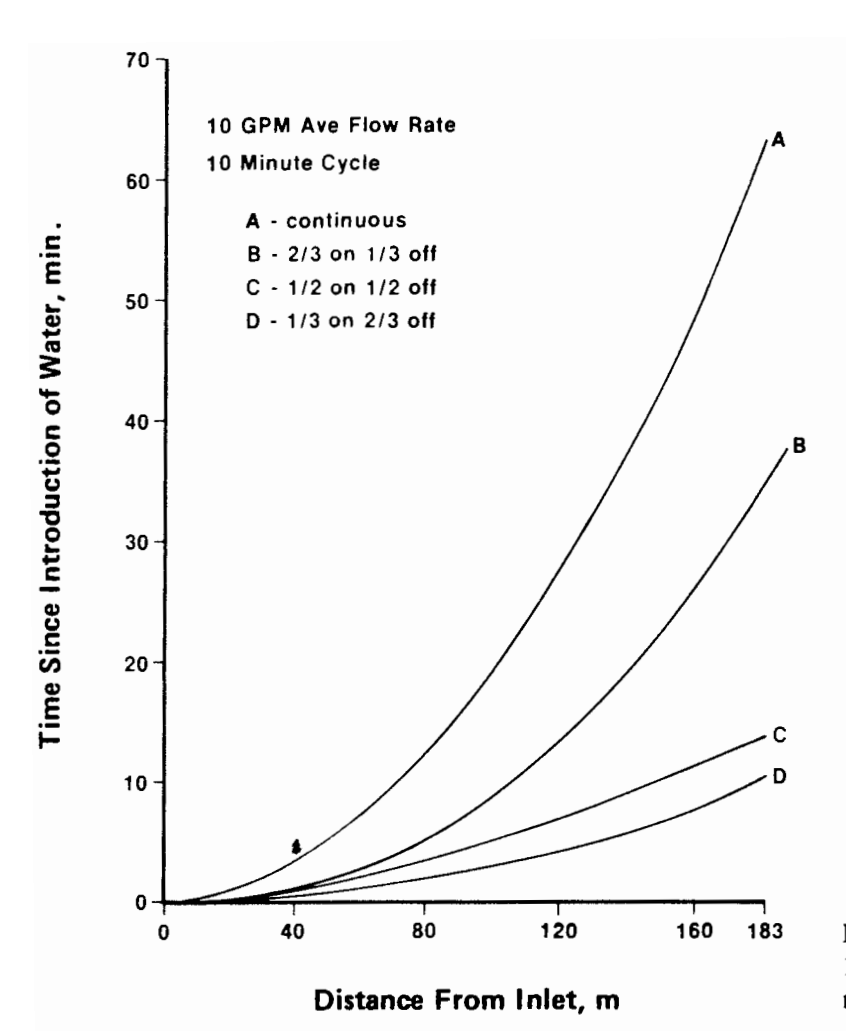


Figure 9.3 Advance rates on July 12, 1979, second irrigation nonwheel furrows. (After Allen, 1980.)

min, a factor-of-2 variability. The results of both the Allen (1980) and Poole (1981) field tests have been summarized by Bishop et al. (1981).

The final field trials of the surge flow concept during the early period were conducted by Coolidge (1981) and later summarized by Coolidge et al. (1982). The results of Allen (1980) and Poole (1981) clearly demonstrated that intermittent application of water in furrows substantially reduced infiltration rates on the silt loam soil. Coolidge (1981) installed the surge flow system at another USU field having the same soil type but having only 100-m furrows on a 1% slope. primary objectives were to substantiate the effect of surging on spatial variability and to determine, if possible, the relative importance of on- and off-time. The spatial variability was again significantly lower under a surged regime than under continuous flow (the standard deviations were 53 to 86% lower). The effect on infiltration was again observed in advance rate and tailwater conditions. For example, Fig. 9.5 shows the tailwater hydrographs from a surged and a continuous flow furrow. The instantaneous inflows were both 0.3 liters/s and the surged cycle time was 20 min. It is quite clear that the basic intake rate following several surges is approximately one-fourth the value under the continuous flow regime. Coolidge (1981) also concluded that on-time significantly affected surge flow systems but that off-time did not. Apparently, the reduction in infiltration rates, by whatever means, occurred very quickly following the furrow recession.

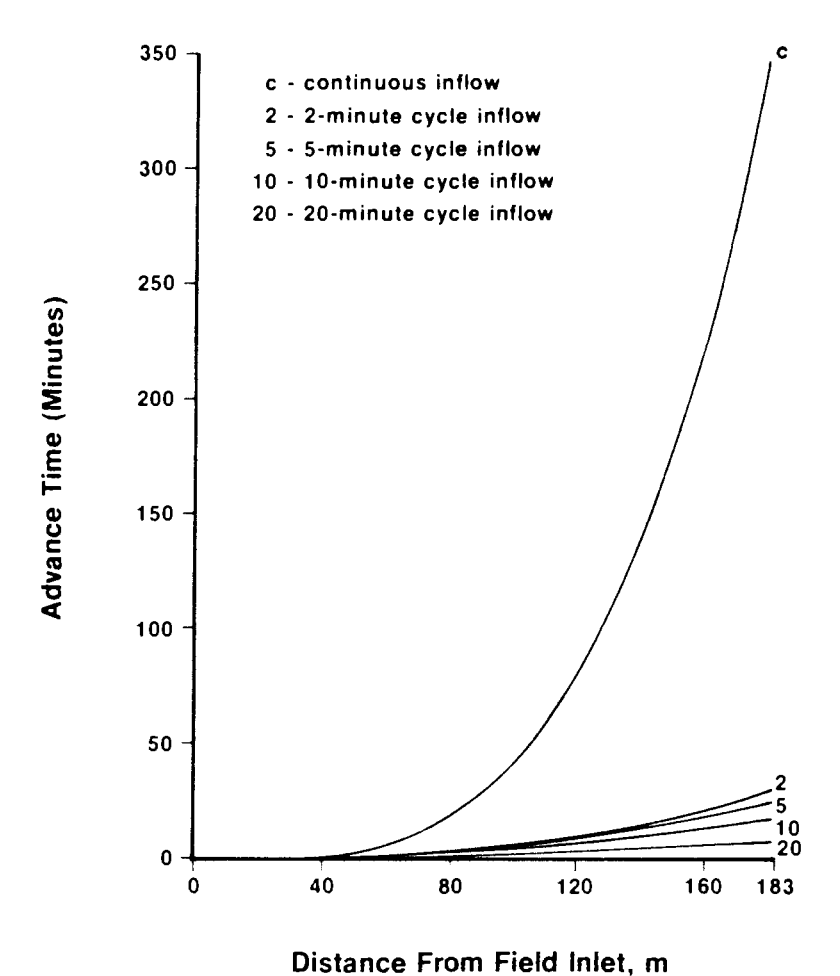


Figure 9.4 Advance rates on July 3 and 4, 1979, first irrigation in the non-wheel furrows. (After Poole, 1981.)

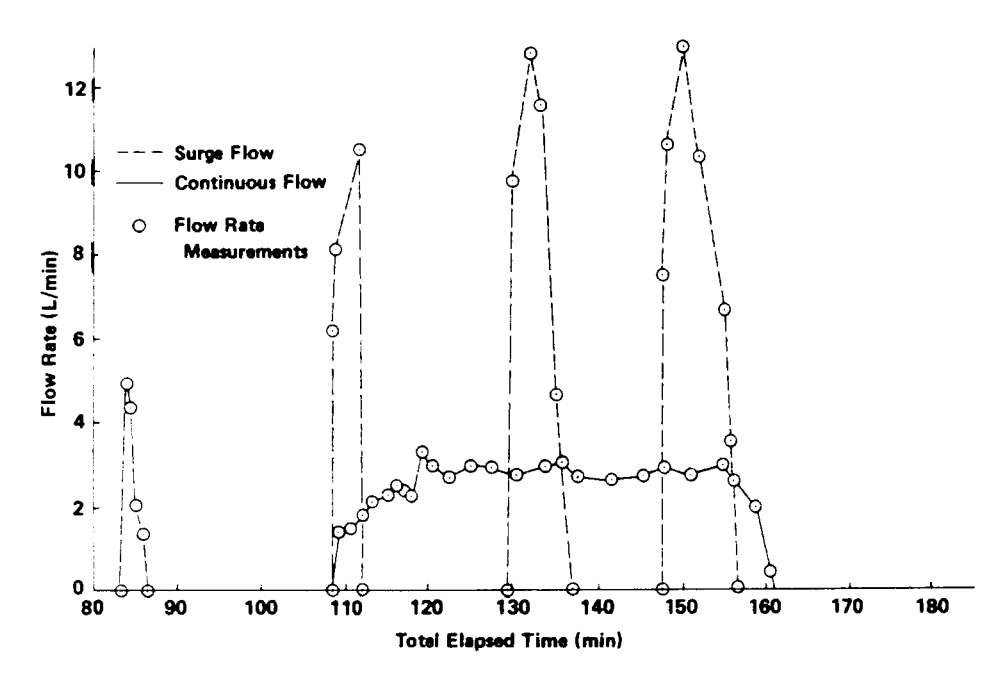


Figure 9.5 First irrigation runoff hydrographs associated with continuous and surge flow furrow data. (From Coolidge et al., 1982, with permission of ASCE.)

These early field evaluations have now been supplemented by numerous other tests under a wide range of field conditions (Walker et al., 1982; Podmore and Duke, 1982; and various others reporting only to the W163 project). The results have generally been mixed and few as significant as those at USU in 1979 and 1980. The following conclusions can be derived from field studies to date:

- 1. Intermittent flow over the field surface significantly reduces intake. The effect of surging is probably associated with the accelerated development of a thin surface seal comprised of very fine soil particles created by the water movement. During the drainage period, the buildup of negative pressure consolidates this thin seal, thereby reducing the permeability.
- 2. By reducing infiltration rates, it becomes easier to complete the advance phase. Advance rates are very sensitive to the discharge, so that as surge flow reduces infiltration, the hydraulic performance of the system improves.
- 3. The surge flow regime reduces the temporal and spatial variability exhibited in advance rates. Elliott and Walker (1982) showed that variations in the field's basic intake rate were often statistically insignificant. The surge flow effect in this regard may therefore be attributed to the lower time required to reach a steady or basic intake rate.

## **DEVELOPMENT OF SURGE FLOW SIMULATION MODELS**

In reviewing the testing at the end of the 1980 irrigation season, a number of intriguing questions emerged, such as the effect in other soils and surface irrigation systems, the management of cycle times and ratios to maximize uniformity and efficiency, and the structural elements needed to implement surge flow practices. Further, if the concept proved effective and feasible for a broad range of conditions, a major issue was how to design a surge flow surface irrigation system. As a result, two decisions were set in motion. The first was to expand the scope of surge flow research by promoting regional research coordination. This led to the formation of the Agricultural Experiment Station–USDA Regional Project W163, "Surge Flow Surface Irrigation." Most of the research reported since 1982 falls under this project. The second decision, limited to Utah State University, was to redirect research efforts toward the development of computer-based simulation models of surged operations.

The modeling of surge flow systems was divided into three phases: (1) field data collection for model verification; (2) model formulation and debugging; and (3) model analysis of operational factors.

## **Verification Data**

A review of the hydraulics of surface irrigation, such as in Chapters 12 to 16, indicates that the data necessary to evaluate an irrigation event would include an inflow-outflow hydrograph, advance and recession trajectories, flow geometry, field slope, length, and roughness and infiltration characteristics. These conditions

require a maximum of 16 individual parameters whose variations can vary by as much as an order of magnitude. Thus, developing a comprehensive understanding of their interrelationships would require an enormously expensive and time-consuming field investigation program.

The alternative to research through field evaluation is through theoretical study. Mathematical relationships are formulated and then verified by selective comparison with field observations. Field data collection is still required, but less often and more carefully determined. If it can be shown that a mathematical model accurately simulates a broad range of field data, it can be assumed that it will also simulate any combination of data falling within the limits. Modeling is relatively inexpensive and has the additional advantage that once verified, a multitude of analyses can be performed to investigate changes in both design and operational conditions.

Two field studies were conducted in 1981 to generate data for model testing. The first was on a field near Flowell, Utah, in which a conversion from a sideroll sprinkle to a furrow irrigation system was being made to allow corn production. The field was about 360 m long with a slope of 0.8%. The soil was a sandy loam. Upon irrigating the furrows the first time, the irrigator was not able to complete the advance phase without resorting to repeated "bumping," even though the individual furrow discharges ranged as high as 2.5 to 3.0 liters/s. Utah State University was invited to test the surge flow technique on this field in the hopes that it might increase uniformity and efficiency enough to compete with a center-pivot sprinkle system being considered as an option. The water supply for the entire farm was derived from a large well. A 75-hp pump was used to lift the water into a buried pipe network feeding the surface irrigation system via 10-in. gated pipe. To utilize the sprinkle systems, a 50-hp pump was used to pressurize the flow.

The second site was about 5 miles south of Kimberly, Idaho, and was selected in cooperation with researchers at the Snake River Conservation Research Center. USDA. The field was topographically similar to the Flowell field, but the soil was a silty-clay loam. Again, the irrigator had difficulty completing the advance phase and had practiced bumping. The field itself had just been plowed-out of many years of alfalfa production and the soil structure was very stable. At the time of the study, a first irrigation was being applied to a bean crop on part of the field and corn crop on the other. The water supply for the farm was derived from a gravity-flow mutual ditch association acquiring water from the Snake River.

The testing at each site involved several stages. The irrigator was asked about the discharge being used so that the surge flow trials could use the same instantaneous flows. The field was staked along the furrow lengths in 30-m intervals and the slope surveyed. Small cutthroat and trapezoidal flumes were installed at the inlet and outlet of the test furrows to record the inflow-outflow hydrograph. The individual furrow cross sections before and after irrigation were measured with the profilometer described in Chapter 4, and independent infiltration measurements were made with the recirculating infiltrometer, also described in Chapter 4. The comparison of surge and continuous flow irrigation regimes involved a cycle time of 20 to 120 min and a cycle ratio of 0.5. Replications were

Development of Surge Flow Simulation Models

219

divided into wheel compacted and noncompacted furrows, and a range of discharges was utilized. The advance and recession trajectories of each surge and continuous flow treatment were observed and recorded.

Figures 9.6 and 9.7 are two examples of the wheel and nonwheel results at the Flowell site. The solid lines represent the surge by surge advance-recession trajectories, and the superimposed dashed line is the advance trajectory of a continuous flow treatment having similar conditions. The problem of furrow irrigation at the site is most evident in Fig. 9.6. The flow simply stops advancing at about 280 m. By surging with 40-min cycles, the advance phase was completed in nine surges. Using the field discharge of 2 liters/s for 180 min yielded an average applied depth of 6 cm per furrow, or since the irrigated furrow spacing was 1.5 m, an average field depth of 4 cm. During the same elapsed time, the continuous flow furrow received twice as much water and only wetted 78% of the furrow. The average depth applied was 10 cm,  $2\frac{1}{2}$  times as much as the surged furrows.

Figures 9.8 and 9.9 illustrate two of the test results gathered from Kimberly. In Fig. 9.8, a 1.0- liter/s flow was applied to noncompacted furrows. Again the solid lines and dashed lines represent surged and continuous flow measurements. However, in this case, the furrow inflow was not sufficient, and although the surging

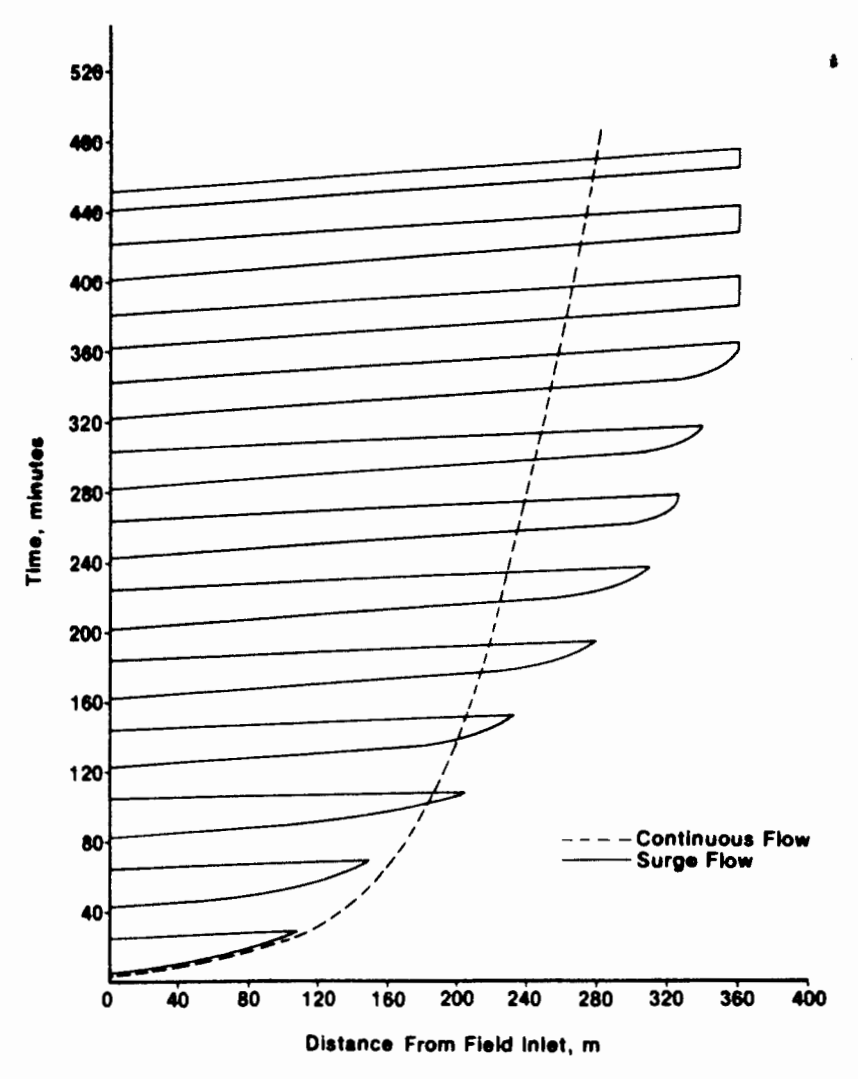


Figure 9.6 Advance and recession trajectories for continuous and surged nonwheel furrows at Flowell, Utah.

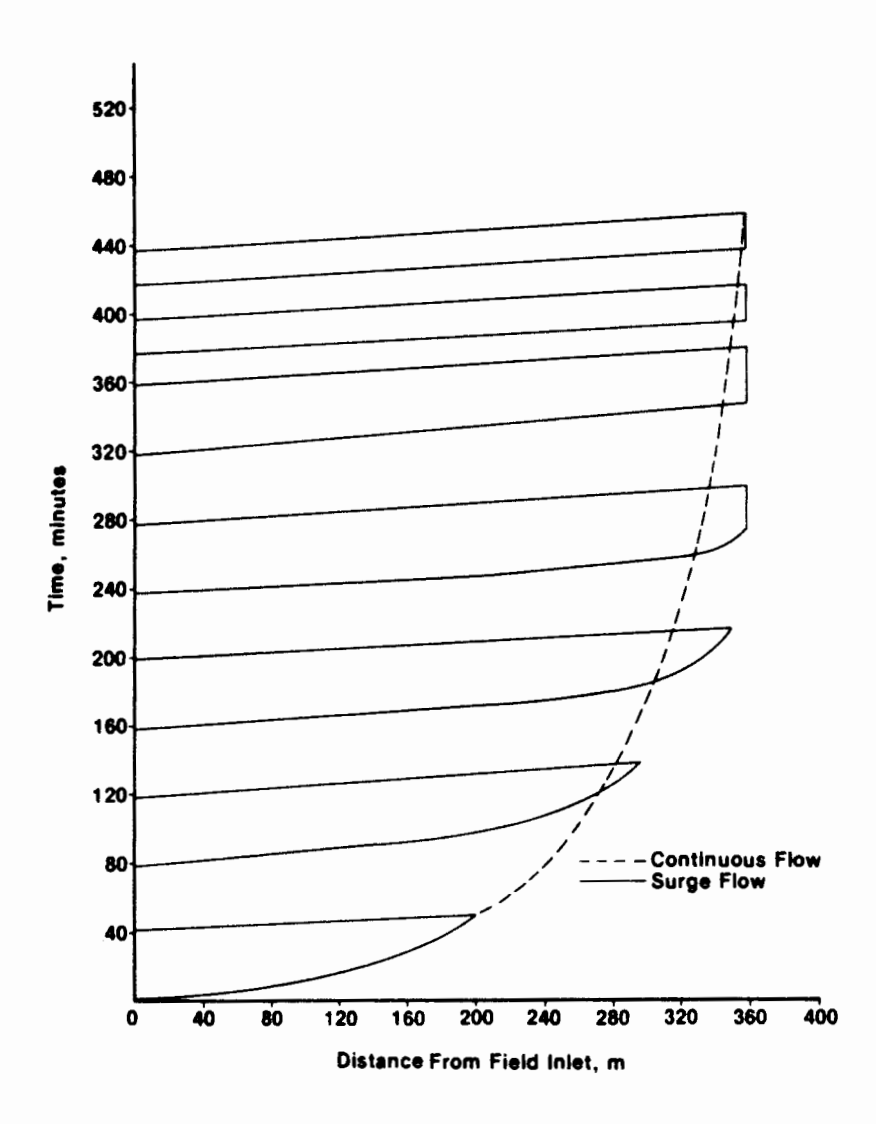


Figure 9.7 Comparison of advance rates under continuous and surged wheel furrows at Flowell, Utah.

treatment was creating the desired effect, it did not result in a solution to the problem. Figure 9.9 on the other hand illustrates in the case of a wheel compacted furrow the more typical result of surging in tighter soils. A 40-min surged flow completed the advance time in about the same interval as the continuous flow, but with one-half the total volume applied.

There have been many surge and continuous flow comparisons (Izuno et al., 1985; Evans et al., 1985; Wallender, 1985; Blair and Smerdon, 1985; and others who have reported only to the W163 project at the time of this book). The results confirm the results reported above to varying degrees. In a small number of tests, the surging has been less effective. Examining all the results in a qualitative manner has led to the observation that soil aggregate stability and texture have a significant effect on the surging effectiveness. In relatively stable sandy loam soils, infiltration rates decrease at much slower rates than in unstable clay loam soils. Part of the decrease in infiltration rates is due to the restructuring of the furrow surface due to the water's mechanical breakdown of the soil aggregates. The primary effect of surge flow is to consolidate the disturbed soil surface during the drainage period. Since the less stable soils exhibit more rapid change in surface permeability, the effect of surge flow is less than in sandy soil.

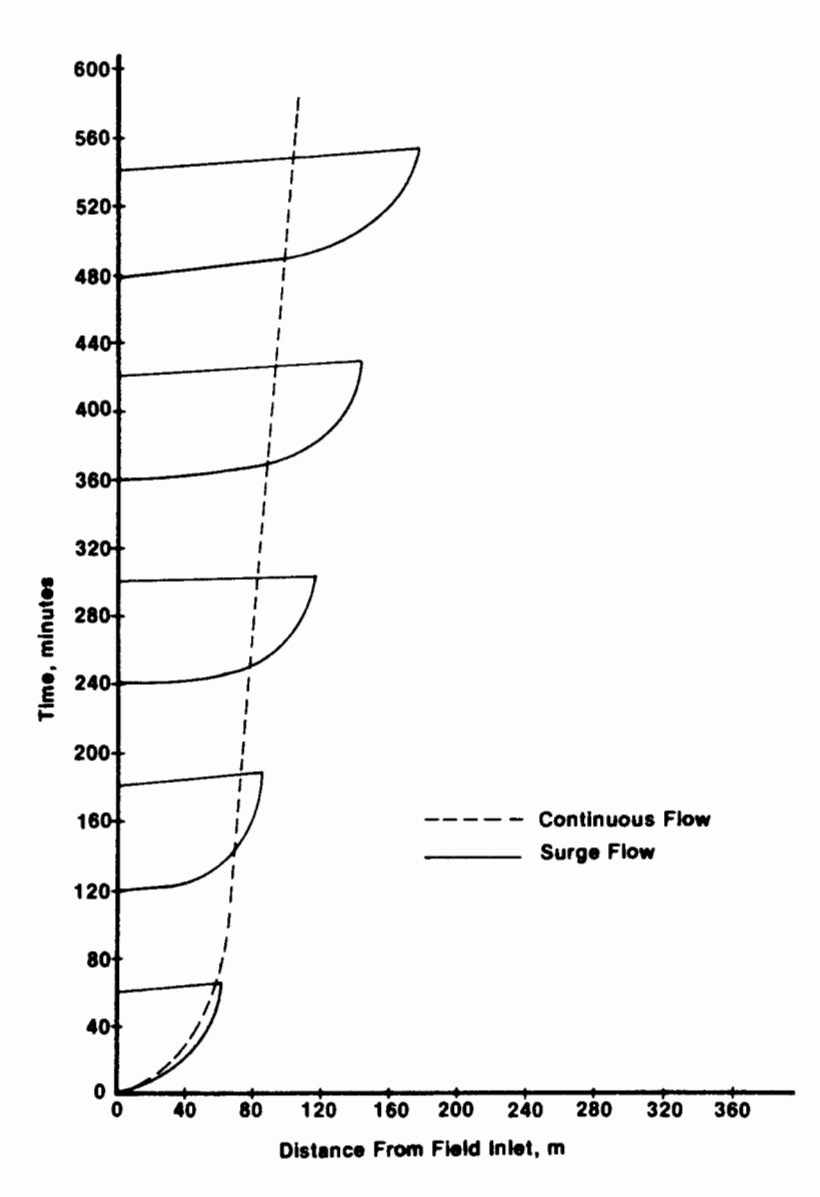


Figure 9.8 Continuous and surged flow advance and recession for nonwheel furrows near Kimberly, Idaho.

A summary of the field measurements at Flowell and Kimberly for selected tests is given in Tables 9.1 and 9.2. These data were used to verify the hydraulic models described in Chapters 14 to 16 for both continuous and surge flow conditions.

#### **Model Modification and Verification**

The first successful effort to modify one of the hydraulic models for surge flow simulation was reported by Walker and Lee (1981). This report described a kinematic-wave model which used zero-inertia-type first-order integration of the continuity equation. Since that time, a revised kinematic-wave model has been verified (Walker and Humpherys, 1983). Essafi (1983) formulated a recursive volume balance model and successfully verified it for surge flow conditions. Oweis (1983) expanded the zero-inertia model to surge flow conditions, and Haie (1984) did the same for a fully hydrodynamic model. Thus four levels of surface irrigation hydraulics have been developed: (1) the volume balance model, (2) the kinematic-wave model, (3) the zero-inertia model, and (4) the hydrodynamic model. The

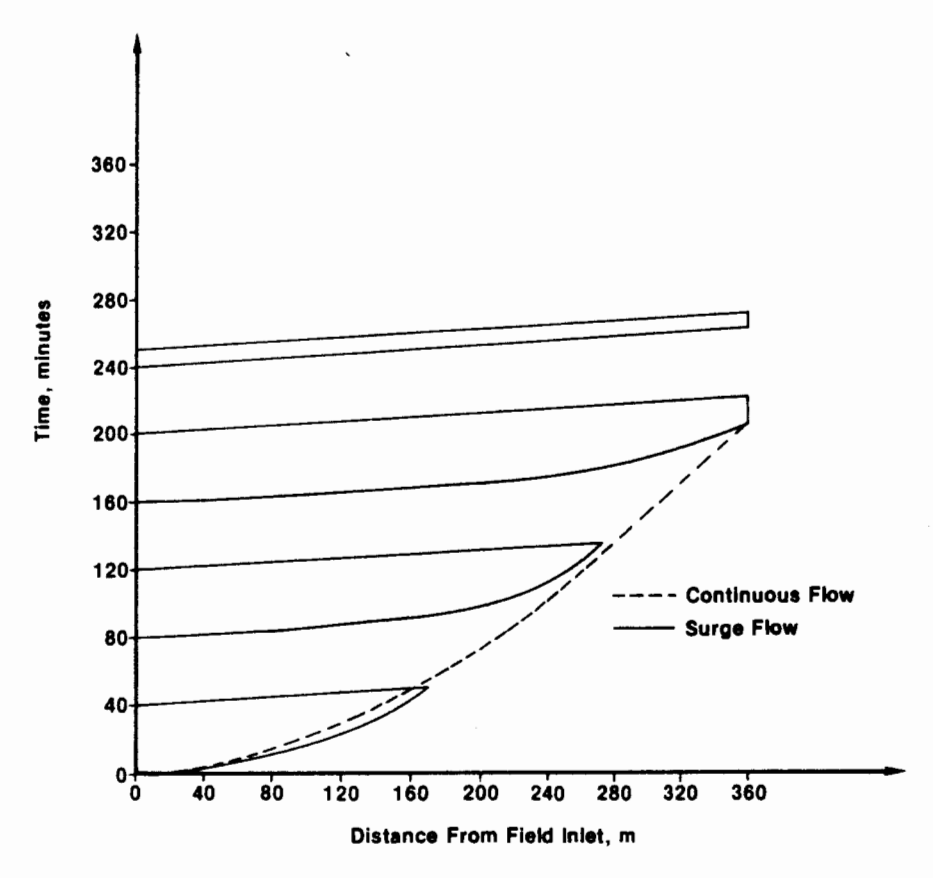


Figure 9.9 Wheel furrow advance trajectories for continuous and surged furrows near Kimberly, Idaho.

TABLE 9.1 FURROW MODELING INPUT DATA FOR CONTINUOUS FLOW

Model input parameters	Flowell nonwheel furrow	Flowell wheel furrow	Kimberly nonwheel furrow	Kimberly wheel furrow
Soil type	Sandy Ioam	Sandy loam	Silty-clay loam	Silty-clay loam
Inflow (liters/s)	2.0	2.0	0.8	1.5
Field length (m)	250	360	360	360
Field slope (m/m)	0.008	0.008	0.0104	0.0104
Manning's n	0.04	0.04	0.04	0.04
Hydraulic section parameters				
$\rho_1$	0.3269	0.3269	0.6644	0.6644
$\rho_2$	2.734	2.734	2.8787	2.8787
Furrow geometry parameters				
$\sigma_1$	0.782	0.782	0.962	0.962
$\sigma_2$	0.536	0.536	0.6046	0.6046
Time of cutoff (min)	350	400	400	200
Kostiakov-Lewis infiltration Function parameters				
$k  (m^3/m/min)$	0.002169	0.0028	0.00701	0.00884
a	0.673	0.534	0.533	0.212
$f_0$ (m <sup>3</sup> /m/min)	0.000222	0.00022	0.00017	0.00017

Source: After Walker and Humpherys (1983).

TABLE 9.2 FURROW MODELING INPUT DATA FOR SURGED FLOW

Input parameters	Flowell nonwheel furrow	Flowell wheel furrow	Kimberly nonwheel furrow	Kimberly wheel furrow
Soil type	Sandy loam	Sandy loam	Silty-clay loam	Silty-clay loam
Inflow (liters/s)	2.0	2.0	0.8	1.5
Field length (m)	360	360	360	360
Field slope (m/m)	0.008	0.008	0.0104	0.0104
Manning's n	0.04	0.04	0.04	0.04
Hydraulic section parameters				
$\rho_1$	0.3269	0.3269	0.6644	0.6644
$\rho_2$	2.734	2.734	2.8787	2.8787
Furrow geometry parameters				
$\sigma_{i}$	0.782	0.782	0.962	0.962
$\sigma_2$	0.536	0.536	0.6046	0.6046
Continuous flow intake parameters				
$k \text{ (m}^3/\text{m}/\text{min)}$	0.002169	0.00280	0.00701	0.00884
a	0.673	0.534	0.533	0.212
$f_0(\text{m}^3/\text{m}/\text{min})$	0.000222	0.000222	0.00017	0.00017
Surge flow intake parameters				
$k \text{ (m}^3/\text{m/min)}$	0.003561	0.00459	0.00494	0.00625
a	0.322	0.356	0.493	0.196
$f_0  (\mathrm{m}^3/\mathrm{m}/\mathrm{min})$	0.00018	0.00018	0.00012	0.00012
Cycle time (min)	40	80	80,120	80
Cycle ratio	0.5	0.5	0.5	0.5

Source: After Walker and Humpherys (1983).

volume balance and kinematic-wave models are general for furrow irrigation, capable of simulating both continuous and surged flow systems accurately, but limited to sloped fields. The lower limit on slope depends somewhat on the infiltration rates but is on the order of 0.1% and less. Both models determine the distribution of infiltrated water and runoff hydrographs.

The zero-inertia and hydrodynamic models are more general in that they are not limited by furrow systems or by slope. Thus these models can simulate continuous and surge flow practices in furrow, border, and basin irrigation systems.

Surge flow modifications. Each of the four models incorporates a common strategy for computing infiltration. Field observations, particularly those by Malano (1982) and Walker et al. (1982), indicated that the cycled wetting of soil can be represented by basically two independent functions. However, it appeared that neither function adequately handled the second wetting since the wetted perimeter changes signficantly between the first and third surges.

In a furrow section where the discharge is relatively constant from surge to surge, infiltration can be evaluated by two Kostiakov-Lewis equations:

$$Z_c = k\tau^a + f_0\tau \tag{9.1}$$

$$Z_s = k'\tau^{a'} + f_0^r \tau \tag{9.2}$$

where  $Z_c$  and  $Z_s$  are the infiltrated volumes per unit of furrow length  $(L^2)$  for dry, continuous flow conditions and wet, intermittent flow conditions, respectively. The parameters k, k', a, a',  $f_0$ , and  $f'_0$  are the empirical parameters particular to the soil type and the effect of cycled wetting and drying. For Eq. 9.2, the intake opportunity time,  $\tau$ , is cumulative; that is, the sum of opportunity time over the number of surges applied.

The flow rate in a dry furrow section being initially wetted by a surge is substantially lower than will occur in that section during succeeding surges. Field observations indicate that infiltration can be described by a function somewhere between Eqs. 9.1 and 9.2 for the second surge cycle. In the present version of the models, these changes are approximated using Eq. 9.1 for the dry sections, Eq. 9.2 for the third and succeeding surges, and a transition equation for the second surge.

Letting  $x_{i-2}$  and  $x_{i-1}$  be the advance distances of the i-2 and i-1 surges, the transition function is written

$$T = \begin{cases} \left(\frac{x_{i-1} - x}{x_{i-1} - x_{i-2}}\right)^{\lambda} & x_{i-2} \le x \le x_{i-1} \\ 0 & x < x_{i-2} \text{ or } x > x_{i-1} \end{cases}$$
 (9.3)

in which x is the location of the computational point of interest during the current time step (i) and  $\lambda$  is an empirical nonlinear distribution constant. Then the infiltration equation coefficients for the transition infiltration function are:

$$k'' = k + (k - k')T (9.4)$$

$$a'' = a + (a - a')T$$

and (9.5)

$$f_0'' = f_0 + (f_0 - f_0')T (9.6)$$

In order to provide a nonlinear transition, values of  $\lambda$  in Eq. 9.3 can range from 2 to 5.

Infiltration equations, such as Eq. 9.1, are based on cumulative opportunity time. The infiltrated volume added by a particular surge must therefore be computed as a difference. For instance, if at point x, the opportunity time prior to the ongoing surge is  $\bar{\tau}$  and the opportunity time created by the present surge is  $\tau$ , the infiltrated volume added during the present surge is

$$Z(t) = Z(\bar{\tau} + \tau) - Z(\tau) \tag{9.7}$$

**Model verification.** To evaluate the various models, seven sets of continuous flow and four sets of surged flow tests data, given in Tables 9.1 and 9.2, were

evaluated. The continuous flow testing is described in Chapters 14 to 16. A selected set of the surge flow testing will be given here.

Figure 9.10 illustrates the surge-by-surge advance and recession trajectories for a Flowell wheel furrow test. The results were similar for the other Flowell and Kimberly data. The combined kinematic-wave simulations of surge flow are shown in Fig. 9.11 with the actual and predicted surge advance front locations plotted. Three replications of the Flowell nonwheel furrow tests and two of the Kimberly nonwheel furrow tests are shown.

The results of the recursive volume balance modeling (Essafi, 1983), the zero-inertia modeling (Oweis, 1983), and the hydrodynamic modeling (Haie, 1984) are all essentially the same.

In visually inspecting the field measurements of individual surge advance and recession trajectories, it was concluded that the spatial variability in the soil intake properties has more impact on model performance for surge flow than for continuous flow conditions. The relatively simple approximations contained in Eqs. 9.3 to 9.6 provide a limited capability to deal with this problem but have proved adequate in most cases. However, a substantial research effort is needed to clarify the infiltration processes for surge flow. In the interim, the models should be adequate in most cases to describe the consequences of alternative surge flow practices and to indicate the potential advantage or disadvantage of a surge practice over a continuous flow regime.

The recession phase in surge flow is very important since a significant fraction of the surge-to-surge extension of the field coverage actually occurs during this phase (i.e., simultaneous advance and recession). The models evaluate this phase of the irrigation very well in the cases studied. However, recession is very difficult

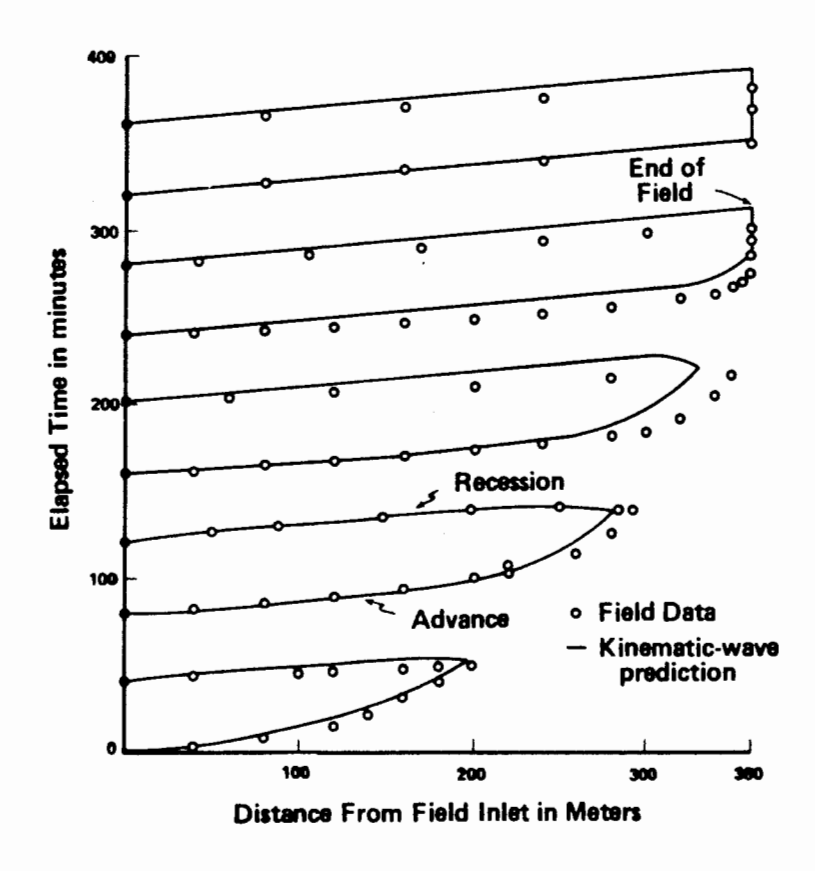


Figure 9.10 Measured and kinematicwave model simulation of surge flow advance and recession data for the Flowell wheel furrow. (From Walker and Humpherys, 1983, with permission of ASCE.)

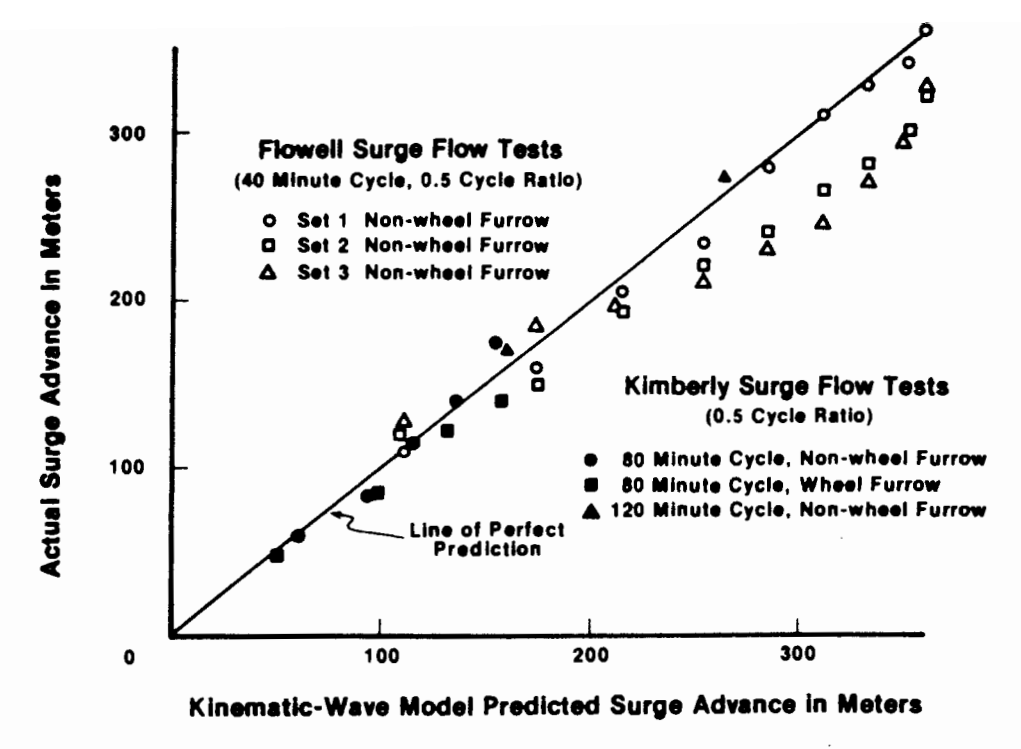


Figure 9.11 Comparison of measured and calculated surge advance fronts for the kinematic-wave evaluation of the Flowell, Utah, and Kimberly, Idaho, tests. (From Walker and Humpherys, 1983, with permission of ASCE.)

to monitor in the course of taking field measurements and in sloping furrow systems the total process is relatively short. Under surge flow conditions, the model appeared to simulate field observations quite well, particularly the extension of the wetted area during the recession phase.

One important conclusion that emerged from these studies is that any of the models should be satisfactory tools for predicting water advance, intake, and runoff for sloped furrow irrigated systems. Their accuracy is demonstrated with data encompassing a relatively wide range of field and soil conditions. The simpler models are easier to program and execute more rapidly, but do not have the generality of the more complex models.

Current versions of the USU models allow evaluation of cutback under surge flow by reducing either the cycle time or the inflow discharge. All of the models compute the tailwater hydrographs and can therefore evaluate the effects of various cutback options as a means to reduce runoff losses.

## SURGE FLOW MANAGEMENT

The practice of surge flow offers the furrow irrigator, and quite possibly other surface irrigators as well, a means to significantly improve irrigation efficiency and thereby lower water, energy, fertilizer, and labor costs. On freshly tilled fields, particularly for lighter-textured soils, surging will improve the hydraulics of the advance phase, allowing the irrigator to water the entire length of the field more uniformly and with smaller depths of application. During subsequent irrigations

when advance is less difficult, the surge flow regime becomes one of the most effective means of minimizing field tailwater. It should be noted, however, that surge flow management is more complex than traditional surface irrigation practices. In addition to selecting inflow rates and total times of application as in existing management scenarios, surge flow management also requires the selection of cycle time, cycle ratio, and a cutback strategy.

To illustrate some of the basic concepts of surge flow management, in the following discussion we first outline the management philosophies and then consider a specific example.

## Management Strategies

Like all other irrigation systems, surge flow systems are subject to optimization; that is, the system performance varies with both field and operational conditions. Application efficiency can often be increased 5 to 10% by careful selection of a single parameter such as cycle time. The controlling variable appears to be the depth of application required to replenish the root zone water supply. Generally, large depths are more efficiently applied with long cycle times and small depths with short cycle times. Thus the management practices achieving optimal surge flow performance are defined in relation to the required application. For the purposes of the USU surge flow program, the "required application" is considered to be the situation where 90% or more of the root zone deficit at the downstream end of the field has been satisfied.

Advance hydraulics become the central issue for the irrigator as watering begins. Given the depth to be applied, the advance-phase hydraulics must be optimized by proper selection of inflow rates and cycle time. These parameters vary as the field length, soil infiltration characteristics, the effect of surging on infiltration characteristics, furrow shape and size, and surface debris vary. A significant fraction of advance under surge flow occurs after an individual surge is terminated. In other words, water is often advancing along the downstream end of the furrow and receding near the upper end. To make this process work effectively, the volume of water added to the furrow in each surge must be large in comparison to the infiltration along the already wetted length of the furrow and the volume of water needed to fill furrow dead storage in the section previously wetted. Thus for light-textured soils, and long and clogged furrows, inflow rates and cycle times should be large. For the opposite case (heavy soils, short, small, clean furrows), smaller flows and cycle times can be used.

When the water reaches the end of the furrows, the irrigator has several decisions to make. If the system must continue applying water for some period in order to refill the root zone, tailwater losses are likely to be substantial unless the flows are cut back. When these depths have been applied, the system needs to be rotated to the next series of sets. Because of the influence of cycled wetting on infiltration, this cutoff time is difficult to ascertain. Nevertheless, there are four post-advance water management alternatives.

First, the cycle time can be reduced to the point where the furrow infiltration absorbs most if not all of the surge. This is primarily an alternative for longer

furrows on lighter soils. Second, the cycle time can be reduced to the point where individual surges combine along the furrow, creating a relatively steady flow at the end of the furrows. This is the original surge flow concept. Some systems may allow opening of furrow inlets on the next advance-phase sets, thereby providing a continuous flow cutback. Third, the last advance surge can be prolonged enough to refill the root zone. This takes advantage of the differences in infiltration rates between dry and previously wetted regions. Finally, the irrigator has the option of simply continuing the advance cycling until the irrigation is completed.

It might be noted that optimizing surge flow management can only be guaranteed either by simulation model analysis or by extensive field experiences. It is doubtful that field experience can be generalized sufficiently to account for field-to-field and year-to-year variations. Modeling, on the other hand, requires definition of infiltration characteristics field to field, irrigation to irrigation, and year to year. Thus the irrigator and the irrigation engineer are confronted by a difficult design/management problem. None of the simulation models has been programmed for determining optimal surge flow configurations.

Given the complexities of surge flow and the time-space variations inherent with surface-irrigated systems, the eventual application of technology will involve self-calibrated control systems (SCCS). The SCCS would involve (1) a computer-assisted control-logic device housing the surge flow software currently encompassed by the simulation models, (2) field advance-recession and soil moisture sensors to monitor how fast the water fronts are moving (both surface and subsurface), and (3) an automated headland facility monitored and actuated by the controller.

The SCCS would initiate irrigation using default values of flow, cycle time, and so on. Information from the first surge would be processed to determine the dry furrow infiltration parameters and from the second and third to determine the effect of surging. The computer would then estimate the performance of current settings as well as optimized settings. Then if sufficient improvements can be made, the controller would change the system configuration to achieve the desired results. At the end of an irrigation, the system would shut down and begin monitoring crop water use so that the next irrigation can be planned.

There will be other surge flow management issues raised and resolved before practice is fully implemented. For example, leaching salts from the soil profile using surge flow or adding fertilizers through the system are yet to be studied. Some surface-irrigated field conditions may not benefit from surge flow; some sprinkle and trickle systems may be replaced with a surge system. In any event, the concept of surge flow is a significant step forward in surface irrigation automation.

## The Flowell Case Study

To illustrate the advantage of surge flow, data from the Flowell tests have been reevaluated for the typical first-irrigation, wheel furrow condition. Three furrow irrigation configurations were studied. The first was conventional continuous flow without cutback at the end of the advance phase (the infiltration rates are so high that cutting back tends to dewater the end of the furrows, resulting in poor uni-

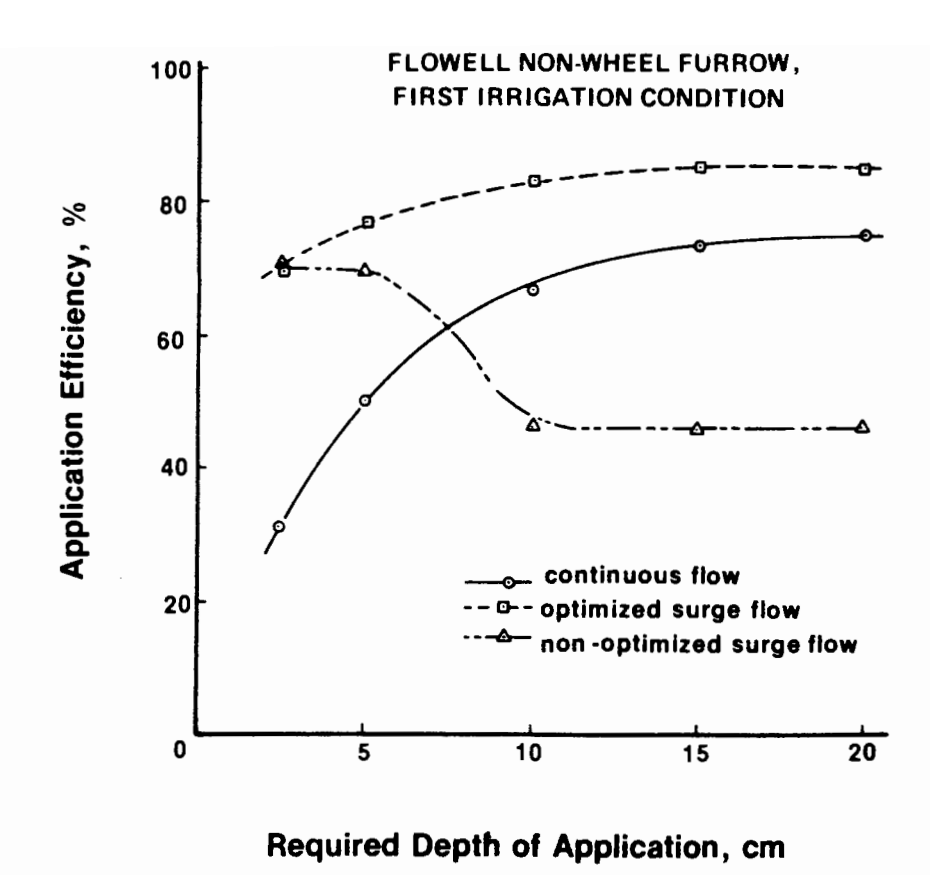


Figure 9.12 Comparison of attainable application efficiencies under continuous and surge flow management for Flowell nonwheel furrows under first irrigation conditions.

formity). The second is a surge flow regime without any type of cutback, and the third is an optimized surge flow regime (optimal cycle times and cutback regime based on each required depth of application). For this case study, inflow to each furrow was set at the maximum allowable nonerosive discharge.

Figure 9.12 shows the performance of the three scenarios in terms of application efficiency  $(E_a)$  as a function of required depth of application. Application efficiency is the ratio of root zone storage to total water applied. Under continuous flow,  $E_a$  increased rapidly from a 2.5-cm (1-in.) application (32%) to a 10-cm (4in.) application (67%). At higher applications,  $E_a$  increased by another 10%. For non-cutback surge flow (60-min cycles) using the same inflow, the  $E_a$  at lower depths is substantially better than continuous flow. In fact, in a 2.5-cm application, the surge flow system is nearly twice that of the continuous flow. However, as the required application increases, the non-cutback surge system suffers a decline in effectiveness due to high tailwater losses. Because surging reduces intake rates, it is difficult to apply a large depth and thus surge flow systems are expected to irrigate more frequently then traditional practices. If the cutback option is added to the surge flow, substantial overall improvements in application efficiency are made. As will be seen shortly, the gain is due primarily to much higher uniformities. The specific values of cycle time vary by required depth under the optimal strategy. At low depths a 60-min cycle (30 min off) was used. At 10-cm depths, the optimal cycle increased to 180 min.

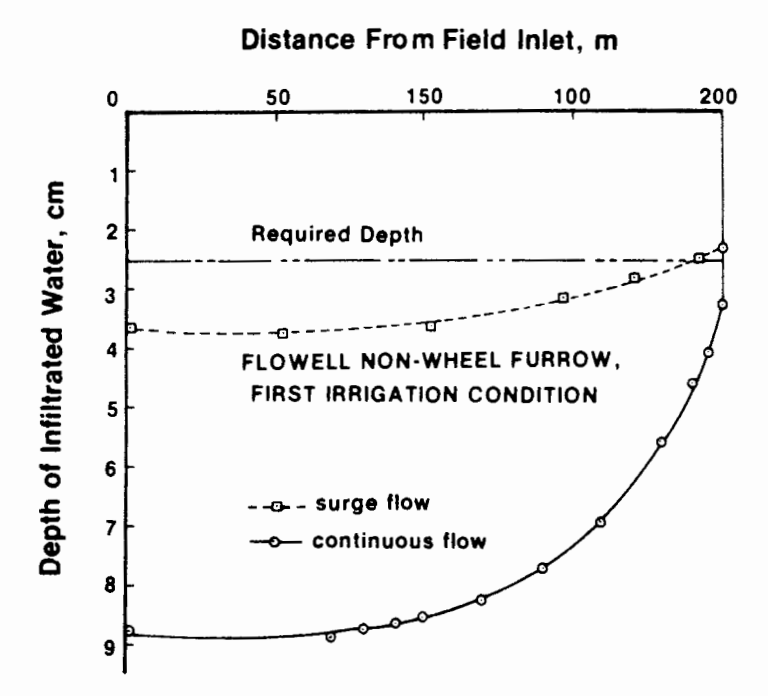


Figure 9.13 Distribution of infiltrated water under continuous and surge flow for a 2.5-cm application (Flowell non-wheel, first-irrigation conditions.)

The subsurface profiles and tailwater hydrographs for a required application of 2.5 cm and 10 cm are plotted in Figures 9.13 to 9.16 for the continuous and optimal surge flow system. As illustrated, the major source of inefficiency for low application depth is deep percolation. For higher applications it is field tailwater. High tailwater losses and low deep percolation losses appear to be a significant feature of surge flow, and as noted previously, tailwater management must be an integral component of surge flow management.

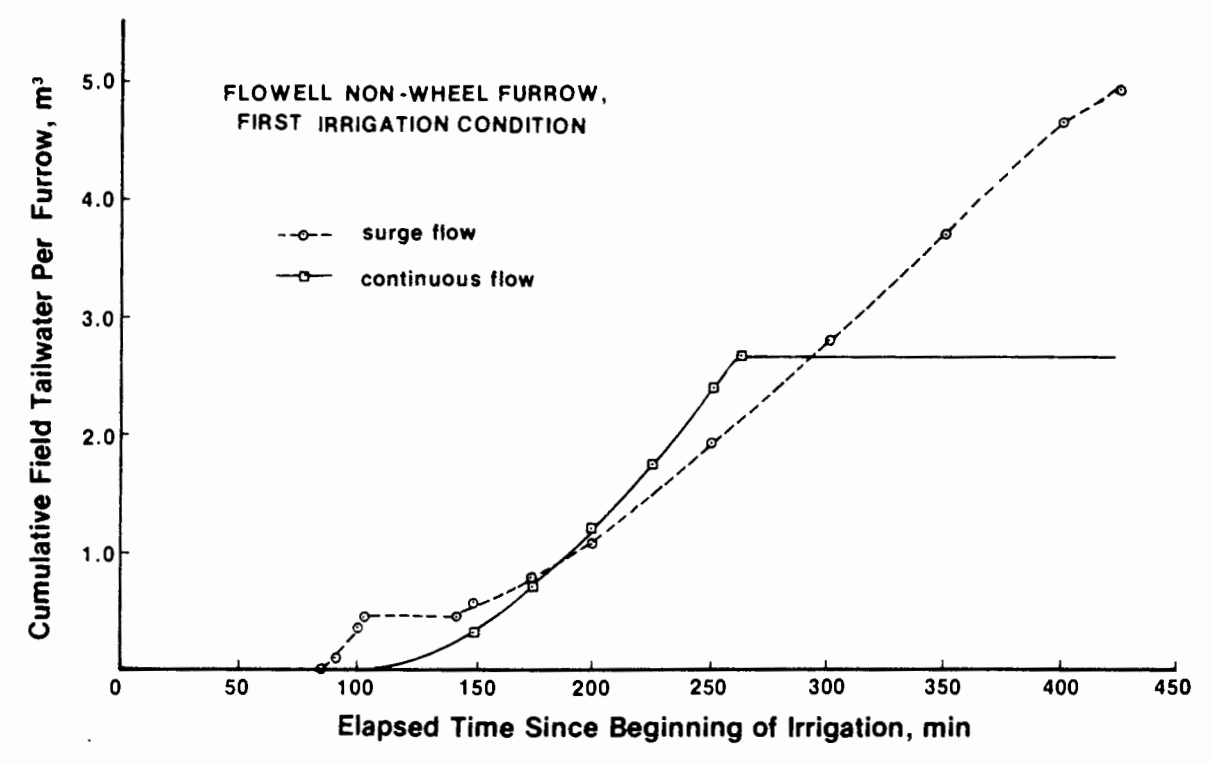


Figure 9.14 Estimated tailwater hydrographs from the Flowell field under continuous and surge flow for a 2.5-cm application.

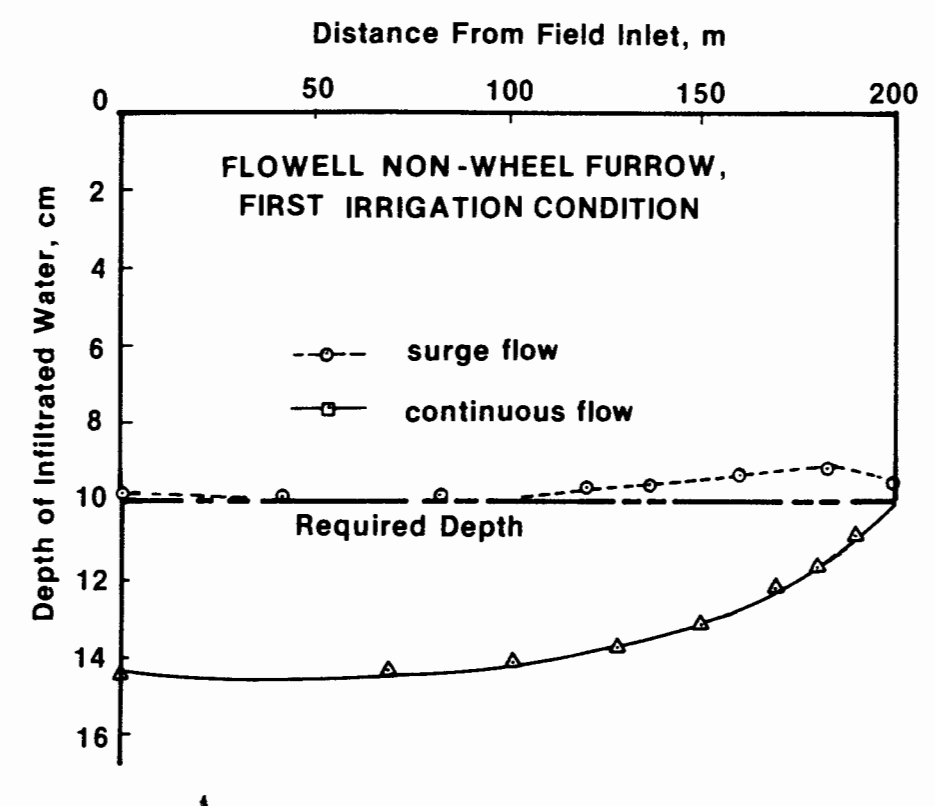


Figure 9.15 Subsurface profiles for a 10-cm application under continuous and surge flow for the Flowell nonwheel, first-irrigation conditions.

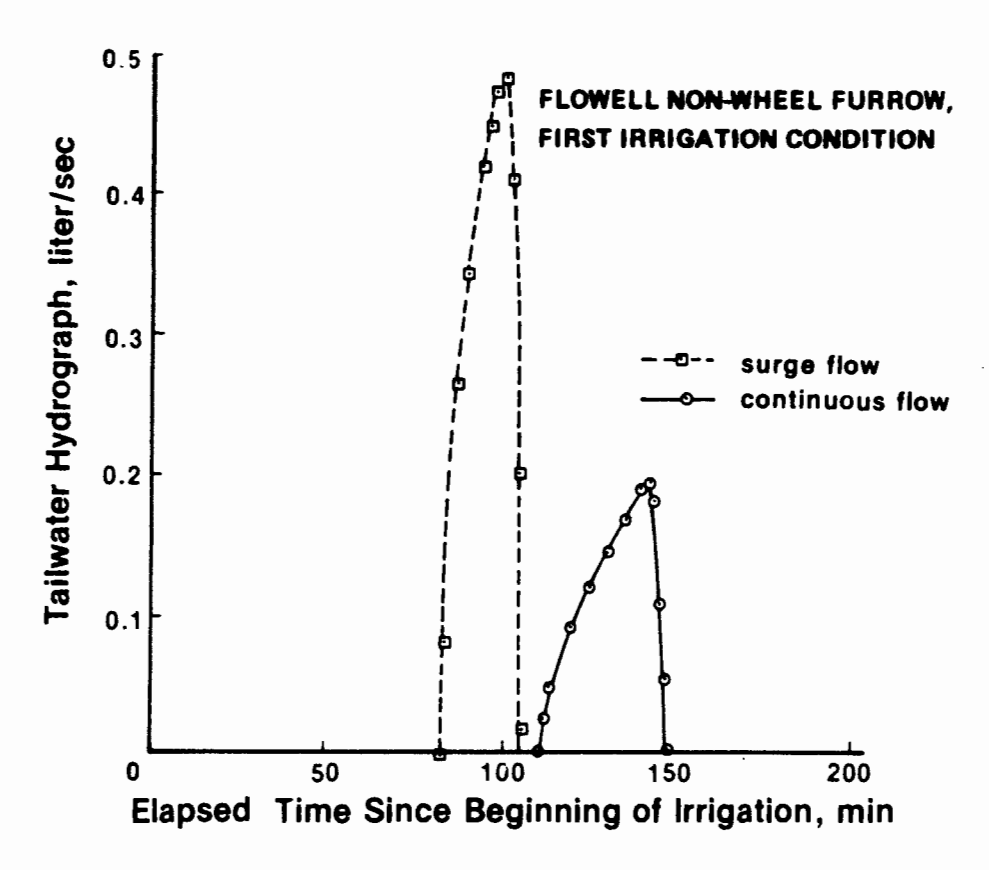


Figure 9.16 Cumulative tailwater losses under continuous and surge flow for a 10-cm application at the Flowell test site.

For other field conditions, such as heavier soils or longer furrow lengths, the tailwater issue is expected to be more pronounced. For these situations, the irrigator may need to reduce the cutback cycle ratio to one-third or one-fourth. To do this for a one-third cycle ratio it will be necessary to irrigate six sets through the advance phase and then cycle through two sets of three banks during the cutback period.

#### SUMMARY

Surge flow offers a number of unique opportunities for water management as well as some problems. These will vary from soil to soil and from farm to farm. Some of the important issues have been discussed and illustrated; others will arise as the concept is applied in other locations. Irrigators, state and federal extension personnel, and irrigation equipment manufacturers in Texas have collectively moved the concept from the research to the commercial level. As others implement surge flow, additional important contributions will be made. Hopefully, researchers will continue to develop a better design and management understanding to serve the many needs of irrigated agriculture. We at Utah State University are gratified by results of our early research and testing. We look forward to a major contribution by surge flow irrigation.

### REFERENCES

- ALLEN, N. L. 1980. Advance Rates in Furrow Irrigation for Cycled Flow. M.S. thesis, Utah State University, Logan, Utah.
- BISHOP, A. A., W. R. WALKER, N. L. ALLEN, and G. J. POOLE. 1981. Furrow Advance Rates under Surge Flow Systems. ASCE J. Irrig. Drain. Div. 107 (IR3):257-264.
- BLAIR, A. W., and E. T. SMERDON. 1985. Effect of Surge Cycle Ratio and Cycle Time on Infiltration. *Proc. ASCE Irrig. Drain. Div. Spec. Conf.*, San Antonio, Texas.
- COOLIDGE, P. S. 1981. Advance Rates under an Automated Pulsed Flow Irrigation System. M.S. thesis, Utah State University, Logan, Utah.
- COOLIDGE, P. S., W. R. WALKER, and A. A. BISHOP. 1982. Advance and Runoff in Surge Flow Furrow Irrigation. ASCE J. Irrig. Drain. Div. 108 (IR1):35-42.
- ELLIOTT, R. L., and W. R. WALKER. 1982. Field Evaluation of Furrow Infiltration and Advance Functions. *Trans. ASAE* 25 (2):396-400.
- Essafi, B. 1983. A Recursive Volume Balance Model for Continuous and Surge Flow Irrigation. M.S. thesis, Utah State University, Logan, Utah.
- Evans, R. G., J. A. Aarsted, D. E. Miller, and M. W. Kroeger. 1985. Crop Residue Effects on Furrow Irrigation Advance and Infiltration. Pap. 85-2586. ASAE Winter Meeting, Chicago, Ill.
- HAIE, N. 1984. Hydrodynamic Simulation of Continuous and Surged Surface Flow. Ph.D. dissertation, Agricultural and Irrigation Engineering Department, Utah State University, Logan, Utah.

- IZUNO, F. T., T. H. PODMORE, and H. R. DUKE. 1985. Infiltration under Surge Irrigation. Trans. ASAE 28(2):517-521.
- Malano, H. M. 1982. Comparison of the Infiltration Process under Continuous and Surge Flow. Thesis, Utah State University, Logan, Utah.
- Owers, T. Y. 1983. Surge Flow Furrow Irrigation Hydraulics with Zero-Inertia. Ph.D. dissertation, Utah State University, Logan, Utah.
- PODMORE, T. H., and H. R. DUKE. 1982. Field Evaluation of Surge Irrigation. Pap. 82-2012. ASAE Summer Meeting, Madison, Wis., June 27-30.
- POOLE, G. J. 1981. Infiltration and Advance under Surge Flow Furrow Irrigation. M.S. thesis, Utah State University, Logan, Utah.
- STRINGHAM, G. E., and J. KELLER. 1979. Surge Flow for Automatic Irrigation. *Proc.* 1979 ASCE Irrig. Drain. Div. Spec. Conf. Albuquerque, N.M., July.
- WALKER, W. R., and A. S. HUMPHERYS. 1983. Kinematic-Wave Furrow Irrigation Model. ASCE J. Irrig. Drain. Div. 109(IR4): 377-392.
- WALKER, W. R., and T. S. Lee. 1981. Kinematic-Wave Approximations of Surged Furrow Advance. Pap. 81-2544. ASAE Winter Meeting, Chicago, Ill., December 15-18.
- Walker, W. R., H. Malano, and J. A. Replogle. 1982. Reduction in Infiltration Rates due to Intermittent Wetting. Pap. 82-2029. ASAE Summer Meeting, Madison, Wis., June 27-30.
- WALLENDER, W. W. 1985. Furrow Model with Spatially Varying Infiltration. Pap. 85-2589. ASAE Winter Meeting, Chicago, Ill.

## Headland Facilities

## INTRODUCTION

Many structures have been developed to accommodate the application of water onto croplands using the various surface irrigation methods. The commonly used surface irrigation water delivery subsystems were illustrated in Chapter 3. The variety of available structures provide considerable flexibility in selecting proper systems to meet individual farm needs.

Well-designed headland facilities should facilitate efficient operation of the irrigation system by: (1) providing complete control of the water; (2) measuring the amount of water delivered to each farm; (3) delivering water to each field when needed; (4) delivering the proper flow rate and volume of water to meet crop water requirements; (5) distributing water uniformly onto each field; and (6) incorporating recycled tailwater if available.

The two general types of headland distribution systems employed in conjunction with surface-irrigated fields are open-channel and low-pressure pipeline. For both systems, the water supply must be free of debris and most sediment.

## **TURNOUT STRUCTURES**

Some examples of canal turnout structures are shown in Fig. 3.5. Although many other configurations have been employed around the world, the combination of a gate and short length of pipe is very typical. The gate at the inlet of the closed

conduit is used to control the discharge rate and the short length of closed conduit (culvert) is used to convey the irrigation water through the canal bank.

For the turnout gate, Eq. 4.47 would be used if free flow exists, while Eq. 4.48 would apply for submerged flow conditions. The geometry of the gate, gate frame, and turnout structure determine the coefficient of discharge,  $C_d$ . A conservative estimate of  $C_d$  would be 0.6, but values near 0.7 are quite common, and even higher values are sometimes encountered. If the gate manufacturer has not hydraulically calibrated the gate and gate frame combination, the value of  $C_d$  should be determined from laboratory or field calibration, or a conservative estimate of  $C_d$  will have to be assumed for purposes of design. By hydraulically calibrating the combination of gate, gate frame, and turnout structure, the gate can then also be used as a flow measurement device.

In order to design the culvert, references on culvert hydraulics should be consulted (e.g., American Concrete Pipe Association, 1970).

## **DEBRIS AND SEDIMENT REMOVAL**

Open-channel sources of irrigation water often contain large quantities of debris and sediment, such as weeds, moss, seed, silt, or sand. Too much debris can result in serious operational problems by causing blockages in control and conveyance structures. Sediment loads can reduce the capacity of the conveyance network.

The design of debris and sediment control structures is still more an art than a science. Thus much can be learned by observing the operational effectiveness of a wide variety of structures. These observations are reflected in the variety of structures that have been found to operate reasonably well. For small irrigation systems, the concern of the designer is with trashracks, screening devices, and sediment control structures.

The purpose of a trashrack is to keep large debris from entering the irrigation water delivery subsystem. The size of the trashrack openings is dependent on the type and quantity of debris expected. The designer prefers that the smallest openings be used without resulting in rapid clogging of the trashrack. Usually, the average velocity through the trashrack opening is designed for 60 cm/s or less. The U.S. Army Corps of Engineers (1959) have utilized previous research findings in developing the relationships shown in Fig. 10.1 between the trashrack closed area coefficient,  $A_r$ ,

$$A_r = \frac{\text{area of the bars}}{\text{area of the section}}$$
 (10.1)

and the head loss coefficient,  $K_r$ , for various bar geometries,

$$K_r = \frac{h_L}{v^2/2g} \tag{10.2}$$

The curve in Fig. 10.1 marked L/T = 1.0 pertains to circular rods, such as reinforcing steel rods. However, this graph can also be used for wire-mesh fabric.

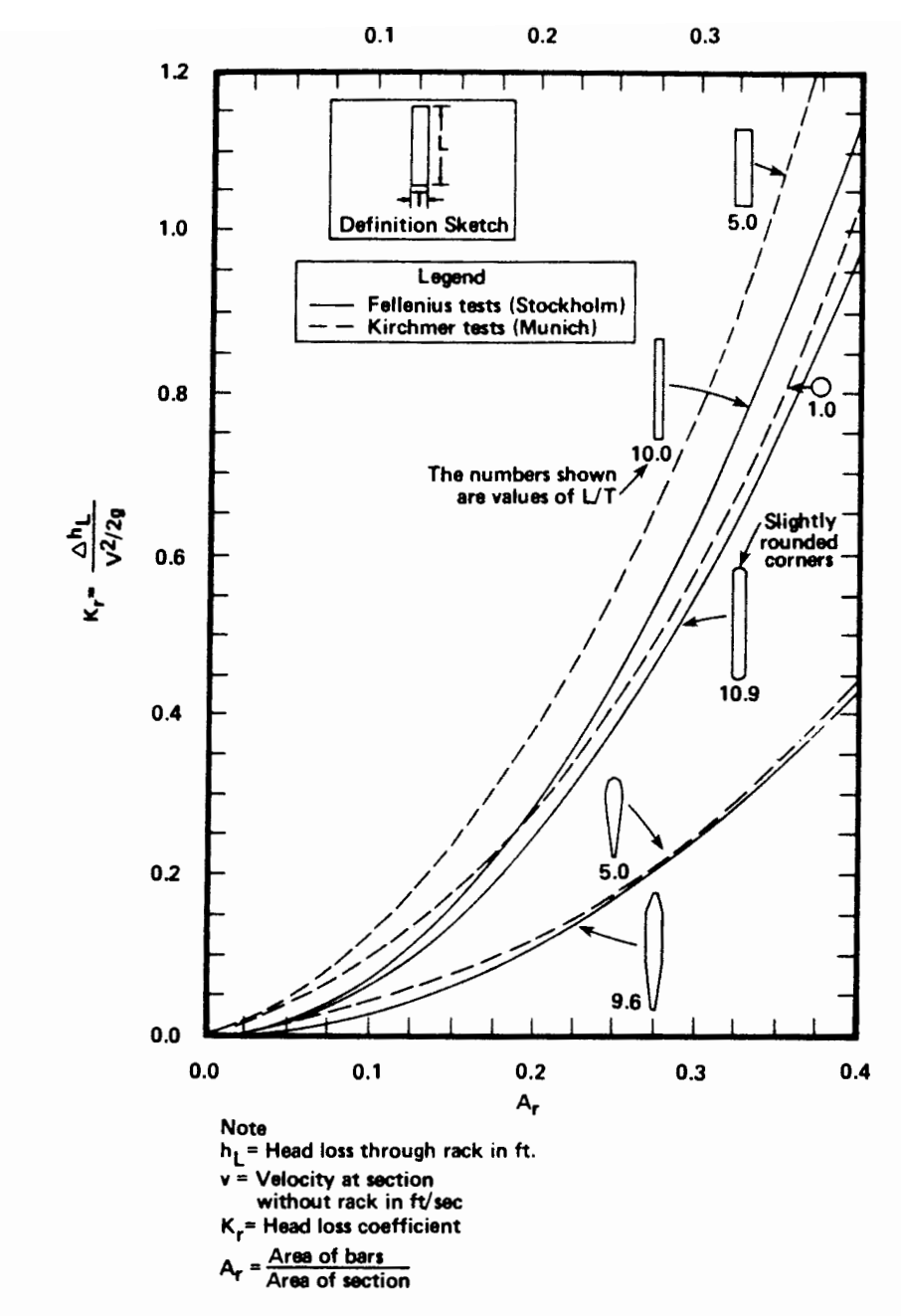


Figure 10.1 Trashrack head losses for various bar shapes. (From U.S. Army, Corps of Engineers, Waterways Experiment Station, 1959.)

The value of A, for various wire-mesh fabrics would have to be obtained from the manufacturers.

A hydromechanically operated trash cleaner is shown in Fig. 10.2. The water flow in the irrigation channel rotates the paddlewheel. The trash cleaner brushes are rotated by means of a wheel-and-sprocket drive between the paddlewheel and the brushes.

Some of the screening devices, and combinations of screening and desilting structures, are illustrated in Figs. 10.3 to 10.14. These structures were developed by agencies such as the USDA to meet a variety of needs so that in any particular "site-specific" situation, the designer may want to incorporate some features from

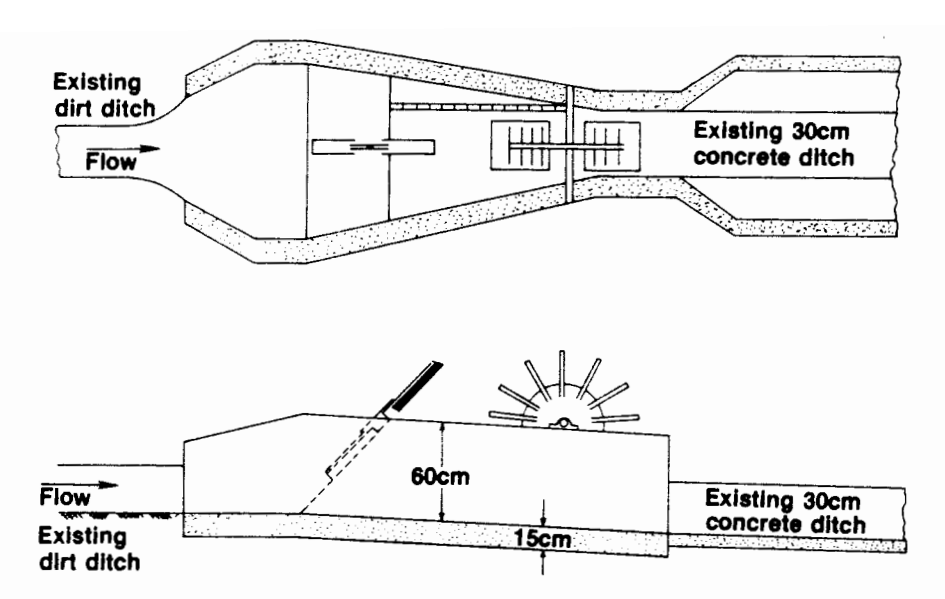


Figure 10.2 Typical hydromechanical trash removal device where the water flow moves the paddlewheel, which in turn rotates the trash cleaner brushes by means of a chain and sprocket. (From Skogerboe et al., 1981.)

various structures in developing an "individualized" design. The outlets from most of these structures can be used for conveyance via pipeline to a pump, gated pipe, open-channel section, and so on. Provisions for flow measurement can be made at the inlet using a weir plate or in the outlet pipeline by installing a propeller meter or a Venturi meter. The structures for precipitating sediments may, or may not, be of sufficient size, depending on the sediment load. If the sediment loads are too great, the structure must be cleaned often (in some cases, every day). Unfortunately, the sizing of small desilting basins is still primarily an art, so if local experiences are not already available, the designer must experiment with alternative designs, usually erring on the side of ensuring that the structures are sufficiently large.

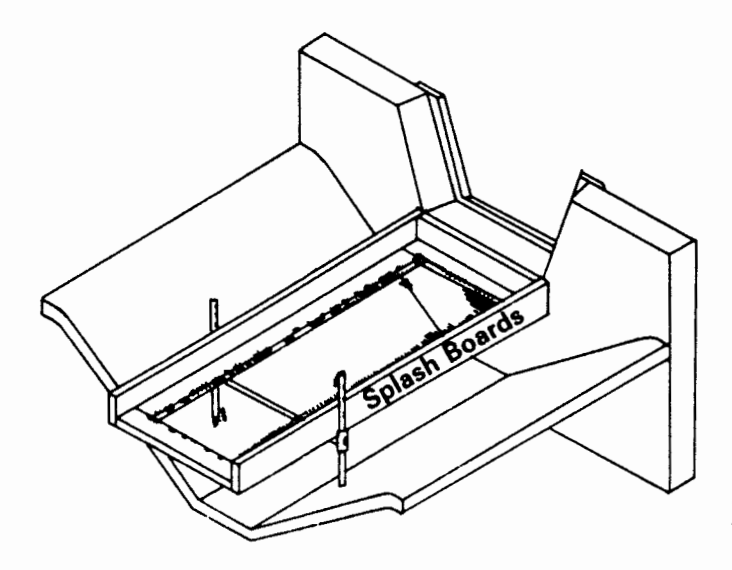


Figure 10.3 Horizontal debris and weed-seed screen.

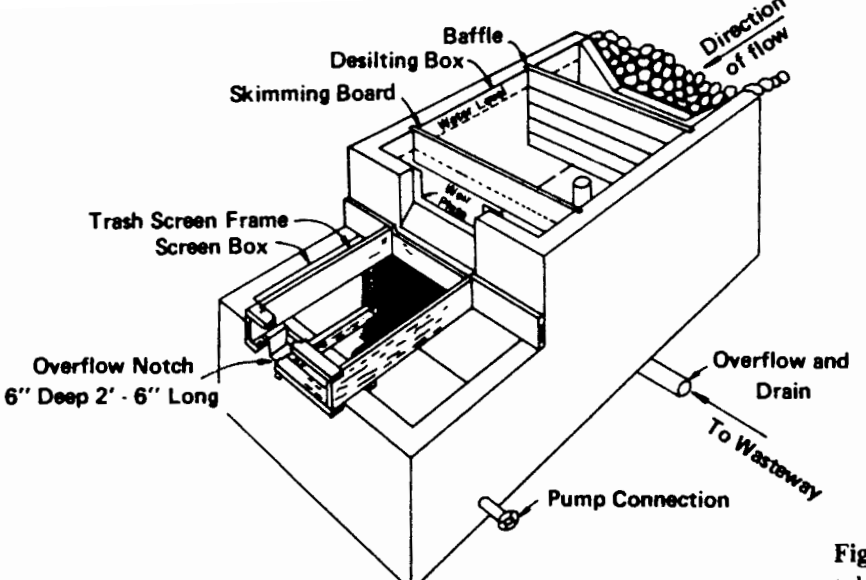


Figure 10.4 Desilting box and horizontal trash screen.

## **OPEN-CHANNEL IRRIGATION DISTRIBUTION**

## **Description**

The type of farm irrigation distribution system in widespread use throughout the world is the open-channel system. The channels may be permanent or temporary installations. In some cases, permanent channels are used to convey water from the farm turnout or other supply source to the individual fields, and temporary channels are used to distribute water on the various fields.

Earth channels are designed and constructed to carry the required discharge capacity without erosion. If earth channels must be placed on slopes so steep that high velocities will occur, structures to control erosion will be required. Drop

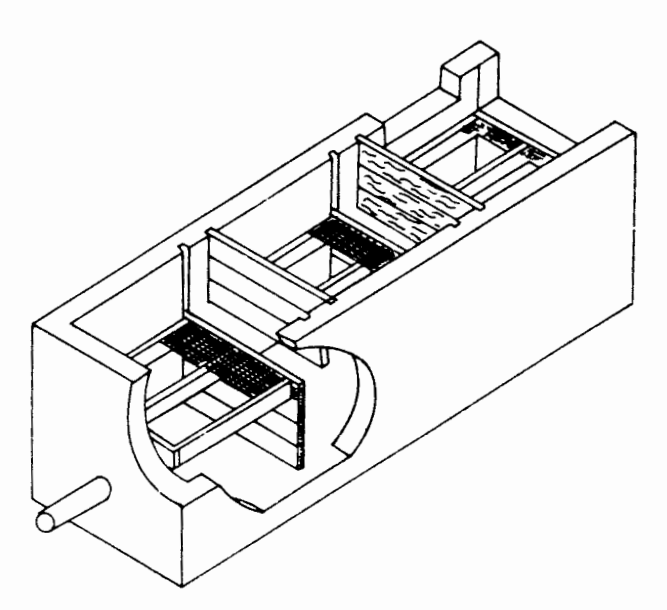


Figure 10.5 Desilting and screening box.

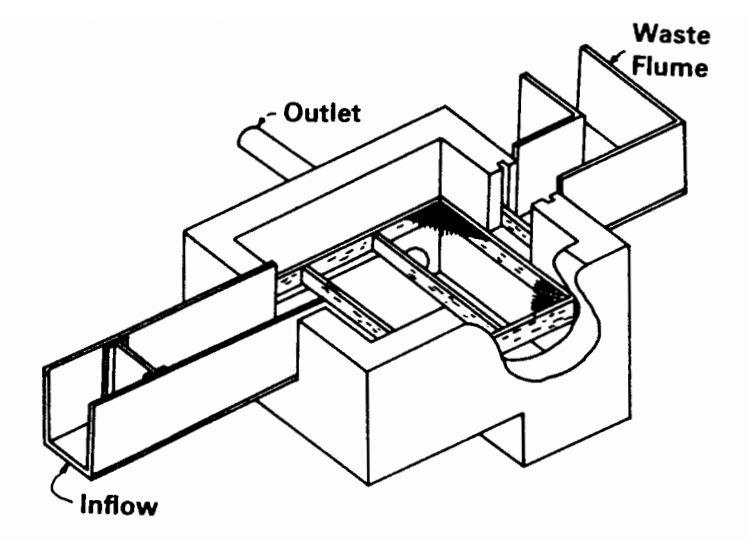


Figure 10.6 Permanent horizontal screen structure for debris removal.

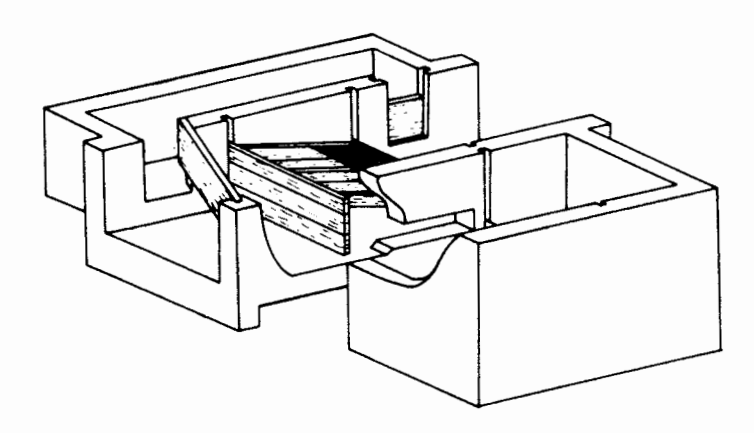
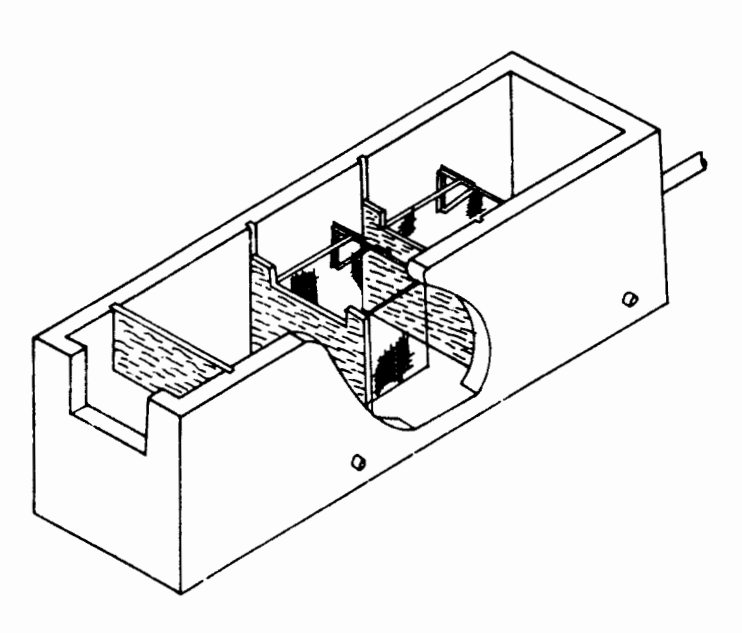


Figure 10.7 Trash screen and desilting box for a pumping station.



**Figure 10.8** Basket-type screening structure.

240 Headland Facilities Chap. 10

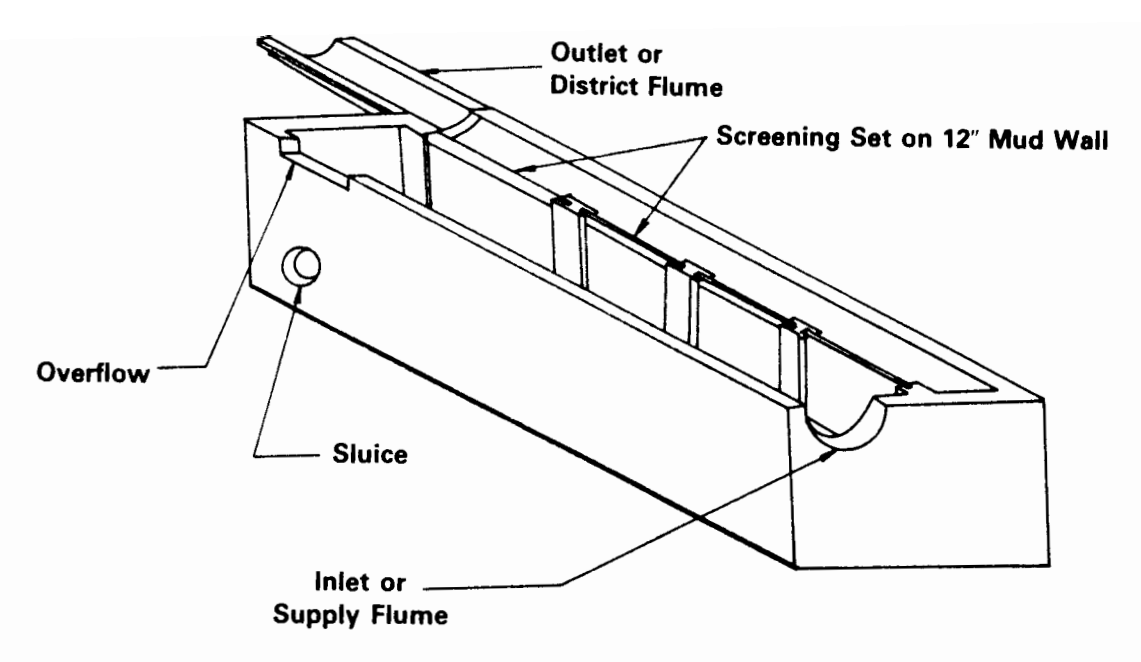


Figure 10.9 Longitudinal screening box for head-water diversion.

structures are often used for this purpose. The channels can be constructed in sections that have little or no slope and the water flows from one section to another over vertical drops with stilling basins at the foot of each drop to prevent washing. On steep slopes requiring frequent drop structures, it may be more economical to use lined canals, chutes, or buried pipelines even though an energy dissipation structure will be required at the outlet to still the water before it enters another section of earth channel.

Irrigation channels constructed in porous soils, or through gravelly or sandy areas, often have excessive seepage losses. These losses can be reduced by installing some type of watertight lining, or by the use of pipelines. Concrete or

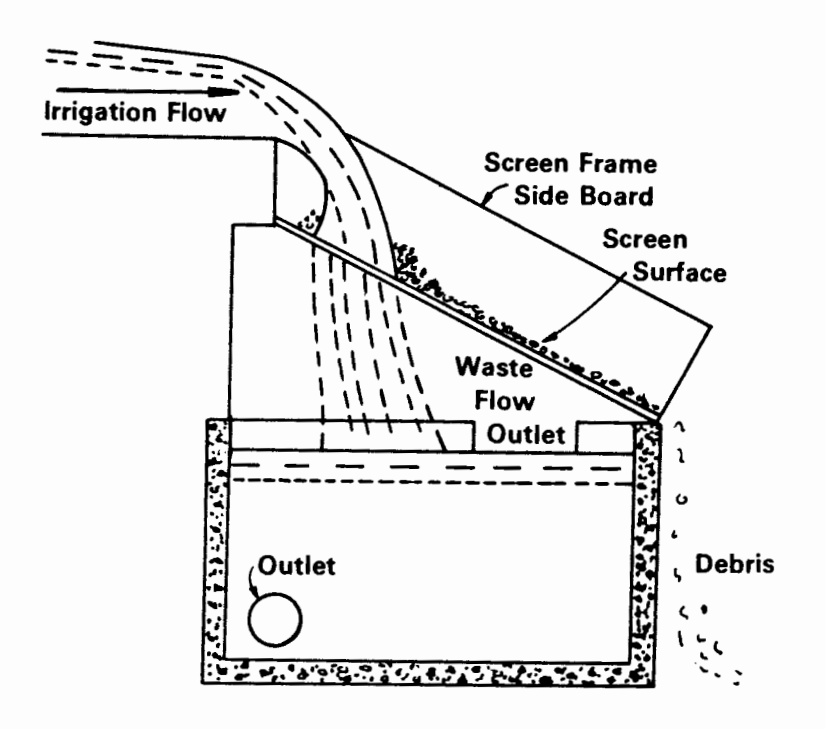


Figure 10.10 Free-fall inclined screen structure with debris removal by gravity.

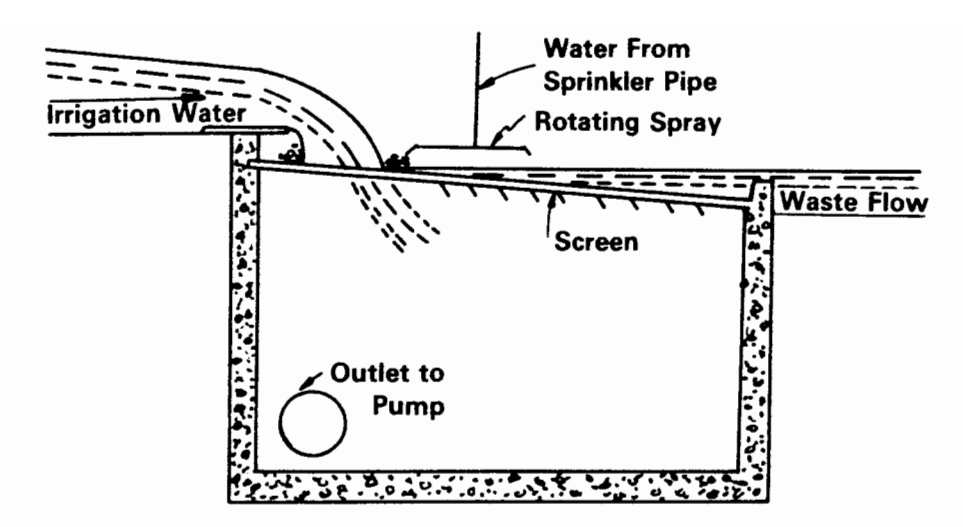


Figure 10.11 Free-fall inclined screen structure with debris removal by sprinkler.

brick-and-mortar are the materials most commonly used for lining. Another material being employed more and more for seepage control lining is asphalt, which is used in asphaltic concrete or in the form of sheets, planks, or membranes. Other membranes are made from butyl rubber or plastic. These materials provide good channel seals but are more easily damaged than concrete. Thin membranes are covered with earth or sand to protect them from sunlight and from trampling by stock. Often, a satisfactory seal is provided by lining the bottom and sides of a channel with a layer of clay soil to a depth of about 15 cm. Clay linings are usually placed so that they can be covered with several centimeters of coarse-textured soils, sand, or gravel. Such linings are easily damaged by maintenance operations and by vegetation, but under ordinary circumstances, initial installation costs are less than for any other type of lining.

For an open-channel irrigation distribution system, certain structures are needed

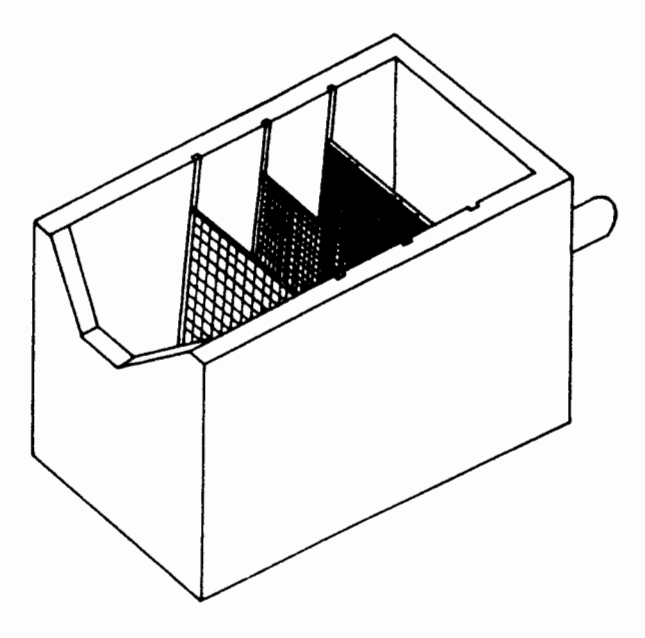


Figure 10.12 Multiple inclined screen box structure.

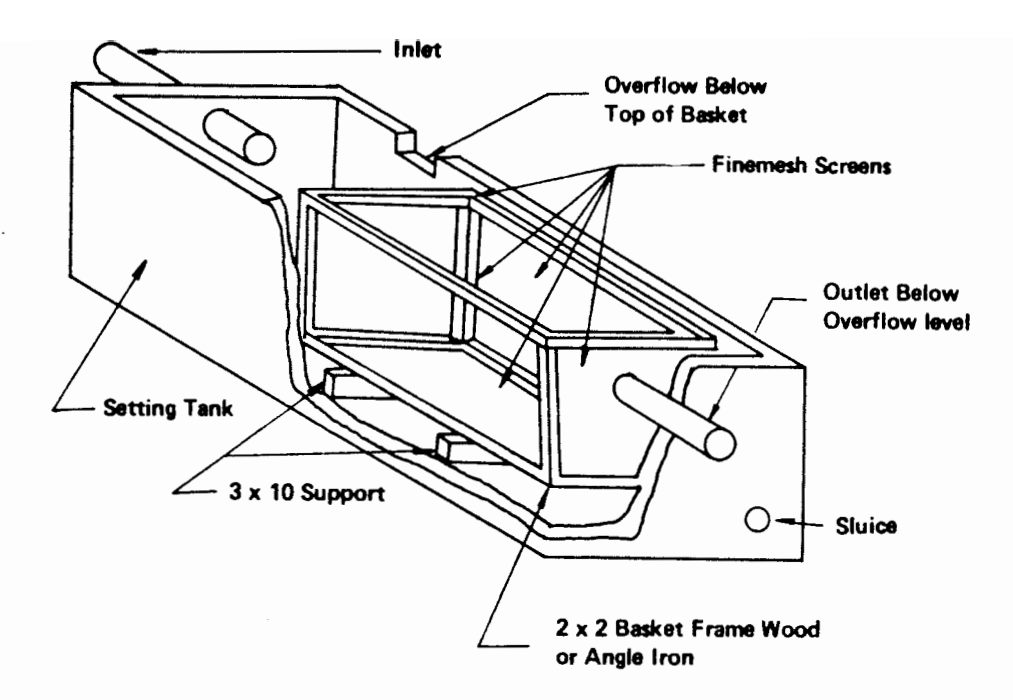


Figure 10.13 External basket-type screen structure.

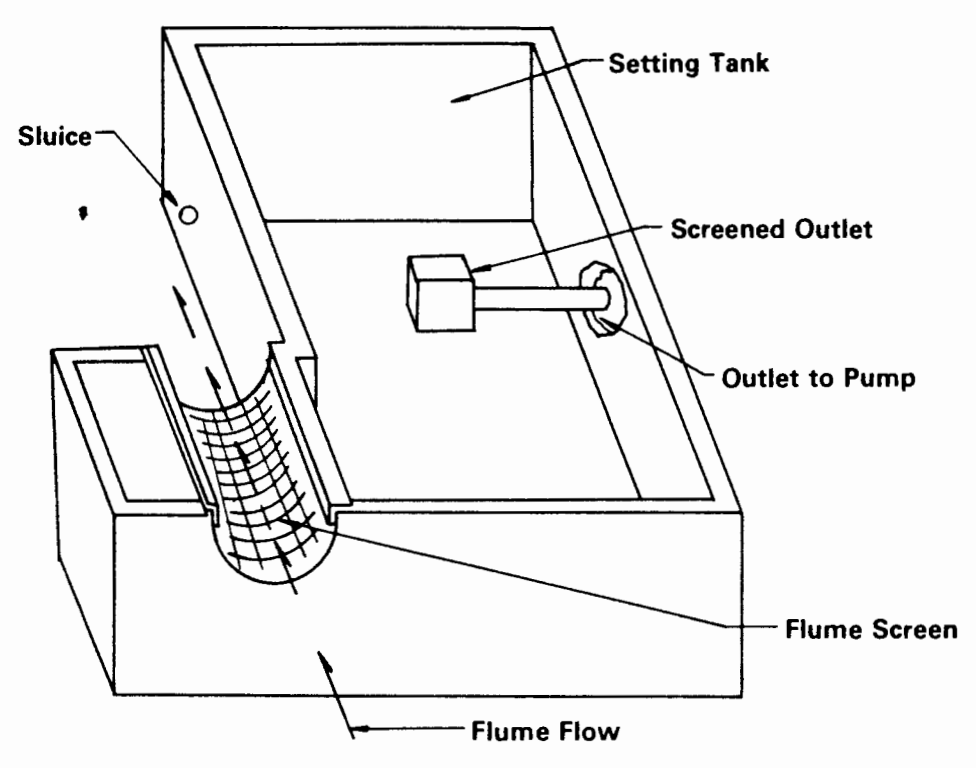


Figure 10.14 Diversion structure for screening open-channel flow into a pipeline inlet box.

to control and manage the irrigation water supply efficiently. Division boxes are installed to divide the water supply between two or more supply channels. Turnouts are installed to control flows into laterals or into field head ditches. Check structures are used for retarding or entirely blocking the flow in a channel. Portable checks, such as canvas or plastic dams or metal sheets, can be used in the smaller channels or ditches.

Weirs, flumes, or other measuring devices are installed in the open-channel system as needed to measure the flow to each individual field. If the entire irrigation water supply is delivered to one field at a time, only one measuring installation may be required. However, if the water supply is divided between two or more channels, additional measuring devices will be required. Weirs can often be built into other structures, such as drops, checks, or turnouts.

Equipment to control the flow of water from field head ditches into individual furrows, corrugations, or border strips facilitates irrigation. Siphons that lay over the channel bank are often used for channels in unstable soils. Plastic, metal, or rubber siphons are available in a wide variety of sizes and with flow capacities ranging from 0.1 to 100 liters/s. For stable soil conditions, spiles or furrow tubes placed through the ditch bank can be used. For border or basin methods of irrigation, concrete or metal pipe or wood boxes are often used to control the flows out of the field head ditch with simple slide gates being used to regulate the flow; but more frequently for irrigated basins, the earthen channel bank is cut to allow water to run onto the basin.

#### **Channel Sections**

The Manning formula is most commonly used for describing flow in open channels.

$$v = \frac{\sqrt{S_0}}{n} R^{0.67} \tag{10.3}$$

where

v = average velocity, m/s

 $S_0$  = dimensionless slope of the energy gradient

n = roughness coefficient

R = hydraulic radius given by

$$R = \frac{A}{\text{WP}} \tag{10.4}$$

where A is the cross-sectional flow area in  $m^2$ , and WP is the wetted perimeter in meters. The discharge form of the Manning formula is

$$Q = \frac{\sqrt{S_0}}{n} A R^{0.67} \tag{10.5}$$

The accuracy of the results from using the Manning formula is dependent on the designer's ability to select an appropriate value of the roughness coefficient, n. Tables of representative values of n for various open-channel boundary conditions are listed in numerous publications. A composite of listed values of n are given in Table 10.1.

The U.S. Soil Conservation Service has prepared design charts for concretelined channel sections. Figures 10.15 to 10.18 are design curves for trapezoidal sections having bottom widths of 1, 2, 3, or 4 ft (30, 60, 90, and 120 cm), side slopes of 1:1, and a roughness coefficient of 0.014.

# **Check-Drop Structures**

In the design of irrigation, drainage, and soil conservation systems, the problem of controlling flow velocities sufficiently to minimize erosion is continually confronted. Under many such conditions, drop structures have been successfully used to prevent excessive scour by dissipating a substantial fraction of the energy within the structure itself. Generally, the energy dissipation is accomplished with a hydraulic jump. Experimental studies have concerned themselves primarily with the very large conveyance works. In the few applications to smaller irrigation channels, little general design information is available.

A typical vertical drop structure as shown in Fig. 10.19 includes an inlet section, a drop section in which the flow is lowered, a stilling basin where the excess energy is dissipated, and an outlet section through which the water is discharged.

The inlet section of a drop structure can consist of an ap-Inlet section. proach channel having a geometry similar to irrigation watercourses or laterals, in which the water drops off the end of the channel (Figs. 10.19 and 10.20). Numerous drop structure inlets in irrigation systems are used as check structures, thereby resulting in a number of possible conditions regarding the jet entering the stilling basin (Fig. 10.21). Usually, a turnout structure will be located immediately upstream from the check structure to regulate the diversion into farm supply channels, which also affects upstream water levels in the lateral or watercourse. The flow passing over the check is usually less than the design discharge for the channel, whereas the check structure might be removed when the full discharge capacity of the channel is to be conveyed downstream. The inlet to the drop must also be considered a control for the upstream channel to prevent channel scouring. inlet should be symmetrical about the channel centerline and when possible, located a sufficient distance downstream from horizontal bends in order to limit undesirable wave action due to unsymmetrical flow.

For the flow condition shown in Fig. 10.21, critical depth occurs in the vicinity of the constriction. Both rectangular and trapezoidal check structures are commonly used in irrigation systems; the critical depth and its location for such geometries can easily be computed with an accuracy sufficient for design purposes. The drop height, H, is measured from the crest of the overflow section to the floor of the stilling basin (Fig. 10.21).

# TABLE 10.1MANNING ROUGHNESS COEFFICIENT, n, FOR VARIOUS OPEN-CHANNELCONDITIONS

I.		en Channels, Lined (Straight Alignment)	
	Α.	Concrete, with surfaces as indicated	
		1. Formed, no finish	0.013 - 0.017
		2. Trowel finish	0.012 - 0.014
		3. Float finish	0.013 - 0.015
		4. Float finish, some gravel on bottom	0.015 - 0.017
		5. Gunite, good section	0.016 - 0.019
		6. Gunite, wavy section	0.018 - 0.022
	В.	Concrete, bottom float finished, sides as indicated	
		1. Dressed stone in mortar	0.015 - 0.017
		2. Random stone in mortar	0.017 - 0.020
		3. Cement rubble masonry	0.020 - 0.025
		4. Cement rubble masonry, plastered	0.016 - 0.020
		5. Dry rubble (riprap)	0.020 - 0.030
	C	Gravel bottom, sides as indicated:	
	С.	1. Formed concrete	0.017-0.020
		2. Random stone in mortar	0.020-0.023
		3. Dry rubble (riprap)	0.023-0.033
	_		
	D.	Brick	0.014 - 0.017
	Ε.	Asphalt	
		1. Smoot <b>b</b>	0.013
		2. Rough	0.016
	F.	Wood, planed, clean	0.001 - 0.013
		Concrete-lined excavated rock	
	Ο.	1. Good section	0.017-0.020
		2. Irregular section	0.022-0.027
**	_	· ·	0.022-0.027
II.		en Channels, Excavated (Straight Alignment, Natural Lining)  Earth, uniform section	
	Α.	•	0.016 0.019
		1. Clean, recently completed	0.016-0.018
		2. Clean, after weathering	0.018-0.020
		3. With short grass, few weeds	0.022-0.027
		4. In gravelly soil, uniform section, clean	0.022 - 0.025
	В.	Earth, fairly uniform section	
		1. No vegetation	0.022 - 0.025
		2. Grass, some weeds	0.025 - 0.030
		3. Dense weeds or aquatic plants in deep channels	0.030 - 0.035
		4. Sides clean, gravel bottom	0.025 - 0.030
		5. Sides clean, cobble bottom	0.030 - 0.040
	C.	Dragline excavated or dredged	
		1. No vegetation	0.028 - 0.033
		2. Light brush on banks	0.035 - 0.050
	D	Rock	
	υ.	1. Based on design section	0.035
		2. Based on actual mean section	0.005
		a. Smooth and uniform	0.035-0.040
		b. Jagged and irregular	0.040-0.045
	Г		CLO10 - OLO10
	E.	Channels not maintained, weeds and brush uncut	0.000 0.130
		1. Dense weeds, high as flow depth	0.080-0.120
		2. Clean bottom, brush on sides	0.050-0.080

Headland Facilities Chap. 10

2 Clear hatter house on sides highest store of flow	0.070. 0.110
3. Clean bottom, brush on sides, highest stage of flow	0.070-0.110
4. Dense brush, high stage	0.100 - 0.140
III. Channels with Maintained Vegetation	
(Values shown are for velocities of 2 and 6 ft/s)	
A. Depth of flow up to 0.7 ft	
1. Burmudagrass, Kentucky bluegrass, buffalograss	
a. Mowed to 2 in.	0.070-0.045
b. Length 4-6 in.	0.090 - 0.050
2. Good stand, any grass	
a. Length about 12 in.	0.180 - 0.090
b. Length about 24 in.	0.200-0.100
3. Fair stand, any grass	
a. Length about 12 in.	0.140-0.080
b. Length about 24 in.	0.250 - 0.130
B. Depth of flow 0.7-1.5 ft	
Bermudagrass, Kentucky bluegrass, buffalograss	
a. Mowed to 2 in.	0.050-0.035
b. Length 4-6 in.	0.060-0.040
2. Good stand, any grass	
a. Length about 12 in.	0.120-0.070
b. Length about 24 in.	0.020 - 0.100
3. Fair stand, any grass	
a. Length about 12 in.	0.100 - 0.060
b. Length about 24 in.	0.170 - 0.090

**Drop section.** Basic hydraulic information is also needed for designing the vertical drop section. The flow depth in the stilling basin before a jump,  $y_1$ , and the nappe trajectory length,  $L_d$ , are the important design dimensions that must be determined.

In vertical drops, the aerated free-falling nappe will occur beginning at the crest of the drop section. A theoretical equation was developed (White, 1943) for determining the flow depth in a rectangular stilling basin preceding a hydraulic jump:

$$\frac{y_1}{y_c} = \frac{\sqrt{2}}{1.06 + \sqrt{H/y_c + 3/2}} \tag{10.6}$$

in which  $y_c$  is the critical depth. The total energy of the flow is found by the specific energy equation,

$$\frac{E_1}{y_c} = \frac{y_1}{y_c} + \frac{v_1^2}{2gy_c} \tag{10.7}$$

where  $E_1$  is the specific energy at the prejump location. Since the Froude number of the point is described by  $F_1 = (y_c/y_1)^{1.5}$ , the relative specific energy,  $E_1/y_c$ , retained by the flow leaving the section of impingement is readily calculated from

$$\frac{E_1}{y_c} = \frac{y_1}{y_c} \left[ 1 + 0.5 \left( \frac{y_c}{y_1} \right)^3 \right]$$
 (10.8)

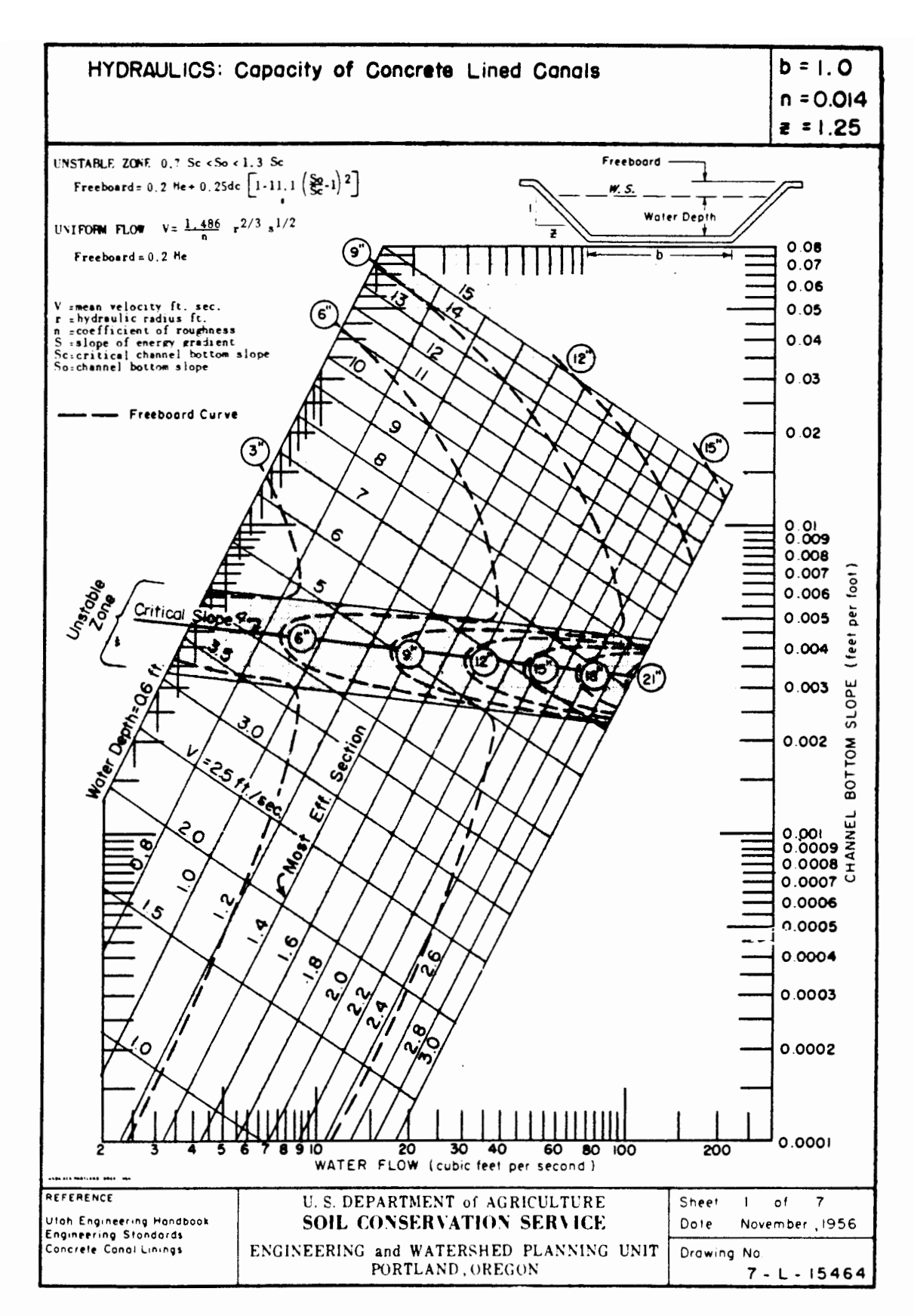
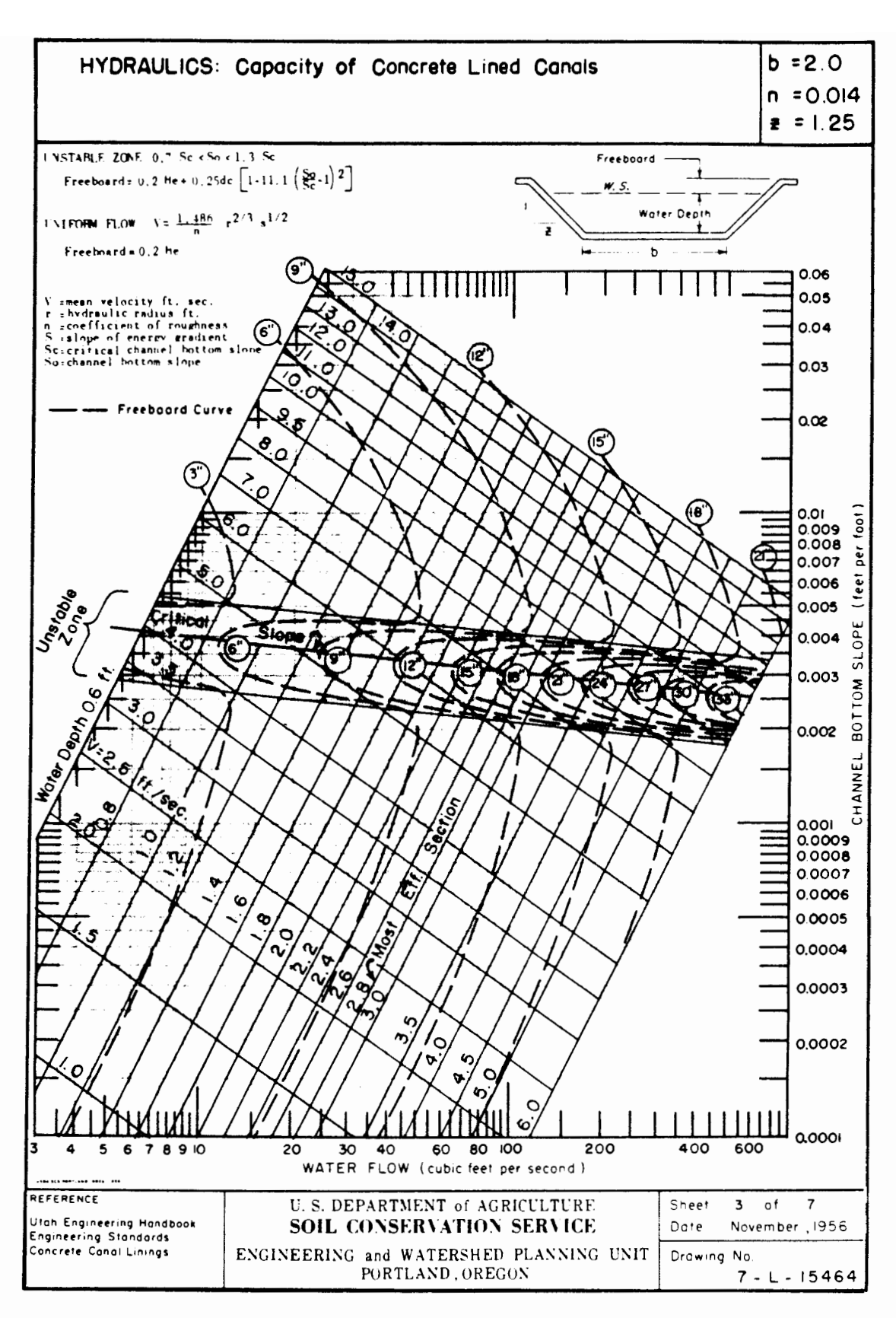


Figure 10.15 Hydraulic design curves for concrete-lined trapezoidal channel sections with 1-ft bottom width.



**Figure 10.16** Hydraulic design curves for concrete-lined trapezoidal channel sections with a 2-ft bottom width.

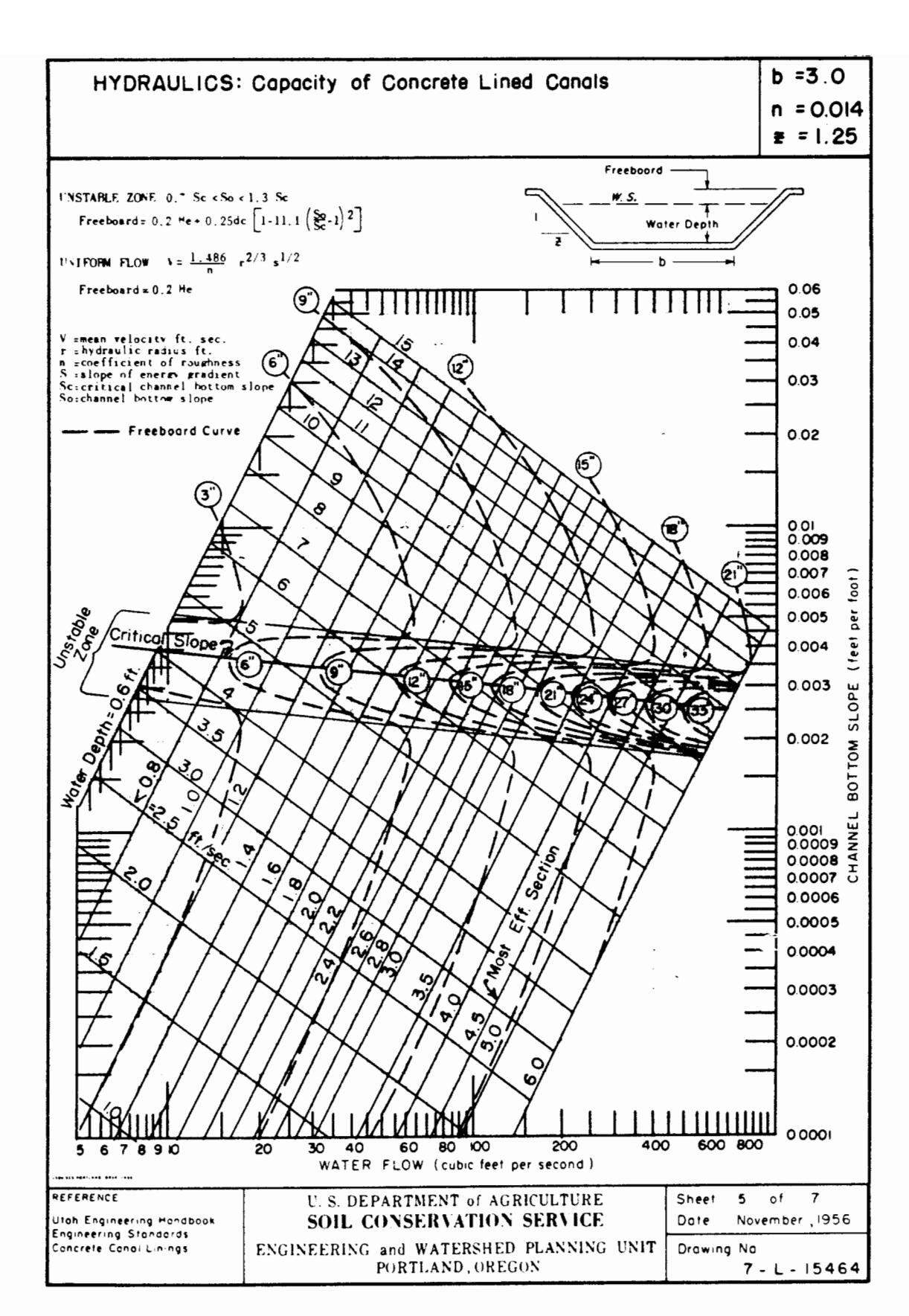


Figure 10.17 Hydraulic design curves for concrete-lined trapezoidal channel sections with a 3-ft bottom width.

250 Headland Facilities Chap. 10

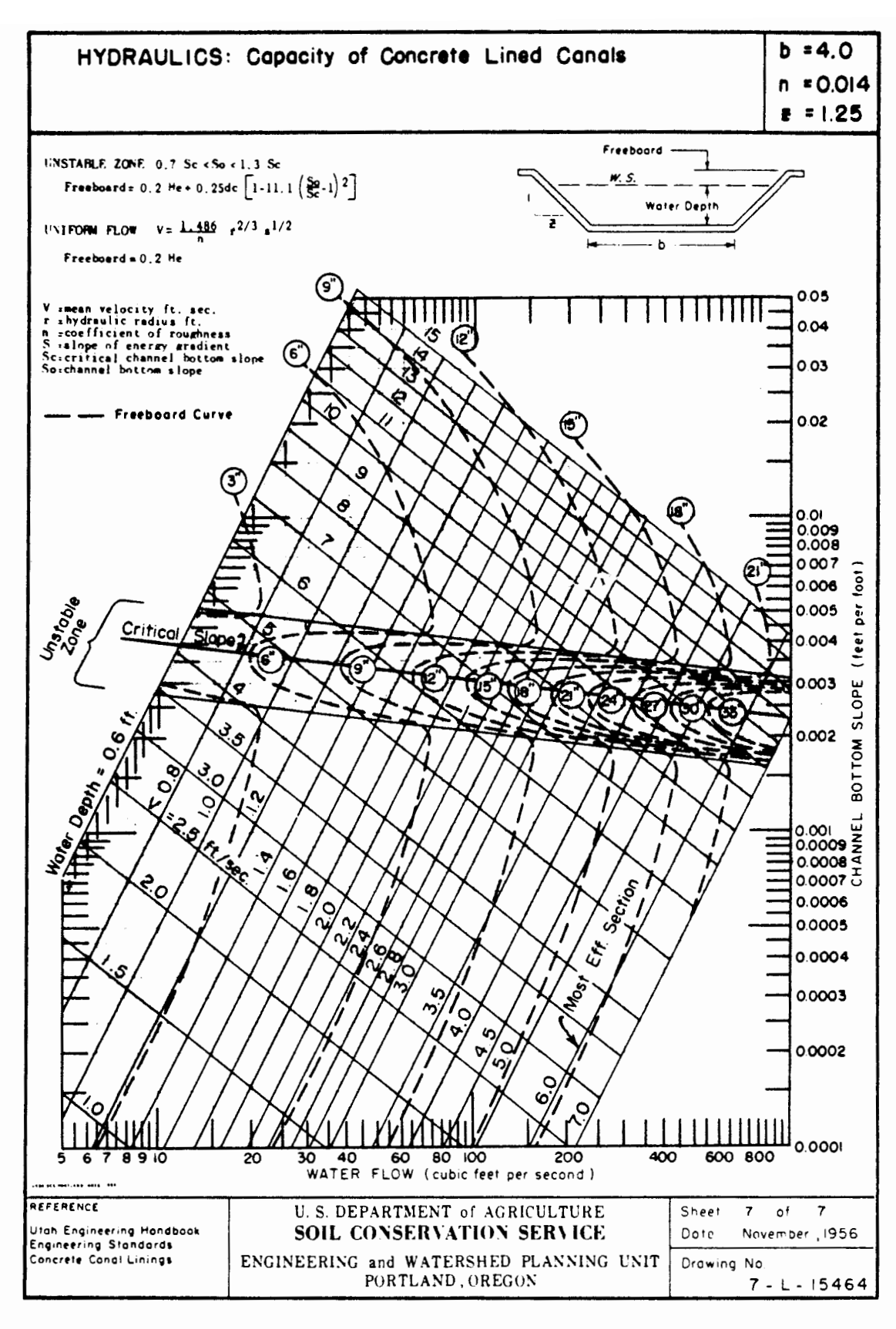
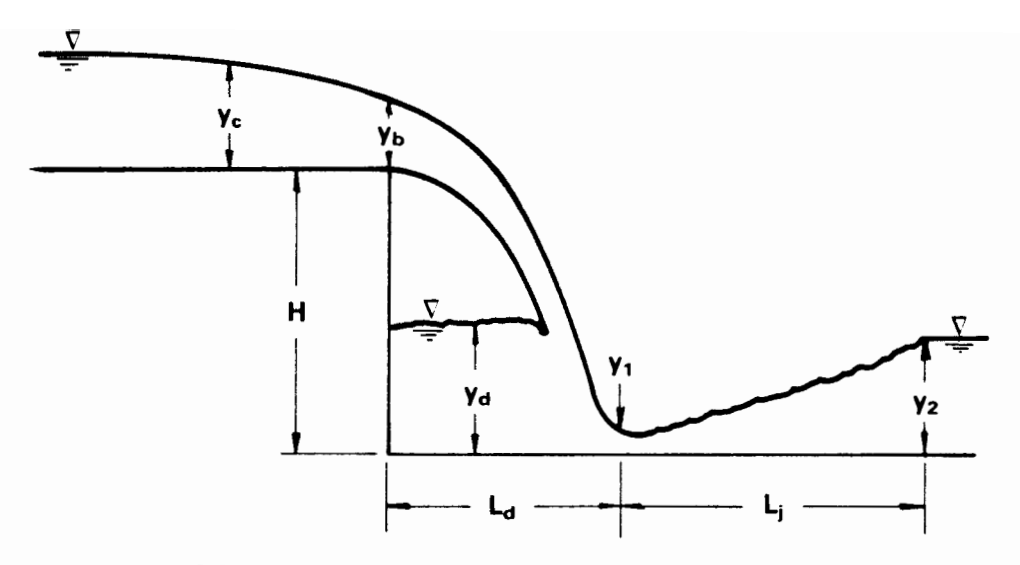


Figure 10.18 Hydraulic design curves for concrete-lined trapezoidal channel sections with a 4-ft bottom width.



**Figure 10.19** Schematic drawing of a typical vertical-drop structure in an irrigation system.

This equation agrees quite well with experimental work by Moore (1943), as shown in Fig. 10.22, in which the values of  $H/y_c$  versus  $E/y_c$  for both experimental data and theoretical values are plotted.

With normal flow conditions for nonweir approach sections, the critical depth for rectangular cross sections can be computed. Then the flow depth preceding the hydraulic jump can be determined using Eq. 10.6.

Rand (1955) utilized experimental results by himself and others to develop the relation

$$\frac{y_1}{H} = 0.54 \left(\frac{y_c}{H}\right)^{1.275} \tag{10.9}$$

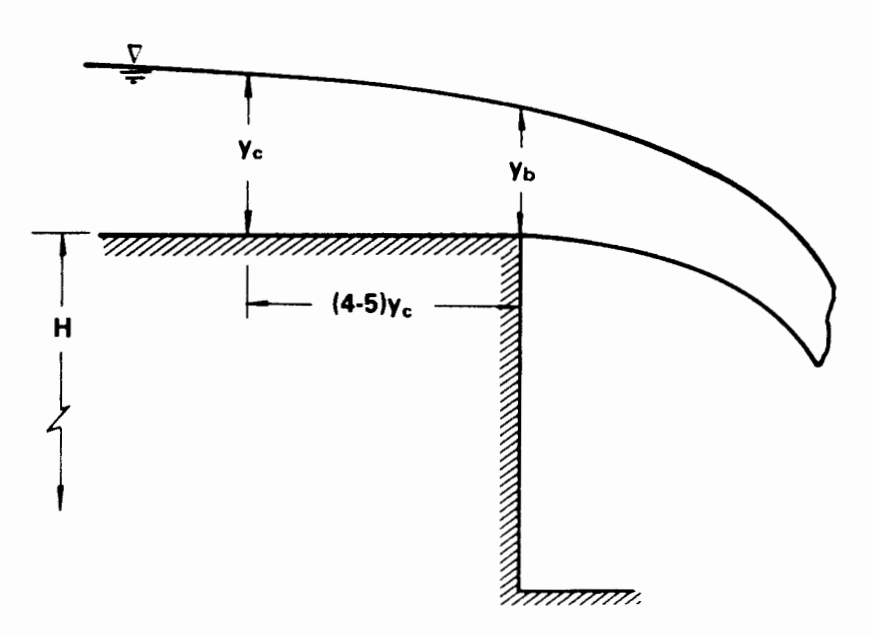


Figure 10.20 Free overfall at a vertical-drop structure.

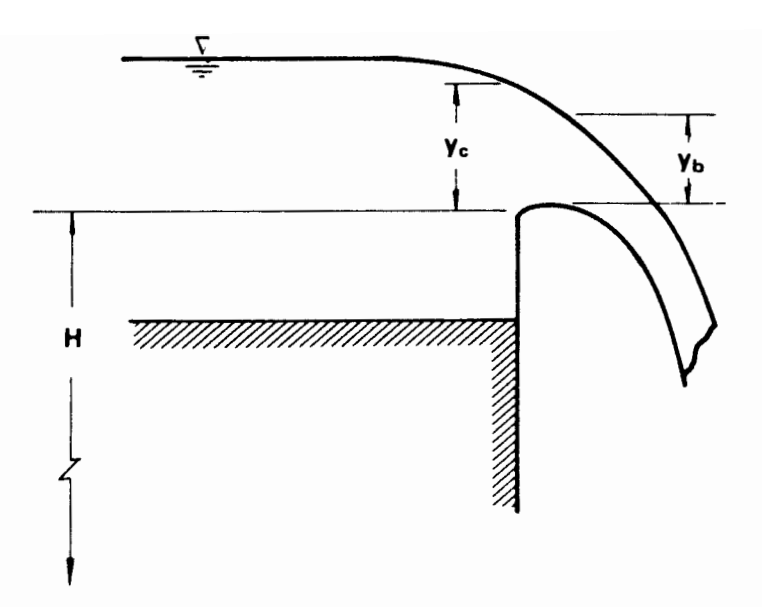


Figure 10.21 Check structure overfall.

Aletraris (1983) collected considerable data on small vertical drop structures, and a comparison of his data with Rand and White is shown in Fig. 10.23. The line of best fit for the Aletraris data has the relation

$$\frac{y_1}{H} = 0.53 \left(\frac{y_c}{H}\right)^{1.319} \tag{10.10}$$

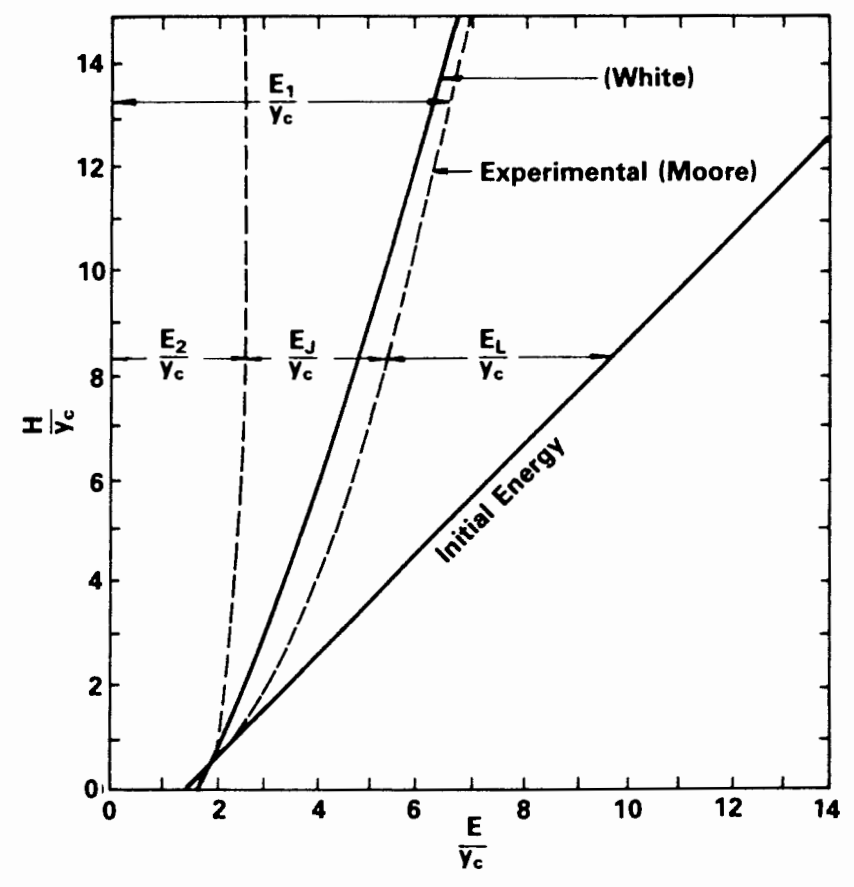


Figure 10.22 Energy dissipation at the base of the free overfall.

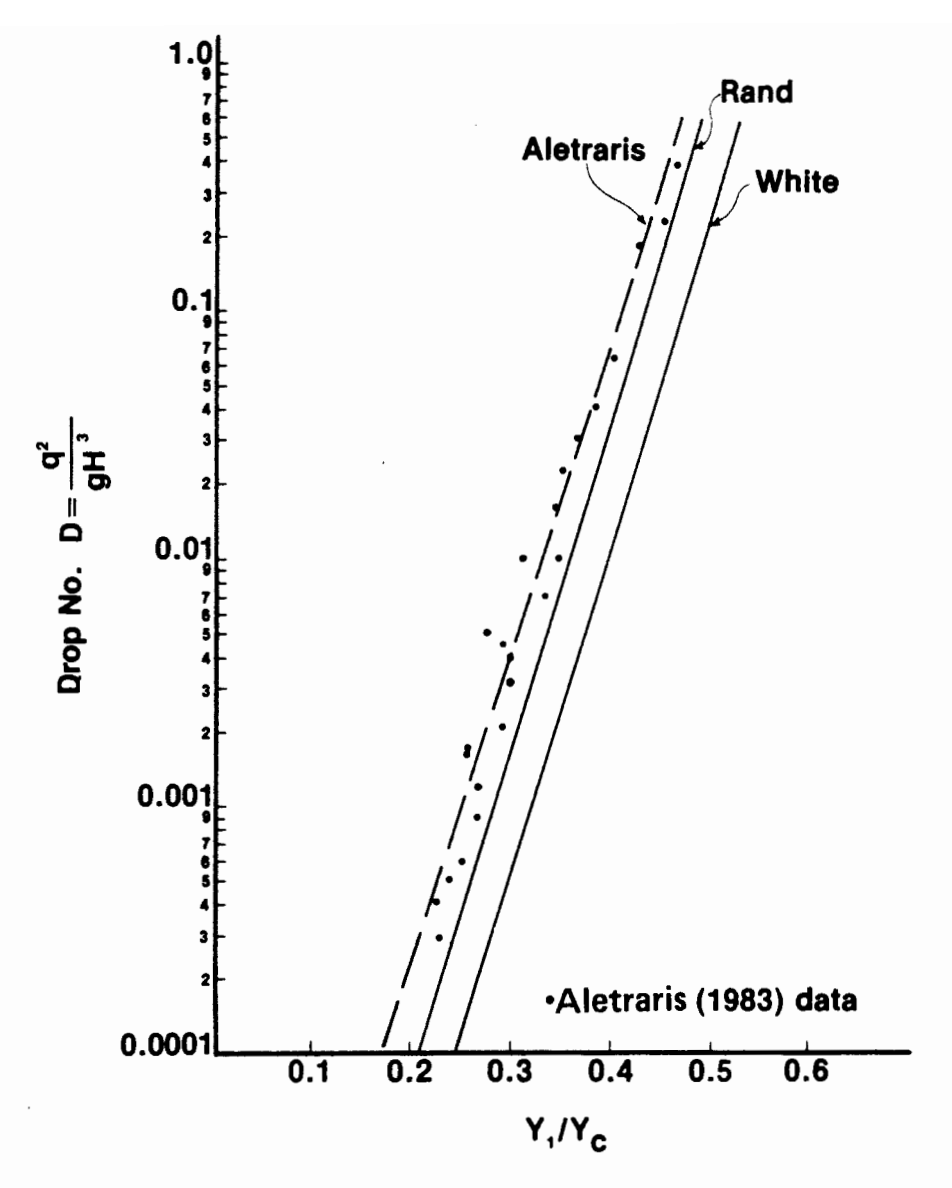


Figure 10.23 Relative depth of flow before the hydraulic jump in relation to the drop number. (From Aletraris, 1983.)

**Stilling basin**. In a vertical drop, the length of the stilling basin consists of two parts: the nappe trajectory length,  $L_d$ , and the hydraulic jump length,  $L_j$ , as shown in Fig. 10.19. The nappe trajectory length,  $L_d$ , can be defined as the distance from the crest to the place where the jet strikes the basin floor. To determine the nappe trajectory length, equations describing the nappe of a freely falling jet were used.

The investigations by Donnelly and Blaisdell (1965) express the nappe trajectory length as an equation for nappe trajectory. The equation for  $L_d$  is

$$L_d = \frac{X_f + X_s}{2} {10.11}$$

in which  $X_f$  is the horizontal distance from drop crest to the upper surface of the

254 Headland Facilities Chap. 10

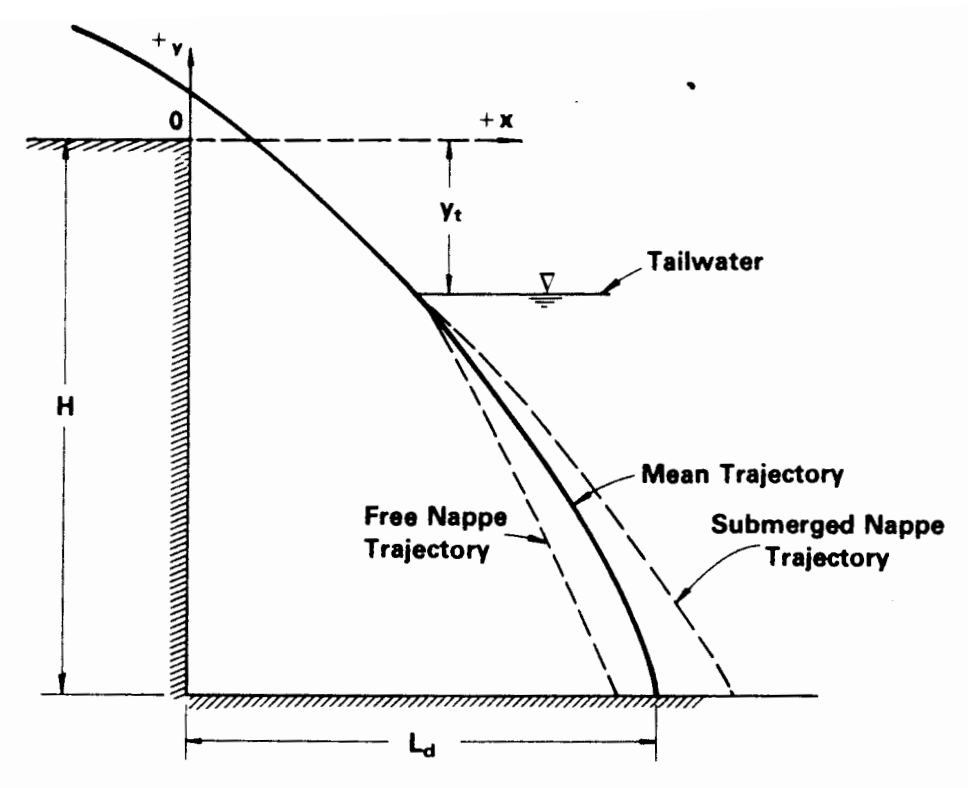


Figure 10.24 Nappe trajectory of flow over a vertical drop.

free-falling nappe at the elevation of the stilling basin shown in Fig. 10.24. The equation for  $X_f$  is

$$\frac{X_f}{y_c} = -0.406 + \left(3.195 - 4.386 \frac{H}{y_c}\right)^{0.5}$$
 (10.12)

The equation for the upper surface of the submerged nappe trajectory above the tailwater level is the same as that for the free-falling nappe. The point at which the upper nappe impinges on the tailwater is

$$\frac{X_t}{y_c} = -0.406 + \left(3.195 - 4.386 \frac{y_t}{y_c}\right)^{0.5} \tag{10.13}$$

in which  $X_t$  is the horizontal distance from the drop crest to the point at which the surface of the upper nappe plunges into the tailwater, and  $y_t$  is the vertical distance from the crest to the tailwater surface, as shown in Fig. 10.24.

At a point where the upper surface of the submerged nappe trajectory strikes the stilling basin floor, the equation is

$$\frac{X_s}{y_c} = \frac{0.691 + 0.228(X_t/y_c) - H/y_c}{0.185 + 0.456(X_t/y_c)}$$
(10.14)

where  $X_s$  is the horizontal distance from the drop crest to the point where the upper surface of the submerged nappe strikes the stilling basin floor. Therefore, from Eq. 10.11, the nappe trajectory length,  $L_d$ , can be determined when the discharge and height of the vertical drop are given. The equation has been com-

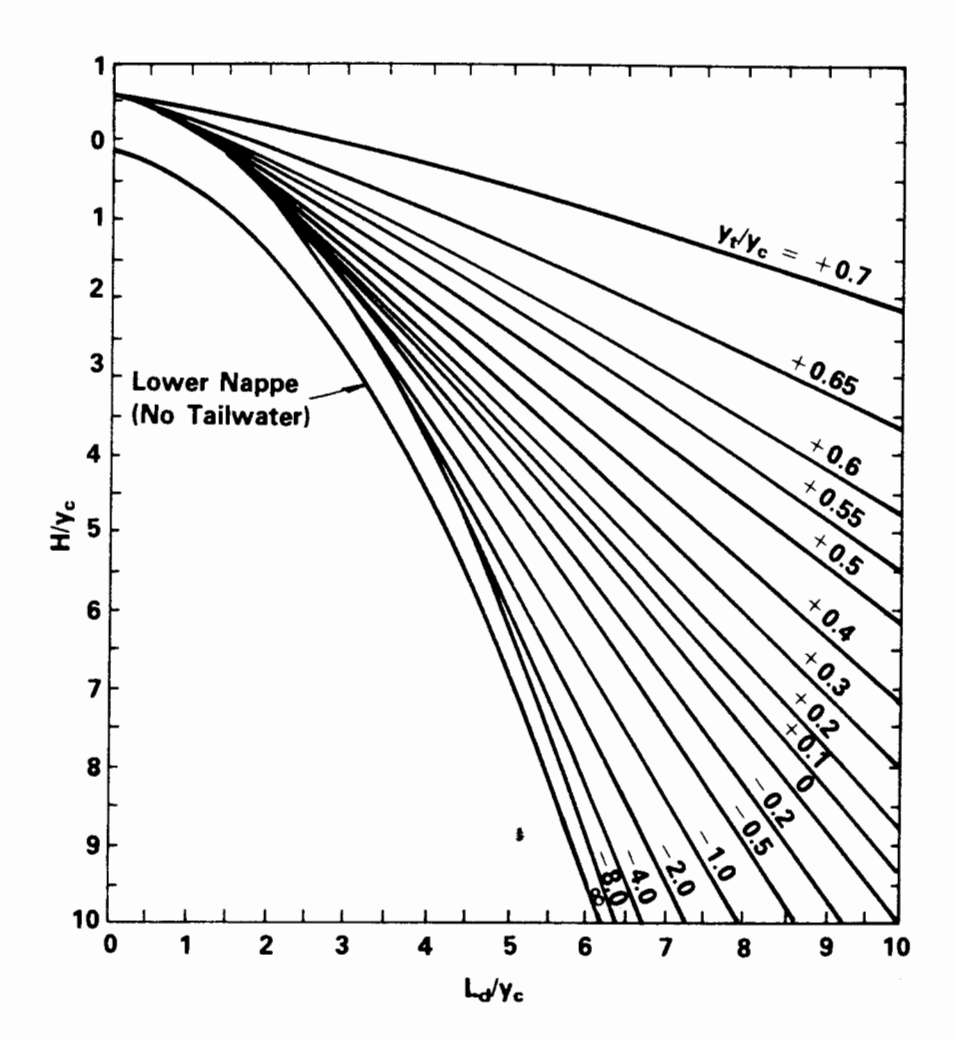


Figure 10.25 Graphical solution to nappe trajectory over a vertical drop.

puted and plotted in Fig. 10.25. It should be noted that the origin of points x and y is at the crest of the drop, so that the values of H and  $y_t$  in Eqs. 10.12 to 10.14 are negative.

Katsaitis (1966) has used the dynamic equations of motion to develop an equation to determine the nappe trajectory length for the weir condition at a vertical check-drop crest (Fig. 10.21). The definition sketch of flow over a weir (Fig. 10.26) can be used to describe the development of an equation for determining  $L_d$ . (The reference point for the equation is the centroid of the jet cross section, where the lower nappe has reached its highest elevation):

$$L_d = (0.627H_0Z)^{0.5} + 0.5H_0' (10.15)$$

The analysis above is based on an aerated nappe. In practice, if the nappe is not fully aerated, the free jet will strike the stilling basin floor at a shorter distance from the overflow crest, and the computation of  $L_d$  using Eq. 10.15 would result in a conservative design.

Instead of using Eq. 10.15, another possibility is to compute  $L_d$  from Eqs. 10.11 to 10.14 (or Fig. 10.25) and then add the distance  $H_0/2$ , which can be computed easily compared to  $H_0'/2$ .

Headland Facilities Chap. 10

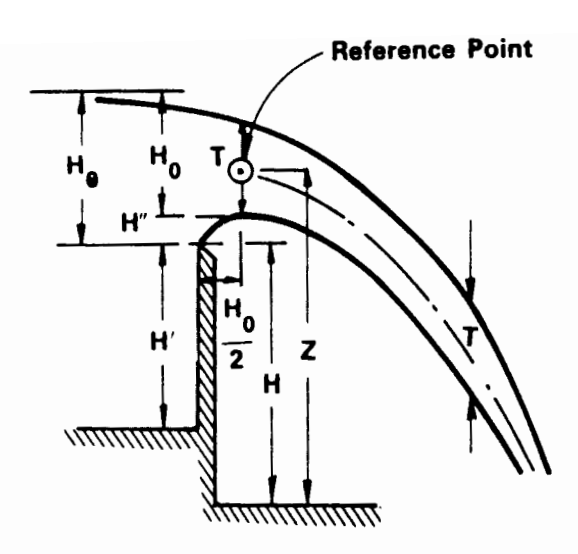


Figure 10.26 Definition sketch for free jet flow over a weir.

Rand (1955) introduced the concept of a drop number, D, defined as

$$D = \frac{q^2}{gH^3} \tag{10.16}$$

Rand related the nappe trajectory length with the drop number by the equation

$$\frac{L_d}{H} = 4.30D^{0.27} \tag{10.17}$$

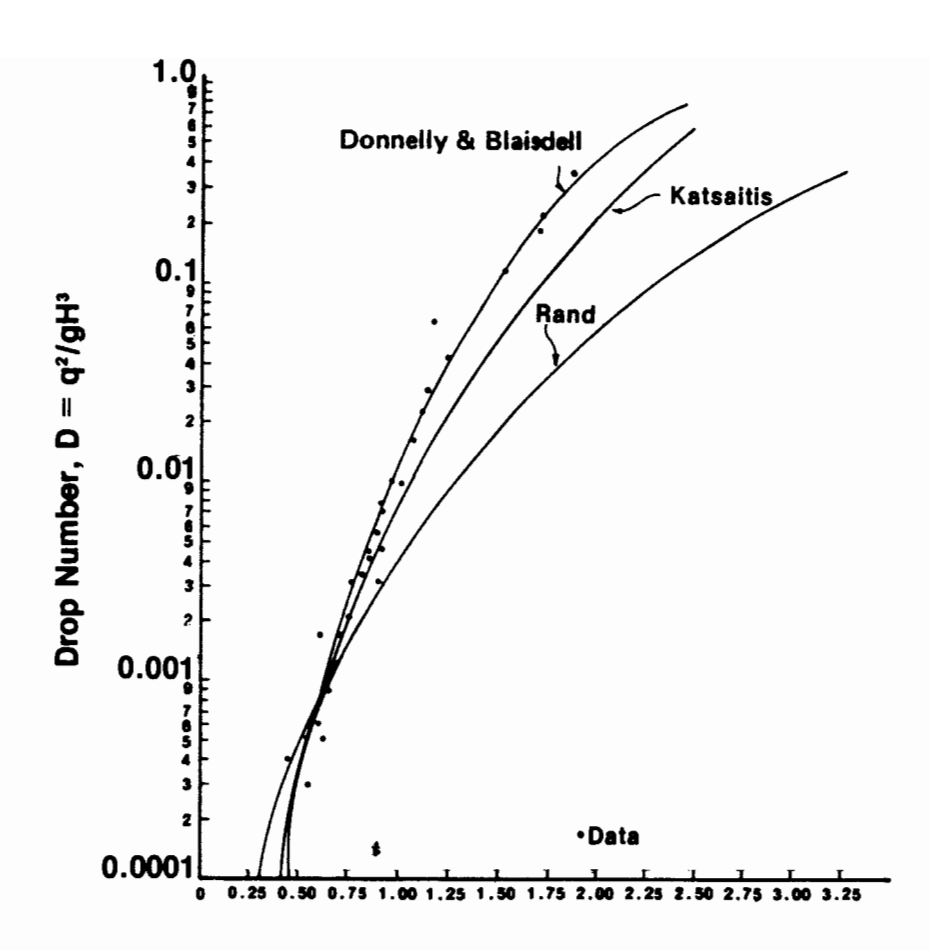
Aletraris (1983) collected laboratory data for small vertical-drop structures. As shown in Fig. 10.27, the laboratory data of Aletraris correspond very closely to the equations presented by Donnelly and Blaisdell (Eqs. 10.11 to 10.14).

**Pool Depth.** Very little information has been collected on the depth of standing water behind the free vertical overfall, which is the pool depth,  $y_d$ . Moore (1943) conducted 10 tests using drop heights of 0.5 and 1.5 ft. The recent work by Aletraris (1983) provides the necessary information on relative pool depth,  $y_d/H$ , as a function of the drop number, D, in Fig. 10.28.

Hydraulic Jump. The flow depth after the hydraulic jump,  $y_2$ , can be determined by the sequent depth ratio,  $y_2/y_1$ , in which the subscripts refer to the sections after and before the jump, respectively. The most common technique used to describe the sequent depth ratio is through the use of the momentum principle of the flow, which results in the following equation:

$$\frac{y_2}{y_1} = \frac{1}{2} \left( \sqrt{1 + 8F_1^2} - 1 \right) \tag{10.18}$$

Experiments were conducted by the U.S. Bureau of Reclamation (Peterka, 1964) to verify Eq. 10.18. The agreement between theory and experimental values is excellent over the entire range, indicating that the equation is applicable even when the flow enters the jump at an appreciable angle to the horizontal. Silvester



### Relative Nappe Trajectory Length, Ld/H

**Figure 10.27** Relative nappe trajectory length in terms of the drop number. (From Aletraris, 1983.)

(1964) has probably presented the most complete analysis, together with a substantial literature review and generalization of experimental data.

The length of the hydraulic jump,  $L_j$ , may be defined as the distance measured from the front face of the jump to a point on the surface immediately downstream from the roller (Chow, 1959). The length cannot be determined easily by theory, but it has been investigated experimentally by many researchers.

Investigators have proposed that the length of hydraulic jump is a function of the Froude number and the height of the hydraulic jump. The experimental data on the length of the hydraulic jump can be plotted conveniently with the Froude number,  $F_1$ , against a dimensionless ratio,  $L_i/(y_2 - y_1)$ ,  $L_i/y_1$ , or  $L_i/y_2$ .

From the experimental results of the USBR, the plot of  $F_1$  versus  $L_j/y_1$  is probably the best, for the resulting curve can be best defined by the data. However, for practical purposes, the plot of  $F_1$  versus  $L_j/y_2$  is desirable because the resulting curve shows a fairly flat portion for the range of Froude numbers that produce a well-established hydraulic jump. This curve was developed primarily for the hydraulic jump occurring in a rectangular channel and thus may be applied for determining the length of hydraulic jump in a horizontal stilling basin.

A number of empirical relations are available to determine the length of the hydraulic jump, but the usual practice is to use a length from five to six times the

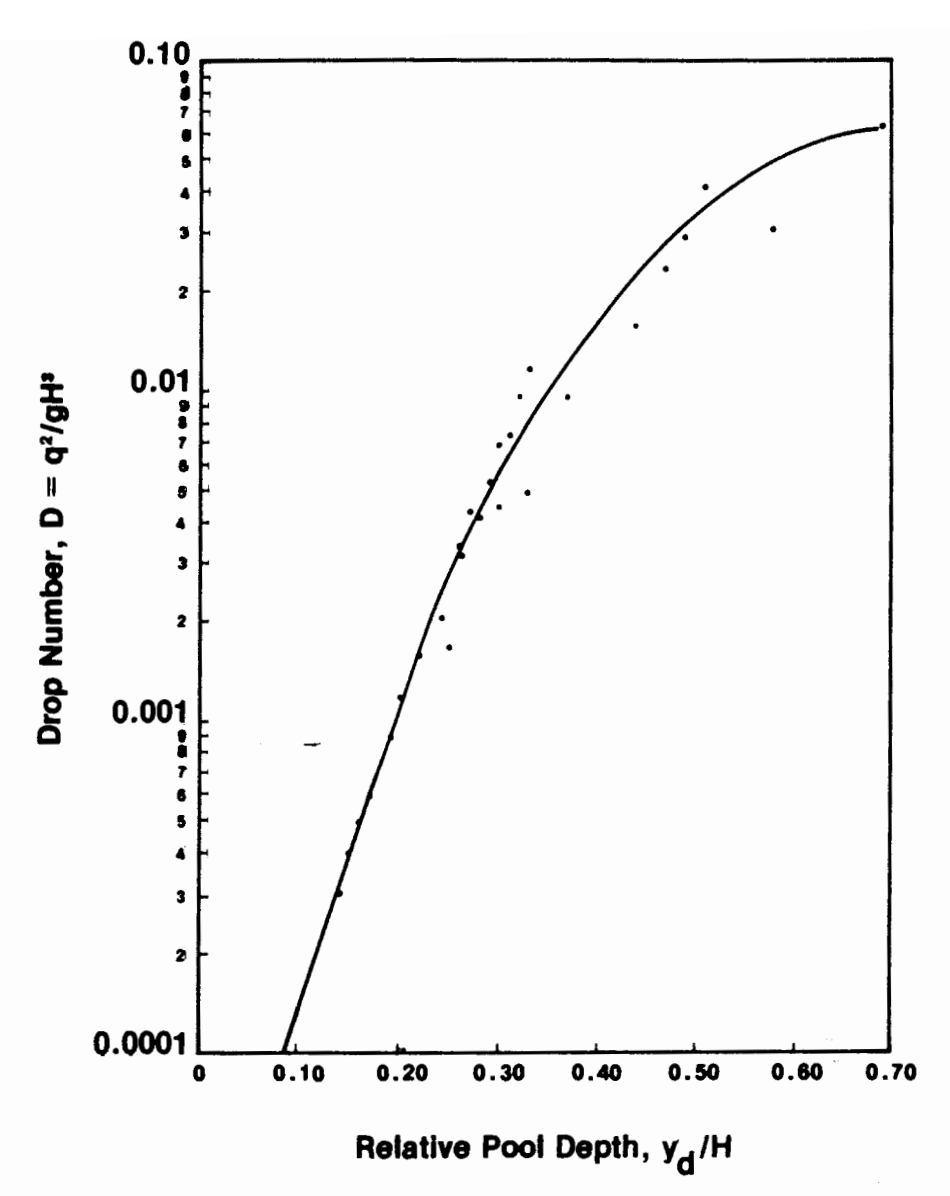


Figure 10.28 Pool depth behind a free vertical overfall in terms of the drop number. (From Aletraris, 1983.)

difference between the conjugate depths of the hydraulic jump  $(y_2 - y_1)$ . Peterka (1964) has provided most of the currently available experimental data regarding hydraulic jump length. An analysis of the experimental data indicates that a good relationship between the length of the jump and the height of the jump existed.

Figure 10.29 shows a plot of  $L_j/y_2$  versus Froude number,  $F_1$ , including the relation recommended by the USBR. However, recent work by Aletraris (1983) shows the length of hydraulic jump for small vertical-drop structures.

**Basin Length.** The nappe trajectory length can be determined by Eq. 10.11 or Eq. 10.15. Using these equations, relations between the dimensionless length ratio,  $L_d/y_2$ , and the Froude number,  $F_1$ , can be developed as shown in Fig. 10.29. The Aletraris curve is recommended for Froude numbers less than 7 and the Zurich Lab curve when the Froude number is greater than 7.

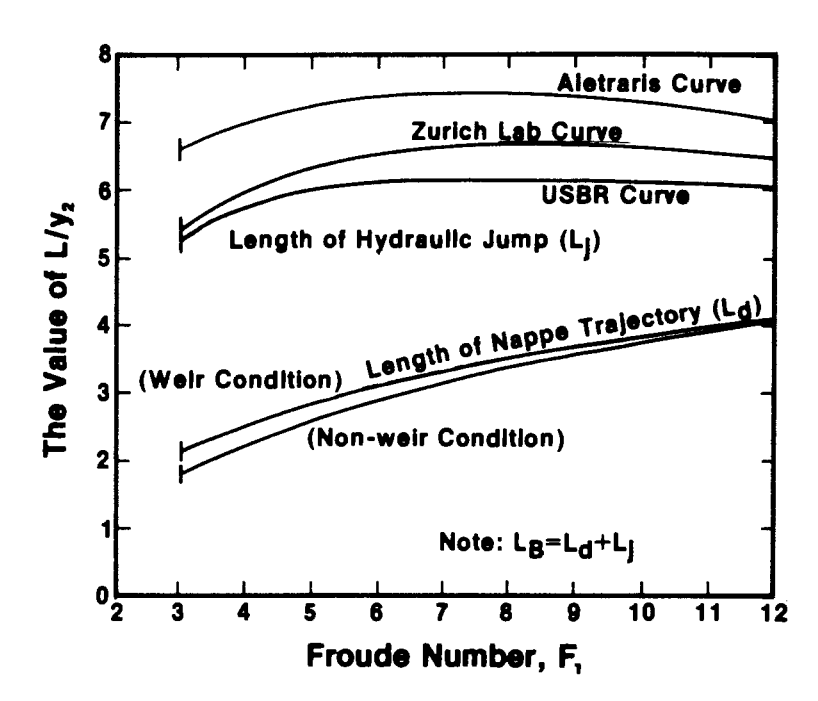


Figure 10.29 Relation between the length ratio  $L/y_2$  and Froude number for determining the stilling basin length for a vertical-drop structure.

**Tailwater.** The formation of the hydraulic jump at the base of a stilling basin depends on the relationship between the tailwater depth of the flow and the conjugate depth.  $y_2$ , of the hydraulic jump. The conjugate depth of the hydraulic jump depends entirely on upstream conditions. Therefore, in designing a stilling basin using the hydraulic jump as an energy dissipator, the conditions both upstream and downstream should be considered.

There may be three alternative patterns of tailwater depth that affect the hydraulic jump in a drop structure:

- 1. The case where the tailwater surface elevation is equal to the water surface elevation of the conjugate depth of the hydraulic jump,  $y_2$
- 2. The case where the tailwater surface elevation is less than the conjugate depth water surface elevation
- 3. The case where the tailwater surface elevation is greater than the conjugate depth water surface elevation

When the tailwater surface elevation is equal to the conjugate depth,  $y_2$ , the hydraulic jump will occur in the stilling basin. For scour protection purposes, this is an ideal case. An objection to this condition, however, is that a little difference between the actual and assumed values of the pertinent hydraulic coefficients may cause the jump to move downstream from its estimated position. Consequently, some means for controlling the position of the hydraulic jump is always necessary.

When the tailwater surface elevation is less than the conjugate depth of the hydraulic jump, the hydraulic jump will move downstream to a point where Eq. 10.18 is again satisfied. This case must, if possible, be avoided in design, because the turbulence of the flow acting on an unprotected downstream channel will result in severe erosion. To prevent this condition, the designer should use a control structure in the channel bottom, which will increase the tailwater and thus ensure a hydraulic jump within the protected stilling basin. When the tailwater is nearly

sufficient to cause the jump to form, baffles or sills may be placed on the floor of the basin to increase the tailwater depth.

The next important case is the pattern in which the tailwater surface elevation is greater than  $y_2$ . In this case, the hydraulic jump will be forced upstream and may finally be drowned out at the stilling basin, becoming a submerged jump. This is the safest case in design because the position of the submerged jump can be fixed most readily and a high degree of energy dissipation results. When the vertical drop is used, high tailwater depths approaching the level of the approach channel bed will result in the jet moving along the water surface, thereby causing downstream bank erosion, which is a situation that should be avoided.

In practical design work, the designer should always be aware of the relationship between tailwater and conjugate depth of the hydraulic jump, and adjust the design to fit these conditions.

# Riprap Protection

The use of natural open channels for the transportation of water presents the possibility of scour. Loose boundary channels are constantly shifting alignment due to this phenomenon while man-made channels through natural earth must be carefully designed either to keep local velocities below those causing scour (critical) or to maintain an equilibrium between deposition and entrainment at any one point. Where the discharge cannot be controlled to keep velocities below a critical value, some means of channel protection must be employed.

Rock (riprap) has been used for lining floodway channels, river improvements, and below irrigation structures as a means of protection against the scouring action of flowing water. Obviously, very large boulders would prevent scour, but to reduce costs, it is desirable to know the smallest rock that can safely be used in a particular design situation. The problem then is to establish the laws and relationships that allow prediction of the flow conditions under which a given size particle will be moved from its position.

An anonymous (1936) Soviet article listed (Table 10.2) competent mean velocities for natural roughness elements from 0.005 to 200 mm (0.0002 to 8 in.). The most significant aspect of this publication was the inclusion of the depth of flow as a parameter describing the particle size that could be moved by the flow.

Neill (1967, 1968) has conducted experiments to determine a relationship between mean competent velocity,  $V_{mc}$ , and the diameter of natural gravels,  $D_s$ . The results of this experimental work, together with the results of other investigators, are shown in Fig. 10.30.

When the required size of riprap is considerably larger than the base material underlying the riprap blanket, a filter layer of material may be required between the base material and the riprap in order to prevent leaching. Leaching is the process by which the finer material underlying the riprap is picked up and carried away by turbulent eddies, waves, jets, and surges that penetrate the riprap blanket through the interstices of the rock particles. Leaching can be minimized if the riprap blanket is thick enough, the interstices are closed or reduced in size, a protective layer of intermediate-sized material is interposed between the base ma-

**TABLE 10.2** USSR DATA ON PERMISSIBLE VELOCITIES FOR NONCOHESIVE PARTICLES

		Particle diameter			
Material	mm	in.	velocity (ft/s)		
Silt	0.005	0.0002	0.49		
Fine sand	0.05	0.002	0.66		
Medium sand	0.25	0.01	0.98		
Coarse sand	1.00	0.04	1.80		
Fine gravel	2.50	0.1	2.13		
Medium gravel	5.00	0.2	2.62		
Coarse gravel	10.00	0.4	3.28		
Fine pebbles	15.0	0.6	3.94		
Medium peb- bles	25.0	1.0	4.59		
Coarse pebbles	40.0	1.6	5.91		
Large pebbles	75.0	3.0	7.87		
Large pebbles	100.0	4.0			
Large pebbles	150.0 200.0	6.0 8.0	10.83 12.80		

USSR corrections of permissible velocity for noncohesive materials

Average depth								
Meters	0.30	0.60	1.00	1.50	2.00	2.50	3.00	
Feet	0.98	1.97	3.28	4.92	6.56	8.20	9.84	
Correction factor	0.8	0.9	1.00	1.1	1.15	1.20	1.25	

terial and the riprap, or the base material is sufficiently cohesive to prevent unraveling and erosion of the individual particles.

The criteria which are frequently used to determine whether or not a filter layer is required can be defined as

$$\frac{D_{15} \text{ riprap}}{D_{85} \text{ base}} < 5 \tag{10.19}$$

$$5 < \frac{D_{15} \text{ riprap}}{D_{15} \text{ base}} < 40 \tag{10.20}$$

$$\frac{D_{50} \text{ riprap}}{D_{50} \text{ base}} < 40 \tag{10.21}$$

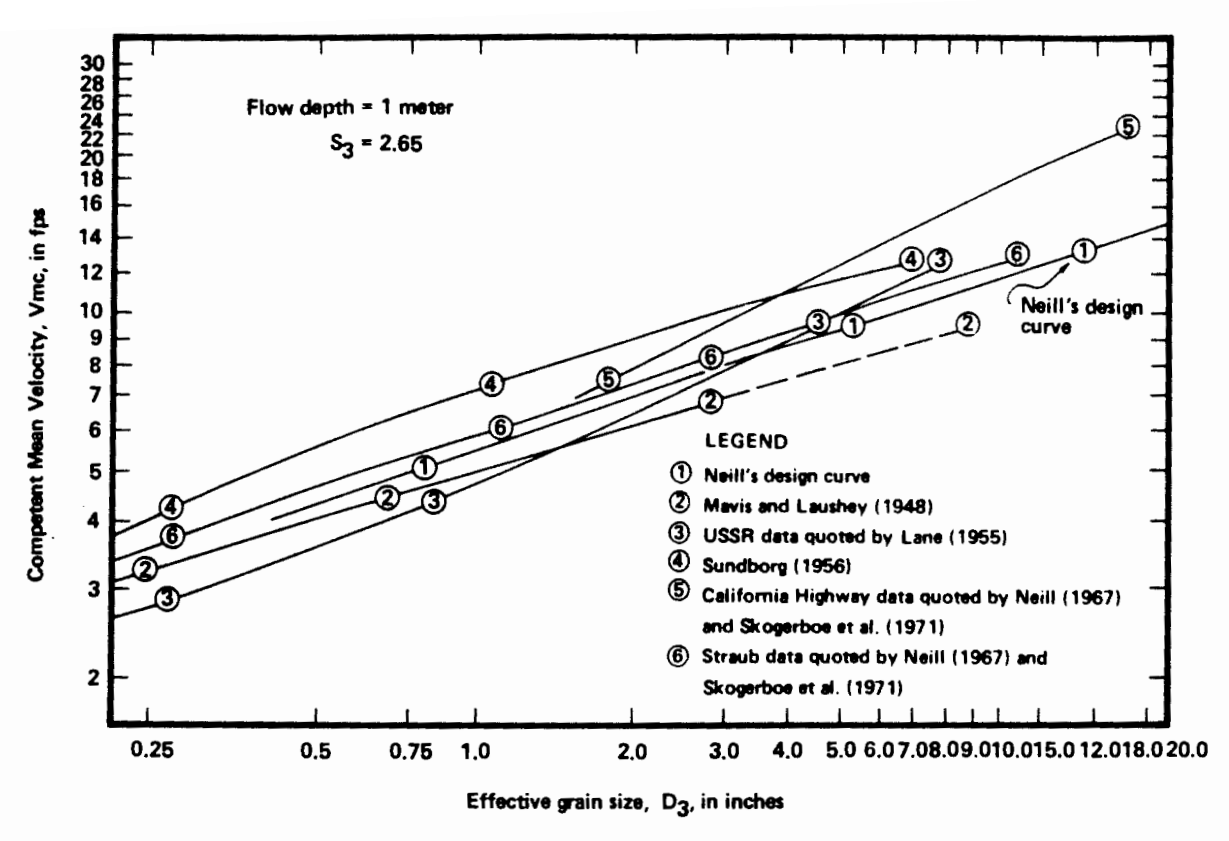


Figure 10.30 Plot of Neill's design curve and comparable data by others for riprap protection in open channels.

in which  $D_{15}$ ,  $D_{50}$ , and  $D_{85}$  are the sizes of riprap and base material of which 15, 50, and 85% are finer. If these criteria (Eqs. 10.19 to 10.21) are not met, a filter layer is necessary. In fact, the possibility exists that more than one filter layer may be required; the criteria above must be met by each successive filter layer.

If, for example, a filter layer is required, the criteria given by Eqs. 10.19 to 10.21 must be modified according to the following equations:

$$\frac{D_{15} \text{ riprap}}{D_{85} \text{ filter}} < 5 \tag{10.22}$$

$$5 < \frac{D_{15} \text{ riprap}}{D_{15} \text{ filter}} < 40 \tag{10.23}$$

$$\frac{D_{50} \text{ riprap}}{D_{50} \text{ filter}} < 40 \tag{10.24}$$

$$\frac{D_{15} \text{ filter}}{D_{85} \text{ base}} < 5 \tag{10.25}$$

$$5 < \frac{D_{15} \text{ filter}}{D_{15} \text{ base}} < 40 \tag{10.26}$$

$$\frac{D_{50} \text{ filter}}{D_{50} \text{ base}} < 40$$
 (10.27)

If only one filter layer is required, the use of Eqs. 10.22 to 10.27 will yield a range of particle size distributions that will be satisfactory for the filter material.

Recommendations regarding the thickness of the riprap blanket or filter layer vary. The range is about 1.3 to 2 times the  $D_{50}$  size of the material. Other recommendations state that the thickness of the material should be equal to the maximum particle size or 1.5 times the maximum particle size.

A natural, built-in series of filter layers is graded riprap, which varies in size from the maximum required by the foregoing criteria down to the maximum size in significant quantity in the base material. All intermediate sizes also need to be present so that the riprap is well graded and maximum density. Such material is usually available at the lowest price as pit-run sand, gravel, cobbles, and boulders, or as crusher-run material from a rock crusher plant.

# **Spiles and Siphon Tubes**

Spiles and siphon tubes are frequently used to transfer water from a field head ditch into individual furrows. Free flow and submerged flow conditions for spiles and siphon tubes are illustrated in Fig. 10.31. The appropriate hydraulic formulas are Eq. 4.41 for free-flow conditions and Eq. 4.42 for submerged-flow conditions. The discharge capacity for commonly used diameters and lengths of siphon tubes is shown in Fig. 10.32. For design purposes, Fig. 10.32 could also be used for spiles, which would be a conservative estimate of discharge capacity since the straight spile tubes would have less head loss than the curved siphon tubes. Frequently, small sliding gates will be installed at the inlet of each spile to control the discharge capacity.

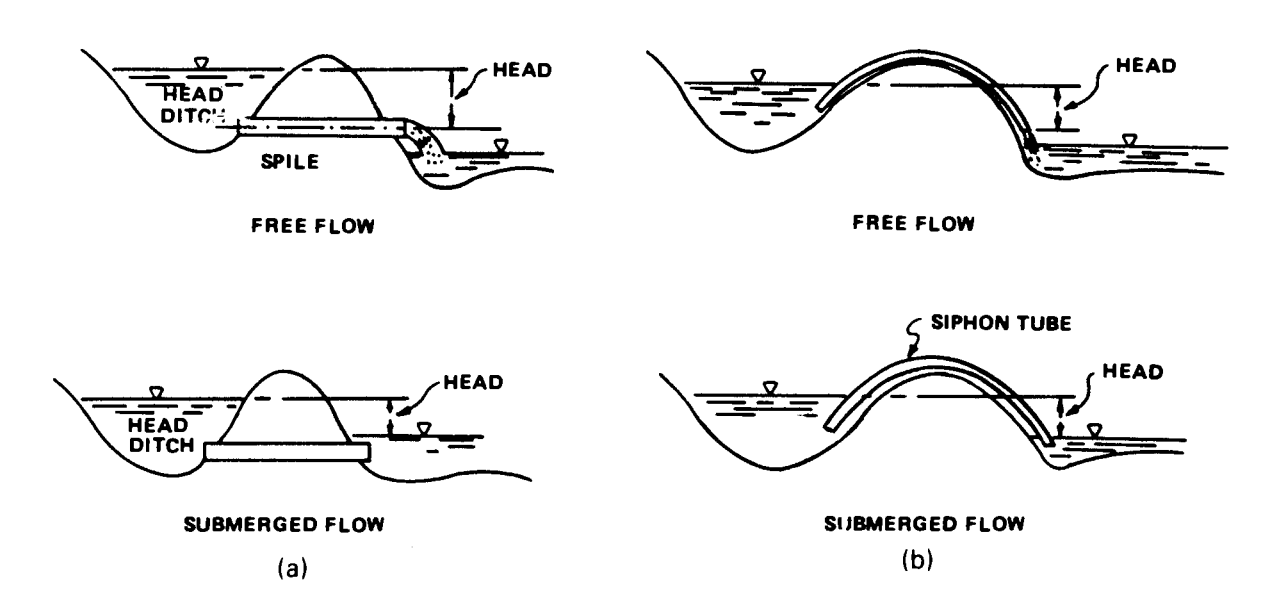


Figure 10.31 Free-flow and submerged-flow conditions for spiles and siphon tubes. (a) Spile. (b) Siphon tube.

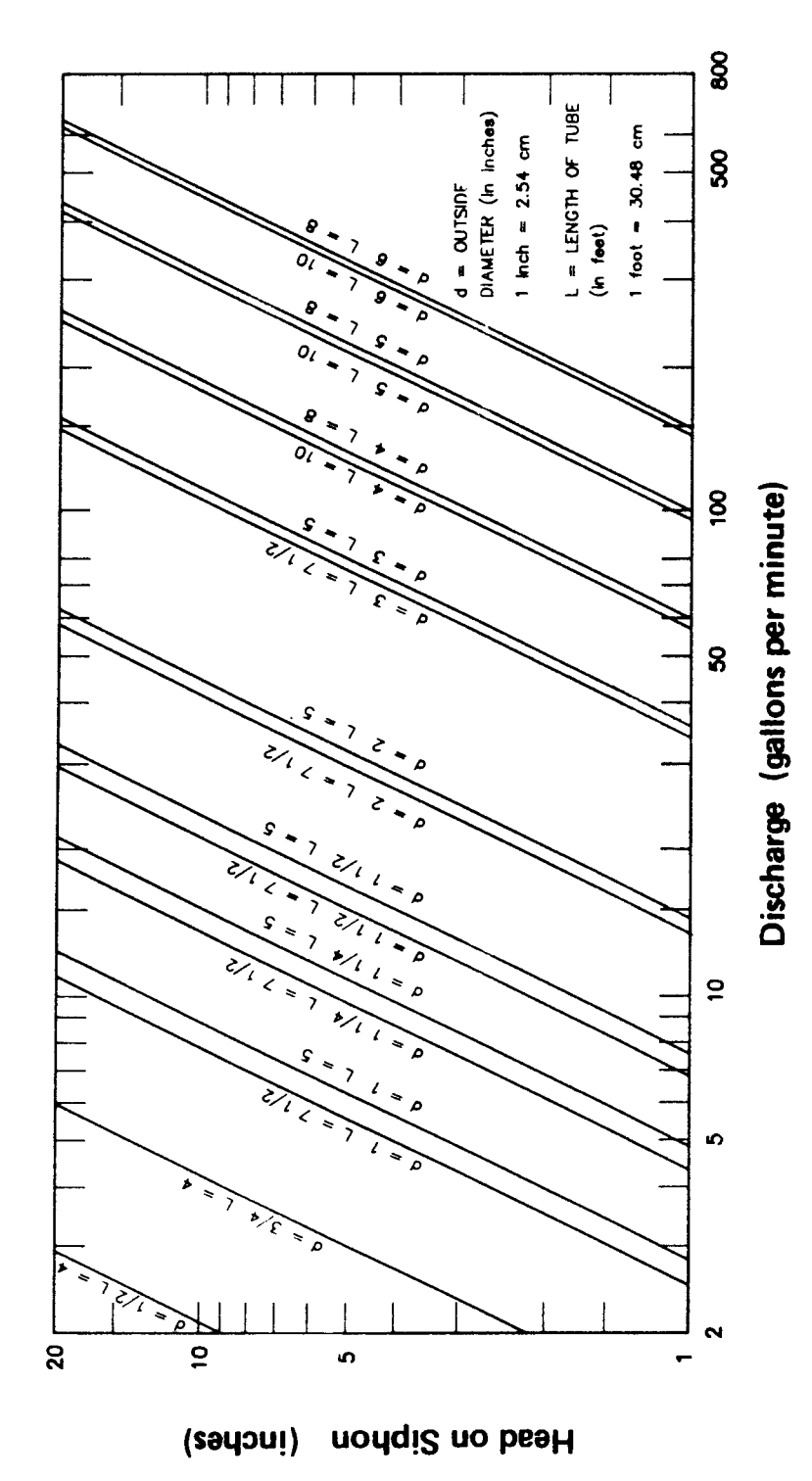


Figure 10.32 Discharge capacity of various diameters and lengths of aluminum siphon tubes. (From U.S. Department of Agriculture, Soil Conservation Service, 1962.)

## **CLOSED CONDUIT IRRIGATION DISTRIBUTION**

## **Low-Pressure Pipeline Systems**

An efficient means of conveying and distributing irrigation water to the farm is through the use of a low-pressure pipeline system. This method practically eliminates evaporation and seepage losses. Also, maintenance work is reduced, water control is easier, and the channel bank weed problem is eliminated.

Low-pressure pipeline systems may be permanent, semiportable, or portable installations. Permanent systems usually consist of buried PVC pipe supply and distribution lines. However, metal, fiber, or concrete pipe also may be used for this type of installation.

In semiportable systems, a buried pipe is used for the supply lines to the individual fields and some type of quick-coupling metal pipe or flexible pipe is laid on the surface to distribute water on the fields. In the fully portable systems, metal or flexible surface pipe is used for both supply and distribution.

Low-pressure pipeline systems must be operated, as the name implies, at low internal pressures. Normally, they are designed for operating heads not to exceed 6 m (20 ft). On sloping land, where excessive pressure heads may be developed, open standpipes or regulating valves are installed to prevent pressure buildup. Pipelines fed directly from pumps should also have facilities for automatically controlling the maximum pressure.

Pipeline systems fed from an open canal, river channel, lake, or other source where trash or debris may collect should be equipped with a trash screen. If the water carries sand or silt, a settling basin may also be needed. If the water source is at a high enough elevation to provide 0.5 m or more of drop at the pipe inlet, a self-cleaning screen can be installed that will require little operating attention. Debris in the pipeline can cause a great deal more trouble and work than manually cleaning a screen.

Measurement of water in low-pressure pipeline systems is just as important as in open-channel systems. Sometimes, the same type of measuring devices that are used in open-channel systems are suitable. For example, a weir or a Parshall flume could be installed at the pipeline inlet structure. Weirs may also be installed in overflow-type standpipes or control boxes. To measure flows in the pipe, some type of flow meter is needed. Several types of meters are manufactured for this purpose.

Where branch lines take off from the main supply line, standpipes or control boxes equipped with gates or valves must be installed to control the flows. Metal slide gates can be used, and automatic control can be provided by installing a float valve arrangement.

There are a number of ways to deliver the water from the pipeline to the field surface. Where permanent buried pipelines deliver the water to the top of the field, riser pipe and alfalfa valves can be used. For the border method of irrigation, these risers should usually be spaced so that there will be a separate valve for each border strip. Where flows of more than about 60 liters/s (2 ft<sup>3</sup>/s)

266

are needed on a border strip, two or more risers should be used to reduce erosion and to provide a more uniform spread of water. For the basin, or level border, method of irrigation, risers are often placed in the ridge at the intersection of four basins and each of the basins is irrigated in turn from the same riser.

If risers and alfalfa valves are being used for hay and pasture crops, they can also be adapted for irrigating furrow row crops by attaching hydrants to the risers and using gated surface pipe to deliver water to each individual furrow. The hydrants and the gated pipe are portable and can be moved from place to place on the field, or from field to field. The risers and alfalfa valves can also be used to deliver water into small level ditches or equalizing basins across the upper end of the furrows. Siphons or spiles can then be used to control the flows into individual furrows in an open-channel system.

When low-pressure pipeline systems are installed for furrow irrigation in orchards, the risers often are extended above the ground surface to form "distribution pots." These pots are equipped with small metal slide gates through which flows to individual furrows are controlled. Generally, the risers are placed in line with the tree rows and one or two furrows on each side of the tree row are fed from a single pot. Another method of controlling the flows in furrow irrigated orchards is the use of a small riser and valve for each furrow instead of large risers and alfalfa valves spaced farther apart. One- to 4-cm-diameter galvanized pipe risers and a simple nonclogging valve are often used.

### **Closed Conduit Hydraulics**

Low-pressure pipeline irrigation systems utilize closed conduits to transport water from the irrigation supply to the individual fields and across the top of the fields (headland facilities). Energy losses occur in the pipeline due to friction and elevational changes. For instance, consider a pipe of constant diameter D, lying on a slope and carrying a discharge as shown in Fig. 10.33. The change in energy in

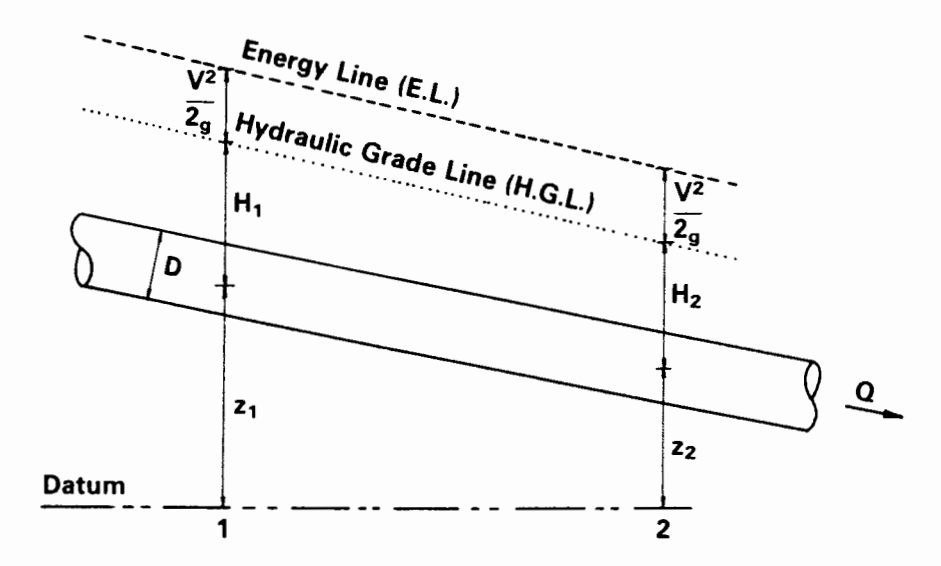


Figure 10.33 Schematic definition sketch for closed conduit flow.

the pipeline between two points, 1 and 2, is described by the Bernoulli equation (Vennard, 1965):

$$Z_1 + H_1 + \frac{v^2}{2g} = Z_2 + H_2 + \frac{v^2}{2g} + h_f$$
 (10.28)

where

Z = elevation above an arbitrary datum, m

H =pressure head defined as the pressure divided by the specific weight of water, m

v = velocity of flow, m/s

 $g = \text{gravitational constant}, 9.81 \text{ m/s}^2$ 

 $h_f$  = frictional headloss, m

If flow is constant in the pipe, Eq. 10.28 can be simplified and rewritten in terms of the pressure head at point 1 as follows:

$$H_1 = H_2 + h_f + (Z_2 - Z_1) (10.29)$$

The pressurized irrigation system designer has two principal hydraulic problems: (1) evaluation of pipe flow without multiple outlets (mains, submains, and auxiliaries), (2) evaluation of pipe flow with multiple outlets (e.g., gated pipe). The basis for design will be the selection of pipe sizes such that energy losses do not exceed prescribed limits, thereby ensuring that efficiencies and uniformities will be high.

Fundamental flow equations. The flow of water in closed conduits is always accompanied by a loss of pressure head due to friction. The magnitude of the loss depends on the interior roughness of the pipe walls, the diameter of the pipe, the viscosity of the water, and the flow velocity. These factors are generally lumped into friction coefficients based on experimental data. However, such coefficients do not completely account for the aging processes, in which deposits and roughening occur with time.

There are several common equations for computing headloss in pipelines. In this text, the Darcy-Weisbach formula will be used:

$$h_f = f \frac{L}{D} \frac{v^2}{2g} \tag{10.30}$$

where

L = pipe length, m

D = pipe diameter, m

f = friction factor

The friction coefficient, f, is determined as a function of the Reynolds number and the relative roughness of the pipe. Standard curves are presented in most hydraulic reference texts in a figure called a "Moody diagram." Absolute roughness,  $\epsilon$ , for various commercial types of pipelines is listed in Table 10.3, while the relative roughness is shown in Fig. 10.34. Since a large part of irrigation piping is plastic, the smooth pipe relationships in the Moody diagram can be used to

**TABLE 10.3** ABSOLUTE ROUGHNESS,  $\varepsilon$ , FOR VARIOUS TYPES OF PIPE

	Values of	s of ε (ft)			
Kind of pipe or lining (new)	Range	Design value			
Brass	0.000005	0.000005			
Copper	0.000005	0.000005			
Concrete	0.001 - 0.01	0.004			
Cast iron					
Uncoated	0.0004 - 0.002	0.0008			
Asphalt-dipped	0.0002 - 0.0006	0.0004			
Cement-lined	0.000008	8000008			
Bituminous-lined	0.000008	0.000008			
Centrifugally spun	0.00001	0.00001			
Galvanized iron	0.0002 - 0.0008	0.0005			
Wrought iron	0.0001 - 0.0003	0.0002			
Commercial and welded steel	0.0001 - 0.0003	0.0002			
Riveted steel	0.003 - 0.03	0.006			
Transite	0.000008	0.000008			
Wood stave	0.0006 - 0.003	0.002			

estimate f (Watters and Keller, 1978). The first step in these calculations is to compute the Reynolds number:

$$R_e = 1.26 \times 10^6 \frac{Q}{D} \tag{10.31}$$

where

 $R_e$  = Reynolds number Q = pipe discharge, lps

 $\widetilde{D}$  = inside pipe diameter, mm

Then the value of f is determined as follows:

$$f = \frac{64}{R_e}$$
 for  $R_e < 2100$  (10.32)

$$f = 0.04 2100 < R_e < 3000 (10.33)$$

$$f = \frac{0.32}{R_e^{0.25}} \qquad 3000 < R_e < 10^5 \tag{10.34}$$

and

$$f = \frac{0.13}{R_e^{0.172}} \qquad 10^5 < R_e < 10^7 \tag{10.35}$$

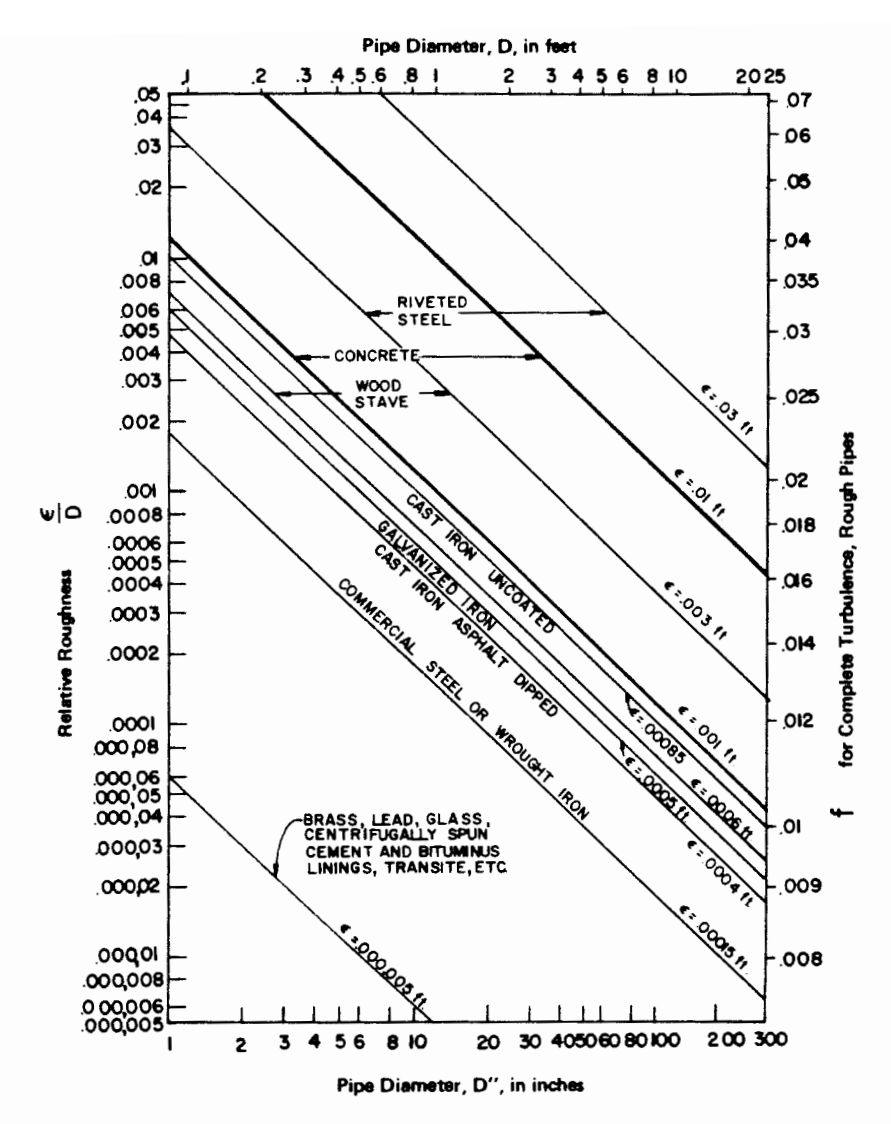


**Figure 10.34** Relative roughness factors for new, clean pipes. (From Moody, 1944.)

Equations 10.32 to 10.35 can be substituted back into Eq. 10.17 resulting in the following simplified expression:

$$h_f = \frac{A_i Q^{P_{i-3}} L}{D^{P_i}} \tag{10.36}$$

where

i	$A_i$	$P_{\iota}$	$R_{\epsilon}$	$P_i - 3$
1	$4.1969 \times 10^{3}$	4.000	$R_e < 2100$	1.000
2	$3.3051 \times 10^{6}$	5.000	$2100 < R_e < 3000$	2.000
3	$7.8918 \times 10^{5}$	4.750	$3000 < R_c < 10^5$	1.950
4	$9.5896 \times 10^{5}$	4.828	$10^{5} < R_{\nu} < 10^{7}$	1.828

Friction losses are also induced in pipelines due to fittings, bends, changes

270 Headland Facilities Chap. 10

in cross-sectional area, and entrances. These losses ( $h'_f$  in meters) are generally evaluated as a function of velocity head in the pipe as follows:

$$h_f' = K_f \frac{v^2}{2g} ag{10.37}$$

The  $K_f$  values for various conditions can be summarized as follows (Pair et al., 1975).

- 1. Entrances: inward-projecting pipe:  $K_F = 0.78$  square-edged inlets:  $K_F = 0.50$  slightly rounded inlets:  $K_F = 0.23$  bell-mouthed inlets:  $K_F = 0.04$
- 2. Bends: sharp 90°:  $K_F = 1.50$ ; long 90°:  $K_F = 0.25$  sharp 60°:  $K_F = 1.20$ ; long 60°:  $K_F = 0.20$  sharp 30°:  $K_F = 0.90$ ;
- 3. Sudden enlargements: (v = velocity of smaller pipe)

$$K_F = \left[1 - \frac{(d_1)^2}{(d_2)^2}\right]^2 \tag{10.38}$$

where  $d_1 = \text{small-pipe diameter (ID)}$  $d_2 = \text{large-pipe diameter (ID)}$ 

4. Sudden contractions (v = velocity of smaller pipe)

$$0.10 < K_F < 0.50$$

5. Irrigation fittings (see Table 10.4)

Head loss in pipes with multiple, equally spaced outlets. The flow of water in a pipe having multiple, equally spaced outlets will have less head loss than a similar pipe transmitting the entire flow over its length because the flow steadily diminishes each time an outlet is passed. To determine the actual head loss, computations should start at the distal outlet and work upstream utilizing one of the equations just discussed. It should be noted that energy losses due to structure of the outlet itself are usually neglected. Christiansen (1942) developed the concept of an "F factor" which accounts for the effect of the outlets. When the first outlet is one outlet spacing from the lateral or manifold inlet,

$$F = \frac{1}{P_i - 2} + \frac{1}{2N} + \frac{\sqrt{P_i - 2}}{6N^2}$$
 (10.39)

where F is the fraction of the head loss under constant discharge conditions expected with the multiple outlet case, and N is the number of outlets along the pipe.

In many cases, the first outlet is only one-half the spacing from the inlet end. In this case a different F factor (F') is defined as

$$F' = \frac{2N}{2N-1} F - \frac{1}{2N-1} \tag{10.40}$$

**TABLE 10.4** VALUES OF THE COEFFICIENT,  $K_F$ , FOR VARIOUS IRRIGATION FITTINGS AND DIAMETERS

			Nomi	nal diamete	er (mm)					
Fitting or valve	76.2	101.6	127	152.4	177.8	203.2	254			
Bends										
Return flanged	0.33	0.30	0.29	0.28	0.27	0.25	0.24			
Return screwed	0.80	0.70								
Elbows										
Regular flanged 90°	0.34	0.31	0.30	0.28	0.27	0.26	0.25			
Long radius flanged 90°	0.25	0.22	0.20	0.18	0.17	0.15	0.14			
Long radius flanged 45°	0.19	0.18	0.18	0.17	117	0.17	0.16			
Regular screwed 90°	0.80	0.70								
Long radius screwed 90°	0.30	0.23								
Regular screwed 45°	0.30	0.28								
Tees										
Flanged line flow	0.16	0.14	0.13	0.12	0.11	0.10	0.09			
Flanged branch flow	0.73	0.68	0.65	0.60	0.58	0.56	0.52			
Screwed line flow	0.90	0.90								
Screwed branch flow	1.20	1.10								
Valves										
Globe flanged	0.70	6.3	6.0	5.8	5.7	5.6	5.5			
Globe screwed	6.0	5.7								
Gate flanged	0.21	0.16	0.13	0.11	0.09	0.075	0.06			
Gate screwed	0.14	0.12								
Swing check flanged	2.0	2.0	2.0	2.0	2.0	2.0	2.0			
Swing check screwed	2.1	2.0								
Angle flanged	2.2	2.1	2.0	2.0	2.0	2.0	2.0			
Angle screwed	1.3	1.0			•					
Foot	0.80	0.80	0.80	0.80	0.80	0.80	0.80			
Strainers—basket type	1.25	1.05	0.95	0.85	0.80	0.75	0.67			

Source: From U.S. Department of Agriculture, Soil Conservation Service (1960).

The pressure head loss in the pipe having multiple outlets is found by computing the head loss using the inlet discharge and then multiplying this value by F or F'.

The flow conditions in lateral and manifold lines are generally steady and spatially varied, with decreasing discharge along the line (Wu and Gitlin, 1975). Under these conditions, the energy gradient will not be linear as implied by Eq. 10.28, but will be of an exponential type.

The total head loss,  $h_f$ , at the end of a multiple outlet pipe is found as follows:

$$h_f = \frac{A_i (q/s_s)^{P_i - 3}}{D^{P_i}} \frac{L^{P_i - 2}}{P_i - 2}$$
 (10.41)

where  $A_i$  and  $P_i$  are defined from inlet Reynold numbers

q = average outlet discharge, liters/s

 $s_s$  = outlet spacing, m

D = pipe diameter, mm

The friction drop ratio,  $R_l$ , is defined as the friction loss at any point l along the pipe from the inlet,  $(h_f)_l$ , divided by the total loss,  $h_f$ .

$$R_{l} = \frac{(h_{f})_{l}}{h_{f}} = 1 - \left(\frac{L - l}{L}\right)^{P_{l-2}}$$
 (10.42)

The pressure distribution in the lateral or manifold can be described by combining Eqs. 10.29 and 10.30 and expressing the result in terms of the pressure at a distance l meters from the pipe inlet:

$$H_{l} = H_{1} - R_{l}h_{f} + (Z_{1} - Z_{2})\frac{l}{L}$$
 (10.43)

where  $H_1$  is the pressure at the inlet in meters, and  $Z_1$ , and  $Z_2$  are the elevations at the pipe inlet and its distal end, respectively, in meters. Equation 10.43 incorporates two assumptions that need mention. In the development of Eq. 10.42, the outlet discharge is assumed uniform. The relationship between pressure and discharge for most closed conduits with multiple, equally spaced outlets is described by

$$q = K_d H^c (10.44)$$

where

q = outlet discharge, liters/s

 $K_d$  = coefficient of discharge

 $c = \text{discharge exponent}, \ 0 < c < 1.0 \ \text{for most outlets and quite commonly}, \ c = 0.5$ 

Thus a discharge variation is present and can be estimated from Eqs. 10.43 and 10.44. The evaluation of the results by Wu and Gitlin (1975) show reasonable accuracy. The simplicity of the analysis in design or evaluation computations support its general use. It has been assumed in the preceding analysis that kinetic-energy change is negligible. Usually, the velocity head in irrigation systems is relatively small in comparison to pressure and elevation changes. This assumption makes the estimation of pressure in Eq. 10.43 conservative and tends to offset the effects of assuming uniform discharge from the outlets.

# Valves and Hydrants

The following information and design data are taken from the report "Concrete Pipe for Irrigation" by Arthur F. Pillsbury (1953).

Alfalfa valves (Fig. 10.35) are used to distribute water into border strips, checks, or large basins. Alfalfa valves should be placed approximately 3 in. (7 to 8 cm) below the ground surface to help minimize erosion. The flow rate for an alfalfa valve can be computed by the following relationship, which is similar to Eq. 4.42:

$$Q = C_d A (2g \Delta h)^{0.5} (10.45)$$

where the coefficient of discharge,  $C_d$ , is equal to 0.7, A is defined as the circumference times the amount the valve is opened, and  $\Delta h$  is the difference in head

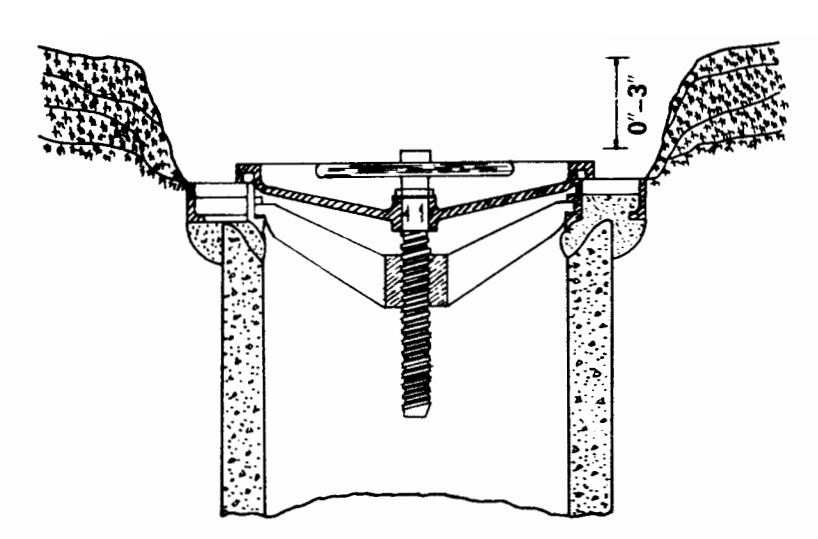


Figure 10.35 Cross-sectional elevation of typical alfalfa valve hydrant.

between the riser ( $h_u$  in Eq. 4.42) and the depth of water above the alfalfa valve ( $h_d$  in Eq. 4.42). Distribution to furrows can be accomplished by placing an adaptor hydrant head on the alfalfa valve which can distribute the flow through a pipe or gate pipeline (Fig. 10.36), as well as being used to control the discharge onto basinor border-irrigated fields.

Orchard valves (Fig. 10.37) are used for single ditches, large furrows, or into basins, checks, or border strips. Orchard valves can also be adapted for furrow or pipe irrigation with a portable hydrant or adaptor and a sheet metal stand. The capacity of an orchard valve can be computed using  $C_d = 0.6$ .

In a low-pressure system, risers without a valve may be used to distribute the flow. A riser hydrant consists of a riser with two or more slide gates to discharge the flow into a furrow (Fig. 10.38). A riser hydrant is used where the pipeline is always under low pressure, and no orchard valve in the riser is necessary. The design capacity of slide gates is obtained from the assumption that velocities below 90 cm/s will not cause excessive erosion, but the erosion potential is highly dependent on the soil type and vegetation, so that special measures may be required to prevent, or at least minimize, the degree of erosion.

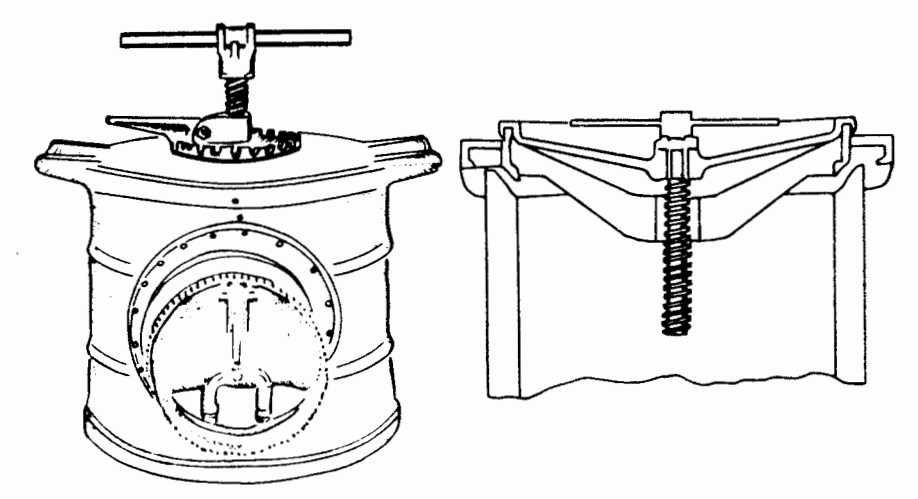
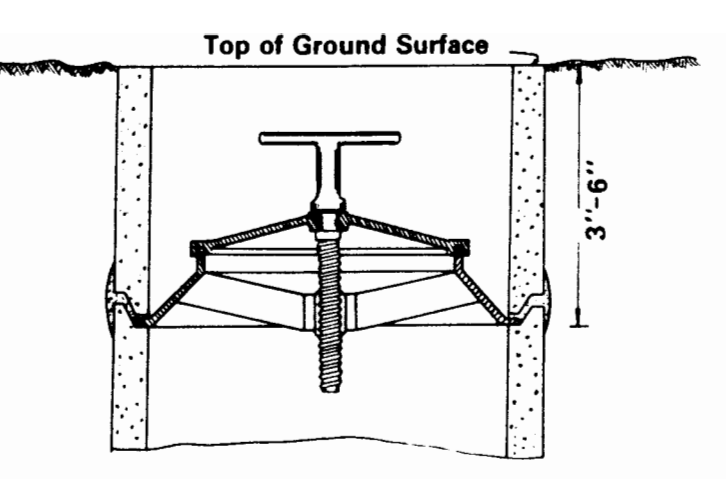


Figure 10.36 Portable hydrant and alfalfa valve working together, the hydrant being quickly attached for flow control.



**Figure 10.37** Cross-sectional elevation of an orchard valve hydrant.

An open pot hydrant is a combination of an orchard valve and a riser hydrant (Fig. 10.39). The orchard valve is usually adjusted to keep the water level 2 to 8 cm above the slide gate outlets. Such low head simplifies regulation of the outlets. The orchard valve regulates the flow into the pot, and the slide gates regulate the flow into individual furrows. For best control, the orchard valve is adjusted to keep the water surface only 2 to 5 cm above the slide gates. The slide gates should be located on the inside of the pots and at ground surface elevation, to minimize erosion of the adjacent soil. The size of pot depends on the number and size of the side gates to be used. Again,  $C_d = 0.6$  is used for design purposes.

A capped riser or pot hydrant is similar to the riser hydrant in Fig. 10.38 but is more permanently capped over to prevent debris from falling in and plugging the slide gates. Slide gate outlets and the concrete cap are mortared to a length of ordinary concrete irrigation pipe. Having slide gates in a short section of pipe with larger diameter than the riser makes the riser hydrant a "capped pot hydrant." The disadvantages of this structure are less control of the flow, and more erosion of adjacent soil since the slide gates must be on the outside.

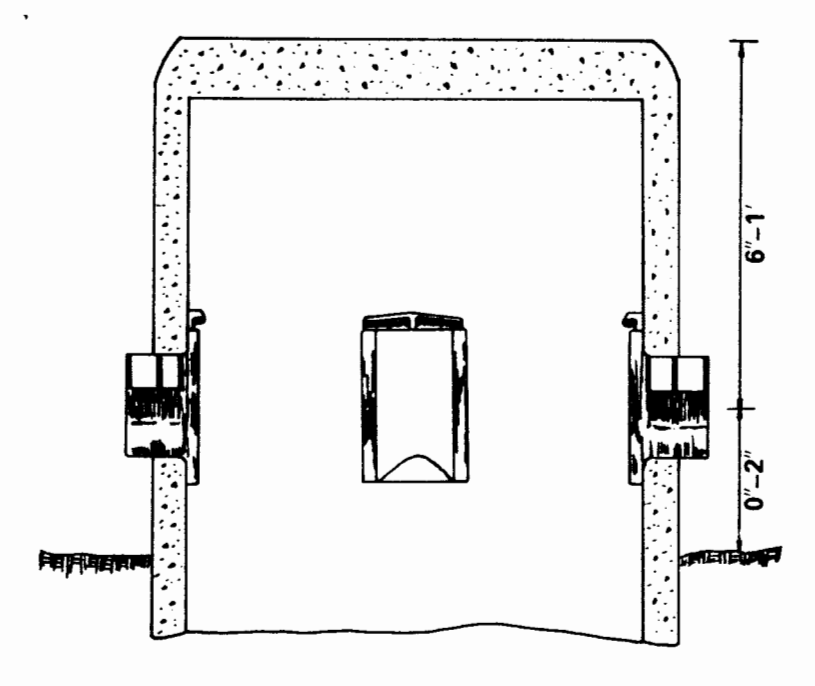


Figure 10.38 Riser hydrant.

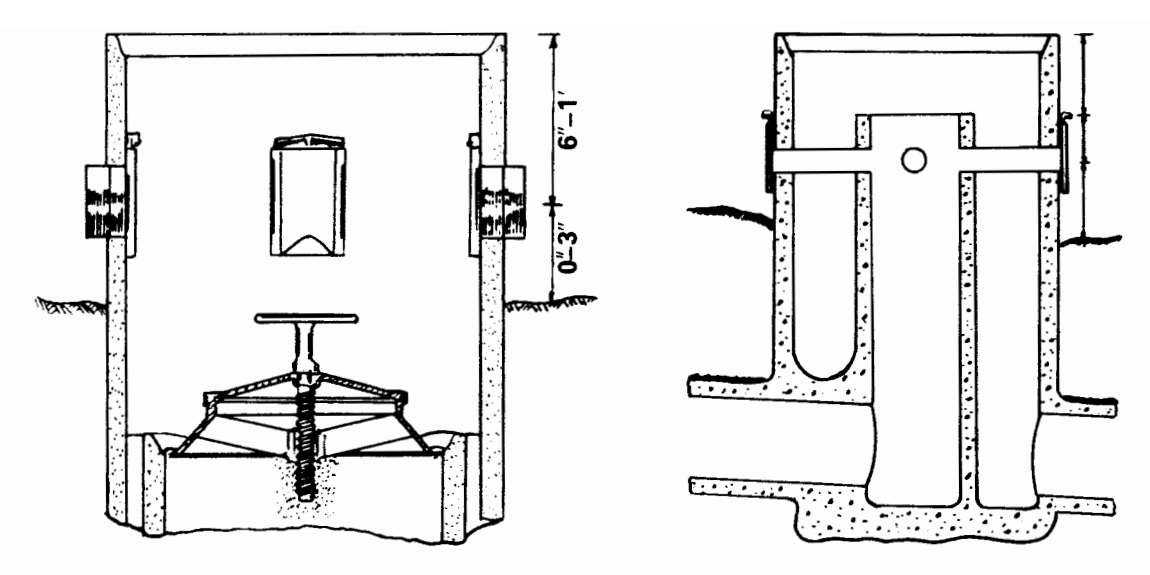


Figure 10.39 Open-pot hydrant with orchard valve on top of riser and three slide gate outlets on the pot.

Figure 10.40 Overflow pot hydrant.

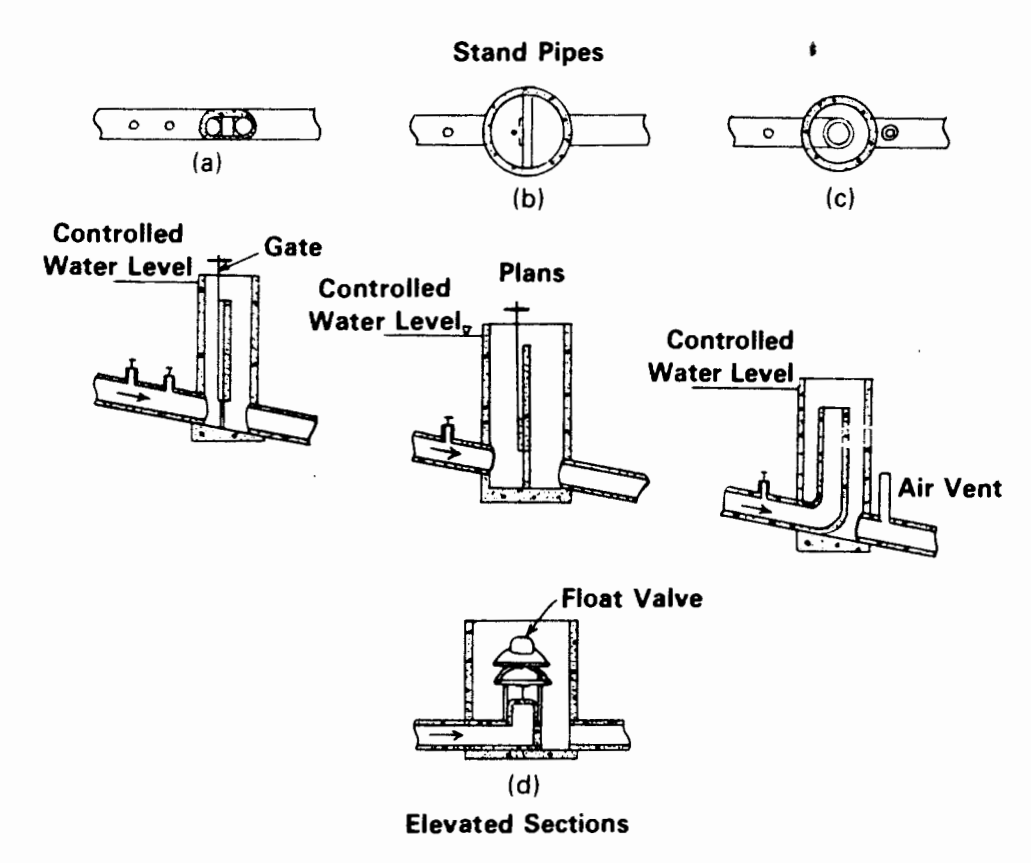


Figure 10.41 Four types of pressure relief and water-level-control stand pipes. (a) Gate-operated stand pipe made of precast "T" and branch pipe section elements. (b) Large-diameter basin-type stand pipe with partition wall (the partition wall may be with or without a control gate). (c) Stand pipe made of two upright pipes (internal pipe is an extension of the upstream pipe and external to the downstream pipe. (d) Stand pipe with a float valve for automatic control of the water level in accordance with the downstream water requirement.

Overflow pot hydrants are best for use on steep slopes. The overflow pot hydrant is a combination of the open pot hydrant and the overflow stand (Fig. 10.40). This structure simplifies regulation of small flows where pipelines are on relatively steep slopes.

Overflow stands (Fig. 10.41) can operate both as a check and a drop structure in addition to the usual functions of a stand. As a check structure, it regulates pressures to maintain constant upstream flow out of hydrants and/or into laterals. As a drop structure, it creates a drop in the hydraulic gradient, thus limiting pipeline pressures. This structure is not required on flat areas or on very slight slopes.

#### **EXAMPLE PROBLEMS**

#### Example 10.1

A new turnout structure is to be constructed from an earthen irrigation canal that has a normal water surface (NWS) elevation of 432.6 m, a maximum water surface (MWS) elevation of 432.8 m, and a bed elevation of 431.7 m. There is an existing control structure 875 m downstream from the site of this new turnout structure, and the water surface elevation corresponding to a design discharge of 70 liters/s (2.47 ft<sup>3</sup>/s) is 431.4 m. The structures will include a trashrack, screens, circular control gate, pipeline, and concrete-lined channel, as shown in Fig. 10.42.

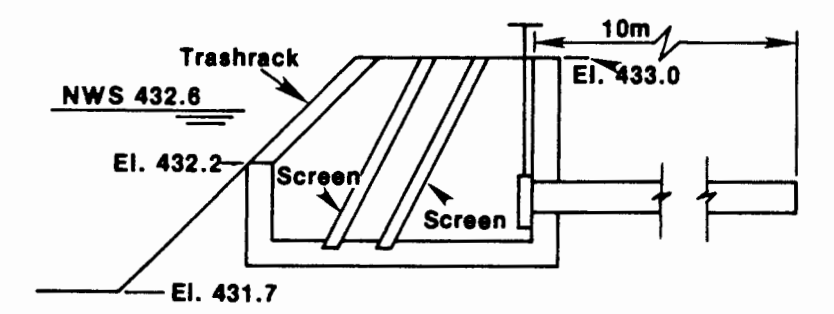


Figure 10.42 Definition sketch for example turnout structure.

Trashrack. A multiple inclined screen box structure similar to Fig. 10.12 will be designed consisting of a trashrack, two screens, and a circular control gate. The crest elevation of the inlet wall should be set so that the sediment bedload in the earthen canal will not enter the turnout structure. For this example problem, this crest elevation will be set at 432.2 m; however, an elevation of 432.0 m might also be satisfactory. The floor elevation of the turnout structure will be set later.

This irrigation conveyance system will have to be designed using the canal normal water surface elevation of 432.6 m. Thus the depth of flow at the trashrack will be 0.4 m (432.6 - 432.2). The trashrack will be constructed of 5-mm  $\times$  5-cm steel bars turned on edge and spaced on 25-mm centers. From Eq. 10.1,

$$A_r = \frac{5 \text{ mm}}{25 \text{ mm}} = 0.2$$

$$\frac{L}{T} = \frac{50 \text{ mm}}{5 \text{ mm}} = 10$$

From Fig. 10.1, for  $A_r = 0.2$  and L/T = 10,

$$K_{-} = 0.28$$

The average velocity through the trashrack openings should be 60 cm/s or less. This corresponds to an approach velocity of 48 cm/s  $[60(1 - A_r)]$ . The minimum width,  $W_{\min}$ , of the trashrack can be calculated from the continuity equation:

$$0.070 \text{ m}^3/\text{s} = W_{\min}(0.4 \text{ m})0.48 \text{ m/s}$$

Then solving for  $W_{\min}$  yields

$$W_{\min} = 0.36$$

Therefore, a trashrack width of 40 cm will be used. The approach velocity to the trashrack is

$$V = \frac{Q}{A} = \frac{0.070 \text{ m}^3/\text{s}}{0.4 \text{ m} (0.4 \text{ m})} = 0.44 \text{ m/s}$$

and the velocity head is

$$\frac{V^2}{2g} = \frac{(0.44 \text{ m/s})^2}{2(9.81 \text{ m/s}^2)}$$
$$= 0.0098 \text{ m}, \text{ say } 10 \text{ mm}$$

The head loss through the trashrack is

$$(h_L)_T = K_r \frac{V^2}{2g}$$
  
= 0.28 (10 mm)  
= 2.8 mm, say 3 mm

Therefore, the elevation downstream from the trashrack is 432.597 m (432.6 - 0.003).

**Screens.** Two screens will be used, with the first having a closed area coefficient,  $A_r$ , of 0.30, while  $A_r = 0.40$  for the second screen. (Manufacturers' catalogs should be consulted for this information.) Assume that the approach velocity for each screen is the same as for the trashrack, which will result in the head loss being overestimated since the floor elevation in the turnout structure is lower than the inlet crest. From Eq. 10.1, using L/T = 1.0,

$$K_r = 0.58$$
 (first screen)  
 $K_r = 1.03$  (second screen)  
 $h_L = 0.58(10 \text{ mm})$  (first screen)  
 $= 5.8 \text{ mm}$ , say 6 mm  
 $h_L = 1.03(10 \text{ m})$  (second screen)  
 $= 10.3 \text{ mm}$ , say 10 mm

Total head loss for the screens is 16 mm and the water surface elevation downstream from the second screen is 432.581 m (432.597 - 0.016).

Concrete-Lined Channel. Before designing the size of the circular control gate and the pipeline, the concrete-lined channel will be designed because the head loss will probably be much greater. Figures 10.15 to 10.18 can be used. For example, using Fig. 10.15, for a channel bottom width of 1.0 ft (30.5 cm) and a discharge of 2.47 ft<sup>3</sup>/s (70 liters/s):

$$S_0 = \begin{cases} 0.0001 & \text{for water depth} = 1.25 \text{ ft} \\ 0.001 & \text{for water depth} = 0.75 \text{ ft} \end{cases}$$

For S = 0.001, the head loss in 860 m would be 0.86 m, which would result in a water surface elevation downstream from the pipeline of 431.96 m (431.1 m + 0.86 m), which would be satisfactory for this problem.

Use a concrete-lined channel having a 30-cm bottom width, z = 1.25, water depth = 22.5 cm, and freeboard = 7.5 cm.

$$A = 0.30 \text{ m}(0.225 \text{ m}) + 1.25(0.225 \text{ m})0.225 \text{ m}$$

$$= 0.0675 \text{ m}^2 + 0.0633 \text{ m}^2 = 0.1303 \text{ m}^2$$

$$P = 0.30 \text{ m} + 2(0.225 \text{ m}) \sqrt{(1.25)^2 + (1)^2}$$

$$= 1.02 \text{ m}$$

$$R = \frac{A}{P} = \frac{0.1303 \text{ m}^2}{1.02 \text{ m}} = 0.1277 \text{ m}$$

Using Eq. 10.5 gives us

$$S_0 = \frac{Q^2 n^2}{A^2 R^{4/3}}$$

$$= \frac{(0.070)^2 (0.014)^2}{(0.1303)^2 (0.1277)^{4/3}}$$

$$= 8.743 \times 10^{-4}$$

In approximately 862 m of channel length, the energy loss would be

$$h_L = 862 \text{ m}(8.743 \times 10^{-4}) = 0.754 \text{ m}$$

Therefore, the water surface elevation at the beginning of this concrete-lined channel would be 432.154 (431.4 + 0.754 m).

Circular Gate and Pipeline. The same diameter will be used for the circular control gate and the pipeline. The required size will be dependent on the available head loss, which in this case is 0.427 m (432.581 - 432.154). Equation 10.45 will be used for the circular control gate, where  $C_d$  normally varies between 0.6 and 0.8, but  $C_d = 0.6$  will be used as a conservative estimate for this problem. Equations 10.31 and 10.36 will be used for calculating the energy loss in the pipeline,  $K_F = 0.50$  will be used for the entrance loss, and  $K_F = 1.0$  will be used for the exit loss. The computations for various diameters are summarized in Table 10.5.

The water surface elevation upstream from the circular control gate is 432.581, while the water surface elevation downstream from the pipeline (which corresponds with the water surface elevation at the head of the concrete-lined channel) is 432.154. Therefore, the maximum allowable head loss for the circular gate and pipeline is 0.427 m (432.581 m - 432.154 m). Consequently, the 30-cm-diameter circular gate and pipeline will be used because the total head loss is 0.239 m. The difference between 0.427 m and 0.239 m (0.188 m) is a measure of how much clogging of the trashrack and screens can occur and still maintain the design discharge capacity.

The width of the trashrack was established as 40 cm. Although the diameter of the circular gate is only 30 cm, the manufacturers' catalogs would have to be consulted to

TABLE 10.5 SUMMARY OF HEAD LOSS CALCULATIONS FOR EXAMPLE 10.1

	Diameter (cm)			
Item	10	20	30	40
Circular gate				
$C_d$	0.6	0.6	0.6	0.6
$\Delta h$ (m)	11.25	0.703	0.139	0.044
Pipeline				
Entrance				
$K_F$	0.5	0.5	0.5	0.5
$h_{L}(\mathbf{m})$	2.024	0.126	0.025	0.008
Friction				
$R_e$	$8.82 \times 10^{5}$	$4.41 \times 10^{5}$	$2.94 \times 10^{5}$	$2.205 \times 10^{5}$
f	0.01235	0.0139	0.0149	0.01566
<i>L</i> (m)	10.0	10.0	10.0	10.0
L/D	100.0	50.0	33.3	25.0
$V^2/2g$	4.049	0.253	0.050	0.016
$h_f(\mathbf{m})$	4.999	0.176	0.025	0.001
Exit				
$K_F$	1.0	1.0	1.0	1.0
$h_L$ (m)	4.049	0.253	0.050	0.016
Total loss (m)	22.322	1.258	0.239	0.069

determine whether or not the gate frame is 40 cm wide, or less. If so, the width of the turnout structure would be 40 cm. If the gate frame is wider than 40 cm, the width of the turnout structure would be made wide enough to accommodate the gate frame.

Finally, the floor elevation of the turnout structure must be set. The primary consideration is having the crown of the pipeline below the floor of the concrete-lined channel, which is at elevation 431.929 m (432.154 m - 0.225 m). The invert of the pipeline would then be at elevation 431.629 m (431.929 m - 0.300 m), or lower. Again, the gate manufacturers' catalogs would have to be consulted to determine how much space is required below the pipeline invert to accommodate the gate frame. Assume that the floor elevation of the turnout structure can be 431.5 m and then let the pipeline invert be 431.6 m.

The final design is shown in Fig. 10.43. Note that the length of the stilling basin downstream from the pipeline is relatively short, only 50 cm. This allows the far wall to act as an impact wall for the jet issuing from the pipeline, thereby dissipating the excess energy and minimizing the turbulence that will occur in the concrete-lined channel.

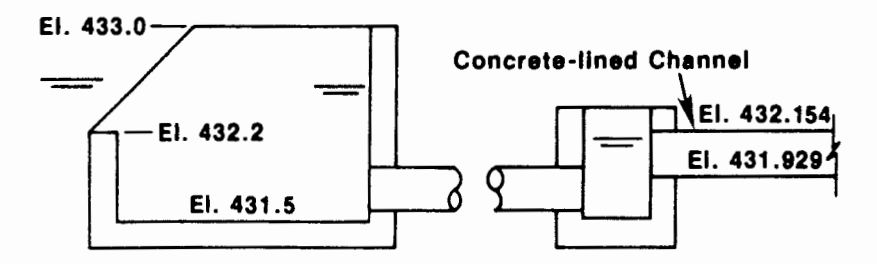


Figure 10.43 Final design for example turnout structure.

#### Example 10.2

A vertical-drop structure is needed along an irrigation channel. The maximum discharge

rate is 240 liters/s. The inlet floor elevation is 65.5 m and the tailwater elevation is 64.8 m. The maximum width that can be readily accommodated is 50 cm.

Using the maximum width, the unit discharge is

$$q = \frac{240 \text{ liters/s}}{50 \text{ cm}} = \frac{0.240 \text{ m}^3/\text{s}}{0.50 \text{ m}} = 0.48 \frac{\text{m}^3/\text{s}}{\text{m}}$$

$$V_c = \frac{\sqrt[3]{q^2}}{g} = \frac{\sqrt[3]{(0.48 \text{ m}^2/\text{s})^2}}{9.81 \text{ m/s}^2} = 0.286 \text{ m}$$

The primary difficulty in this problem is that the drop height, H, is not specified. Therefore, a trial-and-error solution is required. As an initial trial, assume that H = 1.0 m, thereby resulting in a floor elevation of 64.5 m for the vertical-drop structure.

The results of Aletraris (1983) will be used in the design. From Eq. 10.10,

$$\frac{y_1}{H} = 0.53 \left(\frac{y_c}{H}\right)^{1.319} = 0.53 \left(\frac{0.288 \text{ m}}{1 \text{ m}}\right)^{1.319} = 0.102$$

Since H = 1 m,  $y_1 = 0.102$  m, the ratio  $y_2/y_1$  can be computed from Eq. 10.18 after calculating the Froude number,  $F_1$ .

$$F_{1} = \frac{\sqrt{V}}{gy_{1}} = \frac{\sqrt{q/y_{1}}}{gy_{1}} = \frac{\sqrt{q}}{gy_{1}^{2}} = \frac{\sqrt{0.48 \text{ m}^{2}/\text{s}}}{9.81 \text{ m/s}^{2}(0.102 \text{ m})^{2}} = 2.17$$

$$\frac{y_{2}}{y_{1}} = \frac{1}{2}\sqrt{1 + 8F_{1}^{2} - 1}$$

$$= \frac{1}{2}\sqrt{1 + 8(2.17)^{2} - 1} = 2.61$$

Therefore.

and

$$y_2 = y_1 \frac{y_2}{y_1} = 0.102 \text{ m}(2.61) = 0.266 \text{ m}$$

#### Example 10.3

The range of allowable size distributions for a filter material is to be determined. A sample of a local source of riprap was run through a series of sieves and the weight of sample retained on each sieve is listed below. A representative sample of the soil through which the channel is to be excavated yielded the size distribution listed in the following table.

Channel excavation		Riprap		
Sieve opening (in.)	Weight retained (g)	Sieve opening (in.)	Weight retained (lb)	
0.50	68	18	77	
0.25	141	15	108	
0.125	182	12	124	
0.08	217	9	67	
0.03	161	6	34	
0.02	133	3	21	
0.01	90	2	10	
	992	1	4	
			445	

For a given open channel, it was determined that the required riprap size at the design discharge have a minimum value of  $D_{50}$  of 11.5 in. First of all, a determination must be made if a filter layer is required. Then, if a filter is required, the gradation requirements for the filter layer must be established to ensure that the base material will not be eroded.

The criteria that are frequently used in determining whether a filter layer is required can be defined by Eqs. 10.19 to 10.21. If a filter layer is required, Eqs. 10.22 to 10.27 can be used to determine the size distribution of the particles for the filter material.

From the data obtained by the sieve analysis, the values of  $D_{15}$ ,  $D_{50}$ , and  $D_{85}$  can be calculated.

Channel excavation (in.)	Riprap (in.)
$D_{15} = 0.0245 D_{50} = 0.11$	$D_{15} = 8.8 D_{50} = 14.0$
$D_{85} = 0.335$	$D_{85} = 18.3$

These values are then used in Eqs. 10.19 to 10.21 to determine if a filter is needed.

$$\frac{D_{15} \text{ riprap}}{D_{85} \text{ base}} < 5 \frac{8.8 \text{ in.}}{0.335 \text{ in.}} = 26.3 \text{ which is not less than 5}$$

$$5 < \frac{D_{15} \text{ riprap}}{D_{85} \text{ base}} < 40 \frac{8.8 \text{ in.}}{0.0245 \text{ in.}} \stackrel{\text{t}}{=} 359 \text{ which is not less than 40}$$

$$\frac{D_{50} \text{ riprap}}{D_{50} \text{ base}} < 40 \frac{14 \text{ in.}}{0.11 \text{ in.}} = 127 \text{ which is not less than 40}$$

Therefore, it can be concluded that a filter is required.

Knowing that a filter is required, the next step is to determine the values of  $D_{15}$ ,  $D_{50}$ , and  $D_{85}$  for a suitable filter material. By using Eqs. 10.22 to 10.27, these gradation values can be calculated. From Eq. 10.22,

$$\frac{D_{15} \text{ riprap}}{D_{05} \text{ filter}} < 5$$

Solving for  $D_{85}$  filter, this becomes

$$D_{\rm ks}$$
 filter  $> \frac{D_{\rm 15} \text{ riprap}}{5}$ 

Therefore,

$$D_{85}$$
 filter  $> \frac{8.8 \text{ in.}}{5} > 1.76 \text{ in.}$ 

So  $D_{85}$  filter must be greater than 1.76 in.

From Eq. 10.23,

$$5 < \frac{D_{15} \text{ riprap}}{D_{15} \text{ filter}} < 40$$

Solving for  $D_{15}$  filter, this becomes

$$D_{15}$$
 filter  $< \frac{D_{15} \text{ riprap}}{5}$ 

and

$$D_{15}$$
 filter  $> \frac{D_{15} \text{ riprap}}{40}$ 

Therefore,

$$D_{15}$$
 filter  $< \frac{8.8 \text{ in.}}{5} = 1.76 \text{ in.}$ 

and

$$D_{15}$$
 filter  $> \frac{8.8 \text{ in.}}{40} = 0.22 \text{ in.}$ 

From Eq. 10.24,

$$\frac{D_{50} \text{ riprap}}{D_{50} \text{ filter}} < 40$$

Solving for  $D_{50}$  filter,

$$D_{50} > \frac{D_{50} \operatorname{riprap}}{40}$$

$$D_{50}$$
 filter  $> \frac{14.0 \text{ in.}}{40} = 0.35 \text{ in.}$ 

Therefore, the filter that will work with the riprap is described as follows: 0.22 in.  $< D_{15}$  filter < 1.76 in.;  $D_{50}$  filter > 0.35 in.;  $D_{85}$  filter > 1.76 in. From Eq. 10.25,

$$\frac{D_{15} \text{ filter}}{D_{85} \text{ base}} < 5$$

Solving for  $D_{15}$  filter, we have

$$D_{15}$$
 filter < 5 ( $D_{85}$  base)

Therefore,

$$D_{15}$$
 filter < 5 (0.335 in.) = 1.68 in.

From Eq. 10.26,

$$5 < \frac{D_{15} \text{ filter}}{D_{15} \text{ base}} < 40$$

Solving for  $D_{15}$  filter, this becomes

$$D_{15}$$
 filter  $> 5(D_{15}$  base)

and

$$D_{15}$$
 filter  $< 40(D_{15}$  base)

Therefore,

$$D_{15}$$
 filter > 5(0.0245) = 0.123 in.

$$D_{15}$$
 filter  $< 40(0.0245) = 0.98$  in.

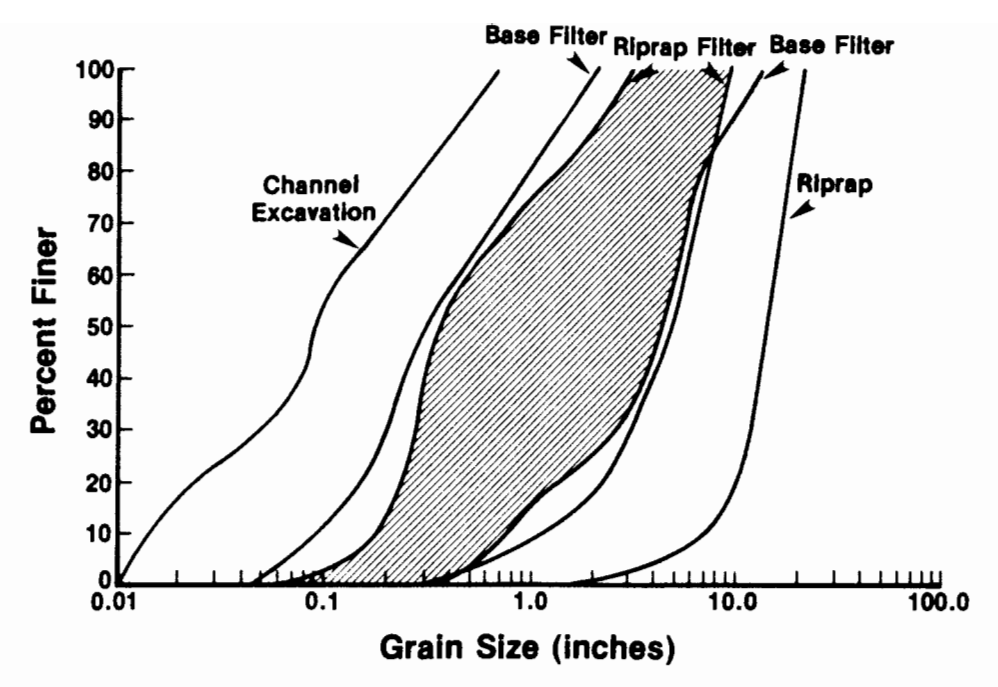


Figure 10.44 Distribution of filter grain sizes in Example 10.3.

From Eq. 10.27,

$$\frac{D_{50} \text{ filter}}{D_{50} \text{ base}} < 40$$

Solving for  $D_{50}$  filter, we have

$$D_{50}$$
 filter < 40 ( $D_{50}$  base)

so

$$D_{50}$$
 filter  $< 40(0.11) = 4.4$  in.

Therefore, the filter that must be used with the base is described as follows:

$$0.123 \text{ in.} < D_{15} \text{ filter} < 0.98 \text{ in.} D_{50} \text{ filter} < 4.4 \text{ in.}$$

To obtain a better feeling for how all the numbers are related to each other, they are plotted in Fig. 10.44. Here the upper and lower limits of  $D_{15}$ ,  $D_{50}$ , and  $D_{85}$  that were calculated are plotted and smooth curves are drawn through the points. The area between the highest minimum-size curve and the lowest maximum-size curve (crosshatched area) is the range through which the values for the filter material may vary.

#### Example 10.4

A 20-cm-diameter pipeline is to be laid horizontally ( $S_0 = 0$ ) across the head of a furrow-irrigated field. Gated slots are spaced 80 cm apart along this pipeline, which corresponds with the furrow spacing. One set consists of a 60-m field width. The furrow inflow is to be 1.2 liters/s. When a gated slot is fully open, the discharge rating is

$$q = 0.82H^{0.5}$$

where q is in liters/s and H is in meters. What is the minimum required pressure head at the inlet to this gated pipeline?

The minimum pressure will occur at the end of the gated pipeline. The required pressure head at the last gated slot will be

$$H = \left(\frac{q}{0.82}\right)^2 = \left(\frac{1.2 \text{ liters/s}}{0.82}\right)^2 = 2.142 \text{ m}$$

First, the friction loss in the pipeline will be determined from Eq. 10.30 assuming no outlets:

number of furrows = 
$$\frac{60 \text{ m}}{0.8 \text{ m}}$$
 = 75

Therefore,

$$Q = 75 \text{ furrows} \left( \frac{1.2 \text{ liters/s}}{\text{furrow}} \right) = 90 \text{ liters/s}$$

From Eq. 10.18,

$$R_e = 1.26 \times 10^6 \left( \frac{90 \text{ liters/s}}{200 \text{ mm}} \right) = 5.67 \times 10^5$$

From Eq. 10.22,

$$f = \frac{0.13}{(5.67 \times 10^5)^{0.172}} = \frac{0.13}{9.764} = 0.0133$$

To determine the velocity head:

$$V = \frac{Q}{A} = \frac{0.090 \text{ m}^3/\text{s}}{\pi (0.2\text{m})^2/^4} = 2.865 \text{ m/s}$$

$$\frac{V^2}{2g} = \frac{(2.865 \text{ m/s})^2}{2(9.81 \text{ m/s}^2)} = 0.146 \text{ m}$$

Therefore, the head loss without outlets is

$$h_f = (0.0133) \frac{60 \text{ m}}{0.2 \text{ m}} (0.146 \text{ m}) = 0.583 \text{ m}$$

The F factor for 75 multiple outlets is calculated from Eq. 10.39:

$$F = \frac{1}{1.828 + 1} + \frac{1}{2(75)} + \frac{(1.828 - 1)^{0.5}}{6(75)^2}$$

$$= 0.3536 + 0.0067 + 0.00006(75)^2$$

$$= 0.3603, \text{ say } 0.36$$

Thus the head loss with multiple outlets is

$$(h_f)_{75} = 0.36h_f = 0.36(0.583 \text{ m}) = 0.210 \text{ m}$$

Consequently, the minimum required pressure head at the beginning of the gated pipeline,  $(H_i)_{\min}$ , is

$$(H_i)_{\min} = 0.210 \text{ m} + 2.142 \text{ m} = 2.352 \text{ m}$$

### **HOMEWORK PROBLEMS**

- 10.1. A turnout structure similar to Example 10.1 is to be designed. Using the same trashrack and screens, and the same diameter (30 cm) of circular control gate and pipeline, what would be the maximum discharge from this system if the pipeline discharged freely into the atmosphere? Use the maximum water surface elevation in the canal of 432.8 m. What is the maximum discharge corresponding to the normal water surface elevation?
- 10.2. Using Figures 10.15 to 10.18, draw sketches to the same scale (1:10) comparing b = 1.0, 2.0, 3.0, and 4.0 ft for a channel slope of 0.0005 and a discharge rate of 15 ft<sup>3</sup>/s. Include freeboard. If the concrete thickness were 2.5 in., how many cubic yards of concrete would be required for each 100 ft of length? How many cubic meters of concrete are required for each 100 m of channel length?
- 10.3. Compute the total length of a vertical-drop structure having drop heights of 1, 2, 4, and 6 ft and unit discharge rates of 2, 5, 10, and 20 ft<sup>3</sup>/s per foot. Plot the data with drop height on the abscissa and  $L_d + L_i$  on the ordinate.
- 10.4. Compare the total length  $(L_d + L_j)$  of a vertical-drop structure having drop heights of 25, 50, 100, and 200 cm and unit discharge rates of 200, 500, 1000, and 2000 liters/s per meter. Plot the data with drop height, H, on the abscissa and  $L_d + L_j$  on the ordinate. Then plot the drop number, D, on the abscissa and  $L_d + L_j$  on the ordinate.

Sieve opening (mm)	Weight retained (g)
25	42
20	64
15	87
10	93
5	78
2	59
1	43
0.5	17

Show on semilogarithmic paper, with grain size on the logarithmic abscissa scale and percent finer on the ordinate, the range of allowable particle sizes between base and riprap materials.

- 10.6. Calculate the discharge for the 4-in.-inside-diameter siphon shown in Fig. 10.45. Assume an entrance loss coefficient of 0.8, bend loss coefficient of 0.2, and a friction factor, f = 0.02.
- 10.7. A PVC pipeline 250 m in length lies on a 1.2% slope downhill and has an inside diameter of 152.4 mm. The pipeline inlet is connected to a reservoir having a water level 30 m above the pipe inlet. The lower end of the pipeline discharges freely into a drain. Neglecting entrance losses, what is the flow rate in the pipeline?
- 10.8. If the lower end of the pipeline of Problem 10.7 were plugged, and outlets were cut every 5 m beginning 5 m from the reservoir, what would the pressure be at the lower end of the pipeline if the discharge rate was measured as 100 liters/s?

286 Headland Facilities Chap. 10

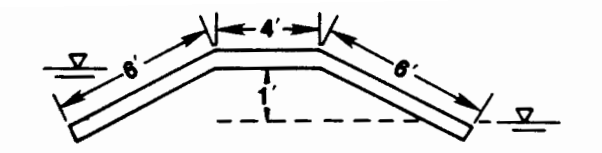


Figure 10.45

- 10.9. A gated pipeline, 177.8 mm inside diameter, runs downhill on a 1.5% slope for 120 m. The gated slots have an average discharge of 2 liters/s and a spacing of 1.5 m. What is the total change in pressure from the inlet to the distal end?
- 10.10. One of the gated slots from a gated pipeline was rated in the field and the following data collected for the full-open position:

Pipeline pressure (lb/in.²)	Discharge (gal/min)
2	8.6
4	12.3
6	14.4

Derive values of  $K_d$  and c in Eq. 10.44 analytically by using the data for pipeline pressures of 2 and 6 psi. Then, derive values of  $K_d$  and c graphically by plotting all the data on logarithmic paper.

### REFERENCES

- ALETRARIS, S. S. 1983. Energy Dissipation Parameters for Small Vertical Drop Structures. Unpublished M.S. thesis, Department of Agricultural and Irrigation Engineering, Utah State University, Logan, Utah.
- AMERICAN CONCRETE PIPE ASSOCIATION. 1970. Concrete Pipe Design Manual. American Concrete Pipe Association, Arlington, Va.
- CHOW, V. T. 1959. *Open Channel Hydraulics*. McGraw-Hill Book Company, New York, pp. 393-431.
- CHRISTIANSEN, J. E. 1942. Irrigation by Sprinkling. Bull. 670. California Agricultural Experiment Station, Berkeley, Calif.
- DONNELLY, C. A., and F. W. BLAISDELL. 1965. Straight Drop Spillway Stilling Basin. ASCE J. Hydraul. Div. 91(HY3):101-131.
- KATSAITIS, G. D. 1966. The Use of Dissipation Bars in Channel Drop Structures. J. Inst. Eng. Aust. January-February, pp. 9-18, Pap. 2005.
- LANE, E. W. 1955. Design of Stable Channels. Trans. ASAE 120:1234-1260.
- MAVIS, F. T., and L. M. LAUSHEY. 1948. A Reappraisal of the Beginnings of Bed Movement—Competent Velocity. International Association for Hydraulic Structures Research. Stockholm, Sweden.
- Moody, L. F. 1944. Friction Factors for Pipe Flow. Trans. ASME, 66:673.
- MOORE, W. L. 1943. Energy Loss at the Base of a Free Overfall. Trans. Am. Soc. Civ. Eng. 108:1343-1392, Pap. 2204.

- Neill, C. R. 1967. Mean-Velocity Criterion for Scour of Coarse Uniform Bed Material. *Proc. XII IAHR Cong.* 3:46-54, Pap. C6.
- NEILL, C. R. 1968. A Re-examination of the Beginning of Movement for Coarse Granular Bed Materials. Rep. Int. 68. Hydraulics Research Station, Wallingford, Berkshire, England.
- PAIR, C. H., W. H. HINZ, C. REID, and K. R. FROST (eds.). 1975. Sprinkler Irrigation. Sprinkler Irrigation Association, Silver Spring, Md.
- Peterka, A. J. 1964. Hydraulic Design of Stilling Basin and Energy Dissipators. Eng. Monogr. 25. U.S. Bureau of Reclamation, Denver, Colo., September, pp. 1-222.
- PILLSBURY, A. F. 1953. Concrete Pipe for Irrigation. Circ. 418. University of California.
- RAND, W. 1955. Flow Geometry at Straight Drop Spillways. ASCE J. Hydraul. Div. 81:1-13, September, Proc. Pap. 791.
- SILVESTER, R. 1964. Hydraulic Jump in All Shapes of Horizontal Channels. ASCE J. Hydraul. Div. 90(HY1):23-55, Pap. 3754.
- SKOGERBOE, G. V., S. S. KUNDU, and E. G. KRUSE. 1981. Monitoring and Evaluation of On-Farm Irrigation Improvements in the Grand Valley Salinity Control Project. Report AER80-81 GVS-SSK-EGK 4. Department of Agricultural and Chemical Engineering, Colorado State University, Fort Collins, Colo. March.
- SKOGERBOE, G. V., V. T. SOMORAY, and W. R. WALKER. 1971. Check-Drop-Energy Dissipator Structures in Irrigation Systems. Water Manage. Tech. Rep. 9, Water Management Research Project, Colorado State University, Fort Collins, Colo.
- SUNDBORG, A. 1956. The River Klaralven—A Study of Fluvial Processes. Institution of Hydraulics, Bull. 52, Royal Institute of Technology, Stockholm, Sweden.
- U.S. ARMY, CORPS OF ENGINEERS. 1959. Hydraulic Design Criteria. Waterways Experiment Station, Vicksburg, Miss.
- U.S. DEPARTMENT OF AGRICULTURE, SOIL CONSERVATION SERVICE. 1960. Sprinkler Irrigation. Irrigation, *National Engineering Handbook*. U.S. Government Printing Office, Washington, D.C., Sec. 15, Chap. 11.
- U.S. DEPARTMENT OF AGRICULTURE, SOIL CONSERVATION SERVICE. 1962. Measurement of Irrigation Water. Irrigation, *National Engineering Handbook*. U.S. Government Printing Office, Washington, D.C., Sec. 15, Chap. 9.
- VENNARD, J. E. 1965. Elementary Fluid Mechanics. John Wiley & Sons, Inc., New York.
- WATTERS, G. Z., and J. KELLER. 1978. Trickle Irrigation Tubing Hydraulics. Pap. 78-2015. ASAE Summer Meeting, Utah State University, Logan, Utah, June.
- WHITE, M. P. 1943. Energy Loss at the Base of a Free Overfall. Trans. Am. Soc. Civ. Eng. 108:1361-1364, Discussion of Pap. 2204.
- Wu, I., and H. M. GITLIN. 1975. Energy Gradient Line for Drip Irrigation Laterals. ASCE J. Irrig. Drain. Div., 101(IR4):323-326, Tech. Note.

# Fundamentals of Surface Irrigation Hydraulics

# INTRODUCTION

Water flowing across a soil surface is both spatially varied and unsteady. The discharge at a specific point changes with time due to the time-dependent intake behavior of the soil. At the advancing end of the water body, particularly, depth also changes with time and space. Equations describing continuity of mass, momentum, and/or energy for this flow condition have been developed and verified in many literature sources. The two equations that result are known commonly as the Saint-Venant equations, after A. J. C. Barre de Saint-Venant (Chow, 1959).

The development of the Saint-Venant equations is repeated in this section to review basic principles of open-channel hydraulics pertinent to surface irrigation and to provide the basis for subsequent simplifications. The derivations are based on the assumption that the channel is prismatic and the bed slope is relatively small. A dimensional format is used to present these derivations in order to give the reader a better frame of reference. However, as these relations are utilized to study the performance of a surface irrigation system, it becomes very difficult to evaluate the general behavior of the model because of the large number of parameters. Strelkoff and Clemmens (1981) note that transforming the equations of motion into a dimensionless form reduces the number of independent parameters, and thereby places the problem of discerning general model behavior at a tractable level. One of the many nondimensional transformations of the Saint-Venant equations is presented and discussed at the end of this chapter to demonstrate the concepts involved.

### THE CONTINUITY EQUATION

An infinitesimal fluid element within a furrow flow is shown in Fig. 11.1. At time, t, the conditions at the element inlet are Q, y, T, and I, representing discharge, depth, top width, and infiltration rate per unit length, respectively. To simplify the mathematical description of these conditions, the changes with space are written as

$$f_x = \frac{\partial f}{\partial x} \tag{11.1}$$

and with time as

$$f_t = \frac{\partial f}{\partial t} \tag{11.2}$$

where the parameter f is the symbolic representation of the various hydraulic parameters. Therefore, at time t the conditions at the right-hand side of the element (outflow) are  $Q + Q_x dx$ ,  $y + y_x dx$ ,  $T + T_x dx$ , and  $I + I_x dx$ . Since the discharge equals the product of velocity times area, inlet, and exit parameters for area and velocity can be described as A and  $A + A_x dx$ , and v and  $v + v_x dx$ , respectively. If it is assumed that the furrow is prismatic, then

$$\partial A = T \partial y \tag{11.3}$$

The changes in the flow during a time interval, dt, are assumed to be reflected by the numerical average of the conditions at time t and at time t + dt. For instance, the total inflow during the interval,  $V_{\rm in}$ , is

$$V_{\rm in} = \frac{Q + (Q + Q_t dt)}{2} dt = \left(Q + \frac{Q_t}{2} dt\right) dt \tag{11.4}$$

Figure 11.1 Fluid element within an unsteady, spatially varied furrow flow.

Similarly, for the surface outflow,  $V_{out}$ , and infiltration,  $V_I$ :

$$V_{\text{out}} = \frac{(Q + Q_x dx) + (Q + Q_x dx) + (Q + Q_x dx)_t dt}{2} dt$$

$$= \left[ Q + Q_x dx + \frac{(Q + Q_x dx)_t dt}{2} \right] dt$$
(11.5)

$$V_{I} = \frac{1}{2} \left[ \frac{I + (I + I_{x} dx)}{2} + \frac{(I + I_{t} dt) + (I + I_{x} dx) + (I + I_{x} dx)_{t} dt}{2} \right] dx dt$$

$$= \left[ I + \frac{I_{x} dx}{2} + \frac{I_{t} dt}{4} + \frac{(I + I_{x} dx)_{t} dt}{4} \right] dx dt$$
(11.6)

It can be assumed that second-order differentials and third-order differential products are negligible in comparison with other terms in Eqs. 11.4 to 11.6. Using this assumption, the change in the volume stored within the element during the period dt is

$$dV_s = V_{in} - V_{out} - V_I$$

$$= -O_s dx dt - I dx dt$$
(11.7)

or

$$\frac{dV_s}{dt} = -(Q_x + I) dx \tag{11.8}$$

The storage within the element at time t is

$$V_{s|t} = \frac{A + (A + A_x dx)}{2} dx$$
 (11.9)

and at time t + dt is

$$V_{s|_{t+dt}} = \frac{(A + A_t dt) + (A + A_x dx) + (A + A_x dx)_t dt}{2} dx$$
 (11.10)

Again, neglecting second-order differentials and third-order differential products yields the following expression for the change in element storage during the dt interval:

$$\frac{dV_s}{dt} = \frac{V_{s|_{t+dt}} - V_{s|_t}}{dt}$$

$$= A_t dx$$
(11.11)

Equations 11.8 and 11.11 can be combined and rearranged. After dividing by dx and returning to normal mathematical conventions, the continuity equation is written:

$$\frac{\partial A}{\partial t} + \frac{\partial Q}{\partial x} + I = 0 \tag{11.12}$$

#### **MOMENTUM EQUATION**

The conservation of momentum in the fluid element in Fig. 11.1 follows Newton's second law, which states that the unbalanced force acting on the element must be compensated for by the time rate of change of momentum. In the expanded view (Fig. 11.2) of the fluid element shown earlier in Fig. 11.1, three forces act on the surface of the element: (1) the component of the element's weight acting in the direction of flow, (2) the pressure forces acting on each end of the element, and (3) the viscous or shear forces along the wetted perimeter. It will be assumed that the momentum associated with water infiltrating from the element is negligible.

# Weight Forces

If the slope of the lower boundary,  $S_0$ , is small, so that it can be approximated by the sine of the slope angle, the component of weight in the direction of flow at time t is the average flow area multiplied by the specific weight of water and the length, dx:

$$F_{w|_{t}} = \gamma \frac{A + (A + A_{x} dx)}{2} dx S_{0}$$
 (11.13)

in which  $F_w$  is the gravitational force and  $\gamma$  is the specific weight of water. At time t + dt, the gravitational force is

$$F_{w|_{t+dt}} = \gamma \frac{(A + A_t dt) + (A + A_x dx) + (A + A_x dx)_t dt}{2} dx S_0 \qquad (11.14)$$

Adding and averaging Eqs. 11.13 and 11.14 and dropping second-order differentials as well as differential products yields the average weight force:

$$F_{w} = \gamma A S_0 \, dx \tag{11.15}$$

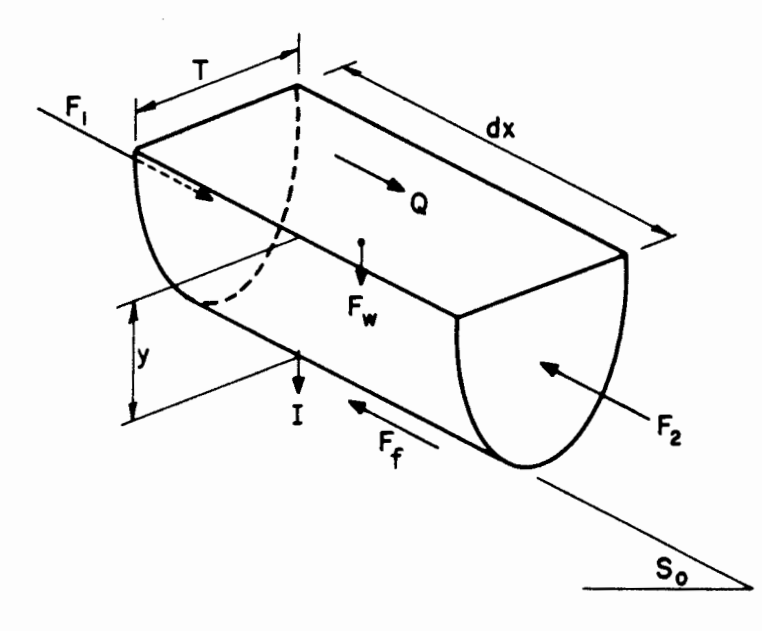


Figure 11.2 Expanded view of the fluid element within an unsteady, spatially varied furrow flow.

#### **Pressure Forces**

The pressure forces acting on the element ends,  $F_1$  and  $F_2$ , are the product of specific weight, distance from the water surface to the centroid of the end areas, h, and the end area, A. At time t, the expression for  $F_1$  is

$$F_1|_t = \gamma hA \tag{11.16}$$

At time t + dt,  $F_1$  is

$$F_1|_{t+dt} = \gamma [hA + (hA), dt]$$
 (11.17)

Consequently, the average pressure force at the inlet end of the element is

$$F_1 = \frac{F_1|_t + F_1|_{t+dt}}{2} = \gamma hA + \frac{1}{2\gamma(hA)_t} dt$$
 (11.18)

The same development can be made for the downstream force,  $F_2$ , as follows:

$$F_{2}|_{t} = \gamma [hA + (hA)_{x} dx]$$
 (11.19)

$$F_{2|_{t+dt}} = \gamma [hA + (hA)_{x} dx] + \gamma [hA + (hA)_{x} dx], dt \qquad (11.20)$$

and

$$F_2 = \gamma(hA) + \gamma(hA)_x dx + \frac{\gamma(hA)_t dt}{2}$$
 (11.21)

If Eq. 11.21 is subtracted from Eq. 11.18, the result is the average net force on the fluid element during the period dt:

$$F_p = F_1 - F_2 = -\gamma (hA)_x dx$$

$$= -\gamma A \left( h_x + \frac{hA_x}{A} \right) dx$$
(11.22)

It is desirable to express Eq. 11.22 in terms of depth defined from the bottom channel, y, instead of from the surface, to avoid an additional variable. The depth can be defined as

$$y = h + d \tag{11.23}$$

in which d is the distance from the channel bottom to the area centroid. Thus

$$h = y - d \tag{11.24}$$

Noting that

$$d = \frac{1}{A} \int_0^A d' \ dA' \tag{11.25}$$

in which d' and A' are variables of integration, leads to the following form of Eq. 11.22:

$$F_{p} = -\gamma A \, dx \left[ \left( y - d \right)_{x} + \left( \frac{y - d}{A} \right) A_{x} \right]$$

$$= -\gamma A \, dx \left[ \left( y - \frac{\int_{0}^{A} d' \, dA'}{A} \right)_{x} + \left( \frac{y - \left( \frac{1}{A} \right) \int_{0}^{A} d' \, dA'}{A} \right) A_{x} \right]$$

$$= -\gamma A \, dx \left[ y_{x} - \frac{A \left( \int_{0}^{A} d' \, dA' \right)_{x} - \left( \int_{0}^{A} d' \, dA' \right) A_{x}}{A^{2}} \right]$$

$$+ \frac{y A_{x}}{A} - \frac{A_{x} \int_{0}^{A} d' \, dA'}{A^{2}} \right]$$

$$= -\gamma A \, dx \left[ y_{x} - \frac{1}{A} \left( \int_{0}^{A} d' \, dA' \right)_{x} + \frac{y A_{x}}{A} \right]$$

$$(11.26)$$

The Leibnitz rule for differentiating the integral in Eq. 11.26 can be applied as follows:

$$\left(\int_0^A d' \ dA'\right)_x = \int_0^A d'_x \ dA' + \left. d'A_x \right|_{d'=y}$$

$$- \left. d'A_x \right|_{d'=0}$$

$$= yA_x + \int_0^A d'_x \ dA'$$
(11.27)

The second term on the right side of Eq. 11.27 can be assumed negligible in comparison to the first. The assumption allows the second and third terms in the brackets in Eq. 11.26 to cancel, resulting in

$$F_p = -\gamma A y_x \, dx \tag{11.28}$$

#### **Friction Forces**

It is generally assumed that the unsteady shear forces are equal to those under steady flow conditions as long as the flow is gradually varied (Chow, 1959). Using average weight and pressure forces from Eqs. 11.15 and 11.28, the steady flow momentum equation is written as follows:

$$\gamma A S_0 \, dx - \gamma A y_x \, dx - F_f = \rho [-Qv + Qv + (Qv)_x \, dx] \qquad (11.29)$$

in which  $F_f$  is the shear force. Simplifying and solving for  $F_f$  yields

$$F_f = \gamma A \, dx \left( S_0 - y_x - \frac{v v_x}{g} \right) \tag{11.30}$$

The energy equation for steady flow conditions is

$$S_0 dx + y + \frac{v^2}{2g} = y + y_x dx + \frac{v^2}{2g} + \left(\frac{v^2}{2g}\right)_x dx + S_f dx$$
 (11.31)

where  $S_f$  is the friction loss per unit length (friction slope). Solving for  $S_f$  gives

$$S_f = S_0 - y_x - \frac{vv_x}{g} \tag{11.32}$$

Thus, by substituting Eq. 11.32 into Eq. 11.30, the average friction or shear forces during the interval are

$$F_f = \gamma A S_f \, dx \tag{11.33}$$

The friction slope under steady flow conditions can be described by three popular equations. They are:

Chezy equation: 
$$v = C\sqrt{RS_0}$$
 (11.34)

Manning equation: 
$$v = \frac{1}{n} R^{0.67} S_0^{0.5}$$
 (11.35)

Darcy-Weisbach equation: 
$$v = \frac{\sqrt{8RgS_0}}{f}$$
 (11.36)

where

v = average channel velocity, m/s

R = hydraulic radius, m

 $S_0$  = channel slope

C =Chezy's friction coefficient

n = Manning's friction coefficient

f = Darcy-Weisbach friction factor

A great deal of research has been conducted to develop rational expressions for the friction factors and the reader interested in a thorough discussion is referred to Chow (1959). The relationship between C, n, and f can be summarized as

$$C = \frac{1}{n} R^{1.67} \tag{11.37}$$

$$f = \frac{8gn^2}{R^{0.33}} \tag{11.38}$$

However, it should be noted that these friction factors change with several conditions such as flow depth. Chow (1959) presents a lengthy discussion of friction coefficients, but it is more applicable to large open channels and will not be given here.

# **Unsteady Momentum**

The development of Wilke (1968) uses an unsteady momentum principle which equates the rate of change of momentum of a fluid element in motion past a fixed point to the sum of momentum change within the element and the momentum flux across the element boundaries.

The average momentum fluxes into and out of the element during the period dt are

$$\left[\frac{d(mv)}{dt}\right]_{\text{in}} = \rho Q v + \frac{1}{2\rho} (Qv)_{t} dt$$

$$\left[\frac{d(mv)}{dt}\right]_{\text{out}} = \frac{1}{2\rho} \left[ (Q + Q_{x} dx)(v + v_{x} dx) \right]$$

$$+ \frac{1}{2\rho} \left[ Q + Q_{x} dx + (Q + Q_{x} dx)_{t} dt \right]$$

$$\cdot \left[ v + v_{x} dx + (v + v_{x} dx)_{t} dt \right]$$

$$(11.39)$$

If second-order differentials and third-order differential products are considered negligible, the net flux across the element boundaries is the difference between Eqs. 11.40 and 11.39:

$$\left[\frac{d(mv)}{dt}\right]_{\text{net}} = \rho(Qv_x dx + vQ_x dx) \tag{11.41}$$

The average momentum change within the fluid element during the period can be developed as follows. At the time t, the momentum within the element is

$$(mv)_{t} = \left[\frac{1}{2\rho} (A + A + A_{x} dx) dx\right] \left[\frac{1}{2} (v + v + v_{x} dx)\right]$$
(11.42)

Writing a similar expression for t + dt, neglecting higher-order differentials and subtracting Eq. 11.42 from the result yields the change of momentum within the element:

$$(mv)_{t+dt} - (mv)_t = \frac{\rho v A_t \, dx \, dt + \rho A v_t \, dx \, dt}{dt}$$
 (11.43)

Then adding Eqs. 11.43 and 11.41, the unsteady momentum is given by

$$\frac{d(mv)}{dt} = \rho(Qv_x dx + vQ_x dx + vA_t dx + Av_t dx)$$
 (11.44)

It is now possible to combine the results of developing Eqs. 11.15, 11.28, 11.33, and 11.44 into the basic momentum equation:

$$\gamma A dx S_0 - \gamma A y_x dx - \gamma A S_f dx = \rho (Q v_x + v Q_x + v A_t + A v_t) dx \qquad (11.45)$$

Dividing by  $\gamma A dx$  yields

$$S_0 - y_x - S_f = \frac{vv_x}{g} + \frac{vQ_x}{gA} + \frac{vA_t}{gA} + \frac{v_t}{g}$$
 (11.46)

The discharge, Q, is generally a more readily identified variable than flow velocity, v. Consequently, the expression of the momentum equation can be written as a function of discharge by replacing  $v_t$  and  $v_x$  by the following expressions:

$$v_{t} = \frac{1}{A^{2}} \left( AQ_{t} - QA_{t} \right) \tag{11.47}$$

and

$$v_x = \frac{1}{A^2} (AQ_x - QA_x) \tag{11.48}$$

Then, utilizing Eq. 11.3 to replace  $A_x$  by  $(Ty_x)$  and v = Q/A, the discharge form of the momentum equation is

$$\frac{1}{Ag}Q_t + \frac{2Q}{A^2g}Q_x + (1 - F^2)y_x = S_0 - S_f \qquad (11.49)$$

where the squared Froude number,  $F^2$ , is

$$F^2 = \frac{Q^2 T}{A^3 g} \tag{11.50}$$

It should be worth noting that other investigators often derive Eq. 11.46 from the energy relations and then use the continuity equation to replace  $A_t$ . This introduces a term containing the infiltration function vI/2Ag into the result. The momentum derivation of Eq. 11.46 can also be modified to include such a term, but it would be vI/Ag. Nevertheless, the results are generally insensitive to this term in Eq. 11.46 (Farrell, 1963; Kincaid et al., 1972; Bassett, 1972).

### **NONDIMENSIONALIZATION OF BASIC EQUATIONS**

As noted previously, the nondimensional expression of the governing equations provides the means to more systematically study the surface irrigation system's response to design and operational parameter changes. Several approaches have been described in the literature for accomplishing the nondimensional transformation. The approach taken in this chapter is one of the more recent.

The dimensional variables in the continuity and momentum equations can be nondimensionalized by dividing them by "characteristic" variables which are representative of some basic features of the surface irrigation system. The procedure is to first define a set of nonzero characteristic variables, nondimensionalize the flow equations, and then determine the relationships between the characteristic variables and the physical problem variables.

To begin work on the continuity and momentum equations, dimensionless discharge, area, depth, time, hydraulic radius, distance, infiltrated volume per unit length, and top width are defined as follows:

$$Q^* = \frac{Q}{Q_c} \qquad R^* = \frac{R}{R_c}$$

$$A^* = \frac{A}{A_c} \qquad x^* = \frac{x}{x_c}$$

$$y^* = \frac{y}{y_c} \qquad \tau^* = \frac{\tau}{t_c}$$

$$t^* = \frac{t}{t_c} \qquad Z^* = \frac{Z}{Z_c}$$

$$(11.51)$$

in which the starred variables are nondimensional, and those subscripted by c are the nonzero characteristic variables.

Substituting Eq. 11.51 into Eq. 11.12 yields

$$\frac{Q_c}{x_c} \frac{\partial Q^*}{\partial x^*} + \frac{A_c}{t_c} \frac{\partial A^*}{\partial t^*} + \frac{Z_c}{t_c} \frac{\partial Z^*}{\partial \tau^*} = 0$$
 (11.52)

in which  $\partial Z/\partial \tau$  replaces I. Similarly, for Eq. 11.49,

$$\frac{Q_c \partial Q^*}{A_c g t_c A^* \partial t^*} + \frac{2Q_c^2 Q^{*2} \partial Q^*}{A_c^2 x_c g A^{*2} \partial x^*} + 1 - \frac{Q_c^2 T_c Q^{*2} T^*}{A_c^3 g A^{*3}} \frac{y_c}{x_c} \frac{\partial y^*}{\partial x^*}$$

$$= S_0 - \frac{Q_c^2 n^2}{A_c^2 R_c^{1.33}} \frac{Q^{*2}}{A^{*2} R^{*1.33}}$$
(11.53)

Since the characteristic variables for the hydraulic conditions would be independent of time only at the field inlet, their expression can be set to the inlet flow conditions (subscripted with 0), and related by uniform flow conditions. Thus

$$y_c = y_0$$
  $Q_c = Q_0$  (11.54)  
 $R_c = R_0$   $A_c = A_0$   $T_c = T_0$ 

After Eq. 11.54 is incorporated, Eqs. 11.52 and 11.53 can be rearranged as follows. First Eq. 11.52 can be written:

$$\frac{\partial A^*}{\partial t^*} + V_1^* \frac{\partial Q^*}{\partial r^*} + V_2^* \frac{\partial Z^*}{\partial \tau^*} = 0$$
 (11.55)

in which

$$V_1^* = \frac{Q_0 t_c}{A_0 x_c} \tag{11.56}$$

and

$$V_2^* = \frac{Z_c}{A_0} \tag{11.57}$$

Similarly, Eq. 11.53 becomes

$$\frac{F_0^2}{V_1^*} \frac{V_3^*}{A^*} \frac{\partial Q^*}{\partial t^*} + F_0^2(2V_3^*) \frac{Q^*}{A^{*2}} \frac{\partial Q^*}{\partial x^*} + (1 - F_0^2 F^{*2}) \frac{\partial y^*}{\partial x^*} = \frac{S_0 x_c}{v_0} - \frac{S_0 x_c}{v_0} S_f^*$$
(11.58)

where

$$V_3^* = \frac{A_0}{T_0 y_0} \tag{11.59}$$

$$S_f^* = \frac{Q^{*3}}{A^{*2}R^{*1.33}} \tag{11.60}$$

and

$$F_0^2 = \frac{Q_0^2 T_0}{A_0^3 g} \tag{11.61}$$

$$F^{*2} = \frac{Q^{*2}T^*}{A^{*3}} \tag{11.62}$$

The characteristic variables  $Q_c$  and  $y_c$  were defined earlier as the field inlet values under uniform flow conditions. To define the characteristic distance,  $x_c$ , and the characteristic time,  $t_c$ , Souza (1981) and Strelkoff and Clemmens (1981) suggest that the dimensionless volume  $V_1^*$  of Eq. 11.56 and the ratio  $S_0x_c/y_0$  in Eq. 11.58 be set equal to unity. Thus

$$x_c = \frac{y_0}{S_0} \tag{11.63}$$

and the characteristic time,  $t_c$ , is defined by Eq. 11.56 as

$$t_{\mathbf{e}} = \frac{y_0 A_0}{S_0 Q_0} \tag{11.64}$$

The characteristic infiltrated volume per unit length,  $Z_c$ , in Eq. 11.57 can be defined in a number of ways. For this chapter, it can be assumed that

$$Z_c = kt_c^a + f_0 t_c (11.65)$$

where the Kostiakov-Lewis equation is used generally.

The results of the foregoing transformation allow Eqs. 11.55 and 11.58 to be simplified to the following,

$$\frac{\partial A^*}{\partial t^*} + \frac{\partial Q^*}{\partial x^*} + V_2^* \frac{\partial Z^*}{\partial \tau^*} = 0 \tag{11.66}$$

and

$$F_0^2 \left( \frac{V_3^*}{A^*} \frac{\partial Q^*}{\partial t^*} + \frac{2V_3^* Q^*}{A^{*2}} \frac{\partial Q^*}{\partial x^*} - F^* \frac{\partial y^*}{\partial x^*} \right) + \frac{\partial y^*}{\partial x^*} = 1 - S_f^*$$
 (11.67)

Equations 11.66 and 11.67, together with the appropriate boundary conditions, can be solved with the same result as Eqs. 11.12 and 11.49.

#### REFERENCES

\$

- BASSETT, D. L. 1972. Mathematical Model of Water Advance in Border Irrigation. *Trans.* ASAE 15(5):992-995.
- CHOW, V. 1959. Open Channel Hydraulics. McGraw-Hill Book Company, New York.
- FARRELL, D. A. 1963. Analysis of Border Irrigation. Trans. 5th Congress of ICID 4(6):16.57-16.81.
- KINCAID, D. C., D. F. HEERMANN, and E. G. KRUSE. 1972. Hydrodynamics of Border Irrigation. *Trans. ASAE* 15(4):674-680.
- Souza, F. 1981. Non-linear Hydrodynamic Model of Furrow Irrigation. Unpublished Ph.D. dissertation, Department of Land, Air and Water Resources, University of California, Davis, Calif.
- STRELKOFF, T., and A. J. CLEMMENS. 1981. Dimensionless Stream Advance in Sloping Borders. ASCE J. Irrig. Drain Div. 107(IR4):361-382.
- WILKE, O. C. 1968. A Hydrodynamic Study of Flow in Irrigation Furrows. Tech. Rep. 13. Water Resources Institute, Texas A & M University, College Station, Tex., July.

# The Hydrodynamic Model: Characteristic Approach

### INTRODUCTION

Strelkoff (1970) outlines four categories of solution for the equations of motion and evaluates the stability and computational requirements of each. In later papers by Bassett (1972), Kincaid et al. (1972), and Katapodes and Strelkoff (1977), experience had reduced the alternatives to special forms of the method of characteristics. Recently, Souza (1981) solved the equations using the deformable control volume or integral approach of Strelkoff and Katapodes (1977). The characteristic method discussed in this chapter, and the deformable control volume (DCV) approach is considered separately in Chapter 13.

The Saint-Venant equations have been in existence for many years in the fields of open-channel hydraulics and watershed hydrology. Surface irrigation involves several unique characteristics that influence the mathematical treatment of these equations. First, the land slope is generally small such that the sine of the slope angle is essentially equal to the land slope itself. Under these conditions and the fact that the irrigated surfaces are relatively rough, the flow can be expected to remain in the subcritical range except for a small region near an advancing front.

The second unique aspect of surface irrigation is that primary emphasis must be given to the spatial and temporal distribution of infiltrated water rather than surface water. In other words, surface irrigation is considered an unsteady gradually and spatially varied flow problem in which particular interest is focused on spatial variation due to infiltration. The term "gradually varied" implies a number of important assumptions that affect the application of these principles for surface irrigation hydraulics. Two of specific interest are: (1) the friction slope at a section

is assumed to be the same as for a uniform flow having similar flow velocity, and (2) the channel is prismatic. While these assumptions are maintained for mathematical simplicity, they are by no means accurate for surface-irrigated systems. The roughness of the soil surface changes a great deal during an irrigation and from irrigation to irrigation. Furthermore, furrow irrigation systems generally exhibit substantial changes in furrow shape and alignment during irrigation. However, since we do not have the information to correct for these effects and they do not appear to hinder our basic modeling accuracy, it is usually sufficient to admit their existence.

The third unique feature of surface irrigation applications of overland flow principles is the management of flow and duration of flow. An irrigator modifies the flow rate and its duration in order to minimize the nonproductive use of water (field tailwater and deep percolation). Consequently, the sphere of interest extends beyond attempting to understand the hydraulic processes to also managing them for more efficient use of water, energy, labor, capital, and fertilizer resources.

In the introduction to their paper, Katapodes and Strelkoff (1977) concisely state the impact that the foregoing characteristics place on investigating surface irrigation systems. The models used to analyze the problem were given four objectives and a primary purpose. The objectives are:

- 1. To describe the physical processes on a sound theoretical basis with minimal arbitrary or experimental parameters
- 2. To numerically evaluate the mathematical model in a manner that achieves numeric stability and accuracy
- 3. To include each physical phase of surface irrigation (i.e., advance, ponding, depletion, recession)
- 4. To achieve simplicity in computer structure and rapid execution of computations to minimize expense

The primary purpose of the model is to gain a better understanding of the interrelationships among processes and parameters and thereby provide useful evaluations of the simplifications which are necessary to develop design and operational programs.

#### **CHARACTERISTIC EQUATIONS**

Equations 11.12 (continuity) and 11.46 (momentum) are first-order, nonlinear partial differential equations without a known closed-form solution. The method of characteristics converts the equations into ordinary differential equations for which there exists a great deal of knowledge. Because both equations must be satisfied simultaneously for each time and space coordinate, it is assumed that the simultaneous solution can be written as a linear combination of the two equations. Strelkoff (1970) reviews in great detail the mathematical theory upon which this assumption is based. Wilke (1968), Kincaid et al. (1972), and numerous others have used the result to formulate the characteristic equations for border irrigation.

For this discussion, it is convenient to utilize Eqs. 11.12 and 11.46 in their velocity-depth form. Equation 11.12 becomes

$$\frac{\partial y}{\partial t} + \frac{v}{\partial x} \frac{dy}{dx} + \frac{A}{T} \frac{\partial v}{\partial x} + \frac{I}{T} = 0$$
 (12.1)

Equation 11.46 can be written as

$$\frac{1}{g}\frac{\partial v}{\partial t} + \frac{v}{g}\frac{\partial v}{\partial x} + \frac{v}{Ag}\left(\frac{\partial Q}{\partial x} + \frac{\partial A}{\partial t}\right) + \frac{\partial y}{\partial x} - (S_0 - S_f) = 0$$
 (12.2)

Then utilizing Eq. 11.12 to replace the bracketed terms in the third component of Eq. 12.2 yields

$$\frac{1}{g}\frac{\partial v}{\partial t} + \frac{v}{g}\frac{\partial v}{\partial x} + \frac{\partial y}{\partial x} - \left(S_0 - S_f + \frac{vI}{Ag}\right) = 0 \tag{12.3}$$

Equations 12.1 and 12.3 can be written as a linear combination:

$$L_1 + \lambda L_2 = 0 \tag{12.4}$$

where  $L_1$  equals Eq. 12.3 multiplied by g and  $L_2$  equals Eq. 12.1. After grouping terms together we have

$$\left[\frac{\partial v}{\partial t} + \left(v + \frac{\lambda A}{T}\right)\frac{\partial v}{\partial x}\right] + \lambda \left[\frac{\partial y}{\partial t} + \left(v + \frac{g}{\lambda}\right)\frac{\partial y}{\partial x}\right] - g\left(S_0 - S_f + \frac{vI}{Ag}\right) + \frac{\lambda I}{T} = 0 \quad (12.5)$$

The total change in velocity and depth equals the sum of the partial changes with respect to time and distance. Velocity, for example, follows

$$\frac{dv}{dt} = \frac{\partial v}{\partial t} + \frac{\partial v}{\partial x}\frac{dx}{dt}$$
 (12.6)

The first term in Eq. 12.5 is therefore dv/dt if

$$\frac{dx}{dt} = v + \frac{\lambda A}{T} \tag{12.7}$$

Similarly, the second bracketed term is dy/dt if

$$\frac{dx}{dt} = v + \frac{g}{\lambda} \tag{12.8}$$

Since both conditions must hold,

$$v + \frac{\lambda A}{T} = v + \frac{g}{\lambda}$$

$$\lambda = \pm \sqrt{\frac{gT}{A}}$$
(12.9)

Equation 12.9 is substituted back into Eqs. 12.7 and 12.8, yielding

$$\frac{dx}{dt} = v \mp c \tag{12.10}$$

in which

$$c = \sqrt{\frac{gA}{T}} \tag{12.11}$$

Equation 12.4 is thereby converted to two ordinary differential equations using these results:

$$\frac{dv}{dt} + \frac{g}{c}\frac{dy}{dt} + \frac{Ig}{Tc} - g\left(S_0 - S_f + \frac{vI}{Ag}\right) = 0$$
 (12.12)

along

$$\frac{dx}{dt} = v + c \tag{12.13}$$

and

$$\frac{dv}{dt} - \frac{g}{c}\frac{dy}{dt} - \frac{Ig}{Tc} - g\left(S_0 - S_f + \frac{vI}{Ag}\right) = 0$$
 (12.14)

along

$$\frac{dx}{dt} = v - c \tag{12.15}$$

Equations 12.12 and 12.14 can be simplified somewhat through the use of the differential formulas (Katapodes and Strelkoff, 1977)

$$\frac{d(v+2c)}{dt} = g\left[S_0 - S_f + \frac{I}{Ag}(v-c)\right]$$
 (12.16)

$$\frac{d(v-2c)}{dt} = g \left[ S_0 - S_f + \frac{I}{Ag} (v+c) \right]$$
 (12.17)

where both Eqs. 12.16 and 12.17 are defined along the characteristic directions described by Eqs. 12.13 and 12.15.

A number of investigators have solved Eqs. 12.13, 12.15, 12.16, and 12.17 for overland flow conditions. Wilke (1968) attempted to simulate furrow irrigations without success. Bassett and Fitzsimmons (1976), Kincaid et al. (1972), and Katapodes and Strelkoff (1977) are examples of border and basin irrigation simulations. The approach of Katapodes and Strelkoff (1977) will serve to illustrate the characteristic solution of utilizing the plane flow condition of border and basins.

#### **NUMERICAL SOLUTION FOR PLANE FLOW**

The flow of water in borders and basins is similar to flow in very wide rectangular channels and can therefore be studied by examining the flow of a unit width. Equations 12.16 and 12.17 become

$$\frac{d(v + 2c)}{dt} = g \left[ S_0 - S_f + \frac{I(v - c)}{c^2} \right]$$
 (12.18)

and

$$\frac{d(v-2c)}{dt} = g \left[ S_0 - S_f + \frac{I(v+c)}{c^2} \right]$$
 (12.19)

where

$$c = \sqrt{gy} \tag{12.20}$$

and

$$S_f = \frac{v^2 n^2}{y^{1.33}} \tag{12.21}$$

The solution proposed by Katapodes and Strelkoff (1977) of Eqs. 12.18 and 12.19 utilized a finite difference approximation with second-order accuracy achieved by a quadratic interpolation scheme. The x axis was divided into N+1 computational nodes (node 1 corresponding to the left boundary and node N+1 to the right boundary). Since the water surface profiles at the advancing or receding fronts are significantly more varied than away from the fronts, node spacing is weighted toward the region of most rapid change. For advance, a parameter  $r_t < 1.0$  is defined such that the spacing between the nodes 1 and 2 is

$$\Delta x_2 = \frac{x_{N+1} - x_1}{1 + \sum_{k=1}^{N-1} r_i^k}$$
 (12.22)

where  $x_{N+1}$  and  $x_1$  are the distance at the advancing front and left boundary, respectively. Then the remaining node spacings are computed sequentially by

$$\frac{\Delta x_k}{\Delta x_{k-1}} = r_t \qquad k = 3, 4, \dots, N+1 \tag{12.23}$$

Equations 12.22 and 12.23 thus define the x coordinates of each node as illustrated in Fig. 12.1. When the surface flow is receding,  $r_t$  is redefined as a value of greater than 1.0 which reverses the nonlinear spacing of the nodes.

It can be seen that the x plane is divided into a moving grid system. The division of the t plane is made in a linear fashion by constant time steps, although the step size can be modified periodically.

Referring to Fig. 12.1, the solution advances from time  $t_j$  to  $t_j + \Delta t = t_{j+1}$  by a reverse extension of the characteristics from each node along  $t_j$  axis. At time  $t_j$ , the two characteristics emanating from  $x_l$  and  $x_r$  intersect at node m on the  $t_{j+1}$  line and therefore provide the solution at that point through Eqs. 12.18 and 12.19. In finite difference form, Eqs. 12.18, 12.19, 12.13, and 12.15 are

$$A_1 = F_m - F_l - \frac{\Delta t}{2} (f_m + f_l)$$
 (12.24)

$$A_2 = H_m - H_r - \frac{\Delta t}{2} (h_m + h_r)$$
 (12.25)

$$A_3 = x_m - x_l - \frac{\Delta t}{2} \left( \alpha_m + \alpha_l \right) \tag{12.26}$$

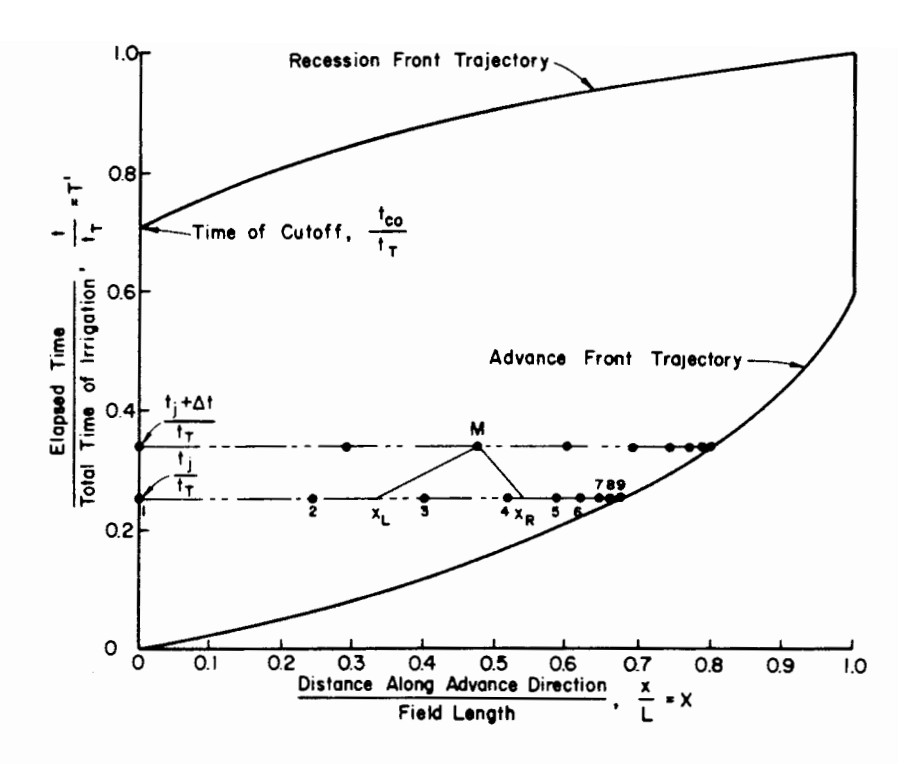


Figure 12.1 Dimensionless space-time plane showing numerical solution procedure for the Saint-Venant equation.

and

$$A_4 = x_m - x_r - \frac{\Delta t}{2} (\beta_m + \beta_r)$$
 (12.27)

in which

$$F = v + 2c \tag{12.28}$$

$$H = v - 2c \tag{12.29}$$

$$\alpha = v + c \tag{12.30}$$

$$\beta = v - c \tag{12.31}$$

$$f = g \left[ S_0 - S_f + \frac{I(v - c)}{c^2} \right]$$
 (12.32)

$$h = g \left[ S_0 - S_f + \frac{I(v+c)}{c^2} \right]$$
 (12.33)

Equations 12.24 to 12.33 are now a set of simultaneous nonlinear algebraic equations in the unknowns  $y_m$ ,  $v_m$ ,  $x_l$ , and  $x_r$ . Thus, at each node where these equations apply, a solution procedure such as Newton-Raphson can be employed to solve the four equations in the four unknowns. There are, however, three cases where these relations do not apply. First, during the first time step, there is an undefined distance over which the flow advances. Second, at the left boundary, Eq. 12.26 is undefined since  $x_i$  would project outside the domain of the physical problem. Third, at the right boundary Eq. 12.27 is not defined because x, would project beyond either the water front or the downstream field boundary. Consequently, equations for initial and boundary conditions must be developed for the numerical solutions.

One other problem of only minor consequence needs mention here. Equations 12.24 to 12.33 require that both velocity and depth be known at the points  $x_l$  and  $x_r$ . Several writers have used a linear interpolation scheme, while Katapodes and Strelkoff (1977) use a second-order polynomial to improve accuracy somewhat.

Before proceeding with a discussion of the initial and boundary conditions, it may be helpful to briefly review the Newton-Raphson procedure.

The Newton-Raphson technique has been used by many of the investigators studying surface irrigation hydraulics and found to converge rapidly and execute efficiently. The procedure begins by defining two matrices, A and U. The matrix A consists of four elements  $(A_1, A_2, A_3, A_4)$  from Eqs. 12.24 to 12.27 which are functions of a second matrix, U, comprised of the problem variables  $(y_m, v_m, x_l, and x_r)$ . The solution to the four equations occurs when the values of  $y_m, v_m, x_l$  and  $x_r$  are such that A = (0, 0, 0, 0). If the function represented by A is expanded in a Taylor series with only the first two terms retained, the result is

$$\mathbf{A}[\mathbf{U}]_{i+1} = \mathbf{A}[\mathbf{U}]_i + (\nabla_u \mathbf{A}_i) \Delta \mathbf{U}$$
 (12.34)

where the notation  $A(U)_{i+1}$  and  $A(U)_i$  refers to the value of the matrix A at succeeding iterations, and  $\Delta U$  is the change in the U matrix  $(\Delta y_m, \Delta v_m, \Delta x_l, \Delta x_r)$ . The term  $(\nabla_u A_i)$  is called the "Jacobian matrix,"  $J_i$ , which is

$$\mathbf{J}_{i} = \begin{bmatrix} \frac{\partial A_{1}}{\partial y_{m}} & \frac{\partial A_{1}}{\partial v_{m}} & \frac{\partial A_{1}}{\partial x_{l}} & \frac{\partial A_{1}}{\partial x_{r}} \\ \frac{\partial A_{2}}{\partial y_{m}} & \frac{\partial A_{2}}{\partial v_{m}} & \frac{\partial A_{2}}{\partial x_{l}} & \frac{\partial A_{2}}{\partial x_{r}} \\ \frac{\partial A_{3}}{\partial y_{m}} & \frac{\partial A_{3}}{\partial v_{m}} & \frac{\partial A_{3}}{\partial x_{l}} & \frac{\partial A_{3}}{\partial x_{r}} \\ \frac{\partial A_{4}}{\partial y_{m}} & \frac{\partial A_{4}}{\partial v_{m}} & \frac{\partial A_{4}}{\partial x_{l}} & \frac{\partial A_{4}}{\partial x_{r}} \end{bmatrix}$$

$$(12.35)$$

To solve Eq. 12.34, the values of  $A[U]_{i+1}$  are set equal to zero to reflect the anticipated solution. Then the relation can be rearranged as follows:

$$\mathbf{A}[\mathbf{U}]_i = -\mathbf{J}_i \,\Delta \mathbf{U} \tag{12.36}$$

which is a system of four linear equations in four unknowns  $(\Delta y_m, \Delta v_m, \Delta x_l, \Delta x_r)$  that can be solved by procedures such as Gaussian elimination. Katapodes and Strelkoff (1977) give the 16 derivatives in Eq. 12.35. For each node 2 through N, Eq. 12.36 is solved iteratively until the iterations converge within the tolerance set by the investigator. At nodes 1 and N+1, initial and boundary equations are written and the Jacobian matrix is redefined.

#### **Initial Conditions**

Between time equal to zero,  $t_0$ , and  $t_1 = t_0 + \Delta t$ , flow is introduced into the border. Inertial and acceleration forces are large relative to resistance forces, and the flow profile is highly curved. As the flow advances, the resistance forces quickly become the dominant processes affecting the flow and a more stable flow profile occurs. Mathematically, the transient nature of the initial conditions will cause large errors in predicting the hydraulic conditions unless the computational scheme is unconditionally stable itself. Katapodes and Strelkoff (1977) state that the procedure outlined herein is stable, and therefore, the error input through the definition of initial conditions vanishes with time by the self-correcting mechanism of mathematical stability. As a result, initial conditions used need not be more than simple approximations of the actual flow.

In the simplest case, the velocity is assumed to be constant during the first time increment, and the inlet depth is assumed to vary instantaneously from zero at  $t_0$  to critical depth at  $t_1$ . During the interval, the flow advances to a distance  $x_2$  at a rate  $v_1$  which because of the constant-velocity assumption, equals the velocity in the flow behind the advancing tip. In addition, the friction slope is generally much greater than the bed slope, which can thereby be neglected. Equation 12.2 reduces to an ordinary differential equation:

$$\frac{dy}{dx} = -S_f = -\frac{v_1^2 n^2}{y^{1.33}} \tag{12.37}$$

The depth of flow at a distance x from the inlet is found by integrating Eq. 12.37. Similarly, the volume of surface storage within that distance is found by integrating the result. The origin of reference is transferred to the advance front for ease of integration by defining the variable  $\phi$ :

$$\phi = x_2 - x \tag{12.38}$$

where x is the variable distance from the inlet and

$$d\Phi = -dx \tag{12.39}$$

The first integration then describes depth as a function of distance:

$$\int y^{1.33} \, dy = v_1^2 n^2 \int d\phi \tag{12.40}$$

or

$$y = \left[\frac{7}{3}v_1^2n^2\phi\right]^{0.428} \tag{12.41}$$

At the inlet,  $\phi = x_2$ , and the depth  $y_1$  is

$$y_1 = \left[\frac{7}{3} v_1^2 n^2 x_2\right]^{0.428} \tag{12.42}$$

The volume in surface storage in the portion of the profile between the tip and the inlet,  $V_s$ , is found by integrating the right side of Eq. 12.41:

$$V_{s} = \int_{0}^{x_{2}} \left[ \frac{7}{3} v_{1}^{2} n^{2} \phi \right]^{0.428} d\phi$$

$$= \frac{7}{10} \left[ \frac{7}{3} v_{1}^{2} n^{2} \right] x_{2}^{1.42} = 0.7 y_{1} x_{2}$$
(12.43)

The depth at the inlet is assumed to be at the critical depth:

$$y_1 = y_c = \left(\frac{q_1^2}{g}\right)^{0.33} \tag{12.44}$$

A similar analysis is made of the volume of water infiltrating the soil,  $V_1$ . The time-dependent infiltration function is assumed to be the Kostiakov relation, and the advance rate is assumed to be a constant,  $v_1$ , as above. Then

$$t_x = \frac{x}{v_1} \tag{12.45}$$

in which  $t_x$  is the time required for the advance to reach the distance x. The infiltrated depth can then be written as a function of x only:

$$Z(x) = \frac{k(x_2 - x)^a}{v_1^a}$$
 (12.46)

Integrating, we obtain

$$V_{I} = \int Z(x) dx = \frac{k}{v_{1}^{a}} \int_{0}^{x} 2(x_{2} - x)^{a} dx$$

$$= \frac{k}{v_{1}^{a}} \frac{x_{2}^{1+a}}{1+a}$$
(12.47)

and

$$V_I = \frac{Z_1 x_2}{1 + a} \tag{12.48}$$

where  $Z_1$  is the infiltrated depth at the inlet during the first time interval. Equations 12.43 and 12.48 can be set equal to the total inflow  $(q_1t_1)$  and solved for  $x_2$  to estimate the location of the advancing front for the first time increment:

$$x_2 = \frac{q_1 t_1}{0.7 y_1 + [Z_1/(1+a)]}$$
 (12.49)

# **Boundary Conditions**

The mathematical problem at the left and right boundaries is solved by writing appropriate boundary conditions describing advance, ponding, depletion, and recession phases of the irrigation event.

The left boundary consists of the field inlet during advance, ponding, and depletion and the receding edge during recession. While the left boundary is at the field inlet, Eqs. 12.24 and 12.26 are not defined as noted previously and Eqs. 12.25 and 12.27 have three unknowns,  $y_m$ ,  $v_m$ , and  $x_r$  ( $y_1$ ,  $v_1$ , and  $x_r$ ). A third equation can be written from the inflow hydrograph:

$$A_5 = v_1 - \frac{q_1|_{t_{l-1}}}{y_1} \tag{12.50}$$

The Jacobian matrix is now a  $3 \times 3$  matrix with the differentiation of Eq. 12.50 filling the top row.

At the time of cutoff,  $t_{co}$ , the inlet discharge and velocity are set instantly to zero. Equations 12.25 and 12.27 then only have two unknowns  $(y_1 \text{ and } x_r)$  and can be solved directly without a boundary equation. As the depth gradually diminishes until it approaches zero (depletion phase), the left boundary begins receding along the direction of flow (recession phase). Because zero depth is computationally impossible to achieve with the numerical procedure, the analysis sets an arbitrarily small value of depth at which recession has been assumed to be completed. The boundary is then moved to the next computational node by setting the velocity at that node equal to zero. If the  $r_i$  in Eq. 12.22, which is defined as a value greater than 1 at the beginning of recession, is chosen properly, the discrete changes in the receding front are smoothed.

The right boundary condition during advance can be considered the same as the initial condition during the advance phase. Once the leading edge reaches the end of the field, the boundary condition must be changed according to one of two possibilities: (1) either the tailwater drains from the field, or (2) a barrier stops the forward flow and the ponding phase begins. Although some judgment may be required, it is generally adequate to assume that tailwater exits the field at normal depth. [Although if the end of the field is an abrupt drop, the end depth will be about 0.7 times the critical depth (Kwun, 1975).] At the right boundary Eqs. 12.25 and 12.27 are undefined, leaving Eqs. 12.24 and 12.26 with three unknowns,  $v_{N+1}$ ,  $y_{N+1}$ , and  $x_l$ . A third expression for velocity at the right boundary based on a uniform flow assumption can be written as follows:

$$A_6 = v_{N+1} - \frac{S_0^{.5}}{n} y_{N+1}^{.66}$$
 (12.51)

The Jacobian matrix for the right boundary solution following the completion of advance is based on the differentiation of Eqs. 12.24, 12.26, and 12.51. If the field end is blocked, Eqs. 12.24 and 12.26 reduce to two unknowns,  $y_{N+1}$  and  $x_l$ , and can be solved directly.

#### SUMMARY

Many concepts that appear promising at the mathematical level are impractical when implemented due to the expense of the computer execution. The characteristic method for solving the hydrodynamic model is one such case. For events

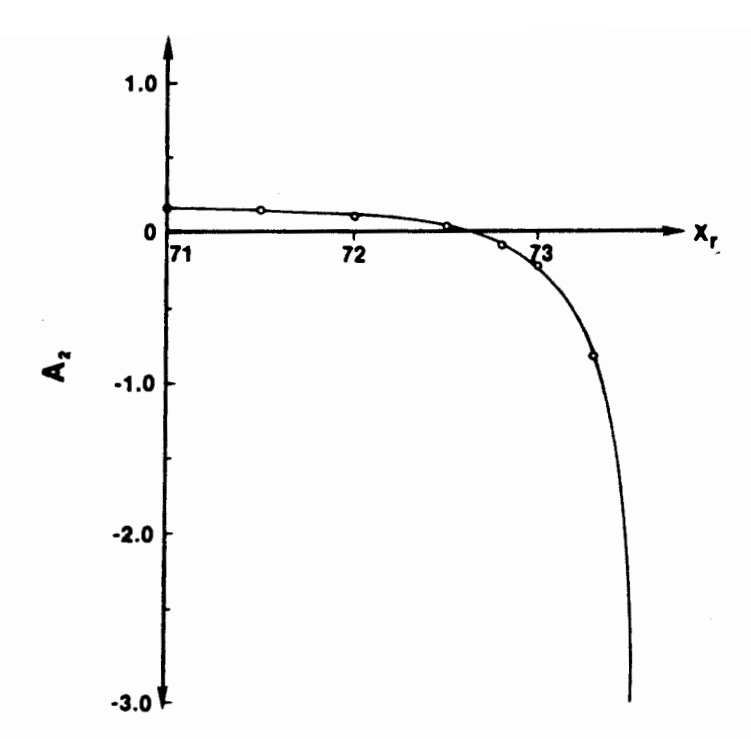


Figure 12.2 Relationship of  $A_2$  to  $x_r$ .

covering many hours, maximum time steps have seldom exceeded 20 to 30 s. Thus the number of Newton-Raphson solutions of four algebraic equations is very large, causing corresponding expenses to soar for any but the simplest irrigation tests. However, were it just a matter of large execution times, the characteristic approach would still be viable in surface irrigation engineering since the advances in computer technology would soon make the model feasible to utilize. Unfortunately, the characteristic approach has a fundamental mathematical problem.

For nodes close to the advancing tip, the relationships between the derivatives of Eqs. 12.24 to 12.27 and the associated y, v,  $x_r$ , and  $x_l$  parameters are not well behaved. An illustration is given in Fig. 12.2 for the  $A_2$  function versus  $x_r$  (Haie, 1984). As can be seen, unless the initial approximation of  $x_r$  is very good, the Newton-Raphson procedure is likely to enter the region of extremely steep gradients and fail to converge. Of a number of methods evaluated to ensure convergence, the most reliable alternative was to maintain very small (5 to 10 s) time steps so that step-to-step changes in the flow profile were small. Even so, as the structure of the problem changes due to different inflows, intake characteristics, and so on, a convergence problem near the tip may be encountered even at smaller time steps.

Although the characteristic approach to surface irrigation modeling is at present impractical, especially given the effectiveness of the integral solution described in Chapter 13, the principles are important for the study of surface irrigation and have therefore been included in this text. The insights and experience acquired while attempting to formulate a workable hydrodynamic model using the characteristic approach substantially aided the development of the other models described in the following chapters.

Summary

#### REFERENCES

- BASSETT, D. L. 1972. Mathematical Model of Water Advance in Border Irrigation. Trans. ASAE 15(5):992-995.
- BASSETT, D. L., and D. W. FITZSIMMONS. 1976. Simulating Overland Flow in Border Irrigation. *Trans. ASAE* 19(4):666-671.
- HAIE, N. 1984. Hydrodynamic Simulation of Continuous and Surged Surface Flow. Ph.D. dissertation, Agricultural and Irrigation Engineering Department, Utah State University, Logan, Utah.
- KATAPODES, N. D., and T. STRELKOFF. 1977. Hydrodynamics of Border Irrigation—Complete Model. ASCE J. Irrig. Drain. Div. 103(IR3):309-324.
- KINCAID, D. C., D. F. HEERMANN, and E. G. KRUSE. 1972. Hydrodynamics of Border Irrigation. *Trans. ASAE* 15(4):674–680.
- KWUN, S. 1975. Design of Irrigation Drop Structures: CID. Water Manag. Tech. Rep. 33. Colorado State University, Fort Collins, Colo., March.
- Souza, F. 1981. Nonlinear Hydrodynamic Model of Furrow Irrigation. Unpublished Ph.D. dissertation, Department of Land, Air and Water Resources. University of California, Davis, Calif.
- STRELKOFF, T. 1970. Numerical Solution of Saint-Venant Equations. ASCE J. Hydraul. Div. 96(HY1):223-252.
- STRELKOFF, T., and N. D. KATAPODES. 1977. Border Irrigation Hydraulics with Zero-Inertia. ASCE J. Irrig. Drain. Div. 103(IR3):325-342.
- WILKE, O. C. 1968. A Hydrodynamic Study of Flow in Irrigation Furrows. Tech. Rep. 13. Water Resources Institute, Texas A & M University, College Station. Tex., July.

1

İ

# The Hydrodynamic Model: Eulerian Integration

# THE DEFORMABLE CONTROL VOLUME

The Eulerian integration approach is a numerical approximation of the Saint-Venant equations based on the concept of a deforming control volume comprised of individual deforming cells. The principal deformation can occur at the system inlet, in which case the cells have a forward velocity (an analysis called the Lagrangian system) or it can occur at the downstream boundary and the cells are stationary (Eulerian system). The zero-inertia model discussed in the following chapter is based on the Lagrangian system, so the development herein will be limited to the Eulerian system.

Conceptually, the approach considers the surface and subsurface water profile along the wetted portion of the field during sequential time steps. Figure 13.1 illustrates the flow profile at two times,  $t_{i-1}$  and  $t_i$ , and identifies the cells comprising the profiles. During each time step, the flow advances an incremental distance,  $\delta x$ .

One typical cell in the profile has been extracted in Fig. 13.2 for closer examination. The cell was formed during the (k-1)th time step and is shown for the (i-1)th and ith time step. The J, M, L, R notation is introduced for each cell to identify the physical parameters with respect to time and space. A parameter subscripted by a J or M refers to conditions at time  $t_{i-1}$  and at the left and right boundaries of the cell, respectively. Similarly, L and R are subscripts at the left and right cell boundaries at time  $t_i$ . Combining of all the cells together yields a time-space grid as shown in Fig. 13.3, from which the advance and recession trajectories can be plotted.

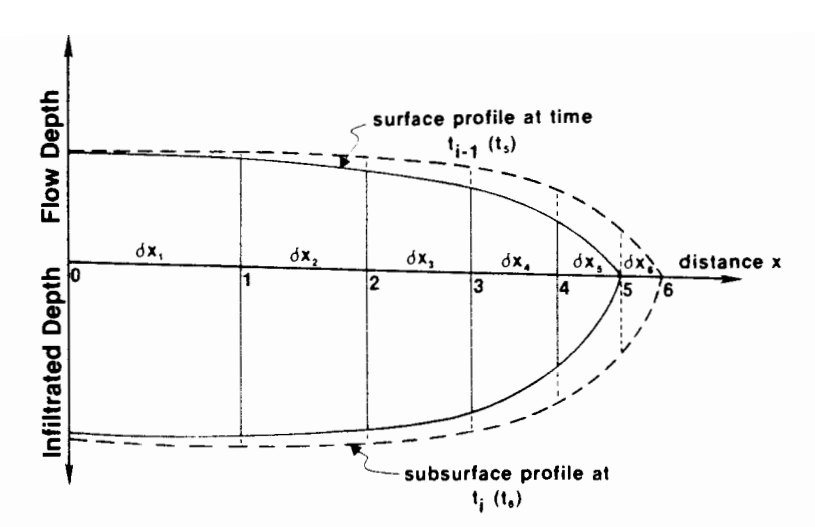


**Figure 13.1** Typical surface and subsurface flow profile expansion under surface-irrigated conditions.

There are two approaches that might be followed to relate the equation of motion to the multicell deforming control volume. The first involves an integral method using first-order approximations. The second, which will be followed here, is patterned after the original development in Chapter 11. Both lead to exactly the same result. The interested reader may wish to consult the dissertation by Souza (1981) for a description of the integral approach.

#### **DEFINITION OF CONTINUITY**

The continuity relation states simply that inflow minus outflow must equal a change in cell volume. During the interval  $t_i - t_{i-1}$ , the net inflow volume is written:

net inflow volume = 
$$\left[\theta(Q_L - Q_R) + (1 - \theta)(Q_J - Q_M)\right] \delta t$$
 (13.1)

where

 $\delta t = \text{in the time step size}, t_i - t_{i-1}$ 

Q = flow across the respective cell boundaries

 $\dot{\theta}$  = time-averaging coefficient to account for the nonlinear variation in the flow profile over time

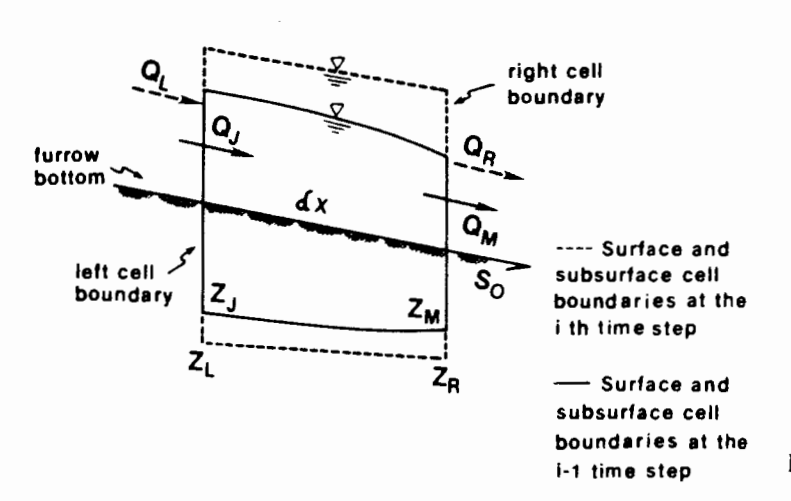
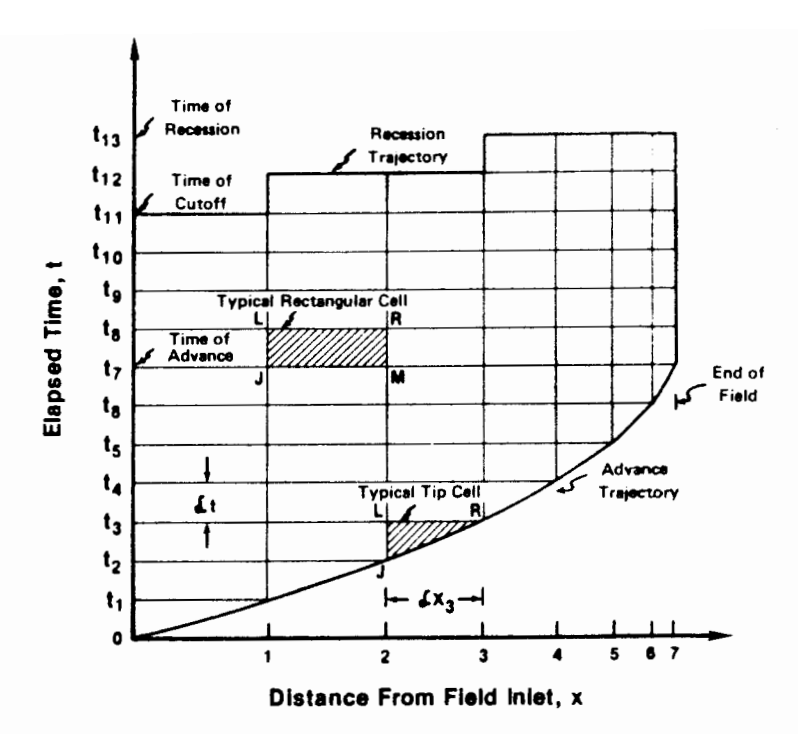


Figure 13.2 Deforming flow cell.



**Figure 13.3** Eulerian space-time solution grid.

The change in cell volume during  $\delta t$  is

$$\Delta \text{ volume} = \text{volume} \mid_{t_{l}} - \text{volume} \mid_{t_{l-1}}$$

$$= [\phi(A_{L} + Z_{L}) + (1 - \phi) (A_{R} + Z_{R})] \delta x \qquad (13.2)$$

$$- [\phi(A_{J} + Z_{J}) + (1 - \phi) (A_{M} + Z_{M})] \delta x$$

where

A = cross-sectional flow area

Z = infiltrated volume per unit length

 $\delta x = \text{length of the cell}$ 

 $\phi$  = space-averaging coefficient to account for nonlinear variation in the flow profile over the cell

Equating Eqs. 13.1 and 13.2 yields the continuity relationship:

$$[\theta(Q_{L} - Q_{R}) + (1 - \theta) (Q_{J} - Q_{M})] \delta t - [\phi(A_{L} + Z_{L} - A_{J} - Z_{J}) + (1 - \phi) (A_{R} + Z_{R} - A_{M} - Z_{M})] \delta x = 0$$
 (13.3)

#### **MOMENTUM EQUATION**

Newton's second law states:

$$F_W + F_p - F_f = \frac{d(mv)}{dt}$$
 (13.4)

where  $F_w$  = net weight force acting on the cell in the direction of flow

 $F_p$  = net pressure force acting on the cell

 $\vec{F}_f$  = friction force along the cell-soil boundary

m =mass of fluid in the cell

v = velocity of fluid in the cell

It is again assumed that momentum removed from the system due to infiltration is negligible, the bed slope angle is small enough to be approximated by the bed slope,  $S_0$ , and the friction force can be approximated by that which would occur under a similar but steady condition. It is further assumed, as previously, that the time-dependent change in momentum is equal to the net momentum flux into the cell plus the net change of momentum within the cell.

# **Weight Forces**

Weight forces acting in the direction of flow are described as follows:

$$F_W = \gamma A S_0 \,\delta x \tag{13.5}$$

in which  $\gamma$  is the specific weight of water. Writing Eq. 13.5 for the spatial averages at times  $t_{i-1}$  and  $t_i$  and then time averaging to determine the condition during the interval gives

$$F_W = [\theta \{ \phi A_1 + (1 - \phi) A_R \} + (1 - \theta) \{ A_1 + (1 - \phi) A_M \}] \gamma S_0 \delta x \qquad (13.6)$$

## **Pressure Forces**

The basic relation describing the pressure force acting on a cell boundary is

$$F_p = \gamma h A \tag{13.7}$$

where h is the vertical distance from the water surface to the centroid of the cross-sectional flow area, A. To reference the centroid from the same datum as flow depth, the following transformation is introduced:

$$h = y - d \tag{13.8}$$

where

$$d = \frac{1}{A} \int_0^A y' \ dA' \tag{13.9}$$

in which y' and A' are the integrands of depth and area. For most surface irrigation conditions, the flow geometry can be represented as power functions of depth or area. For instance, the top width of the flow, T, can be given by

$$T = \mu_1 y^{\mu_2} \tag{13.10}$$

Since dA = T dv,

$$A = \int \mu_1 y^{\mu_2} dy = \frac{\mu_1}{1 + \mu_2} y^{\mu_2 + 1}$$
 (13.11)

$$d = \frac{1}{A} \int_0^y y' T' \ dy' = \frac{1}{A} \int_0^y \mu_1 y'^{\mu_2 + 1} \ dy' = \frac{\mu_2 + 1}{\mu_2 + 2} y \tag{13.12}$$

and

$$h = \frac{y}{\mu_2 + 2} = \frac{(\mu_2 + 1)^{\frac{1}{\mu_2 + 1}}}{(\mu_2 + 2)\mu_1^{\frac{1}{\mu_2 + 1}}} A^{\frac{1}{\mu_2 + 1}}$$
(13.13)

Simplification of the equation above can be made by defining the pressure force in terms of the pressure, P:

$$F_p = \gamma P = \gamma \varepsilon_1 A^{\varepsilon_2} \tag{13.14}$$

where

$$\varepsilon_1 = \frac{1}{\mu^2 + 2} \left( \frac{\mu_2 + 1}{\mu_1} \right)^{\frac{1}{\mu_2 + 1}} \tag{13.15}$$

and

$$\varepsilon_2 = \frac{\mu_2 + 2}{\mu_2 + 1} \tag{13.16}$$

The net pressure force acting on the cell during the time interval is equal to the time averaged force at the cell inlet minus the time-average force at the outlet:

$$F_{p} = \gamma \{ [\theta P_{L} + (1 - \theta)P_{J}] - [\theta P_{R} + (1 - \theta)P_{M}] \}$$

$$= \gamma [\theta (P_{L} - P_{R}) + (1 - \theta)(P_{J} - P_{M})]$$
(13.17)

## **Friction Forces**

The general expression for the friction force is

$$F_f = \gamma A S_f \, dx \tag{13.18}$$

where  $S_f$  is the friction slope developed from the Manning formula:

$$S_f = \frac{Q^2 n^2}{A^2 R^{4/3}} \tag{13.19}$$

and R and n are the hydraulic radius and resistance coefficient, respectively. The product of area and friction slope is occasionally referred to as the drag, D. Because the friction force applies along the length of the cell's wetted surface with the soil, the average force must be the result of a spatial and time-average combination of the cell boundary conditions. Thus at times  $t_i$  and  $t_{i-1}$ ,

$$F_{f|_{t_{i}}} = \gamma [\phi D_{L} + (1 - \phi)D_{R}] \delta x$$

$$F_{f|_{t_{i-1}}} = \gamma [\phi D_{J} + (1 - \phi)D_{M}] \delta x$$
(13.20)

so that during the interval  $\delta t$ ,

$$F = \theta F_f|_{t_t} + (1 - \theta)F_f|_{t_{t-1}}$$
 (13.21)

$$= \gamma \{\theta[\phi D_{L} + (1 - \phi)D_{R}] + (1 - \theta)[\phi D_{J} + (1 - \phi)D_{M}]\} \delta x \qquad (13.22)$$

# **Unsteady Momentum**

Reiterating the assumption regarding the unsteady momentum (right-hand side of Eq. 13.4), we have

$$\frac{d(mv)}{dt} = \frac{\Delta(mv)_{\text{out}} - \Delta(mv)_{\text{in}}}{\delta t} + \frac{mv|_{t_i} - mv|_{t_{i-1}}}{\delta t}$$
(13.23)

The momentum flux in or out of the cell is the product of mass times velocity at the cell boundary. Thus, during the time step the average flux out of the cell is

$$\Delta(mv)_{\text{out}} = \frac{\rho[\theta Q_{\text{R}} v_{\text{R}} \delta t + (1 - \theta) Q_{\text{M}} v_{\text{M}} \delta t]}{\delta t}$$

$$= \rho \left[\theta \left(\frac{Q^2}{A}\right)_{\text{R}} + (1 - \theta) \left(\frac{Q^2}{A}\right)_{\text{M}}\right]$$
(13.24)

Similarly,

$$\frac{\Delta(mv)_{\rm in}}{\delta t} = \rho \left[ \theta \left( \frac{Q^2}{A} \right)_{\rm L} + (1 - \theta) \left( \frac{Q^2}{A} \right)_{\rm J} \right]$$
 (13.25)

The change in momentum within the cell involves the spatial average conditions at the endpoints of the time interval:

$$\frac{(mv)|_{t_t}}{\delta t} = \frac{\rho \delta x}{\delta t} \left[ \phi A_L v_L + (1 - \phi) A_R v_R \right]$$

$$= \rho \left[ \phi Q_L + (1 - \phi) Q_R \right] \frac{\delta x}{\delta t}$$
(13.26)

and similarly,

$$\frac{(mv)}{\delta t}\bigg|_{t=1} = \rho[\phi Q_{\rm J} + (1-\phi)Q_{\rm M}] \frac{\delta x}{\delta t}$$
 (13.27)

Adding Eqs. 13.24 to 13.27 gives

$$\frac{d(mv)}{dt} = \rho \left\{ \theta \left[ \left( \frac{Q^2}{A} \right)_{R} - \left( \frac{Q^2}{A} \right)_{L} \right] + (1 - \theta) \left[ \left( \frac{Q^2}{A} \right)_{M} - \left( \frac{Q^2}{A} \right)_{J} \right] \right\} 
+ \rho \left[ \phi (Q_{L} - Q_{J}) + (1 - \phi) (Q_{R} - Q_{M}) \right] \frac{\delta x}{\delta t}$$
(13.28)

# Final Momentum Equation

The addition of Eqs. 13.6, 13.17, and 13.22, which can be equated to Eq. 13.28, yields the momentum equation. After dividing through by  $\gamma \delta x$  and combining terms, the equation is

$$\frac{1}{g} \frac{\left[ \phi(Q_{L} - Q_{J}) + (1 - \phi)(Q_{R} - Q_{M}) \right]}{\delta t} + \frac{\theta[(P + Q^{2}/Ag)_{R} - (P + Q^{2}/Ag)_{L}]}{\delta x} + \frac{(1 - \theta)[(P + Q^{2}/Ag)_{M} - (P + Q^{2}/Ag)_{J}]}{\delta x} - S_{0} \{\theta[\phi A_{L} + (1 - \phi)A_{R}] + (1 - \theta)[\phi A_{J} + (1 - \phi)A_{M}]\} + \theta[\phi D_{L} + (1 - \phi)D_{R}] + (1 - \theta)[\phi D_{J} + (1 - \phi)D_{M}] = 0$$
(13.29)

## **NUMERICAL SOLUTION**

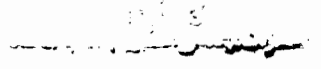
The continuity and momentum equations developed in this chapter are finite difference approximations of the equations developed in Chapter 11. They are nonlinear and algebraic. The characteristic solution given in Chapter 12 yielded four nonlinear algebraic equations in four unknowns at each node, whereas Eqs. 13.3 and 13.29 contain only two. The fundamental difference is that construction of the solution over incremental time steps can be based on known conditions at known locations rather than interpolated conditions at unknown locations. This substantial simplification allows an implicit solution (conditions at all nodes can be found simultaneously rather than node by node).

The Newton-Raphson procedure is again used for solving the equations. The matrix that results is banded and is therefore amenable to a particularly efficient Gaussian elimination method called the Preissmann double-sweep algorithm (Liggett and Cunge, 1975).

The solution begins with an initial condition, proceeds through the advance phase by adding a new cell for each time step, continues through the wetting or ponding and depletion phase with a fixed number of cells, and then computes the recession during which the number of cells decline. Equations 13.3 and 13.29 are written for each cell and supplemented by upstream and downstream boundary conditions. Figure 13.3 shows the cells in the t-x plane. There are at time  $t_i$ , N cells defined with nodes or cell boundaries numbered 0 at the left boundary to N at the right. At nodes 1 - N - 1, there are two unknowns, Q and A, at time  $t_i$  with Q and A known at  $t_{i-1}$ . It is assumed that infiltration is a unique function of opportunity time, and therefore these variables are known at all nodes and at both times.

At the left boundary, the inflow is specified by a hydrograph and the only unknown is area. At the right boundary, Q and A are defined according to the structure of the boundary and the phase of irrigation being computed. During

Numerical Solution 31



advance, Q and A at the right boundary are zero (tip cell) but the incremental advance  $\delta x$  is unknown. Following advance, one or the other is specified by the condition at the end of the field. If the field is free draining, A is often expressed as a function of Q by assuming a uniform flow exit. If the field is diked, Q is zero. Thus the analysis contains one unknown at the first and last nodes (0 and N) and two at all nodes 1 to N-1, totaling 2N unknowns. Considering each cell, Eqs. 13.3 and 13.29 (or their boundary conditions counterparts) yield 2N equations, thereby balancing the solution.

Before examining the specific elements of the solution, it is necessary to illustrate the double sweep form of the implicit Newton-Raphson scheme.

# Newton-Raphson Procedure

For the first cell, Eqs. 13.3 and 13.29 can be equated to a parameter  $P_1$  and a parameter  $R_1$ , both of which are zero when the solution to the equation is achieved. As the solution moves from time to time, solution of the two equations begins with an approximation to the unknown variables  $(A_L, Q_L, A_R, \text{ and } Q_R)$  which when substituted into the equations would yield the residuals  $P_1$  and  $R_1$ . The Newton-Raphson procedure utilizes the results of this analysis to improve the solution systematically until  $P_1 = R_1 = 0$ .

The residuals  $P_1$  and  $R_1$  can be written in terms of a Taylor Series expansion as follows:

$$P_1^{n+1} = P_1^n + (\nabla P_1^n) \Delta P_1^n \tag{13.30}$$

and

$$R_1^{n+1} = R_1^n + (\nabla R_1^n) \Delta R_1^n \tag{13.31}$$

where the superscripts refer to the iteration; that is, the residuals at the improved solution  $(P_1^{n+1} \text{ and } R_1^{n+1})$  are functions of the current solution:

$$P_1^n = P(A_L^n, Q_L^n, A_R^n, Q_R^n)$$
 (13.32)

and

$$R_1^n = R(A_L^n, Q_L^n, A_R^n, Q_R^n)$$
 (13.33)

The gradient terms,  $\nabla P_1^n$  and  $\nabla R_1^n$ , are the Jacobian matrices:

$$\nabla P_1^n = \left(\frac{\partial P_1}{\partial A_L}, \frac{\partial P_1}{\partial Q_L}, \frac{\partial P_1}{\partial A_R}, \frac{\partial P_1}{\partial Q_R}\right)^n \tag{13.34}$$

and

$$\nabla R_1^n = \left(\frac{\partial R_1}{\partial A_1}, \frac{\partial R_1}{\partial Q_1}, \frac{\partial R_1}{\partial A_R}, \frac{\partial R_1}{\partial Q_R}\right)^n \tag{13.35}$$

Finally, the difference term  $\Delta P_1^n$  and  $\Delta R_1^n$  are the matrices

$$\Delta P_{1}^{n} = (A_{L}^{n+1} - A_{L}^{n}, Q_{L}^{n+1} - Q_{L}^{n}, A_{R}^{n+1} - A_{R}^{n}, Q_{R}^{n+1} - Q_{R}^{n})$$

$$= (\delta A_{L}, \delta Q_{L}, \delta A_{R}, \delta Q_{R})$$
(13.36)

and similarly,

$$\Delta R_1^n = (\delta A_1, \delta Q_1, \delta A_R, \delta Q_R) = \Delta P_1^n \tag{13.37}$$

Because it is expected that  $P_1^{n+1}$  and  $R_1^{n+1}$  will eventually equal zero, they are set equal to zero at each iteration, thereby making Eqs. 13.30 and 13.31 two linearized equations in the unknowns  $\delta A_L$ ,  $\delta Q_L$ ,  $\delta A_R$ ,  $\delta Q_R$ . Writing Eqs. 13.30 and 13.31 in an expanded form yields

$$\left(\frac{\partial P_{1}}{\partial A_{L}}\right)^{n} \delta A_{L} + \left(\frac{\partial P_{1}}{\partial Q_{L}}\right)^{n} \delta Q_{L} + \left(\frac{\partial P_{1}}{\partial A_{R}}\right)^{n} \delta A_{R} + \left(\frac{\partial P_{1}}{\partial Q_{R}}\right)^{n} \delta Q_{R} = -P_{1}^{n}$$
(13.38)

and

$$\left(\frac{\partial R_{1}}{\partial A_{L}}\right)^{n} \delta A_{L} + \left(\frac{\partial R_{1}}{\partial Q_{L}}\right)^{n} \delta Q_{L} + \left(\frac{\partial R_{1}}{\partial A_{R}}\right)^{n} \delta A_{R} + \left(\frac{\partial R_{1}}{\partial Q_{R}}\right)^{n} \delta Q_{R} = -R_{1}^{n}$$
(13.39)

For convenience, Eqs. 13.38 and 13.39 for each cell can be represented as follows:

$$A_{i} \delta A_{i-1} + B_{i} \delta Q_{i-1} + C_{i} \delta A_{i} + D_{i} \delta Q_{i} = -P_{i}$$
 (13.40)

and

$$E_{i} \delta A_{i-1} + F_{i} \delta Q_{i-1} + G_{i} \delta A_{i} + H_{i} \delta Q_{i} = -R_{i}$$
 (13.41)

where j = 1, 2, 3, ..., N.

Equations 13.40 and 13.41 are written for each cell, resulting in the matrix structure shown by Elliott (1981) in Fig. 13.4. The first and last lines correspond to the boundary conditions. At the inlet, during the on-time for instance, it is assumed that a linear combination of the discharge and area variables exists:

$$\delta Q_0 = S_1 \, \delta A_0 + T_1 \tag{13.42}$$

At the field inlet, discharge is assumed to be independent of area and  $S_1 = 0$ .  $T_1$  represents the change in inflow rates reflected by the inflow hydrograph.

At the downstream boundary Eq. 13.42 is used directly for the advancing tip and the runoff or diked conditions. During advance, both area and discharge are zero at the tip, but the incremental advance distance,  $\delta x_N$ , is unknown. Letting  $\delta \delta$  be exchanged for  $\delta Q_N$  yields

$$\delta\delta = S_{N+1} \, \delta A_N + T_{N+1} \tag{13.43}$$

where  $T_{N+1}$  will equal  $\delta\delta$  since  $\delta A_N$  equals zero.

The Preissmann double-sweep solution of the linearized equations assumes that the assumption of Eqs. 13.42 and 13.43 holds at all nodes:

$$\delta Q_{i-1} = S_i \, \delta A_{i-1} + T_i \qquad (1 \le j \le N) \tag{13.44}$$

The following description of the technique is taken from Elliott (1981).

Numerical Solution 321

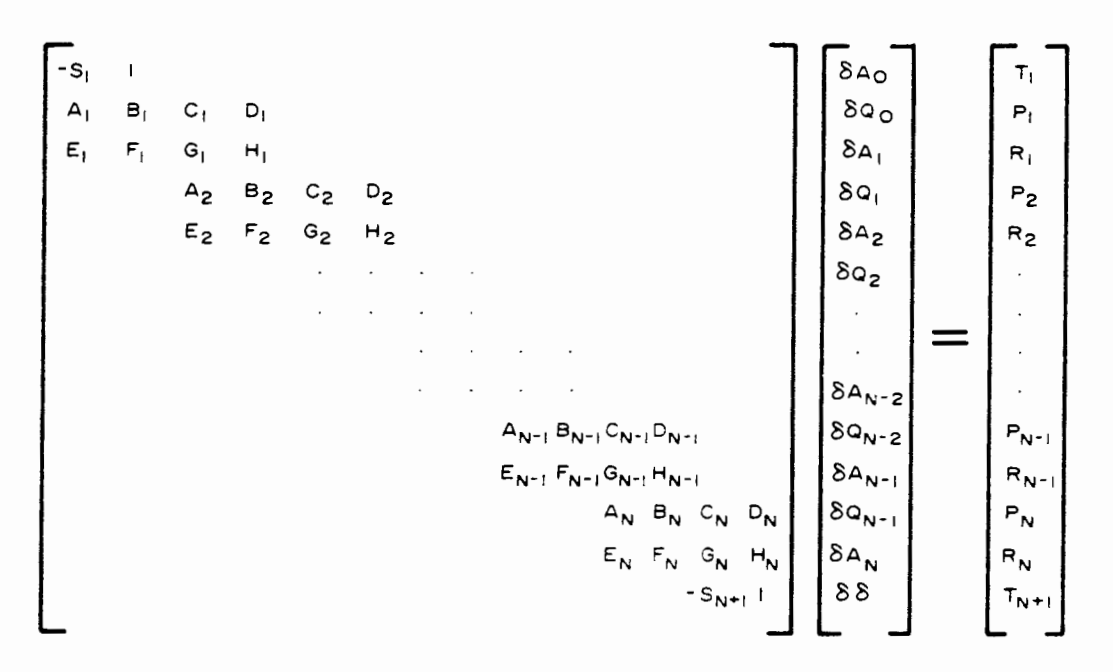


**Figure 13.4** Matrix representation of the implicit equations and boundary conditions for solving the Saint-Venant equations. (After Elliott, 1981.)

The first "sweep" of the procedure begins by substituting Eq. 13.42 into Eq. 13.40 and solving for  $\delta A_0$ . The results:

$$\delta A_0 = \frac{-P_1 - B_1 T_1 - C_1 \,\delta A_1 - D_1 \,\delta Q_1}{A_1 + B_1 S_1} \tag{13.45}$$

Then Eqs. 13.42 and 13.45 are substituted into Eq. 13.41 and solved for  $\delta Q_1$ , yielding

$$\delta Q_1 = \frac{(U_1 C_1 - G_1) \, \delta A_1 - R_1 + F_1 T_1 + U_1 (P_1 + B_1 T_1)}{H_1 - U_1 D_1} \tag{13.46}$$

where

$$U_1 = \frac{E_1 + F_1 S_1}{A_1 + B_1 S_1} \tag{13.47}$$

Equation 13.46 may also be written as

$$\delta Q_1 = S_2 \, \delta A_1 + T_2 \tag{13.48}$$

where

$$S_2 = \frac{U_1 C_1 - G_1}{H_1 - U_1 D_1} \tag{13.49}$$

and

$$T_2 = \frac{-R_1 - F_1 T_1 + U_1 (P_1 + B_1 T_1)}{H_1 - U_1 D_1}$$
 (13.50)

The following recursive formulas are thus established:

$$U_{j} = \frac{E_{j} + F_{j}S_{j}}{A_{i} + B_{j}S_{i}}$$
 (13.51)

$$S_{i+1} = \frac{U_i C_i - G_i}{H_i - U_i D_i} \tag{13.52}$$

and

$$T_{j+1} = \frac{-R_j - F_j T_j + U_j (P_j + B_j T_j)}{H_j - U_j D_j}$$
(13.53)

Knowing  $S_1$  and  $T_1$ , these three equations can be applied recursively from j = 1 through j = N, constituting the "first sweep" of the algorithm. It should be noted that the S and T arrays must be stored, but the value of U at each step need not be remembered. As noted previously,  $S_1 = 0$  and the case of a constant inflow rate,  $T_1$ , is also equal to zero.

At the end of the first sweep, the values of  $S_{N+1}$  and  $T_{N+1}$  are known, which allows computation of  $\delta\delta$  or  $\delta A_N$ , depending on the downstream condition. Equations 13.44 and 13.45 suggest the following formulas for determining the unknown values of  $\delta A$  and  $\delta Q$  at each node:

$$\delta A_{k-1} = \frac{-P_k - B_k T_k - C_k \, \delta A_k - D_k \, \delta \delta}{A_k + B_k S_k} \qquad (k = N)$$
 (13.54)

or

$$\delta A_{k-1} = \frac{-P_k - B_k T_k - C_k \, \delta A_k - D_k \, \delta Q_k}{A_k + B_k S_k} \qquad (N > k \ge 1)$$
 (13.55)

and

$$\delta Q_{k-1} = S_k \, \delta A_{k-1} + T_k \tag{13.56}$$

This second sweep is conducted by applying these equations recursively from k = N through k = 1.

Having computed all values of  $\delta A$ , and  $\delta Q$ , as well as  $\delta x_N$ , if applicable, the improved solution is determined by

$$A_j^{n+1} = A_j^n + \delta A_j \qquad (0 \le j \le N)$$

$$Q_j^{n+1} = Q_j^n + \delta Q_j \qquad (1 \le j \le N)$$
(13.57)

and

$$\delta x_N^{n+1} = \delta x_N^n + \delta \delta$$

Then the residuals  $P_i$  and  $R_j$  can be calculated and compared to a preselected convergence criterion to determine when the Newton-Raphson procedure has produced the solution.

Numerical Solution 323

## **Initial Conditions**

During the first time, J, M, and R subscripted variables in both of the motion equations are zero. Equation 13.3 reduces to

$$\theta Q_{\rm L} - (A_{\rm L} + Z_{\rm L}) \frac{\delta x_1}{\delta t} = 0$$
 (13.58)

and Eq. 13.29 to

$$\frac{1}{g} \Phi Q_{L} \frac{\delta x}{\delta t} - \theta \left( P + \frac{Q^{2}}{Ag} \right)_{I} - \theta \Phi (S_{0} A_{L} - D_{L}) \delta x_{1}$$
 (13.59)

in which the unknowns are  $\delta x_1$  and  $A_L$ . Equations 13.38 and 13.39 can be written as

$$\left(\frac{\partial P_1}{\partial A_L}\right) \delta A_L + \left(\frac{\partial P_1}{\partial \delta x_1}\right) \delta \delta x_1 = -P_1 \tag{13.60}$$

and

$$\left(\frac{\partial R_1}{\partial A_L}\right) \delta A_L + \left(\frac{\partial R_1}{\partial \delta x_1}\right) \delta \delta x_1 = -R_1$$
(13.61)

These equations can be solved directly for the two unknowns using Cramer's rule for  $\delta A_{\rm L}$  and  $\delta \delta x_{\rm 1}$ , and then used in Eq. 13.57 to iteratively solve for  $A_{\rm L}$  and  $\delta x_{\rm 1}$ :

$$\delta A_{\rm L} = \frac{P_1(\partial R_1/\partial \delta x_1) - R_1(\partial P_1/\partial \delta x_1)}{\frac{\partial P_1}{\partial \delta x_1} \frac{\partial R_1}{\partial A_{\rm L}} - \frac{\partial R_1}{\partial \delta x_1} \frac{\partial P_1}{\partial A_{\rm L}}}$$
(13.62)

and

$$\delta \delta x_1 = \frac{R_1(\partial P_1/\partial A_L) - P_1(\partial R_1/\partial A_L)}{\frac{\partial P_1}{\partial \delta x_1} \frac{\partial R_1}{\partial A_L} - \frac{\partial R_1}{\partial \delta x_1} \frac{\partial P_1}{\partial A_L}}$$
(13.63)

## **Downstream Boundary Conditions**

Most surface irrigation systems will have two downstream boundary conditions: (1) a tip cell during the advance phase, and (2) a rectangular cell at the field boundary. In the latter case, several configurations are possible but usually limited to a diked condition ( $Q_N = 0$ ) or a uniform flow exit. However, in some conditions the outflow may pass over or through a structure with a different hydraulic characteristic than a free-draining field boundary. In this case, it is necessary to establish a discharge rating for the structure to use as the downstream boundary condition.

During the advance phase, Eqs. 13.58 and 13.59 are applied across the tip cell. With the boundary condition that  $Q_R$ ,  $A_R$ ,  $Q_M$ , and  $A_m$  are zero, the procedure solves only for  $Q_L$ ,  $A_L$ , and  $\delta x$ .  $\delta x$  is utilized as the parameter in place of  $A_R$  in the double sweep procedure.

When the flow reaches the end of the field, the M and R variables will not be zero for all time steps. For this condition, which can be generalized for the free-draining, diked, or controlled conditions, the boundary condition may be written

$$Q_N = \alpha A_N^m \tag{13.64}$$

For the free-draining case, the uniform flow can be used to define  $\alpha$  and m as

$$\alpha = \frac{(\rho_1 S_0)^{0.5}}{n} \tag{13.65}$$

and

$$m = \frac{\rho_2}{2} \tag{13.66}$$

where as defined previously,  $S_0$  is the slope, n is the resistance coefficient, and  $\rho_1$ ,  $\rho_2$  are characteristics of the hydraulic section:

$$A^2 R^{1.33} = \rho_1 A^{\rho_2} \tag{13.67}$$

For controlled field runoff, it is necessary to define  $\alpha$  and m for the particular characteristics of the control section. If the field is diked,  $\alpha$  can be set to zero. If  $Q_r$  is substituted for  $Q_R$  in Eqs. 13.38 and 13.39, it is assumed that

$$\frac{\delta Q_r}{\delta A_R} = \left(\frac{dQ}{dA}\right)_R \tag{13.68}$$

or by using Eq. 13.64,

$$\frac{dQ_r}{dA_R} = m\alpha A_R^{m-1} \tag{13.69}$$

so that

$$\delta Q_r = \delta A_R \frac{dQ_r}{dA_R} = \delta A_R (m\alpha A_R^{m-1})$$
 (13.70)

Then the resulting forms of Eqs. 13.38 and 13.39 become

$$\frac{\partial P_1}{\partial A_L} \delta A_L + \frac{\partial P_1}{\partial Q_L} \delta Q_L + \left( \frac{\partial P_1}{\partial A_R} + m\alpha A^{m-1} \frac{\partial P_1}{\partial Q_R} \right) \delta A_R = -P_1 \qquad (13.71)$$

$$\frac{\partial R_1}{\partial A_L} \delta A_L + \frac{\partial R_1}{\partial Q_L} \delta Q_L + \left( \frac{\partial R_1}{\partial A_R} + m\alpha A_R^{m-1} \frac{\partial R_1}{\partial Q_R} \right) \delta A_R = -R_1 \qquad (13.72)$$

Numerical Solution 325

## **SUMMARY**

The deformable control volume approach has an important advantage over the characteristic approach. The number of computational unknowns is only half as large, allowing the solution to be implicit. Experience to date also indicates more numerical stability and substantially lower execution costs.

One disadvantage is that a new cell appears for each advance phase time step. This can offset the advantages noted above but need not do so. Because of the rectangular grid, the number of cells can be reduced during the computational process by writing the equation of motion between alternate nodes.

## REFERENCES

- ELLIOTT, R. L. 1981. Zero-Inertia Furrow Irrigation Modeling Applied to the Derivation of Infiltration Parameters. Ph.D. dissertation, Colorado State University, Fort Collins, Colo.
- Flow Equations. In *Unsteady Flow in Open Channels*, Vol. 1, K. Mahmood and V. Yevjevich (eds.). Water Resources Publications, Fort Collins, Colo.
- Souza, F. 1981. Non-linear Hydrodynamic Model of Furrow Irrigation. Unpublished Ph.D. dissertation, Department of Land, Air and Water Resources, University of California, Davis, Calif.

# The Zero-Inertia Model

## INTRODUCTION

The hydrodynamic model described in Chapters 12 and 13 is often expensive to operate and may be difficult to utilize because of its complexity. A simplified solution proposed by Strelkoff and Katapodes (1977), called the "zero-inertia" model, is based on the assumption that the inertial and acceleration terms in the momentum equation would be negligible in most surface irrigated conditions. The two equations for the zero-inertia model are

$$\frac{\partial A}{\partial t} + \frac{\partial Q}{\partial x} + \frac{\partial Z}{\partial \tau} = 0 \tag{14.1}$$

and

$$\frac{\partial y}{\partial x} = S_0 - S_f \tag{14.2}$$

The numerical solution of Eqs. 14.1 and 14.2 has been presented by Strelkoff and Katapodes (1977). Several other investigators have made or suggested refinement and verified the model against field data. For instance, Clemmens and Fangmeier (1978) improved the numerical solution associated with a diked-end condition which creates a ponding condition following completion of the advance phase. Clemmens (1979), Elliott et al. (1982), and Oweis (1983) applied the zero-inertia model to other surface-irrigated conditions, including furrows. In every case studied thus far, the model has worked exceptionally well. Analyses of the zero-inertia model itself have been made by several investigators through nondi-

mensionalizing the solutions and then studying the general model response (Katapodes and Strelkoff, 1977; Clemmens, 1979; Strelkoff and Clemmens, 1981; Elliott et al., 1982). From these dimensionless evaluations have come design methodologies for level basins (Clemmens and Strelkoff, 1979) and for sloping borders and basins (Strelkoff and Clemmens, 1981).

The aim of this chapter is to present the basic zero-inertia model, the most common numerical solution, and an illustration of its predictive capability. The first explanations of this model were limited to basin or border systems, which are considered as plane flow regimes. Later studies, such as those of Elliott et al. (1982) and Oweis (1983), generalized the procedure for furrows. Since the plane flow condition is a simplified case of the furrow simulation, the descriptions that follow will be made considering furrow irrigation. Later in the chapter we describe some of the unique features associated with border and basins.

## GENERAL MATHEMATICAL APPROACH

The method of solving Eqs. 14.1 and 14.2, now parabolic rather than hyperbolic, involves a computational definition of surface and subsurface profiles similar to the complete hydrodynamic model of Chapter 13. The time steps are also held constant but need not be if advantages arise for variable time increments such as accuracy during advance and recession. The evaluation of space increments are based on the incremental advance during successive time steps,  $\delta t$ .

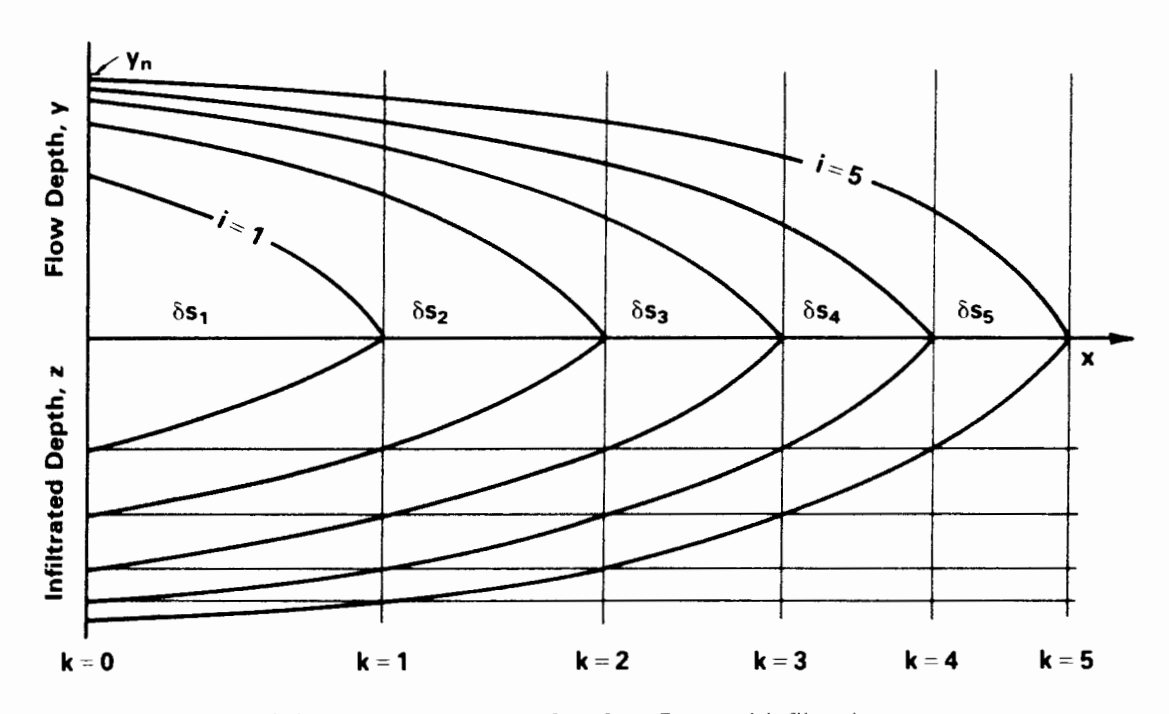


**Figure 14.1** Schematic progression of surface flow and infiltration over constant time steps.

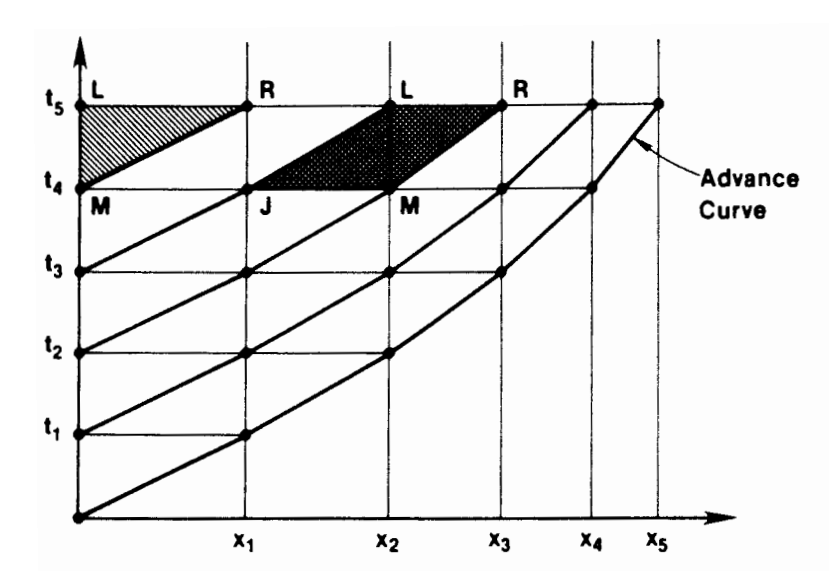


Figure 14.2 Zero-inertia *t-x* grid system. (From Strelkoff and Katapodes, 1977, with permission of ASCE.)

#### The Advance Phase

Consider the flow profile during five successive time intervals, as shown in Fig. 14.1. During the first time step,  $\delta t_1$ , the surface and subsurface profiles extend themselves a distance  $\delta x_1$ . At a subsequent time,  $t_i$  the advance distance,  $x_i$ , is

$$x_i = \sum_{k=1}^i \delta x_k \tag{14.3}$$

in which  $\delta x_k$  is the kth space increment defined by the advance during the time interval when i = k.

The Strelkoff-Katapodes model examines the irrigation as a deforming control volume bounded by the field inlet or the receding front at the left, the advancing tip or the end of the field at the right, the water surface profile at the top, and the infiltrating front at the bottom. In this analysis, the primary deformation comes at the left boundary during advance, creating a control volume of moving cells formed at the left boundary during each time step through advance and then declining during recession. In the mathematical sense, an oblique cell structure is established to advance the solution from time to time in the x-t plane (Fig. 14.2).

Consider a single cell between the left and right boundaries of the control volume as illustrated in Fig. 14.3. The cell is shown at times  $t_{i-1}$  and  $t_i$ . At time  $t_{i-1}$ , the left boundary of the cell is at  $x_{k-2}$  and the right is at  $x_{k-1}$ . The areas of flow and infiltrated volumes per unit length at both times are shown subscripted by J, M, L, and R in order to again identify the time and boundary being studied. The flux of water into and out of the cell volume is also shown, but it should be noted that flux is defined with respect to a fixed spatial coordinate and not the cell boundary. The conservation of mass principle requires that the change in flux be accompanied by a change in volume. The net flow across each boundary is the difference between the discharge, Q, and the flux represented by the movement of the boundary.

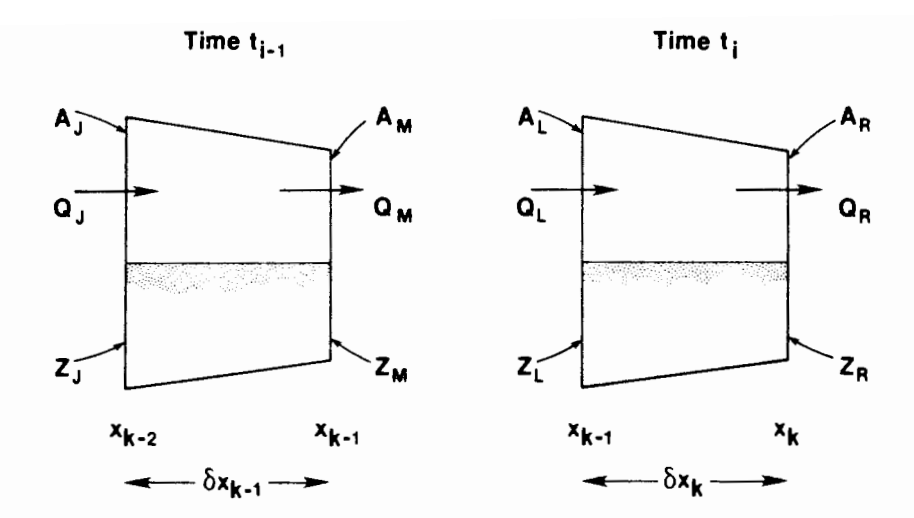


**Figure 14.3** Definition sketch of a single cell at two successive time intervals. (From Elliott et al., 1982, with permission of ASCE.)

At the time  $t_i$ , the net change in flow into the cell is

$$\left[Q_{L}-(A_{L}+Z_{L})\frac{\delta x_{k-1}}{\delta t}\right]-\left[Q_{R}-(A_{R}+Z_{R})\frac{\delta x_{k}}{\delta t}\right]$$
(14.4)

and for  $t_{i-1}$ ,

$$\left[Q_{J}-(A_{J}+Z_{J})\frac{\delta x_{k-1}}{\delta t}\right]-\left[Q_{M}-(A_{M}+Z_{M})\frac{\delta x_{k}}{\delta t}\right] \qquad (14.5)$$

The average of Eqs. 14.4 and 14.5 multiplied by the time interval,  $\delta t$ , is the change in volume that occurs within the cell. Since the upper and lower boundaries are nonlinear, weighting factors,  $\phi$  and  $1 - \phi$ , are utilized to define the spatial average  $(0 \le \phi \le 1)$ .

The change in cell volume can also be calculated by multiplying the average surface and subsurface depths by the space increment. Again the boundary non-linearity suggests the use of time-averaging weighting factors,  $\theta$  and  $1-\theta$ , where  $0 \le \theta \le 1$ . The change in volume during the time interval can thus be written and equated to the result of combining Eqs. 14.4 and 14.5 to yield the mass balance relation:

$$\frac{\delta x_{k}}{\delta t} [(A_{L} + Z_{L}) \phi + (A_{R} + Z_{R})(1 - \phi)] - \frac{\delta x_{k-1}}{\delta t} [(A_{J} + Z_{J}) \phi + (A_{M} + Z_{M})(1 - \phi)]$$

$$= \theta \left\{ \left[ Q_{L} - (A_{L} + Z_{L}) \frac{\delta x_{k-1}}{\delta t} \right] - \left[ Q_{R} - (A_{R} + Z_{R}) \frac{\delta x_{k}}{\delta t} \right] \right\}$$

$$+ (1 - \theta) \left\{ \left[ Q_{J} - (A_{J} + Z_{J}) \frac{\delta x_{k-1}}{\delta t} \right] - \left[ Q_{M} - (A_{M} + Z_{M}) \frac{\delta x_{k}}{\delta t} \right] \right\}$$
(14.6)

The first cell of the control volume is also described in terms of its mass balance by Eq. 14.6 but can be simplified somewhat by the fact that its left boundary (the field edge) is stationary. Furthermore, in the context of a deforming control

volume, each additional cell incorporated during each time step "grows" from the left side of the profile. In other words, the volume of the cell at the beginning of the time step is zero, which leads to the following version of Eq. 14.6:

$$\frac{\delta x_1}{\delta t} \left[ (A_L + Z_L) \phi + (A_R + Z_R) (1 - \phi) \right]$$
 (14.7)

$$=\theta\left\{Q_{\rm L}-\left[Q_{\rm R}-(A_{\rm R}+Z_{\rm R})\frac{\delta x_1}{\delta t}\right]\right\}+(1-\theta)\left\{Q_{\rm J}-\left[Q_{\rm M}-(A_{\rm M}+Z_{\rm M})\frac{\delta x_1}{\delta t}\right]\right\}$$

For the right boundary of the control volume, the tip cell must be described (Fig. 14.4). The flow is highly nonlinear both with respect to the surface profile and the infiltration wetting front. The shape of the surface profile cannot usually be assumed to be independent of the infiltration characteristics, but given the assumptions already inherent in the analysis, a detailed tip description is probably not warranted. The Strelkoff-Katapodes model assumes that both surface and subsurface profiles can be described by simple monomial power functions as follows:

$$\frac{A}{A_{N-1}} = \left(\frac{x_N - s}{x_N - x_{N-1}}\right)^{\beta} \tag{14.8}$$

and

$$\frac{Z}{Z_{N-1}} = \left(\frac{x_N - s}{x_N - x_{N-1}}\right)^{\alpha} \tag{14.9}$$

where

N =number of cells

 $s = \text{distance parameter } (x_{N-1} \le s \le x_N)$ 

 $\alpha$ ,  $\beta$  = shape factors whose definition depends on the flow geometry and the infiltration parameters

To develop expressions for  $\alpha$  and  $\beta$ , the methodology for describing cross-sectional shape and friction slopes must be introduced.

The number of dependent variables in Eqs. 14.1 and 14.2 can be reduced by

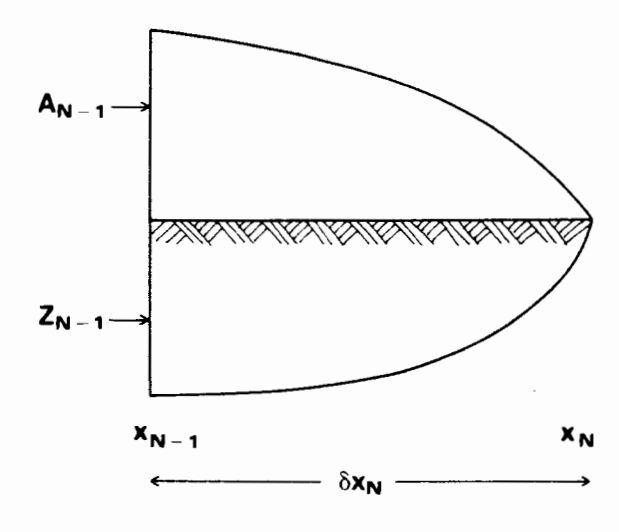


Figure 14.4 Surface and subsurface profiles near the advancing front. (From Elliott et al., 1982, with permission of ASCE.)

mathematically relating depth of flow, y, to the cross-sectional area of flow using a simple power function:

$$y = \sigma_1 A^{\sigma_2} \tag{14.10}$$

in which  $\sigma_1$  are  $\sigma_2$  are empirical fitting constants.

Friction slope is defined using the Manning equation:

$$S_f = \frac{Q^2 n^2}{A^2 R^{4/3}} \tag{14.11}$$

in which n is Manning's roughness and R is the hydraulic radius. It is also reasonable to assume that the wetted perimeter may be written as a power function of y (or of A), so that the denominator in Eq. 14.11 also becomes a function of A:

$$A^2 R^{4/3} = \rho_1 A^{\rho_2} \tag{14.12}$$

in which  $\rho_1$  and  $\rho_2$  are again fitting constants. The four parameters  $(\sigma_1, \sigma_2, \rho_1,$  and  $\rho_2)$  can be used to describe flow geometry in the governing equations, but must be held constant for any given irrigation event.

Returning to the variables  $\alpha$  and  $\beta$  in Eqs. 14.8 and 14.9, their values can be determined by integrating the equations to find the volume of surface and subsurface storage:

$$\int_{x_{N-1}}^{x_N} A \ ds = \frac{A_{N-1}(x_N - x_{N-1})}{1 + \beta} = \frac{A_{N-1} \delta x_N}{1 + \beta}$$
 (14.13)

$$\int_{x_{N-1}}^{x_N} Z \, ds = \frac{Z_{n-1}(x_N - x_{N-1})}{1 + \alpha} = \frac{Z_{N-1} \, \delta x_N}{1 + \alpha} \tag{14.14}$$

where the terms  $1/(1 + \beta)$  and  $1/(1 + \alpha)$  are the surface and subsurface shape factors in the region of the advancing tip.

Elliott et al. (1982) assumed that in the region of the advancing tip, the friction slope is usually much greater than the field slope, so that Eq. 14.2 with Eq. 14.10 substituted for y can be approximated by

$$\frac{\partial(\sigma_1 A^{\sigma^2})}{\partial s} = \frac{-Q^2 n^2}{\rho_1 A^{\rho_2}} = \frac{-v^2 n^2}{\rho_1 A^{\rho_2-2}}$$
(14.15)

where v is the average flow velocity, Q/A. At the time the flow reaches the point  $x_N$ , the differential of Eq. 14.15 is (after separation of variables)

$$A^{\sigma_2 + \rho_2 - 3} dA = \frac{-v^2 n^2}{\sigma_2 \sigma_1 \rho_1} ds$$
 (14.16)

which when integrated between s and  $x_N$ , assuming that velocity is uniform in the tip region, yields

$$\frac{A}{A_{N-1}} = \left(\frac{x_N - s}{x_N - x_{N-1}}\right)^{\frac{1}{\sigma_2 + \rho_2 - 2}}$$
(14.17)

Thus in Eq. 14.8,  $\beta$  is

$$\beta = \frac{1}{\sigma_2 + \rho_2 - 2} \tag{14.18}$$

For the parameter  $\alpha$ , Eq. 6.13 can be written

$$\int_{x_{N-1}}^{x_N} (k\tau^a + f_0\tau) \ ds = \frac{Z_{N-1} \delta x_N}{1+\alpha}$$
 (14.19)

where

$$\tau = \delta t - t, \tag{14.20}$$

in which  $\delta t$  is the time for the flow to advance from  $x_{N-1}$  to  $x_N$  and  $t_s$  is the time for the flow to advance from  $x_{N-1}$  to s. If the rate of advance is effectively linear in the interval, then

$$t_s = \frac{\delta t(s - x_{N-1})}{\delta x_N} \tag{14.21}$$

Substituting Eqs. 14.20 and 14.21 into Eq. 14.19, and then solving the integral, results in the following expression:

$$\frac{k(\delta t)^a \delta x_N}{1+a} + \frac{f_0 \delta t \delta x_N}{2} = \frac{Z_{N-1} \delta x_N}{1+\alpha}$$
 (14.22)

For the usual case,

$$\frac{k(\delta t)^a}{1+a} >> \frac{f_0 \delta t}{2} \tag{14.23}$$

so that

$$Z_{N-1} \approx k(\delta)^a \tag{14.24}$$

and Eq. 14.22 reduces to

$$\frac{k(\delta t)^a}{1+a} = \frac{k(\delta t)^a}{1+\alpha} \tag{14.25}$$

Thus the approximate value of  $\alpha$  is the infiltration exponent, a.

The continuity equation can now be written for the tip cell by integrating Eqs. 14.8 and 14.9 and then equating the results with the net flux relation:

$$\left(\frac{A_{L}}{1+\beta} + \frac{Z_{L}}{1+\alpha}\right) \frac{\delta x_{N}}{\delta t} - \left(\frac{A_{J}}{1+\beta} + \frac{Z_{J}}{1+\alpha}\right) \frac{\delta x_{N-1}}{\delta t}$$

$$= \theta \left[Q_{L} - (A_{L} + Z_{L}) \frac{\delta x_{N-1}}{\delta t}\right] + (1-\theta) \left[Q_{J} - (A_{J} + Z_{J}) \frac{\delta x_{N-1}}{\delta t}\right]$$
(14.26)

In summary, the continuity equation is described by Eqs. 14.6, 14.7, and 14.26 during the advance phase and correspond to the interior cells, the first cell,

and the tip cell, respectively. Similar approximations must also be made for Eq. 14.2.

Utilizing Eqs. 14.10 and 14.11, Eq. 14.2 can be written

$$\frac{\partial(\sigma_1 A^{\sigma_2})}{\partial x} = S_0 - \frac{Q^2 n^2}{\rho_1 A^{\rho_2}} \tag{14.27}$$

For all cells except the tip, Eq. 14.27 can be numerically integrated by first writing the equation in the following finite difference form:

$$\frac{\sigma_1 A_{\rm R}^{\sigma_2} - \sigma_1 A_{\rm L}^{\sigma_2}}{\delta x_k} = S_0 - \left[ \phi \frac{Q_{\rm L}^2 n^2}{\rho_1 A_{\rm L}^{\rho_2}} + (1 - \phi) \frac{Q_{\rm R}^2 n^2}{\rho_1 A_{\rm L}^{\rho_2}} \right]$$
(14.28)

For the tip cell, Eq. 14.8 is differentiated with respect to s and then defined at  $x_{N-1}$ :

$$\frac{\partial A}{\partial s}\Big|_{s=x_{N-1}} = \frac{-\beta A_{N-1}}{x_N - x_{N-1}} \left(\frac{x_{N-s}}{x_N - x_{N-1}}\right)^{\beta - 1}\Big|_{s=x_{N-1}} = \frac{-\beta A_L}{\delta x_N}$$
 (14.29)

Thus

$$\frac{\partial(\sigma_1 A^{\sigma_2})}{\partial x} = \frac{-\beta \rho_2 \sigma_1 A_L^{\sigma_2}}{\delta x_N}$$
 (14.30)

so that Eq. 14.27 for the tip cell becomes

$$\frac{-\beta \rho_2 \sigma_1 A_{\rm L}^{\sigma_2}}{\delta x_N} = S_0 - \frac{Q_{\rm L}^2 n^2}{\rho_1 A_{\rm L}^{\rho_2}}$$
(14.31)

At any time during the advance phase of the irrigation, the number of equations equals the number of unknowns. Equations 14.6 and 14.28 are written for each intermediate cell, 1 < k < N. Equations 14.7 and 14.28 are written for the first cell and Eqs. 14.26 and 14.31 are written for the tip cell. Thus the number of equations is 2N. The unknown variables are area, A, and discharge, Q, at all interior nodes, area at the field inlet, and the incremental advance distance,  $\delta x_N$ , for the tip cell. The number of unknowns is therefore also 2N.

# The Ponding Phase

When the irrigation water advances to the end of the field, the advance phase is completed and the ponding phase begins. The duration of the ponding phase is the subsequent interval until the flow is cut off at the field inlet.

The basic zero-inertia mathematics do not change during ponding with two exceptions. First, the downstream boundary is no longer an advancing tip but a stationary field boundary which may either allow water to drain from the field (tailwater boundary) or prevent runoff (diked boundary). The second exception is that the control volume need no longer deform in the dimension parallel to the field surfaces, so that cells may be defined in the oblique or rectangular fashion. The number of cells is fixed during the ponding phase. For furrow-irrigated systems, the diked-end condition is not common and would be particularly difficult

to model inasmuch as the downstream water surface would quickly submerge the furrows.

Various investigators have proposed different methods to characterize the downstream boundary for the tailwater condition. The simplest and most indicative of most field conditions is to assume the flow leaves the field under a uniform flow regime. The area at the last node would therefore be a direct function of the flow rate at the node. This effectively replaces the two equations describing the tip cell and reduces the problem unknown by two (the  $\delta x_N$  is no longer unknown). Some zero-inertia models alter the *t-x* computational grid during the ponding phase to create rectangular cells rather than the oblique cells shown in Fig. 14.2.

Because the cells can be considered in fixed positions, Eq. 14.6, which now represents all the cells except the first one, reduces to

$$\frac{\delta x_k}{\delta t} \left[ \phi (A_L + Z_L - A_J - Z_J) + (1 - \phi)(A_R + Z_R - A_M - Z_M) \right]$$

$$= \theta (Q_L - Q_R) + (1 - \theta)(Q_J - Q_M)$$
(14.32)

Equation 14.7 can still be used to describe the continuity equation for the inlet triangular cell. Equation 14.28 can be used as the motion equation for all cells.

# The Depletion Phase

When sufficient water has been applied to the field, the irrigator shuts off the inflow and the irrigation enters the depletion phase. The motion of water along the furrow continues, but at the inlet the area begins to diminish. The equations describing the flow are the same as those utilized during the advance and ponding phases. Equation 14.7, the continuity relation for the first cell, is modified by forcing  $Q_L$  equal to zero. The inlet area,  $A_L$ , then begins to decline. When it has approached zero, the depletion phase has been completed. In actual practice, to avoid numerical instabilities in many zero-inertia models, the depletion phase is considered completed when  $A_L$  has reduced to 5 to 10% of the original inlet flow area.

## The Recession Phase

In the absence of inertial effects, the water level at the field inlet decreases gradually following the cessation of inflow. Conceptually at least, the field dewaters progressively from the inlet end, the process known as recession.

Recession is largely a qualitative process. As the flow depths reduce and the velocities slow down, it is very difficult to observe the location of the "trailing edge" one would expect. Variations in intake rate, field slope, and roughness create conditions where recession actually occurs simultaneously over a fairly wide reach of the field (say 1 to 10 m). Simple rules such as defining recession when 50% of the lateral soil surface is dewatered are often followed, but two or more observers will locate recession substantially different.

At the time of cutoff, the field inlet boundary conditions are modified to reflect the cessation of inflow. Rather than attempt to continue the calculations at each station until the depth at the inflow to each cell is actually zero, Strelkoff and Katapodes (1977) suggest limiting the computations to the time where the depth is 5% of the original normal depth at that point. The remaining water is then assumed to infiltrate directly in place. When the area at a node becomes "zero" by the definition above, the number of cells is reduced by one (calculations initiate at the next downstream node), and the procedure continues. This is often accomplished by moving the "inlet" boundary downstream, thereby moving the triangular first cell along the grid. The rate of recession then becomes the rate the triangular cell is moved.

Recession may also occur from the downstream end of the furrow, where infiltration rates are higher. In this case, the downstream node where the area and discharge approach the limit is neglected in subsequent calculations and the number of nodes diminished by one.

## **NUMERICAL SOLUTION**

The zero-inertia models which use the approach described above result in 2N, nonlinear algebraic equations to be solved simultaneously at each time step. To streamline these solutions, the equations can be linearized and then solved as a set of simultaneous linear equations. The following discussion follows the original works of Strelkoff and Katapodes (1977) and Elliott et al. (1982).

The linearization process begins by defining a new set of variables as follows:

$$A_{\mathsf{L}} = A_{\mathsf{J}} + \delta A_{\mathsf{L}} \qquad (1 < k \le N) \tag{14.33}$$

$$A_{\rm R} = A_{\rm M} + \delta A_{\rm R} \qquad (1 \le k \le N)$$
 (14.34)

$$Q_{\rm L} = Q_{\rm J} + \delta Q_{\rm L} \qquad (1 < k \le N)$$
 (14.35)

$$Q_{\rm R} = Q_{\rm M} + \delta Q_{\rm R} \qquad (1 \le k \le N)$$
 (14.36)

$$\delta x_N = \delta x_{N-1} + \delta \delta \tag{14.37}$$

$$A_{\rm L} = A_{\rm M} + \delta A_{\rm L} \qquad (k = 1)$$
 (14.38)

$$Q_{\rm L} = Q_{\rm M} + \delta Q_{\rm L} \qquad (k = 1)$$
 (14.39)

in which k represents the cell index, and N is the number of cells on a given time line. The new variables  $(\delta A_L, \delta A_R, \delta Q_R, \delta Q_R)$  and  $\delta \delta$  serve to relate the unknowns of the problem  $(A_L, A_R, Q_L, Q_R, \delta Q_R)$  to their known values at the preceding time  $(A_J, Q_J, A_M, Q_M, \delta Q_M)$  and  $\delta X_{N-1}$ . Equations 14.33 to 14.35 can then be substituted into Eqs. 14.6, 14.7, 14.26, 14.28, and 14.31, thereby replacing the unknown variables with the new  $\delta$  variables. To simplify the resulting equations, second-order products involving  $\delta$  variables are neglected and a sum raised to a power as approximated by the first two terms of a binomial expansion.

The accuracy of the approximations is enhanced when the  $\delta$  variables have

magnitudes which are small in comparison to those of the known variables and thus the use of oblique rather than rectangular cells in the computational grid. During advance,  $A_L$  is likely to have a value nearer  $A_J$  than to  $A_M$ . The resulting linear equations are as follows (after Elliott et al., 1982). For the first cell (k = 1),

$$[\phi w_{1}] \delta A_{L} + [(1 - \phi - \theta)w_{1}] \delta A_{R} - \theta \delta Q_{L} + \theta \delta Q_{R} = \phi w_{1}(Z_{M} - Z_{L})$$

$$(14.40)$$

$$(14.40)$$

$$(-\sigma_{1}\sigma_{2}A_{M}^{\sigma_{2}-1} - \phi\rho_{2} \frac{S_{fM}}{A_{M}} \delta x_{1}) \delta A_{L} + \left[\sigma_{1}\sigma_{2}A_{M}^{\sigma_{2}-1} - (1 - \phi)\rho_{2} \frac{S_{fM}}{A_{M}} \delta x_{1}\right] \delta A_{R}$$

$$+ \left(2\phi \frac{S_{fM}}{Q_{M}} \delta x_{1}\right) \delta Q_{L} + \left[2(1 - \phi)\frac{S_{fM}}{Q_{M}} \delta x_{1}\right] \delta Q_{R} = \delta x_{1}(S_{0} - S_{fM})$$

$$(14.41)$$

For all interior cells (1 < k < N),

$$(\phi w_k + \theta w_{k-1}) \, \delta A_L + \left[ (1 - \phi - \theta) w_k \right] \, \delta A_R - \theta \, \delta Q_L + \theta \, \delta Q_R$$

$$= \left[ \phi w_k + (1 - \phi) w_{k-1} \right] \left( A_M + Z_M - A_J - Z_J \right) + Q_J - Q_M$$
(14.42)

and

$$\left(-\sigma_{1}\sigma_{2}A_{J}^{\sigma_{2}-1} - \phi\rho_{2}\frac{S_{fJ}}{A_{J}}\delta x_{k}\right)\delta A_{L} + \left[\sigma_{1}\sigma_{2}A_{M}^{\sigma_{2}-1} - (1 - \phi)\rho_{2}\frac{S_{fM}}{A_{M}}\delta x_{k}\right]\delta A_{R} 
+ \left(2\phi\frac{S_{fJ}}{Q_{J}}\delta x_{k}\right)\delta Q_{L} + \left[2(1 - \phi)\frac{S_{fM}}{Q_{M}}\delta x_{k}\right]\delta Q_{R}$$

$$= \sigma_{1}\left(A_{J}^{\sigma_{2}} - A_{M}^{\sigma_{2}}\right) + \delta x_{k}[S_{0} - \phi S_{fJ} - (1 - \phi)S_{fM}]$$
(14.43)

For the last cell  $(k \neq N)$ ,

$$\left[ \left( \frac{1}{1+\beta} + \theta \right) w_{N-1} \right] \delta A_{L} - \theta \delta Q_{L} + \left[ \frac{A_{J}}{(1+\beta) \delta t} + \frac{Z_{J}}{(1+\alpha) \delta t} \right] \delta \delta 
= Q_{J} - (A_{J} - Z_{J}) w_{N-1}$$
(14.44)

$$\left(\frac{-\beta\sigma_{2}^{2}\sigma_{1}A_{J}^{\sigma_{2}-1}}{\delta x_{N-1}} - \frac{\rho_{2}S_{fJ}}{A_{J}}\right)\delta A_{L} + \frac{2S_{fJ}}{Q_{J}}\delta Q_{L} - \frac{S_{0} - S_{fJ}}{\delta x_{N-1}}\delta \delta = \frac{\beta\sigma_{2}\sigma_{1}A_{J}^{\sigma_{2}}}{\delta x_{N-1}} + S_{0} - S_{fJ}$$
(14.45)

in which

$$w_k = \frac{\delta x_k}{\delta t} \tag{14.46}$$

$$w_{k-1} = \frac{\delta x_{k-1}}{\delta t} \tag{14.47}$$

Numerical Solution 337

$$S_{fJ} = \frac{Q_J^2 n^2}{\rho_1 A_J^{\rho_2}} \tag{14.48}$$

$$S_{fM} = \frac{Q_{\rm M}^2 n^2}{\rho_1 A_{\rm M}^{\rho_2}} \tag{14.49}$$

In arriving at Eqs. 14.40 to 14.49, it is noted that the t-x grid is formulated such that

$$Z_{\rm L} = Z_{\rm J} \tag{14.50}$$

$$Z_{\rm R} = Z_{\rm M} \tag{14.51}$$

Since the soil infiltration characteristics are considered to be spatially uniform, Eqs. 14.50 and 14.51 seem quite reasonable. However, in the case of furrow irrigation, it is generally recognized that infiltration is also a function of wetted perimeter. Therefore, inherent in Eqs. 14.50 and 14.51 is the additional assumption that the rise in flow depth (and area) with time has been the same at nodes L and J. Again, it is apparent that this assumption is most valid when  $\delta A_L$  and  $\delta A_R$  are relatively small, meaning that  $A_L \approx A_J$  and  $A_R \approx A_M$ .

The solution for each time increment makes use of the known values of the variables at the preceding time. To initiate this process, a solution is required for the first time step. The appropriate continuity equation is

$$\delta V = \delta x_1 \left( \frac{A_L}{1+\beta} + \frac{Z_L}{1+\alpha} \right) \tag{14.52}$$

where  $\delta V$  is the inflow volume during the first time increment. When Eq. 14.31 is written for N=1, the momentum equation becomes

$$-\frac{\beta \rho_2 \sigma_2 A_{\rm L}^{\sigma_2}}{\delta x_1} = S_0 - \frac{Q_{\rm L}^2 n^2}{\rho_1 A_1^{\rho_2}}$$
 (14.53)

These two simultaneous equations are nonlinear in the unknowns  $\delta x_1$  and  $A_L$  and are solved by a Newton-Raphson technique.

For all time steps after the first one, 2N linear algebraic equations in 2N knowns are to be solved. The 2N unknowns are  $\delta A$  for nodes 1 through N,  $\delta Q$  for nodes 2 through N, and  $\delta \delta$ . It should be noted that  $\delta A_R$  and  $\delta Q_R$  in one cell are equal to  $\delta A_L$  and  $\delta Q_L$  in the next cell downstream. If node (N) is at the advancing front, the boundary condition dictates that both  $A_N$  and  $Q_N$  be equal to zero. The upstream boundary condition provides the value of  $\delta Q_1$ .

This system of equations can be solved with any standard matrix solution technique. However, the banded nature of the coefficient matrix (five diagonals) allows the use of the Preissman double-sweep algorithm (described in Chapter 13). Once values have been obtained for  $\delta\delta$  and the arrays  $\delta A$  and  $\delta Q$ , Eqs. 14.33 to 14.37 are used to determine  $\delta x_N$  and the values of A and Q at each node. After advancing in time, the elements of the new coefficient matrix are calculated and the double-sweep algorithm is again applied. This procedure is repeated until the flow has receded following the cutoff of flow at the inlet.

## **MODEL VERIFICATION**

The accuracy of the zero-inertia model must be based on fairly complete sets of irrigation data. Among other things, these data sets must include a value for Manning's n, a description of furrow geometry (unless the data are from borders or basins), and an infiltration function representative of the field conditions. Because one or more of these items is often unavailable, the process of model testing is often difficult.

A facility for conducting surface irrigation experiments at the University of Arizona provided a high degree of uniformity in both channel slope and cross section (Roth et al., 1974). The published data from seven precision border irrigations on bare soil have been used by several researchers in the verification of zero-inertia border-irrigation models (Clemmens, 1979; Strelkoff and Katapodes, 1977). Fangmeier and Ramsey (1978) reported the results of precision furrow-irrigation experiments. The advance curves predicted by the zero-inertia model also agreed well with these experimental observations (Elliott et al., 1982).

Because the lengths of run in the Arizona tests were only about 90 m, much shorter than most furrows used in American agriculture, the corresponding advance times were on the order of only 30 min. Elliott et al. (1982) tested the model (advance phase) using data from furrow evaluations at three Colorado farms. Although these evaluations should be more representative of field conditions, there is an accompanying sacrifice in the accuracy with which model input parameters may be determined. Oweis (1983) utilized the same data as Elliott et al. (1982) but included an analysis of the complete irrigation.

During the summer of 1979, Colorado State University researchers made comprehensive furrow irrigation evaluations at three Colorado locations (Walker and Skogerboe, 1981). Each of these farms is privately owned, and an attempt was made to follow the farmer's normal irrigation practices. At each site, six furrows (two groups of three furrows each) were studied throughout the irrigation season. Table 14.1 provides general information concerning each of the study sites.

Since well over 100 individual furrow evaluations were made, all the data sets could not realistically be used in analyzing the model. Recognizing that the infiltration characteristics of the first irrigation of the season often differ significantly from those later in the season, Elliott et al. (1982) randomly selected one furrow evaluation from the first irrigation event at each of the three farms. In addition, one other furrow test was randomly chosen from the data set for each farm. The model input data for these six evaluations are given in Table 14.2.

The tabulated inflow rate,  $Q_0$ , is the average of the field flow rate measurements made during the advance phase. The furrow slope,  $S_0$ , was determined by performing a least-squares linear regression on the elevation data. Accurate field measurements of Manning's n are difficult to obtain, and the furrow evaluations were not designed for making such measurements. Binder (1981) and Neff (1981) used a constant Manning's n of 0.02 for all three study sites. This value of n was assigned to three of the furrow data sets, but n is presumably greater than 0.02

Model Verification 339

Spacing between wetted furrows 0.762 1.524 1.524 (E) Furrow length (m) 425 450 350 350 625 625 9 TABLE 14.1 GENERAL INFORMATION ON THE COLORADO STUDY SITES Number of irrigation events studied  $\infty$   $\infty$   $\infty$ group number Furrow <del>(</del>5 Crop Corn Corn Corn (3) Loamy sand clay loam Soil type Clay loam Loam to 5 Grand Junction, CO Fort Morgan, CO and location Farm name Lucerne, CO Matchett Benson Printz

TABLE 14.2 COLORADO FURROW EVALUATION DATA ON MODEL TESTING

(1)	(2)	(3)	(4)	(5)	(9)	(7)
	Irrigation 1, group 1,	Irrigation 5, group 2,	Irrigation 1, group 4,	Irrigation 2, group 3,	Irrigation 1, group 1,	Irrigation 8. group 2.
Parameter	furrow 5	furrow 1	furrow 5	furrow 5	furrow 1	furrow 3
$Q_{ m o}$ (liters/s)	2.78	1.17	0.85	0.92	4.81	2.77
S <sub>0</sub> (m/m)	0.0044	0.004	0.0092	0.0095	0.0023	0.0025
u	0.03	0.02	0.03	0.02	0.03	0.02
G,	0.92	0.72	0.87	2.18	1.78	1.13
$\sigma_{\hat{i}}$	0.65	0.64	0.56	0.79	0.72	0.75
ď	0.46	0.34	0.30	1.35	0.92	0.73
p;	2.86	2.84	2.73	3.00	2.91	2.98
$k(m'/m/min^a)$	0.0252	0.0173	0.0011	0.0033	0.0078	0.0161
u	0.02	0.01	0.48	0.40	0.40	0.02
$f_0(\mathbf{m}^3/\mathbf{m}/\mathbf{min})$	0.00023	0.00008	0.00003	0.00003	0.00141	0.00040

during the first irrigation of the season. Thus a discretionary n value of 0.03 was used in the three furrows, which represent the initial irrigation events of the season.

Furrow geometry data were obtained at several stations along the furrow, usually both before and after the irrigation event. The device used was a profilometer described in Chapter 4.

In these Colorado studies, as well as those in Arizona, advance data were used in deriving the values of the infiltration parameters  $(a, k, \text{ and } f_0)$ . Therefore, comparisons between observed field advance and model predictions of advance, including those made in previous research, do not provide a truly independent corroboration of a model. However, the procedure outlined by Ley (1978) requires only two data points on the observed advance curve, the times of advance to the middle and end of the irrigated run. Also, the volume balance methodology includes two critical assumptions which are not made in the zero-inertia approach: (1) the functional form of the advance relationship is a power curve, and (2) the average area of surface storage in the furrow is a constant. Additionally, the furrow outflow volume is an important field measured quantity in Ley's volume balance method, but it is not one of the inputs to the zero-inertia advance model. For the foregoing reasons, analysis of the Colorado furrow data was considered to provide a valid, although not completely independent, test of the model.

With the data from Table 14.2 serving as inputs to the model, an advance and recession curve was generated for each of the six furrow tests. Three of these curves together with the field data are plotted in Figs. 14.5 to 14.7. The terminology for test numbers, "Printz 8-2-3," refers to the Printz location, eighth irri-

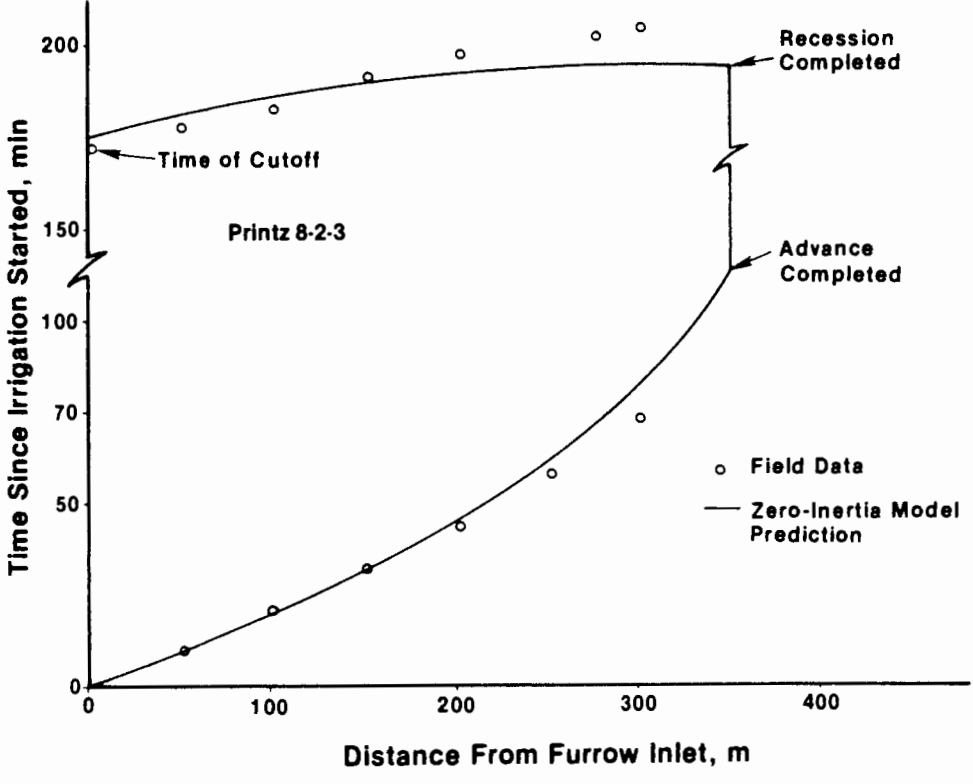


Figure 14.5 Comparison of measured and the zero-inertia calculated advance and recession for Colorado test Printz 8-2-3. (After Oweis, 1983.)

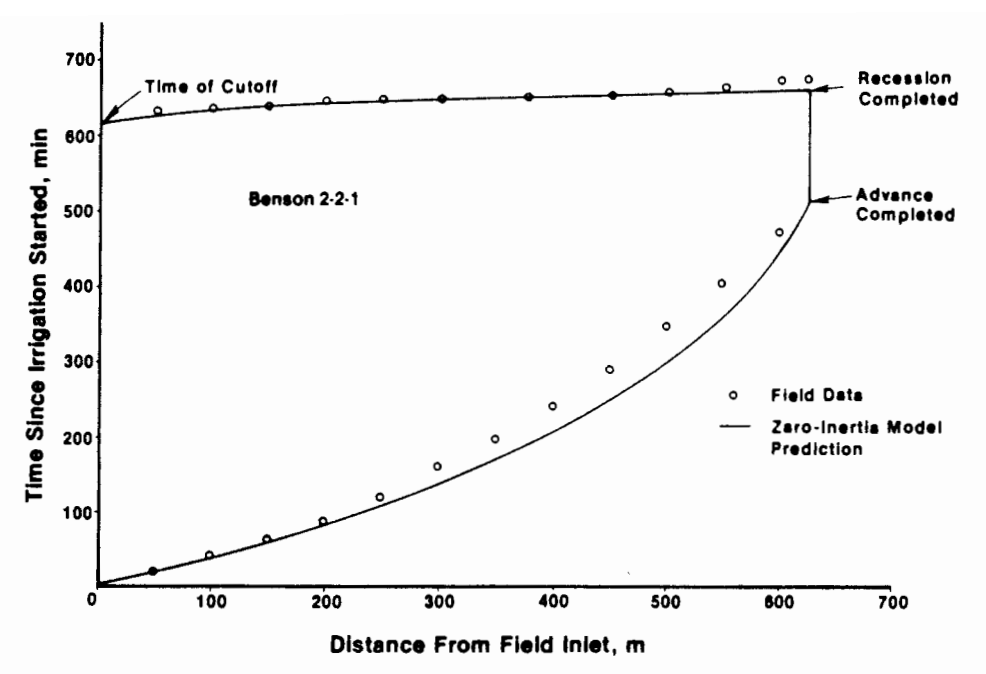


Figure 14.6 Measured and estimated advance and recession trajectories for Colorado test Benson 2-2-1. (After Oweis, 1983.)

gation, second furrow group, and third furrow in that group. In general, the model predictions are consistent with the field observations. The model underestimated the advance rate in some cases and overestimated it in others. Recession was simulated accurately in all cases. Since the model seemed to estimate the early stages of advance much better than the later stages, it is evident that examining longer runs is important in the process of model testing.

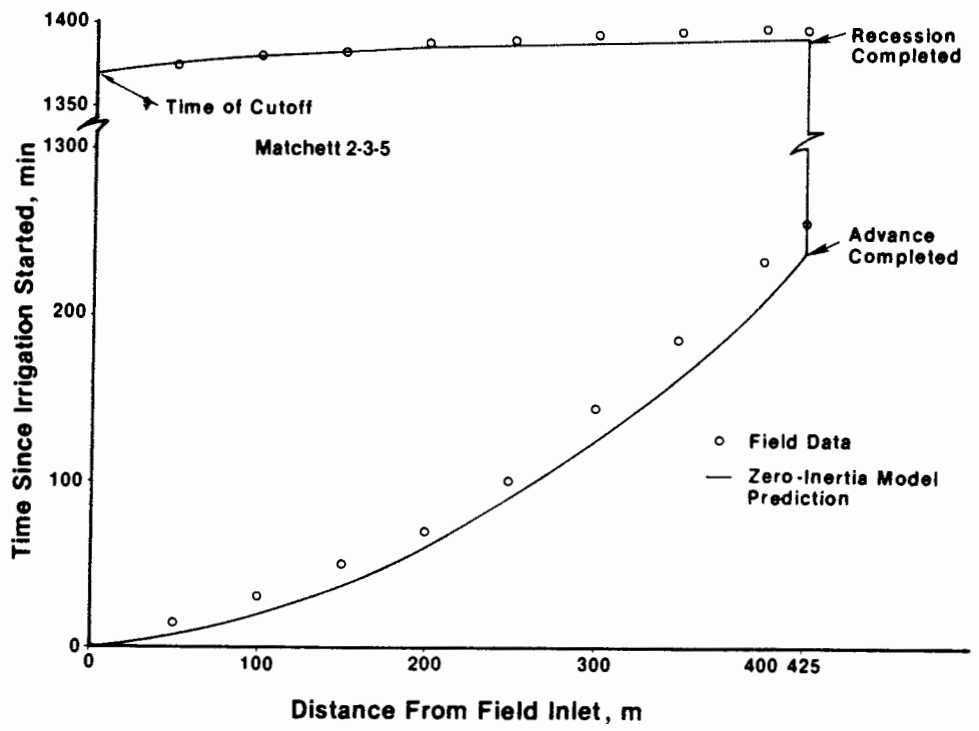


Figure 14.7 Zero-inertia analysis of Colorado test Matchett 2-3-5. (After Oweis, 1983.)

Model Verification 343

When field data are used to test a mathematical model, it is often difficult to assess the values of model input parameters. Additionally, parameters which are considered to be constant may actually exhibit considerable spatial variability. Thus the model validation process may be partly a reflection of the accuracy of input parameter determinations. However, the zero-inertia model was tested over a range of field conditions, and its overall predictive capability indicates that the model is sound.

## REFERENCES

- BINDER, C. W. 1981. Improving Furrow Irrigation Performance through Management Decisions. Unpublished M.S. thesis, Colorado State University, Fort Collins, Colo.
- CLEMMENS, A. J. 1979. Verification of the Zero-Inertia Model for Surface Irrigation. Trans. ASAE 22(6):1306-1309.
- CLEMMENS, A. J., and D. D. FANGMEIER. 1978. Discussion of Strelkoff and Katapodes (1977). ASCE J. Irrig. Drain. Div. 104(IR3):337-339.
- CLEMMENS, A. J., and T. STRELKOFF. 1979. Dimensionless Advance for Level-Basin Irrigation. ASCE J. Irrig. Drain. Div. 105(IR3):259-273.
- ELLIOTT, R. L., W. R. WALKER, and G. V. SKOGERBOE. 1982. Zero-Inertia Modeling of Furrow Irrigation Advance. ASCE J. Irrig. Drain. Div. 108(IR3):179-195.
- FANGMEIER, D. D., and M. K. RAMSEY. 1978. Intake Characteristics of Irrigation Furrows. *Trans. ASAE* 21(4):696-700.
- KATAPODES, N. D., and T. STRELKOFF. 1977. Dimensionless Solution of Border Irrigation Advance. ASCE J. Irrig. Drain. Div. 103(IR4):401–407.
- LEY, T. W. 1978. Sensitivity of Furrow Irrigation Performance to Field and Operation Variables. Unpublished M.S. thesis, Colorado State University, Fort Collins, Colo.
- NEFF, M. E. 1981. The Cost-Effectiveness of Alternate Furrow Irrigation Evaluation Procedures. Unpublished M.S. thesis, Colorado State University, Fort Collins, Colo.
- Owers, T. Y. 1983. Surge Flow Furrow Irrigation Hydraulics with Zero-Inertia. Ph.D. dissertation, Agricultural and Irrigation Engineering Department, Utah State University, Logan, Utah.
- ROTH, R. L., D. W. FONKEN, D. D. FANGMEIER, and K. K. ATCHISON. 1974. Data for Border Irrigation Models. *Trans. ASAE* 17(1):157–161.
- STRELKOFF, T., and A. J. CLEMMENS. 1981. Dimensionless Stream Advance in Sloping Borders. ASCE J. Irrig. Drain. Div. 107(IR4):361-382.
- STRELKOFF, T., and N. D. KATAPODES. 1977. Border Irrigation Hydraulics with Zero-Inertia. ASCE J. Irrig. Drain. Div. 103(IR3):325-342.
- WALKER, W. R., and G. V. SKOGERBOE. 1981. Evaluating Furrow Irrigation Systems for Regional Water Quality Planning. Rep. EPA-600/2-81. U.S. Environmental Protection Agency, Office of Research and Development, Robert S. Kerr Environmental Research Laboratory, Ada, Okla.

# The Kinematic-Wave Model

#### INTRODUCTION

A number of surface irrigation analyses ignore the momentum equation and become categorized as "kinematics." Without the momentum equation, or at least the zero-inertia assumption of how depth changes with respect to distance (Eq. 14.2), nothing can be stated regarding the shape of the surface water profile and thus the volume of surface storage. To avoid being left with an undeterminant continuity equation, two replacement assumptions for the momentum equation have been developed. The first approach is to assume that the average cross-sectional flow area is constant and thereby independent of advance distance and time. This methodology is discussed in Chapter 16.

The second kinematic approach is to assume that a unique relation exists describing discharge as a function of flow depth. This approach is called the kinematic-wave model because it in reality projects the movement of a kinematic shock wave. However, because one of the uniform flow equations (Manning, Chezy, or Darcy-Weisbach) usually provides the basis of the necessary stage-discharge relation, these models are often referred to as "uniform depth" or "uniform flow" models.

In this chapter, two mathematical solutions are presented for furrow irrigation (noting again that the free-draining border case is a simplified solution of the furrow case). The first is the traditional method of characteristics solution, and the second is based on the deformable control volume approach of Chapters 13 and 14.

## THE CHARACTERISTIC SOLUTION

The kinematic-wave model was initially developed for hydrologic applications (Lighthill and Whitham, 1955; Woolhiser and Liggett, 1967) and then applied to sloping, free-draining borders (Smith, 1972; Chen, 1970). The extension to furrows is made in the same manner presented in Chapter 14 for zero-inertia analysis. Again assuming that simple power functions will adequately describe relations between depth, area, top width, hydraulic radius, and so on, the depth-area and hydraulic section-area relation are rewritten here:

$$y = \sigma_1 A^{\sigma_2} \tag{15.1}$$

and

$$A^2 R^{1.33} = \rho_1 A^{\rho_2} \tag{15.2}$$

where

y = flow depth, m

A =flow cross-sectional area, m<sup>2</sup>

R = hydraulic radius, m

 $\sigma_1, \sigma_2, \rho_1, \rho_2$  = empirical data fitting parameters

The Manning formula for describing uniform flow in open channels provides a convenient area-discharge function:

$$S_0 = \frac{Q^2 n^2}{A^2 R^{1.33}} = \frac{Q^2 n^2}{\rho_1 A^{\rho_2}}$$
 (15.3)

where

 $Q = \text{furrow discharge, m}^3/\text{s}$ 

n = Manning resistance coefficient

 $S_0$  = average furrow slope

Equation 15.3 can be solved for Q and written in the following form:

$$Q = \alpha A^{m+1} \tag{15.4}$$

where

$$\alpha = \frac{(\rho_1 S_0)^{.5}}{n} \tag{15.5}$$

and

$$m + 1 = \frac{\rho_2}{2} \tag{15.6}$$

The basic kinematic equation is mass continuity; Eq. 14.1 is repeated here for convenience:

$$\frac{\partial A}{\partial t} + \frac{\partial Q}{\partial x} + \frac{\partial Z}{\partial \tau} = 0 \tag{15.7}$$

where t is time (min) and Z is the cumulative infiltration (m<sup>3</sup>/min/m). The infiltration rate in furrows,  $\partial Z/\partial \tau$ , can be described by whatever function is desired. The Kostiakov-Lewis relation is used in the following development. In most

kinematic analyses of furrows, the definition of the parameters, a, k, and  $f_0$  is made at a flow rate typical of the normal irrigating condition. Thus, given the simplifications made to reach a kinematic level, infiltration can be represented as

$$\frac{\partial Z}{\partial \tau} = ak\tau^{a-1} + f_0 \tag{15.8}$$

and the adjustments for wetted perimeter changes can be neglected.

Substituting Eqs. 15.4 and 15.8 into Eq. 15.7 and then simplifying results in a continuity equation written as a function of time and area:

$$\frac{\partial A}{\partial t} + \alpha (m+1)A^m \frac{\partial A}{\partial t} + (ak\tau^{a-1} + f_0) = 0$$
 (15.9)

Noting that

$$\frac{dA}{dt} = \frac{\partial A}{\partial t} + \frac{dx}{dt} \frac{\partial A}{\partial x} \tag{15.10}$$

then

$$\frac{dA}{dt} = (ak\tau^{a-1} + f_0) \tag{15.11}$$

when

$$\frac{dx}{dt} = \alpha(m+1)A^m \tag{15.12}$$

In other words, Eq. 15.11 holds along the "characteristic" described by Eq. 15.12.

The solution of Eqs. 15.11 and 15.12 describes the trajectory of a kinematic shock moving at a rate equal to the average flow velocity immediately behind the shock. Thus

$$\frac{dx_s}{dt_s} = \frac{Q_s}{A_s} = \alpha A_s^m \tag{15.13}$$

in which  $Q_s$  and  $A_s$  are the discharge and cross-sectional areas at the shock.

A discussion of the kinematic-wave solution for border irrigation is given by Smith (1972) and Bassett et al. (1980). Equations 15.11 to 15.13 differ only in that the dependent parameter is area rather than depth, so the computation grid is the same in both cases. Bassett et al. (1980) list two major disadvantages in the kinematic-wave analysis. First, it is limited to sloped conditions, and second, it cannot handle downstream boundary conditions which affect the flow upstream. The minimal slope depends on roughness, inflow, and infiltration characteristics.

Among the first investigators to consider the kinematic-wave model for surface irrigation was Chen (1970). In his conclusions, he stated that "the kinematic-wave method may only be valid for supercritical flow. For other than supercritical flow, the more hydrodynamic approach should be adopted." However, the work by Woolhiser and Liggett (1967) indicates the accuracy of the method in terms of a normalizing function developed for the equations of motion. Smith (1972) also

cites this work along with a similar experiment by Tinney and Bassett (1961). The normalizing function written by Woolhiser and Liggett (1967) is

$$K = \frac{S_0 L_p}{Y_0 F_0^2} \tag{15.14}$$

where

 $S_0$  = slope of the soil surface

 $L_p$  = length of wetted surface

 $\dot{Y}_0$  = normal depth of flow at plane outlet

 $F_0$  = normal-depth Froude number

Woolhiser and Liggett (1967) state that the kinematic-wave method can be accurate if K > 50. Tinney and Bassett (1961) evaluate the errors inherent with the method based on a somewhat similar function:

$$K_0 = \frac{S_0 L_p}{Y_0} = K F_0^2 \tag{15.15}$$

Their results indicate errors of less than about 10% when k > 2. For the Froude numbers generally encountered in surface irrigation systems (often less than 0.2), one can see that both assessments are approximately the same.

Katapodes and Strelkoff (1977) compared the kinematic-wave model with zero-inertia and hydrodynamic solutions, all of which had been nondimensionalized. These results for borders indicate that the kinematic-wave analysis is closer to the more complete solution for large times and advance distances. Also, the higher the slope, the better the kinematic-wave analysis.

#### **Numerical Solution Procedure**

The solution of Eq. 15.9 using the approach of Smith (1972) involves mathematically constructing the characteristic net in the x-t plane as shown in Fig. 15.1. The spatial scale is divided into uniform increments,  $\Delta x$ , and the time steps,  $\Delta t$ , are left variable with the exception of the time increment,  $\Delta t_1$ , defined relative to the field inlet location. To develop the computational procedure, consider that the conditions along the j-1=3 characteristic are known from the field inlet to the wavefront. Notation will involve subscripts to represent spatial coordinates and superscripts to represent temporal coordinates.

The area of flow at the field inlet can be calculated from Eq. 15.3 and will remain constant from characteristic to characteristic as long as the flow is steady. Thus for j = 4,

$$A_1^i = A_1^{i-1} (15.16)$$

and

$$t_1^j = t_1^{j-1} + \Delta t_1 \tag{15.17}$$

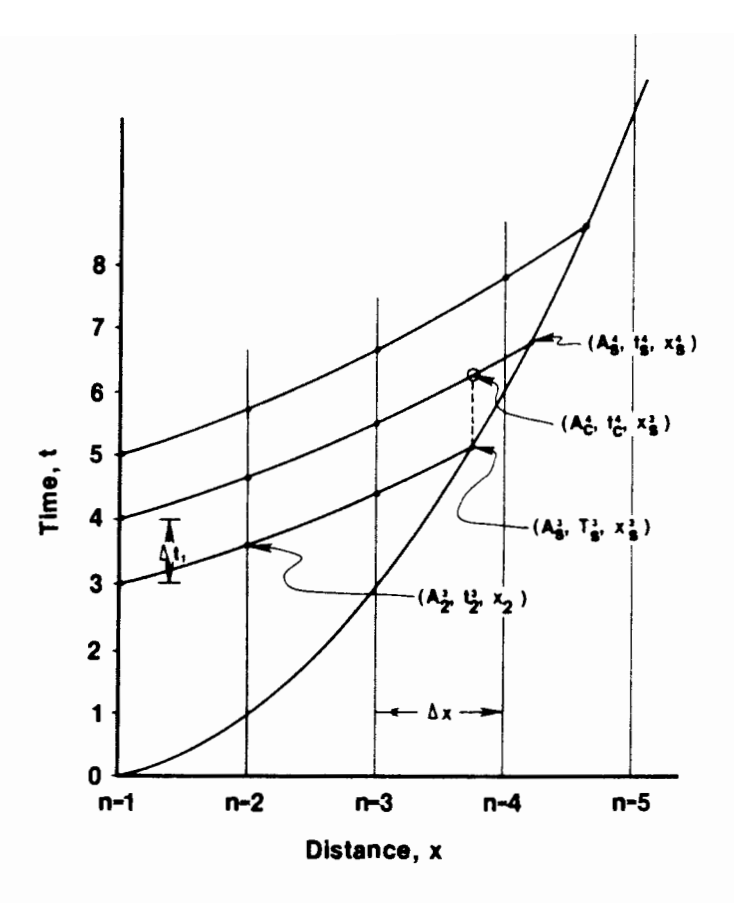


**Figure 15.1** Characteristic *t-x* grid for kinematic-wave model of the advance phase.

Equations 15.11 and 15.12 written in general finite difference form are

$$\frac{x_{n+1} - x_n}{t_{n+1}^j - t_n^j} = \frac{(m+1)\alpha}{2} \left[ (A_{n+1}^j)^m + (A_n^j)^m \right]$$
 (15.18)

and

$$\frac{A_{n+1}^{j} - A_{n}^{j}}{t_{n+1}^{j} - t_{n}^{j}} = -f[\tau_{n}^{j}, \tau_{n+1}^{j}]$$
(15.19)

in which

$$f[\tau_n^j, \tau_{n+1}^j] = \frac{\int_{\tau_n^j}^{\tau_{n+1}^j} \frac{\partial Z}{\partial t} dt}{\tau_{n+1}^j - \tau_n^j}$$

$$= f_0 + \frac{k[(\tau_{n+1}^j)^a - (\tau_n^j)^a]}{\tau_{n+1}^j - \tau_n^j}$$
(15.20)

For the case of n = 1 or the first computation for the j = 4th characteristic, Eqs. 15.18 and 15.19 involve two unknowns,  $t_2^j$  and  $A_2^j$ , which can be evaluated by simultaneous solution of the two nonlinear algebraic equations. The computations then proceed to n = 2 and subsequently along the characteristic until the depth and time variables are identified at each spatial node.

When the computational procedures reach the point where the next logical extension is the location of the advancing front, Eqs. 15.18 and 15.19 are found to contain three unknowns  $t_s^j$ ,  $x_s^j$ ,  $A_s^j$ . To overcome the problem, the conditions on the (j = 4)th characteristic are defined at the location of the advancing front on the previous characteristic  $(x_s^{j-1})$ . In Fig. 15.1 this point is shown as the open circle having data points  $A_c^4$ ,  $t_c^4$ , and  $x_s^3$ . This point is defined by Eqs. 15.18 and 15.19 in the manner described above for the previous points on the characteristic. Then to define the conditions at the advancing front and its location, Eqs. 15.18 and 15.19 are written along with the finite difference form of Eq. 15.13 to give three equations in the three unknowns. Thus

$$\frac{x_s^j - x_s^{j-1}}{t_s^j - t_c^j} = \frac{(m+1)\alpha}{2} \left[ (A_s^j)^m + (A_c^j)^m \right]$$
 (15.21)

$$\frac{A_s^j - A_c^j}{t_c^j - t_c^j} = -f(\tau_c^j, 0)$$
 (15.22)

and

$$\frac{x_s^j - x_s^{j-1}}{t_s^j - t_s^{j-1}} = \frac{\alpha}{2} \left[ (A_s^j)^m + (A_s^{j-1})^m \right]$$
 (15.23)

A detailed discussion of the wetting, depletion, and recession phases of a characteristic simulation will not be given here. Lee (1982) developed a nondimensional kinematic-wave model using the characteristics method, which included each of the four phases of an irrigation. The interested reader may wish to consult this work. However, the following development using a deformable control volume approach results in a much more useful model which will be given primary emphasis.

#### THE DEFORMABLE CONTROL VOLUME APPROACH

The deformable control volume approach described in Chapter 13 can also be directly applied to the kinematic-wave analysis. As before, computations proceed at specified time steps with the spatial coordinates referenced to the incremental advance during a corresponding time increment. This approach offers three important advantages over a characteristic approach. Recession is more easily incorporated because the only dependent variable is area at the spatial coordinates along the known time line, rather than area and time along characteristic lines. Numerical stability is better guaranteed for the initial conditions and for the cases where advance is very slow (steep advance trajectories) or where slope and soil conditions vary along the furrow.

As with the hydrodynamic and zero-inertia models, the cell definition can be either oblique or rectangular. Both configurations have been developed by the writers, and the rectangular (Eulerian coordinates) has served best. Walker and Lee (1981) describe the oblique model and its testing. The focus of this chapter is on the Eulerian grid system.

Chapter 13 contains the essential equations used in the kinematic-wave model. To free the reader from the inconvenience of continually referring back, the development will be repeated here.

## The Advance Phase

The volume of water in surface and subsurface storage at any time during advance is represented by an expanding control volume consisting of deforming cells. One such cell was depicted in Fig. 13.2. In the Eulerian system, there are three typical cells which comprise the control volume. These cells are drawn in Fig. 15.2. The

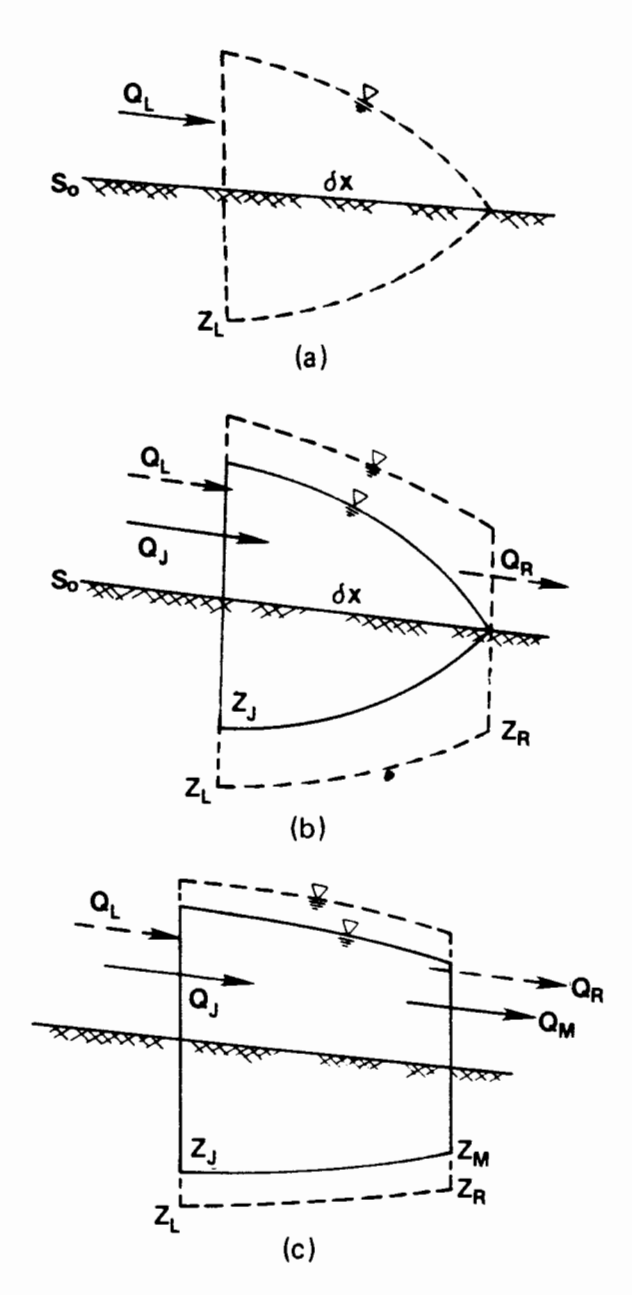


Figure 15.2 (a) Eulerian tip cell. (b) Eulerian penultimate. (c) Eulerian intermediate cell.

subscripts, J, M, L, and R are again used to distinguish which boundary is being considered and whether the time is the beginning or ending of the interval.

The first cell is an advancing tip which forms at the right boundary during each time step. The tip cell is also the initial condition of the analysis. The second cell is a transition cell which begins the time step as the tip cell for the previous step and evolves into a rectangular cell during the current time step. The remaining cells are rectangular and lie behind the tip and transition cells in the flow profile. Considering each cell simultaneously leads to a computational grid in the t-x plane, as illustrated in Fig. 15.3.

The derivation of the kinematic-wave equations follows the same methodology as outlined in Chapter 14 and are equivalent to those expressions. The solutions for this model will be explicit.

The continuity equation for the general rectangular cell (Eq. 13.3) is

$$[\theta(Q_{L} - Q_{R}) + (1 - \theta)(Q_{J} - Q_{M})] \delta t$$

$$- [\phi(A_{L} + Z_{L} - A_{J} - Z_{J})$$

$$+ (1 - \phi)(A_{R} + Z_{R} - A_{M} - Z_{M})] \delta x_{k-1} = 0$$
(15.24)

The left boundary condition defines  $Q_J$  and  $Q_L$  and therefore  $A_J$  and  $A_L$  through Eq. 15.4. Thus Eq. 15.24 is nonlinear in  $A_R$ . Substituting Eq. 15.4 for discharge and solving for  $A_R$  gives

$$A_{\rm R}^{m+1} + C_1 A_{\rm R} + C_2 = 0 ag{15.25}$$

where

$$C_1 = \frac{1 - \phi}{\alpha \theta} \frac{\delta x_{k-1}}{\delta t} \tag{15.26}$$

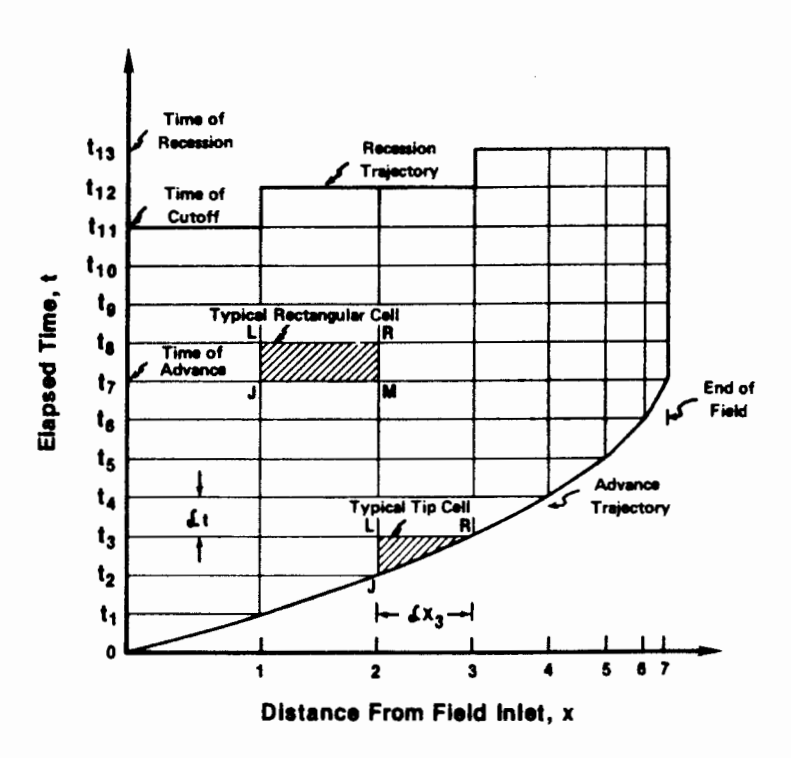


**Figure 15.3** Eulerian *t-x* solution grid for the kinematic-wave model.

and

$$C_{2} = -A_{L}^{m+1} - \frac{1-\theta}{\theta} A_{J}^{m+1} + \frac{1-\theta}{\theta} A_{M}^{m+1} + \frac{1-\theta}{\theta} A_{M}^{m+1} + \frac{1-\theta}{\theta} (A_{L} + Z_{L} - A_{J} - Z_{J}) \frac{\delta x_{k-1}}{\delta t} + \frac{1-\phi}{\theta \alpha} (Z_{R} - A_{M} - Z_{M}) \frac{\delta x_{k-1}}{\delta t}$$
(15.27)

Equation 15.25 is solved explicitly for each node k,  $1 \le k < N - 1$ , using the Newton-Raphson technique.

The boundary conditions for the kinematic-wave model are the same as for the zero-inertia and hydrodynamic models, although limited to a free draining at the end of the furrow.

For the tip cell, area and discharge are both zero for conditions J, M, and R, thereby further simplifying Eq. 15.24 to

$$\theta Q_L \, \delta t - \phi A_L \, \delta x_N - \phi Z_L \, \delta x_N = 0 \tag{15.28}$$

where again  $\theta$  and  $\phi$  are used to average the rapidly changing flow profile. Since  $A_L$  would be known from the solution at the previous cell and  $Z_L$  is a unique function of opportunity time, the single remaining unknown,  $\delta x_N$ , can be solved for directly (again utilizing Eq. 15.4):

$$\delta x_N = \frac{\theta \alpha A_L^{m+1} \, \delta t}{\phi A_L + \phi Z_L} \tag{15.29}$$

Equation 15.29 is also used during the first time step to find  $\delta x_1$ . In this case  $\theta$  must also be viewed as a factor accounting for the possibility that the inflow rate may not be fully established during the first time step.

If the advance phase is completed prior to the time of cutoff, or during recession, the right boundary condition changes from an advancing tip cell to a condition representative of the downstream field condition. For this model the free-draining downstream boundary condition is approximated by assuming the flow leaves the field at normal depth. The rectangular cells are maintained, but computations are terminated at the cell whose right side is equal to or just beyond the field boundary.

## The Ponding, Depletion, and Recession Phases

When the flow is shut off at the furrow inlet, it is assumed that the area at the left boundary,  $A_L$ , goes to zero immediately. Most field observations indicate that this is a fairly good approximation in sloping furrow situations, particularly when the model time step is on the order of 1 min. Computations follow the same steps as during the advance phase. In the current version, model computations are skipped where the areas have declined to 5% or less of the original inflow area and recession is completed when none of the grid point areas exceed this cutoff

TABLE 15.1 KINEMATIC-WAVE INPUT DATA

Model input parameters	Flowell nonwheel furrow	Flowell wheel furrow	Kimberly nonwheel furrow	Kimberly wheel furrow
Soil type	Sandy loam	Sandy loam	Silty-clay loam	Silty-clay loam
Inflow (liters/s)	2.0	2.0	0.8	1.5
Field length (m)	250	360	360	360
Field slope (m/m)	0.008	0.008	0.0104	0.0104
Manning's n	0.04	0.04	0.04	0.04
Hydraulic section parameters				
$ ho_1$	0.3269	0.3269	0.6644	0.6644
$\rho_2$	2.734	2.734	2.8787	2.8787
Furrow geometry parameters				
$\sigma_{\scriptscriptstyle 1}$	0.782	0.782	0.962	0.962
$\sigma_2$	0.536	0.536	0.6046	0.6046
Time of cutoff (min)	350	400	400	200
Kostiakov-Lewis infiltration function parameters				
k (m³/m/min²)	0.002169	0.0028	0.00701	0.00884
a	0.673	0.534	0.533	0.212
$f_0$ (m <sup>3</sup> /m/min)	0.000222	0.00022	0.00017	0.00017

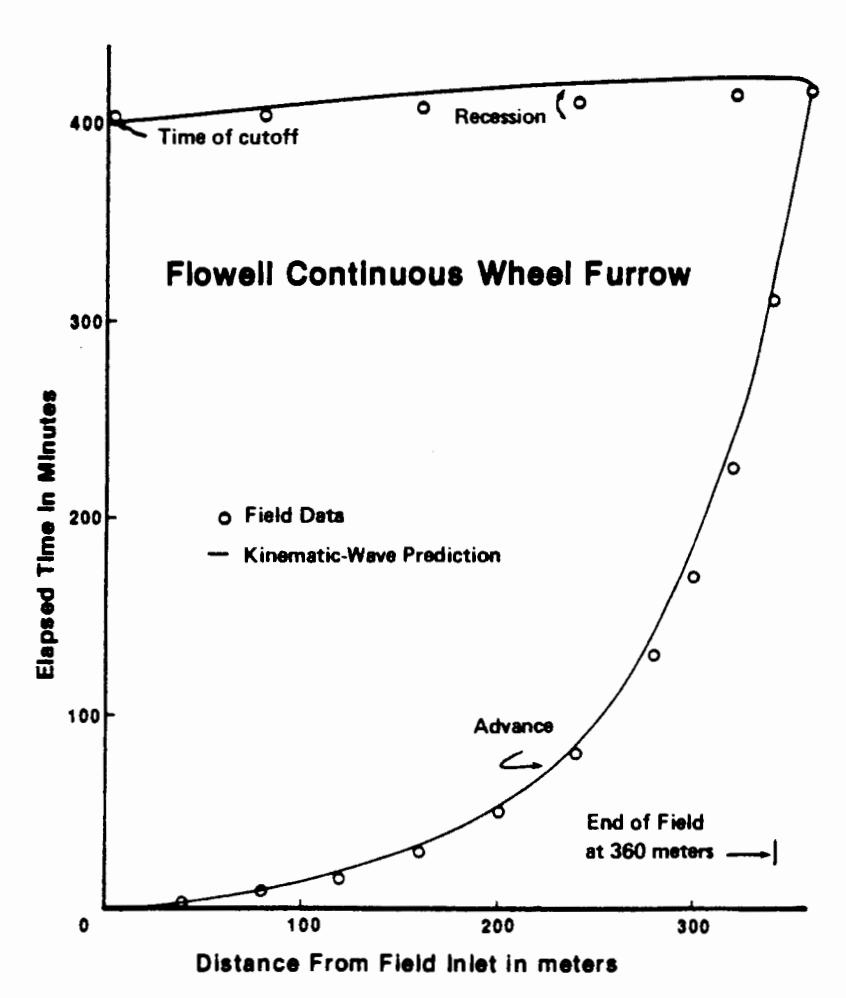


Figure 15.4 Comparison of predicted and measured advance and recession trajectories for Flowell wheel furrow. (From Walker and Humpherys, 1983, with permission of ASCE.)

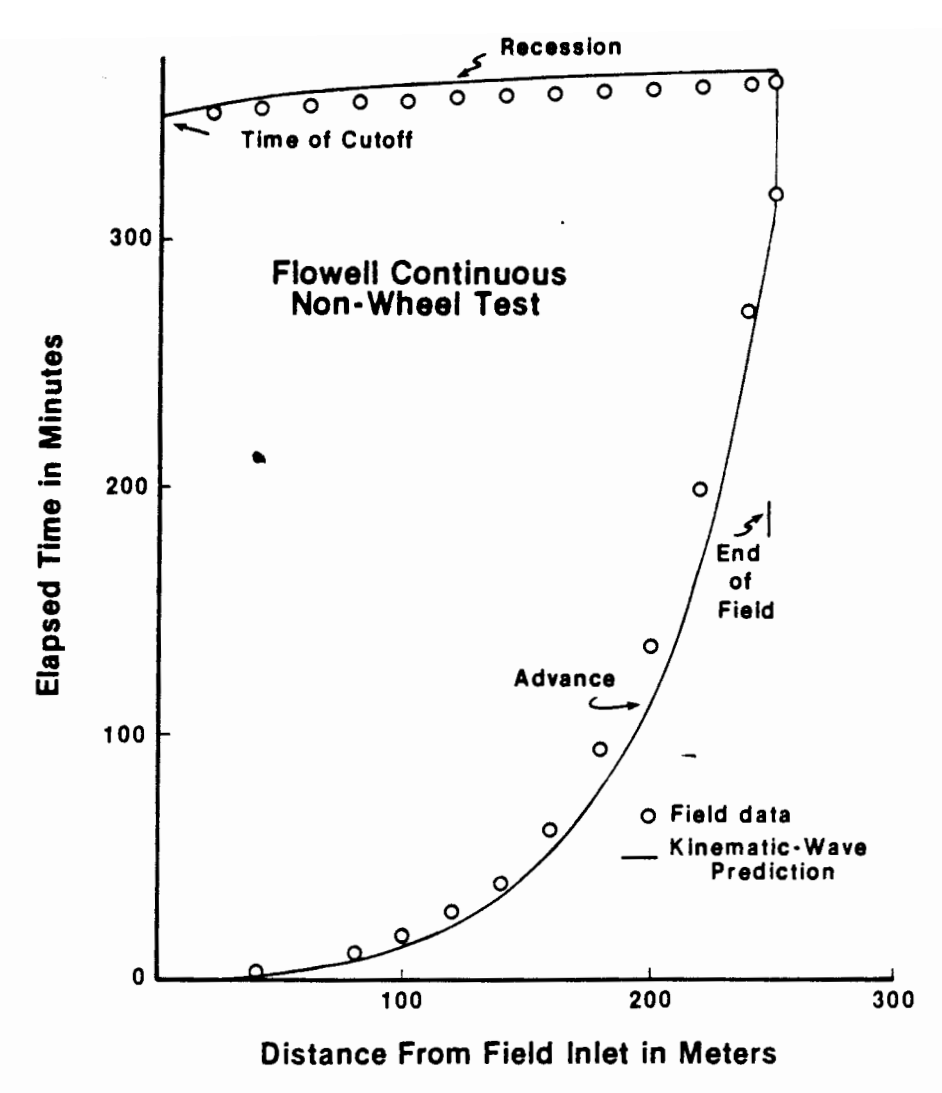


Figure 15.5 Advance and recession trajectories as measured and predicted for the Flowell nonwheel furrow.

value. The model predicts both front and rear recession, although frontal recession is usually a small part of this recession phase.

## **VERIFICATION**

The field data described in Tables 14.1 and 14.2 have also been used to verify the kinematic-wave models. For the purposes of this chapter, the control volume version was applied to four Utah and Idaho tests described in Table 15.1 as reported by Walker and Humpherys (1983). The results are shown in Figs. 15.4 to 15.7.

The uniform flow assumption greatly simplifies the analysis of furrow irrigation hydraulics and as shown, it yields very good results. Although the model provides a good estimation of recession, it should be noted that such field measurements are difficult to make. The relatively accurate simulation of advance over distances much longer than typically published in the literature is probably most indicative of the model's utility. As more field data become available, the limitations of the

Verification 355

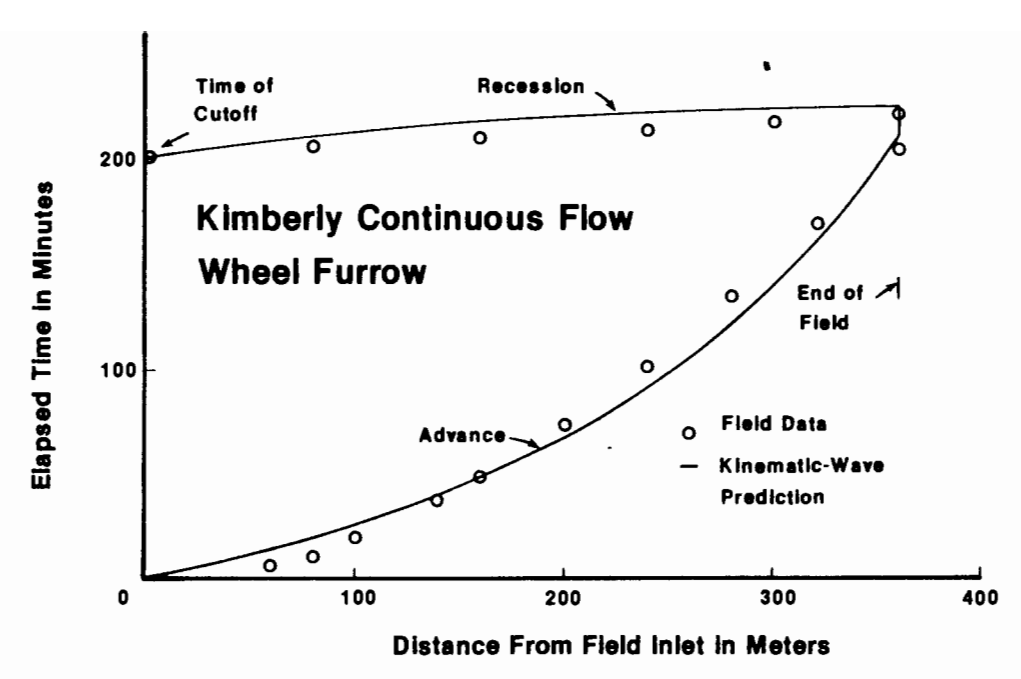
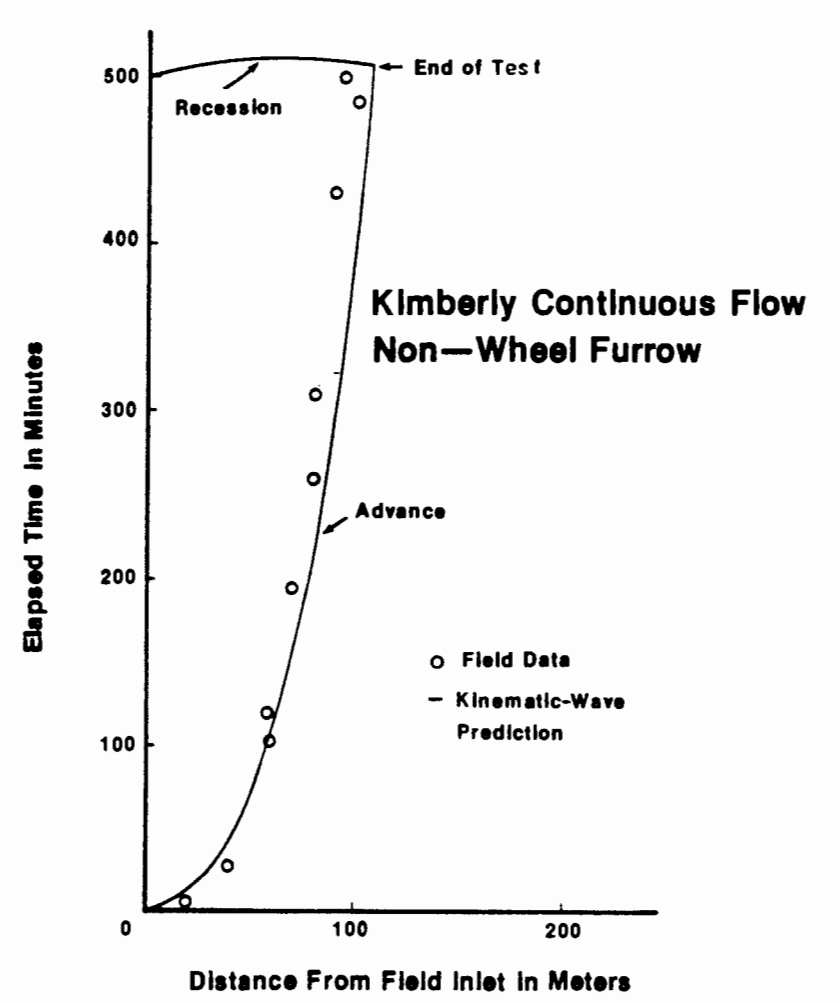


Figure 15.6 Kinematic-wave model analysis of advance and recession data for the Kimberly wheel furrow. (From Walker and Humpherys, 1983, with permission of ASCE.)



**Figure 15.7** Comparison of measured and modeled condition for the Kimberly nonwheel test.

model will be identified with the expectation that the most serious difficulties will be associated with nearly level fields.

#### REFERENCES

- BASSETT, D. L., D. D. FANGMEIER, and J. STRELKOFF. 1980. Hydraulics of Surface Irrigation. In *Design and Management of Farm Irrigation Systems*. ASAE Monogr. 3. St. Joseph, Mich., Chap. 12.
- CHEN, C. L. 1970. Surface Irrigation Using Kinematic-Wave Method. ASCE J. Irrig. Drain. Div. 96(IR1):39-46, Proc. Pap. 6284.
- KATAPODES, N. D., and T. STRELKOFF. 1977. Dimensionless Solution of Border Irrigation Advance. ASCE J. Irrig. Drain. Div. 103(IR4):401-407.
- LEE, T. S. 1982. Kinematic-Wave Simulation of Furrow Advance and Recession. M. S. thesis, Agricultural and Irrigation Engineering Department, Utah State University, Logan, Utah.
- LIGHTHILL, M. J., and R. B. WHITHAM. 1955. On Kinematic Waves: I. Flood Movement in Long Rivers. *Proc. Roy. Soc. London* A229:201-316.
- SMITH, R. E. 1972. Border Irrigation Advance and Ephemeral Flood Waves. ASCE J. Irrig. Drain. Div. 98(IR2):289-305.
- TINNEY, E. R., and D. L. BASSETT. 1961. Terminal Shape of Shallow Liquid Front. ASCE J. Hydraul Div. 87(HY5):117-133.
- WALKER, W. R., and A. S. HUMPHERYS. 1983. Kinematic-Wave Furrow Irrigation Model. ASCE J. Irrig. Drain. Div. 109(IR4):377-392.
- WALKER, W. R., and T. S. LEE. 1981. Kinematic-Wave Approximation of Surged Furrow Advance. ASAE Pap. 81-2544. ASAE Winter Meeting, Chicago, Ill.
- WOOLHISER, D. A., and J. A. LIGGETT. 1967. Unsteady, One Dimensional Flow over a Plane—The Rising Hydrograph. Water Resour. Res. 3(3):753-771.

## The Volume Balance Model

### INTRODUCTION

The momentum equation (Eq. 11.49) describes the temporal and spatial changes in velocity and depth as water flows over the irrigated field. The zero-inertia and kinematic-wave models neglect individual terms in order to develop solutions more amenable to numerical solution. The volume balance approach neglects the entire equation and replaces the dynamic behavior with what might be called gross assumptions in the mathematical sense. These assumptions have been given substantial coverage in the technical literature and have generated an interesting discussion as to their validity and applicability.

The volume balance model has been the basis for most design and field evaluation procedures and has been proven with field and laboratory data. It allows quick and reliable definition of infiltration rates over the length of the field, and it is easily extended to indications of uniformity and efficiency parameters. The review of this technique which follows is given in a historical context so that the contributions of several important investigations can be placed in perspective.

#### **DEVELOPMENT OF MASS CONTINUITY**

The volume balance model is applied primarily to the advance phase, and can be written for the border, basin, or furrow condition. At a time, t, water entering the field will progress a distance, x, toward the lower end as illustrated by Fig. 16.1. It is implicit that the discharge at the field inlet,  $Q_0$ , is steady, so that at

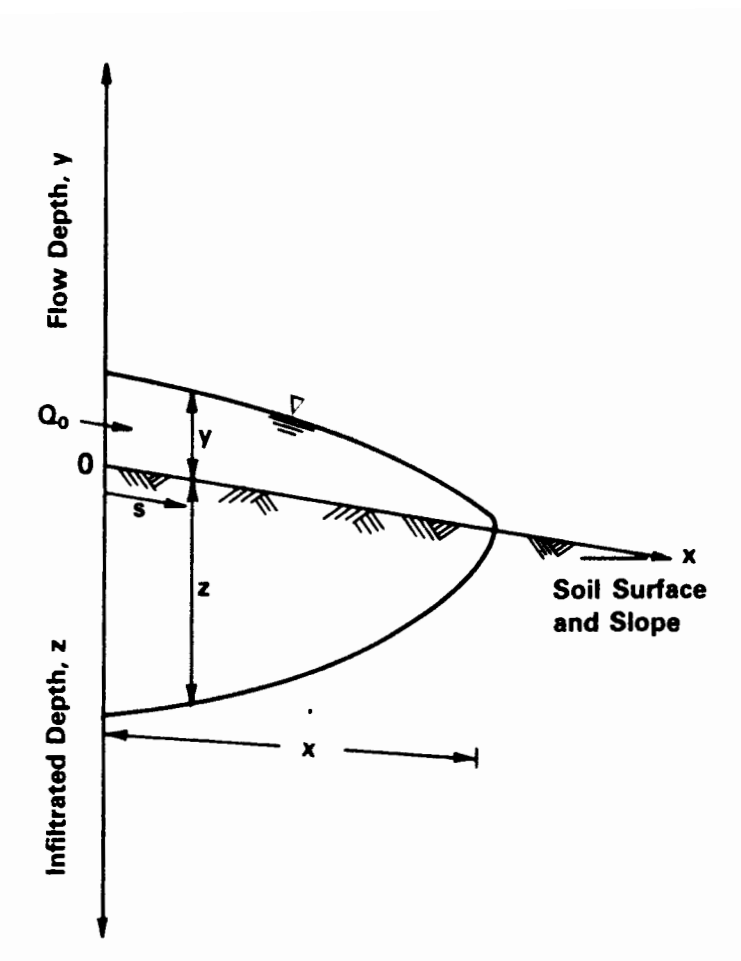


Figure 16.1 Definition sketch of an advancing flow down a border, basin, or furrow. (After Essafi, 1983.)

time, t, the product of  $Q_0$  and t equals the volume of water on the soil surface,  $V_{\nu}(t)$ , plus the volume infiltrated,  $V_{z}(t)$ , which are both time dependent. Thus

$$Q_0 t = V_v(t) + V_z(t) (16.1)$$

and this is equivalent to the integrated form of Eq. 11.12.

The volume of water above the soil surface is found by integrating the flow area over the advance distance:

$$V_{y}(t) = \int_{0}^{x} A(s, t) ds$$
 (16.2)

in which s is the integrand of x and A is the cross-sectional area. In the absence of a momentum or energy relation to describe the temporal and spatial distribution of A, the volume balance model assumes that the average area,  $\overline{A}$ , is constant. The usual practice is to define  $\overline{A}$  as follows:

$$\overline{A} = \sigma_y A_0 \tag{16.3}$$

where  $\sigma_v$  is the "surface water profile shape factor" (i.e., the ratio of average area to the inlet area,  $A_0$ ). The inlet area,  $A_0$ , is assumed to be a function of the normal depth associated with the discharge, slope, roughness, and hydraulic radius at the field inlet. Equation 16.2 reduces to

$$V_{v}(t) = \sigma_{v} A_{0} x = \overline{A} x \tag{16.4}$$

The volume of infiltrated water is found by integrating the infiltrated volume per unit length, Z(s, t), over the advance length:

$$V_z(t) = \int_0^x Z(s, t) \, ds \tag{16.5}$$

in which a unit width of unity is implied for border and basin irrigation. For furrow systems, the furrow spacing can be considered the unit width. It is again assumed that Z(s, t) is independent of surface water depth and dependent only on intake opportunity time,  $t - t_s$ , where  $t_s$  is the time when the advancing front reaches the distance, s.

Combining each of the water volumes during the advance stage into a new representation of Eq. 16.1 yields

$$Q_0 t = \overline{A}x + \int_0^x Z(t - t_s) ds$$
 (16.6)

Equation 16.6 is called the Lewis-Milne equation after two investigators who were apparently the first to suggest it (Lewis and Milne, 1938).

As a matter of interest that will be dealt with in more detail later, a subsurface shape factor,  $\sigma_z$ , can also be defined:

$$\sigma_z = \frac{\int_0^x Z(t - t_s) \, ds}{Z_0 x} \tag{16.7}$$

in which  $Z_0$  is the infiltrated depth at the field inlet. The Lewis-Milne equation written in terms of both shape factors is

$$Q_0 t = \sigma_y A_0 x + \sigma_z Z_0 x \tag{16.8}$$

## **NUMERICAL SOLUTIONS**

The second term on the right-hand side of Eq. 16.6 shows a distance integral of a time-dependent function. An analytic solution must therefore incorporate a functional dependence of advance rate with time, but as Hart et al. (1968) point out, this overconditions the problem. However, this problem is encountered only at the start of advance or during very rapid advance. Volume balance analyses by investigators such as Hall (1956), Philip and Farrell (1964), Wilke and Smerdon (1965), and Hart et al. (1968) wished to solve the Lewis-Milne equation without resorting to an assumption regarding the advance rate functional form. Their papers are largely theoretical and conceptual in nature. Parallelling these works were field data collection activities and follow-up mathematical analyses which led to the alternative volume balance models. Examples include Kiefer (1959) and Fok and Bishop (1965). These works note that measured advance is well approximated by a power function which can be used with a Kostiakov infiltration function to derive much simpler analytic volume balance expressions. As each of

these two approaches began to appear in the literature, discussions followed arguing the merits of the various assumptions and conclusions drawn from field data. With the benefit of another 15 years of experience coupled with additional field evaluations, many of the original questions have been resolved. Basically, at small times either the advance or infiltration must be left in indeterminate form, whereas at large times both processes can be defined without problems developing. It should be noted that spatial scales are not important factors when the analysis can shift from one phase to the other. Gerards (1978) and Elliott and Walker (1982) both showed that water advance over a wet surface, which occurs over relatively short time intervals, cannot be effectively modeled if both infiltration and advance functional forms are assumed.

Hart et al. (1968) recognized these interrelationships and went a long way toward reconciliation of the literature. In the following paragraphs, four basic volume balance models will be summarized: (1) the recursive approach. (2) the kernel function approach, (3) the Laplace transform approach, and (4) the power advance approach.

## The Recursive Approach

Hall (1956) described a recursive method of solving the border advance problem using the same assumptions as those of Lewis and Milne (1938). The flow into the border was assumed steady and stored on the surface within a constant average cross-sectional area. The intake characteristic was assumed to be known from either field measurements or previous experience and was considered indicative of the average field condition. The basic approach is developed on constant increments of time  $\Delta t$ . At a time when the flow has advanced a distance,  $\dot{x}$ , the number of time and space increments is  $n = t/\Delta t$ . The spatial increments decrease in width from field inlet to the advancing front. Figure 16.2 illustrates graphically what will be developed subsequently in terms of a recursive mathematical calculation. Although the approach was developed for border irrigation advance, it will be generalized in this chapter to the furrow case and include the subsequent irrigation phases.

**Advance phase.** During the first time increment, the water at the inlet infiltrates to a depth equal to  $Z_1$  and advances to a distance  $\Delta x_1$ . Writing a mass balance for the condition at the end of the time step and solving for the unknown,  $\Delta x_1$ , yields

$$\Delta x_1 = \frac{Q_0 \, \Delta t}{\sigma_y A_0 + \sigma_z Z_1 + \text{pf}} \tag{16.9}$$

where

 $A_0$  = cross-sectional flow area at the field inlet defined by the normal depth at that point

 $\sigma_z$  = subsurface shape factor for the tip cell at any time

pf = "puddle factor" to account for dead storage on the soil surface

Numerical Solutions 361

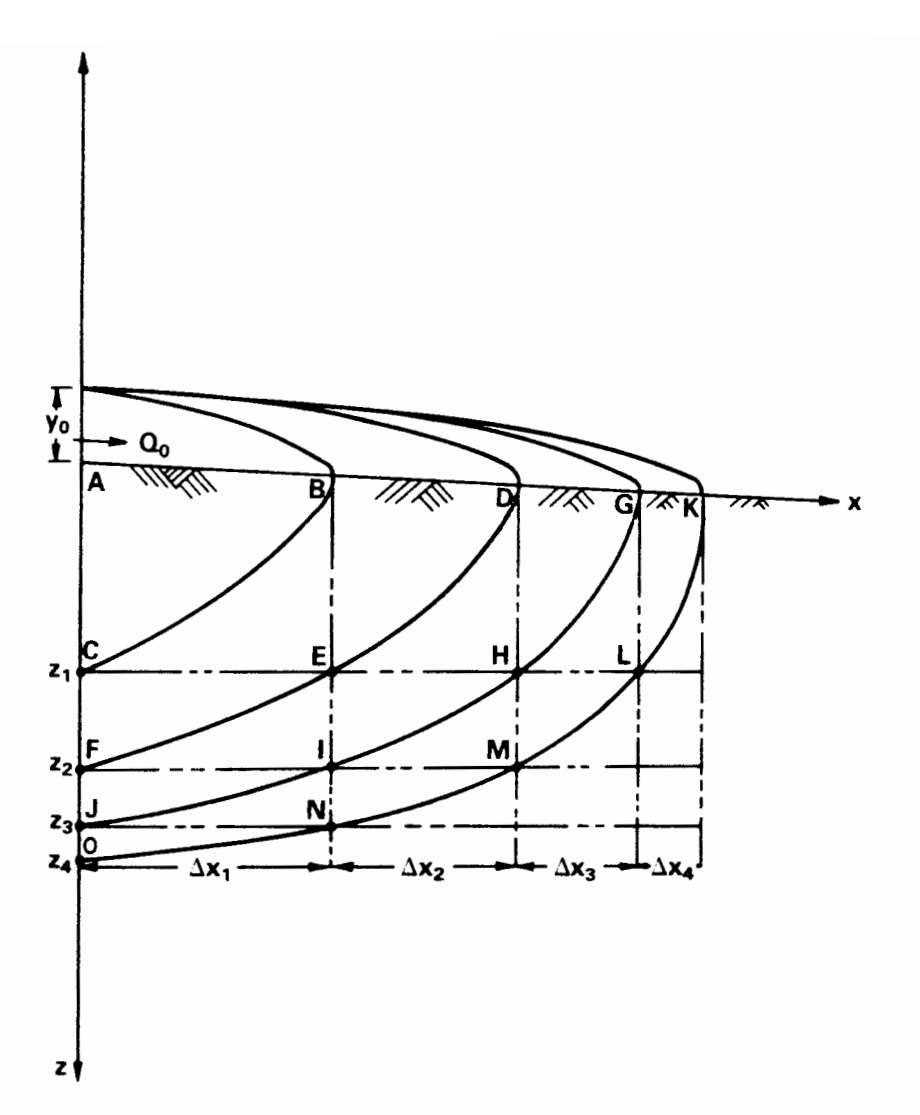


**Figure 16.2** Definition sketch for the Hall approach to solving the volume balance advance problem. (After Hall, 1956.)

Hereafter, the water represented by the puddle factor will be lumped with  $\sigma_y A_0$ . The parameter  $\sigma_z$  is best defined by reference to Fig. 16.2 as follows:

$$\sigma_z = \frac{\text{area } ABC}{\text{area } ABEC} = \frac{BDE}{BDHE} = \frac{DGH}{DGLH}$$
 (16.10)

During the second time step, and subsequently, the changes in surface and subsurface volumes are determined. The change in surface volume is simply  $A\Delta x_2$ , while the change in subsurface volume must be integrated to find the change in volume in each segment except the tip where the  $\sigma_1$  parameter is used. For example, consider the fourth time step in Fig. 16.2. The change in surface inflow,  $Q_0\Delta t$ , equals the change in surface storage,  $A\Delta x_4$ , plus the change in subsurface storage, area JIHGKLMNO. Thus, using the trapezoidal rule for the subsurface volume, we have

$$Q_0 \Delta t = A \Delta x_4 + \sigma_z Z_1 \Delta x_4 + \frac{[(Z_4 - Z_3) + (Z_3 - Z_2)]A \Delta x_1}{2} + \frac{[(Z_3 - Z_2) + (Z_2 - Z_1)] \Delta x_2}{2} + \frac{[(Z_2 - Z_1) + (Z_1 - 0)] \Delta x_3}{2}$$
(16.11)

or

$$\Delta x_4 = \frac{Q_0 \, \Delta t - a_4 \, \Delta x_1 - a_3 \, \Delta x_2 - a_2 \, \Delta x_3}{A + \sigma_2 Z_1} \tag{16.12}$$

in which

$$a_i = \frac{Z_i - Z_{i-2}}{2} \tag{16.13}$$

These results can be written in general form as follows:

$$\Delta x_i = \frac{Q_0 \, \Delta t}{A + \sigma_z Z_1} - \sum_{k=1}^{i-1} \left[ \frac{Z_{i-k+1} - Z_{i-k-1}}{2(A + \sigma_z Z_1)} \, \Delta x_k \right]$$
(16.14)

**Wetting.** Ley (1978) and Essafi (1983) added two modifications to the recursive analysis: (1) a generalized flow geometry to handle furrow irrigation; and (2) wetting, depletion, and recession phase simulation. The model of Ley (1978) assumes a completed advance phase, while Essafi's (1983) model allows a more general solution in which the cutoff can occur prior to the end of the advance phase. In the following paragraphs, only the post-advance phase condition will be described.

The interval between the time the advancing front reaches the end of the field,  $t_L$ , and the time of cutoff,  $t_{co}$ , is the wetting phase. Of interest during this time is the continued development of the subsurface moisture profile and the runoff hydrograph if the field is free draining. Essafi (1983) segregated surface and subsurface storage from tailwater by allowing the computational field length to extend indefinitely as illustrated in Fig. 16.3. Then the numerical integration is made by parts to identify the three components. For instance, during time step i = N + 3 (N being the number of time steps during the advance phase) the flow advances the distance  $\Delta x_{N+3}$  as shown. The volume that would infiltrate along the entire computational length,  $x_{N+3}$ , is the area ABCDEF as determined by

$$V_{ABCDEF} = \frac{1}{2} \sum_{k=1}^{N+2} (Z_{N+4-k} - Z_{N+2-k}) \Delta x_k + \sigma_z Z_1 \Delta x_{N+3}$$
 (16.15)

The infiltrated volume during the time step in the reach beyond the actual field length (area ABCF) is determined by

$$V_{ABCF} = \frac{1}{2} \sum_{k=1}^{2} (Z_{4-k} - Z_{2-k}) \Delta x_{k+N} + \sigma_z Z_1 \Delta x_{N+3}$$
 (16.16)

Numerical Solutions 363

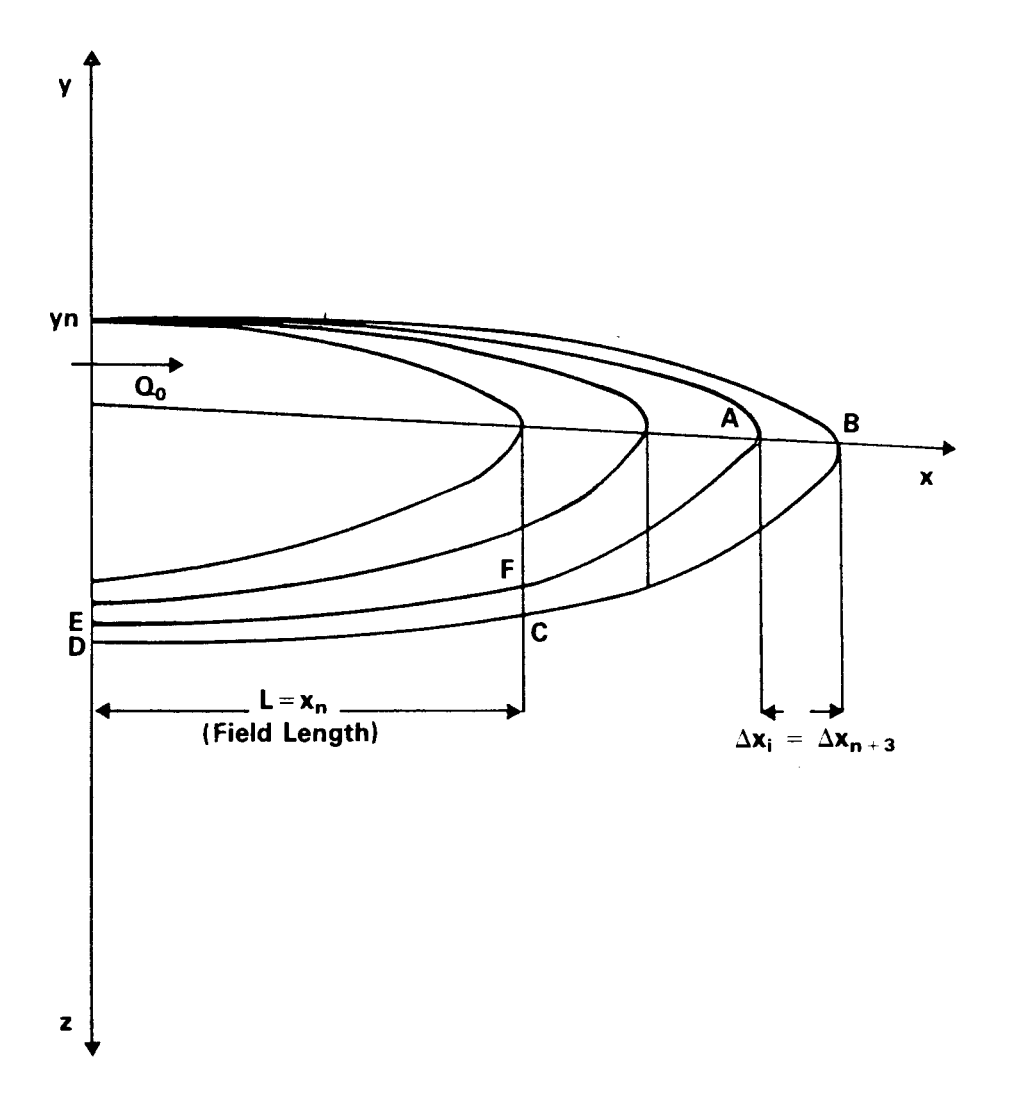


Figure 16.3 Definition sketch for the computation of runoff during the storage phase. (After Essafi, 1983.)

Thus the volume of tailwater during the time step,  $V_{R(N+3)}$ , is given by

$$V_{R(N+3)} = V_{ABCF} + \overline{A} \Delta x_{N+3}$$
 (16.17)

The runoff rate,  $Q_{R(N+3)}$ , is equal to  $V_{R(N+3)}$  divided by the time step. Finally, the actual volume of water that infiltrates in the soil between the two ends of the field during  $\Delta t$  is given by

$$V_{\rm inf} = V_{\rm ABCDEF} - V_{\rm ABCF} \tag{16.18}$$

## **Depletion and Recession Phases**

**Depletion phase.** The depletion and recession phases are patterned after the algebraic border model presented by Strelkoff (1977). Several assumptions are made. First, the surface profile at  $t_{co}$  is a straight line with endpoints corresponding to uniform flow conditions. Second, the tailwater discharge is constant during the depletion phase. Third, the combined runoff and infiltration are identically equal to the pre-cutoff inflow rate. Figure 16.4 is a schematic of this process.

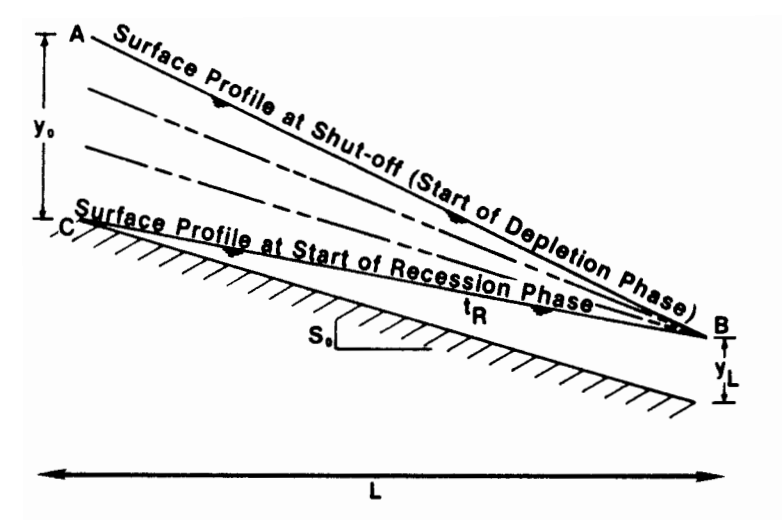


Figure 16.4 Schematic representation of the water surface profiles during the depletion phase. (After Essafi, 1983.)

Summarizing the third assumption mathematically gives us

$$Q_{\rm R}|_{t_{\rm ex}} = Q_0 - I|_{t_{\rm ex}} L \tag{16.19}$$

where

$$I|_{t_{co}} = \frac{I|_{t_{co}} + I|_{(t_{co} - t_{L})}}{2}$$
 (16.20)

and

$$I|_{t} = akt^{a-1} + f_0 (16.21)$$

Ley (1978) utilized a power function to describe area in terms of depth rather than vice versa.

$$A = \sigma_1' y^{\sigma_2'} \tag{16.22}$$

from which the volume of water in a furrow at the time of cutoff,  $V_f$ , was determined to be

$$V_f = 2L \left( \frac{y_L d_1 + y_0 d_0}{3} + \frac{y_0 d_1 + y_L d_0}{6} - \frac{a_2}{b_2 + 1} d_0^{b_2 + 1} \right)$$
 (16.23)

in which

$$d_0 = \frac{\sigma_1' \, \sigma_2'}{2} \, y_0^{\sigma_2'^{-1}} \tag{16.24}$$

$$d_1 = \frac{\sigma_1' \sigma_2'}{2} y_L^{\sigma_2^{j-1}} \tag{16.25}$$

$$b_2 = \frac{1}{\sigma_2' - 1} \tag{16.26}$$

and

$$a_2 = \left(\frac{2}{\sigma_1' \sigma_2'}\right)^{b_2} \tag{16.27}$$

Numerical Solutions 365

The volume of water leaving the furrow during the depletion phase is  $V_D$ :

$$V_D = V_f (1.0 - \sigma_v) \tag{16.28}$$

which in conjunction with Eq. 16.19 defines the length of the depletion phase, called the recession long time,  $t_{LAG}$ :

$$t_{\text{LAG}} = \frac{V_D}{Q_0} \tag{16.29}$$

**Recession phase.** In their solutions of the recession problem. Strelkoff (1977) and Ley (1978) made the assumption that the water surface profiles during the recession phase are straight lines parallel to the profile at the end of the depletion phase (Fig. 16.5). Recession rates were computed using a recursive method in which the receded distance is fixed and the time the receding edge reaches this distance is computed. For purposes of simplicity, the distances that are considered are those computed at each time step during the advance phase.

The volume of water remaining in the furrow expressed as a function of the furrow length covered by water,  $V_{fr}(l_i)$ , is given by

$$V_{fr}(l_i) = 2a_1 S_y^{\sigma_2'} l_i^{(\sigma_2'+1)} \frac{1}{\sigma_2'(\sigma_2'+1)}$$
 (16.30)

in which

$$l_i = L - x_i \tag{16.31}$$

$$S_y = \frac{yL}{L} \tag{16.32}$$

and

$$a_1 = \frac{\sigma_1' \sigma_2'}{2} \tag{16.33}$$

Ley (1978) introduced an adjustment factor to Eq. 16.30 to ensure that the volume of water in the furrow at the beginning of the recession could be obtained either by Eq. 16.30 or from the depletion-phase computations. This correction factor was called the volume balance factor,  $C_f$ .

$$C_f = \frac{V_f - V_D}{V_{fr}(L)} {16.34}$$

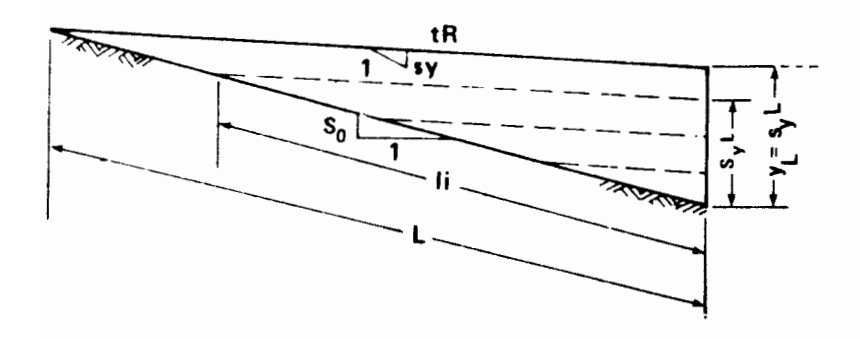


Figure 16.5 Schematic representation of the water surface profiles during the recession phase. (After Essafi, 1983.)

Equation 16.34 is used to multiply Eq. 16.30 in order to equate the two indicators of furrow storage.

Essafi (1983) presented the following summary of the recession computation. First, the furrow length is divided into reaches corresponding to the values of  $\Delta x_i$  determined during the advance phase. Then  $l_i$  is found from Eq. 16.31, where  $x_i = \sum_{j=1}^{i} \Delta x_j$ . For each value of  $l_i$ , the runoff rate is computed assuming that the depth of water at the downstream is equal to the product of the water surface slope,  $S_v$ , and  $l_i$ .

An average infiltration rate, I, is also computed for each value of  $l_i$ . Ley (1978) introduced a linear adjustment factor to take into account the variations in the wetted parameters:

$$I = I \left| t_{R} \frac{WP(l_{i})}{WP_{max}} \right|$$
 (16.35)

 $I|t_R$  is defined from Eq. 16.20 with  $t_R$  substituted for  $t_{co}$ .

 $WP_{max}$  is the average wetted perimeter of the furrow at the time of cutoff and is assumed to correspond with the average of the flow depths at the two ends of the furrow:

$$WP_{\text{max}} = \gamma_1 \left( \frac{y_0 + y_L}{2} \right)^{\gamma_2} \tag{16.36}$$

where  $\gamma_1$  and  $\gamma_2$  are empirical furrow geometry parameters, with  $y_n$  and  $y_L$  being the normal depths at the upper parameters and lower ends of the furrow, respectively, at the time of cutoff (m).

 $\operatorname{WP}(l_i)$  is the average wetted perimeter of the section of furrow still covered by water (m). It is calculated by Simpson's rule, with zero as a depth of flow at the upstream end of the furrow section and normal flow depth for the runoff rate at the downstream end. The value obtained is adjusted by a multiplication by  $C_f$  in order to account for the water surface profile shape.

For each value of  $l_i$ , the volume of water still remaining in the furrow is then computed using Eq. 16.30. The average rate water removed from each segment of the furrow is calculated as the average value of the runoff and infiltration rates determined for the two successive values of  $l_i$ . The time required to remove the volume of water within the furrow segment is determined by first computing the volume at two successive values of  $l_i$  and then dividing the difference by the average removal rate. This procedure is continued until the furrow is drained. The array of points  $(x_i, t_i(i))$  define the recession trajectory.

## The Kernel Function Approach

Hart et al. (1968) nondimensionalized Eq. 16.6 for the border irrigation case using the Kostiakov intake equation (first term of Eq. 11.65). The characteristic time scale, T, and distance scale, X, were chosen as follows:

$$T = \left(\frac{\overline{y}}{k}\right)^{1/a} \tag{16.37}$$

Numerical Solutions 367

and

$$X = \frac{q}{\overline{y}} \left(\frac{\overline{y}}{k}\right)^{1/a} \tag{16.38}$$

where  $\bar{y}$  is the average depth of flow and q is the discharge per unit width. Utilizing Eqs. 16.36 and 16.37 to nondimensionalize Eq. 16.6 results in

$$x^* = t^* - t^{*a} \int_0^{x^*} \left(1 - \frac{t_s^*}{t^*}\right)^a ds^*$$
 (16.39)

in which

$$x^* = \frac{x}{X}$$
  $t^* = \frac{t}{T}$   $t_s^* = \frac{t_s}{T}$   $s^* = \frac{s}{X}$  (16.40)

The variable of integration in Eq. 16.39 can be changed to yield

$$x^* = t^* - t^{*a+1} \int_0^1 (1 - \alpha)^a \frac{dx^*}{dt^*} \bigg|_{\alpha t^*} d\alpha$$
 (16.41)

where  $\alpha = t_s^*/t^*$ . The term  $(1 - \alpha)^a$  is a kernel function whose behavior varies from a straight-line function of  $\alpha$  when a = 1.0 to a convex function for a < 1.0. Hart et al. (1968) point out that the equations above are not valid when a = 0, but state that the a = 0 is not likely to occur.

At very small values of  $t^*$ ,  $dx^*/dt^*$  can be considered equal to unity. The resultant solution to Eq. 16.41 is then

$$x^* = t^* \left( 1 - \frac{t^{*a}}{a+1} \right) \tag{16.42}$$

Hart et al. (1968) show the behavior of Eq. 16.42 compared to a numerical solution of Eq. 16.39 to indicate that it is indeed asymptotic for small values of  $t^*$ .

The numerical results for large values of  $t^*$  indicated that the relationship between advance and time appeared to have a power function shape of the form

$$s^* = pt_s^{*r} \tag{16.43}$$

When this assumption is made, the resulting analysis is equivalent to the power advance approach, discussed later. To illustrate this, the transformation of Eq. 16.39 proceeds as follows:

$$ds^* = \frac{ds^*}{dt_s^*} dt_s^* = \frac{ds^*}{dt_s^*} \frac{dt_s^*}{d\alpha} d\alpha = rpt_s^{*r-1} t^* d\alpha$$
 (16.44)

Then noting that  $t_s^* = \alpha t^*$ , Eq. 16.41 becomes

$$x^* = t^* - t^{*a} \int_0^1 (1 - \alpha)^a \, rpt^{*r} \alpha^{r-1} \, d\alpha \qquad (16.45)$$

or

$$x^* = t^* - t^{*a} p t^{*r} r \int_0^1 (1 - \alpha)^a \alpha^{r-1} d\alpha$$
 (16.46)

where the integral is the beta function and will be shown later; r times the beta function is the subsurface shape factor proposed by Kiefer (1959) and Fok and Bishop (1965). Equation 16.46 can be written in similar dimensional form if a power law advance is assumed (Gerards, 1978):

$$\bar{y}x = qt - Z_0 xr \int_0^1 (1 - \alpha)^a \alpha^{r-1} d\alpha$$
 (16.47)

Hart et al. (1968) inserted Eq. 16.42 into a simplified expression for the subsurface shape factor, organized terms, and concluded that the dimensionless time must vanish. They then performed the preceding transformations in a slightly different way and produced a somewhat different conclusion. If the Lewis-Milne equation is written

$$\overline{y}x = qt - \sigma_z Z_0 x \tag{16.48}$$

and then nondimensionalized by first dividing through by y and then X to yield

$$x^* = t^* - \sigma_z t^* a x^* \tag{16.49}$$

the subsurface shape factor is

$$\sigma_z = \frac{(t^*/x^*) - 1}{t^{*a}} \tag{16.50}$$

Another expression for  $\sigma_z$  is found by equating the second term on the right-hand side of Eq. 16.49 to its counterpart in Eq. 16.41:

$$\sigma_z t^{*a} x^* = t^{*a+1} \int_0^1 (1 - \alpha)^a \frac{dx^*}{dt^*} \bigg|_{\alpha t^*} d\alpha \qquad (16.51)$$

and thus

$$\sigma_z = \frac{t^*}{x^*} \int_0^1 (1 - \alpha)^a \frac{dx^*}{dt^*} \bigg|_{\alpha t^*} d\alpha$$
 (16.52)

If Eqs. 16.49, 16.50, and 16.43 are combined, the result is Eq. 16.46, as one would expect. However, Hart et al. (1968) reasoned that at large times ( $t^* >> 1$ ), Eq. 16.50 could be approximated by

$$\sigma_z = \frac{t^*/x^*}{t^{*a}} \tag{16.53}$$

where the negative 1 is omitted. When Eqs. 16.43, 16.49, and 16.53 are combined, the result is

$$1 = t^{*a+r-1} pr \int_0^1 (1 - \alpha)^a \alpha^{r-1} d\alpha$$
 (16.54)

Then stating that this equation holds only if r = 1 - a, the following solution is derived for large times:

$$x^* = \frac{\sin \pi a}{\pi a (1 - a)} t^{*1 - a} \tag{16.55}$$

Numerical Solutions 369

In summary, then, the kernel function approach of Hart et al. (1968) yields two values of the subsurface shape factor,  $\sigma_z$ :

$$\sigma_z = \frac{1}{1+a}$$
 for  $t^* << 1$  (16.56)

and

$$\sigma_z = \frac{\pi a (1 - a)}{\sin \pi a}$$
 for  $t^* >> 1$  (16.57)

It is interesting to note in concluding the discussion of the model proposed by Hart et al. (1968) that they compared these various modifications against a completely numerical solution. The results indicated that  $\sigma_z$  increased with increases in dimensionless time,  $t^*$ , whereas each of the other models based on the assumption of a power law advance indicates that  $\sigma_z$  is independent of time.

## The Laplace Transform Approach

Twenty-five years after the appearance of the Lewis-Milne equation, Philip and Farrell (1964) presented the first analytical solution. Laplace transforms involving the Faltung theorem were applied to the equation using a number of different infiltration functions.

The convolution or Faltung theorem of the Laplace transformation states that (Philip and Farrell, 1964)

$$L[F] = \int_0^\infty e^{-st} F(t) dt \qquad (16.58)$$

where

L[F] = Laplace transformation on the function F

t = time coordinate

s = spatial coordinate

The Laplace transformation of Eq. 16.6 for the border irrigation case is, after simplification,

$$\frac{x}{q} = L^{-1} \left( \frac{1}{s^3 L[Z] + y s^2} \right) \tag{16.59}$$

When the infiltration function, Z, is represented by the Kostiakov relation, L[Z] is

$$L[Z] = \frac{k\Gamma(1+a)}{s^{1+a}}$$
 (16.60)

Substituting Eq. 16.60 into Eq. 16.59 results in the following convergent expansion:

$$\frac{x}{q} = \frac{t}{y} \sum_{n=0}^{\infty} \frac{(-kt^{a}/y)\Gamma(1+a)^{n}}{\Gamma(2+na)}$$
 (16.61)

Although Eq. 16.61 is convergent, it does so very slowly for the large times

associated with irrigation events. Philip and Farrell (1964) propose asymptotic expansions for both short- and long-time solutions.

## The Power Advance Approach

Anyone who has participated in the field evaluation of a surface irrigation being operated under what might be called "traditional" practices will be impressed by the very large variabilities in the parameters usually assumed constant in mathematical treatments. Roughness, slope, cross-sectional shape, and infiltration characteristics vary widely and arguments over the mathematical adequacy of certain assumptions seem pointless. The poorest assumption that may be made, yet the one where mathematical treatments always begin, is that an equation such as the Kostiakov-Lewis infiltration model can adequately describe the actual process with regard to time and space. The rate at which water covers the field (advance), on the other hand, is readily measured and is well represented by a power law function (Eq. 16.43), an exponential function such as proposed by Singh and Chauhan (1972), or other nonlinear models. It is not surprising, then, to find investigators such as Fok and Bishop (1965), who utilize a measured power advance function, retaining the traditional expressions for infiltration and constancy of surface crosssectional area. These assumptions do not satisfy the volume balance concept at small times but repeatedly represent actual irrigation performance well. dition, they are by far the most useful in extending advance hydraulics to measures of system performance.

Wilke and Smerdon (1965) approached the problem by computing the first 400 terms of Eq. 16.61 for five values of  $kt^a/\bar{y}$  ranging from 1.25 to 1.75 and five values of a, ranging from 0.2 to 0.7. They then plotted dimensionless curves of  $qt/\bar{y}x$  versus  $kt^a/\bar{y}$ . Noticing that the nonlinearity was not great, they approximated the curves with straight lines passing through the point  $qt/\bar{y}x = 1.0$  and  $kt^a/\bar{y} = 0.0$ , which in effect eliminates the time dependence of the slope of these lines. The slope, or subsurface shape factor  $\sigma_z$ , was correlated with the intake characteristic, a, yielding

$$\sigma_z = \frac{0.618 - 0.142 \ln (a)}{\ln(a)} \tag{16.62}$$

Fok and Bishop (1965), as noted, started their analysis by assuming a power law advance, substituted this into the Lewis-Milne equation, expanded the infiltrated volume portion in a binomial series, and integrated the result by parts. These results for the subsurface shape factor are

$$\sigma_z = \frac{\frac{1}{r} - \frac{a}{r+1} + \frac{a(a-1)}{2(r+2)} - \frac{a(a-1)(a-2)}{6(r+3)}}{a+1}$$
(16.63)

which was approximated quite well by the Kiefer (1959) factor:

$$\sigma_z = \frac{a - (a - 1) r + 1}{(a + 1) (r + 1)} \tag{16.64}$$

Numerical Solutions 371

A somewhat more concise formulation was given by Hart et al. (1968) as part of Eq. 16.46:

$$\sigma_z = r \int_0^1 (1 - \alpha)^a \alpha^{r-1} d\alpha \qquad (16.65)$$

Gerards (1978) followed Hart et al. (1968) in the use of Eq. 16.65 and reminded his readers that the integral is a beta function which can be used effectively in the definition of application efficiency and uniformities. It should come as no surprise that the  $\sigma_z$ , as defined by Eqs. 16.62, 16.64, and 16.65, have differed only by normal numerical error in comparisons with field data found in Hart et al. (1968), Fok and Bishop (1965), and Singh and Chauhan (1972). Equations 16.64 and 16.65, however, require that both a and r be known, or that a relationship between the two be defined. Fok and Bishop (1965) proposed

$$r = \exp(-0.6a) \tag{16.66}$$

Gerards (1978) compared Eq. 16.64 using Eq. 16.66 to Eq. 16.62 and a numerical solution to Eq. 16.65. The differences over a range of a values were insignificant.

#### **VERIFICATION**

The recursive volume balance developed by Essafi (1983) was tested with data from the Colorado State University study and against simulation generated by the kinematic-wave and zero-inertia models. The results of advance and recession

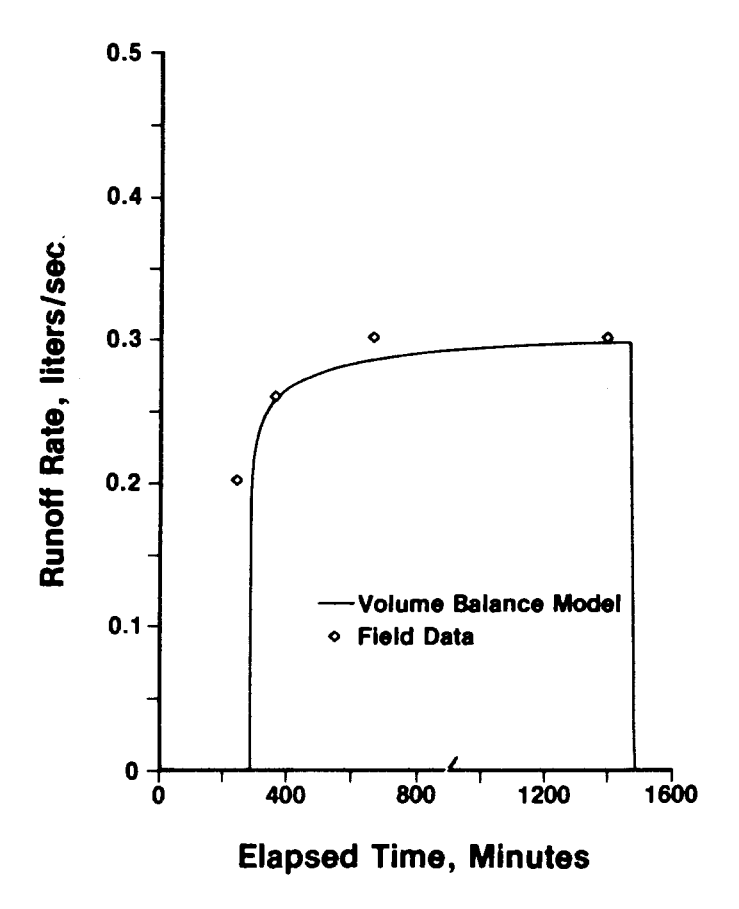


Figure 16.6 Predicted and observed runoff hydrograph for Matchett 8-3-1 test. (After Essafi, 1983.)

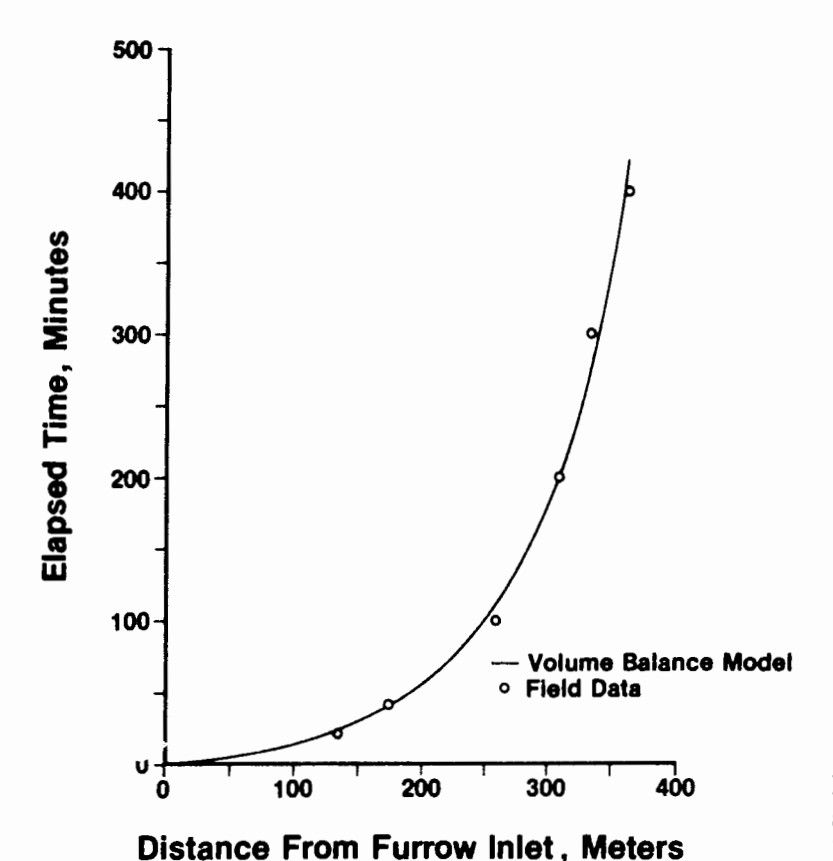


Figure 16.7 Predicted and observed advance for a wheel furrow, Flowell, Utah. (After Essafi, 1983.)

trajectory analysis were generally good. Essafi (1983) also verified the model by comparing predicted and measured tailwater hydrographs. While the results showed more error than in predicting advance and recession, the results were still acceptable. Figure 16.6 shows a tailwater hydrograph comparison for the Matchett 8-3-1 test in Colorado. The model input data were given previously in Table 14.2. This is one of the best results obtained, but not atypical.

None of the Colorado data sets involve completely independent measurements as discussed by Elliott and Walker (1982). Figure 16.7 shows the recursive volume balance model analysis of one set of Utah data (Table 15.1) in which all data, including infiltration, were measured independently. Figure 16.7 therefore constitutes a realistic verification of the volume balance approach in graded furrows.

#### REFERENCES

ELLIOTT, R. L., and W. R. WALKER. 1982. Field Evaluation of Furrow Infiltration and Advance Functions. *Trans. ASAE* 15(2):396–400.

Essafi, B. 1983. A Recursive Volume Balance Model for Continuous and Surge Flow Irrigation. Unpublished M.S. thesis, Utah State University, Logan, Utah.

Fok, Y., and A. A. BISHOP. 1965. Analysis of Water Advance in Surface Irrigation. *ASCE J. Irrig. Drain. Div.* 91(IR1):99-117.

GERARDS, J. L. M. H. 1978. Predicting and Improving Furrow Irrigation Efficiency. Unpublished Ph.D. dissertation, Colorado State University, Fort Collins, Colo.

- HALL, W. A. 1956. Estimating Irrigation Border Flow. Agric. Eng. 37(4):263-265.
- HART, W. E., D. L. BASSETT, and T. STRELKOFF. 1968. Surface Irrigation Hydraulics-Kinematics. ASCE J. Irrig. Drain. Div. 94(IR4):419-440.
- KIEFER, F. W. 1959. Average Depth of Absorbed Water in Surface Irrigation. Civil Engineering Department, Utah State University, Logan, Utah.
- LEWIS, M. R., and W. E. MILNE. 1938. Analysis of Border Irrigation. Agri. Engr. 19:267-272.
- LEY, T. W. 1978. Sensitivity of Furrow Irrigation Performance to Field and Operation Variables. Unpublished M.S. thesis, Colorado State University, Fort Collins, Colo.
- PHILIP, J. R., and D. A. FARRELL. 1964. General Solution of the Infiltration-Advance Problem in Irrigation Hydraulics. *Geop. Res.* 69(4):621-631.
- SINGH, P., and H. S. CHAUHAN. 1972. Shape Factors in Irrigation Water Advance Equation. ASCE J. Irrig. Drain. Div. 98(IR3):443-458.
- STRELKOFF, T. 1977. Algebraic Computation of Flow in Border Irrigation. ASCE J. Irrig. Drain. Div. 103(IR3):325-342.
- WILKE, O. C., and E. T. SMERDON. 1965. A Solution to the Irrigation Advance Problem. ASCE J. Irrig. Drain. Div. 91(IR3):23-34.

#### Absolute roughness of pipe, 269 measurement of, 73-79Ackers, P., 64 modification of, 126 Adjusted infiltration approach, 113-16 surface storage volume estimation Advance phase: and, 105-6, 108-12 characteristic approach to the in surge flow systems, 214–18, hydrodynamic model and, 220-23, 226, 228-30 305 - 10trajectory calculation, 140-42 characteristic approach to the volume balance model and, 358kinematic-wave model and, 63, 367-73 349 - 50zero-inertia model and, 328–34 deformable control volume Agricultural Experiment Stationapproach to the kinematic-**USDA** Regional Project wave model and, 351-56 W163, 218 Eulerian integration approach to Air-operated butterfly valves, the hydrodynamic model and, 200 - 203324 - 25Aletraris, S. S., 253, 254, 257-59 field surface amendments and, 38 Alfalfa valves, 44, 267, 273-74 field system evaluation and, 106-9 Alfaro, J. F., 18 infiltration evaluation and, 114, Allen, N. L., 214, 216 Aluminum Specialties, Inc., 194 116 - 20inlet discharge control practices American Concrete Pipe Association, and, 38 236 irrigation scheduling and, 206-7, American Society of Agricultural 209 Engineers (ASAE), 54, 56, 57

Ampt, G. A., 17 Border irrigation, 32, 35, 137 Anderson, C. L., 187 evaluation of system, 122-23 Application efficiency, 22-25, 135 examples of, 35, 36 estimation of, 122 field distribution systems for, 41, surge flow systems and, 228, 230 Application uniformity, 22-25 infiltration measurement for, 88 Applied irrigation water, depth of, 9 land leveling and, 35, 38 Arizona, University of, 339 volume balance field design for, Ashcroft, G. L., 16 148 - 50Asphalt channel lining, 242 Bos, M. G., 22, 62, 64, 71 Automation, 142 Brick-and-mortar channel lining, 242 controllers, 202-5 Broad-crested weirs, 57–62 open-channel headland facility, Bulk density measurement, 97 193-97 Butterfly valves, air-operated, pipeline, 197-203 200 - 203surge flow (see Surge flow surface Butyl rubber channel lining, 242 irrigation) Basin irrigation, 32–35, 137 **Calibration**, 192, 205–6 advance trajectory for, 107 Canal turnout structures, 40, 235-36 evaluation of systems, 123-24 Capped pot hydrants, 275 examples of, 34 Carlyle Tire and Rubber Company, field distribution systems for, 41, Carter, R. W. C., 64, 66 infiltration measurement for, 88 Chamberlain, A. R., 52, 55 land leveling and, 35, 38 Channels, open (see Open-channel limitations of, 35 irrigation distribution) recession phase measurement for, Characteristic approach to the hydrodynamic model, 301-11 recession trajectory for, 107–9 characteristic equations, 302-4 volume balance field design for, numerical solution for plane flow, 150 - 52304 - 10water advance measurement for, Characteristic approach to the 74, 76 kinematic-wave model, 346–50 Basin length, 259 Characteristic equations, 302-4 Basket-type screening structures, 240 Chauhan, H. S., 371, 372 Bassett, D. L., 297, 301, 347, 348 Check structures, 42, 244, 245, 247, Beggs, R. A., 15 252 - 61Bennett, R. S., 50 Chemical properties of soil, 19–20 Binder, C. W., 339 Chemical weathering, 2 Bishop, A. A., 360, 369, 371, 372 Chen, C. L., 346, 347 Blair, A. W., 221 Chezy equation, 295, 345 Blaisdell, F. W., 254, 257 Chow, V. T., 258, 289, 294, 295 Blocked furrow method, 90–91 Christiansen, J. E., 22, 118, 271 Bodman, G. B., 15, 16 Clay channel lining, 242 Bondurant, J. A., 90 Clemmens, A. J., 289, 299, 327, 339

Closed-conduit flow-measuring	Cunge, J. A., 319
devices (see Flow	Cutback furrow design, 144-46
measurement, closed-conduit)	Cutback irrigation, 38
Closed-conduit irrigation distribution,	Cut/fill ratio adjustment, 186-87
264-77	Cutoff time, 138
hydrants, 267, 274–77	border irrigation, 149-50
hydraulics, 267–73	furrow irrigation, 143–48
low-pressure pipeline systems.	modification of, 125
264-65, 267-73	Cutthroat flumes, 41, 50, 52-54
valves, 265, 267, 272-76	Cylinder infiltrometers, 81–87
Coleman, E. A., 15, 16	
Colorado Valve Company, 198	Darcy-Weisbach equation, 268, 295,
Compatibility of system, 3	345
Complete-irrigation case, 120–22	Debris removal, 236–43
Concrete-lined channels, 241-42,	Deep percolation, depth of, 9-11
248-51	Deep percolation losses, 127
"Concrete Pipe for Irrigation"	Deep percolation ratio (DPR):
(Pillsbury), 273	defined, 25
Continuity equation:	estimation of, 122
development of, 290-91	Deformable control volume
(see also Characteristic approach to	approach:
the hydrodynamic model;	Eulerian system (see Eulerian
Eulerian integration approach	integration approach to the
to the hydrodynamic model;	hydrodynamic model)
Kinematic-wave model;	to the kinematic-wave model,
Volume balance model; Zero-	350-55
inertia model)	Depletion phase:
Continuity principle, 10	characteristic approach to the
Controllers, 202-5	hydrodynamic model and,
Control systems, self-calibrated	309-10
(SCCS), 229	deformable control volume
Conveyance structures, 40, 41	approach to the kinematic-
Coolidge, P. S., 216	wave model and, 353
Corey, A. T., 5	Eulerian integration approach to
Criddle, W. D., 38	the hydrodynamic model and
Crop evapotranspiration (see	319
Evapotranspiration)	measurement of, 78
Crop factors in system selection, 5	recursive approach to the volume
Cropping patterns, 136, 137	balance model and, 364-66
Crop water requirements, 207	zero-inertia model and, 335
Cross-sectional surface flow area,	Desilting boxes, 239, 240
77 – 79	Discharge rate, modification of, 125
Crusting, 4–5	Distribution, 40-41, 43-45 (see also
Cultural practices, 136	Closed-conduit irrigation
Cumulative infiltration, 14–16,	distribution; Open-channel
113–14, 116	irrigation distribution)

Distribution pots, 267	Fangmeier, D. D., 118, 327, 339
Distribution pois, 207  Distribution uniformity, 23–24	Farrell, D. A., 297, 360, 370
Diversion structures, 39–40	Field capacity, 11–13
Division structures, 42, 244	defined, 12
Donnelly, C. A., 254, 257	measurement of, 97
Doorenbos, J., 20	Field distribution systems, 40–41,
Double-pond method, 87, 88	43–45 (see also Closed-conduit
Drainage requirement, depth of, 10,	irrigation distribution; Open-
21	channel irrigation distribution)
Driving hammers, 82, 83	Field length, 142
Drop-closed gates, 195, 197	Field measurement techniques.
Drop-open gates, 193–96	47–98 (see also Flow
Drop structures, 42, 239, 241, 245,	measurement, closed-conduit;
247, 252–61	Flow measurement, free-flow
Duke, H. R., 218	and submerged-flow;
Duke, 11. K., 216	Infiltration measurement;
Earth channels (see Open-channel	·
· •	Irrigation event measurement; Soil-water measurement)
irrigation distribution)	Field operations, 188–89
Earth requirements, miscellaneous, 189	Field operations, 188–89
Economic conditions, 136	,
	Field slope, 4, 180, 86
Economics of irrigation systems, 3-4 Efficiency (see Application efficiency)	Field subdivision 187 88
	Field subdivision, 187–88 Field surface amendments, 38–39
Electrical conductivity (EC), 21 Elliott, R. L., 22, 107, 114, 118, 119,	
218, 321, 327, 331, 332, 336,	Field system evaluation, 104–27 advance-recession trajectories,
337, 339, 361, 373	106-8
Energy costs, 6	advance-surface storage
2.	assessment, 108–12
Epp-fly gated pipe valve, 202, 203 Erodibility, 4–5	basin irrigation, 123–24
Essafi, B., 222, 226, 363, 372, 377	border irrigation, 122–23
Eulerian integration approach to the	furrow irrigation, 121–22
hydrodynamic model, 313–26	infiltration (see Infiltration
continuity definition, 314–15	evaluation)
deformable control volume, 313–	inflow-outflow analysis, 105-6
14	modifying hydraulic conditions.
momentum equation, 315–19	125–27
numerical solution, 319–25	surface irrigation results, 120–21
Evans, R. G., 193–95, 221	Fitzsimmons, D. W., 304
Evapotranspiration:	Flow control, on-off, 39–40
calculation of, 207	Flow cross section, 140–41
depth of, 9, 20–21	Flow depth measurement, 78
potential, 20–21	Flow equations:
External influences on system	closed-conduit distribution, 268–73
selection 5-6	open-channel distribution 244-45

Flow measurement, closed-conduit.	field surface amendments and, 38–39
	infiltration measurement for,
orifices, 71	89–93
propeller meters, 72–74	
Venturi meters, 71–73	pipeline automation for, 197–203
Flow measurement, free-flow and	recession phase measurement for,
submerged-flow, 47–70	80
flumes (see Flumes)	surge flow (see Surge flow surface
free-flow vs. submerged-flow,	irrigation)
48–49	volume balance design, 142–48
orifices, 41, 47–48, 67–70	water advance measurement for,
weirs, 47, 64–67	74, 75
Flow principles (see Saint-Venant	Furrow profilometers, 78, 90
equations)	Furrow slope, 142
Flumes, 41, 47, 49–64, 244	
cutthroat, 41, 50, 52-54	Garton, J. E., 144, 145
H, 63–64	Gated-pipe furrow irrigation systems
modified broad-crested weirs,	43, 45
57-63	Gated pipe outlets, 202, 203
Parshall, 41, 49-52	Gates:
trapezoidal, 54-57	drop-closed, 195, 197
Fok, Y., 360, 369, 371, 372	drop-open, 193–96
Free-draining border irrigation	slide, 195, 197, 198
design, 148-50	Gerards, J. L., 361, 369, 372
Free-flow conditions vs. submerged-	Gitlin, H. M., 273
flow conditions, 48-49 (see	Graded border irrigation, 4
also Flow measurement, free-	Gravimetric sampling, 94
flow and submerged-flow)	Green, W. H., 17
Friction forces, 294-95, 317-18	
Friction losses, 270–71	Green and Ampt equation, 17, 18
Friction slope, 301-2	
Froude numbers, 259, 260	Hachum, A. Y., 18
Furrow infiltrometers (see	Haie, N., 222, 226
Infiltrometers)	Haise, H. R., 81, 197, 198, 202-4
Furrow irrigation, 3, 32, 35–37, 137	Hall, W. A., 360
advantages of, 35-36	Hammers, 82, 83
cross-sectional area determination	Hanks, R. J., 16
for, 77–79	Hansen, V., 15
disadvantages of, 36	Hart, W. E., 5, 22, 186, 360, 361,
evaluation of system, 121–22	367–70, 372
examples of, 37	Head ditch outlets, 40–41, 43, 44
field distribution systems for,	Head ditch water level, 144
43–45	Headland facilities, 235–77
field shape and, 4	canal turnout structures, 40,
field shape and, 4	235–36
neia siope ana, 4	233-30

Headland facilities (cont.) closed-conduit (see Closed-conduit irrigation distribution)	Infiltration evaluation, 111, 113-20 adjusted infiltration approach, 113-16
debris and sediment removal, 236-43	from advance data, 114, 116-20 Infiltration measurement, 80-93
open-channel (see Open-channel irrigation distribution)	blocked furrow method, 90–91 cylinder infiltrometers, 81–87
Head loss, 271–73	importance of, 80-81
H flumes, 63–64	inflow-outflow methods, 88-90
Holtan, H. N., 63	ponding methods, 87-89
Horton, R. E., 18	recycling furrow infiltrometers,
Humpherys, A. S., 193, 200, 201,	92-93
222, 223	Infiltration opportunity time, 15, 16
Hyatt, M. L., 52	Infiltrometers:
Hydrants, 267, 274–77	cylinder, 81–87
Hydraulic conductivity, 19	recycling, 92–93
Hydraulic jump, 257–61	Inflatable pneumatic O-rings,
Hydrodynamic model:	197–200
characteristic approach (see	Inflow-outflow analysis, 105-6
Characteristic approach to the	Inflow-outflow methods, 88–90
hydrodynamic model)	Inflow rates:
Eulerian approach (see Eulerian	basin irrigation, 151
integration approach to the	border irrigation, 148–50
hydrodynamic model)	furrow irrigation, 143–48
surge flow, 222, 224–27	Inlet discharge control practices, 38
Hydrographs, inflow-outflow, 105-6,	Intake opportunity time, 135, 139–40
120-21	Iraq, 1
Hydromechanical trash cleaners, 237,	Irrigation, 1-6
238	objectives of, 2–3
	selection of method, 3–6
Infiltrated water, depth of, 10	surface (see Surface irrigation
Infiltration:	systems)
basic rate of, 14–15, 105, 106,	Irrigation and Drainage Specialty
119-20	Conference (1979), American
cumulative, 14–16, 113–14, 116	Society of Civil Engineers, 212
evaluation of (see Infiltration evaluation)	Irrigation distribution, 40-41, 43-45 (see also Closed-conduit
irrigation requirement and, 13-18	irrigation distribution; Open-
irrigation scheduling and, 206-7	channel irrigation distribution)
measurement of (see Infiltration measurement)	Irrigation efficiency and uniformity, 22-25
modification of, 126	Irrigation event measurement, 73-81
surge flow systems and, 216, 218,	Irrigation events (see Advance phase;
221, 223–25	Depletion phase; Ponding
uncertainty of rate of, 37	(wetting) phase; Recession
Infiltration equations, 16-18	phase)
•	

Irrigation requirement, 8-25	Land leveling, 38, 138, 178–89
application uniformity and	basin irrigation and, 35, 38
efficiency, 22–25	border irrigation and, 35, 38
defined, 25	cut/fill ratio adjustment, 180,
drainage, 21	186-87
evapotranspiration, 20-21	earth requirements, miscellaneous,
infiltration, 13–18	189
soil chemical properties, 19-20	field operations, 188-89
soil moisture, 11–14	field slope selection, 180–86
soil physical properties, 19	field subdivision, 187–88
water balance, 9-11	general considerations, 179
Irrigation scheduling, 137, 192-93,	land survey and mapping, 180-81
206-9	laser-controlled equipment, 35, 38,
Izuno, F. T., 221	188-89
	maintenance, 189
Jacobian matrix, 307, 310	steps in, 180
Jensen, M. E., 20	Land surveying and mapping, 180-81
	Laplace transform approach to the
Votemedes N. D. 201 202 204 207	volume balance model,
Katapodes, N. D., 301, 302, 304, 305,	370-71
307, 308, 327, 328, 336, 339,	Laser-controlled land leveling
348 Votesitie G. D. 254	equipment, 35, 38, 188-89
Katsaitis, G. D., 256	Leaching, 2
Keller, J., 23, 113, 202, 212, 214, 269	Leaching requirement (LR), 21
Kernel function approach to the	Lee, T. S., 222, 350
volume balance model, 367-70	Length of run, modification of,
	125–26
Kiefer, F. W., 360, 369 Kincaid, D. C., 297, 301, 302, 304	Lewis, M. R., 361
Kindsvater, C. E., 64, 66	Ley, T. W., 118, 342, 363, 365, 366
Kinematic-wave model, 345–57	Liggett, J. A., 319, 346-48
characteristic solution approach,	Lighthill, M. J., 346
346–50	Low-pressure pipeline systems,
deformable control volume	264-65, 267-73
approach, 350–55	
surge flow, 222, 224–27	Maintenance, land leveling and, 189
verification of, 355–57	Malano, H. M., 224
Kostiakov, A. V., 17	Malsajan, V. I. K., 43
Kostiakov equation, 113, 139, 346	Management, 37–39
Kovda, V. A., 1	Management allowed deficit (MAD),
Krautz, D. G., 43	13, 14
Kundu, S. S., 107	Manning equation, 109, 140-41,
Kwun, S., 310	244–45, 295, 345
	Manning roughness coefficient, 246-47
Labor requirements, 6	Mapping, 180-81
Lagrangian system, 313	Marr. J. C., 186

Merriam, J. L., 23, 95, 113 Open-channel lining, 241–42 Open pot hydrants, 275, 276 Mesopotamia, 1 Miller, R. D., 15 Opportunity time, 78, 80, 81 Milne, W. E., 361 Orchard valves, 274, 275 Modified broad-crested weirs, 57–62 Orifices: Modifying hydraulic conditions, closed-conduit, 71 125 - 27free-flow and submerged-flow, 41. Momentum equation: 47-48, 68-70 development of, 292–97 O-rings, inflatable pneumatic, (see also Characteristic approach to 197 - 200Outlet box with gate control, 43 the hydrodynamic model; Eulerian integration approach Outlets, head ditch, 40-41, 43, 44 to the hydrodynamic model; Overflow pot hydrants, 276, 277 Kinematic-wave model; Zero-Overflow stands, 277 inertia model) Overland flow principles (see Saint-Monitoring, 208–10 Venant equations) Moody diagram, 268–70 Oweis, T. Y., 222, 226, 327, 339 Moore, W. L., 252 Parshall, R. L., 49 Nappe trajectory length, 254-56 Parshall flumes, 41, 49–52 Neff, M. E., 339 Permanent wilting point, 11–14 Neill, C. R., 261, 263 defined, 12 Net irrigation requirements, 137 measurement of, 97-98 Net precipitation, depth of, 10 Peterka, A. J., 257, 259 Neutron probes, 94-95 Philip, J. R., 17, 18, 360, 370 Newton-Raphson procedure, 140, Pillsbury, A. F., 273 306, 307, 311, 319–23 Piped delivery systems, 39–40 Nondimensionalization of basic automated, 197-203 equations, 297–99 furrow irrigation systems, 43, 45 low-pressure, 264-65, 267-73 On-off flow control, 39–40 Pipe outlet with gate control, 43 Open-channel headland facility Plane method, 181-84 automation, 193-97 Plastic channel lining, 242

Open-channel irrigation distribution,

channel sections, 244-45, 248-51

check structures, 40, 42, 244, 245,

description of, 239, 241, 242, 244

drop structures, 40, 42, 239, 241,

247, 252-61

division structures, 42, 244

245, 247, 252–61 riprap protection, 261-64 deformable control volume siphon tubes, 44, 244, 264-67 approach to the kinematicspiles, 44, 264, 265, 267 wave model and, 353

Pneumatic O-rings, inflatable,

characteristic approach to the

hydrodynamic model and,

197 - 200

Podmore, T. H., 218

309 - 10

Point gage, 83, 84, 87, 89 Ponding methods, 87–89

Ponding (wetting) phase:

Eulerian integration approach to the hydrodynamic model and, 319 measurement of, 78 recursive approach to the volume balance model and, 363-64 zero-inertia model and, 334–35 Pool depth, 257 Poole, G. J., 214, 215, 217 Potential evapotranspiration, 20–21 Pot hydrants, 275–77 Power advance approach to the volume balance model. 371 - 72Precipitation, depth of, 9 Precipitation intercepted by plants, depth of, 9 Precipitation that infiltrates soil, depth of, 9 Precipitation that occurs as surface runoff, depth of, 9 Preisman double-sweep algorithm, 319 - 23Preliminary design, 136–37 Pressure forces, 293-94, 316-17 Pressure-relief stand pipes, 276 Profilometers, furrow, 78, 90 Propeller meters, 72–73 Pruitt, W. O., 20 Ramsey, M. K., 118, 339 Rand, W., 252 Recession phase, 81 characteristic approach to the hydrodynamic model and, 305, 306, 309 - 10deformable control volume approach to the kinematicwave model and, 353-56Eulerian integration approach to

the hydrodynamic model and,

field system evaluation and, 106-9

recursive approach to the volume balance model and, 366–67

measurement of, 78, 80

surge flow system and, 220-23, 226 - 27zero-inertia model and, 335-36 Rectangular thin-plate weirs, 64-66 Recursive approach to the volume balance model, 361–67 Recycling furrow infiltrometers. 92 - 93Relative roughness of pipe, 268, 270 Replogle, J. A., 54, 57, 58, 60 Richard, F., 15 Richards equation, 16–17 Riprap protection, 261-64 Riser hydrants, 274, 275 Riser outlets, 43, 44 Risers, 267, 274, 275 Robinson, A. R., 52, 55 Rock protection, 261–64 Root growth patterns, 19 Rooting depths of selected crops, 14 Roth, R. L., 339 Roughness of pipe, 268–70

Saint-Venant, A. J. C. Barre de, 289 Saint-Venant equations, 301 continuity equation, development of, 290-91 momentum equation, development of, 292-97 nondimensionalization of basic equations, 297–99 (see also Characteristic approach to the hydrodynamic model; Eulerian integration approach to the hydrodynamic model; Kinematic-wave model; Volume balance model; Zeroinertia model) Saline soils, 19 Salt balance, 21

Saline soils, 19
Salt balance, 21
Salt concentration (loading), 2, 21
Saturated zone, 15, 16
Scheduling, irrigation, 137, 192-93, 206-9
Scour, 261

Screens, 238-43	Sorptivity, 18
Sediment removal, 236-43	Souza, F., 299, 301, 314
Self-calibrated control systems	Spiles, 44, 264, 265, 267
(SCCS), 229	Sprinklers, 4
Shen, J., 66	Staking process, 180–81, 184–85
Siltation, 2	Station controllers, 204
Silvester, R., 257-58	Strelkoff, T., 123, 289, 299, 301, 302,
Simulation models, surge flow, 218-	304, 305, 307, 308, 327, 328,
27	336, 339, 348, 364, 366
Singh, P., 371, 372	Stringham, G. E., 202, 212, 214
Single-pond method, 87, 88	Structural elements, 39–46
Siphon tubes, 44, 244, 264-67	Subdivision of field, 187–88
Skogerboe, G. V., 40, 42, 44, 50, 52,	Submerged-flow conditions vs. free-
107, 238, 339	flow conditions, 48-49 (see
Slack, D. C., 15, 17	also Flow measurement, free-
Slide-gate turnouts, 195, 197, 198	flow and submerged-flow)
Slope:	Surface irrigation system operation,
of furrow, 142	192-210
of land, 4, 180-86	calibration, 192, 205-6
Smerdon, E. T., 221, 360, 371	conceptual approach, 192-93
Smith, R. E., 346–48	controllers, 202-5
Snake River Conservation Research	irrigation scheduling, 192-93,
Center, 219	206-9
Sodic soils, 19	monitoring and evaluation, 208-10
Sodium adsorption ratio (SAR), 19	open-channel headland facility
Soil characteristics:	automation, 193-97
irrigation requirement and, 11-20	pipeline automation, 197-203
system selection and, 4-5	Surface irrigation systems, 32-46
Soil chemical properties, 19-20	advantages of, 6
Soil Conservation Service, 55, 57, 71,	automated (see Automation)
245, 248-51	defined, 6
Soil cooling, 2	design of (see Volume balance field
Soil infiltration (see Infiltration)	design)
Soil moisture:	disadvantages of, 6
irrigation requirement and, 11-14	evaluation of (see Field system
measurement of, 94-96	evaluation; Irrigation
Soil moisture deficit (SMD), 13	requirement)
Soil moisture holding capacity, 4	field measurement techniques (see
Soil moisture storage, depth of	Flow measurement, closed-
change in, 9, 10	conduit; Flow measurement,
Soil physical properties, 19	free-flow and submerged-flow;
Soil-water measurement, 93-98	Infiltration measurement;
bulk density. 97	Irrigation event measurement;
field capacity, 97	Soil-water measurement)
permanent wilting point, 97-98	field system evaluation (see Field
soil moisture content, 94–96	system evaluation)

hydraulics (see Saint-Venant Thin-plate weirs, rectangular, 64–66 equations) Tinney, E. R., 348 irrigation requirement (see Topographic limitations, 4 Irrigation requirement) Topography: operation of (see Surface irrigation information on, 136 system operation) modification of (see Land leveling) results of, 120-21 Total available water (TAW), 13 structural elements, 39-46 Total dissolved solids (TDS), 21 subsystems, 32, 33 Touch-and-feel method, 95, 96 surge flow (see Surge flow surface Transition zone, 15, 16 irrigation) Transmission zone, 15, 16 types of (see Basin irrigation; Transmissivity, 18 Border irrigation; Furrow Transpiration, depth of, 9 Trapezoidal broad-crested weirs, irrigation) volume balance field design (see 58 - 62Volume balance field design) Trapezoidal flumes, 54-57 water supply and management, Trashracks, 236-37 37 - 39Trickle irrigation, 4 Surface storage volume estimation, Trout, T., 57 105-6, 108-12Turnout structures, 40, 235-36 Surface water storage, 105-6 Surge flow surface irrigation, 212-33 Under-irrigation case, 120-22 conceptual development, 212-14 Uniformity, application, 22-24 early field tests, 214-18 U.S. Army Corps of Engineers, 236 management of, 227-33 U.S. Bureau of Reclamation, 64, 71, simulation models, development 257, 258 of, 218-27 U.S. Department of Agriculture Surveying, 180-81 (USDA): System controllers, 203-4 Agricultural Experiment Station Regional Project W163, 218 Agricultural Research Service, 193, Tailwater ratio (TWR): 195-97, 202-4 defined, 25 inflatable pneumatic O-ring of, estimation of, 122 197 - 200Tailwater removal and reuse systems, Snake River Conservation 45 - 46Research Center, 219 Tailwater reuse, furrow systems with, Soil Conservation Service, 55, 57, 146 - 4771, 245, 248–51 Tailwater runoff: U.S. Salinity Laboratory, 21 depth of, 10

## Valves:

air-operated butterfly, 200-203 alfalfa, 44, 267, 273-74

Unsteady momentum, 296-97, 318

Utah State University, 214, 218, 219

modification of, 126-27

231 - 33

120 - 21

surge flow systems and, 216, 217,

Tailwater runoff hydrographs, 105-6,

Tailwater storage and recycling, 39

Valves (cont.)	Wastewater recovery and reuse, 39
in closed-conduit distribution	Water advance (see Advance phase)
systems, 265, 267, 272-76	Water balance, 9-11
Epp-fly, 202, 203	Water control structures, 40, 42
inflatable pneumatic O-ring,	Water delivery subsystem, 32
197-200	Water-level-control stand pipes, 276
orchard, 274, 275	Waterlogging, 2, 11
in surge flow systems, 212-14	Water-operated Snake River valves,
water operated Snake River, 198,	198, 200, 201
200, 201	Water removal subsystem, 32
Van Bavel, C. H. M., 94, 95	Water requirement efficiency:
Venturi meters, 71–73	defined, 25
Vertical infiltration, 16	estimation of, 122
V-notch weirs, 66–68	Water resources, nature of, 136, 137
Volume balance, 105	Water supply, 37
Volume balance equation, 116-18	furrow irrigation design and,
Volume balance field design, 134–52	147-48
basin irrigation, 150-52	system selection and, 5
border irrigation, 148-50	Water supply subsystem, 32
computations, 139-42	Water use subsystem, 32
design data, 135-36	Watters, G. Z., 269
detailed (see Headland facilities;	Weight forces, 292, 316
Land leveling)	Weirs, 47, 64-67, 244, 265
furrow irrigation, 142–48	Wetting front, 15, 16
preliminary, 136–37	Wetting phase (see Ponding phase)
rationale for, 138–39	Wetting zone, 15, 16
Volume balance model, 358–73	Whitham, R. B., 346
mass continuity development, 358-	Wild flooding, 32
60	Wilke, O. C., 296, 302, 304, 360, 371
numerical solutions, 360-72	Willardson, L. S., 22, 45
surge flow, 222, 224-27	Wu, I., 273
verification, 372–73	
Volumetric moisture content, 11-13	Zono inantia madal 227 44
	Zero-inertia model, 327–44
Wolken W D 22 107 114 119	general mathematical approach, 328-36
Walker, W. R., 22, 107, 114, 118, 119, 218, 222-24, 339, 350,	numerical solution, 336–37
	surge flow, 222, 224–27
361, 373	•
Wallender, W. W., 221	verification of, 339–44